FACTORS AFFECTING THE DRAINAGE OF GAS FROM COAL AND METHODS TO IMPROVE DRAINAGE EFFECTIVENESS

A thesis submitted in fulfilment of the requirements for the award of the degree

DOCTOR OF PHILOSOPHY

from

UNIVERSITY OF WOLLONGONG

by

DENNIS JOHN BLACK

B. Eng. (Hons) (Mining), Assoc. Dip. Mine Ventilation, Grad. Dip. Mgt

School of Civil, Mining and Environmental Engineering

2011

AFFIRMATION

I, Dennis John Black, declare that this thesis, submitted in fulfilment of the requirements for the award of Doctor of Philosophy, in the Department of Civil, Mining and Environmental Engineering, University of Wollongong, is wholly my own work unless otherwise referenced or acknowledged. The document has not been submitted for qualifications at any other academic institution.

Dennis J. Black

The following publications are the result of this thesis project:

Black, D J, 2007. Gas management challenges at West Cliff Colliery, *ACARP Gas and Outburst Seminar* (ed: J Hanes), Mackay, Queensland, 29 June, pp 98-106.

Black, D J and Aziz, N I, 2008. Improving UIS gas drainage in underground coal mines, in *Proceedings of the 8th Underground Coal Operator's Conference COAL2008*, University of Wollongong, (eds: N I Aziz and J A Nemcik), Wollongong, 14-15 February, pp 186-196.

Black, D J and Aziz, N I, 2008. The evolution in coal mine gas extraction – a response to economic, environmental and community pressures, in *Proceedings of the 16th Coal Congress of Turkey*, Chamber of Mining Engineers of Turkey, Zonguldak, Turkey, 26-28 May, pp 149-156.

Black, D J and Aziz, N I, 2008. Improving UIS gas drainage in underground coal mines, in *Proceedings of the 16th Coal Congress of Turkey*, Chamber of Mining Engineers of Turkey, Zonguldak, Turkey, 26-28 May, pp 157-170.

Black, D J and Aziz, N I, 2008. Development of hydraulic fracturing in high stress conditions in Australian underground coal mines, in *Proceedings of the 16th Coal Congress of Turkey*, Chamber of Mining Engineers of Turkey, Zonguldak, Turkey, 26-28 May, pp 171-184.

Black, D J and Aziz, N I, 2008. Gas drainage improvement in underground coal mines, in *Proceedings of the 1st ASIA Pacific Coalbed Methane Symposium*, University of Queensland, Brisbane, 22-24 September, Paper No. 043.

Black, D J and Aziz, N I, 2008. Hydraulic fracturing in underground coal mines, in *Proceedings of the 1st ASIA Pacific Coalbed Methane Symposium*, University of Queensland, Brisbane, 22-24 September, Paper No. 044.

Black, D J and Aziz, N I, 2009. Reducing coal mine GHG emissions through effective gas drainage and utilisation, in *Proceedings of the 9th Underground Coal Operator's Conference COAL2009*. University of Wollongong, (eds: N I Aziz and J A Nemcik), Wollongong, 12-13 February, pp 217-224.

Black, D J and Aziz, N I, 2009. Reducing coal mine GHG emissions through effective gas drainage and utilisation, in *Proceedings of the 2009 International Coalbed & Shale Gas Symposium*, University of Alabama, Tuscaloosa, 18-22 May, Paper No. 0912.

Black, D J and Aziz, N I, 2009. Developments in coal mine methane drainage and utilisation in Australia, in *Proceedings of the Ninth International Mine Ventilation Congress*, Department of Mining Engineering, Indian School of Mines University, Dhanbad, India, 10-13 November, pp 445-460.

Black, D J and Aziz, N I, 2010. Outburst threshold limits – current research outcomes, in *Proceedings of the 10th Underground Coal Operator's Conference COAL2010*,

University of Wollongong, (eds: N I Aziz and J A Nemcik), Wollongong, 11-12 February, pp 203-209.

Black, D J and Aziz, N I, 2010. Impact of coal properties and operational factors on mine gas drainage, in *Proceedings of the 10th Underground Coal Operator's Conference COAL2010*, University of Wollongong, (eds: N I Aziz and J A Nemcik), Wollongong, 11-12 February, pp 229-240.

Black, D J and Aziz, N I, 2010. Coal properties and mine operational factors that impact gas drainage, in *Proceedings of the 13th U.S. / North American Mine Ventilation Symposium* (eds: S Hardcastle and D L McKinnon), Sudbury, Ontario, 13-16 June, pp 251-258.

Black, D J and Aziz, N I, 2011. Actions to improve coal seam gas drainage performance, in *Proceedings of the 11th Underground Coal Operator's Conference COAL2011*. University of Wollongong, (eds: N I Aziz, R J Kininmonth, J A Nemcik and T X Ren), Wollongong, 10-11 February, pp 309-316.

Black, D J, Aziz, N I and Florentin, R M, 2010. Assessment of factors impacting coal seam gas production, in *Proceedings of the 2010 International Coalbed & Shale Gas Symposium*, University of Alabama, Tuscaloosa, 17-21 May, Paper No. 1004.

Black, D J, Aziz, N I and Florentin, R M, 2010. Use of early stage gas emission data for estimating total gas content, in *Proceedings of the 2010 International Coalbed & Shale Gas Symposium*, University of Alabama, Tuscaloosa, 17-21 May, Paper No. 1005.

Black, D J, Aziz, N I, Jurak, M J and Florentin, R M, 2009. Outburst threshold limits – are they appropriate?, in *Proceedings of the 9th Underground Coal Operator's Conference COAL2009*, University of Wollongong, (eds: N I Aziz and J A Nemcik), Wollongong, 12-13 February, pp 185-192.

Black, D J, Aziz, N I, Jurak, M J and Florentin, R M, 2009. Gas content estimation using initial desorption rate, in *Proceedings of the 9th Underground Coal Operator's Conference COAL2009*, University of Wollongong, (eds: N I Aziz and J A Nemcik), Wollongong, 12-13 February, pp 193-198.

Black, D J, Aziz, N I and Ren, T X, 2011. Enhanced gas drainage from undersaturated coalbed methane reservoirs, in *Proceedings of the 3rd Asia Pacific Coalbed Methane Symposium*, University of Queensland, Brisbane, 3-6 May, Paper No. 50.

The following presentations are the result of this thesis project:

Black, D J, 2007. Gas management challenges at West Cliff Colliery, paper presented to the Gas and Outburst Committee Seminar, Wollongong, New South Wales, 27 June, pp 13-21.

Black D J, 2010. Appropriate risk control and drainage to avoid gas outbursts, paper presented to Mining Ventilation 2010, Brisbane, 01 September.

ACKNOWLEDGEMENTS

I would like to acknowledge and thank my thesis supervisor Assoc. Professor Naj Aziz, Department of Civil, Mining and Environmental Engineering, University of Wollongong for his generous support, guidance and friendship throughout this study.

I would also like to acknowledge and thank my wife Dr Sarah Toole and children, Angus and Emma, for their support during the considerable time involved in completing this PhD study.

I would also like to acknowledge and thank the Australian Coal Association Research Program (ACARP) for the financial support provided to me through the ACARP post-graduate scholarship C18004. I would like to acknowledge and thank Mr Roger Wischusen (ACARP), Dr Chris Harvey (Gujarat NRE) and Assoc. Professor Naj Aziz who monitored the progress of my study on behalf of ACARP project C18004.

The work completed during this study was recognised with an award from the Royal Society of New South Wales in 2010 which is appreciated.

I would also like to acknowledge and thank the following people and organisations who have provided assistance and support to this study:

- Mr Matthew Jurak and Ms Kate Lennox, former undergraduate students from the Department of Civil, Mining and Environmental Engineering and Mr Adrian Hutton , formerly of the School of Geosciences, University of Wollongong;
- Mr Robert Seeley, Mr Andrew Filipowski, Mr Murray Bull, Mr Sal Castelo, Mr Mike Armstrong, Mr Hugo Kaag, Mr David Benson and Mr David Ashelford (formerly of GeoGAS), from BHP Billiton Illawarra Coal;
- Mr Andrew Newland from Newtuk Consulting;
- Mr Paul Maddocks from Xstrata Coal NSW;
- Mr Peter Liston, Mr Ken Lewthwaite and Mr Wayne Green from Peabody Energy Australia; and
- Mr Bruce Robertson formerly from Anglo American Metallurgical Coal.

I would also like to acknowledge the keen eye of Mr Bob Kininmonth and express my thanks for assisting with the editing of this PhD thesis.

ABSTRACT

The relationship between gas production from underground-to-inseam (UIS) drainage boreholes and various coal seam properties and operational factors were examined. Gas production from 279 UIS gas drainage boreholes was collated and assessed relative to a variety of coal geological properties and operational factors. The reasons for poor coal seam gas drainage performance from particular zones were investigated and actions to improve gas drainage performance have been recommended. Investigation were focussed on gas drainage performance from the Bulli seam of the Sydney Basin, focussing on West Cliff Colliery, where gas production was highly variable and many zones found to be difficult to drain.

The degree of saturation (DoS) was found to have a significant impact on coal seam gas drainage, with decreased gas production from highly undersaturated zones with low permeability. Within West Cliff Colliery, in the areas where gas drainage was found to be particularly difficult, conventional UIS drainage was shown to be incapable of reducing the reservoir pressure below the critical desorption point prior to roadway development.

From analysis of operational factors, drainage time was found to have a significant impact on gas production and appeared to be closely related to DoS indicating that coal with lower DoS required increased drainage time. Borehole length and orientation were found to have some impact on gas production with maximum gas production achieved from boreholes between 500 and 1 000 m long oriented between 5 and 60^{O} to the face cleat and between 0 and 40^{O} to the maximum horizontal stress. Boreholes drilled up-dip, with an apparent dip between 0.0 and $+3.0^{O}$ achieved increased gas production and the relationship was strongest in highly undersaturated coal. In saturated coal the initial gas flow rate tends to be high and the increased gas flow velocity supports the borehole to self-clear water and fines. With increasing age, gas flow velocity reduces which appears to affect the ability of the borehole to self-clear, particularly in boreholes oriented down-dip. Undulations such as troughs existing along the length of the boreholes also allow water and fines to accumulate which impedes gas drainage. No evidence was found to support a relationship between applied suction pressure and gas production. However where high suction pressure is applied to boreholes increased

leakage may occur. A new method for enhancing coal seam gas production using cyclic injection of inert gas is proposed.

The nature of coal seam gas emission from both fast and slow desorption gas testing methods was investigated using results from 4 185 gas tests collected from eight Australian underground coal mines, four located in Queensland and four in New South Wales.

The following equations were found to best represent the average relationship between each gas content component and the total measured gas content (Q_M):

- $Q_1 = 0.0064 \times Q_M{}^{2.0227}$
- $Q_2 = 0.0257 \times Q_M{}^{1.9692}$
- $Q_3 = 1.1631 \times Q_M{}^{0.7529}$

The following equations were proposed for use in estimating average and maximum Q_M based on Q_1 and initial desorption rate (IDR):

- $Q_{M(ave)} = 9.3729 \times Q_1{}^{0.3328}$
- $Q_{M(max)} = 2.5665 \times \ln(IDR) + 2.1686$
- $Q_{M(ave)} = 0.7413 \times \sqrt{IDR}$

- The relationship between Q_M and desorption rate index (DRI) was investigated and found to be different from the relationship presented in 1995, which is the basis for the DRI900 methodology used to determine outburst threshold limit values (TLV) applicable to non-Bulli seam mines. The impact of recent increases to outburst TLV at several Bulli seam mines and the relationship between Q_M and DRI identified during this study suggests that a TLV applicable to the Bulli seam may be directly transferrable to non-Bulli seam mines.
- From analysis of 3 355 fast desorption test results the relationship between Q_M and DRI was found to be independent of gas composition and represented by the following equation:
  - $Q_M = 0.008 \times DRI$

The following relationships were identified from analysis of slow desorption data.

- A linear relationship exists between Q_2 and Q_M that is independent of changes in seam gas composition. The rate of gas desorption was shown to be faster from

samples with increased Q_M. Extending total desorption time beyond 200 days was shown to have little impact on Q_2 or the Q_2:Q_M ratio.

- From analysis of Q_2 and the Q_2:Q_M ratio, no relationship was found between vitrinite content, porosity and mineral matter content of each sample, suggesting the nature of desorbed gas emission was independent of coal petrography.
- Q_3 did not vary significantly in response to increasing Q_M whereas the Q_3:Q_M ratio reduced. The results indicate coal samples with high Q_M, having increased DoS, desorb gas at a faster rate resulting in the Q_3:Q_M ratio being less than from samples with low Q_M that desorb gas at a slower rate. The relationship between Q_3 and Q_M appeared to be independent of changes in seam gas composition. Extending the total desorption time beyond 200 days had little effect on residual gas content.
- From analysis of Q_3 and the Q_3:Q_M ratio relative to the measured vitrinite content, porosity and mineral matter content of the coal samples, it was found that residual gas content was independent of coal petrography.

To reduce the risk of gas loss into solution from prolonged contact with the current conventional slow desorption testing apparatus; consideration should be given to the use of electronic gas testing apparatus for continual analysis of the desorbed gas from coal.

TABLE OF CONTENTS

LIST OF FIGURES

LIST OF TABLES

LIST OF SYMBOLS AND ABBREVIATIONS

ACIRL	Australian Coal Industry Research Laboratories
BHPBIC	BHP Billiton Illawarra Coal
Φ	porosity (%)
CBM	coalbed methane
cc/g	cubic centimetres per gram
cm	centimetre
$CO_{2\text{-}e}$	carbon dioxide equivalent
D50	initial 50 days of gas production from UIS drainage boreholes
daf	dry and ash free
DRI	desorption rate index (ml)
DTV	defined threshold value
ECBM	enhanced coalbed methane
g	gram
GHG	greenhouse gas
Gt	gigatonnes ($1x10^9$ tonnes)
IDR	initial gas desorption rate ($\sqrt{ml \div \sqrt{min} \div kg}$)
IDR30	gas desorbed from sample in initial 30 secs of testing (m^3/t)
kPa	kilopascal
L/s	litres per second
L/min	litres per minute
LWD	logging-while-drilling
m	metre
mm	millimetre
m/day	metres per day
m^3	cubic metre
m^3/m	cubic metre per metre
m^3/t	cubic metre per tonne
m/s	metres per second
mD	milli Darcy
MPa	megapascal
MRD	medium radius drilling
Mt	megatonne ($1x10^6$ tonnes)
Mtpa	million tonnes per annum
MWD	measure-while-drilling
nm	nanometre ($1x10^{-9}$ m)
NCM	non-coal matter
NTP	normal temperature and pressure (20^OC and 101.325 kPa)
P	absolute gas pressure
Pa	Pascal
P_{CDP}	critical desorption pressure
P_i	initial reservoir pressure

P_L	Langmuir pressure constant
P_O	atmospheric pressure (101.325 kPa)
Q_1	gas lost during coal core sample recovery (m^3/t)
Q_2	gas released from coal core sample during desorption testing (m^3/t)
Q_3	gas released from coal sample after crushing (m^3/t)
Q_M	total measured gas content; sum of Q_1, Q_2 and Q_3 (m^3/t)
STIS	surface to inseam
T	absolute strata temperature (^OK)
TLV	outburst threshold limit value
ρ	rho - density (t/m^3)
ROM	run-of-mine
rpm	revolutions per minute
μm	micrometre, or micron ($1x10^{-6}$ m)
UIS	underground to inseam
V_i	*in situ* gas content
V_L	Langmuir volume constant
V_{sat}	saturated gas content
WCC	West Cliff Colliery

CHAPTER ONE – GENERAL INTRODUCTION

1.1 COAL MINING IN AUSTRALIA

Australia was the fourth largest coal producing country behind China, the Russian Federation and the United States of America in 2008 with raw coal production totalling 497 Mt. Total saleable production was 337 Mt of which 261 Mt was exported, making Australia the world's largest coal exporter. The total revenue from export coal sales was $32.3 billion making coal Australia's highest value export commodity (ABARE, 2010).

Australia has significant black coal resources. At the end of 2008, Australia's reported recoverable economic demonstrated resources of black coal totalled 39.2 Gt with 8.3 Gt of sub-economic demonstrated resources and a further 66.6 Gt of recoverable inferred resources (ABARE, 2010). The majority of Australia's economic black coal resources exist in Queensland and New South Wales, which jointly produced 98% of Australian black coal (ABARE, 2009a and 2009b). Figure 1.1 shows the location of coal resources, operating mines, and coal deposits within Australia, highlighting the intensity of coal mining activity in the Bowen and Sydney basins (ABARE, 2010). The majority of Australia's metallurgical (coking) coal is produced in Queensland, while New South Wales produces predominantly thermal (steaming) coal. In addition, brown coal is mined in Victoria and South Australia, where it is used for domestic electricity generation.

Open cut mining accounts for approximately 75% of total saleable coal production with the balance from underground mines. In 2008, there were 123 black coal mines operating in Australia comprising 79 open cut and 44 underground mines. Of the 44 underground mines, 30 utilised the longwall mining method (Cram, 2009). Underground mining is typically used to extract coal seams which are beyond the economic depth limit of open cut mining methods.

The productivity of underground mines, regardless of the mining method, is significantly impacted by the prevailing geological conditions, such as faults and dykes, the presence of coal seam gas, and the relative ease with which these gases can be drained.

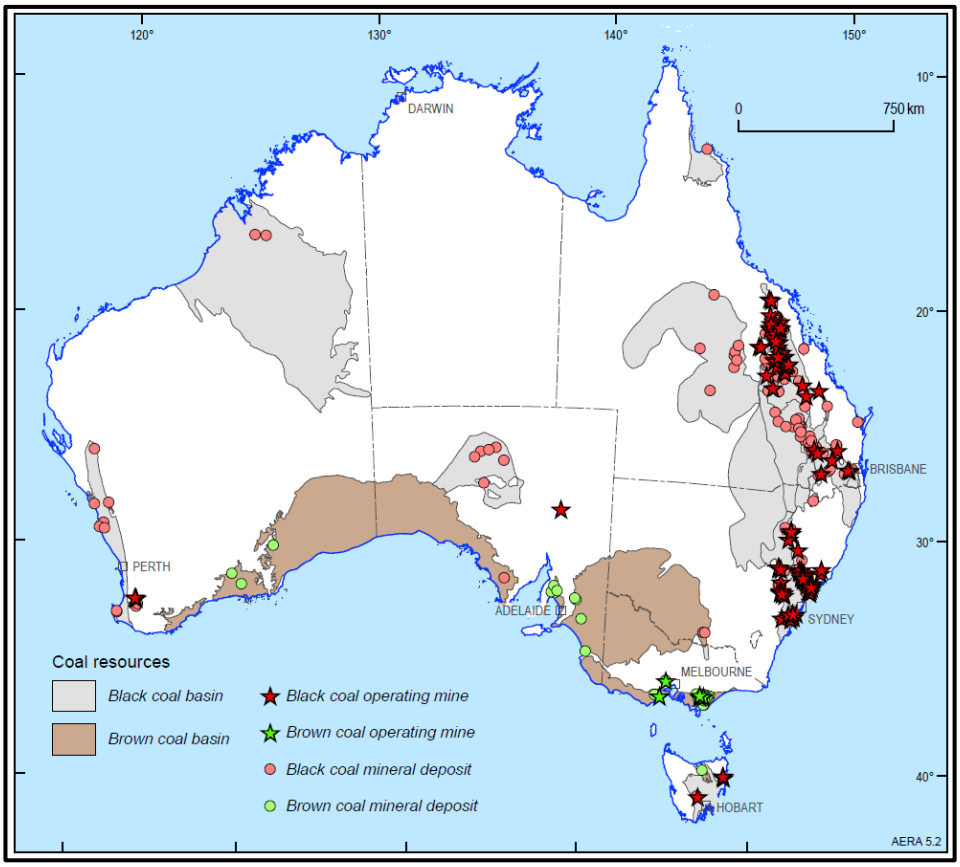

Figure 1.1: Australia's operating black and brown coal mines as at December 2008 (ABARE, 2010)

It is estimated that 40% of Australian longwall mines require regular gas drainage to manage coal seam gas emissions. Mines that use gas drainage include Grasstree, North Goonyella, Moranbah North, Oaky No.1, Oaky North and Newlands in Queensland and Appin, Mandalong, Metropolitan, South Bulga, Tahmoor, United, and West Cliff in New South Wales.

Gas emission from coal mining, both open cut and underground, has been identified as a potentially significant source of greenhouse gas emission with the most common coal seam gas, methane (CH_4), having a global warming potential 21 times that of carbon dioxide (CO_2). In 2007, total fugitive gas emission from Australian coal mining was estimated at 26.8 $MtCO_{2\text{-}e}$, representing approximately 5% of Australia's total greenhouse gas emissions of 547 $MtCO_{2\text{-}e}$ (AGDCC, 2009).

1.2 COAL SEAM GAS DRAINAGE AND UTILISATION

Coal seam gas represents a potentially significant risk to the safety and productivity of coal mining operations. In the two years to December 2010 more than 561 lives were lost in coal mines as a direct result of methane gas explosions and outbursts. More than 317 lives were lost in China (ILN, 2009a; ILN, 2009b; ILN, 2009c; Hays, 2010; ILN 2010a; ILN, 2010b; ILN, 2010h and ILN, 2010i), 38 in Columbia (ILN, 2010c), 32 in Indonesia (ILN, 2009d), 29 in New Zealand (ILN, 2010g), more than 66 in Siberia (ILN, 2010d), 20 in Slovakia (BBC, 2010), 30 in Turkey (ILN, 2010e), and 29 in the United States (ILN, 2010f).

High levels of methane and carbon dioxide gas, typically in close proximity to geological structures, have been identified as a major contributing factor in the coal and gas outburst phenomenon (Lama, 1995c). In Australia, the Bulli seam, located in the southern Sydney Basin, is extremely prone to the occurrence of coal and gas outbursts. In the history of mining in the Bulli seam 12 lives have been lost as a result of outbursts (Harvey and Singh, 1998).

In addition to the explosion and outburst risk, accumulations of methane and carbon dioxide in underground mines have the potential to exceed the diluting capacity of the mine ventilation system, thus exceeding prescribed maximum concentration limits. Where such concentration limits are exceeded coal production is required to cease until the gas concentration in the mine ventilation air is reduced below the statutory limit. In gassy and highly permeable coal seams reliance on the ventilation system alone to effectively manage high gas emission may result in frequent, prolonged production delays. In such mines gas drainage is used to reduce the gas loading of the mine ventilation system, to improve ventilation air quality and reduce ventilation costs, minimise the risk of a dangerous gas accumulation, reduce the risk of an outburst, and ultimately make mining safer and more efficient (Lama, 1980; Kahil and Masszi, 1982; Clark *et al.*, 1983 and Wood and Hanes, 1983).

Although aware of the relationship between gas and outburst risk, and the impact of gas drainage on reducing this risk, many mine operators failed to implement systems to regularly check and assess the outburst risk ahead of future workings. As a result of the investigation into the last fatal Bulli seam outburst, at West Cliff Colliery on 25 January 1994, a directive was issued to all Bulli seam coal mine operators, under the authority of

the Coal Mines Regulation Act 1982, prescribing Threshold Limit Values (TLV), and other actions, to be implemented to manage risk and prevent future coal and gas outbursts (Clarke, 1994 and NSWDMR, 1995). The TLV represent the maximum allowable gas content, relative to seam gas composition, considered safe for mine operations. Mine operators are required to ensure seam gas content has been reduced below the applicable TLV prior to mining.

In gassy outburst prone coal seams such as the Bulli seam, mine operators use intensive gas drainage drilling programs to collect coal cores for gas content testing, identify structures ahead of the mine workings, and drain gas to below the applicable TLV. These mines typically drill in the order of 100 000 m of inseam boreholes annually for the purpose of coal seam gas drainage. The total cost of gas drainage in such mines was reported to range between $1 and $5 per ROM tonne (Kelly, 1983; Allen, 2002 and Thomson, 2007). The unit cost of drilling underground-to-inseam (UIS) boreholes was reported to range between $50 and $100 per metre (Hanes, 2004 and Benson, 2006). With an annual cost in the order of $5 000 000 to $10 000 000, gas management represents a significant operational cost and the gas drainage program should be effective in reducing coal seam gas content and achieve maximum gas production from every metre drilled.

In the years following the introduction of routine coal seam gas drainage in the early 1980's many investigations have been undertaken to identify the various factors which impact gas drainage performance (Lama, 1980; Lama *et al.*, 1980; Clark, 1983; Clark *et al.*, 1983; Williams *et al.*, 1983; Lama, *et al.*, 1984; Lama, 1988a and Lama, 1995b). The aim of these investigations was to reduce seam gas emissions into mine workings, to reduce the risk of outburst, and generally improve mine safety. More recently the growth of the coalbed methane (CBM) industry has supported research to assess the impact of various coal seam geological properties on CBM production and hence the economic viability of potential gas development projects.

With increasing community and government focus on greenhouse gas emissions from coal mines and the potential for mine operators to incur a financial penalty to offset greenhouse gas emissions there is increased interest in technologies to improve coal seam gas capture and utilisation, thereby reducing coal mine fugitive gas emission (Black and Aziz, 2009).

1.3 GEOLOGY OF THE ILLAWARRA COAL MEASURES

The Illawarra Coal Measures, which are Permian to Triassic in age, form part of the Southern Coalfield, which encompasses the southern portion of the Sydney Basin. The Southern Coalfield is bounded to the west by the towns of Campbelltown and Mittagong, and to the east by Wollongong and Helensburgh, shown in Figure 1.2. There are a number of coal seams in the Illawarra Coal Measures, as shown in Figure 1.3 (Apex Energy NL, 2008). The Bulli seam, which is the focus of this research, is stratigraphically the uppermost coal seam in the sequence.

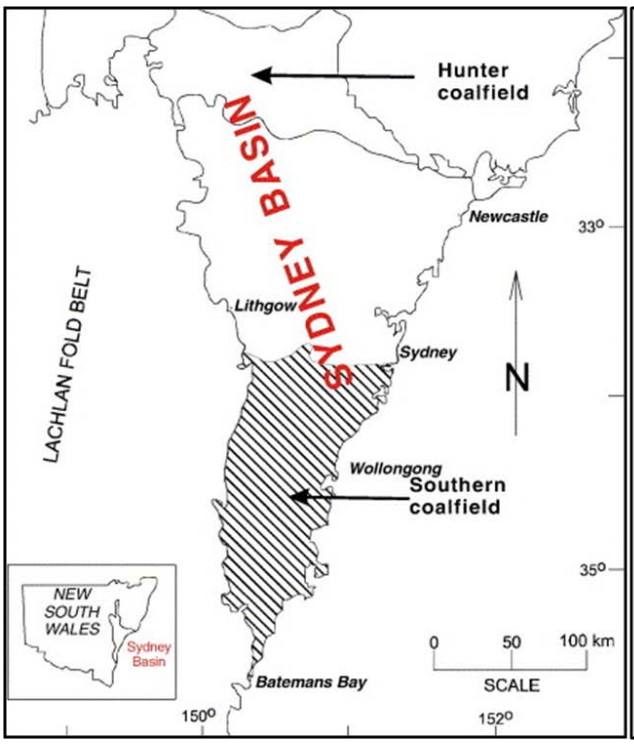

Figure 1.2: Extent of the Southern Coalfield of the Sydney Basin (after Faiz *et al.* 2007b)

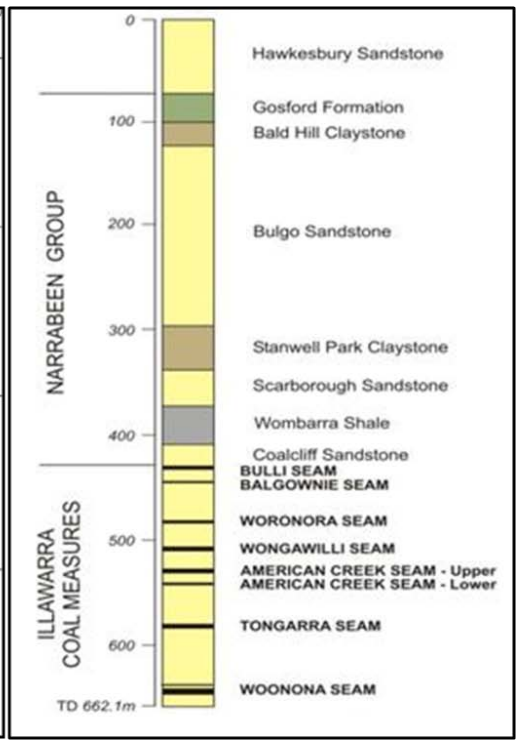

Figure 1.3: Stratigraphic section of the Sydney Basin (after Apex Energy NL, 2008)

The Bulli seam in the area covered by this study has a depth of cover of approximately 450 to 500 m with a regional dip of approximately 1.5^{O} toward the west. The seam gas composition is variable, ranging from almost pure CH_4 in the east to almost pure CO_2 in the west. Table 1.1 lists the minimum and maximum value of various Bulli seam coal properties determined from analysis of coal samples collected from in and around Area 5 at West Cliff Colliery, which is the primary focus of this study (Clark, 1986-2007 and Armstrong and Kaag, 2008).

Table 1.1: Range of coal property values representing West Cliff Colliery, Area 5

Coal Property	Minimum	Maximum
$CH_4/(CH_4+CO_2)$ (%)	6.5	97.8
Gas Content (m^3/t)	5.2	15.7
Permeability (mD)	0.05	6.0
Seam Thickness (m)	2.3	3.2
Ash Content (%)	9.4	14.8
Moisture Content (%)	0.7	1.3
Vitrinite Reflectance ($R_{V(max)}$)	1.23	1.36
Vitrinite (%)	28.9	54.5
Inertinite (%)	45.5	71.1
Mineral Matter (%)	1.8	5.8
Volatile Matter (%)	19.7	25.3

1.4 STATEMENT OF THE PROBLEM

Many Australian underground coal mines are progressing toward areas which require the use of gas drainage to reduce seam gas concentrations below a prescribed TLV. In a number of cases, these mines will encounter areas where the gas is extremely difficult to drain from the coal, ahead of mining. Where difficult drainage areas are encountered, the mine may be faced with significant production delays while intensive drilling is carried out in an attempt to reduce the gas concentrations to an acceptable level. Where intensive additional drilling proves unsuccessful, other high cost, low productivity actions may be taken such as remote mining (Tower/Appin Colliery), grunching (Tahmoor Colliery), cited by Hanes, (2004), and realignment of roadways to avoid the difficult zone (Central Colliery). To avoid such costly delays, mine management may choose to avoid the area completely, resulting in loss of reserves (West Cliff Colliery), loss of potential revenue and ultimately reduced mine life. In extreme cases, an inability to effectively manage gas may lead to mine closure (Leichhardt Colliery and Collinsville Colliery).

Several BHP Billiton mines have previously encountered areas within the Bulli seam where gas drainage was particularly slow and ineffective (Brown, 2007). In these areas lengthy mining delays were incurred, and in the case of West Cliff Colliery the mine plan was changed to avoid the difficult drainage areas which involved reducing the

length of the future longwall panels. The presence of high concentrations of CO_2 in the seam gas was assumed by mine personnel to be the reason for the poor drainage.

The workings in the Bulli seam at West Cliff Colliery (WCC) were classified according to perceived gas drainage risk based on measured gas content in areas where the composition of the seam gas was >60% CO_2. The gas content in the high risk Orange zone (A) was≥10 m^3/t and <10 m^3/t in the moderate risk Yellow zone (B). Figure 1.4 shows the aerial extent of the gas drainage risk zones relative to the Area 5 mine workings (Armstrong and Kaag, 2006). Changing the WCC mine plan to avoid the Orange zone effectively reduced future planned recoverable coal reserves by some 3.5 Mt ROM.

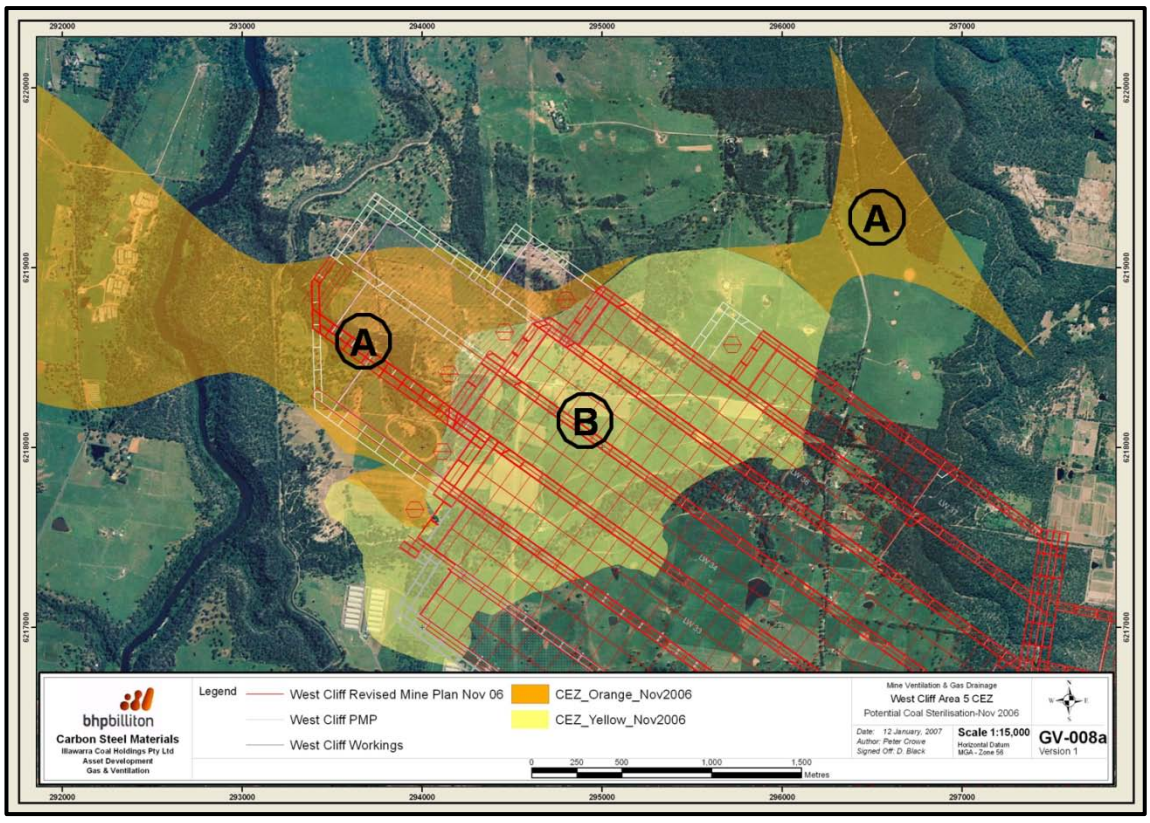

Figure 1.4: Gas drainage risk classification for WCC Area 5 (Armstrong and Kaag, 2006)

1.5 RESEARCH OBJECTIVES

The objectives of this thesis are:

1. To provide new knowledge on the nature of gas emission from coal, in particular the specific geological properties and operational factors that adversely impact gas production from coal;

2. To provide an improved understanding of the characteristics of gas emission from the Bulli seam, in particular the specific geological properties and operational factors that impact coal seam gas drainage, and to recommend a variety of actions to improve drainage effectiveness;
3. To provide new knowledge on the characteristics of gas emission from coal samples during gas content testing;
4. To identify new methods for estimating gas content and the current status of outburst TLV; in particular the impact of recent increases in Bulli seam TLV and identified nature of gas emission from coal on the method used to determine TLV applicable to non-Bulli seam mines is investigated; and
5. To investigate the fast and slow desorption methods for determining gas content to identify differences in the nature of gas emission determined through each test. The accuracy of the two methods is also considered. Changes in the composition of gas liberated from coal during slow desorption testing is assessed relative to changes in gas composition recorded during gas production from inseam drainage boreholes.

1.6 SCOPE

The scope of work to achieve the research objective involved in-mine and laboratory data collection, testing and analysis. The first stage of work, summarised in Figure 1.5, focussed on determining the factors which have greatest impact on gas drainage, based on the collection and analysis of the following:

- Gas production data from UIS gas drainage boreholes;
- Coal core sample gas analysis and coal quality data; and
- Coal properties and characteristics determined from laboratory testing.

From the research conducted during the first stage of the project the relative significance of a variety of factors that impact gas drainage can be explained. Various improvement actions can also be recommended to WCC management to improve the performance and effectiveness of coal seam gas drainage. The results of this research may be used to support extending the length of future longwall panels on the basis of renewed confidence in the ability of the mine to successfully drain gas from the previously sterilised Orange zones in advance of mining, thereby increasing recoverable coal reserves and effectively extending the mine life.

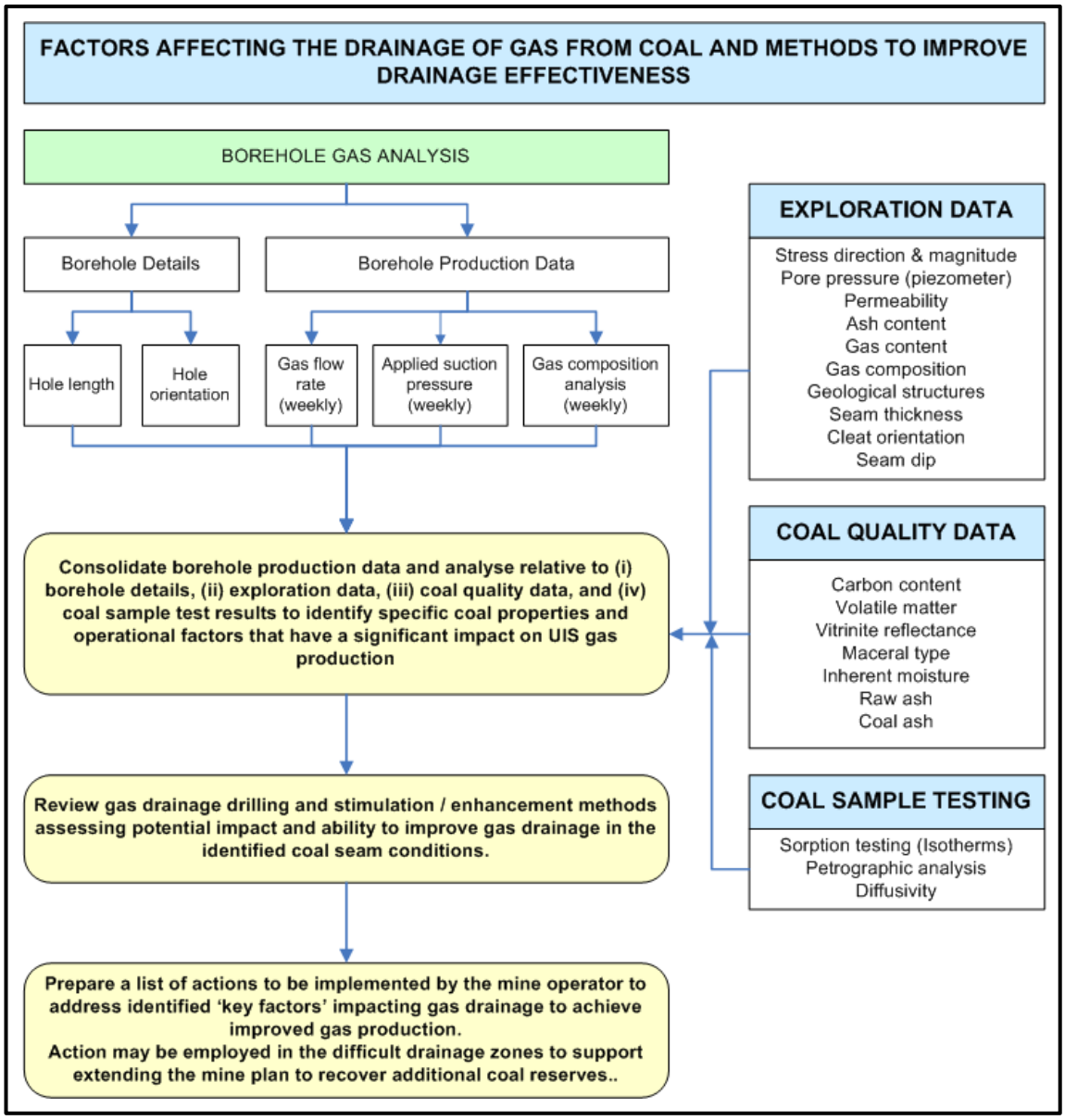

Figure 1.5: Project flowchart (Stage 1) factors that impact on UIS gas drainage

The second stage of the work, summarised in Figure 1.6, involved detailed analysis of the results from core sample gas analysis testing to determine (a) possible differences between the results of various direct gas content measurement techniques, (b) key relationships between gas content components, and (c) the impact of gas composition on gas emission rate. Analysis of the relationship between desorption rate index (DRI) and measured gas content (Q_M) was also considered. The impact of gas composition on the DRI-Q_M relationship and outburst threshold limits was investigated.

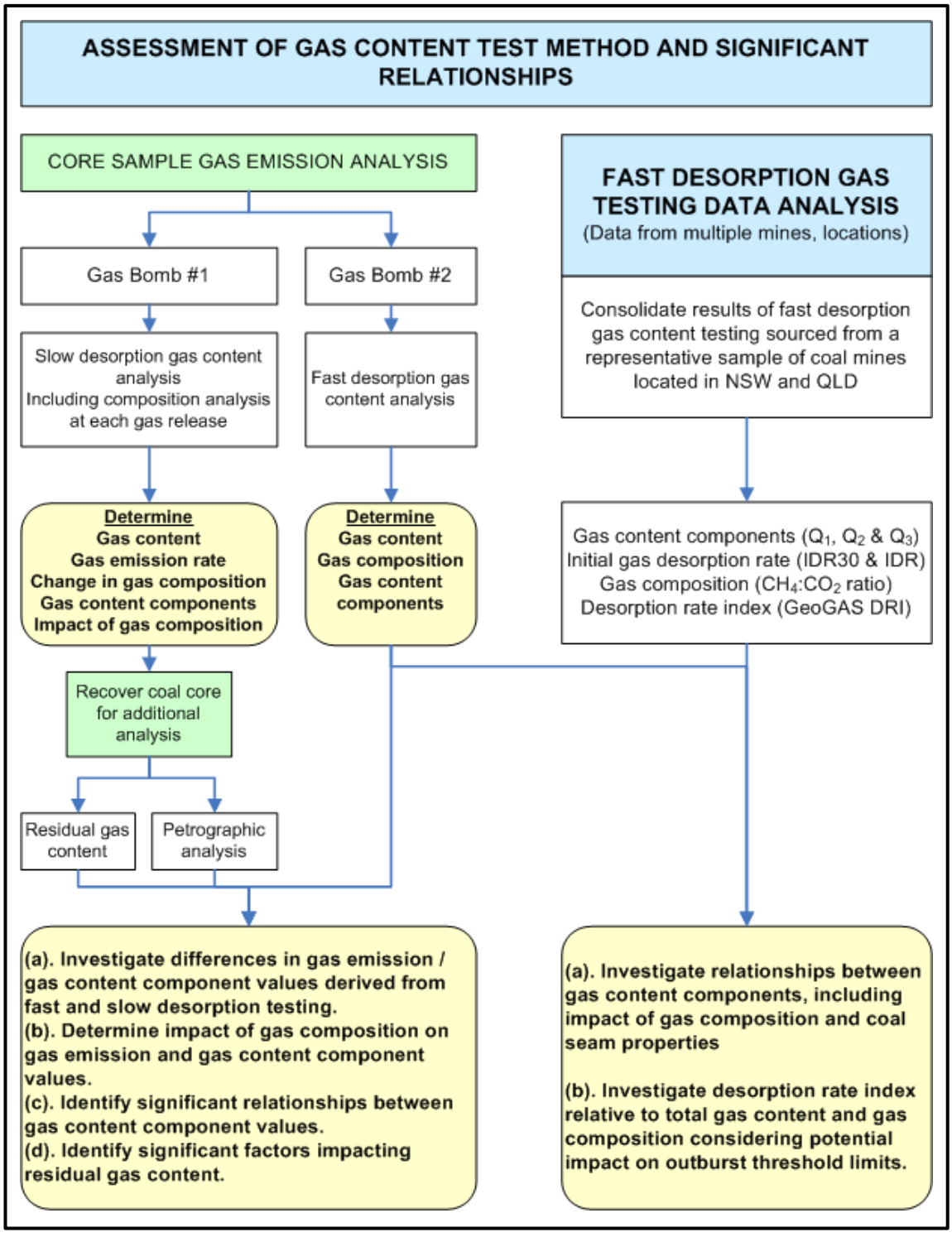

Figure 1.6: Project flowchart (Stage 2) assessment of gas content test data

1.7 THESIS OUTLINE

This thesis is presented in seven chapters. A flow of the arrangement of the thesis is presented in Figure 1.7.

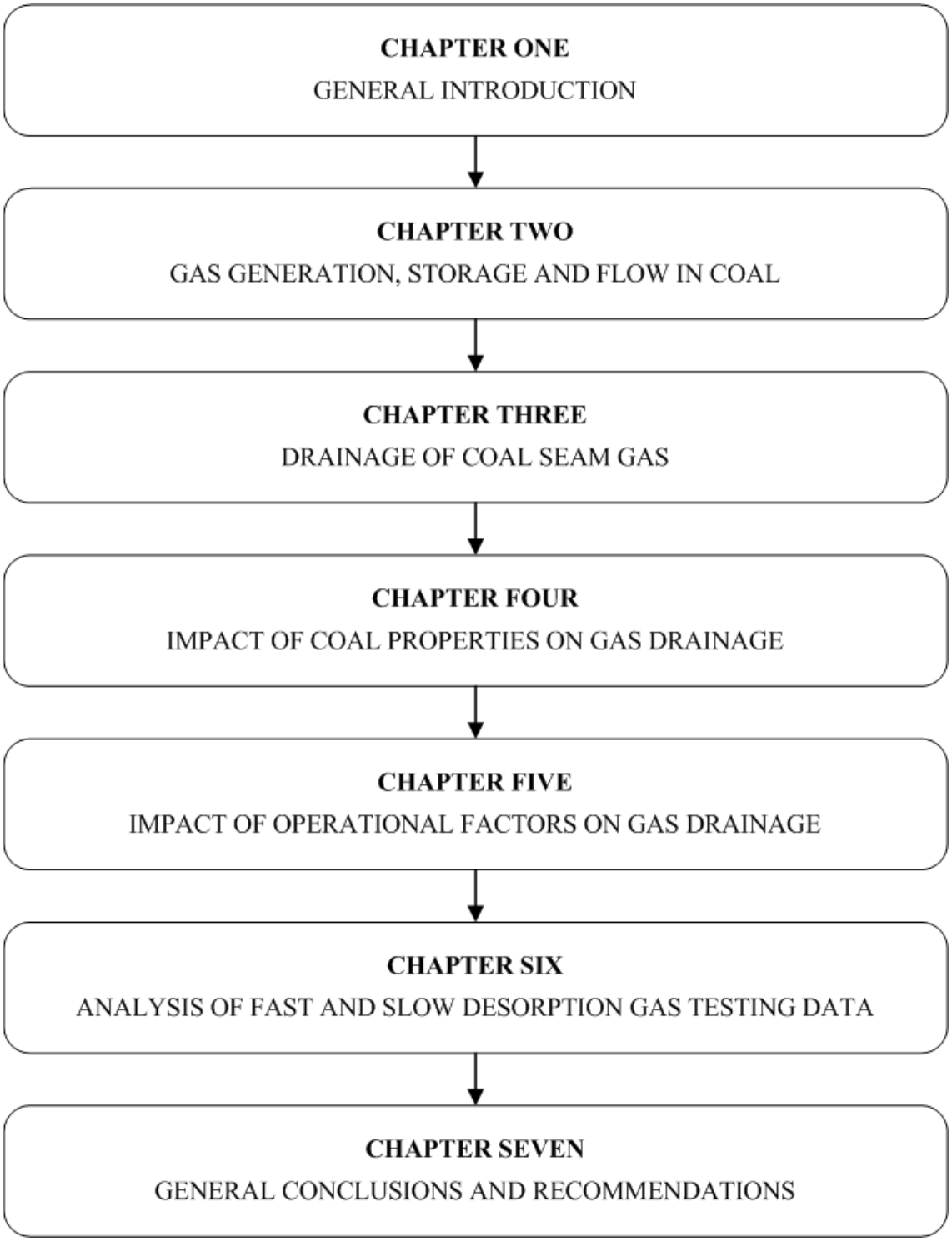

Figure 1.7: Structure of chapters in the thesis

- Chapter 1 presents the general purpose of the research and objectives of the thesis work.
- Chapter 2 describes the mechanisms involved in the generation of coal seam gas, the modes of gas storage and the nature of gas flow and emission from coal.
- Chapter 3 describes the evolution of gas drainage drilling technology from the introduction of routine rotary inseam drilling in the early 1980's through to current directional drilling applications. A variety of methods commonly used to enhance coal seam gas production performance are discussed. A new gas drainage enhancement technique involving the cyclic injection of inert gas is proposed.
- Chapter 4 details the gas production performance from 279 underground-to-inseam (UIS) gas drainage boreholes which form the basis of the analysis to determine the various factors that impact production performance. Data relating to a number of coal seam properties are presented and analysed to determine particular relationships and impact on coal seam gas production.
- Chapter 5 presents data relating to various operational factors and analyses the particular relationship and impact of each on coal seam gas production. Issues relating to the standard of control and management of gas drainage systems and subsequent impact on gas production performance are discussed.
- Chapter 6 presents the results of slow desorption gas testing conducted on 35 coal samples and compares the results to duplicate samples tested using the fast desorption method. The two testing methods are compared and the impact of coal properties on gas emission behaviour and residual gas content are discussed. The results of core sample gas testing, representing more than 4 000 coal samples from eight Australian coal mines, are analysed and significant trends in gas emission behaviour and the impact of gas composition are discussed. An assessment of desorption rate index (DRI) data and the impact on accepted methods for determining outburst threshold limits is discussed.
- Chapter 7 summarises the results and principal conclusions of the research work presented in the thesis and lists suggested areas requiring further research.

CHAPTER TWO – GAS GENERATION, STORAGE AND FLOW IN COAL

2.1 INTRODUCTION

Whether coal seam gas is considered a threat, in the case of coal mine operators, or an opportunity, in the case of coalbed methane gas producers, it is essential that operators and planners understand the principles of gas generation and storage and have the ability to drain gas from the coal seam.

Gas is generated during the coalification process, whereby vegetable matter, known as peat, is altered physically and chemically to form coal. Gas composition is typically greater than 90% methane, with minor amounts of liquid hydrocarbons, carbon dioxide and nitrogen (Jenkins and Boyer, 2008). The amount of gas retained within a particular coal seam, known as gas content, is dependent upon a range of factors that include: seam thickness, depth of burial, bounding strata type, coal geology, coal structure, coal strength, igneous intrusions and the ground stress regime. The processes and properties that control the generation, storage and emission of gas from coal seams are the subject of review and discussion in this chapter.

2.2 THE COALIFICATION PROCESS

Coalification is the process of coal formation through the physical and chemical transformation of peat material. During coalification the peat material undergoes several changes resulting from bacterial decay and the effects of compaction, heat and time (UWYO, 2002a). With increasing pressure, heat and time the complex hydrocarbon compounds in peat material break down and change in a variety of ways. There are two main processes involved in coalification, firstly Diagenesis, followed by Metamorphism (UWYO, 2002a).

The process of bacterial decay, known as Diagenesis, involves two separate stages of biochemical alteration, commencing with aerobic decay followed by anaerobic decay (UWYO, 2002a). Oxygen present in the peat material is consumed during aerobic decay. Once all of the available oxygen has been consumed the aerobic bacteria die and anaerobic bacteria continue the decay process. The decay process produces acid, increasing the pH. Once the pH reaches 4.0 the anaerobic bacteria can no longer survive

and at this point the peat has been transformed into a black, gel-like material, known as Gytta (UWYO, 2002b).

As the depth of burial of the peat material increases due to basin subsidence, the peat enters the geochemical stage of coalification, known as Metamorphism, where the material is subjected to rising temperature and pressure (UWYO, 2002a). During metamorphism hydrocarbons are generated and thermal cracking of the free lipid hydrocarbon fraction and/or cracking of the kerogen fraction of coal generates methane gas (Singh and Singh, 1999).

The generation of coal bed methane during coalification occurs in two ways (Singh and Singh, 1999):

1. Metabolic activity of biological agencies (biological process), and
2. Thermal cracking of hydrogen-rich substances (thermogenic process).

Figure 2.8 shows the relationship between the processes and stages involved in the coalification process along with the products throughout coalification (UWYO, 2002a).

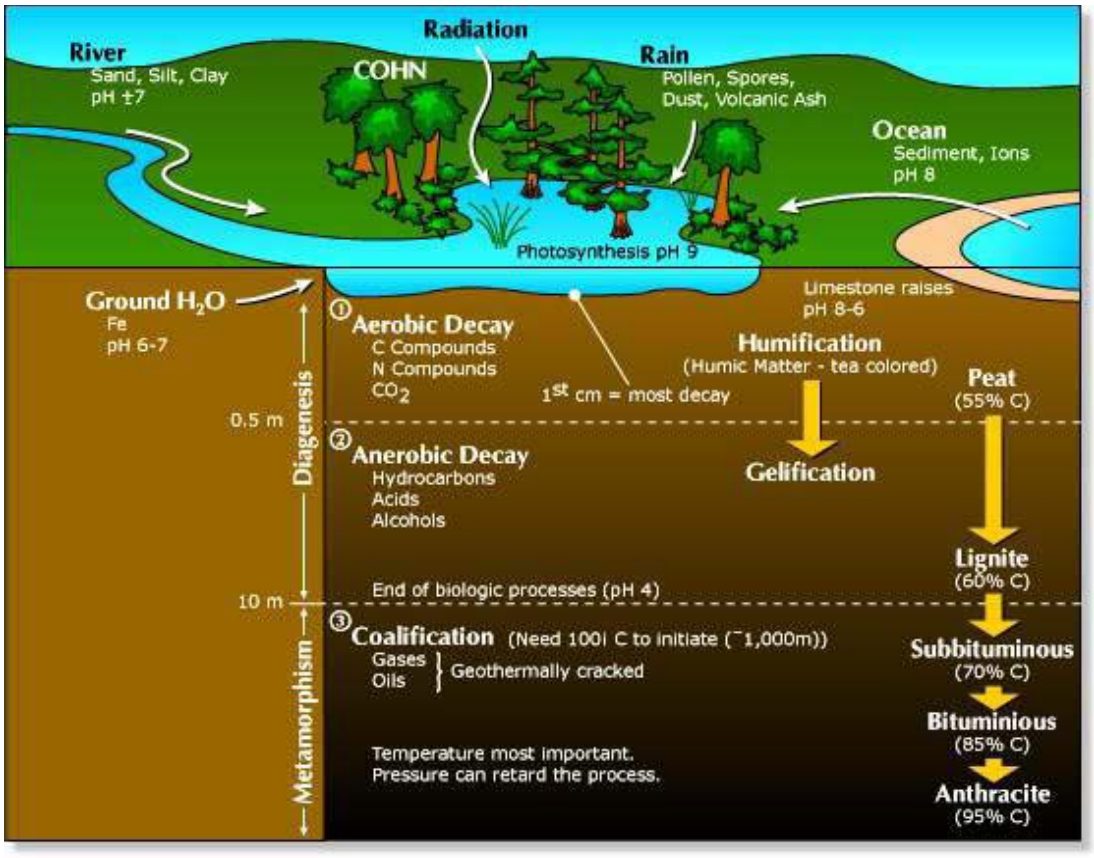

Figure 2.8: Details of the processes, stages and products of coalification (UWYO, 2002a)

2.2.1 Coal Rank

As organic matter progresses through the coalification process it matures and undergoes both physical and chemical change. The degree of alteration, or metamorphism, which occurs as coal matures, is referred to as the "rank" of the coal. The coal rank classifications used to describe coal, in increasing order of alteration and maturity, with the exception of the highest rank Anthracite, are described in Figure 2.9 (Aziz, 2006). Coal rank generally increases in direct correlation to temperature, depth of burial, geothermal gradient, and the length of time the organic material remains in a given regime. Rank is estimated by measuring various rank parameters, which include: carbon content, volatile matter, vitrinite reflectance, moisture content and specific energy (Ward, 1984).

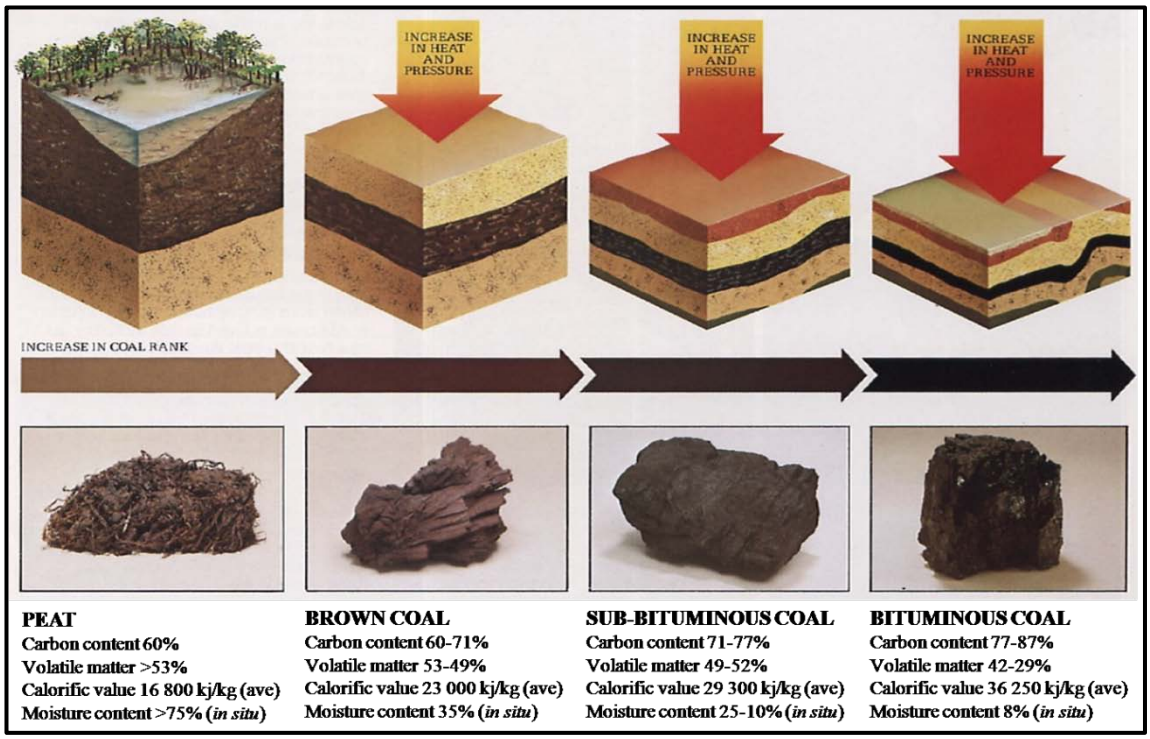

Figure 2.9: Changes in coal composition with increasing rank (Aziz, 2006)

Faiz (1993) suggests vitrinite reflectance is the preferred method of determining coal rank as it is not influenced by the presence of mineral matter or moisture and therefore does not require corrections to be made for these factors, which must be made for the other rank parameters.

Low rank coals are typically soft and friable with a dull earthy appearance and are characterised by high moisture and low carbon content. Higher rank coals are typically

harder and stronger, with a black vitreous lustre and are characterised by reduced moisture levels and increased carbon content.

Variation in coal rank is one of the most important factors that govern the gas storage of coal, whilst another important factor is coal type (Faiz, 1993).

2.2.2 Coal Type

Coal is also classified according to the organic material, called macerals, from which the coal was formed. Macerals are the remains of plants and degraded plant materials, which have characteristic chemical and physical attributes. The three main maceral groups used to describe coal are: Vitrinite, Liptinite and Inertinite. These maceral groups include various maceral sub-groups and individual maceral types. Table 1.2 lists the coal maceral classification detailed in Australian Standard AS2856.2-1998 (SAA, 1998).

Table 1.2: Classification of coal macerals (after SAA, 1998)

COAL MACERAL CLASSIFICATION			
Maceral Group	**Maceral Subgroup**	**Macerals**	
Vitrinite	Telovitrinite	Textinite	Eu-ulminite
		Texto-ulminite	Telocollinite
	Detrovitrinite	Attrinite	Desmocollinite
		Densinite	
	Gelovitrinite	Corpogelinite	Eugelinite
		Porigelinite	
Liptinite	____	Sporinite	Suberinite
		Cutinite	Fluorinite
		Resinite	Exsudatinite
		Liptodetrinite	Bituminite
		Alginite	
Inertinite	Telo-inertinite	Fusinite	Funginite
		Semifusinite	
	Detro-inertinite	Inertodetrinite	Micrinite
	Gelo-inertinite	Macrinite	

The macerals present in coal can be identified through coal petrographic analysis, using reflected light microscopy to view a prepared coal sample. The various maceral types can be identified by shape, morphology, reflectance and fluorescence. The vitrinite maceral group has a generally poor ultraviolet (UV) fluorescence and moderate reflectance, whereas the liptinite maceral group, also known as exinite, has a strong UV

fluorescence and low reflectance, whilst the inertinite maceral group has no UV fluorescence and very high reflectance. Examples of the macerals from the three main maceral groups, as seen under reflected light using oil immersion lenses, are indicated in Figure 2.10 (Esterle, 2007).

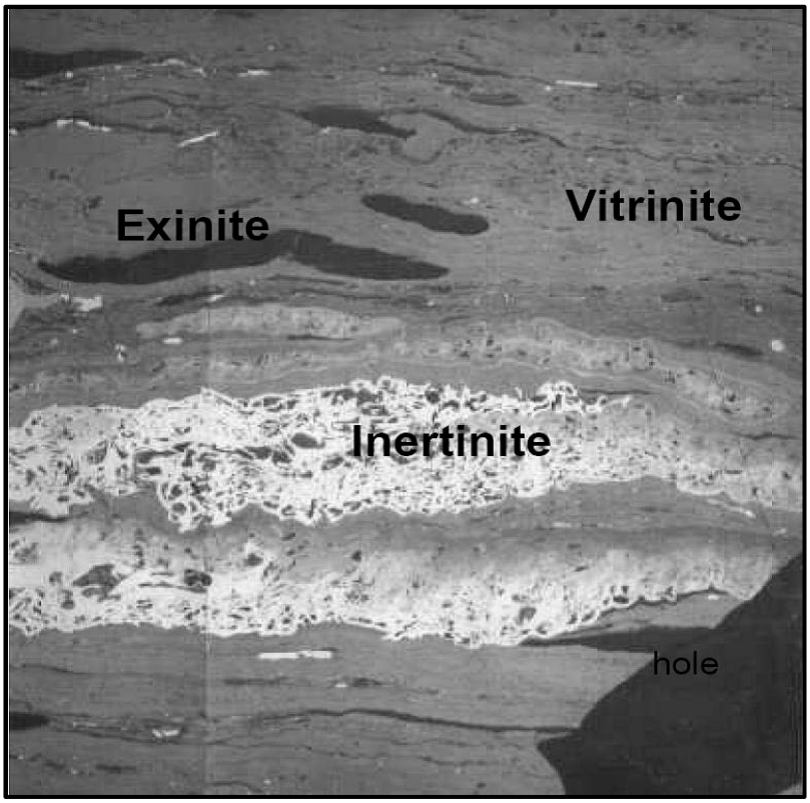

Figure 2.10: Examples of coal maceral type as seen under reflected light microscopy (Esterle, 2007)

Of the three maceral groups, vitrinite, which is predominantly micro-porous, is the largest producer of methane gas, has the greatest sorption capacity, and has a slower desorption rate than inertinite-rich coals, which are predominantly macro-porous and have reduced gas generating potential and sorption capacity (Beamish and Crosdale, 1995; Singh and Singh, 1999; Scott, 2002 and Hartman and Pratt, 2005).

Beamish *et al.* (1993) report vitrinite-rich coals desorb gas more rapidly with increasing rank suggesting this may be due to increased micro-fracturing within the vitrain bands.

2.2.3 Coal Structure

The structure of coal includes a well defined and almost uniformly distributed network of natural fractures known as cleats that develop as a result of physical and chemical change during coalification. Cleat and fracture development is also related to the stress

conditions present during and after coalification (Solano-Acosta *et al.*, 2007). There are two types of cleat, known as face cleat and butt cleat, both of which develop perpendicular to the bedding plane and provide the primary conduit for fluid flow (Mavor *et al.*, 1992 and Jenkins and Boyer, 2008). The face cleat is a more prominent group and is essentially continuous whereas the butt cleat, which is oriented perpendicular to the face cleat, is discontinuous and terminates at intersections with the face cleat, as illustrated in Figure 2.11 (Mavor *et al.*, 1992; Osisanya and Schaffitzel, 1996 and Shi and Durucan, 2003). The spacing between cleats tends to be quite uniform, in the order of millimetres to centimetres (Shi and Durucan, 2003) and cleat aperture is typically less than 0.1 mm (Laubach *et al.*, 1998). Factors that impact on cleat development include coal rank, coal type, seam (ply) thickness and the degree of tectonic and compactional deformation (Laubach *et al.*, 1998).

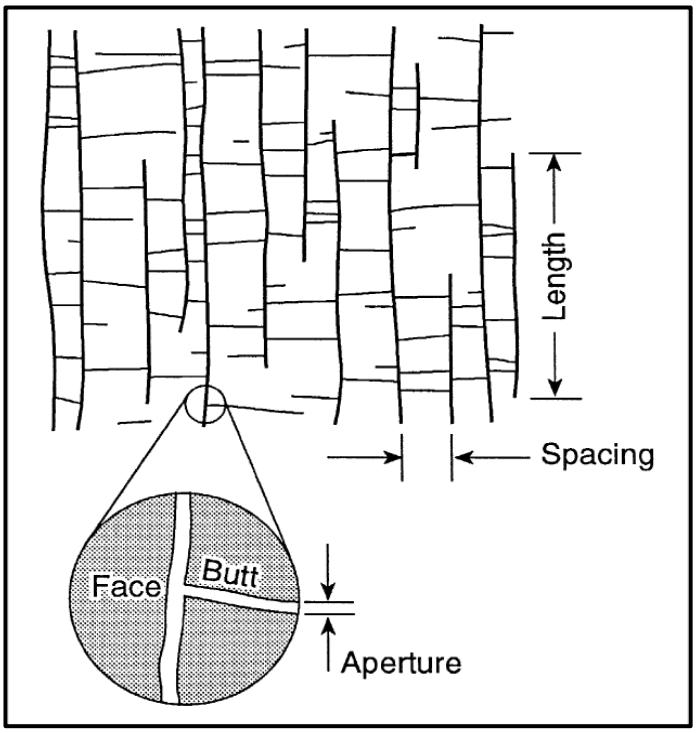

Figure 2.11: Illustration of coal cleat geometry in plan view (Laubach *et al.*, 1998)

Coal has a complex internal pore structure that resembles a molecular sieve, whereby some molecules are able to penetrate the pore structure whilst other, larger molecules cannot (Faiz, 1993 and Lama, 1995a).

Coal contains a mixture of pores which are classified on the basis of pore width (Saghafi *et al.*, 2007). According to the International Union of Pure and Applied

Chemistry, cited in Shi and Durucan (2003), the three pore types used to classify coal include: micro-pores (<2 nm), meso-pores (2-50 nm), or macro-pores (>50 nm). The macro-pore system is comprised of a naturally occurring network of fissures and fractures which is referred to as the cleat system.

The volume of pores in coal is small (less than 10%) and the majority of gas in coal consists of adsorbed gases, which are thought to cover the surfaces of the micro-pores (Shi and Durucan, 2003 and Saghafi *et al.*, 2007). Figure 2.12 shows two separate views of the coal matrix, as seen through an electron microscope (Sereshki, 2005).

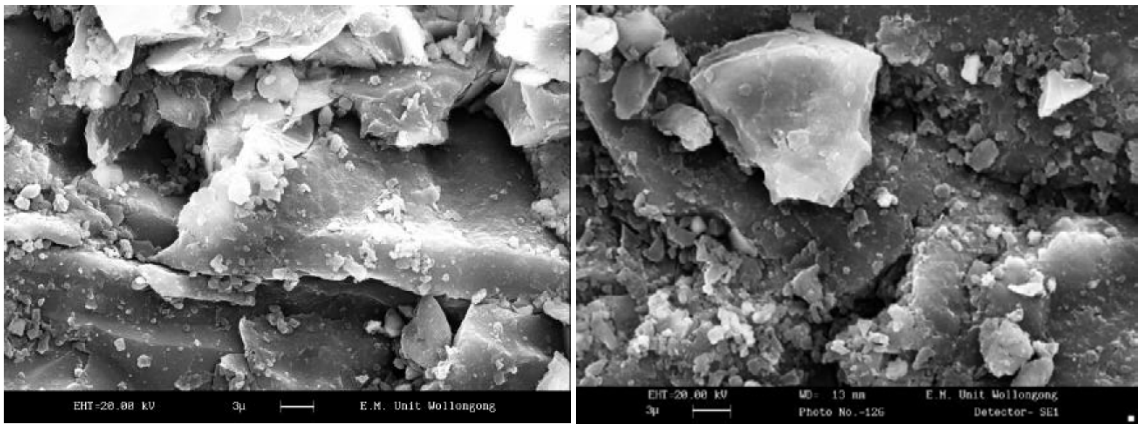

Figure 2.12: Electron micrographs showing the coal matrix (Sereshki, 2005)

2.3 GENERATION OF COAL SEAM GAS

The major component of coal seam gas is methane (CH_4) with lesser amounts of carbon dioxide (CO_2), nitrogen (N_2) and other gases, such as higher hydrocarbons (C_{2+}) (Bishop and Battino, 1989 and Saghafi *et al.*, 2007).

During coalification, gas is generated through separate biological and chemical processes. In the early stages of coalification, whilst at depths typically less than 10 m, biogenic methane is generated through the decomposition of organic matter which typically occurs within a temperature range of 50 to 80^{O}C (Singh and Singh, 1999). The volume of biogenic gas generated represents approximately 10% of the total gas generated in subsequent stages of coalification. As the process of coalification continues, increasing temperature and pressure conditions develop, due to subsidence of the basin/graben, either by increasing overburden thickness or by tectonic activity, which leads to the production of thermogenic methane. Thermogenic gas is produced through the thermal cracking of hydrogen-rich substances. There are two stages of

thermogenic gas production, catagenic and metagenic gas generation, which typically occur within temperature ranges of 80 to 150^{O}C and 150 to 200^{O}C respectively (Singh and Singh, 1999).

A significant amount of gas is generated during the coalification process. Patching (1970) and Thakur and Dahl (1982) suggest the volume of CH_4 generated during coalification is in the order of 1 300 m^3/t, while Eddy *et al.* (1982) suggest the CH_4 generated is in the order of 200 to 765 m^3/t. The current *in situ* gas content of Australian coals was estimated by Lama (1991) to be less than 1.5% of the total gas volume generated during the coalification process. Saghafi *et al.* (2007) suggests the majority of gas produced during coalification was lost from the coal seam due to dissolution in mobile water and migration out of the coal seam.

The volume of gas contained in a coal seam, known as gas content, typically increases with (i) rank of the coal, (ii) depth of burial of the coal seams, provided the roof and overburden are impervious to the gas, and (iii) the thickness of the coal seams (Close and Erwin, 1989 and Singh and Singh, 1999).

2.3.1 Coal Seam Gas in the Bulli seam, southern Sydney Basin

Lama and Saghafi (2002) report mining experience in Australia has demonstrated the gas content in a coal seam can vary significantly over relatively short distances. Bulli seam gas content data gathered during various surface to seam exploration programs (Armstrong and Kaag, 2008) was used to produce the contour plot, shown in Figure 2.13, which highlights the variable gas content within Area 5 at WCC. As shown, the measured gas content (Q_M) ranges from less than 6 m^3/t in the centre of Area 5, increasing toward the east and west, to greater than 15 m^3/t.

Thermal history modelling conducted by Faiz *et al.* (2007b) suggest the majority of the hydrocarbon gases present in the southern Sydney Basin are the result of coalification during the Jurassic and early Cretaceous period, with additional CH_4 gas generated during microbial activity which occurred post-Cretaceous. Analysis of two exploration core samples, EWC58 and EWC61, from WCC, determined the seam gas, which consisted of CO_2, CH_4 and N_2, was a mixture of thermogenic, magmatic and biogenic gases (CSIRO, 2007).

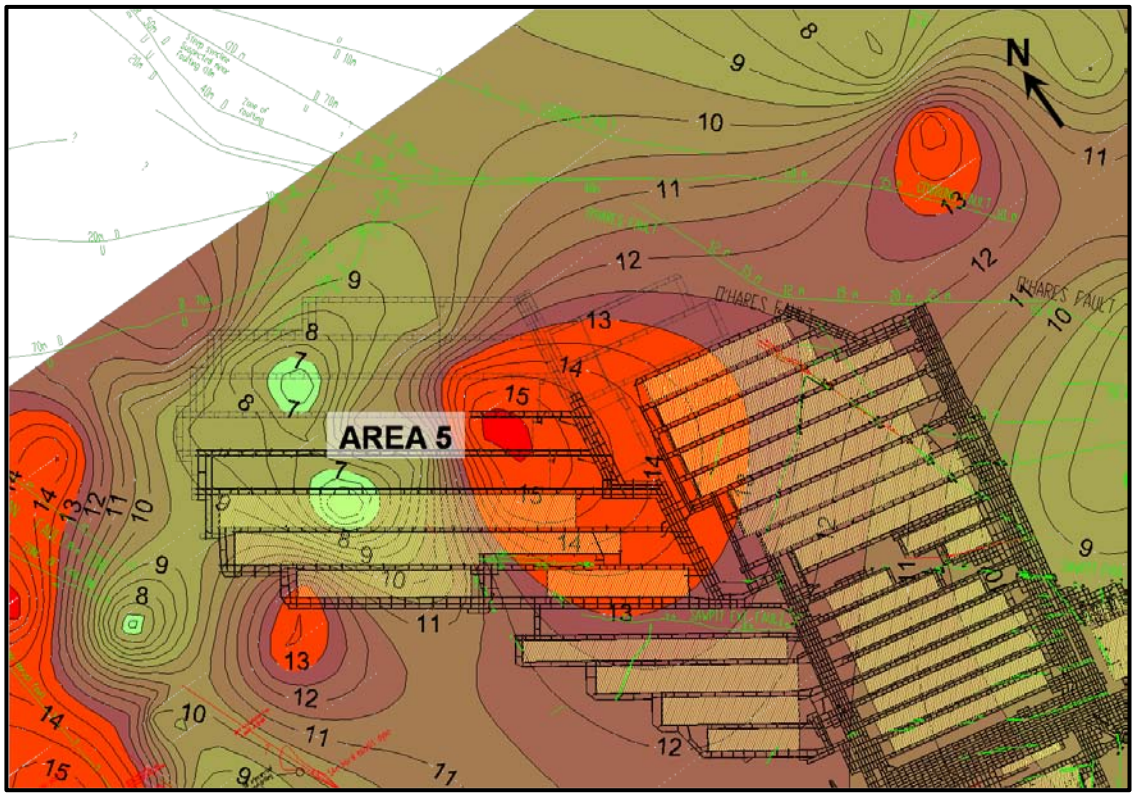

Figure 2.13: Bulli seam gas content contours relative to the WCC mine workings.

Although CH_4 is the dominant seam gas in the Sydney Basin there are many examples where CO_2 is the major coal seam gas component. Faiz and Hutton (1995) and Lama and Bodziony (1996) report changes in seam gas composition within the Illawarra coal measures, in particular that increased CO_2 concentration, was associated with igneous activity and geological structures. Sereshki (2005) and Saghafi *et al.* (2007) also report increased CO_2 concentrations were found to be localised laterally along major faults and other geological structures and in areas subjected to magmatic activity, such as dykes and sills.

The origin of the CO_2 has been the subject of comprehensive investigation, initially due to the association of CO_2 with coal and gas outburst incidents (Lama and Saghafi, 2002), and more recently in the development of enhanced coalbed methane (ECBM) production and geosequestration (Larsen, 2004; Faiz *et al.*, 2007a and Saghafi *et al.*, 2007).

The contour plan, Figure 2.14, prepared using exploration gas composition data (Armstrong and Kaag, 2008) show the variation in gas composition ($CH_4/(CH_4+CO_2)$) within Area 5 at WCC, from CH_4 rich in the east to CO_2 rich in the north-west.

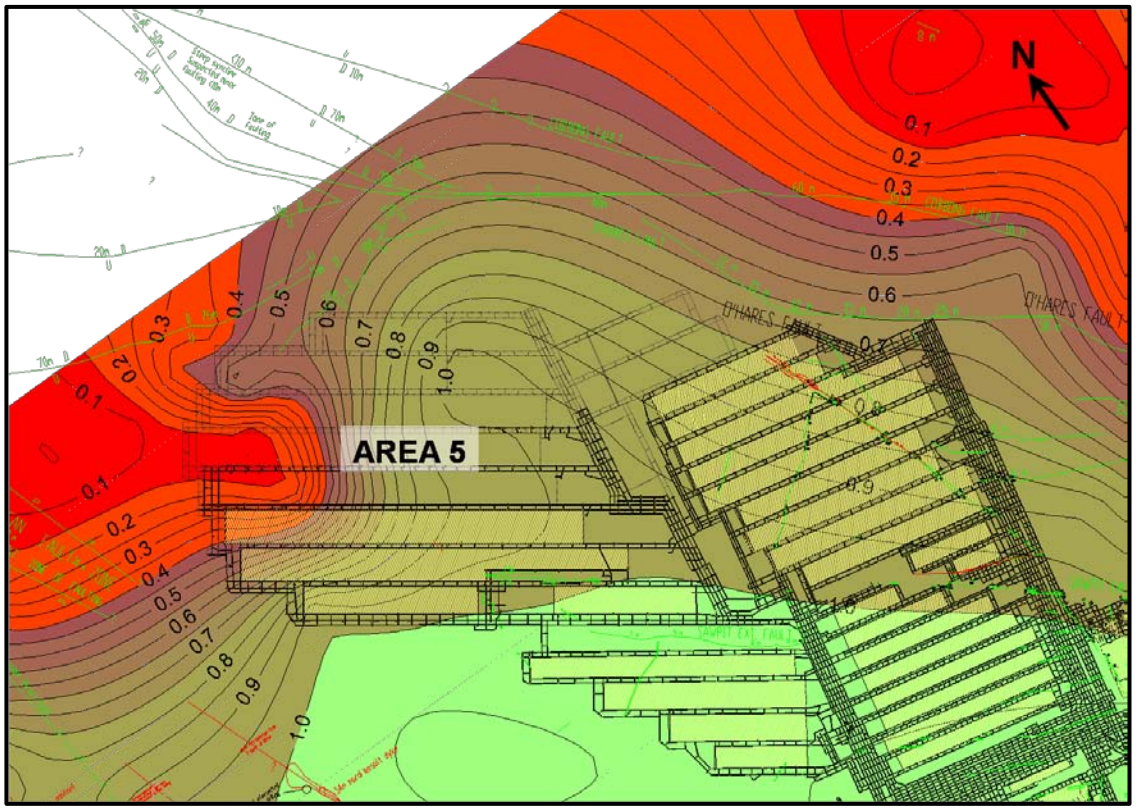

Figure 2.14: Bulli seam gas composition ($CH_4/(CH_4+CO_2)$) relative to WCC mine workings.

Saghafi *et al.* (2007) list four potential sources of CO_2 gas generation in coal seams, which are:

a) Decarboxylation reactions of kerogen and soluble organic matter during burial heating of coal;
b) Mineral reactions such as thermal decomposition or dissolution of carbonates or other metamorphic reactions;
c) Bacterial oxidation of organic matter; and
d) Magmatic intrusion.

Analysis of the ratio of stable isotopes of carbon present in gases may be used to interpret the origin of gas; whether of chemical, physical or biological origin (Lama and Bodziony, 1996). Analysis of the ratio between the Carbon-13 and Carbon-12 isotopes of gas samples sourced from the Sydney Basin indicate the CO_2 is mainly derived from magmatic sources (Lama and Bodziony, 1996 and Saghafi *et al.*, 2007).

Sereshki (2005) suggests the increased CO_2 in the vicinity of dykes and other magmatic intrusions was the result of physio-chemical alteration whereby the coal in the vicinity of the intrusion was heated resulting in the oxidation of carbon and hydrogen. The

chemical processes which have the potential to generate CO_2 in coal are listed in the equations below:

$$C_{(S)} + O_{2(G)} \rightarrow CO_{2(G)} \quad (2.1)$$

$$2C_{(S)} + O_{2(G)} \rightarrow 2CO_{(G)} \Rightarrow 2CO_{(G)} + O_{2(G)} \rightarrow 2CO_{2(G)} \quad (2.2)$$

$$CH_{4(G)} + 2O_{2(G)} \rightarrow CO_{2(G)} + 2H_2O_{(G)} \quad (2.3)$$

where: subscript (S) represents the solid state and (G) represents the gaseous state.

In addition to providing the heat required to support the chemical reactions to generate CO_2, the igneous structures also serve as a barrier, preventing gas migration through the coal seam. The sealing capability and thickness of the seam roof and floor rocks also play a significant role in the accumulation of gas in coal seams (Singh and Singh, 1999).

Faiz *et al.* (2007b) suggest the concentration of CO_2 in the Bulli seam is generally low in synclines and increases toward structural highs, with the highest contents occurring in anticlines and the up-thrown side of some major faults. The distribution of CO_2 in the Bulli seam at WCC is contrary to the suggestion made by Faiz *et al*. (2007b) as the CO_2 concentration increases with seam dip, toward the west. Faiz *et al.* (2007b) also identified areas adjacent to igneous intrusions where the concentration of CO_2 was generally low suggesting long range lateral migration of CO_2 along fractures and through permeable strata, such as interbedded sandstone, prior to diffusion into the micro-pores of adjacent coals.

A major geologically disturbed zone, which includes O'Hares Fault, extends in a south-east to north-west orientation forming the northern limit of the current planned mining area at WCC, shown in Figure 2.14. High concentrations of CO_2 have been measured to the north of these structures. The increased concentration of CO_2 to the north of these structural features supports the claims made by Faiz and Hutton (1995) of increased CO_2 adjacent to structural features that create a barrier to lateral migration. The lateral extension of the CO_2 though the fault zone, toward the west, supports the suggestion made by Faiz *et al.* (2007a) that lateral migration of CO_2 occurs along fractures and through permeable strata.

2.4 GAS STORAGE IN COAL

The capacity of coal to store gas, and its ability to allow movement of gas through its pore systems, are two major factors that influence the storage of gas in coal seams and its subsequent release during coal mining. The gas which is available for storage is however dependent on the gas produced during the coalification, igneous activity and/or igneous sources, and secondary biogenic activity, less that which has been lost due to leakage.

The storage and migration of gas in coal is represented by adsorption and diffusivity measurements, which are considered to be primary reservoir properties (Saghafi *et al.*, 2007). The ability of coal to store gas is influenced by many internal and external properties that include coal type, rank, pore structure, gas type, moisture, stress and the presence of mineralisation within the pores and/or the cleat system (Gurba *et al.*, 2003; Hartman and Pratt, 2005; Sereshki, 2005 and Sagahfi *et al.*, 2007).

It is generally accepted that gas is stored in coal in four separate ways (Curl, 1978; Osisamya and Schaffitzel, 1996 and Mastalerz *et al.*, 2004) that include:

- Adsorption upon internal surfaces (micropores);
- Absorption into the molecular structure of the coal;
- As free gas within the voids, cleats and fractures; and
- As a solute in groundwater present within the coal seam

Gas may also be condensed as a solid or liquid in coal (Crosdale *et al.*, 1998), with CO_2 being stored in the form of carbonate precipitates (Faiz *et al.*, 2007a).

The first two modes listed, adsorption and absorption, account for more than 90% of the gas storage within the coal (Faiz, 1993; Mastalerz *et al.*, 2004 and Schatzel *et al.*, 2008). The volume of gas able to be adsorbed by coal is dependent upon the energy of the free gas, and therefore on temperature and pressure. After sufficient time, at constant temperature and pressure conditions, the rate of adsorption and desorption of gas from the coal pore surfaces reaches equilibrium, i.e. the adsorbed phase and free phase are in kinetic equilibrium.

The most widely used technique to describe gas adsorption onto the internal surface of the micro-porous coal matrix is the adsorption isotherm. The adsorption of gas onto

open surfaces freely exposed to gas can be expressed using the simplified Langmuir equation, shown in Equation 2.4. The Langmuir equation assumes a monomolecular layer is adsorbed on the pore walls and that the isotherm plateau corresponds to the completion of the monolayer (Curl, 1978; Crosdale *et al.*, 1998 and Dutta *et al.*, 2008). The Langmuir isotherm is applicable for gas pressure less than 6 MPa, where the size of the gas molecules and diameter of the coal pores are of the same order of magnitude (Saghafi *et al.*, 2007).

$$V_{sat} = V_L \cdot \frac{P_i}{P_i + P_L} \tag{2.4}$$

where: V_{sat} = saturated gas content (cc/g);

V_L = Langmuir volume constant (cc/g), which represents the maximum gas storage capacity of the coal;

P_i = initial reservoir gas pressure (MPa);

P_L = Langmuir pressure constant (MPa), which represents the gas pressure at which gas storage capacity is half of the maximum storage capacity.

Therefore, where $P_i = P_L$, $V_{sat} = V_L/2$.

The volume of free gas in coal is quite small, and is related to the porosity of the coal matrix, as well as the absolute pressure and temperature of the gas (Lama and Bodziony, 1996). The free gas volume may be calculated using Equation 2.5, cited in Lama and Bodziony (1996), which applies to pores not saturated with water (Faiz *et al.*, 2007a).

$$Q = \Phi \cdot \frac{P}{P_0} \cdot \frac{273}{T} \tag{2.5}$$

where: Q = free gas content (m^3/m^3);

Φ = rock porosity (%);

P = absolute gas pressure (kPa);

P_0 = atmospheric pressure, (101.3 kPa); and

T = absolute strata temperature (^OK).

2.4.1 Gas Sorption Capacity

The term sorption, first proposed by McBain in 1932, cited in Faiz (1993), is used to describe the two primary modes of gas storage within coal; adsorption on surfaces and absorption by penetration into the molecular structure of the coal.

The gas sorption behaviour and the maximum volume of gas adsorbed within the organic matrix of coal are conventionally evaluated through gas sorption testing. Two key parameters are obtained from the gas sorption measurements on coal; these are the gas sorption isotherm and the gas sorption rate (Beamish and Crosdale, 1995).

Many researchers have carried out sorption testing experiments, primarily for the purpose of investigating CO_2 sequestration capability and enhanced coalbed methane (ECBM) production opportunities. It is widely accepted that CO_2 has the greatest sorption capacity of the commonly occurring coal seam gases, being approximately twice the sorption capacity of CH_4 which has approximately double the sorption capacity of N_2 (Levy *et al.*, 1997; Busch *et al.*, 2004; Mastelerz *et al.*, 2004; Faiz *et al.*, 2007a and Saghafi *et al.*, 2007).

Sorption testing was conducted on eight coal samples gathered from Area 5 at WCC. The results, shown in Figure 2.15, are consistent with the results from sorption testing on Bulli seam coal by Lama (1981); Faiz *et al.* (1992); Aziz and Ming-Li (1999); GeoGAS (2004); Faiz *et al.* (2007a) and Saghafi *et al.* (2007).

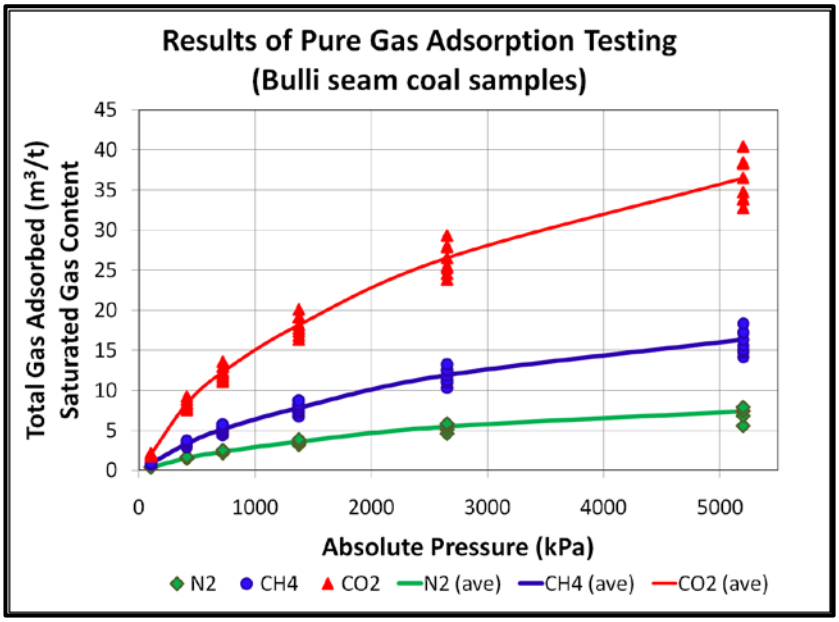

Figure 2.15: Results of pure gas adsorption testing on Bulli seam coal from WCC

2.4.2 Factors Impacting Gas Sorption Capacity

A variety of factors have been listed by past researchers as impacting the ability of coal to store gas. Such factors include coal rank, type, moisture content, mineral content and composition, temperature, depth, porosity, natural fracturing and stress (Faiz *et al.*, 1992; Laxminarayana and Crosdale, 1999 and Hildenbrand *et al.*, 2006).

2.4.2.1 Coal Rank

It is generally accepted that sorption capacity of coal increases with increasing coal rank (Close and Erwin, 1989 and Mastalerz *et al.*, 2004). Testing conducted by Beamish and O'Donnell (1992) and Faiz *et al.* (1992) confirm increasing Langmuir volume relative to increasing fixed carbon content and vitrinite reflectance.

Adsorption testing of coal samples from WCC found little change in the Langmuir volume corresponding to an increase in fixed carbon content and vitrinite reflectance. The data range was however quite narrow with the fixed carbon content ranging from 72 to 78% (daf), volatile matter ranging between 22 and 28% (daf) and vitrinite reflectance ranging between 1.27 and 1.36%. Plots of both fixed carbon content and vitrinite reflectance relative to the Langmuir volume determined for both CH_4 and CO_2 are presented in Appendix 2.1 and Appendix 2,2 respectively.

2.4.2.2 Coal Type

The relationship between gas sorption capacity and the maceral composition of coal has been studied previously by several researchers however the findings are inconsistent.

Testing conducted on low and medium rank coals by Ettinger *et al.* in 1966, cited in Faiz *et al.* (1992), found inertinite-rich coal had greater methane gas sorption capacity than vitrinite-rich coal. Whereas in separate testing, reported by Beamish and O'Donnell (1992); Faiz *et al.* (1992) and Clarkson and Bustin (1999), vitrinite-rich coal was found to have greater methane gas sorption capacity than inertinite-rich coal. Analysis of the sorption data presented by Beamish and O'Donnell (1992) found that although bright coal had greater sorption capacity the difference is not great, with the saturated gas content of the bright coal samples being less than 6% greater than dull coal at 2.5 MPa and 10.0% greater at 4.0 MPa.

Testing on eleven coal samples sourced from mines in Queensland and New South Wales that ranged in inertinite content from 11 to 71% by Faiz *et al.* (1992) concluded the maceral composition had little impact on the gas sorption capacity. The lack of correlation between gas sorption properties and coal maceral content was also identified during separate studies of coal from the southern coalfield of the Sydney Basin (Faiz and Cook, 1991 and Crosdale *et al.*, 1998).

Petrographic analysis was conducted on five coal samples from WCC and the results assessed relative to the Langmuir volume determined from sorption testing using both CH_4 and CO_2. The plots, shown in Appendix 2.3, show that for vitrinite maceral composition ranging from 22 to 61% and inertinite maceral composition ranging from 26 to 73% there was some indication of increasing Langmuir volume corresponding to an increase in bright coal composition however the relationship is not strong.

Laxminarayana and Crosdale (1999) suggest evaluating the impact on gas adsorption capacity of coal type alone is complicated by rank influences. From an assessment of individual ranks, Laxminarayana and Crosdale (1999), determined vitrinite-rich coal had greater gas adsorption capacity in high volatile bituminous coal whereas for medium and low volatile bituminous coal maceral composition had little impact on gas adsorption capacity. While conceding a low number of semi-anthracite and anthracite samples, Laxminarayana and Crosdale (1999), state the samples of this rank indicated a reduction in Langmuir volume in response to increasing vitrinite maceral composition.

Faiz *et al.* (1992) and Mastalerz *et al.* (2004) suggest increased gas sorption capacity corresponding to increased surface area and porosity within the coal structure. In support of this relationship Crosdale *et al.* (1998) suggest the influence of rank and maceral composition on pore structure development was the critical factor controlling gas sorption in coal.

2.4.2.3 Moisture Content

The presence of moisture was considered to have significant impact on the gas adsorption capacity of coal, with sorption capacity decreasing in response to increasing moisture content as both gas and moisture compete for adsorption sites (Beamish and O'Donnell, 1992; Laxminarayana and Crosdale, 1999; Scott, 2002; Busch *et al.*, 2004; Mastalerz *et al.*, 2004; Mazumder et al., 2006 and Crosdale *et al.*, 2008). The capacity

of coal to adsorb gas was greatest when no moisture was present and decreased in response to increasing moisture, until the moisture holding capacity of the coal was reached. Increased moisture beyond this level was reported to have no further impact on methane gas adsorption capacity (Jahediesfanjani and Civan, 2006 and Crosdale *et al.*, 2008).

Lama and Bodziony (1996) state 1% moisture reduced sorption capacity by 25% and 5% moisture reduced the gas adsorption capacity by 55 to 65%. Levy *et al.* (1997) identified a decrease in methane adsorption capacity of Bowen Basin coal samples at a rate of 4.2 m^3/t for each 1% increase in moisture content.

The air dried moisture content of eight WCC coal samples was assessed relative to the Langmuir volume for both CH_4 and CO_2. The plots, presented in Appendix 2.1 and Appendix 2.2 respectively, suggest a reduction in Langmuir volume in response to increasing moisture content, for moisture content within the range 1.0 to 1.7%. For each 1% increase in moisture content the Langmuir volume was found to reduce by an average 4.2 m^3/t, in the case of CH_4 adsorption, and 7.2 m^3/t, in the case of CO_2 adsorption, which for CH_4 adsorption is consistent with the results of Levy *et al.* (1997).

2.4.2.4 Ash and Mineral Content

The presence of mineral matter in coal, expressed as ash content, serves to reduce the gas adsorption capacity of coal (Close and Erwin, 1989; Laxminarayana and Crosdale, 1999; Scott, 2002; Busch *et al.*, 2004 and Mastalerz *et al.*, 2004). Testing conducted by Beamish and O'Donnell (1992) and Faiz *et al.* (1992) recorded reducing Langmuir volume in response to increasing ash and mineral content. Faiz *et al.* (1992) suggest the presence of mineral matter in the coal causes a relative decrease in the meso- and macro-pore volume which leads to the reduction in gas sorption capacity of the coal.

Analysis of coal samples spanning an ash range of 1.5 to 54%, by Laxminarayana and Crosdale (1999), identified a linear decrease in gas adsorption capacity in response to increasing ash content, with the adsorption capacity of methane decreasing 0.38 m^3/t for each 1.0% increase in ash content.

Results of proximate analysis of eight WCC coal samples were assessed relative to the Langmuir volume for both CH_4 and CO_2. The plots, presented in Appendix 2.1 and

Appendix 2.2 respectively, suggest a reduction in Langmuir volume in response to increasing ash content, for ash content spanning 4.8 to 13.6%, although the relationship is not strong.

The relationship between Langmuir volume and coal density was also considered. The results of eight samples, with measured density within the range 1.38 to 1.53 t/m^3, indicate a reduction in Langmuir volume in response to increasing coal density.

Considering the average relationship between Langmuir volume and ash content for the WCC samples, the Langmuir volume reduced by 0.27 m^3/t, in the case of CH_4 adsorption, and 0.43 m^3/t, in the case of CO_2 adsorption, for each 1% increase in ash content, which is consistent with the results of Laxminarayana and Crosdale (1999).

2.4.2.5 Temperature and Pressure

A coal seam exposed to increased temperature and confining pressure has a reduced capacity to store gas (Lama, 1988b and Busch *et al.*, 2004).

Gas sorption testing conducted at different temperatures by Busch *et al.* (2004) found reducing the temperature increased the adsorption capacity of coal and reduced the rate of gas adsorption.

Lama and Bodziony (1996) suggest a linear relationship exists between the gas adsorption capacity of coal and temperature, with adsorption capacity decreasing at a rate of 1.0 m^3/t per 10^OC increase. This result is consistent with testing on Bowen Basin coal samples by Levy *et al.* (1997) that identified a 1.2 m^3/t reduction in CH_4 adsorption capacity per 10^OC increase. Crosdale *et al.* (2008) suggest the relationship is non-linear with adsorption capacity increasing at a greater rate in response to reducing temperature.

2.4.2.6 Sample Particle Size

Mavor *et al.* (1992) suggest the grain size of coal used in adsorption testing affects the measured gas storage capacity with the adsorption capacity of coal samples 25 mm long and 38 mm in diameter having a greater adsorption capacity than crushed samples.

The impact of particle size on gas sorption capacity was disputed by Beamish and O'Donnell (1992) who claimed reducing coal particle size did not increase the gas

adsorption capacity of coal, referring to the results of testing by Bielicki *et al.* in 1972 and Ruppel *et al.* in 1974.

Gamson and Beamish (1992) reported that sorption testing using both small, solid (1 g) blocks and crushed (–250 μm) coal samples confirmed the crushed size fraction displayed a more rapid methane uptake and reached equilibrium faster than the solid samples. A similar relationship was reported by Perkins and Cervik (1969).

Commercial laboratories prefer using coal of smaller particle size due to the reduced time required to achieve saturation. A potential issue associated with the use of finely ground coal samples in sorption testing is the risk of overstating the sorption capacity of the coal. The two situations where sorption capacity may be overstated are (i) loss of coal material during desorption / depressurisation resulting in reduced coal mass (g) relative to the measured adsorbed gas volume (cc), thereby overstating the adsorbed gas content (cc/g or m^3/t), and (ii) the surface area of coal crushed to less than 212 μm is significantly greater than coal in its natural state allowing greater total gas adsorption than would be practically achieved by *in situ* coal. The relatively small coal sample mass used by commercial testing laboratories is also considered a risk to obtaining accurate results from sorption testing as the percentage error inherent in the measurement of the adsorbed gas volume will be greater than for larger sample sizes.

2.4.3 Impact of Gas Sorption on Coal Structure

During the process of adsorption of gas by coal, the coal swells, resulting in an overall volume increase. Analysis of strain response of coal samples during laboratory adsorption testing of CH_4 and CO_2 demonstrated increased swelling in response to CO_2 adsorption (Harpalani and Zhao, 1989; Harpalani and Chen, 1992; Levine, 1996; Larson, 2004 and Reward, 2006). Testing conducted by Levine (1996) and Larson (2004) demonstrated coal swelling in the order of 1% in response to CH_4 and up to 4% in response to CO_2 adsorption. Conversely, during desorption, shrinkage of the coal matrix occurs. Curl (1978) reported the extent of coal shrinkage was in the order of 0.2 to 0.5% of seam thickness.

The adsorption and subsequent swelling of the coal matrix causes a reduction in the permeability of coal, through the squeezing of cleats and pores (Faiz *et al.*, 2007a). However during methane adsorption testing by Harpalani and Zhao (1989), following

an initial decrease in permeability, the permeability was found to increase in response to injection pressure above 2 758 kPa (400 psi).

Testing conducted by Stefanska in 1990 indicated the swelling and shrinkage of coal in response to CO_2 sorption was reversible whereas the swelling–shrinkage response of coal during CH_4 adsorption was not reversible (Harpalani and Chen, 1992). Harpalani and Chen (1992) report the degree of swelling of coal was impacted by rank and moisture content which is to be expected given that both factors affect the sorption capacity of coal. They also state shrinkage of the coal matrix leads to an increase in the size of the cleat aperture, thus increasing the cleat porosity.

During CO_2 sorption testing, Larsen (2004), observed anisotropic swelling in the initial test, with greater swelling perpendicular to the bedding plane than parallel to it, whilst in subsequent sorption testing, using the same sample, the swelling was deemed to be isotropic. From this testing it was suggested that the CO_2 dissolves in the coal, serving as a plasticiser, causing structural rearrangement of the coal. It may however be that irreversible damage had been sustained by the coal matrix during the initial testing and therefore a different response would be inevitable in subsequent testing on the same coal sample.

2.5 GAS FLOW AND EMISSION FROM COAL

The movement of gas through coal is generally considered a two-stage process, involving viscous flow, through cleat and fractures, and diffusion through the coal matrix (Saghafi *et al.*, 2007). Gas molecules diffuse through the coal matrix in response to concentration gradients and upon reaching the cleat system migrate in response to pressure gradients, obeying Darcy's Law (Hadden and Sainato, 1969; Curl, 1978; Beamish and O'Donnell, 1992; Beamish and Crosdale, 1995; Scott, 2002; Shi and Durucan, 2003; Cui and Bustin, 2006; Faiz et al., 2007a; Meszaros *et al.*, 2007 and Solano-Acosta *et al.*, 2007).

Gas desorption from the matrix to the cleat is a complex process in which gas desorbs from the walls of the pores and diffuses through the pore system to the cleat. The nature of the coal pore structure and gas type may result in the diffusive flow being a combination of three distinct diffusion mechanisms, (i) Fickian diffusion, (ii) Knudsen diffusion and (iii) surface diffusion (Saghafi et al., 2007 and Pan *et al.*, 2010).

Gas migration through the cleat system typically occurs at a much faster rate than diffusion through the coal matrix. As most of the gas in coal is stored in micropores, diffusivity is the rate limiting factor for gas flow in most low permeability coals.

Gamson and Beamish (1992) proposed a four tier gas flow model, suggesting the two tier model may not adequately describe the flow of gas through the various microstructures present in coal. The four tier gas flow model proposed is:

1) diffusion at the micropore or matrix level;
2) laminar flow through open, unmineralised microfractures and cavities to the cleat;
3) flow/diffusion of methane through microfractures, cavities and cleats partly blocked by diagenetic minerals; and
4) laminar flow through cleats at the macrofracture level.

Gamson and Beamish (1992) also state gas flow through the microstructure was likely to be impacted by (i) the type of microstructure present, (ii) the density, orientation and continuity of the microstructure, (iii) the degree of infilling in the voids, and (iv) the extent of clay layers present in the coal seam.

Coal seams may contain large volumes of water at *in situ* conditions and the presence of this water within the cleat and pores exerts hydrostatic pressure on the adsorbed gas keeping it from moving out from the internal surfaces of the micropores within the coal (Jahediesfanjani and Civan, 2006; Lamarre, 2007 and Meszaros *et al.*, 2007). Therefore dewatering is necessary to reduce hydrostatic pressure allowing gas molecules to desorb from coal and diffuse through the matrix to the cleat (Osisanya and Schaffitzel, 1996 and Cui and Busten, 2006).

Dougherty and Karacan (2010) describe three distinct phases of a typical coal seam gas production well:

- Phase 1: Water production and reduction of reservoir pressure. During initial production, flow is primarily single phase (water) with negligible gas production.
- Phase 2: Decreasing water production and increasing gas production rate. The relative characteristic and change in rate of gas-water production is governed by the gas-water relative permeability which is a function of fluid saturation (Kissell and Edwards, 1975). The increasing gas production during this phase is also known as

negative decline (Lamarre 2007). The point at which the maximum gas production rate is achieved denotes the end of Phase 2 and start of Phase 3.

- Phase 3: The well has reached maturity and during this phase gas production is in decline. During this latter stage of production flow is primarily single phase (gas) with negligible water production.

Many authors simplify the gas production cycle suggesting insignificant gas production until such time as the reservoir pressure has been reduced to the critical desorption point (Close and Erwin, 1989; Levy *et al.*, 1992; Thungsuntonkhun and Engler, 2001; Lamarre, 2007 and Seidle and O'Connor, 2007). Figure 2.16 indicates the critical desorption point of a typical Bulli seam sample, based on isotherms representing the adsorption capacity for both pure CH_4 and CO_2. Considering the same initial *in situ* gas condition, gas content (10.5 m^3/t) and pressure (3.5 MPa), it can be seen that a CH_4 rich coal requires far less reservoir pressure reduction to reach the critical desorption point than does an equivalent CO_2 rich sample.

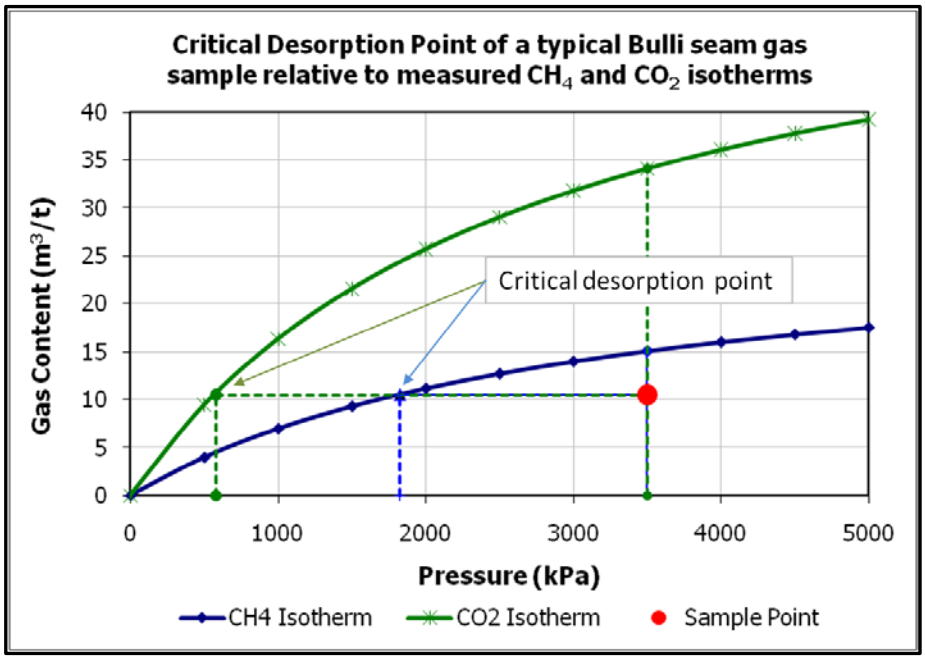

Figure 2.16: Critical desorption point of a typical CH_4 and CO_2 rich Bulli seam coal sample.

2.5.1 Factors Impacting on Gas Emission from Coal

A number of factors impact on the rate of gas emission from coal. The factors considered to have the greatest impact are (i) permeability, which is also impacted by effective stress and pore size, and (ii) degree of saturation.

2.5.1.1 Permeability

Permeability refers to the ability of the coal to transmit gas when a pressure or concentration gradient exists across it. Permeability is generally considered the most critical parameter controlling gas flow in coal (Zutshi and Harpalani, 2005 and Mazumder and Wolf, 2008). Permeability is however a dynamic property therefore any *in situ* measurement simply provides a static snapshot (Zutshi and Harpalani, 2005).

The permeability of coal is dependent upon factors that include effective stress, gas pressure, water content, disturbance associated with drilling and matrix swelling/shrinkage due to adsorption/desorption (Gray, 1987 and Zutshi and Harpalani, 2005). The majority of these parameters change continuously with time making the process of gas flow in coal difficult to predict and model.

Permeability measurements conducted using small coal samples in laboratory conditions have been shown to be inconsistent with measured bulk *in situ* permeability. Testing at Leichhardt Colliery by Gray (1982) measured core permeability less than 5 mD whereas the bulk permeability was found to be in the order of 200 mD for drainage along the cleat.

Gray (1987) demonstrated the presence of two processes impacting the permeability of the cleat structure within a coal seam; the first being the influence of phase effects whereby the degree of water saturation affects the gas and water permeability of the reservoir; and the second, and potentially more significant, being the impact of changes in effective stress. As a function of effective stress, permeability may increase or decrease in response to stress changes associated with drainage thereby influencing the gas production performance from a coal seam reservoir.

2.5.1.2 Coal Structure and Pore Volume

Generally, higher gas production rates may be expected from highly fractured coal with reduced spacing between cleats and increased cleat aperture (Cui and Bustin, 2006 and Solano-Acosta *et al.*, 2007). In such coals there is less distance for the gas to travel by diffusion before exiting the coal matrix and entering the cleat system. Once in the cleat system, provided the aperture of the cleat is wide enough, gas migrates toward points of reduced pressure, such as a drainage boreholes (Cui and Bustin, 2006). However, coal with high cleat porosity is likely to have a high initial stored water volume, requiring

increased dewatering time to reduce cleat pressure and enhance the gas permeability (Cui and Bustin, 2006).

Cui and Bustin (2006) suggest optimal gas production was achieved from coal seams characterised by cleat networks with wide cleat apertures and intermediate cleat spacing. Such coal seams would have high cleat permeability and low cleat porosity, resulting in a short time to achieve peak production and a high production rate during the main stage of production.

Coal seam permeability is also considered to be directional, with greatest permeability being parallel to the major (face) cleat (Hayes, 1982 and Osisanya and Schaffitzel, 1996). Hayes (1982) refers to work at WCC which found gas flow from boreholes drilled parallel to the major (face) cleat was lower and produced for less time than holes drilled perpendicular to the major cleat. Therefore in coal seams with a more developed face cleat, maximum gas production can be expected from boreholes oriented perpendicular to the major (face) cleat (Hayes, 1982 and Osisanya and Schaffitzel, 1996).

Lama *et al.* (1980) observed the cleat system in the Bulli seam at WCC to be equally developed which suggested the orientation of drainage boreholes would have limited affect on gas drainage rate.

2.5.1.3 Effective Stress

In coal seams, permeability is considered to be a function of the effective stress, which is the overburden pressure minus the seam fluid pressure (Osisanya and Schaffitzel, 1996 and Cui and Bustin, 2006). As fluid pressure is reduced and gas is drained from a coal seam two distinct phenomena exert an opposing effect on permeability. During the initial dewatering, decreasing fluid pressure in the cleat and pores of the coal seam results in an increase in effective horizontal stress which serves to reduce permeability. Following initial dewatering, the rate of gas desorption increases and the coal begins to dry causing the coal matrix to shrink, thereby increasing the aperture of the cleats and fractures, thus increasing cleat porosity and hence permeability of the coal (Gray, 1987; Harpalani and Zhao, 1989; Harpalani and Schraufnagel, 1990; Harpalani and Chen, 1992; Mazumder and Wolf, 2008 and Yi *et al.*, 2009).

Sorption testing conducted on coal samples from the Piceance and Black Warrior Basins in the United States, reported by Harpalani (1989) and Harpalani and Zhao (1989), observed an initial reduction in permeability in response to matrix swelling during adsorption, followed by an increase in permeability as the increasing gas pressure overcame the adsorption/swelling, forcing an expansion of the cleat and fractures. During desorption testing the reverse response was observed, with a decrease in permeability during initial gas pressure reduction, due to the closing of the cleats and expansion of the coal matrix, until reaching a pressure of approximately 3.0 MPa, below which there was a rapid increase in permeability, probably due to the desorption of gas from the coal structure and corresponding shrinkage of the coal matrix.

Where matrix shrinkage is less than the compaction forces, permeability may decrease during production, whereas if shrinkage is greater than the compaction forces, permeability may increase (Harpalani and Chen, 1992). Matrix shrinkage can have a significant impact on long term gas production from coal seams and is therefore an important parameter in predicting coal seam gas production (Harpalani and Chen, 1992).

2.5.1.4 Saturation

Gas saturation is a measure of the actual *in situ* gas content of a coal seam relative to the maximum gas storage capacity of that coal under the same environmental conditions. A coal containing the maximum amount of gas at a given reservoir pressure and temperature is said to be ‘saturated’ whereas a coal containing less than this theoretical maximum gas content is said to be ‘undersaturated’. Many coal deposits throughout the world are undersaturated to some degree and require pressure reduction to initiate gas release from the matrix into the cleats (Seidle and O’Connor, 2007). Where the cleat and fractures of an undersaturated coal are water filled, the rate of gas desorption from the coal will be impeded until sufficient water has been removed and the pressure reduced to the critical desorption point (Close and Erwin, 1989; Carlson, 2006; Cui and Bustin, 2006; Lamarre, 2007 and Seidle and O’Connor, 2007). Slightly undersaturated coal behaves in a similar manner to saturated coal with only a short delay prior to first gas production followed by a steady, strong, rising gas production rate. Highly undersaturated coal behaves quite differently and requires extensive dewatering prior to initiation of gas production (Seidle and O’Connor, 2007).

The degree of saturation can be expressed as a ratio of measured to saturated gas content. The saturated gas content of the coal seam can be determined using the Langmuir equation, Equation 2.4. Applying the Langmuir equation to the typical Bulli seam example presented in Figure 2.16, where the initial gas content (V_i) was 10.5 m^3/t and the initial reservoir pressure (P_i) was 3 500 kPa, the saturated gas content (V_{sat}) for CH_4 is 15 m^3/t (V_L = 28.2 m^3/t and P_L = 3 051 kPa) and V_{sat} for CO_2 is 34 m^3/t (V_L = 60.4 m^3/t and P_L = 2 701 kPa). In this example the coal was 70% saturated in CH_4 and 31% saturated in CO_2.

The degree of saturation may also be expressed as a ratio of critical desorption pressure to initial pressure. Critical desorption pressure is related to measured gas content by Langmuir's equation. Solving the Langmuir equation for critical desorption pressure is expressed in Equation 2.6.

$$P_{CDP} = P_L \cdot \frac{V_i}{V_L - V_i} \tag{2.6}$$

where: P_{CDP} = critical desorption pressure (kPa) corresponding to the measured gas content of the coal seam V_i (m^3/t)

Using Equation 2.5, the critical desorption pressure of the typical Bulli seam example is 1 809 kPa for CH_4 and 568 kPa for CO_2. Therefore, in the example the Bulli seam is said to be 51% saturated in gas pressure for CH_4 and 16% saturated in gas pressure for CO_2 which is equivalent to being 49% undersaturated in gas pressure for CH_4 and 84% undersaturated in gas pressure for CO_2.

From a study of the economic impact of gas saturation in the Powder River Basin in the United States, Seidle and O'Connor (2007) concluded that as the degree of saturation reduced, gas production weakened, dewatering time increased and the peak gas production rate reduced. Seidle and O'Connor (2007) also reported that coal which was 60% undersaturated required five times as long to reach peak gas rate and the magnitude was one sixth that of an equivalent saturated coal.

Faiz *et al.* (2007a) and Saghafi *et al.* (2007) investigated the degree of saturation in CO_2 rich areas of the Bulli seam, comparing measured gas content to the saturated gas content determined from CO_2 sorption isotherms. From the measured and saturated gas content values, presented by Faiz *et al.* (2007a) in Figure 2.17, the maximum gas

saturation in areas of high CO_2 composition was found to be less than 60%. Faiz *et al.* (2007a) suggest the undersaturation of CO_2 may be due to restricted accessibility of adsorption sites or leakage of previously existing CO_2 from the coal seam, or a combination of the two. Saghafi *et al.* (2008) report coal seams in the Hunter Valley are generally 20 to 40% saturated.

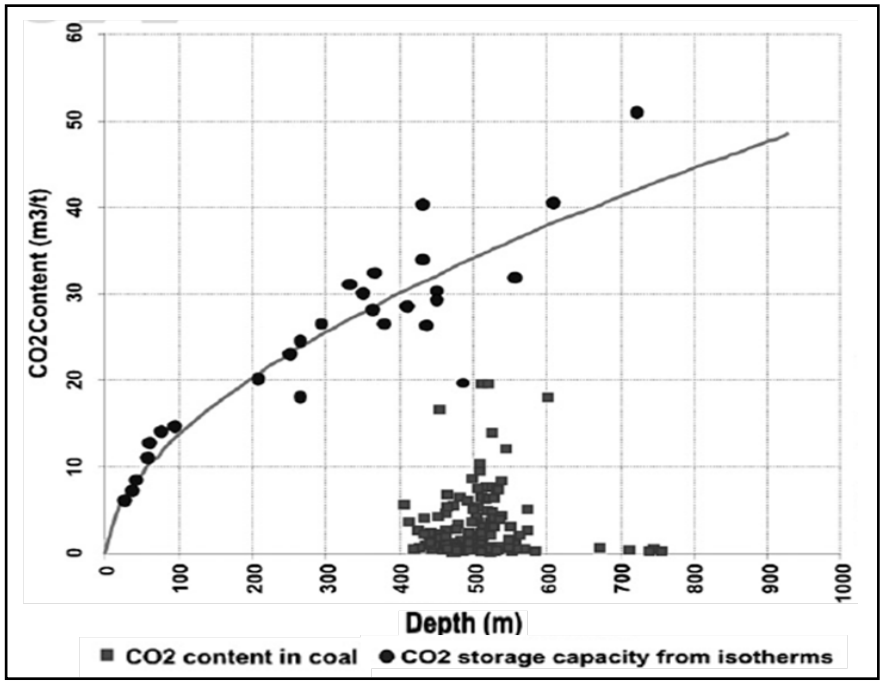

Figure 2.17: Measured CO_2 content relative to saturated storage capacity of Sydney Basin coal samples (after Faiz *et al.*, 2007a)

Figure 2.18 presents total measured gas content of core samples collected from WCC, plotted relative to the sorption isotherms for CO_2 and CH_4. Although not able to be determined the gas content values in this example have been plotted relative to an arbitrary gas pressure of 2 500 kPa. The results highlight the high degree of undersaturation in the CO_2 rich areas relative to the CH_4 rich areas, which is consistent with the findings of Faiz *et al.* (2007a) and Saghafi *et al.* (2007).

Given the high degree of undersaturation in the CO_2 rich areas of the Bulli seam, slow gas drainage rates and low total gas production can be expected. Figure 2.19 presents a comparison of flow rate (L/s) and cumulative gas production (m^3/m) data from similar gas drainage boreholes located in CH_4 rich and CO_2 rich areas of the 518 panel at WCC. From core sample gas analysis the average gas composition at 37 cut-through was 19% CH_4 / 81% CO_2 and at 14 cut-through was 87% CH_4 / 13% CO_2. Comparing the results from the two areas it can be seen that both the gas flow rate and total produced

volume from the highly undersaturated CO_2 rich area was significantly less than the near saturated CH_4 rich area. This result is consistent with the findings of Seidle and O'Connor (2007).

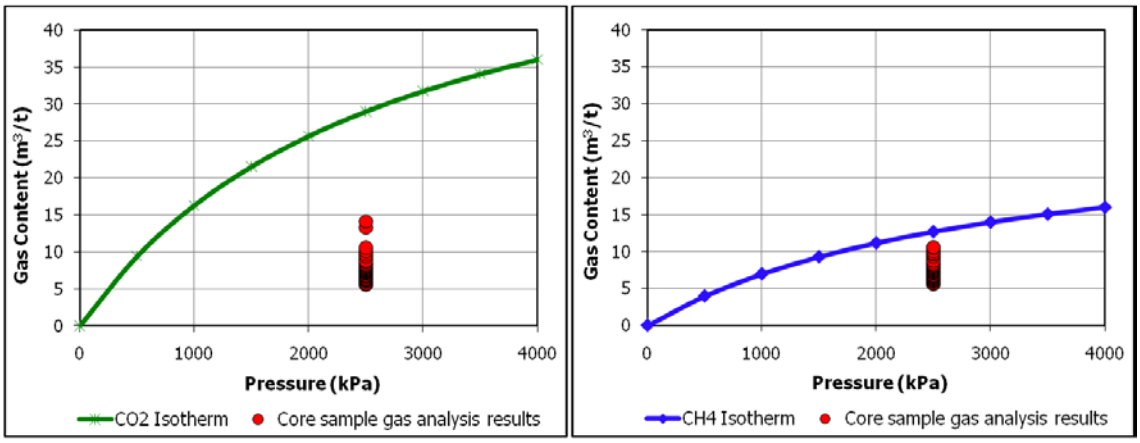

Figure 2.18: Bulli seam gas content relative to CO_2 and CH_4 isotherm indicating degree of saturation

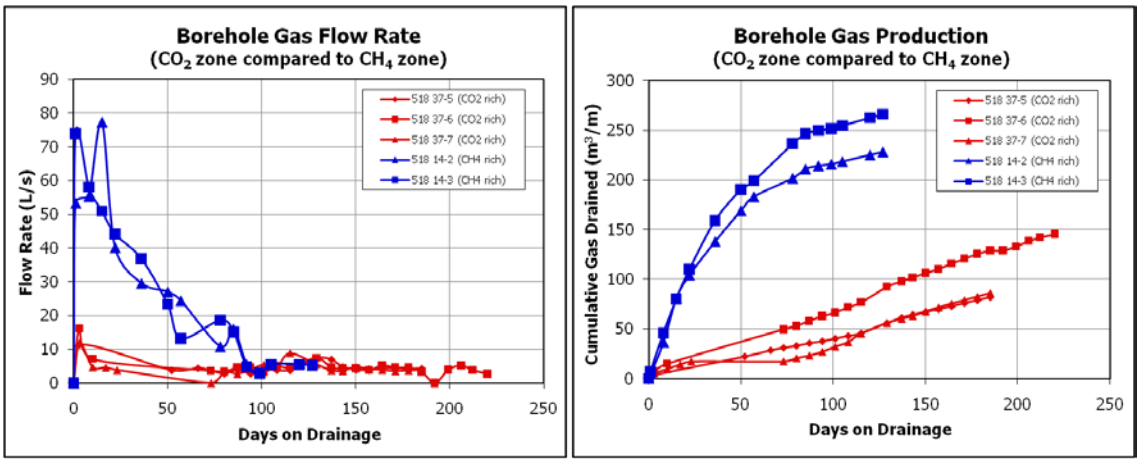

Figure 2.19: Comparison of flow rate and cumulative gas production from inseam gas drainage boreholes in CO_2 and CH_4 zones at WCC

2.6 MEASUREMENT OF COAL SEAM GAS CONTENT

Gas content is an important factor in relation to mine safety and mine planning, and has become increasingly important in coalbed methane resource assessment and recovery operations. Gas content data may be used in the calculation of gas resources and as input data for reservoir modelling and gas production simulators and to evaluate coal seam gas control options in underground coal mining. Various methods used to measure or estimate gas content can be grouped into two categories, (i) direct methods, which measure the volume of gas released from a coal sample sealed in a desorption canister, and (ii) indirect methods, which are based on gas sorption characteristics under given

temperature and pressure conditions, or empirical correlations between gas content and other coal seam parameters such as coal rank, depth of cover and gas emission rate (Lama and Bartosiewicz, 1982 and SAA, 1999).

2.6.1 Direct Method

Measurement of the gas content of a coal samples involves three stages: (i) determining the gas lost from the coal sample during core sample recovery (Q_1), (ii) measuring the gas desorbed from the coal sample while sealed in a desorption canister (Q_2), and (iii) measuring the gas released from a coal sub-sample during crushing (Q_3). The gas content measured during each stage is added to give the total measured gas content (Q_M), Equation 2.7, which for the purpose of this analysis represents the total volume of gas released per unit mass of coal when the ambient gas partial pressure is maintained at one atmosphere.

$$Q_M = Q_1 + Q_2 + Q_3 \tag{2.7}$$

Given the potential for variable temperature and atmospheric pressure conditions during gas content measurement and differences in mineral matter content of the coal samples, the results are typically normalised with Q_M being reported in NTP (20^OC and 101.325 kPa) and 10% non-coal matter (NCM) (Close and Erwin, 1989 and SAA, 1999).

Diamond and Schatzel (1998) list a variety of methods developed to measure gas content subsequent to the introduction of the first method by Bertard *et al.* in 1970. The techniques include:

- Bertard's method;
- US Bureau of Mines direct method;
- US Bureau of Mines modified direct method;
- Smith and Williams method;
- Decline curve method;
- Gas Research Institute method; and
- Australian Standard method.

The fast and slow desorption methods used in Australia to directly measure the gas content of coal samples, as described in Australian Standard AS3980:1999 (SAA,

1999), vary only in the time allowed for gas to desorb from the intact core prior to final crushing. The fast desorption test is typically completed in less than one day whereas slow desorption testing involved a much longer desorption period enabling the rate of gas emission from the intact coal core to be determined. For samples of equivalent Q_M, the Q_2:Q_3 ratio determined from fast desorption testing will be much less than the ratio determined from slow desorption testing. The lost gas volume, Q_1, will be the same regardless of the test method.

2.6.1.1 Lost Gas Component

The lost gas component (Q_1) is the portion of Q_M that escapes from the coal sample during its collection and retrieval, prior to being sealed into a desorption canister. Q_1 cannot be directly measured and therefore must be estimated from gas emission data collected subsequent to the sample being sealed into the desorption canister. It is generally accepted that during initial desorption the volume of gas released is proportional to the square root of desorption time. As described in Australian Standard AS3980:1999 (SAA, 1999) and presented in Figure 2.20, projecting the line of best fit representing initial gas emission from the time the core was sealed into the gas desorption canister (t_i) to the time midway between the commencement and completion of coring the sample (t_0) gives a measure of the gas volume lost during core sample recovery.

Since Q_1 is an estimated quantity, it is generally accepted to be the least accurate component of Q_M (Mavor *et al.*, 1992; Diamond and Schatzel, 1998 and Williams, 2002). Factors considered to impact the accuracy of the Q_1 measurement include sample recovery time, integrity of the coal sample, type of drilling fluid, water saturation and the amount of gas stored as free gas (Diamond and Schatzel, 1998). Close and Erwin (1989) refer to an alternative method for determining Q_1, presented by Smith and Williams based on the assumption that methane diffusion in coal is through a bi-disperse pore structure which is contrary to the unimodal pore theory upon which the more commonly used direct method is based. Comparative analysis of gas content measurement of samples from deep coal seams in the western United States indicated potential problems associated with using the Smith and Williams method when compared to other gas content measurement methods (Diamond and Schatzel, 1998).

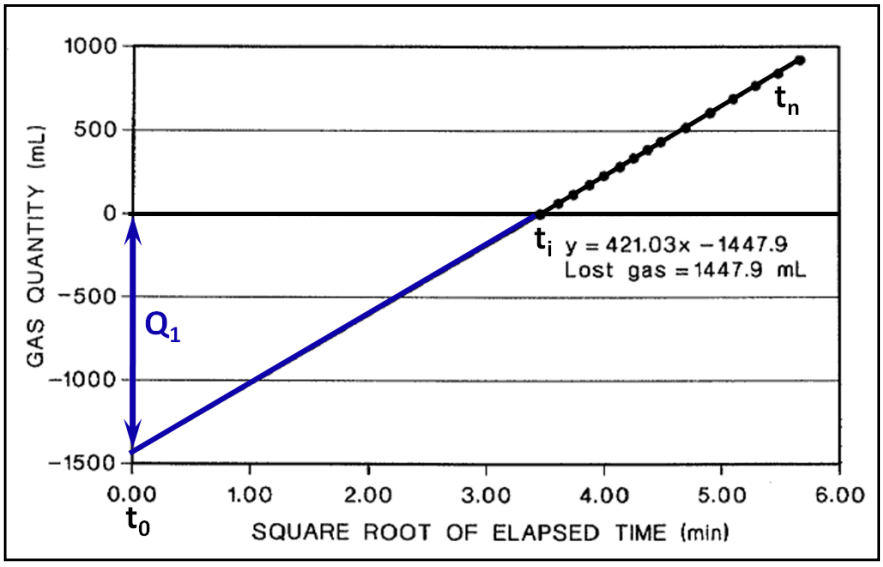

Figure 2.20: Q_1 lost gas determination (after SAA, 1999)

2.6.1.2 Desorbed Gas Component

The desorbed gas component (Q_2) is a measure of the volume of gas released from a coal sample whilst contained in a desorption canister. The duration of the Q_2 test may be short in the case of a fast desorption method, less than one day, or much longer in the case of slow desorption testing, greater than one month. Typically, gas released from a core sample is measured by water displacement using a graduated glass or plastic measuring flask. As shown in Figure 2.21 the measurement apparatus may be setup such that the gas liberated from the core sample within the desorption canister enters the measuring flask via a tube connected to the bottom or top of the measuring flask. Gas entering the top of the cylinder is preferred as the desorbed gas does not bubble through the water column thereby reducing the risk of gas loss through dissolution, particularly in the case of seam gas containing highly soluble CO_2 (SAA, 1999). Measures used to mitigate CO_2 dissolution in water include the use of acidified water in the measuring flask and a layer of linseed oil as a barrier between the water column and the gas entering the top of the flask (Saghafi *et al.*, 1998). An additional measure to minimise gas loss into solution is the periodic release of gas from the desorption canister which involves opening the valve at the top of the desorption canister, measuring the water displacement and noting other environmental conditions such as temperature and atmospheric pressure, then resealing the desorption canister until the next scheduled gas release (McCulloch *et al.*, 1975; Diamond and Schatzel, 1998 and SAA, 1999).

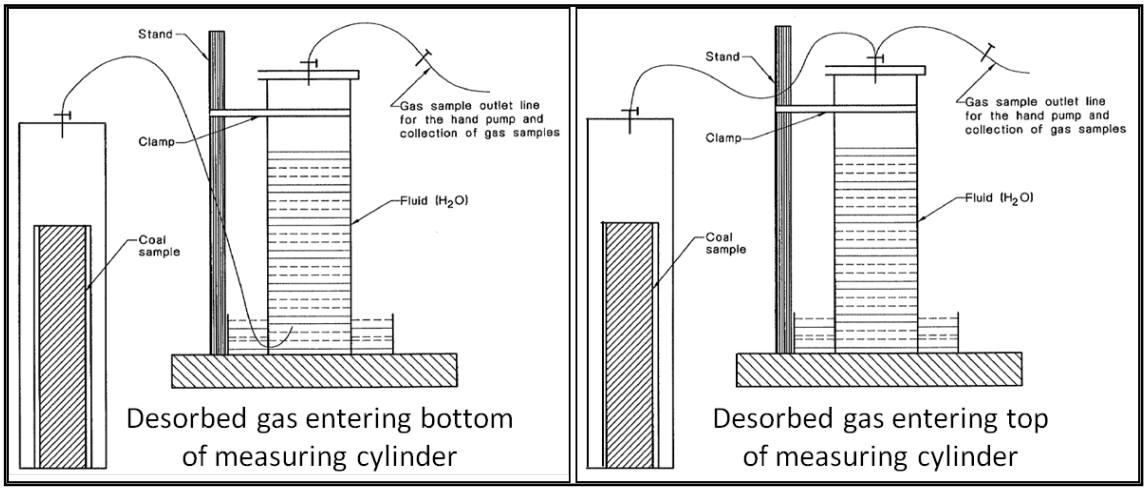

Figure 2.21: Desorbed gas volume measurement apparatus (after SAA, 1999)

An alternative desorbed gas measuring method, referred to as the US Bureau of Mines modified direct method (Diamond and Schatzel, 1998), is claimed to have increased accuracy in the measurement of gas emissions from coal samples, particularly those with low total gas content. The unit, known as the Portable Modified Direct Method Testing Apparatus (Schatzel and Garcia, 1999), abandons the use of a water column for the periodic measurement of gas desorbed from a coal sample instead relying on the ideal gas law and measurement of differential pressures to calculate desorbed gas volume.

McCulloch *et al.* (1975) proposed that desorption measurements should continue until less than 0.05 cm^3/g of gas was liberated per day for five consecutive days. This standard was later revised by Diamond and Levine (1981) who proposed desorption measurement should continue until less than 10 cm^3 of gas was liberated per day for one week. SAA (1999) provides no definitive measure to signal the completion of the desorption test, suggesting the test be deemed complete when the rate of gas evolution approaches an asymptotic value.

2.6.1.3 Crushed Gas Component

The crushed gas component (Q_3) is a measure of the gas liberated from a coal sample following crushing. Following completion of the desorbed gas test the coal core is removed and a representative sub-sample collected and sealed into a crushing or grinding mill. Following crushing the volume of gas liberated from the coal sample is measured using a water column similar to that used in the desorbed gas measurement.

McCulloch *et al.* (1975) first proposed that coal samples be sealed in a crushing vessel filled with N_2 and crushed to less than 200 µm. Diamond and Levine (1981) proposed crushing a sub-sample of up to 1 000 g for one hour to achieve a –200 µm fine powder and allowing the sample to cool to room temperature prior to measuring the liberated gas by way of water displacement. SAA (1999) recommends testing a minimum of two representative sub-samples of similar mass (±5%) weighing between 15 and 300 g, each sub-sample crushed separately to achieve a minimum of 95% of the material –212 µm.

A comparison of Q_3 testing procedures used by three Australian companies reported by Danell *et al.* (2003) identified differences in sample mass, crushing time and cooling time. Although different, the procedures employed by each laboratory were reported to comply with the guidelines detailed in Australian Standard 3980:1999. An assessment of gas content testing on equivalent reference samples by Danell *et al.* (2003) noted consistent differences in the results reported by each of the laboratories involved, with variability of up to 17%. This result was consistent with the expectation of Australian Standard 3980:1999 (SAA, 1999) which suggest inter-laboratory variability of 15%.

In fast desorption testing, given the short desorption time, Q_3 represent a large percentage of Q_M, whereas in slow desorption testing Q_3 is quite low, representing the residual gas content of the sample. Residual gas content is the volume of gas per unit mass of coal that is naturally retained within the coal and not readily released from an intact sample. The residual gas content also represents the portion of Q_M that will not be liberated into the mine atmosphere from mined or intact coal (Diamond and Schatzel, 1998).

Residual gas content is also an important consideration in the evaluation of coalbed methane gas recovery potential as it represents the portion of Q_M that will not readily flow to gas drainage boreholes (Diamond and Schatzel, 1998).

2.6.1.4 Fast Desorption Method

The fast desorption method is the preferred method for gas content measurement used in the Australian underground mining industry due to the relatively short time from core recovery to reporting of gas content and composition. This is particularly important from the point of view of outburst risk management and control as it decreases response

time and reduces the risk of production delays being incurred whilst awaiting the results of gas content measurement.

Past studies by (Saghafi *et al.*, 1998; SAA, 1999; Williams, 2002 and Danell *et al.*, 2003) list potential errors associated with the direct method of gas content testing which include:

- inaccurate estimation of gas lost during sample recovery, prior to sealing the coal sample into an air tight canister;
- inaccurate measurement of liberated gas volume, both in the field and laboratory;
- leakage of gas from desorption canisters;
- loss of gas due to dissolution when in contact with water;
- loss of gas during sample transfer between Q_2 and Q_3 testing;
- inaccurate measurement of temperature and pressure variations during desorption resulting in inaccurate temperature and pressure correction being applied to liberated gas volume; and
- partial pressure effects within sealed desorption canister impeding the rate of gas desorption.

2.6.1.5 Slow Desorption Method

The slow desorption method for gas content testing is not commonly used in the Australian coal mining industry however is a preferred method in the coalbed methane industry. As the name suggests the desorption test period can take many months and frequent desorbed gas volume measurement is required to achieve an accurate gas emission profile from which sorption time can be determined (Close and Erwin, 1989). Sorption time, considered an important factor in coalbed methane reservoir production modelling, is defined as the time taken for the coal sample to desorb 63% of Q_M.

Given the partial pressure effect on gas desorption there is a potentially adverse impact on the rate of desorption resulting from sealing the desorption canister between desorption measurements. Although impacted by the frequency and time between desorption measurements the measured gas emission profile is likely to be somewhat lower than would be the case if the sample were allowed to freely desorb. The measuring apparatus described in the US Bureau of Mines modified direct method, referred to by Diamond and Schatzel (1998) and Schatzel and Garcia (1999), has the

potential to address this issue enabling more accurate recording of the rate of gas emission during gas desorption testing.

2.6.2 Indirect Method

The most accurate measurement of gas content is achieved through direct measurement from borecore samples (Saghafi *et al.*, 2008). Alternatively gas content may be estimated using an indirect method based on sorption isotherm data (Kim, 1977) or empirical relationships between Q_M and other measurable variables such as coal seam depth and coal rank (Diamond *et al.*, 1976).

Sorption isotherms represent the maximum gas storage capacity of a coal sample at varying pressure and constant temperature. Based on knowledge of the isotherm for a particular coal type and details of the gas pressure, or an estimate of gas pressure based on knowledge of seam depth, the maximum gas content can be determined. However many coal seams are undersaturated which, if not accounted for, may result in an over estimate of actual seam gas content (Diamond and Schatzel, 1998). A variety of potential errors are associated with the use of sorption isotherms to determine gas content, which include:

- isotherm data may not be representative of conditions at the sample location due to changes in coal seam gas composition and variable coal characteristics, such as moisture content, temperature, coal rank, and ash content;
- lack of knowledge relating to degree of gas saturation in the coal seam and changes in gas content occurring naturally and due to the effects of mining and near and far field gas drainage; and
- inaccurate measurement or estimation of seam gas pressure at the sample location.

Gas content may also be estimated using an interpolation technique whereby the gas content value is calculated for the target location based on measured gas content results at neighbouring locations (Saghafi *et al.*, 2008).

The use of indirect methods to estimate gas content may be appropriate for use as a preliminary assessment tool for mine planning and gas reservoir assessment, however, given the potential for error, should not be used in detailed planning and economic decision making (Diamond and Schatzel, 1998).

2.7 USE OF GAS CONTENT IN OUTBURST MANAGEMENT

An outburst is a sudden release of gas and coal under pressure from a working face area (BHP, 1995). Various theories have been presented regarding factors that contribute to the occurrence of coal and gas outbursts. Factors considered to have the potential to contribute to an outburst, as reported by Lama (1995c), include the tensile strength of coal, gas emission rate, gas pressure gradient, moisture content and the magnitude of localised stresses. Lama (1995c), referring to the Bulli seam, concluded that seam gas was the most significant factor in outburst occurrence, more so than induced stress. For an outburst to occur in the Bulli seam there must be a large percentage of fine coal and high gas content present. The violence of an outburst is proportional to the gas pressure, content and composition at the point of initiation (BHP, 1995).

The four factors considered to have greatest impact on outburst propensity, the most significant being gas content, are presented in an outburst risk matrix, presented in Figure 2.22, to illustrate the levels of outburst risk (Black *et al.*, 2009).

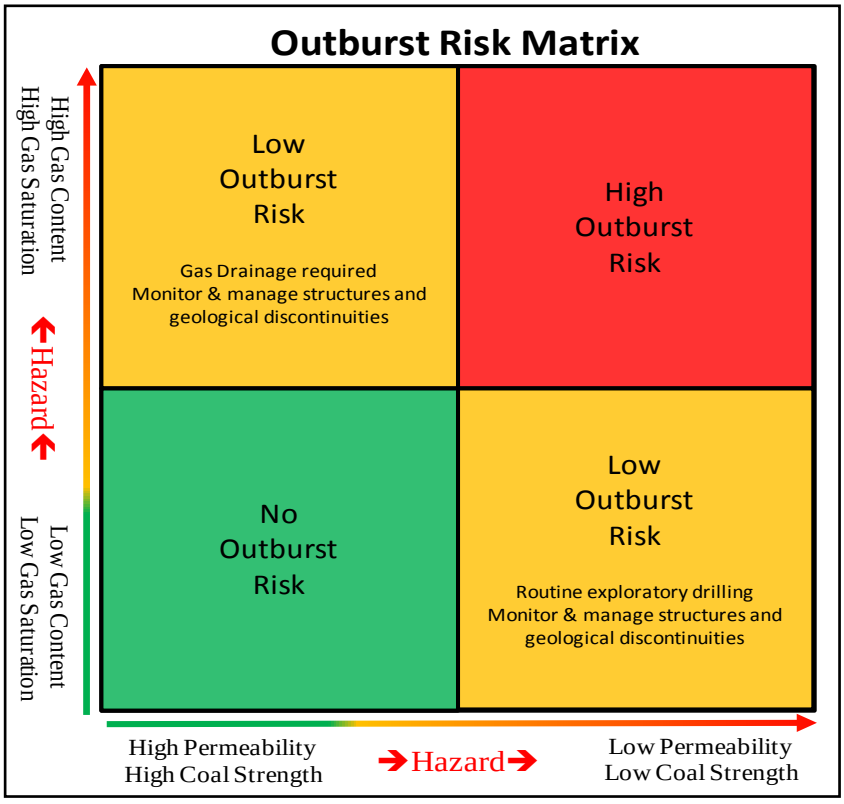

Figure 2.22: Outburst Risk Matrix (after Black *et al.*, 2009)

Virtually all outburst events that have occurred in the Bulli seam have been associated with geological structures and been located in areas where no substantial gas drainage

has been undertaken. There have been 12 outburst related fatalities in Bulli seam mines (Harvey and Singh, 1998) all of which occurred in areas without gas drainage and where CO_2 was the primary seam gas component (Lama, 1995c).

The removal of gas by gas drainage and the reduction of gas content levels to a value considered safe for mining were uncritically accepted by the mining industry (Lama, 1995c).

2.7.1 Outburst Threshold Limit Values – Bulli Seam Mines

Following the last outburst related fatality in Australia, which occurred at WCC on 25th January 1994, the NSW Department of Mineral Resources (DMR) issued a directive to all mines operating in the Bulli seam detailing actions to be implemented to prevent further outburst related fatalities. Arguably the most significant of these actions was the stipulation of limits on seam gas content prior to mining, known as outburst threshold limits (TLV). Figure 2.23 shows the Bulli seam TLV prescribed in the Section 63 notification (Clarke, 1994). The TLV varied linearly based on gas composition, decreasing from a maximum in CH_4 rich conditions to a minimum in CO_2 rich conditions. The Level 1 TLV indicates the maximum gas content limit for normal mining above which outburst mining procedures must be followed. The Level 2 TLV indicates the maximum gas content limit for outburst mining above which mining must only be undertaken using remote operated equipment, with all personnel remaining clear of the outburst risk zone.

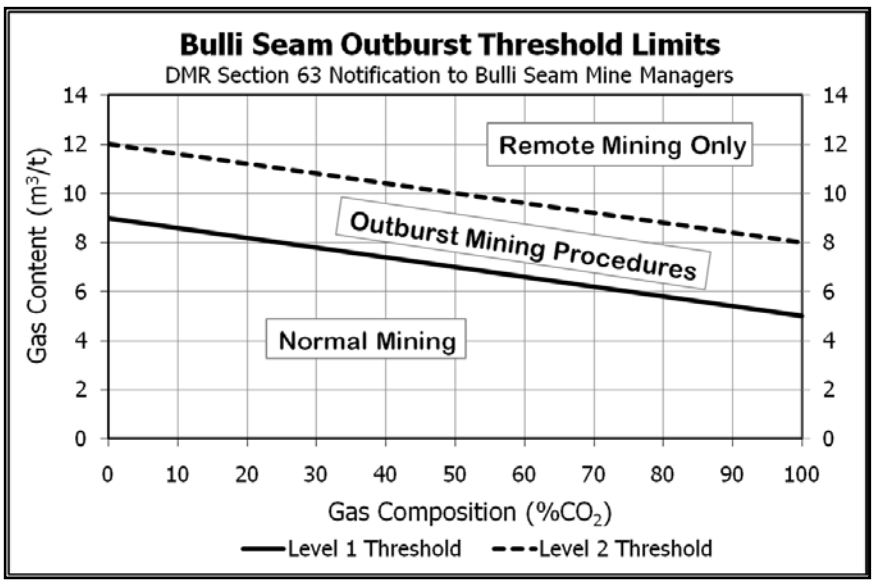

Figure 2.23: Prescribed Bulli seam Outburst Threshold Limits (Clarke, 1994)

The introduction of TLV resulted in a significant increase in the intensity of drilling and gas drainage for the purpose of identifying geological structures and reduction of gas content to below threshold limits. Mine operators developed comprehensive outburst management plans which included standard drilling patterns and routine management controls to deal with the issue of gas content reduction. However the TLV made no allowance for the introduction of intensive inseam gas drainage drilling and the capability of directional drilling technology to aid in locating geological structures and other outburst risk zones.

Lama (1995c) described the process that led to his recommendation of TLV for safe mining of the Bulli seam, based on total gas content. As shown in Figure 2.24, the Level 1 TLV of 6.4 m^3/t for CO_2 and 9.4 m^3/t for CH_4 are considered safe under all circumstances, i.e. when mining in close proximity to geological structures with a development advance rate up to 50 m/d. Lama (1995c) suggested that if the rate of development advance was reduced to 10-12 m/d the Level 1 TLV could be safely increased by 20%. Lama (1995c) also proposed a Level 2 TLV of 10.0 m^3/t and 12.0 m^3/t for CO_2 and CH_4 when it was known that no geological structures were present within 5.0 m of the excavation during roadway development in virgin areas. In presenting the TLV, Lama stated the proposed TLV would include a safety factor of 19% (1.1 m^3/t), considered higher than the error in gas content measurement.

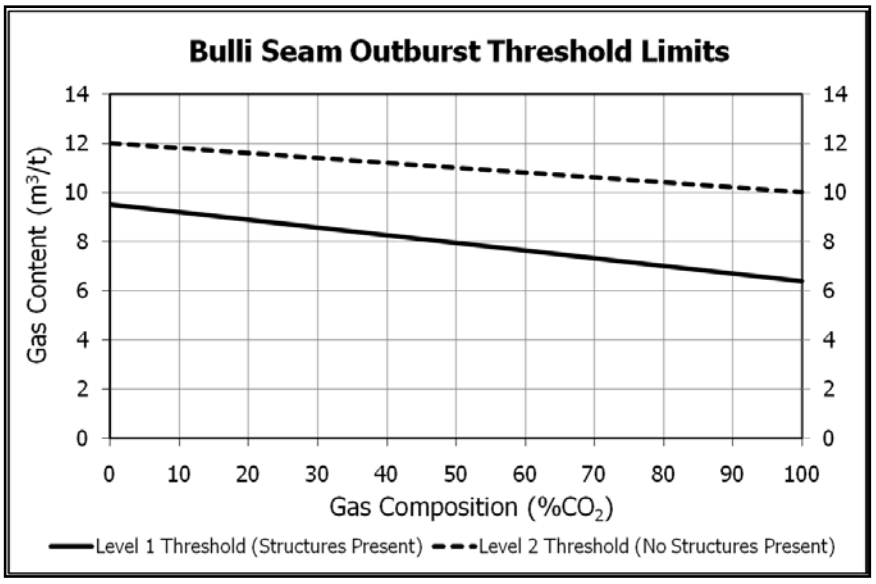

Figure 2.24: Recommended Bulli seam Outburst Threshold Limits (Lama, 1995c)

The methodology used by Lama to determine the proposed TLV was based on operating experience in the Bulli seam, and the inferred gas content and composition of the seam gas present in areas where outbursts had occurred. The fact that there had been no recorded outbursts where gas content was known to be less than the proposed TLV supported the proposed levels.

The difference between the Level 1 TLV presented by Clarke (1994) and Lama (1995c) suggest an additional 'factor of safety' was applied by the DMR to the TLV prescribed for the Bulli seam mines. Although the prescribed TLV was conservative (Black *et al.*, 2009), it achieved the objective of the DMR, in eliminating outburst incidents in the Bulli seam. Favourable conditions present in the mines at that time enabled the seam gas content to be reduced below TLV relatively easily and without delay to mine operations and coal production.

2.7.1.1 Raising Bulli Seam Outburst Threshold Limit Values

In the 15 years following the introduction of TLV there has been significant advances in the technology and production capacity of mining equipment. Mine operators are endeavouring to produce at much faster rates and in many cases the conventional gas drainage management techniques are struggling to achieve sufficient gas content reduction ahead of the advancing mine development. Figure 2.25 shows the annual run of mine production over the 15 year period 1995 to 2009 from longwall mines operating in the Bulli seam (Cram, 1995-2010). Over this period, excluding Tower Colliery which ceased longwall production in 2002, there was an average increase in annual production of 64% from the four operating mines.

In situations where mines experience difficulty reducing the coal seam gas content ahead of mining a typical response has been to increase the density of boreholes by infill drilling to reduce the spacing between boreholes. In addition to increasing the cost of gas drainage and diverting drill rigs from scheduled pre-mine gas drainage drilling elsewhere in the mine, these additional boreholes typically have limited drainage time prior to the arrival of the mining machinery and production delays may still result. In extreme cases operators have chosen to sacrifice coal reserves in favour of redirecting mining effort to areas with more favourable drainage response.

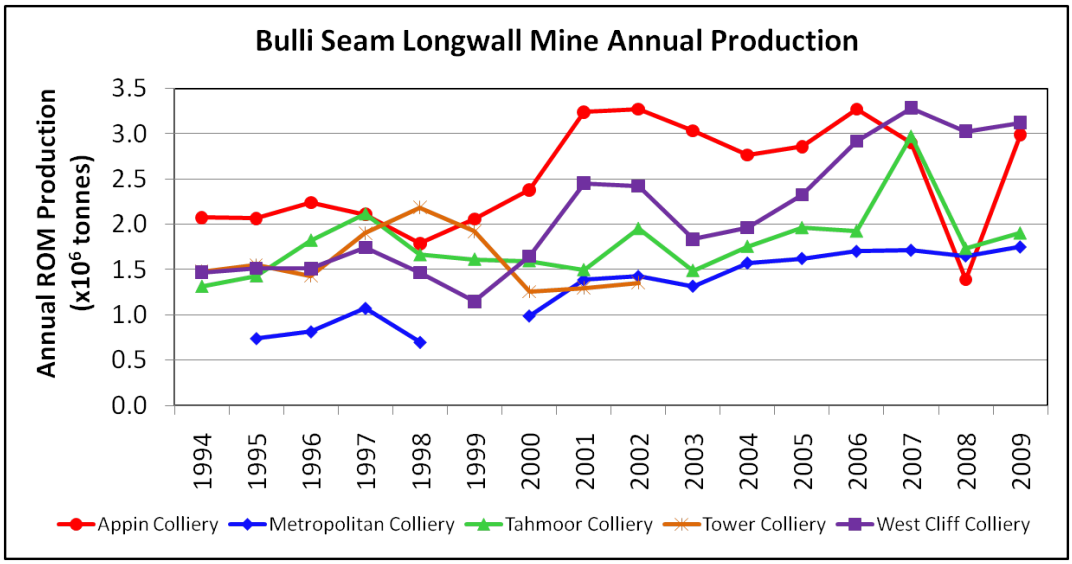

Figure 2.25: Annual Bulli seam Longwall Mine Production (after Cram, 1995-2010)

Two Bulli seam mines completed formal reviews of their respective outburst management plans which supported increasing their respective TLV. Application was made to the DMR seeking approval to vary the TLV from the levels prescribed in the original Section 63 directive of 1994. Increased TLV were approved for Tahmoor Colliery in 2003 and WCC in 2005. Figure 2.26 and Figure 2.27 show the current TLV for Tahmoor and WCC. In the years following the changes to the TLV, both Collieries continue to operate without an outburst incident. Several other Bulli seam mines are now considering undertaking similar reviews.

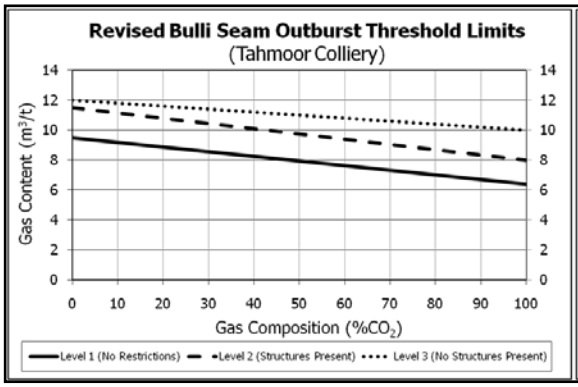

Figure 2.26: Revised Tahmoor Colliery TLV (after Tahmoor Colliery, 2003)

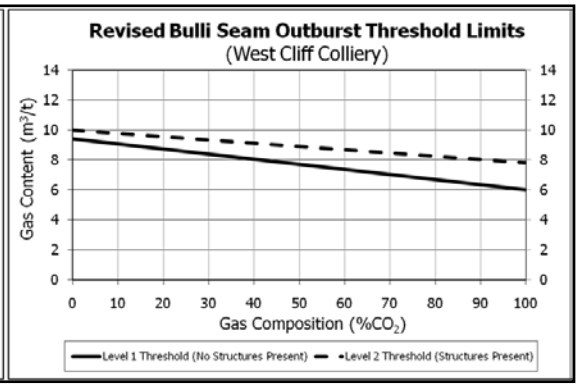

Figure 2.27: Revised WCC TLV (after West Cliff Colliery, 2007)

At Tahmoor Colliery, in addition to the Level 1 TLV, below which no restrictions are placed on mining, two additional TLV levels were introduced. The Level 2 TLV applies to structured coal. Where the measured gas content is greater than Level 1 and less than Level 2, in addition to more intensive drilling and coring, the rate of development

advance is restricted to 12 m/day. The Level 3 TLV applies to coal free of geological structures. Where the measured gas content is greater than Level 1 and less than Level 3, in addition to increased drilling and gas content testing, the rate of development advance is restricted to 25 m/day in each heading and cut-through to a maximum of 75 m in any 24 hour period. In areas where gas content remains above the defined TLV, normal mining is prohibited and grunching is the only approved development mining method.

At WCC, in addition to the Level 1 TLV, one additional TLV was introduced. While no restrictions are placed on the rate of development advance, where the measured gas content is between the Level 1 and Level 2 TLV increased drilling, structure identification and gas content testing is required. Where the gas content remains above the Level 2 TLV normal mining is prohibited and an alternative mining method, such as remote control or grunching, shall be used.

2.7.1.2 Impact of Gas Analysis Measurement Accuracy

The revised TLV at both Tahmoor and WCC do not exceed the TLV recommended by Lama (1995c), who claimed a 19% factor of safety, equating to a tolerance of 1.1 m^3/t error in gas content. Although Australian Standard AS3980:1999 aims to achieve a maximum of 10% variability in the accuracy of gas content measurement, error may arise in the testing process, as reported by Saghafi and Williams (1998) and Danell *et al.* (2003), which if not controlled has the potential to adversely impact the factor of safety.

Increasing the TLV has been demonstrated at both Tahmoor and WCC to be effective in controlling the risk of coal and gas outburst. However any errors arising during gas content measurement resulting in the reported Q_M being less than actual will effectively reduce the inherent factor of safety.

2.7.2 Outburst Threshold Limit Values – Non-Bulli Seam Mines

Williams and Weissman (1995) introduced the concept of using the rate of gas desorption from crushed coal, during Q_3 testing, known as desorption rate index (DRI), to determine TLV applicable to coal mines operating in coal seams other than the Bulli seam. The test involved measuring the volume of gas emitted from a 200 g sub-sample of coal material after crushing for 30 seconds and extrapolating the result to the total gas

content (Q_M) of the full core sample to determine the DRI of the full coal sample (Williams, 1996 and Williams, 1997). The data presented in Figure 2.28, which represents data collected from the 386 panel at WCC (Williams, 2010) demonstrate a strong correlation between Q_M and DRI for both CO_2 rich and CH_4 rich coal samples. The relationship was assumed by Williams and Weissman (1995) to be representative of all Bulli seam conditions.

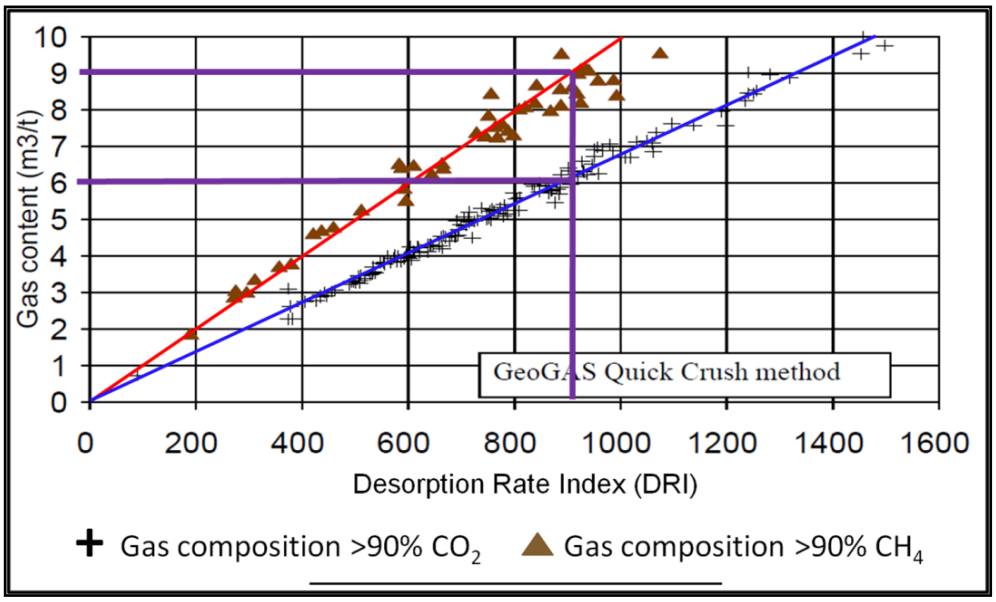

Figure 2.28: Q_M relative to DRI for CO_2 and CH_4 rich coal from 386 panel, WCC (after Williams and Weissman, 1995)

As shown, the Bulli seam TLV of 9 m^3/t (100% CH_4) and 6 m^3/t (100% CO_2) correspond to a common desorbed gas volume of 900 ml. From this assessment, Williams and Weissman (1995) concluded that the Q_M value corresponding to a DRI of 900, based on a unique Q_M-DRI relationship determined specifically for each mine and coal seam, represent the TLV applicable to that coal mine. This method, known as DRI900, which was uncritically accepted by the mining industry for determining outburst TLV applicable to non-Bulli seam mines, is described in Equation 2.8.

$$TLV_{(Bulli)} \xrightarrow{\langle Q_M \leftrightarrow DRI_{Bulli} \rangle} DRI900 \xrightarrow{\langle Q_M \leftrightarrow DRI_{non-Bulli} \rangle} TLV_{non-Bulli} \qquad (2.8)$$

2.7.2.1 Impact of Changes to Bulli Seam Outburst Threshold Limit Values

Assuming the relationship between Q_M and DRI for both CO_2 and CH_4 rich coal samples, presented by Williams and Weissman (1995), remains valid and represents all Bulli seam conditions; the fact that both Tahmoor and WCC are safely operating at

TLV greater than those originally prescribed in 1994 suggest the DRI900 method for determining TLV applicable to non-Bulli seam mines may not fully recognise the use of additional outburst management controls and the use of a Level 2 TLV.

Employing the same process described by Williams and Weissman (1995), to determine DRI values corresponding to Bulli seam TLV; Figure 2.29 show the impact of the raised TLV on the DRI value. In this example, Bulli seam TLV of 12 m^3/t for CH_4 and 8 m^3/t for CO_2 correspond to a DRI value of 1 200. Based on this example using current, acceptable Bulli seam TLV it is suggested that a DRI1200 may also be employed by non-Bulli seam mines to determine applicable Level 2 TLV. It is however important to note that where the gas content in the mining area exceeds the defined Level 1 TLV significant additional outburst management controls play an integral role in the management of outburst risk.

The relationship between Q_M and DRI and the impact on TLV applicable to non-Bulli seam mines is analysed in detail in Chapter 6 using an extensive dataset of fast desorption gas test results gathered from eight Australian underground coal mines.

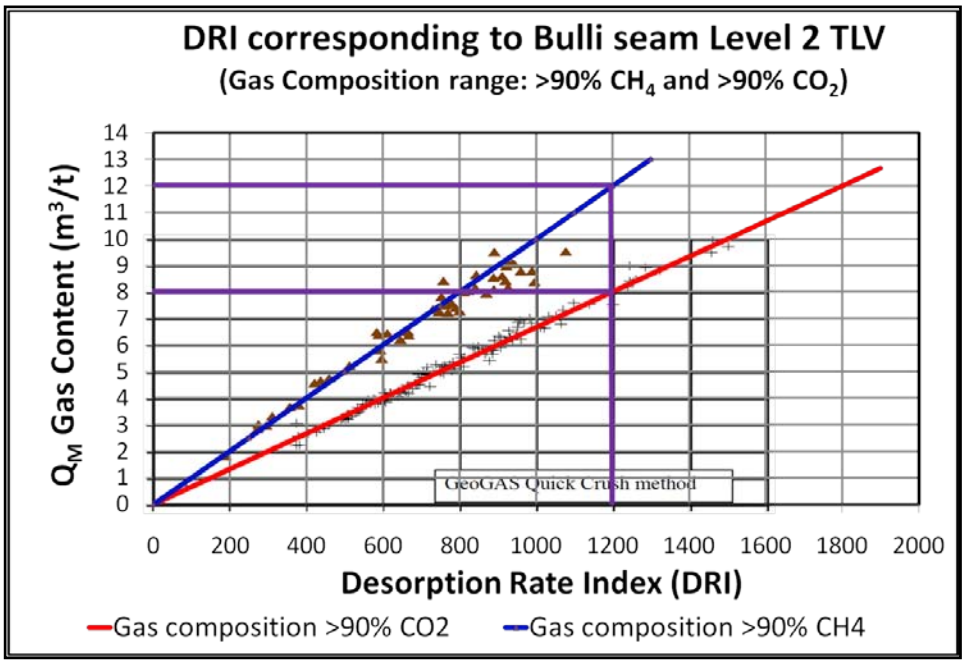

Figure 2.29: Impact of increased Bulli seam TLV on DRI used to determine non-Bulli seam TLV (after Williams and Weissman, 1995)

2.8 SUMMARY

This chapter discussed the generation, storage and emission of gas in coal seams, along with methods used to determine the gas content of coal and the use of gas content in the management of outburst risk in Australian underground mines.

The content and composition of seam gas in the Bulli seam at WCC was shown to vary significantly throughout the current mining area. Langmuir volume (V_L) and Langmuir pressure (P_L) constants were determined from sorption testing on coal samples collected from the mine and assessed relative to various coal properties to assess the impact on sorption capacity. The relationship between the various coal properties and V_L, determined for both CH_4 and CO_2 sorption testing, were in general agreement with the findings of previous studies. V_L was considered to increase with coal rank however given the similar rank of the WCC samples no relationship was evident. Previous work reported both positive and negative relationships between V_L and coal type. The results of this study gave some indication of increasing V_L in response to increase vitrinite content however the relationship was not strong. Consistent with the results of previous work, V_L was found to decrease in response to increasing moisture content with V_L reducing by an average 4.2 m^3/t, in the case of CH_4 adsorption, and 7.2 m^3/t, in the case of CO_2 adsorption, for each 1.0^OC increase in moisture content. Also consistent with the results of previous work, for each 1% increase in ash content V_L reduced by 0.27 m^3/t, in the case of CH_4 adsorption, and 0.43 m^3/t, in the case of CO_2 adsorption. Although not assessed as part of this study V_L was reported to decrease in response to increasing temperature and confining pressure. Testing in QLD and NSW reported a decrease in V_L of 1.0 to 1.2 m^3/t per 10^OC increase in temperature.

The impact of permeability, coal structure, effective stress and degree of saturation on gas emission from coal was also reviewed. Permeability plays a significant role in controlling the flow of gas in coal. Permeability is dynamic and any measurement provides only a snapshot at that moment. Factors that impact permeability include effective stress, gas pressure, water content, drilling induced disturbance and matrix swelling/shrinkage characteristics.

Previous studies suggest optimum gas drainage performance may be achieved from vitrinite rich, high volatile bituminous coal, effectively sealed above and below by impermeable strata to minimise gas leakage, in a relatively low stress environment. The

coal should also have a well defined cleat network free of mineral deposits, with cleat spacing between 0.001 mm and 20 mm and a cleat aperture between 0.05 μm and 20 μm, thereby having high cleat permeability and low cleat porosity.

Saturation has also been shown to have a significant impact on coal seam gas production. Analysis of Bulli seam coal samples from WCC confirms deep undersaturation in CO_2 rich areas, consistent with the results of separate studies of Bulli seam coals. Analysis of UIS borehole gas production from a highly undersaturated, CO_2 rich area of the mine demonstrated a slow drainage rate and low total gas production, consistent with the effect of deep undersaturation as proposed by Seidle and O'Connor (2007).

Methods used to determine gas content were reviewed. Gas content plays an important role in outburst risk management with safe threshold limits being based on maximum acceptable gas content values. The method proposed by Williams and Weissman (1995) to determine TLV for non-Bulli seam mines was based on TLV for CH_4 and CO_2, applied to the observed relationship between Q_M and DRI for each gas, which corresponded to a common DRI value of 900. Assuming the relationship identified in 1995 between Q_M and DRI for CH_4 and CO_2 remains valid and applicable to all current Bulli seam conditions; recent increases in Bulli seam TLV, proven to operate effectively without compromising mine safety, correspond to a DRI value of 1 200. By adopting a Level 2 TLV corresponding to DRI1200, used in conjunction with effective additional outburst risk management controls, mine operations may continue in areas of increased gas content. The relationship between Q_M and DRI and the impact on outburst TLV warrants further investigation and is addressed in Chapter 6.

CHAPTER THREE – DRAINAGE OF COAL SEAM GAS

3.1 INTRODUCTION

Coal mines typically undertake coal seam gas drainage for reasons related to mine safety and to maintain environmental gas concentrations below specified limits in order to minimise gas-related production delays. Gas may be liberated into an operating underground mine from a number of sources, listed below and shown in Figure 2.8.

A. Emission from exposed mine roadways;
B. Emission during coal cutting in both development and longwall panels;
C. Emission into longwall goaf from adjacent gas bearing coal seams and strata;
D. Emission from longwall goaf into connecting airways; and
E. Emission from coal being transported from mine via the coal clearance system.

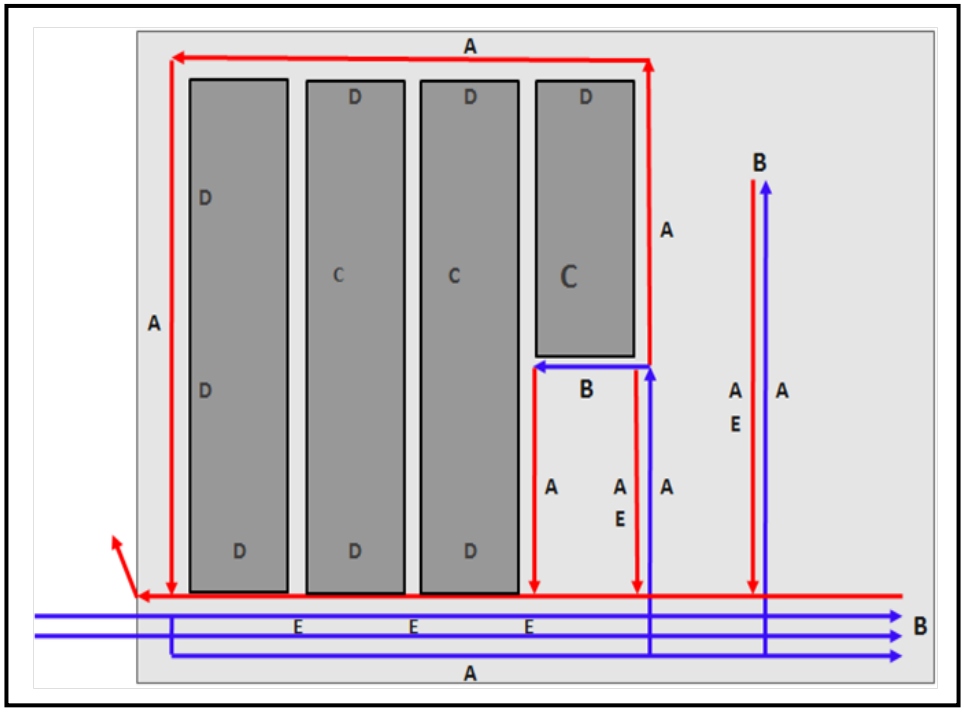

Figure 3.30: Conceptual underground mine layout indicating potential sources of coal seam gas emission (Black and Aziz, 2009)

Where the volume of gas liberated into the mine environment exceeds the diluting capacity of the mine ventilation system three options are available to the mine operator (a) remove the excess gas through systematic gas drainage, (b) dilute the excess gas by increasing the ventilation air quantity, or (c) reduce the rate of gas emission by reducing

the mining rate. As discussed in Chapter 2 gas drainage may also be required to reduce the *in situ* seam gas content to below specified TLV prior to mining.

This chapter discusses the evolution of gas drainage in Australian underground coal mines and describes a variety of drilling and stimulation techniques developed in the oilfield, coalbed methane and shale gas industries which offer potential benefit to coal mine and coal seam gas drainage.

3.2 DRAINAGE OF COAL SEAM GAS FROM UNDERGROUND

3.2.1 Background

On a global scale the Australian underground coal mining industry was slow to adopt the use of systematic gas drainage to control gas emission into mine ventilation and to reduce the outburst risk.

3.2.1.1 Metropolitan Colliery

Following the commencement of operations at Metropolitan Colliery in 1888 coal from the Bulli seam was mined by hand with some single round shotfiring (Ward, 1980). Following a fatal outburst in 1925, which occurred during shotfiring on a fault, the mine introduced the practice of drilling a 43 mm diameter borehole, typically 20 to 25 m ahead of the mining face (Ward, 1980 and Clark, 1983). This practice continued until a fatal outburst incident in 1954, which occurred on a fault where a single borehole had been previously drilled through the fault zone. Mining continued with the use of multi-shot shotfiring, employing a maximum of six shots per round. Full face shotfiring was approved for use in development mining at Metropolitan Colliery in 1961 (Clark, 1983). The use of multi-shot and full face shotfiring, reported to provide increased protection for mine workers, was also considered to have contributed to an increase in the frequency and severity of outbursts (Ward, 1980 and Clark, 1983).

During the 1960's, experiments were conducted at Metropolitan Colliery to determine the impact on gas drainage by increasing the length, diameter and number of boreholes drilled into the working face (Clark, 1983). The use of suction applied to 43 mm pilot pre-drainage boreholes was also examined by Hargraves however results were considered disappointing (Clark, 1980). The perceived failure of pre-drainage boreholes

with applied suction led to drainage boreholes being abandoned at Metropolitan Colliery in favour of inducer shotfiring (Clark, 1983).

The first large diameter borehole was drilled at Metropolitan Colliery using a modified Edeco Hydrac methane drainage drill (Ward, 1980). Boreholes of 300 mm, 450 mm and 600 mm diameter were drilled and assessed (Clark, 1983 and Clark *et al.*, 1983). The use of large diameter boreholes was initially considered successful based on a significant reduction in outburst events during shotfiring in combination with two 300 mm diameter boreholes drilled into the working face (Clark, 1983), one borehole along each rib line (Ward, 1980). Scroll rods were used to drill 300 mm diameter boreholes up to a maximum length of 80 m (Hargraves, 1983) and the scroll design aided in clearing cuttings and any fractured coal created through stress fracturing or in-hole outburst.

In 1968, continuous miners were introduced to development mining at Metropolitan Colliery and used in combination with larger diameter boreholes; however stringent conditions including fixed drainage periods prior to commencement of mining were required (Clark, 1983). Initially, a 60 day minimum drainage period was required prior to mining which was later reduced to 40 days subject to the results from emission value index monitoring. The fixed drainage period was later discontinued in favour of complete reliance on emission value monitoring as the basis for determining outburst risk and whether to mine in a particular heading (Ward, 1980). Where places were slow to drain additional centre holes were drilled or the face was shotfired using full-face rounds (Ward, 1980).

Large diameter boreholes were later considered a limiting factor in the mine's ability to achieve increased production from its development panels. In addition to drilling being time consuming, the boreholes had a tendency to wander off line, strike the roof or floor and fail to achieve the target distance of one pillar advance (Ward, 1980). As development roadways were required to follow the line of the boreholes the panels experienced difficulty maintaining straight roadways which was a particular problem in conveyor roadways (Ward, 1980). The use of large diameter boreholes also required an increased number of roadways in the panel to accommodate the drilling rig and to provide sufficient alternative mining places during the gas drainage period (Ward, 1980 and Clark, 1983).

Issues associated with large diameter boreholes led to Metropolitan Colliery adopting pulsed infusion shotfiring to drain gas from and de-stress the zone immediately ahead of the working face (Ward, 1980 and Clark, 1983). A typical drilling pattern featured three boreholes drilled to a depth of six metres, located mid seam, one hole in the centre of the heading and two flanking holes (Ward, 1980). The process of pulsed infusion shotfiring at Metropolitan Colliery involved drilling the boreholes in a non-production period, followed by sealing and infusing water at a pressure of 1.7 MPa for a period of two hours (Ward, 1980). Charges were then inserted into each borehole and infusion pressure restored and maintained until the holes were fired (Ward, 1980). Further testing and optimisation of the pulsed infusion process considered the pressure and duration of water infusion. Increasing water pressure to 6.2 MPa was found to provide no additional benefit, and following an initial infusion period of 10 minutes minimal additional water was infused into the coal seam (Ward, 1983). Poor roof and rib conditions, linked to the use of pulsed infusion shotfiring, led to reduced productivity at Metropolitan Colliery (Clark, 1983 and Clark *et al.*, 1983) which in turn led to the pursuit of more productive gas drainage and outburst control measures.

During the late 1970's and early 1980's, based on successful overseas experience, Metropolitan Colliery commenced investigations into the use of lateral inseam gas drainage by drilling small diameter boreholes from an adjacent panel to protect an advancing panel (Clark *et al.*, 1983). Initially, 43 mm diameter boreholes were drilled to depths up to 80 m using hand held, compressed air driven Victor borers with an air leg. Reamer bits were used to increase the diameter of the borehole to 100 mm (Clark *et al.*, 1983). A modified Joy roof bolter, mounted horizontally, was later introduced which had the capacity to increase borehole depth to 130 m (Clark, *et al.*, 1983). Trials using the Joy roof bolter produced longer boreholes, with less frequent roof or floor intersection and reduced lateral deviation than was achievable using the Victor borer (Clark *et al.*, 1983).

The benefit of inseam drilling as a means of reducing seam gas emissions at Metropolitan Colliery was recognised in mid-1981 (Clark *et al.*, 1983) and by the end of that year the mine had committed to the implementation of systematic inseam drainage, complete with an underground gas reticulation pipe range and vacuum plant (Clark, 1983).

Investigations followed to improve the effectiveness of inseam gas drainage at Metropolitan Colliery (Clark *et al.*, 1983), significant findings include:

- Multiple boreholes to be drilled in the immediate path of the heading;
- Minimum 50 mm borehole diameter was required to avoid blockages; 75 mm and 100 mm was considered adequate;
- Applied suction to drainage boreholes increases gas production; 13 to 20 kPa was reported to be most productive;
- High standard of borehole installation, sealing and connections to minimise leakage;
- Adequate planning of borehole location;
- Accurate control of borehole trajectory;
- Boreholes to extend a minimum of 10 m beyond the proposed heading distance; and
- Effective water separation was required from individual boreholes as well as along the gas reticulation pipe range.

3.2.1.2 Leichhardt Colliery

From the commencement of operations in 1973, Leichhardt Colliery in Queensland used shotfiring in combination with mechanised mining equipment to induce outbursts (Moore and Hanes, 1980).

Inseam drilling was introduced to Leichhardt Colliery in 1975 to drain gas ahead of roadway development however was discontinued in 1978 following an outburst incident (Moore and Hanes, 1980). Moore and Hanes (1980) describe the sequence of events associated with the incident which may have unnecessarily ended the use of inseam drilling for gas drainage and outburst control at Leichhardt Colliery. When the roadway had advanced to within 30 m of the outburst site ten boreholes, each 28 m long, were drilled and allowed to drain for five months. When mining resumed the roadway was advanced 25 m, to within three metres of the end of the pre-drainage boreholes and five metres short of the outburst site. A further five boreholes were drilled ahead of the roadway, at least four of these boreholes were later thought to have passed below the structured zone associated with the outbursts (Moore and Hanes, 1980). Upon completion of the second set of five boreholes mining resumed immediately, with no

time allowed for gas to drain from the freshly drilled area. The first of a series of outbursts occurred when the roadway had advanced two metres beyond the end of the previously drained boreholes (Moore and Hanes, 1980). In 1979 mining resumed at Leichhardt Colliery and continued until the mine closed in 1982 (BHP Billiton, 2001), utilising full-face shotfiring as the primary mining method (Moore and Hanes, 1980).

3.2.1.3 Collinsville No.2 Colliery

Between 1977 and 1979 investigations were conducted at the Collinsville No.2 Colliery to reduce seam gassiness through water infusion, bleeder holes, pulsed infusion shotfiring and vacuum drainage (Williams *et al.*, 1983 and Beamish *et al.*, 1985). Of the four methods, vacuum drainage using a venturi extractor delivered the most encouraging results, prompting a reassessment of inseam drilling for gas content reduction and outburst control which led to the establishment of an extensive gas drainage research program (Williams *et al.*, 1983). The initial program, using boreholes drilled to depths up to 60 m, investigated the effects of length, spacing, drainage time, orientation, dewatering and vacuum on gas content and seam gas pressure reduction (Williams *et al.*, 1983). To enable improved control of borehole trajectory and increased borehole length a Craelius Diamec 251 electro-hydraulic drill rig was introduced to the mine which featured independent thrust and rotation control (Williams *et al.*, 1983). During the Collinsville trials boreholes of 80 mm diameter were successfully drilled to a distance of 230 m (Williams *et al.*, 1983). The boreholes were surveyed at an interval of 20 to 30 m to determine trajectory using an Eastman single-shot survey tool, pumped into the borehole through the drill rods using drilling water and later recovered using wireline attached to the instrument (Williams *et al.*, 1983).

3.2.1.4 West Cliff Colliery

Systematic gas drainage was adopted at WCC in 1980 with the introduction of Australia's first full scale drainage system complete with surface drainage plant connected to an underground gas reticulation pipe range (Lama, 1983). One of the early drill rigs used at the mine was a compressed air operated Atlas Copco Diamec 250 capable of drilling boreholes to 100 m (Richards, 1980). This drill rig was limited by the high volume of compressed air required to drive the motor and due to the weight of the drill string the boreholes had a tendency to take a downward trajectory and intersect the floor (Richards, 1980). In the 24 months to March 1982, 482 inseam gas drainage

boreholes, with an average length of 105 m, were drilled at WCC (Marshall *et al.*, 1982). By 1982 WCC had experienced 125 outburst events and gas emission from working development faces had increased to a level where mining had to be regularly stopped (Marshall *et al.*, 1982). From analysis of gas emission data collected over a two year period it was recognised that improving the effectiveness of the gas drainage system was the only acceptable control to decrease the intensity and frequency of outbursts, improve mine safety and increase efficiency of coal production (Marshall *et al.*, 1982).

3.2.1.5 Appin Colliery

Appin Colliery introduced methane drainage in 1981, drilling cross-measure boreholes, to support longwall mining (Kelly, 1983). The drained gas was reticulated through an underground pipe network to a surface extraction plant which had a capacity of 5 500 L/s at a maximum suction of 50 kPa (Kelly, 1983). Inseam gas drainage commenced in 1982 using a Kempe U4-450 electro-hydraulic drill rig (Kelly, 1983). In the first year approximately 20 kilometres of inseam drilling had been completed at Appin Colliery, with an average and maximum borehole length of 230 m and 506 m respectively (Kelly, 1983). During this period the majority of boreholes were completed without survey. Once intersected by subsequent mine development, the deviation of the boreholes from the planned trajectory was found to vary from virtually zero to 70 m over a distance of 170 m (Kelly, 1983). Inseam boreholes drilled at Appin Colliery typically deviated toward the direction of the dominant cleat (Kelly, 1983). The type of drill bit used and the degree of wear on the bit also impacted on borehole trajectory (Kelly, 1983). The nature of borehole deviation reported by Kelly was in contrast with more common report of boreholes deviating to the right due to the clockwise rotation of the drill string (Hebblewhite *et al.*, 1982 and Osisanya and Schaffitzel, 1996).

The ability to drill boreholes up to 600 m in length was achieved through the introduction of drill rigs developed in the United States such as the Fletcher degasification drill and the Acker Big John degasification drill (Richards, 1980 and Hebblewhite *et al.*, 1982). The Australian Coal Industry Research Laboratories (ACIRL) acquired an Acker Big John rig in 1980 as part of a research program to improve methane drainage and outburst control (Richards, 1980). Using rotary drilling techniques ACIRL successfully drilled inseam boreholes to a maximum depth of 732 m

(Hebblewhite *et al.*, 1983). During the 1980's inseam rotary drilled boreholes, ranging in length from 250 to 320 m, were used to drain gas from the Bulli seam (Thomson, 1998). Longer boreholes offered increased drainage time however limited trajectory control commonly resulted in boreholes deviating from the planned path (Thomson, 1998). Lateral deviation of boreholes resulted in uneven borehole spacing and non-uniform drainage of the coal seam while vertical deviation commonly resulted in boreholes penetrating the roof or floor strata and not achieving target length (Thomson, 1998). Borehole deviation was considered to be more pronounced in areas of geological complexity resulting in less than adequate drainage in areas of increased outburst risk and outbursts continued to occur (Thomson, 1998).

Drill rig operators controlled borehole trajectory through varying applied thrust and the speed of bit rotation (Richards, 1980). To cause the trajectory of the borehole to rise, thrust was increased and rotation speed reduced and to cause the trajectory of the borehole to fall, thrust was reduced and rotation speed increased (Richards, 1980). Measurement of borehole trajectory was initially achieved through periodic survey using a single shot photographic tool, such as an Eastman single shot survey tool (Richards, 1980; Gray, 1994 and Lama, 1995b). The instrument was inserted into the drill rods and pumped down the drill string by water pressure to a non-magnetic section located behind the drill bit. After a pre-defined delay period, sufficient to allow the instrument to reach the end of the borehole, the camera would capture an image of a gymbled compass and dipmeter (Gray, 1994). Once the image had been captured the instrument would be recovered from the borehole, typically using a trailing wireline, and the photographic plate removed, developed and read (Richards, 1980 and Gray, 1994). Drilling was then resumed and based on the results of the survey corrections made to alter the trajectory of the borehole (Richards, 1980 and Gray, 1994). Although providing valuable information to improve control of borehole trajectory the survey process slowed drilling rate. Following the introduction of borehole survey using the Eastman single shot instrument the drilling rate at Appin Colliery reduced from 150-250 m/shift to 60-90 m/shift (Kelly, 1983).

The lateral position of some rotary drilled boreholes was found to have deviated from the planned trajectory by as much as 45^{O} (Hebblewhite *et al.*, 1982 and Thomson, 1998). When conducting surveys at a regular 10 to 20 m interval, using a single shot survey tool, in boreholes to a total length ranging between 400 and 600 m the horizontal

deviation was found to be within ±15^{O} of the planned trajectory (Hebblewhite *et al.*, 1983). Thomson (1998) suggests the interval between surveys during drilling and survey control had a significant impact on the accuracy of borehole placement relative to the planned trajectory.

3.2.2 Inseam Directional Drilling

Demand for increased productivity and safer mining conditions led to the pursuit of faster, cheaper and more accurate inseam drilling solutions (Thomson, 1998) leading to the replacement of rotary techniques by directional drilling for inseam degasification (Thomson and Adam, 2007). Downhole motor technology was first used in Australia in 1987 to directionally drill cross-measure longholes at Appin Colliery (Lunarzewski, 2001). Downhole motor drilling delivered improved control of borehole trajectory, typically achieving accuracy of ±1.0^{O} azimuth and ±0.5^{O} pitch when surveyed using the pump down single shot instruments (Brunner and Schwoebel, 2010 and Gleeson, 2010).

Directional drilling incorporates a downhole motor used in combination with a bent section of drill pipe, referred to as a bent sub, located behind the motor-bit assembly (Thomson, 2007). In Australia, the 'slide' method is used almost exclusively which involves pushing the drill string, without rotation, behind the rotating drill bit to advance the borehole (Thomson and Qzn, 2009). The vertical and horizontal trajectory of the borehole is controlled by adjusting the orientation of the bent sub. A side force developed between the bent sub housing and the borehole wall exerts a force on the drill bit to advance in the opposite direction, as shown in Figure 3.31 (Kravits and Schwoebel, 1994 and REI Drilling, 2004). Through regular adjustment of the bent sub orientation to control borehole trajectory the resulting borehole is not straight and more a series of subtle bends (Thomson and Qzn, 2009).

The bend angle of a typical bent sub assembly is 1.25^{O} which provides more rapid steering response than earlier designs that used a 1.0^{O} bend angle (Thomson, 1998). High pressure pumps are used to pump drilling fluid, which is typically water, into the borehole through the drill rods at a rate of 3 to 5 L/s and pressure ranging between 2 and 10 MPa (Gray, 1994; Thomson *et al.*, 2005 and Brunner *et al.*, 2008). The action of the high pressure water flowing through the stator-rotor drive unit of the downhole motor converts hydraulic horsepower into mechanical horsepower, providing rotational speed

and torque to the drill bit, without having to rotate the drill rods (Kravits and Schwoebel, 1994 and Kravits *et al.*, 1999). After passing through the downhole motor the water exits the drill rods through the drill bit and flows along the annulus of the borehole flushing drill cuttings from the borehole in the process.

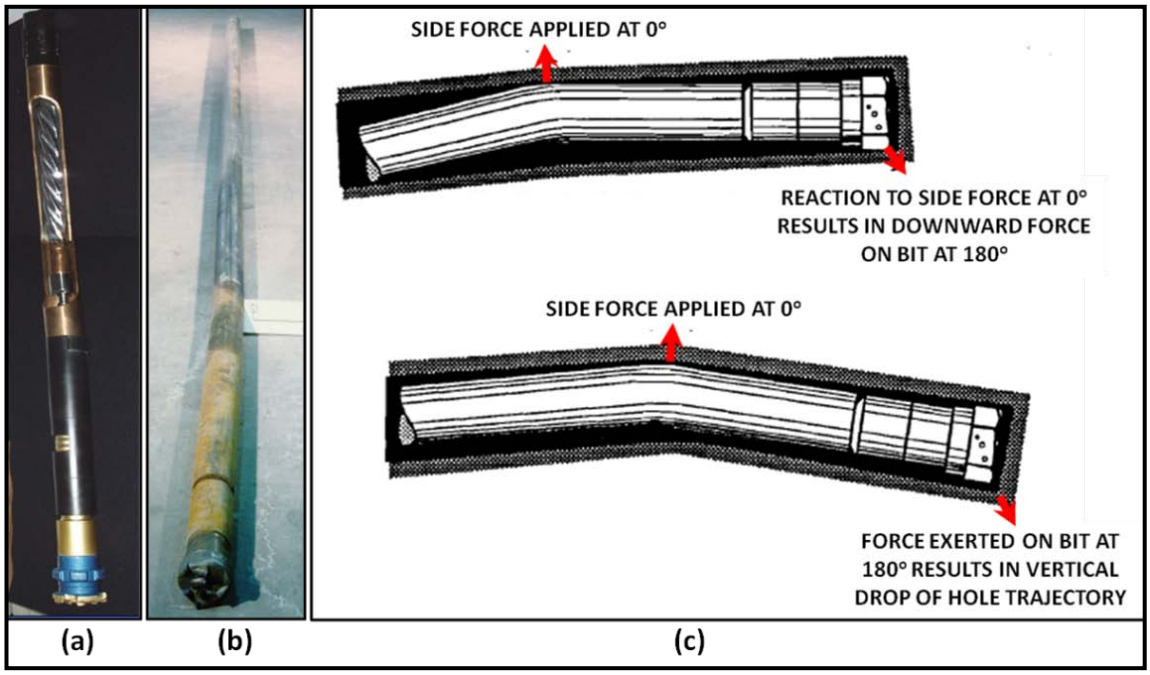

Figure 3.31: (a) Internal view of downhole motor (Brunner, 2005); (b) View of the angle of the bent sub (Hungerford, 2008); (c) Impact of bent sub orientation on borehole trajectory (after Kravits and Schwoebel, 1994)

Borehole inclination, bearing and tool face orientation are monitored using permissible survey tools. The inclination and bearing are used to calculate borehole elevation and coordinates from which the tool face orientation is adjusted to maintain the planned trajectory (Kravits and Schwoebel, 1994). The resulting path of the borehole is tortuous which is a significant factor limiting the length of inseam directionally drilled boreholes due to the increased frictional forces acting on the drill rods, as borehole length increases (Gray, 1994; Thomson, 2007 and Thomson and Qzn, 2009).

Directional drilling of horizontal boreholes in coal involves periodic contact with the roof and floor as a means of determining the position of the borehole within the coal seam (Kravits and Schwoebel, 1994; Kravits *et al.*, 1999 and Gray *et al.*, 2002). Once the roof or floor has been identified, typically by evidence of non-coal material observed in drill cuttings and changes in drilling parameters such as an increase in thrust, the downhole motor is pulled back into the coal seam and a branch, or sidetrack,

initiated to form a new section of borehole (Gray, 1994; Kravits and Schwoebel, 1994 and Kravits *et al.*, 1999). The tortuous path of the borehole created by frequent changes of tool face orientation is exacerbated by branching and periodic roof and floor touches which form multiple peaks and troughs along the length of the borehole. Figure 3.32 presents a section view of an inseam borehole at Myuna Colliery which highlights the extent of vertical deviation along the length of a typical directionally drilled borehole (Brunner *et al.*, 2008). The troughs formed along the borehole create points where water and fines may accumulate and impede gas drainage. This method of controlling boreholes trajectory is generally inefficient, with an estimated 20-30% of total drilling consumed by unplanned branches which also increase drilling time and complexity and create zones of weakness and possible borehole failure (Thomson *et al.*, 2005 and Thomson and Adam, 2007).

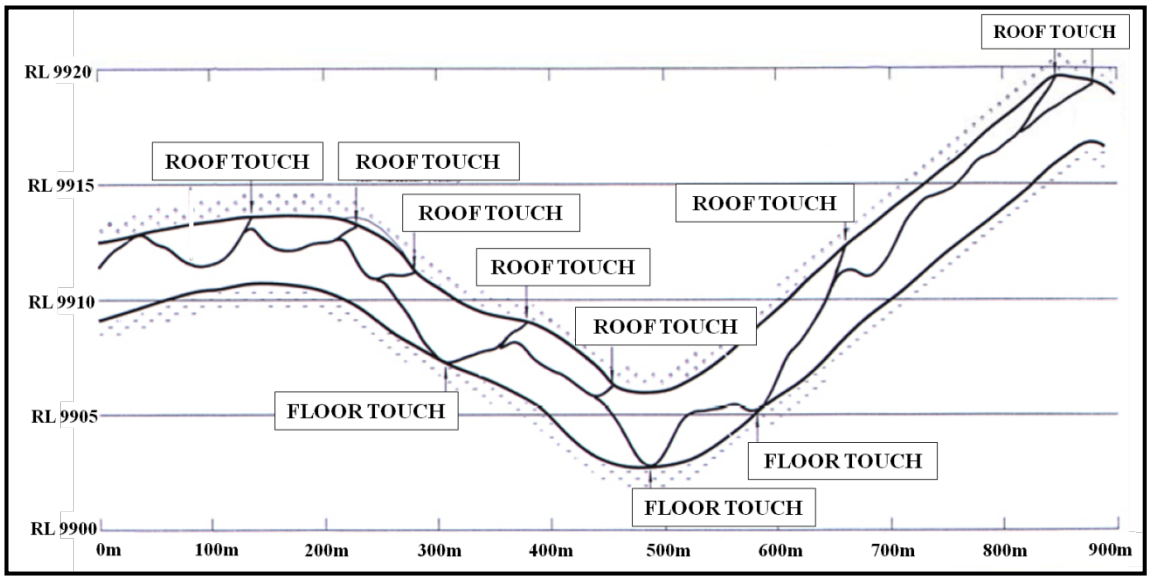

Figure 3.32: Profile of an inseam directionally drilled borehole (after Brunner *et al.*, 2008)

In the 1990's single shot camera survey systems and borehole pitch control stabilisers were replaced by advanced drilling systems comprising high thrust drilling rigs, high strength drill rods and connections, powerful downhole motors and real time electronic downhole survey tools (Thomson, 1998; Thomson *et al.*, 2005 and Brunner *et al.*, 2008).

The DDM-Mecca, developed by Advanced Mining Technologies (AMT), is the only real time electronic downhole survey system approved for use in Australian underground mines to improve control of inseam directional drilling (Thomson *et al.*,

2005). The DDM-Mecca (Directional Drill Monitor using Modular Electrical Connected Cable Assembly) when used in combination with AMT's Drill Guidance System (DGS) may be configured to provide numerical and full colour graphical display of drill rig operating parameters and borehole position and trajectory data acquired by the downhole survey unit (AMT, 2008). The explosion proof, watertight downhole survey unit incorporates a three-axis flux-gate magnetometer and three orthogonal accelerometers which measure the position of the unit relative to the earth's magnetic field and gravitational vector (Kravits *et al.*, 1999). The high resolution survey data is transmitted from the survey unit through the modular cable assembly (MECCA), which is internally fixed along the length of each drill rod and coupled automatically as drill rods are connected, to the up-hole control unit at high baud rates (Kravits, *et al.*, 1999; Monaghan *et al.*, 2003 and Gleeson, 2010). Surveys are typically conducted every three metres along the length of the borehole, as drill rods are added. Using navigational data obtained from the survey the drill rig operator may rotate the drill string to change the toolface orientation and hence drilling direction for the ensuing three metre drilling interval (Kravits *et al.*, 1999 and Monaghan *et al.*, 2003). The time required to collect, transmit, process and display survey data on the up-hole monitoring units is less than five seconds, regardless of borehole length, enabling faster and more accurate control of inseam directional drilling (Kravits *et al.*, 1999 and Monaghan *et al.*, 2003). The DDM-MECCA has improved the accuracy of inseam directional drilling enabling borehole trajectory to be maintained to within $\pm 0.5^{O}$ for azimuth and ± 0.1 to 0.25^{O} for inclination (Kravits *et al.*, 1999; ILN, 2000; Lunarzewski, 2001; AMT, 2008, Brunner *et al.*, 2008; Brunner and Schwoebel, 2010 and Gleeson, 2010).

The development of advanced inseam direction drilling systems delivered substantial increases in drilling rate, borehole length and trajectory control (Brunner et al., 2008) with boreholes greater than 1 500 m able to be drilled successfully (Thomson, 1998; ILN, 2000; Lunarzewski, 2001; Thomson *et al.*, 2007; Brunner *et al.*, 2008 and Thomson and Qzn, 2009). United States based company, Target Drilling Inc., reported an inseam drilling record in March 2008, completing a 1 695 m long directionally drilled gas drainage borehole at the Cumberland mine (Caudill, 2008).

The length of inseam directionally drilled boreholes is limited by the frictional drag forces developed along the length of the holes which must be overcome to advance the drill string (Gray, 2000 and Thomson and Qzn, 2009). Factors that impact the drag force

include borehole geometry, wall roughness, cuttings accumulation, annular pressure and total weight of the drill string (Thomson and Qzn, 2009). There is a limiting condition, known as 'lockup', which occurs when the frictional forces developed along the borehole exceed the axial force exerted by the drill rig leading to helical buckling of the drill pipe within the borehole (Gray, 1994 and Thomson and Qzn, 2009). The rate of change of borehole trajectory and the interval between changes in tool face angle have a dramatic impact on friction developed along a borehole and the thrust and pullout force required to drill and extract rods from the borehole (Gray, 1994). Where multiple bends exist along the length of a borehole the force required to pull the drill string from the borehole will be greater than the push force required during drilling (Gray, 1994). When advancing the drill string into the borehole the drill rods are pushed to the outer side of the bends whereas when recovering the drill string the rods are pulled against the inside of the bends whereby increased friction is developed (Gray, 1994). In such cases it may not be possible to recover the drill string from the borehole making it necessary to abandon the downhole equipment in-hole (Gray, 1994).

During slide drilling, cuttings fall to the bottom of the borehole forming a bed. The cuttings, along with any additional broken coal from weak zones encountered during drilling, accumulate along the length of the length of the borehole increasing the contact surface area and hence friction developed between the drill rods and the borehole (Thomson and Adam, 2007). In cases where the annular pressure exceeds the formation pressure the differential pressure may push the drill string against the side of the borehole further increasing the friction developed during slide drilling (Thomson and Adam, 2007). Excessive friction may lead to a condition known as 'differential sticking' possibly resulting in the drill string being temporarily stuck in the borehole or complete loss of the downhole equipment (Thomson and Adam, 2007). Figure 3.33 illustrates the presence of drill cuttings and high annular pressure acting on the drill pipe that lead to differential sticking during slide drilling (Thomson, 2009).

The standard method for directional drilling used outside of the Australian underground mining industry utilises a 'rotary-slide' technique which produces a smoother borehole with fewer, less dramatic bends (Gray, 1994 and Thomson and Qzn, 2009). The rotary-slide method involves rotating the drill rods at a relatively slow rate, in the order of 80 rpm (Gray, 1994), reverting to slide-only drilling subsequent to changing tool face orientation to set the drilling orientation into the altered trajectory (Thomson and Adam,

2007 and Thomson and Qzn, 2009). In addition to producing straighter boreholes requiring fewer changes to tool face orientation, the rotation of the drill rods reduces the contact surface area and the friction developed between the drill rods and the borehole (Thomson and Adam, 2007). A direct comparison was made between the rotary-slide and slide-only methods drilling parallel longholes in the same coal seam using the same drilling equipment which demonstrated rotary-slide drilling produced significantly longer boreholes than slide-only drilling, with markedly reduced bend rates (Thomson and Qzn, 2009).

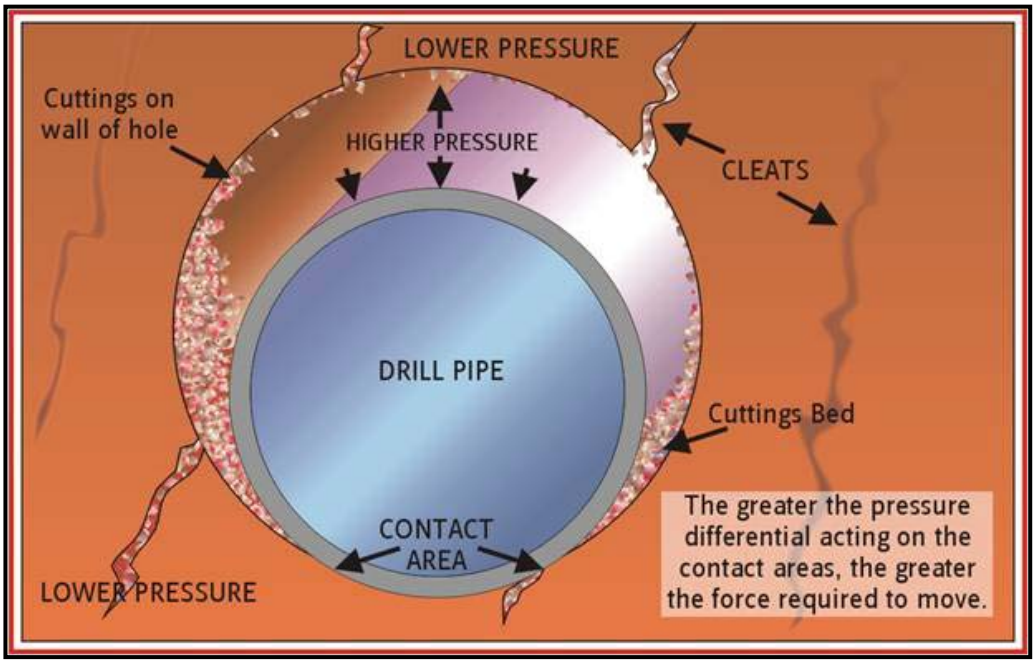

Figure 3.33: Effect of drill cuttings and annular pressure to increase drag forces leading to differential sticking of the drill string (Thomson, 2009)

Inseam directional drilling, under normal conditions, is ‘underbalanced’, whereby formation pressure exceeds the annular pressure of the circulating drilling fluid (Thomson and Qzn, 2009). The higher pressure of the formation in the underbalanced condition creates a pressure differential resulting in the flow of water and gas from the coal seam into the borehole (Thomson and Qzn, 2009). In underbalanced drilling, particularly where the pressure differential is high and when negotiating zones of weak coal and geological structures, the risk of the borehole collapsing around the drill string is increased. Rapid build-up of material within the borehole may disrupt fluid circulation causing increased annular pressure potentially causing differential sticking, mechanical jamming and borehole failure (Thomson and Qzn, 2009).

Where annular pressure exceeds formation pressure an ‘overbalanced’ condition is created (Thomson and Qzn, 2009). In an overbalanced condition the higher pressure of the borehole annulus forces drilling fluids and fines into the cleat and pores of the surrounding coal seam forming a ‘skin’ around the wall of the borehole which adversely impacts future gas drainage (Thomson and Qzn, 2009). Where the rate of fluid loss into the surrounding coal seam is high the velocity of drill fluid circulating in the borehole may be insufficient to effectively clear cuttings from the borehole potentially leading to increased friction and bogging of the drill string (Thomson and Adam, 2007). Figure 3.34 illustrates the nature of fluid and gas flow in underbalanced and overbalanced conditions associated with a localised failure within the borehole (Thomson, 2009).

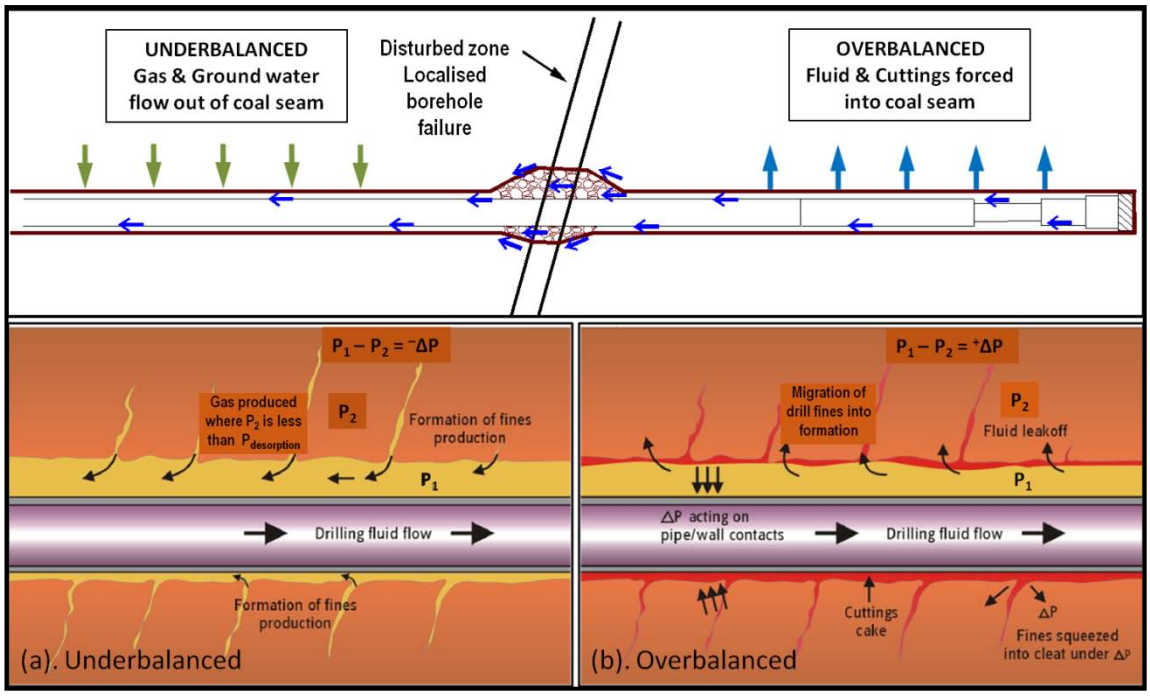

Figure 3.34: Effect of overbalanced and underbalanced drilling conditions (Thomson, 2009)

Drill patterns employed in coal mine gas drainage typically involve inseam boreholes drilled from exposed roadways, across blocks, to drain gas ahead of future mine development. The angle and spacing between boreholes is determined based on empirical data related to coal seam permeability, available drainage time, gas content and past experience (Thomson, 1998). The decision on which drill pattern to use is often based on available access for the drill rig, logistics and efficiencies associated with relocation and site establishment (Thomson, 1998). As shown in Figure 3.35 drill patterns may involve a regular pattern of parallel boreholes, each drilled from a separate site and requiring the drill rig to be repositioned to drill each borehole (Type A),

separate boreholes drilled in a fan pattern from a common drill site (Type B), multiple branches drilled from a common parent borehole (Type C), long boreholes drilled parallel to future mine development panels (Type D), and long exploration boreholes (Type E) (Thomson, 1998). When using long boreholes, such as in Type D, allowance should be made in the mine design and production schedule for increased drainage time, providing an opportunity to drain more gas and offset the increased drilling time and cost.

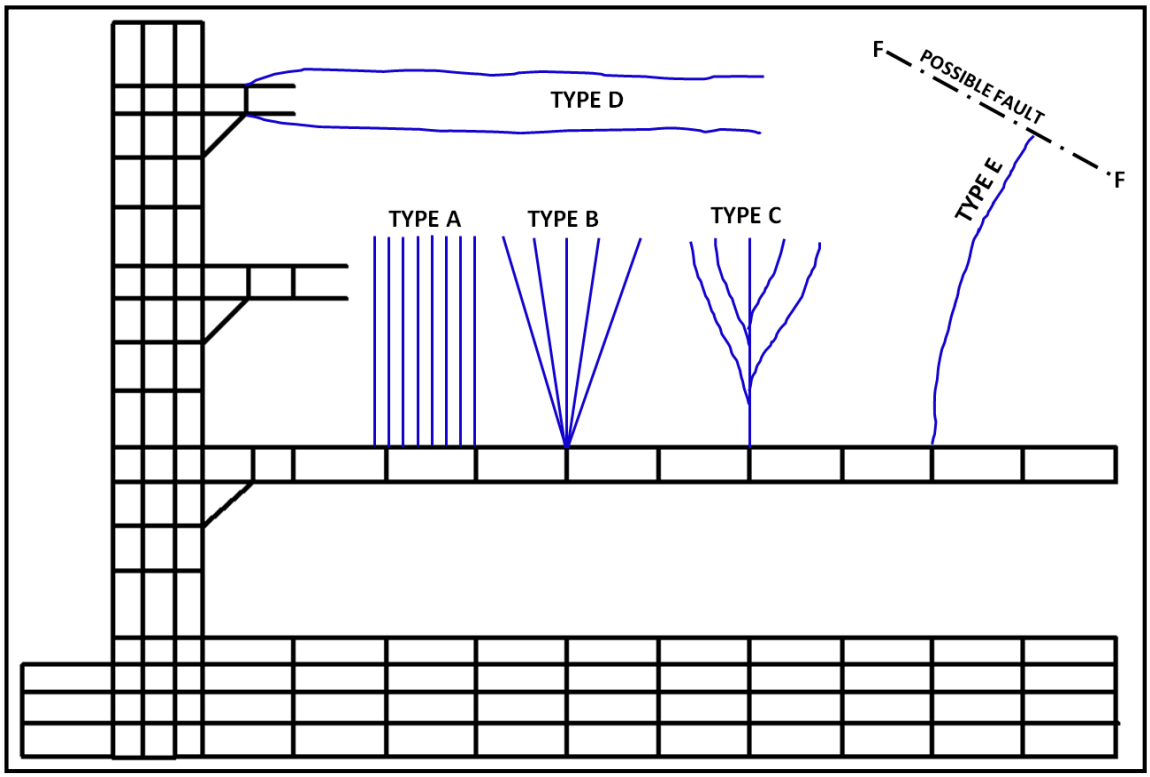

Figure 3.35: Inseam drilling patterns available for coal seam gas drainage (after Thomson, 1998)

3.2.3 Actions to Improve Directional Drilling Capability

Thomson and Qzn (2009) list a variety of weaknesses associated with current inseam drilling practice that include:

- Lack of balance control;
- Limited logging and geosteering capability;
- High risk of bogging and losing drill string downhole;
- Limited use of 'well completion' techniques to optimise seam gas drainage; and
- Continuing safety issues associated with manual drill rod handling.

Adapting available technology for use in an underground coal environment has the potential to address many of the weaknesses listed above to improve the efficiency and effectiveness of inseam directional drilling. Details relating to the geology encountered along the length of the boreholes may also be gathered during or subsequent to the completion of drilling to assist mine planning and aid in identifying potential outburst risk zones.

The use of sensors to monitor torque and thrust, annular pressure and the position of the borehole within the seam, relative to roof and floor, has the potential to improve control and performance of inseam directional drilling systems. Sensors can also detect geological structures encountered along the length of the borehole (Murray *et al.*, 1999). Enhanced drilling systems offer increased control of borehole trajectory with the potential to produce boreholes which are less tortuous, reducing the time and drilling effort presently consumed by branching and regular roof and floor intersections. However merely having advanced systems is no guarantee of success and skilled engineers will be required to generate improved drilling plans taking into account the additional data collected during prior drilling in the area.

The development of semi-automated drilling control systems capable of continuously monitoring and analysing sensors and automatically adjusting thrust, rotation and tool face orientation would enable skilled drill rig operators to maintain optimum drilling performance and produce boreholes with minimal deviation from planned trajectory.

Improving the capabilities of inseam directional drilling has been the focus of numerous research projects spanning more than 15 years. Many promising technologies have been identified and developed, some even being redeveloped, at significant cost. However in the majority of cases the identified technologies have failed to develop and become adopted by industry as standard components of advanced inseam directional drilling systems. It is possible that the potentially damaging effects on gas drainage resulting from current drilling methods, which have experienced little change since being introduced in the mid-1990’s, are not well understood by mine personnel. Unless mining companies demand improved drilling systems and operational controls from drilling contractors it is likely the status quo will continue (Thomson and Qzn, 2009).

3.2.3.1 Torque / Thrust Sensors

The measurement of torque and thrust at the drive motor and across the downhole assembly delivers valuable information relating to weight-on-bit and the level of drag force being experienced by the drill string. Thrust applied to the drill rods by the drill rig which is not transferred to the downhole assembly is consumed by friction along the length of the drill string. Increased friction may be the result of contact rubbing of the drill road against the borehole wall, exacerbated by snaking along the length of the borehole, and a build-up of fines along the borehole. Advanced warning of deteriorating in-hole conditions enables the drill rig operator to take remedial action such as flushing and rotation of the drill string to clear fines and reassess in-hole conditions prior to reaching lock-up. Torque and thrust sensors were first developed for inseam drilling in 1997 under ACARP project C3073 (Gray, 1997) and later tested in 2002 under ACARP project C7023 (Gray *et al.*, 2002). In 2007, prototype instrumentation was developed to monitor torque/thrust sensors located at the borehole collar under an ACARP sponsored project, C14034 (Thomson and Adam, 2007).

3.2.3.2 Annular Pressure Sensors

Measurement of annular pressure within the borehole provides useful information to determine whether drilling is underbalanced, balanced or overbalanced. Where a high differential exists between annular pressure and formation pressure the borehole and surrounding coal may be damaged, affecting drilling performance and future gas drainage. Indication of increasing annular pressure may indicate fines accumulation allowing the drill rig operator to take corrective measures prior to reaching a borehole blocked and lock-up situation.

The torque and thrust sub designed as part of ACARP project C3073 (Gray, 1997) included a pressure transducer which enabled the differential pressure across the sub to be measured (Gray *et al.*, 2002). A separate pressure logging sub, referred to as a ‘P Logger’, was developed as part of a later ACARP sponsored project, C14034, in 2007 (Thomson and Adam, 2007). These systems add to the many real-time pressure logging systems presently being used in oilfield and CBM drilling equipment (Thomson and Adam, 2007).

3.2.3.3 Coal Interface Detection

In order to drill longer boreholes with reduced risk of a lock-up condition developing drag forces must be reduced. This may be achieved by drilling boreholes that are much straighter than are able to be achieved using current drilling and steering practices, whilst minimising deviation from the planned trajectory. Boreholes must be drilled with fewer, less dramatic changes in orientation, and the reliance on regular roof and floor contact to determine the vertical position of the borehole within the coal seam should be eliminated.

A variety of technologies with potential application in coal interface detection (CID), such as natural gamma, focussed gamma, density, dielectric logging and radar logging were tested by Thomson *et al.* (2005) from which gamma and density tools delivered the best results. The results from dielectric tools testing were considered to be encouraging while radar did not produce convincing results and was not considered suitable for use in CID tools in its current form (Thomson *et al.*, 2005). Although recognising the potential of such devices as a means of improving inseam directional drilling capability a significant issue to be addressed is developing the systems to be intrinsically safe (Hatherly *et al.*, 1996; Gray *et al.*, 2002; Thomson *et al.*, 2005 and Thomson and Adam, 2007).

3.3 DRAINAGE OF COAL SEAM GAS FROM SURFACE

A variety of surface-based drilling methods are now available for drilling boreholes to connect to one or more coal seams to support gas drainage ahead of coal extraction. Early surface to seam coal seam gas drainage was achieved using vertical drilling to intersect and drain gas from one or more coal seams. Unless intersecting highly permeable coal seams the rate of gas production from vertical wells was generally low requiring the use of stimulation treatments to enhance gas production. Advances in drilling equipment and directional drilling capabilities led to the development of radius drilling, a method of drilling inseam boreholes from a surface-based drilling rig. Radius drilling enables a borehole to be extended inseam to achieve greater contact with the coal seam gas reservoir and increasing the potential to drain more gas than could be drained using a vertical borehole. Figure 3.36 illustrates the output from gas reservoir modelling, showing the impact on coal seam gas content reduction from the use of vertical wells, short SIS wells and long SIS wells (Thomson, 2007).

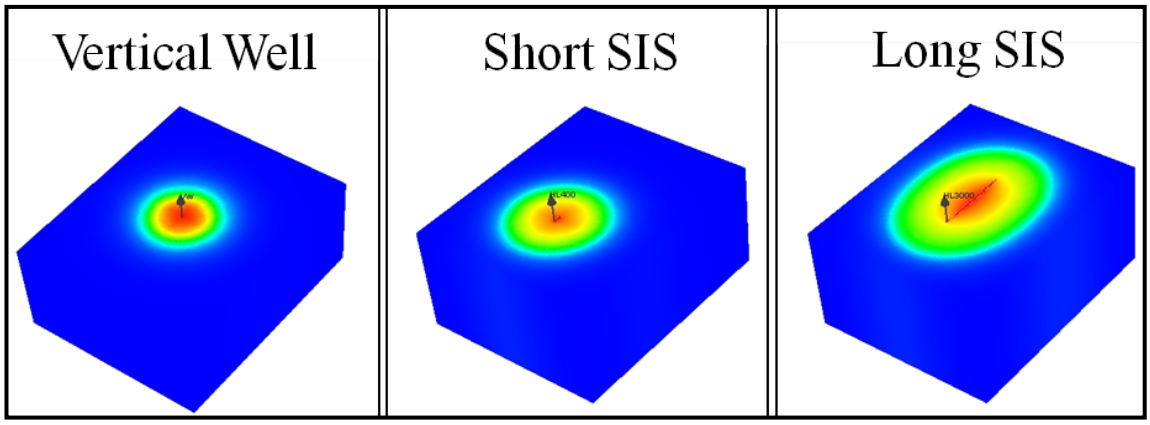

Figure 3.36: Reservoir model output comparing gas content reduction from vertical and SIS boreholes (after Thomson, 2007)

3.3.1 Vertical Drilling

Vertical gas drainage wells are drilled from the surface to penetrate one or more coal seams. Dewatering the borehole causes a pressure drop in the coal seam which leads to gas migration toward the well (Kahil and Masszi, 1982). For a vertical drainage well system to be considered successful each well should produce a large volume of gas which generally requires a long drainage time, typically greater than ten years, to produce sufficient gas for the well to be considered economic in its own right (Kahill and Masszi, 1982). Vertical wells alone, without some form of stimulation treatment such as hydraulic fracturing, seldom produce measurable amounts of gas (Osisanya and Schaffitzel, 1996; Thomson *et al.*, 2003 and Kissell, 2006).

Gas drainage through vertical wells is commonly used in the United States coalbed methane industry however application in Australia has failed to deliver the gas production levels achieved in many gas fields within the United States (Humphries et al., 2006). A number of limitations, listed below, contribute to the limited use of vertical wells for coal seam pre-drainage in the mining industry (Creedy *et al.*, 1997; Wight, 2005 and Meszaros *et al.*, 2007).

- High drilling cost to access deep coal seams;
- Long drainage time required;
- Drilling locations must be coordinated with the long term mine plan;
- Poor response to changes in mine plan at short notice;
- Non-uniform drainage of the coal seam;
- High well density required;

- High surface impact during drilling and gas production;
- Coal seams must have high natural fracture permeability; and
- Reduced permeability in deep coal seams.

Figure 3.37 illustrates the surface impact and high borehole density required to conduct a vertical coal seam gas drainage drilling program (Wight, 2005).

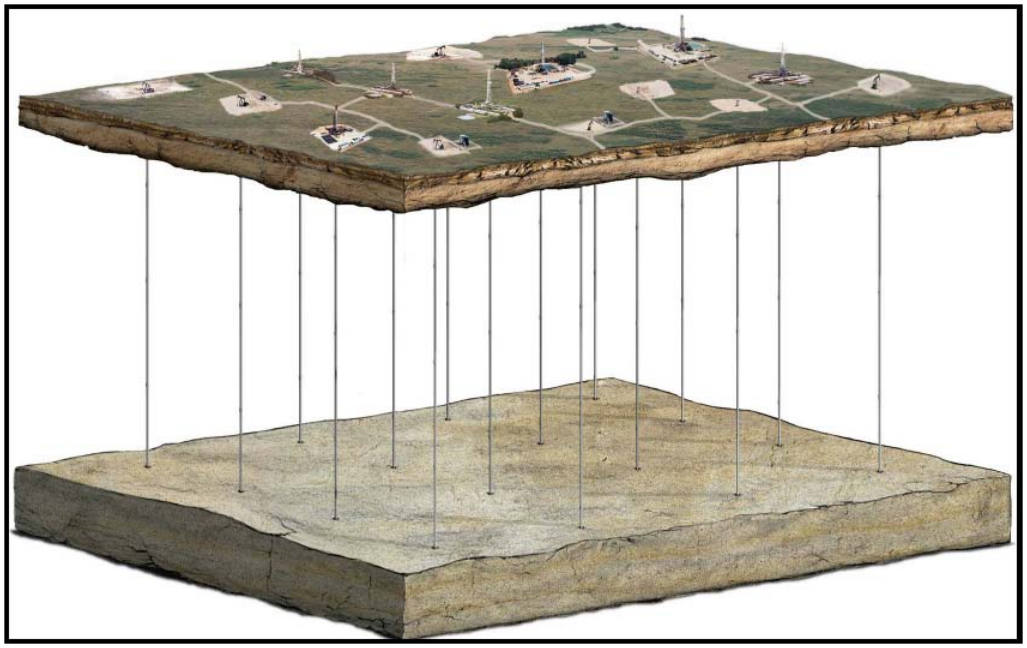

Figure 3.37: Illustration of coal seam gas drainage using vertical boreholes (Wight, 2005)

3.3.2 Radius Drilling

Radius drilling is an alternative method used to drill boreholes for coal seam gas drainage. Subject to the design of the drilling equipment, a borehole initially drilled vertically from the surface is steered through a given radius to intersect the target coal seam horizontally after which drilling continues inseam to the design length. The categories of radius drilling are illustrated in Figure 3.38.

The most common type of radius drilling, medium radius drilling (MRD), was introduced to Australia in the mid-1990's and by the end of that decade had been adapted for use in coal mining applications for strategic long term coal seam pre-drainage (Thomson and MacDonald, 2003). In Australia, the radius of MRD wells varies between 250 to 430 m (Thomson *et al.*, 2003 and Humphries *et al.*, 2006).

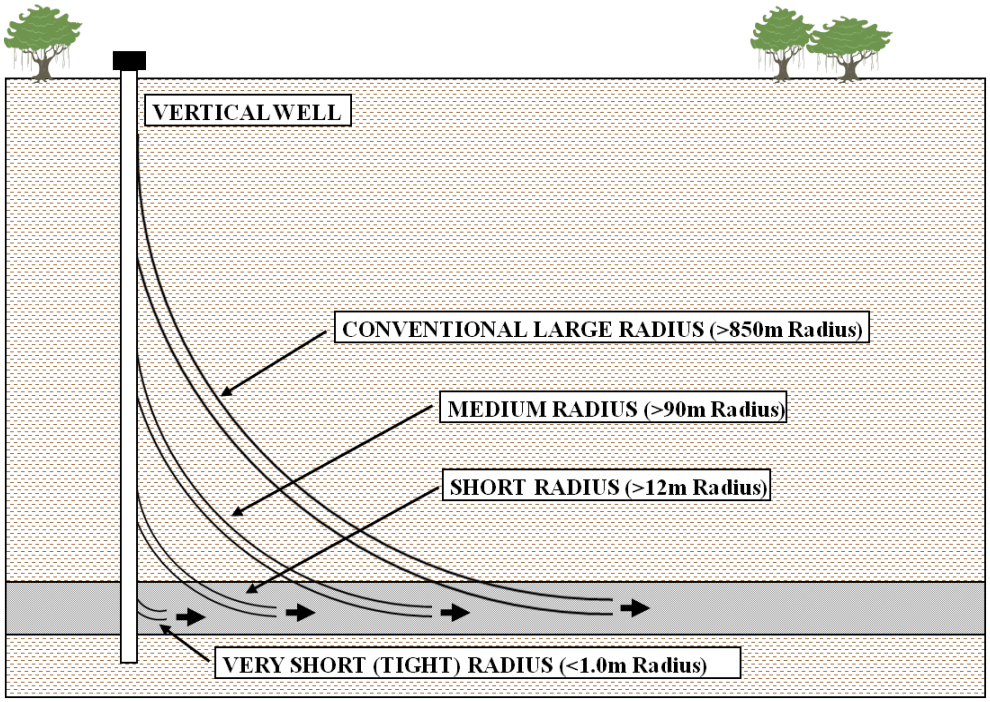

Figure 3.38: Categories of radius drilling (after Logan *et al.*, 1987)

Radius drilled horizontal gas drainage borehole are reported to have several advantages over fracture-stimulated vertical wells (Osisanya and Schaffitzel, 1996; Cameron *et al.*, 2007 and Meszaroz *et al.*, 2007), which include:

- increased coal seam contact, with the potential length of inseam section extending beyond 2 500 m, subject to drill rig capacity, depth of cover and coal seam conditions;
- reduced surface impact and disturbance, requiring fewer surface installations; and
- ability to vary borehole orientation relative to (a) the horizontal stress field to provide maximum wellbore stability, (b) the natural fracture systems within the coal seam to benefit from directional permeability, and (c) the natural dip of the seam to facilitate dewatering.

Cameron *et al.* (2007) and Meszaroz *et al.* (2007) report several disadvantages associated with MRD wells, which include:

- Increased cost compared to fracture stimulated vertical wells;
- Where drainage from multiple coal seams is required, additional drilling on multiple horizons is required which increases total drilling cost;
- Borehole stability can become an issue, particularly in weaker coal, resulting in localised failure during drilling and completion; and

- Dewatering of the inseam section may be required where troughs are present along the inseam section allowing water to accumulate.

The cost of drilling and producing from an MRD well was reported to be in the order of three times the cost of a hydraulically fractured vertical well (Cameron *et al.*, 2007 and Roy, 2008). In a comparison of the two drilling and completion methods in the United States, Cameron *et al.* (2007) reported the peak gas production rate from horizontal wells was up to ten times that from average vertical wells with the average rate being four to five times greater. Early development of MRD wells in the Bulli seam at a depth of 650 m below surface, with an 1 800 m inseam section were reported to be producing at three times the rate of hydraulically fractured vertical wells in the same field (Roy, 2008).

Drilling inseam boreholes from the surface using MRD technology offers significant advantages over existing UIS drilling systems (Gray, 2000). Additives to drilling fluids used in MRD drilling, in conjunction with downhole pressure sensors, allow the pressure within the borehole and the coal seam to be balanced and controlled throughout the drilling phase to avoid the potentially damaging effects of out-of-balance drilling. MRD drilling systems also offer increased control of borehole trajectory to place boreholes within a target drilling horizon. Boreholes with reduced tortuosity and dogleg severity enable increased borehole length to be achieved using existing drilling equipment due to reduced frictional forces developed along the length of the borehole (Meszaroz *et al.*, 2007). Increased control of borehole trajectory is achieved through the use of measure-while-drilling (MWD) and logging-while-drilling (LWD) systems in conjunction with geo-steering software and geo-steering specialists. Many different sensors may be incorporated into MWD and LWD systems to monitor and record drilling performance and geological information, however it is the at-bit gamma ray and dynamic inclination sensors that provide the data necessary to determine borehole position within the coal seam, relative to roof and floor units, from which adjustments can be made to maintain planned borehole trajectory (Meszaroz *et al.*, 2007 and Palmer, 2008).

3.4 MANAGEMENT OF BOREHOLE STABILITY

The stability of coal seam gas drainage boreholes is a particularly significant issue that must be considered and adequately managed during both the drilling and production phases. Creedy *et al.* (1997) suggest the strength of the material being drilled is the most important factor controlling borehole stability as lower strength materials are more likely to fail, particularly those affected by water. The magnitude and orientation of the stress field relative to the borehole can also have a significant impact on resulting stability. Figure 3.39 illustrates the effect of excessive vertical and horizontal stress experienced by a borehole and the resulting stress induced failure (break-out).

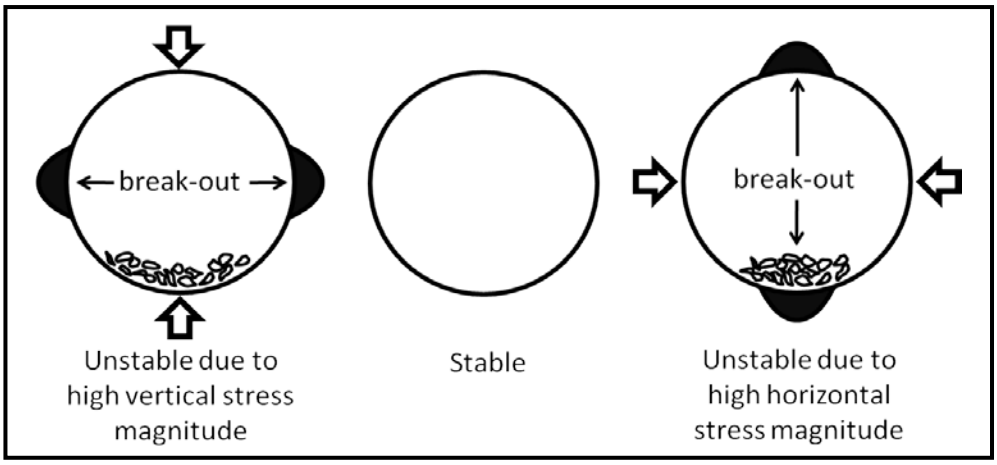

Figure 3.39: Impact of vertical and horizontal stress on borehole stability (after Brown *et al.*, 1996)

Where weak and unstable coal zones exist, a number of potentially serious outcomes may result during and subsequent to drilling (Lama, 1995b), which include:

- Inability to continue drilling to reach target distance preventing gas drainage from the coal beyond the failed zone;
- Inability to clear fines and failed material from the borehole leading to loss of drilling equipment down-hole, which is not only expensive to replace but may also cause problems when mining through the area;
- Accumulation of broken material in a borehole restricts gas flow and reduces gas drainage effectiveness from the coal ahead of the failed zone; and
- Where failed material causes a blockage in the borehole gas pressure may build up in the borehole beyond the failed zone. When mining close to or intersecting the pressurised section of borehole a sudden ejection of explosive gas and coal may occur.

Where potentially unstable conditions exist, a number of techniques may be used to assist in maintaining borehole integrity including grouting and re-drilling, use of slotted casing and borehole liners and the use of special drilling fluids (Creedy *et al.*, 1997 and Palmer, 2008). Avoiding drilling through weak and potentially unstable zones is an alternative technique which involves drilling into the roof and extending the borehole out-of-seam and then re-entering the coal seam on the other side of the potentially unstable area after which drilling continues until the target distance is reached.

Where grout is used to treat unstable coal, or special drilling fluids used to pressurise the borehole to maintain stability during drilling, the permeability of the coal surrounding the borehole and future gas drainage performance is likely to be adversely impacted (Creedy *et al.*, 1997).

Bell and Jones (1989) suggest the pressure in the borehole is a critical factor that must be well understood and appropriately managed during drilling in order to prevent wellbore failure. The management of downhole pressure is commonplace in MRD drilling to avoid permeability damage from over-balance drilling or borehole failure from under-balanced drilling (Humphries *et al.*, 2006). Controlling the downhole pressure during drilling can also assist in the management of differential sticking, fluid loss into the formation, weight transfer and cuttings removal (Thomson and Adam, 2007).

Existing UIS drilling systems typically do not monitor downhole pressure and do not utilise any form of pressure control. The lack of monitoring and control of downhole pressure may result in significant pressure changes during drilling from over-balanced to under-balanced conditions with long term damaging effect on gas production potential and borehole stability. Gray (1998) developed a borehole pressurisation tool, for use in conjunction with UIS drilling systems, reported to enable pressure control during drilling however this tool was never trialled in UIS drilling and did not progress beyond an initial prototype.

3.5 GAS DRAINAGE ENHANCEMENT

A variety of methods are available to enhance gas production from standard vertical and radius drilled boreholes. These methods include under-reamed cavity completion, open-

hole cavity completion, hydraulic fracturing, drilling of multiple lateral branches from a main borehole, and inert gas injection.

Figure 3.40 illustrates the various enhancement methods, with the exception of inert gas injection, ranked according to cost and applicability to varying coal seam permeability conditions (Loftin, 2009 and Johnson, 2010).

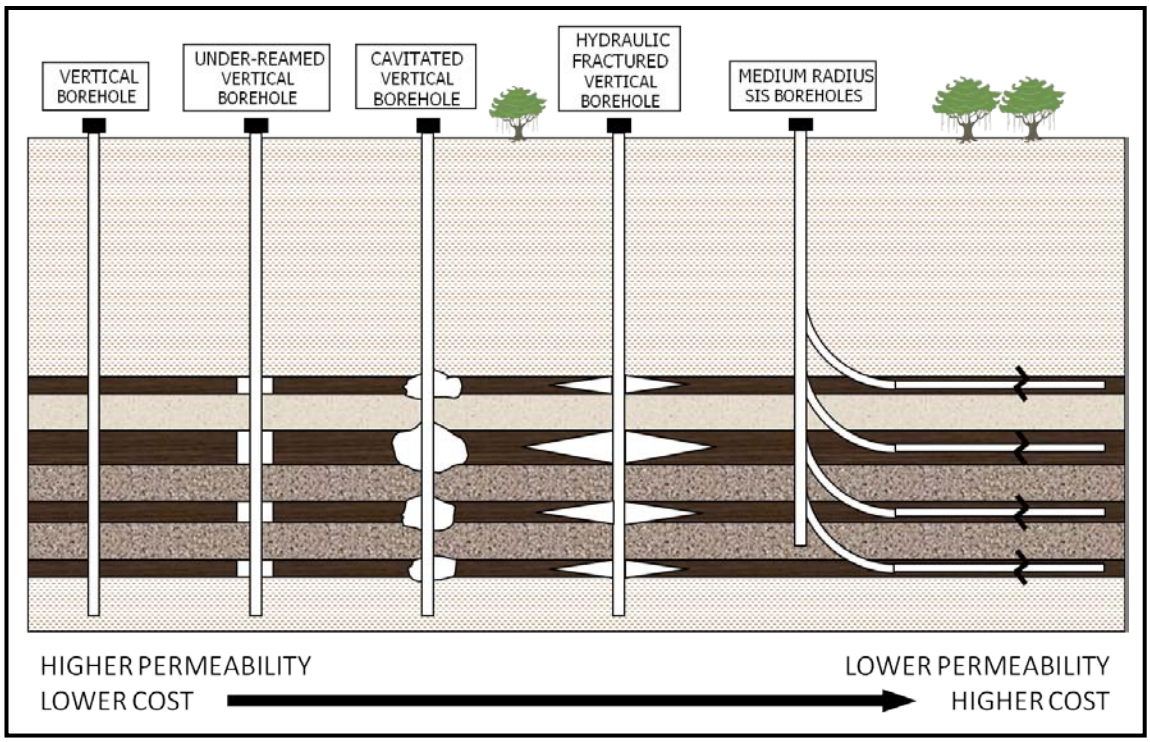

Figure 3.40: Gas drainage enhancement methods ranked according to cost and application relative to coal seam permeability (after Loftin, 2009 and Johnson, 2010)

The success of a particular completion in one coal seam is no guarantee of success in another coal seam therefore it is important that when considering completion methods in a new area that prevailing operational and geological conditions are understood and the selected completion method is adapted to the new environment (Johnson *et al.*, 2006).

3.5.1 Under-Reaming

Under-reaming involves inserting a special reaming tool, typically with three arms which are deployed using drill fluid pressure once the tool is in position in the borehole. The tool is rotated to increase the diameter of the borehole equivalent to the fully deployed diameter of the cutting arms. Upon completion of the cavity the fluid pressure is reduced and the cutting arms retract into the tool (USEPA, 2009). The reaming tool

may then be repositioned to ream a cavity in a separate seam or removed from the borehole. Following under-reaming, slotted casing may be inserted across the coal seam section and the cavity packed with gravel to keep the cavity open (USEPA, 2009).

Reaming tools are available in a variety of designs, each suited for use in specific applications and conditions. The United States based Harvest Tool Company offer jet, rotor and cavity reaming tools in a range of sizes. Figure 3.41 shows a cavity reaming tool manufactured by the Harvest Tool Company in the closed and open positions.

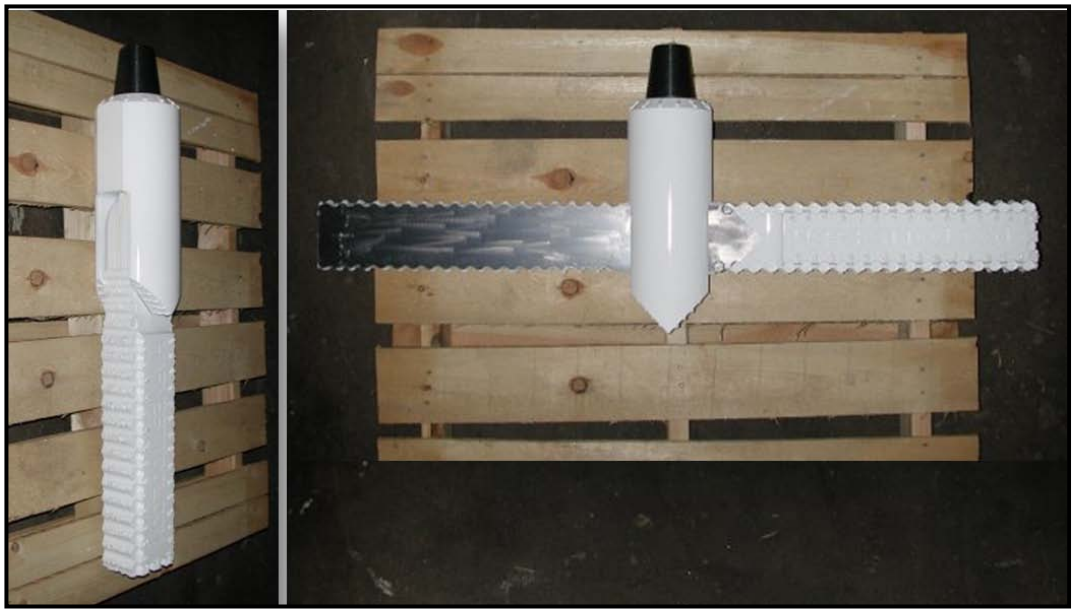

Figure 3.41: Cavity reaming tool in Closed and Open position (Harvest Tool Company, 2010)

Under-reaming is commonly used in CBM projects in the Powder River Basin, United States and in the high permeability coal seams in the Surat Basin, Australia (USEPA, 2009). Figure 3.42 illustrates a typical under-reamed vertical borehole completion used by Arrow Energy in the Surat Basin (Arrow Energy, 2008).

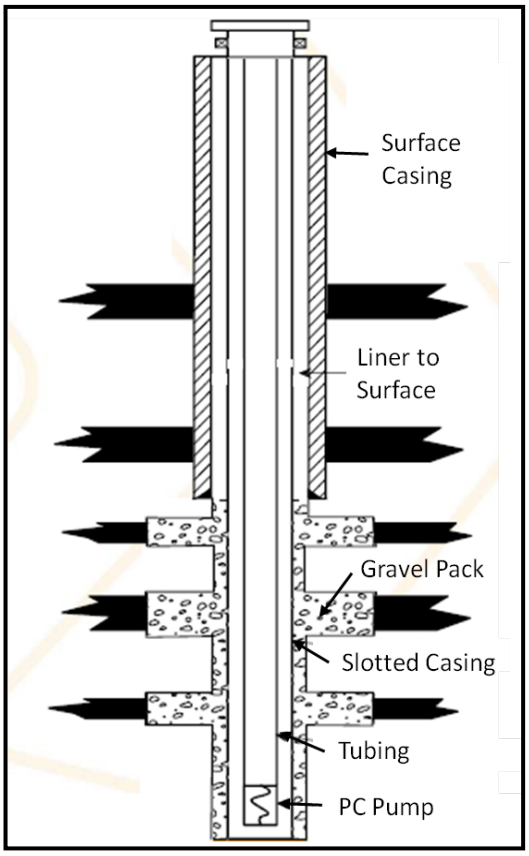

Figure 3.42: Under-reamed vertical gas drainage borehole completion used in the Surat Basin (Arrow Energy, 2008)

3.5.2 Open Hole Cavity Completion

Open hole cavity completion involves creating a cavity in the coal seam sufficiently large enough to remove any coal in contact with the borehole that may have been damaged during the drilling process (Mavor and Logan, 1994). In addition the surface area of the borehole in contact with the natural fracture network of the coal seam is increased (Mavor and Logan, 1994).

Cavities are typically formed through a series of surging events each involving shutting-in the borehole to build up pressure in the coal seam, either by seam gas pressure or by injection of a compressed air or air/water mix, followed by the rapid release of the pressure (Logan *et al.*, 1989 and Mavor, 1994). The rapid depressurisation causes the coal to fracture and slough into the borehole. Broken coal material and groundwater is removed from the borehole using air and/or foam circulating at a high rate (Logan *et al.*, 1989 and Mavor, 1994). Surging continues until the amount of coal recovered from the borehole subsides (Logan *et al.*, 1989 and Mavor, 1994). A perforated liner may then be installed across the open hole interval to protect the borehole from further coal

sloughing that may occur during production. Logan *et al.* (1989) recommend maintaining back pressure on the well during production as a control to reduce the flow of fines into the borehole.

(Mavor *et al.*, 1992 and Mavor, 1994) suggest open hole cavity completion is the preferred method for enhancing gas production from coal seams with moderate permeability such as the coal seams in the Fruitland formation of the San Juan basin, as the cavity completed boreholes often produced gas and water at a significantly greater rate than hydraulically fractured vertical wells in similar geological settings.

3.5.3 Secondary Lateral Drilling

Secondary lateral drilling involves drilling multiple branches from the primary lateral of a horizontal inseam directionally drilled borehole. Drilling secondary laterals effectively increases borehole density and contact with the coal seam gas reservoir to increase total gas extraction potential whilst reducing the number of surface installations required.

Figure 3.43 illustrates a dual seam completion using the quad Z-pinnate pattern developed by CDX Gas which covers an area of 1 280 acres, replacing 16 conventional vertical boreholes at the Pinnacle operations in West Virginia, United States (Wight, 2005).

In addition to having a small surface footprint, Palmer (2008) suggests horizontal drilling, and the use of secondary lateral drilling such as the pinnate pattern, is well suited to gas drainage applications in low permeability, medium thickness coal seams with no geological structures.

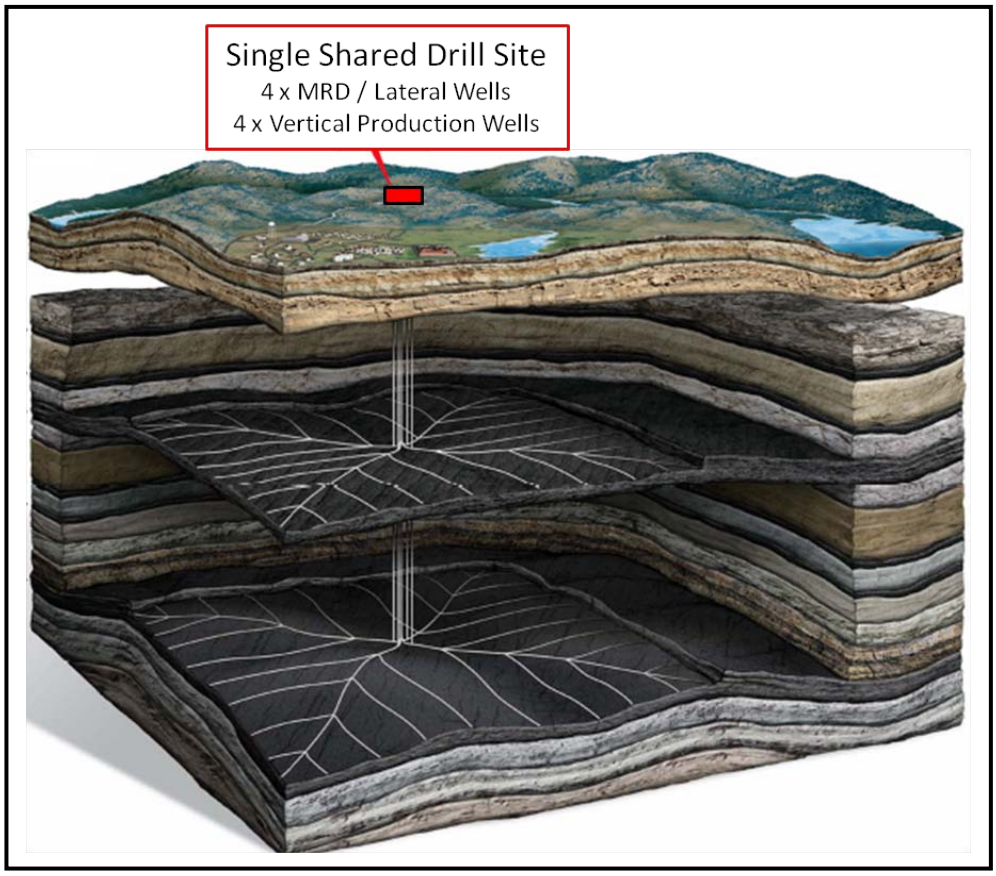

Figure 3.43: Dual seam quad z-pinnate pattern developed by CDX Gas (Wight, 2005)

3.5.5 Hydraulic Fracturing

Hydraulic fracturing involves injecting a suitable fluid or gas at a high rate into a coal seam at a pressure exceeding the minimum *in situ* stress to initiate and propagate a fracture (Kahil and Masszi, 1982 and Stewart and Barro, 1982).

Hydraulic fracturing in a coal seam attempts to (a) bypass any formation damage caused during drilling that would restrict gas flow to the borehole, (b) increase the connection between the borehole and the natural fracture system of the coal seam gas reservoir to stimulate production and accelerate dewatering, and (c) distribute the pressure drawdown over an increased area to reduce fines production (Logan *et al.*, 1989 and Zahid *et al.*, 2007).

The design and execution of an effective hydraulic fracture stimulation program is a complex process. In addition to selecting suitable injection fluid(s) and proppant material type, size and loading schedule, the potentially adverse impacts of high injection pressures, complex fracture systems, screen-outs, and the production of proppant and coal fines post-treatment must also be considered (Holditch *et al.*, 1988).

A number of primary reservoir properties that impact coal seam gas production should also be considered when designing a hydraulic fracturing treatment, such as adsorbed gas content, desorption characteristics, size of area to be drained, reservoir pressure, permeability, pore volume, water saturation of the cleat system and the mechanical properties of the coal (Holditch *et al.*, 1988).

A variety of gases, liquids and gels may be used as injection fluids in hydraulic fracturing (Mavor *et al.*, 1992; Zahid *et al.*, 2007 and Palmer, 2008). Polymers, surfactants, biocides, friction reducers and other chemicals may also be added to injection fluids (Puri *et al.*, 1991). Figure 3.44 lists a variety of injection fluids, ranked in order of increasing proppant carrying capacity and increasing risk of permeability damage and gel residue deposition within the coal structure following injection (Palmer, 2008).

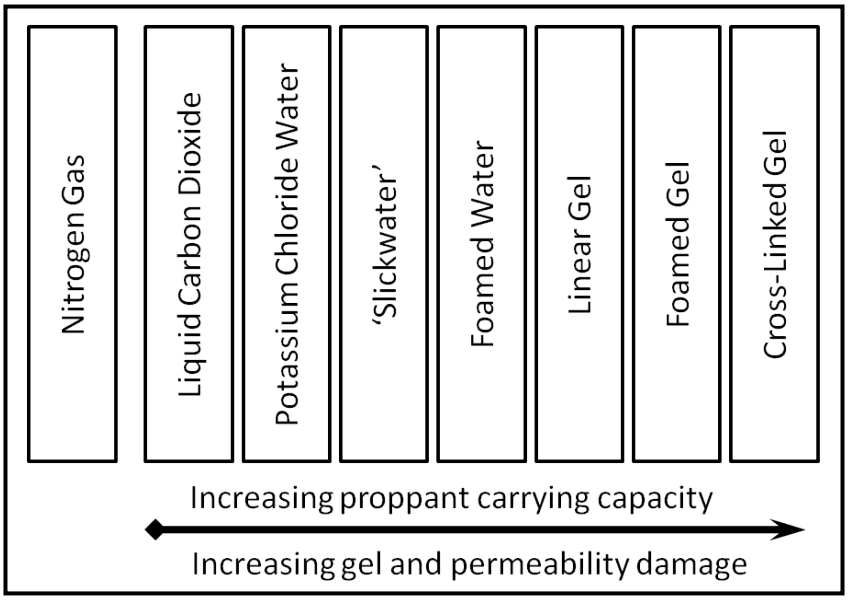

Figure 3.44: Fluids (gases, liquids and gels) used in hydraulic fracturing (after Palmer, 2008)

When using low viscosity fluids, proppant settling occurs rapidly with proppant accumulating within a short distance from the injection borehole, resulting in incomplete placement of proppant within the complete fracture (Holditch *et al.*, 1989; Palmer *et al.*, 1991; Snyder *et al.*, 2007 and Cramer, 2008). A situation where proppant is not carried toward the tip of the fracture and accumulates to block the facture preventing further fluid/proppant injection to extend the fracture is referred to as a 'screenout' (Snyder *et al.*, 2007 and Cramer, 2008). Therefore when using low viscosity injection fluid, a high injection rate is required to minimise leak-off and a light weight

small proppant material with reduced settling rate should be used to achieve deeper penetration of proppant into the fracture (Holditch *et al.*, 1988; Holditch *et al.*, 1989; Palmer *et al.*, 1991; Britt *et al.*, 2006 and Cramer, 2008).

In cases where the formation may be sensitive to aqueous-based fracture fluid systems dry gases such as N_2 may be used (Zahid *et al.*, 2007). Gases are unable to carry proppant therefore the use of gases, such as N_2, for hydraulic fracturing may be classified as a proppant-less, non-reactive stimulation technique (Zahid *et al.*, 2007). The injection of N_2 also serves to reduce the partial pressure of methane and stimulate coal seam gas desorption from the matrix (Badri *et al.*, 2000 and Ham and Kantzas, 2008).

Cross-linked gel and similar high viscosity injection fluids are less susceptible to leak-off and tend to create wider fractures with reduced radial extent than fractures created using less viscous fluids (Elder, 1977; Holditch *et al.*, 1989 and Palmer, 1992). High viscosity injection fluids have strong proppant suspension characteristics therefore maximising proppant transport into the induced fractures (Holditch *et al.*, 1989 and Palmer, 1992). Viscous injection fluids may cause significant damage to the permeability of the coal seam due to invasion of the fluids into the cleat / fracture network, sorption induced swelling and gel plugging of the cleat (Palmer *et al.*, 1991; Puri *et al.*, 1991; Mavor *et al.*, 1992 and Palmer, 1992). When using gelled fluid in hydraulic fracture stimulation adequate breakers must be added during injection to increase the rate of breakdown of the viscous fluid and improve the efficiency of cleanup following injection (Holditch *et al.*, 1989). Gelled fracturing fluids without the addition of sufficient breaker systems remain stable for long periods and may adversely impact gas production from the coal seam (Holditch *et al.*, 1989; Mavor *et al.*, 1992 and Jeffrey *et al.*, 1995).

Figure 3.45 illustrates the zone of potential permeability damage and cleat compression caused by the distribution of pressure during inflation of the hydraulic fracture (Palmer, 1993 and Palmer, 2008).

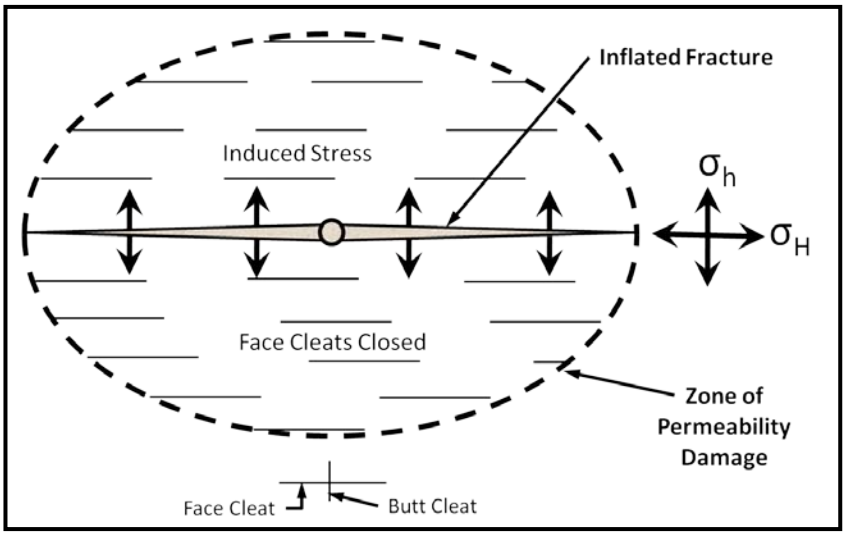

Figure 3.45: Zone of stress induced permeability damage surrounding an inflated hydraulic fracture (after Palmer, 1993)

Solid materials, known as proppant, are commonly added to the stimulation fluid during injection to fill the fracture and prevent it from closing following completion of injection and removal of the injection fluid from the coal seam (Stewart and Barro, 1982). Materials used as proppant commonly include sand or beads formed from glass, plastic or ceramic and each material is available in a range of sizes to suit the particular hydraulic fracture treatment design. The choice of proppant material is an important aspect in the design of a hydraulic fracture treatment. Proppant deposited in an induced fracture must form a permeable channel to increase contact between the borehole and the coal seam gas reservoir to support increased gas extraction (Stewart and Barro, 1982 and Zahid *et al.*, 2007).

Hydraulic fracturing treatments typically comprise multiple stages, the first involving pumping injection fluid, without proppant, to initiate a fracture in the coal seam. If proppant is to be used, proppant material will be added to the injection fluid in stage two. The proppant concentration in the injection fluid is typically increased in each subsequent stage of the hydraulic fracturing treatment (Zahid *et al.*, 2007). Figure 3.46 illustrates fracture growth within a coal seam showing the initial water pad fluid followed by sand proppant delivery into the fracture (USEPA, 2009).

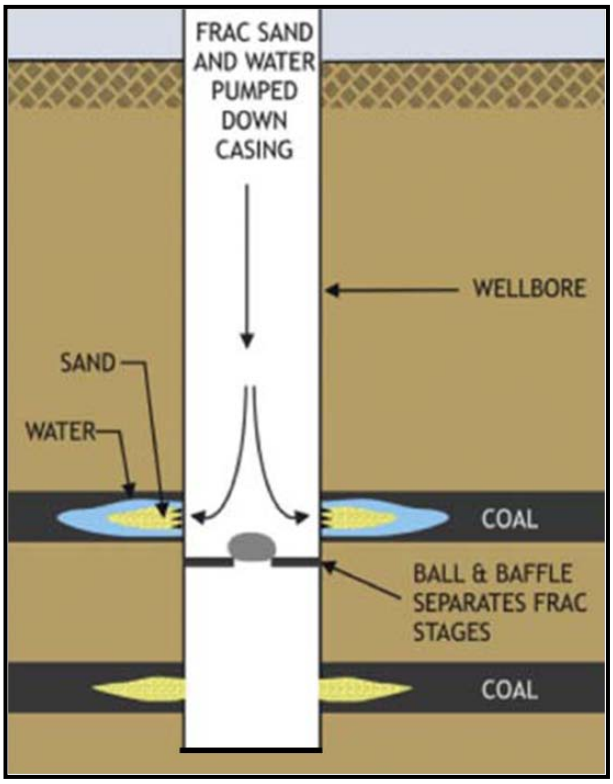

Figure 3.46: Hydraulic fracturing schematic (USEPA, 2009)

Hydraulic fractures are generally considered to create a single, planar, vertical fracture which extends in two wings, in opposite directions, from the injection borehole (USEPA, 2009). Fracture growth typically aligns parallel to the major horizontal stress (Palmer, 2008), as shown in Figure 3.47. However given the complex nature of coal, with multiple pre-existing fracture networks, the growth of a hydraulic fracture can be complex (Holditch *et al.*, 1988; Olsen *et al.*, 2003 and Zahid *et al.*, 2007), as shown in Figure 3.48. Increased leak-off of injection fluid into the formation typically occurs in conjunction with complex fracturing which reduces the effective length and conductivity of the fracture (Holditch *et al.*, 1988 and Mavor *et al.*, 1992).

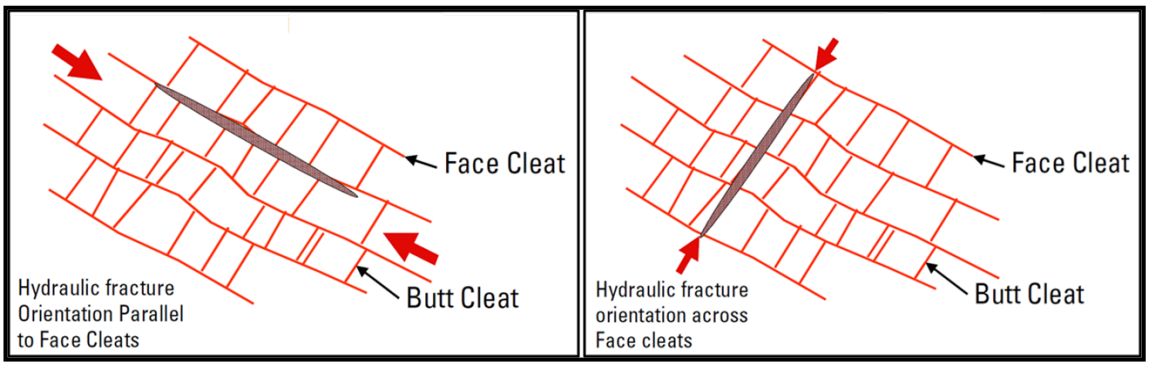

Figure 3.47: Hydraulic fracturing schematic (Olsen *et al.*, 2003)

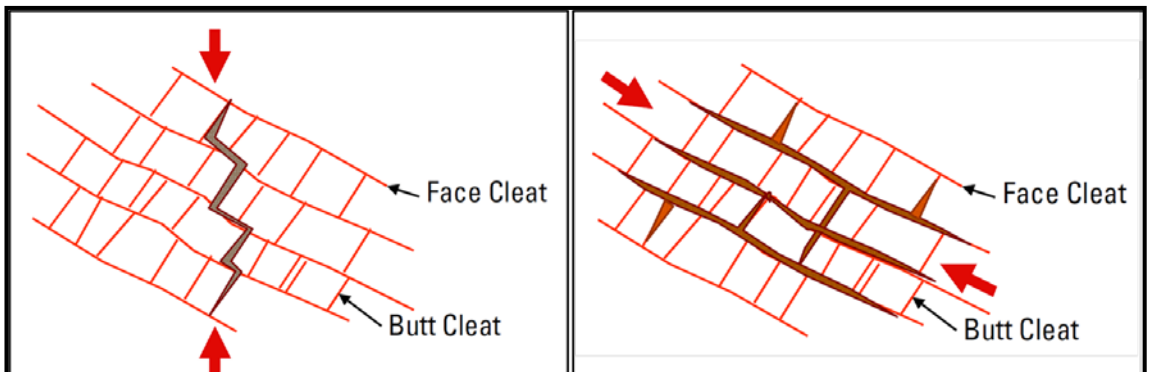

Figure 3.48: Hydraulic fracturing schematic (Olsen *et al.*, 2003)

Where hydraulic fracturing is used to stimulate coal seams at shallow depth and the vertical stress is the minimum principal stress, fracture will preferentially grow horizontally, propagating along a particular ply within the coal seam or along the coal/roof interface (Holditch *et al.*, 1989; Jeffrey *et al.*, 1989 and Mavor *et al.*, 1992). At increased depth fractures are more likely to be vertical, however should the pressure developed within a propagating vertical fracture exceed the magnitude of the vertical stress the fracture can develop a horizontal component, typically referred to as a T-shaped fracture (Jeffrey *et al.*, 1989). In cases where the coal seam is bounded by lower strength roof and floor strata there is an increased risk of the fracture extending beyond the coal seam into these lower strength units (Enever *et al.*, 1995).

Many mine operators express concern regarding the potentially detrimental impact of hydraulic fracturing on future mining conditions, particularly creating geotechnical instability (Kahil and Masszi, 1982 and Carter, 1990). Provided the injection pressure during hydraulic fracturing does not exceed the minimum horizontal stress of the bounding roof or floor strata it is highly probable that the fracture will be contained within the coal seam (Trevits *et al.*, 1982). Many studies have monitored mining conditions in areas subjected to hydraulic fractures and with few exceptions no geotechnical instability or adverse mining conditions attributable to the stimulation treatment have been reported (Elder, 1977; Battino and Hargraves, 1982; Diamond and Oyler, 1987; Jeffrey *et al.*, 1993; Jeffrey *et al.*, 1994; Enever *et al.*, 1995 and Jeffrey *et al.*, 1998). In cases where fractures were observed to have extended beyond the coal seam the majority penetrated pre-existing joints (Diamond and Oyler, 1987).

3.5.7 Enhanced Coalbed Methane (ECBM)

Conventional gas drainage methods rely on decreasing reservoir pressure to stimulate gas desorption in accordance with the sorption isotherm condition for the given coal / gas mix (Durucan and Shi, 2009). Such methods, although relatively simple are not efficient as reduction in reservoir pressure also corresponds to a reduction in the rate of gas production from the borehole (Puri and Stein, 1989). Total coal seam gas production using conventional pressure depletion methods rarely achieve greater than 50% recovery of the initial sorbed gas volume (Stevenson *et al.*, 1993).

Enhanced coalbed methane (ECBM) is a drainage enhancement technique involving the injection of an inert gas, typically CO_2 and/or N_2, into a coal seam to stimulate gas desorption and increase total coal seam gas production (Stevenson *et al.*, 1993 and Durucan and Shi, 2009). The use of ECBM to enhance coal seam gas production was first trialled in 1993 in a small scale N_2-ECBM pilot project in the Fruitland formation, San Juan Basin and CO_2-ECBM pilot project in the Manville formation, Alberta (Ham and Kantzas, 2008 and Saghafi, 2009). A typical ECBM drilling pattern consists of a central gas injection borehole surrounded by a number of dedicated gas production boreholes, used to extract the coal seam gas / injected gas mixture.

The injection of CO_2 or N_2 into the coal seam, referred to as inert gas stripping, reduces the partial pressure of CH_4 in the free gas phase stimulating the desorption of CH_4 from the coal matrix (Brown *et al.*, 1996; Durucan and Shi, 2009 and Saghafi, 2009). The movement of gas through the coal seam 'sweeps' the desorbed seam gas toward the production borehole(s).

The effectiveness of ECBM is highly dependent on prevailing geological conditions, the properties of the coal seam gas reservoir, the layout of the injection and production boreholes and the design of the injection program. To be effective the injected inert gas must be in contact with the coal matrix for sufficient time to stimulate desorption and sweep seam gas from a large area of the coal seam. In cases where the face cleat and geological structures align sub-parallel to the path between the injection and production boreholes the injected gas is more likely to take a direct path toward the production borehole resulting in low sweep efficiency and reduced effectiveness of the ECBM method.

As coal has a strong affinity for CO_2 adsorption some of the CO_2 injected into the coal seam during CO_2-ECBM will compete with CH_4 for sorption sites displacing CH_4 from the coal matrix (Mazumder and Wolf, 2008). The process of CO_2 adsorption does however induce swelling of the coal matrix which can reduce permeability having a detrimental impact on the ability to inject additional gas into the coal seam (Mazumder and Wolf, 2008; Durucan and Shi, 2009; Siriwardane *et al.*, 2009 and Yi *et al.*, 2009). During CO_2-ECBM at the Allison Unit pilot project in the San Juan Basin a reduction in permeability of more than two orders of magnitude was experienced as a result of sorption induced swelling (Durucan and Shi, 2009).

N_2 is considered a superior gas for use in ECBM injection for methane production as it achieves greater sweep efficiency and is less likely to induce sorption related permeability reduction (Oudinot *et al.*, 2007 and Durucan and Shi, 2009). Injection of N_2 following CO_2 at the Tiffany ECBM pilot in the San Juan basin not only reversed the permeability reduction caused by the previous CO_2 injection but enhanced the rate of N_2 injection into the coal seam (Oudinot *et al.*, 2007 and Durucan and Shi, 2009).

Injecting gas into the formation at elevated temperature has also been reported to have a positive effect in increasing gas desorption and total gas production through ECBM, stimulating the movement of gas molecules and reducing the sorption capacity of coal (Every and Dell'Osso, 1977; Puri and Stein, 1989 and Levine, 1992).

The concept of injecting CO_2 through an injection borehole into a coal seam, at a pressure greater than reservoir pressure and less than fracture initiation pressure, to promote CH_4 desorption into the injected fluid, with the CO_2/CH_4 gas mix being extracted through separate production wells was first introduced in the mid-1970's (Every and Dell'Osso, 1977). The injection of other inert gases such as N_2, He, Ar and air into the coal seam through a dedicated injection to strip and remove CH_4 through separate production boreholes without reducing reservoir pressure was proposed by Puri and Stein (1989). Prior to the development of the coalbed methane industry a similar technique involving the injection of heated gases into oil sand strata to increase oil production from adjacent well was proposed by Steffen (1948).

Battino and Hargraves (1982) suggested the potential advantages of inert gas injection to enhance inseam pre-drainage, by injecting gas into a central borehole to accelerate

gas production from adjacent boreholes. Battino and Hargraves (1982) suggested injecting compressed air in CO_2 rich seam gas conditions and N_2 in CH_4 rich seam gas conditions.

The technique proposed by Every and Dell'Osso (1977) differs from current ECBM application in that following injection the fluid is shut-in and held in the coal seam for a period prior to being released through the surrounding production wells with the cycle of injection-hold-release being repeated multiple times. Every and Dell'Osso (1977) claim the process of injection-hold-release achieved greater methane desorption than alternative methods based on continuous injection of inert gas through the coal seam.

Mones (2001 and 2002) introduced the concept of using a common injection-production borehole, initially injecting inert gas into the coal seam, flooding the coal surrounding the borehole to desorb CH_4 from the coal matrix, immediately followed by production of the CH_4 / inert gas mix through the same borehole. Based on simulation Mones (2001 and 2002) suggest the possibility of determining the minimum volume of N_2 required to be injected into a coal seam to achieve maximum CH_4 desorption resulting in the concentration of inert gas in the produced gas being maintained at less than 10%.

An alternative method of ECBM is proposed; known as cyclic inert gas injection (CIGI), this method incorporates many aspects of past research to deliver increased total gas production and permeability enhancement (Black *et al.*, 2010). CIGI involves injecting a heated inert gas, such as N_2, into a coal seam through a dual purpose injection-production borehole at a pressure greater than reservoir pressure and less than fracture initiation pressure to penetrate the cleat and flood the coal structure surrounding the injection borehole. Upon completion of the injection phase the borehole is shut-in for a period to encourage desorption of CH_4 from the coal matrix. After sufficient hold time the borehole is opened producing a mixture of desorbed CH_4 and inert gas. The cycle of inject-hold-produce is repeated multiple times, each cycle increasing the total area affected by the stimulation treatment. Figure 3.49 illustrates the major components of a CIGI project to complete a five cycle coal seam stimulation treatment.

The individual aspects of the CIGI concept which in combination deliver a potentially superior ECBM method for stimulating coal seam gas drainage are listed below:

- Gas injection into the coal seam at a pressure greater than reservoir pressure and less than fracture initiation pressure forces inert gas into the coal seam, opening the cleat and penetrating deep into the formation;
- The presence of fractures and geological discontinuities is not detrimental, they provide additional paths for inert gas penetration into the coal seam;
- Reduced partial pressure of the inert gas within the cleat and fracture network of the coal promotes CH_4 desorption from the coal matrix;
- Heat transfer from injected gas increases the temperature of the coal seam, energising the CH_4 gas molecules and increasing the rate of movement out of the coal matrix;
- Increasing the temperature reduces the sorption capacity of coal which in turn increases the relative degree of saturation of the CH_4 / inert gas mix;
- The sorption isotherm of a CH_4/N_2 gas mix will be lower than for a pure CH_4 isotherm therefore for a given gas content, injecting N_2 will also serve to increase the relative degree of saturation; and
- During the gas production phase a reduction in pressure within the cleat and fracture network will cause the coal matrix to swell having an adverse effect on permeability. However this effect will be counteracted by the matrix shrinkage resulting from CH_4 desorption. After having been subjected to multiple inject-hold-produce cycles the CH_4 content is expected to have been substantially reduced and the resulting shrinkage of the coal matrix will result in a net increase in effective permeability.

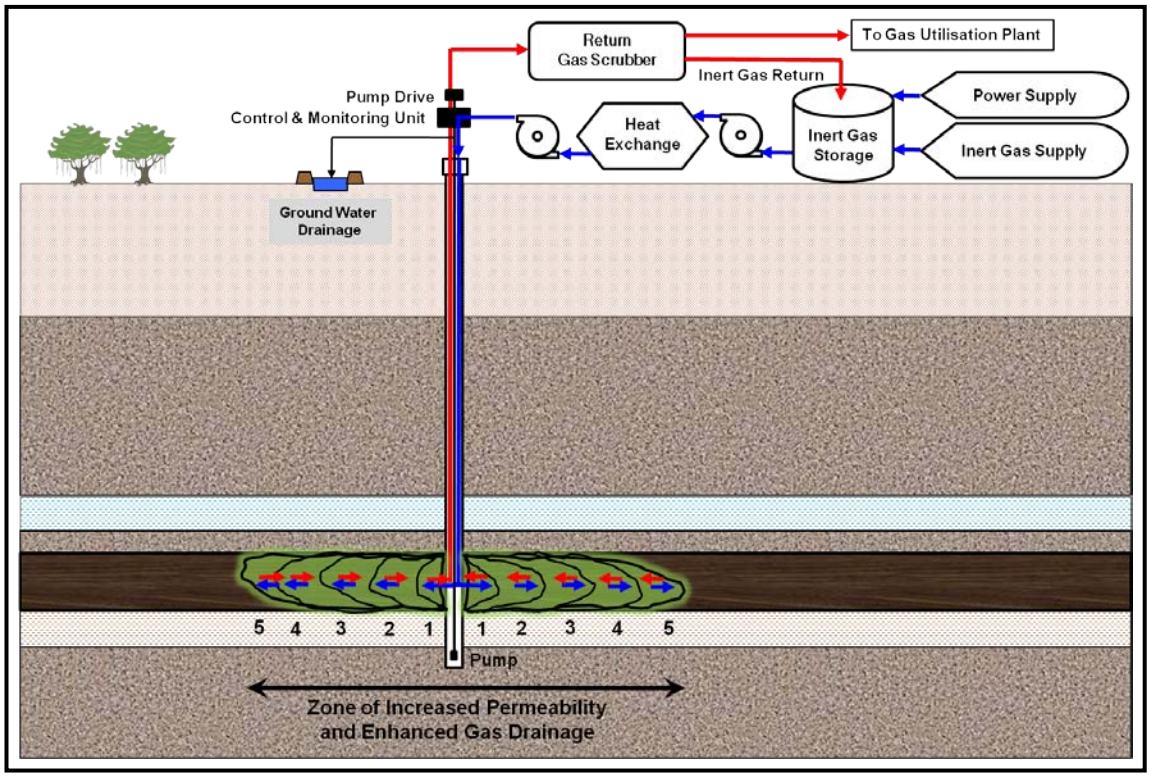

Figure 3.49: Cyclic Inert Gas Injection to enhance coal seam gas drainage (after Black *et al.*, 2010)

3.6 SUMMARY

Drilling boreholes into a coal seam from underground or the surface is now an accepted method for draining coal seam gas to reduce ventilation air methane (VAM) concentrations, reduce gas-related production delays and reduce the risk of initiating a coal seam gas outburst.

Underground to inseam (UIS) drilling is presently the preferred method for gas drainage employed by deep mines working the Bulli seam which feature high gas content, low permeability and limited surface access. The UIS directional drilling systems employed at these mines have undergone little change and technological development since being introduced into Australia in the mid-1990's. Although the control of borehole placement is substantially better than earlier rotary drilling systems which utilised single-shot survey tools, the path of the completed borehole is tortuous with frequent changes in direction, regular branches and roof and floor touches. Drilling in this manner increases the risk of encountering problems such as borehole failure, reduced borehole length, loss of downhole equipment and reduced gas drainage performance. Although various UIS drilling patterns are available each relies on setting up a drill rig in an existing roadway to drill boreholes ahead of future mine workings. The consequence of this

drilling system is limited drainage time, commonly much less than 12 months. In areas where gas drainage occurs at a reduced rate the drainage time may not be adequate to achieve the required minimum gas content reduction, in such cases alternative gas drainage methods such as a surface-based system must be considered.

Various research projects have developed sensors that offer improved control and performance from UIS drilling however to date these sensors have not advanced to become standard inclusions in operating UIS drilling systems.

A number of surface-based drilling and completion methods are available for use in coal seam gas drainage. Surface-based systems are disconnected from underground mining workings and are therefore free from the inherent logistical challenges associated with operating in underground roadways such as limited space and restricted access. Surface-based gas drainage is ideally undertaken many years in advance of mine workings to maximise the gas production potential from each borehole, offsetting the drilling and gas production costs, and reducing the total number of drainage boreholes needed to achieve the required gas content reduction.

A new method for enhancing coal seam gas production using cyclic injection of inert gas is proposed. To improve coal seam gas drainage in advance of underground mine workings, particularly in areas with low permeability and historically poor gas drainage performance, the injection of an inert gas such as N_2 or air is recommended. Using a treatment cycle of inject-hold-produce, repeated multiple times, a substantial reduction in gas content is expected from the treated area. In addition to gas content reduction the cyclic inert gas injection offers the potential to achieve a net increase in effective permeability which supports increased gas desorption long after the ECBM treatment.

The material properties and drainage characteristics of coal can change significantly between seams, between mines and even over short distances within the same seam, in the same mine. The success of a particular gas drainage method in one area does not necessarily guarantee success in a different area. Therefore an essential element in the design of any gas drainage program is to have a clear understanding of the drainage characteristics of the coal throughout the area. In particular, the geological properties and other operational factors that have the greatest impact on gas drainage must be

understood and considered in the selection of an appropriate gas drainage method and the design and management of the overall drainage program.

The following two Chapters analyse the relationship between a variety of operational factors and geological properties affecting inseam gas drainage from the Bulli seam within Area 5 at WCC.

CHAPTER FOUR – IMPACT OF COAL PROPERTIES ON GAS DRAINAGE

4.1 INTRODUCTION

This chapter examines gas production from underground gas drainage boreholes and analyses the relative impact of a variety of coal properties using data collected from and relevant to the Bulli coal seam in the mining area, known as Area 5, at WCC.

Much of the past research has analysed individual coal properties in great detail. These studies have typically been conducted in laboratories using small samples of coal material recovered from exploration drilling or operating mines. Given the structural changes and potential degradation of coal samples during extraction, transport, storage, and preparation for testing, the results from laboratory testing potentially lack transferability and may not be representative of the *in situ* characteristics of gas flow and emission from coal.

4.2 DATA ACQUISITION

Data was obtained from various sources associated with WCC, however it was the availability of extensive gas production data that underpinned this aspect of the research, enabling detailed analysis of the impact of various coal seam properties on borehole gas production performance.

Coal property data was gathered from various sources within BHP Billiton Illawarra Coal and from testing and analysis conducted at the University of Wollongong's Mine Gas Research laboratory.

Table 4.1 lists the coal seam properties considered. Appendix 4.1 provides a summary of gas production and geological property data corresponding to the 279 inseam gas drainage boreholes included in this study.

Table 4.1: Coal seam properties considered in analysis

Coal Rank	Coal Type	Coal Seam Gas
Fixed carbon	Inertinite maceral	Gas content
Volatile matter	Vitrinite maceral	Gas composition
Vitrinite reflectance	Mineral matter	Total gas in place
Ash Content	Permeability	Degree of saturation
Seam (raw) ash	Inherent moisture	
Coal ash		

4.2.1 Inseam Borehole Gas Production Data

The availability of accurate and regular gas flow measurement data is essential to any investigation and analysis of gas drainage performance. Throughout the study area gas flow from inseam boreholes was measured at approximately weekly intervals. The data was consolidated to produce gas production profiles for individual and groups of boreholes, and this data was used to evaluate the individual and combined effects on gas production of the coal properties and other factors considered in this study.

In preparing the dataset, boreholes were excluded if they had experienced substantial periods of either blockage or flooding or had been drilled into a previously drilled area, thereby overlapping other boreholes. Also, where it was obvious from notes made in gas production reports, or from reference to the mine plan, that boreholes had been intersected by compliance boreholes or advancing mine development, all flow data subsequent to such an event was excluded from the dataset.

Data was collected from 279 UIS gas drainage boreholes drilled from 34 drill sites, covering an area of approximately 7.2 km^2. The boreholes span the length of five separate mine development panels, referred to as 516, 517, 518, 519 and 520, with 20 boreholes in 516 panel, 40 boreholes in 517 panel, 80 boreholes in 518 panel, 87 boreholes in 519 panel and 52 boreholes in 520 panel. Figure 4.1 shows the location of the boreholes in each of the five panels relative to current and future planned mine workings.

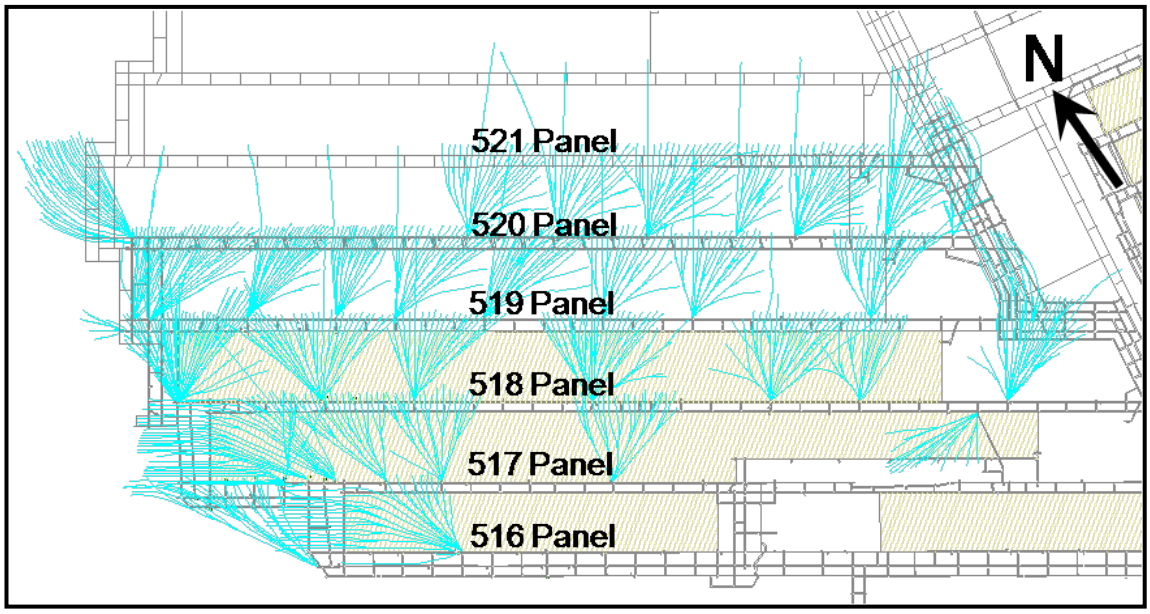

Figure 4.1: Plan of UIS boreholes where flow data was recorded

4.2.2 Coal Property Data

A range of geological, geotechnical and coal quality data was compiled from sources within the various operating and technical areas of BHP Billiton Illawarra Coal. The following data was gathered:

- Gas content and composition from surface to seam exploration drilling;
- Permeability measurement determined from step-rate and injection fall-off testing during surface to seam exploration drilling;
- Stress orientation interpreted from borehole logging subsequent to surface to seam exploration drilling;
- Seam thickness from surface to seam exploration drilling and underground strip sample measurement;
- Seam dip interpretation from top of coal measurement during surface to seam exploration drilling and logging;
- Coal quality and petrographic analysis data from laboratory analysis of coal samples collected during surface to seam exploration drilling and underground strip sampling of the coal seam;
- Hydrostatic pressure change due to mining and gas drainage from piezometers installed in the coal seam subsequent to surface to seam exploration drilling; and
- Cleat orientation and spacing identified from geological mapping of accessible roadways in both the 519 and 520 panels.

Figure 4.2 shows the location of coal samples collected for coal quality analysis. Figure 4.3 shows the location of boreholes used to acquire gas content, gas composition, seam thickness, stress orientation, permeability and hydrostatic pressure data.

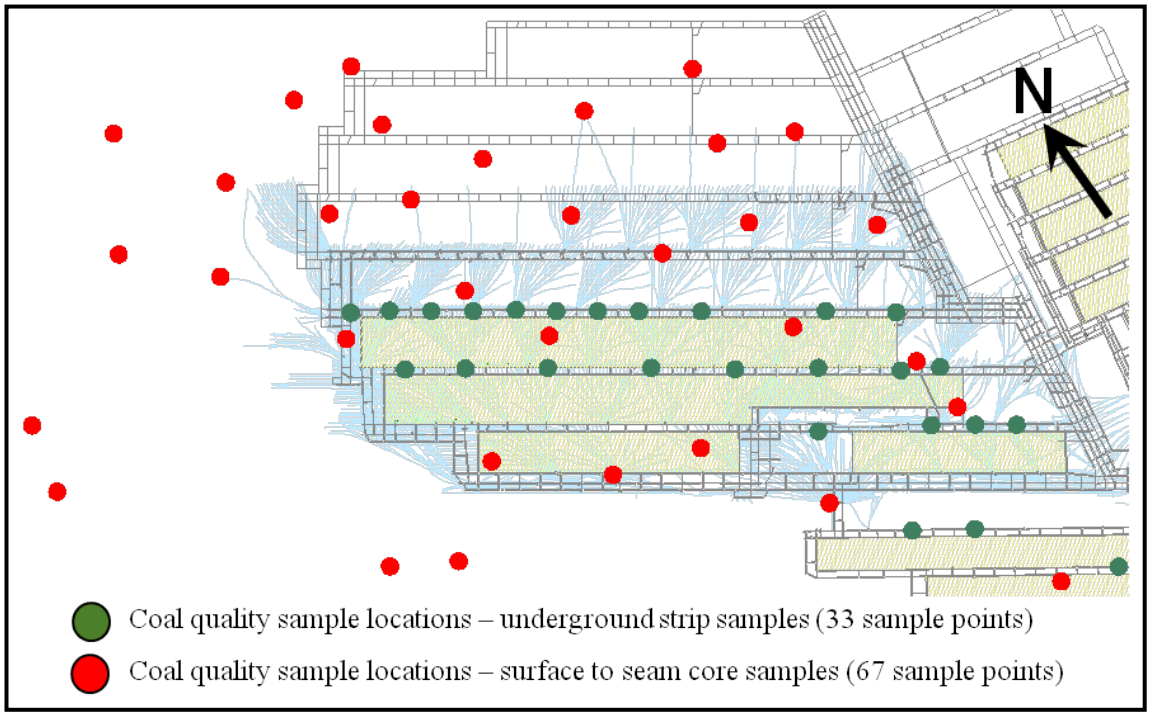

Figure 4.2: Location of coal samples used to acquire coal quality analysis

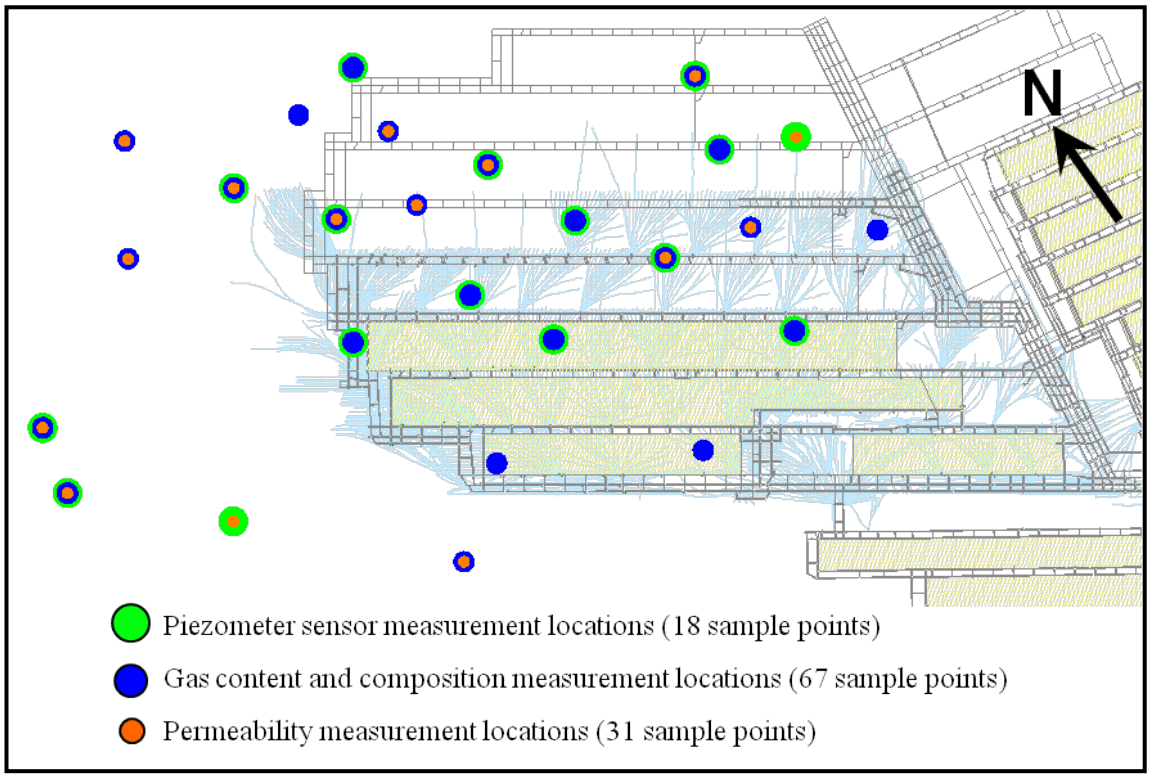

Figure 4.3: Sites used to acquire coal seam geological and geotechnical data

4.3 ANALYSIS OF INSEAM BOREHOLE GAS PRODUCTION

Total gas production is a useful indicator of the overall performance and effectiveness of a borehole during the course of its operating life. The total volume and rate of gas production from the UIS boreholes was found to steadily decrease along the length of the panels. Figure 4.4 and Figure 4.5 show the average total gas production (m^3) and average gas production rate (m^3/m/day) from the boreholes in each of the 34 drill sites, relative to the position of the drill site along each panel.

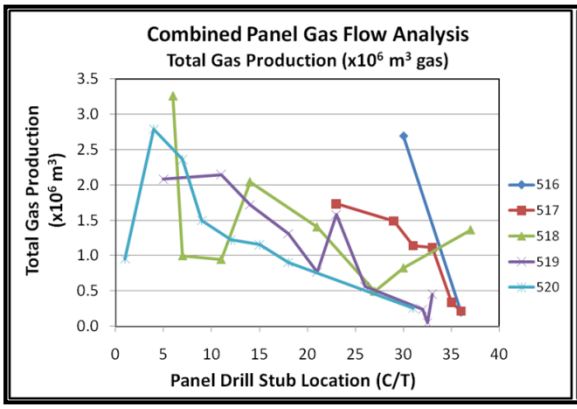

Figure 4.4: Total drill stub gas production relative to panel drill stub location

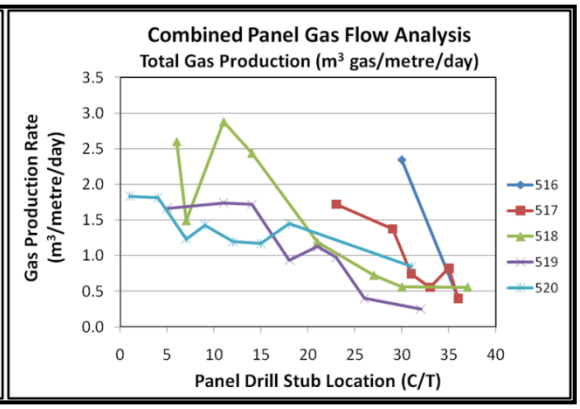

Figure 4.5: Average drill stub gas production rate relative to panel drill stub location

Figure 4.6 show total gas production from each of the 279 boreholes relative to their position along the panels. The data indicate decreasing gas production with distance into the panels. The relationship between borehole location and gas production was further assessed by grouping the boreholes from each of the five panels, based on the cut-through from which the borehole was drilled. Four separate zones were established, each covering a distance of approximately 10 cut-throughs, representing a distance of approximately 1 000 m. Of the 279 total boreholes, 45 were located within the zone 0-10 cut-through, 59 within the zone 10-20 cut-through, 80 within the zone 20-30 cut-through, and 95 within the zone Inbye +30 cut-through. Figure 4.7 shows the span and median gas production within each of the four cut-through zones.

In addition to the high degree of variability, the data highlights the significant number of boreholes that achieved low production. As shown in Figure 4.8, 45% of the boreholes achieved less than 100 000 m^3 total gas production. Figure 4.9 shows the distribution of gas production rate (m^3/m/day) data, which was based on total measured

length, including significant branches, and total effective production life (drainage time).

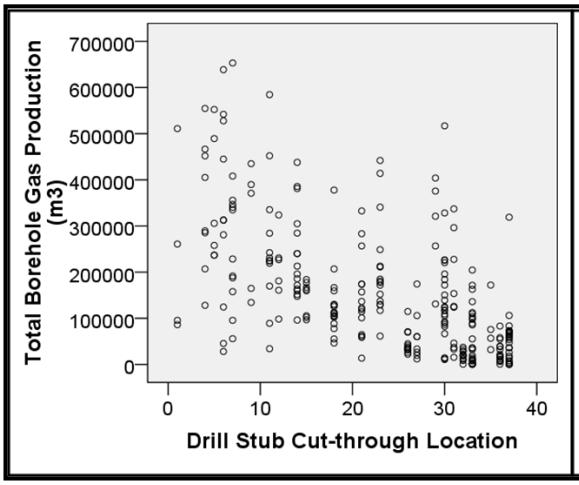

Figure 4.6: Total gas production relative to borehole location along panel

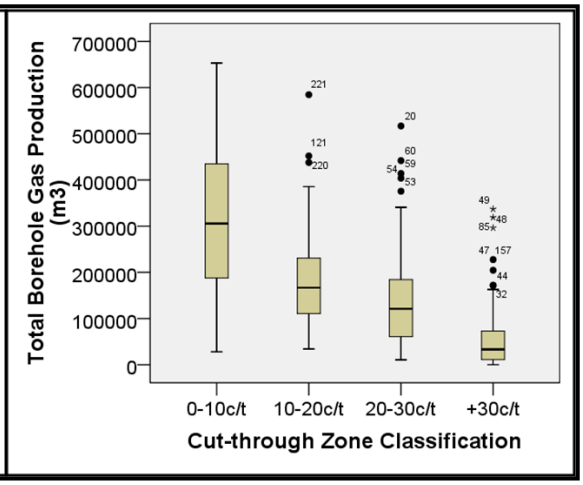

Figure 4.7: Span and median total gas production in each of the four cut-through zones

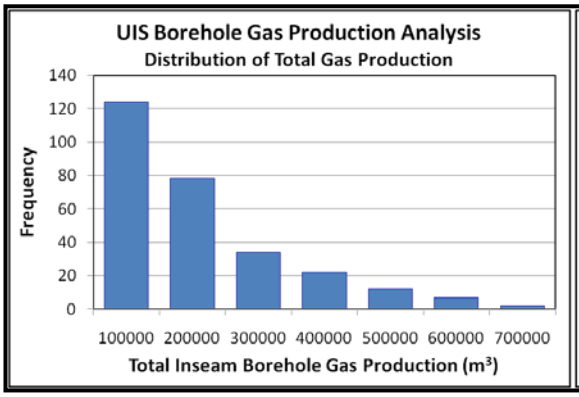

Figure 4.8: Histogram showing distribution of total borehole gas production

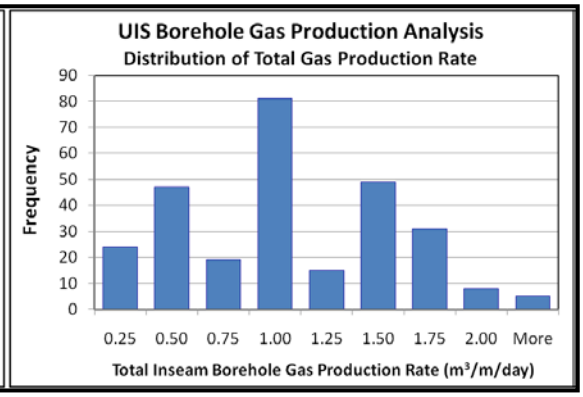

Figure 4.9: Histogram showing distribution of total borehole gas production rate (m^3/m/day)

Although total gas production is an important measure for assessing the complete performance of a borehole, its use as the basis for comparing multiple boreholes must be understood and used with caution. This is due to the variability in production life (drainage time) between boreholes and the non-linear nature of gas emission rate. Gas emission typically commences at a high rate during the initial production phase, decreasing over the productive life of the borehole, to a point where the rate is virtually zero. Figure 4.10 shows the results of gas emission rate measurement from two coal samples sourced from the mining area. Both have similar total desorbed gas content (4.0 m^3/t), which includes both the Q_1 and Q_2 components of Q_M however the gas emission rate differs markedly. Sample WE1189 required 390 days to liberate a combined $Q_1 + Q_2$ gas content of 4.0 m^3/t whereas sample WE1198 required 685 days,

indicating a much slower gas emission rate. In both cases the Q_3 components were similar, liberating approximately 2.0 m^3/t.

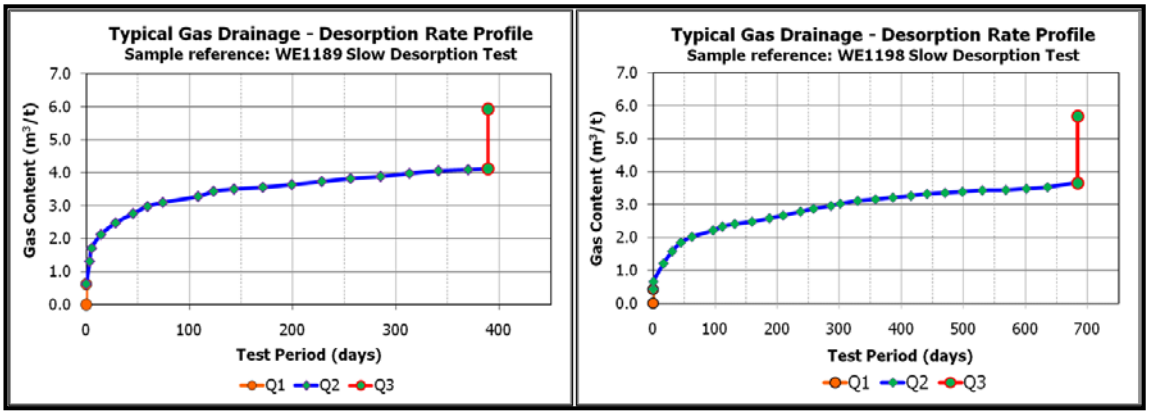

Figure 4.10: Gas emission rate curves from coal samples WE1189 and WE1198

This example highlights the potential risk involved in basing an evaluation of gas production potential entirely on the total desorbed gas content as it does not consider the actual rate of gas emission during the production life of the borehole. In order to account for the potential impact of variable gas emission rates a second measure of gas production performance was devised for use in this study, which is the total volume of gas produced during the first 50 days (D50) of borehole production. The D50 gas production data was determined for 249 of the 279 boreholes.

Analysis of the D50 gas production relative to total gas production indicates a strong correlation (R^2 = 83%) with an average 49% of total gas production liberated within the first 50 production days (Figure 4.11). Considering the relationship between the percentage of the total gas production at D50 and total borehole gas production (Figure 4.12) a high degree of scatter is evident among boreholes producing less than 200 000 m^3, with the percentage of total gas produced at D50 ranging between 10 and 100%. The scatter reduces significantly with increasing total gas production, particularly where total gas production exceeds 200 000 m^3.

Considering the impact of short drainage time on the relationship between D50 and total gas production, a filter was applied to the data to consider boreholes with drainage time exceeding 200 days. Figure 4.13 shows the impact of drainage time on span and median percentage of total gas produced at D50 within the four cut-through zones. Removing the influence of short drainage time it was found that the D50 percentage of total gas

production decreased with distance into the panels, indicating a reduction in gas emission rate.

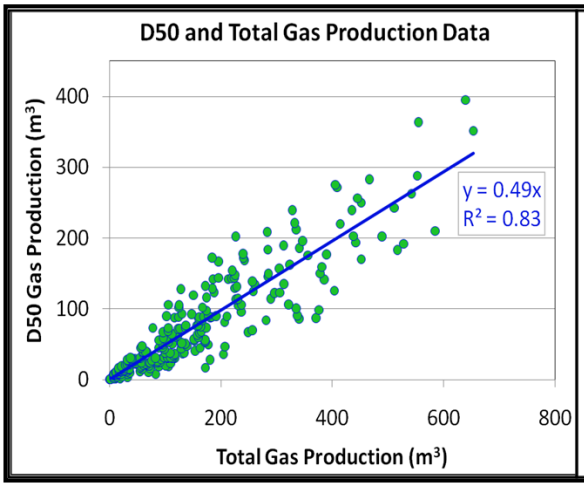

Figure 4.11: Relationship between D50 and total gas production

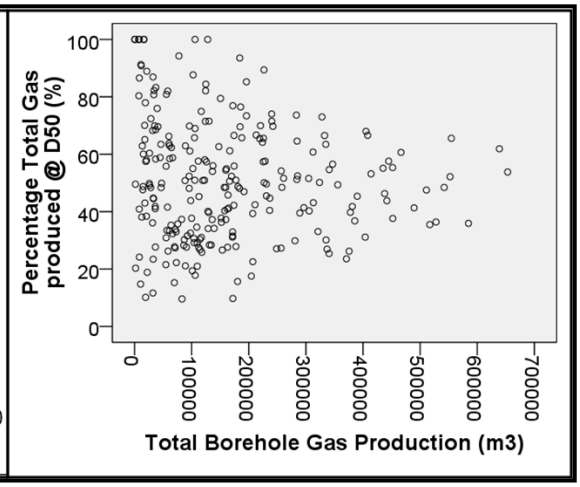

Figure 4.12: Proportion of total gas removed at D50 relative to the total borehole gas production

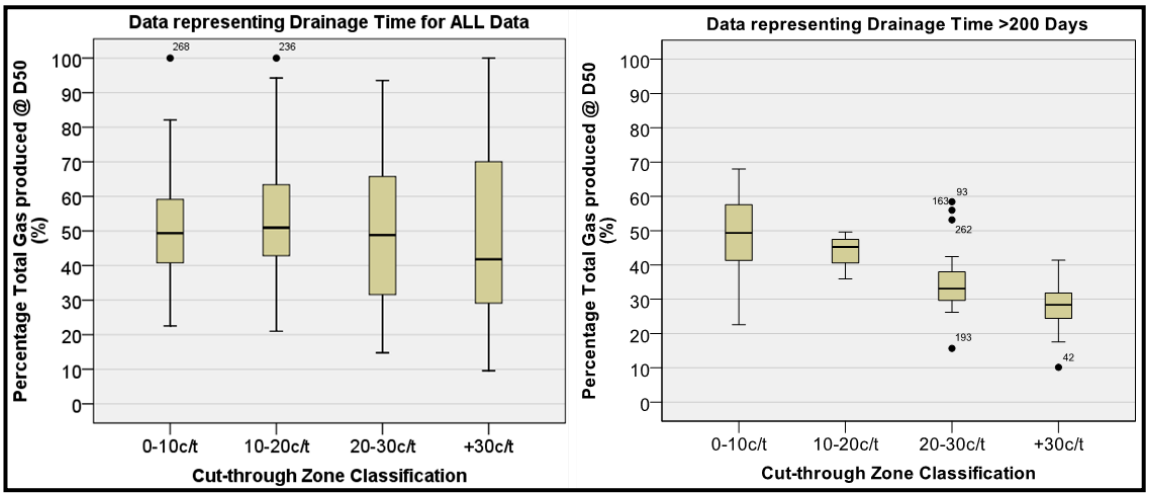

Figure 4.13: Impact of drainage time on span and median D50 percentage of total gas production

4.4 ANALYSIS OF COAL PROPERTIES

Coal quality and petrographic data was gathered from coal analysis testing, reported by Clark (1986-2007). Bulli seam coal samples were gathered from both surface to seam exploration drilling and underground strip samples. Coal property data was gathered from coal samples sourced from within and adjacent to the mining area. The coal property values reported at each sample location represent the weighted average result of all clean coal fractions recorded during laboratory testing and analysis. Grid files and contour plots were generated for each coal property using “Surfer 9” software. Overlaying the gas production boreholes and coal property contours, an average coal

property value was determined for the boreholes within each of the 34 drill sites. The individual coal property values were assessed relative to the gas production from the boreholes drilled from each drill site. Statistical analysis was conducted using "SPSS 17" software to identify and quantify the relationship between gas production and each coal property.

4.4.1 Coal Rank

The term 'rank' is used to classify coal according to the degree of progressive alteration during the coalification process, from lignite to anthracite. Ward (1984) lists five components of coal composition that may be used to classify a particular coal based on its rank. These components include bed moisture, volatile matter, total carbon, specific energy and vitrinite reflectance. Data was available for three of the components, carbon content, volatile matter and vitrinite reflectance. Table 4.2 shows the range of coal rank values recorded at the drill sites within the mine along with the range of rank indicator values for each of low volatile, medium volatile and high volatile A bituminous coal, as stated by Ward (1984). On average it was concluded that the rank of the coal within this mining area was medium volatile bituminous.

Table 4.2: Coal rank classification (after Ward, 1984)

Coal Rank Indicator	**Data range recorded within mining area (%)**	Low volatile bituminous coal (%)	Medium volatile bituminous coal (%)	High volatile A bituminous coal (%)
Carbon content	**67.3 - 70.8**	78 - 86	**69 - 78**	**<69**
Volatile matter	**20.2 - 22.1**	**14 - 22**	22 - 31	>31
Vitrinite reflectance	**1.26 - 1.32**	1.50 - 2.05	**1.10 - 1.50**	0.71 - 1.10

Given the relatively narrow range of data representing each component it was not possible to complete a broad assessment of the relationship between coal rank and gas production.

4.4.1.1 Carbon Content

Table 4.3 provides a summary of the results of carbon content analysis conducted on 56 coal samples, reported by Clark (1986-2007). The carbon content values were used to

generate the contour plot, shown relative to current and future mine workings in Figure 4.14.

Table 4.3: Carbon content data source and summary information (after Clark, 1986-2007)

Carbon content	number of samples	Average (%)	Data range (%)		Sample collection & analysis	
			Minimum	Maximum	From	To
SIS core sample	31	73.4	66.4	90.0	4/11/1987	5/12/2007
UG strip sample	25	69.9	66.1	71.5	8/08/2001	6/08/2007
Combined	56	71.8	66.1	90.0	4/11/1987	5/12/2007

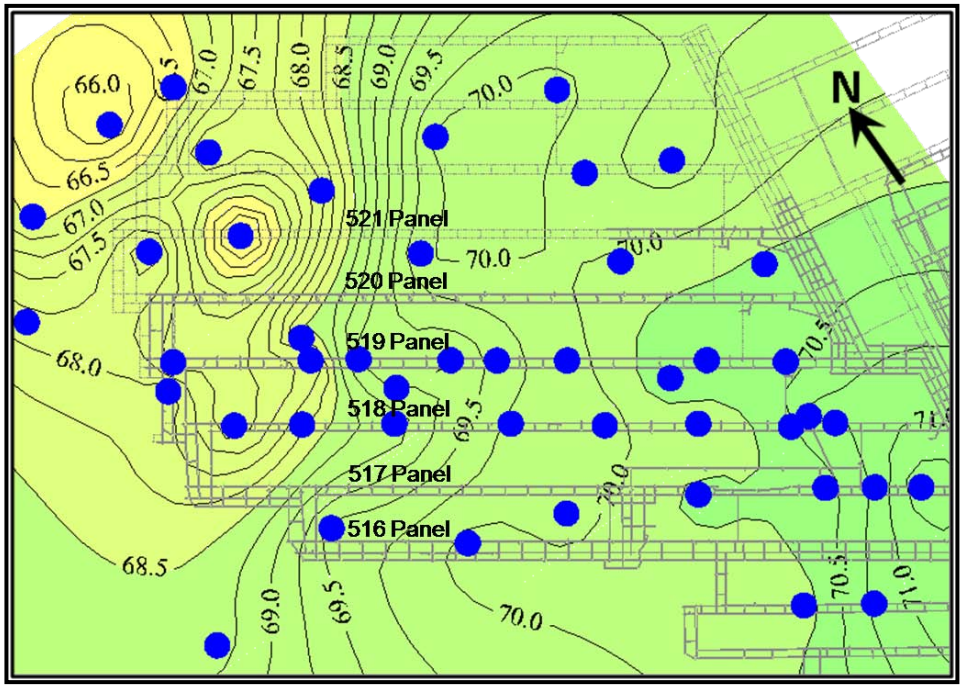

Figure 4.14: Carbon content contours relative to mine workings and coal sample locations

Figure 4.15 and Figure 4.16 show the distribution of estimated average carbon content corresponding to the boreholes in the complete dataset and in each of the four cut-through zones. The average carbon content of all boreholes in the dataset was 69.0%, with the range extending from a low of 67.3% to a high of 70.8%. The carbon content was found to decrease with distance into the panels, with the average in each cut-through zone decreasing from a high of 70.3%, in the 0-10c/t zone, to a low of 67.9%, in the +30c/t zone.

Figure 4.17 and Figure 4.18 show the relationship between carbon content and gas production, with increased total and D50 production from boreholes located in areas of

increased carbon content. Statistical analysis indicated a positive correlation of 0.639 and 0.673 between carbon content and each of total production and D50 production.

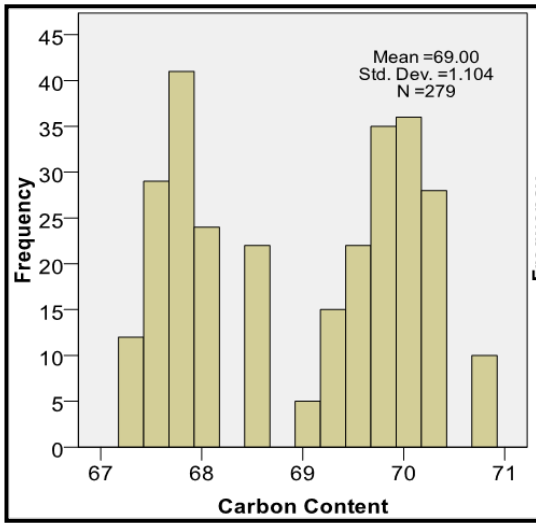

Figure 4.15: Distribution of carbon content for all boreholes within the complete dataset

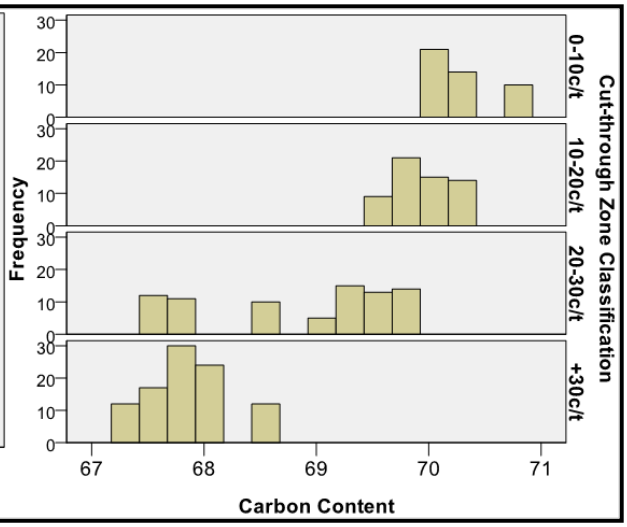

Figure 4.16: Distribution of carbon content for boreholes in each cut-through zone

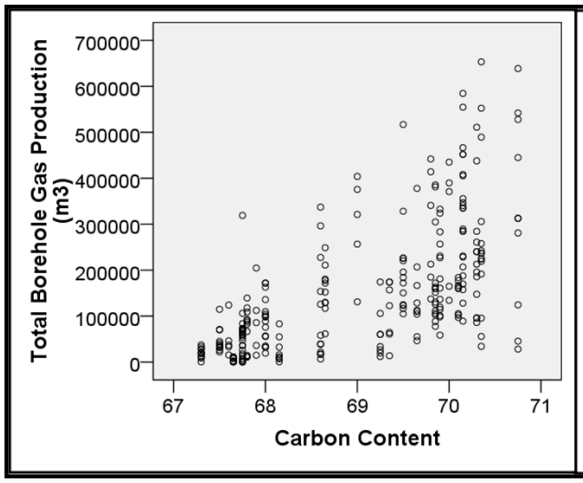

Figure 4.17: Total gas production relative to carbon content

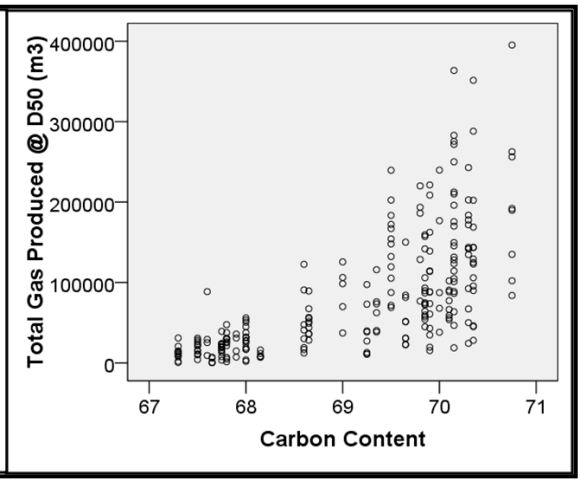

Figure 4.18: D50 gas production relative to carbon content

The relationship between carbon content and both total and D50 gas production within each cut-through zone was also considered. As shown in Figure 4.19 and Figure 4.20 the maximum gas production in each zone was greater in areas of increased carbon content.

This assessment has shown increased gas production was achieved from boreholes located in areas with greater carbon content and the relationship was independent of location along the panels. Therefore in this case the data indicates that carbon content, and hence coal rank, has an impact on gas production.

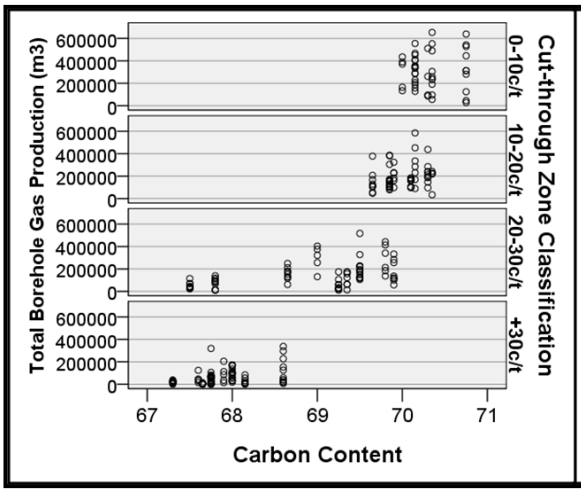

Figure 4.19: Total gas production relative to carbon content in each cut-through zone

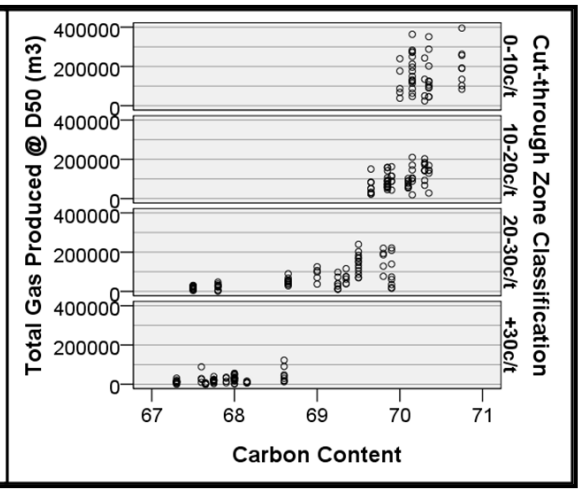

Figure 4.20: D50 gas production relative to carbon content in each cut-through zone

4.4.1.2 Volatile Matter Content

Table 4.4 provides a summary of the results of volatile matter analysis conducted on 64 coal samples, reported by Clark (1986-2007). The volatile matter values were used to generate the contour plot, shown relative to current and future mine workings in Figure 4.21.

Table 4.4: Volatile matter data source and summary information (after Clark, 1986-2007)

Volatile matter	number of samples	Average (%)	Data range (%)		Sample collection & analysis	
			Minimum	Maximum	From	To
SIS core sample	34	22	20.3	25.3	13/08/1986	5/12/2007
UG strip sample	30	21.1	19.7	23.1	8/08/2001	6/08/2007
Combined	64	21.6	19.7	25.3	13/08/1986	5/12/2007

Figure 4.22 and Figure 4.23 show the distribution of estimated average volatile matter content for the boreholes in the complete dataset and in each of the four cut-through zones. The average volatile matter content of all boreholes in the dataset was 21.4%, and the range extended from a low of 20.2% to a high of 22.1%. The volatile matter content was found to increase with distance into the panels, with the average in each cut-through zone increasing from a low of 20.7%, in the 10-20c/t zone, to a high of 21.9%, in the +30c/t zone.

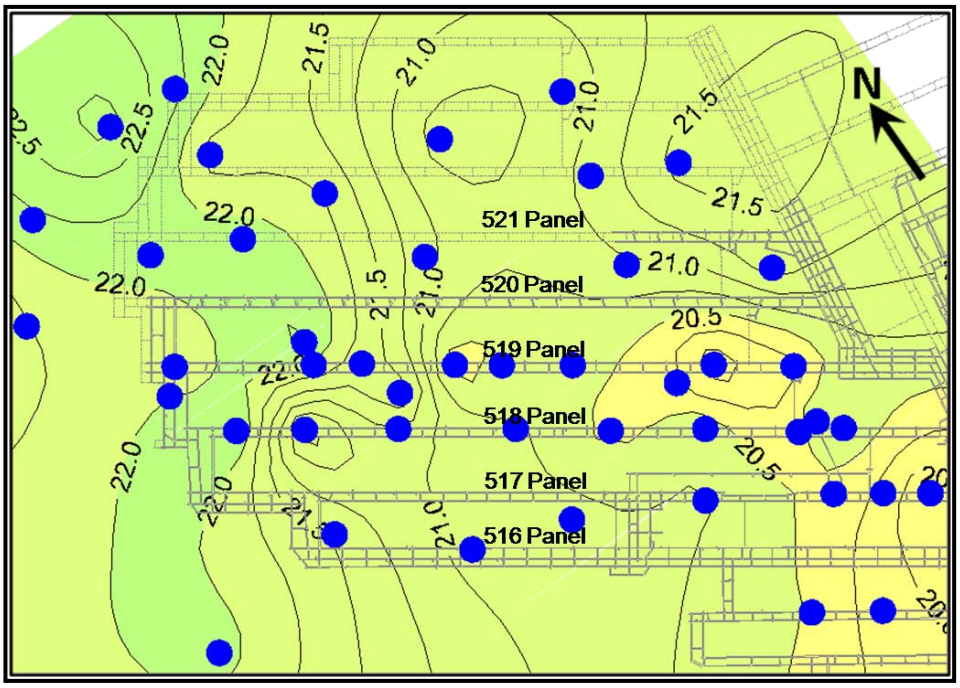

Figure 4.21: Volatile matter contours relative to mine workings and coal sample location

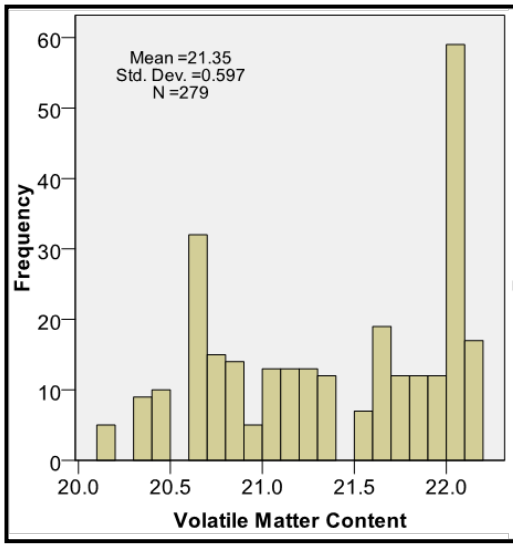

Figure 4.22: Distribution of volatile matter content for all boreholes within the complete dataset

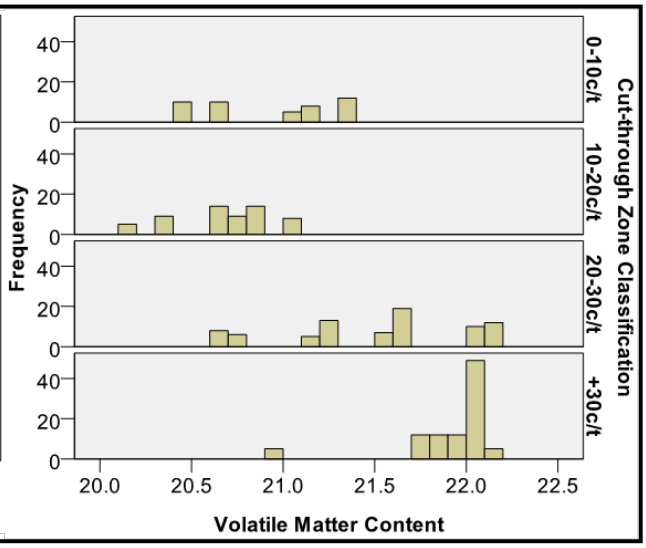

Figure 4.23: Distribution of volatile matter content for boreholes in each cut-through zone

Figure 4.24 and Figure 4.25 show the relationship between volatile matter and gas production, with increased total and D50 production from boreholes located in areas of lower volatile matter content. Statistical analysis identified a negative correlation of –0.577 and –0.576 between volatile matter content and each of total production and D50 production.

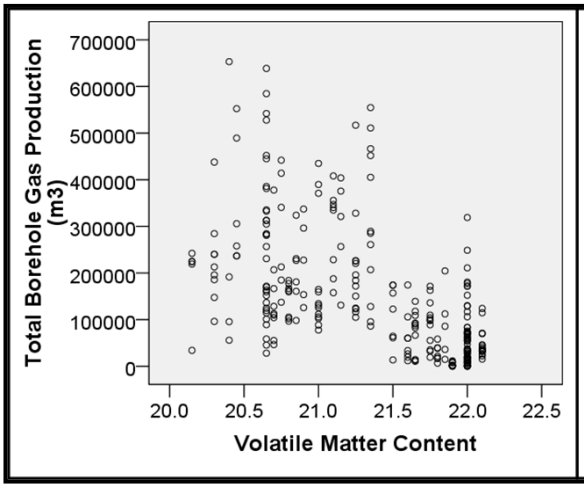

Figure 4.24: Total gas production relative to volatile matter content

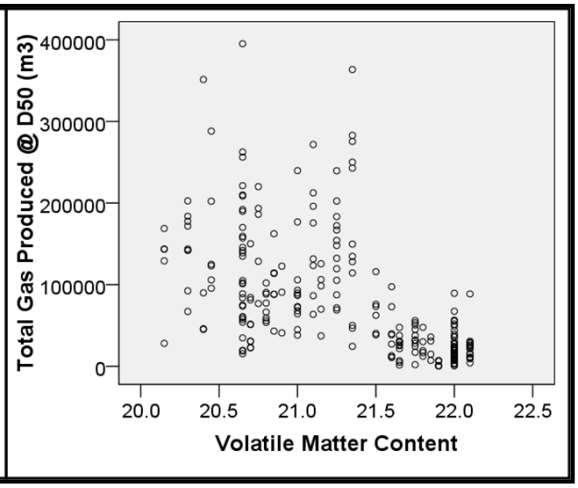

Figure 4.25: D50 gas production relative to volatile matter content

The relationship between volatile matter and both total and D50 gas production within each cut-through zone was also considered. As shown in Figure 4.26 and Figure 4.27 the maximum gas production in each zone tends to be greater in areas of reduced volatile matter content. This relationship is particularly evident in the 20-30c/t and +30c/t zones where the volatile matter spans approximately 1.5%.

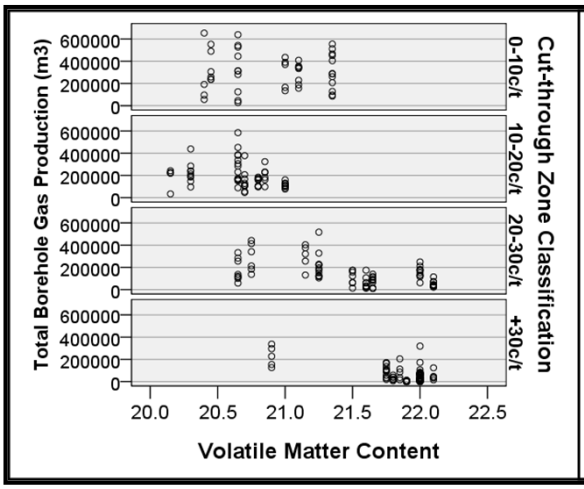

Figure 4.26: Total gas production relative to volatile matter content in each cut-through zone

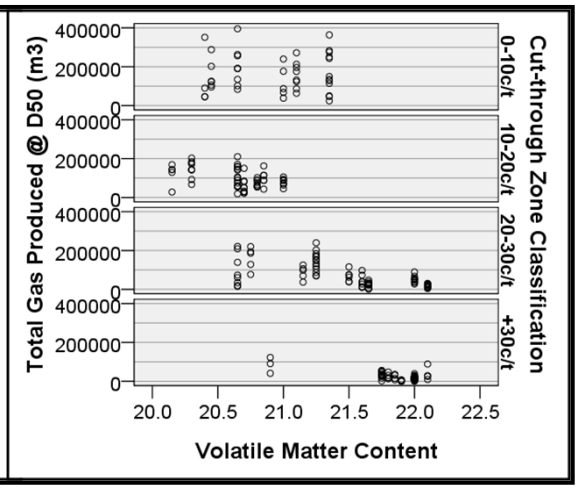

Figure 4.27: D50 gas production relative to volatile matter content in each cut-through zone

This assessment has shown increased gas production was achieved from boreholes located in areas with lower volatile matter content and this relationship appears to be independent of location along the panels. Therefore in this case the data indicates that volatile matter content, and therefore coal rank, has an impact on gas production.

4.4.1.3 Vitrinite Reflectance

Table 4.5 provides a summary of the results of vitrinite reflectance analysis conducted on 57 coal samples, reported by Clark (1986-2007). The vitrinite reflectance values were used to generate the contour plot, shown relative to current and future mine workings in Figure 4.28.

Table 4.5: Vitrinite reflectance data source and summary information (after Clark, 1986-2007)

Vitrinite reflectance	number of samples	Average (%)	Data range (%)		Sample collection & analysis	
			Minimum	Maximum	From	To
SIS core sample	29	1.28	1.22	1.36	13/08/1986	5/12/2007
UG strip sample	28	1.29	1.27	1.33	8/08/2001	6/08/2007
Combined	57	1.29	1.22	1.36	13/08/1986	5/12/2007

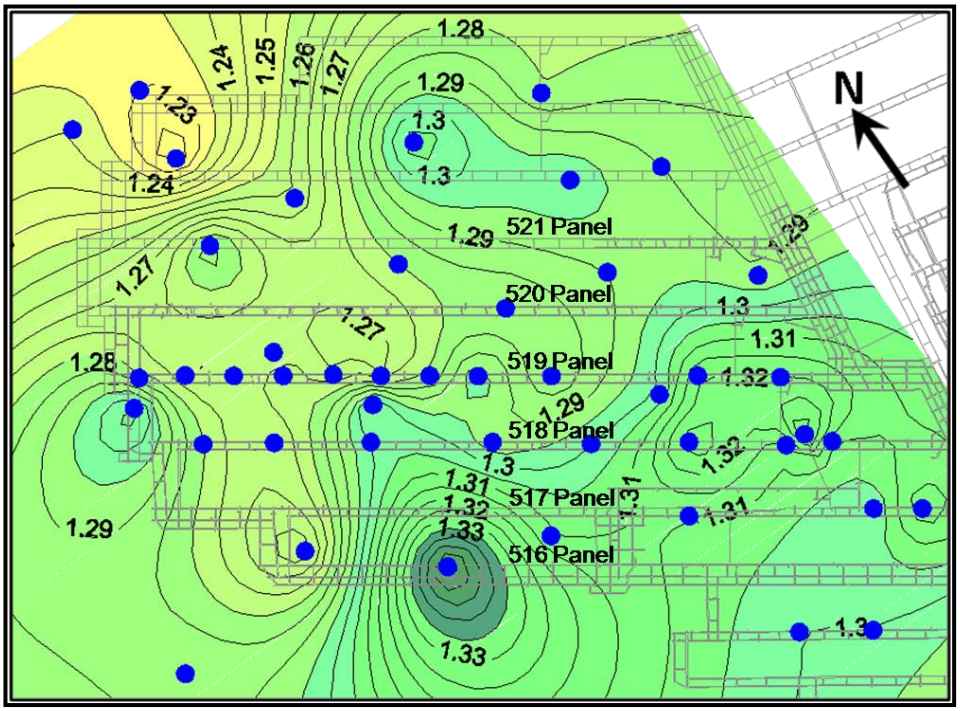

Figure 4.28: Vitrinite reflectance contours relative to mine workings and coal sample location

Figure 4.29 and Figure 4.30 show the distribution of estimated average vitrinite reflectance corresponding to the boreholes in the complete dataset and in each of the four cut-through zones. The average vitrinite reflectance of all boreholes in the dataset was 1.29%, with the range extending from a low of 1.26% to a high of 1.32%. Vitrinite reflectance was found to decrease with distance into the panels, with the average in each cut-through zone decreasing from a high of 1.30%, in the 0-10c/t zone, to a low of 1.28%, in the +30c/t zone.

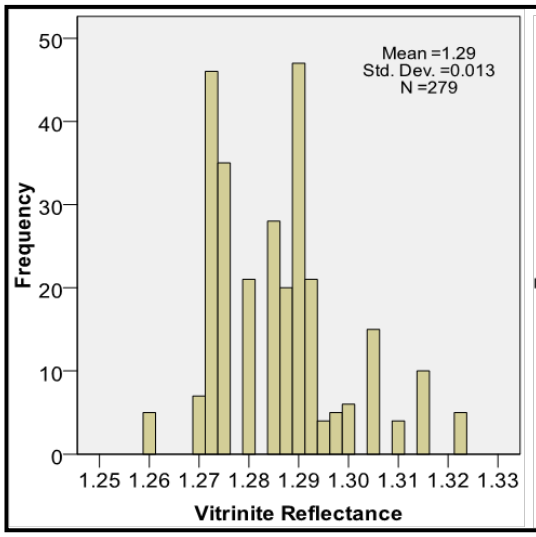

Figure 4.29: Distribution of vitrinite reflectance for all boreholes within the complete dataset

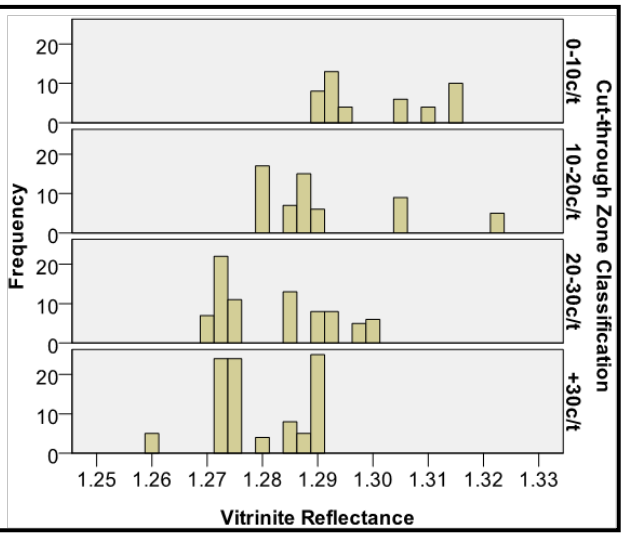

Figure 4.30: Distribution of vitrinite reflectance for boreholes in each cut-through zone

Figure 4.31 and Figure 4.32 show the relationship between vitrinite reflectance and gas production, with increased total and D50 production from boreholes located in areas of greater vitrinite reflectance. Statistical analysis determined a positive correlation of 0.479 and 0.537 between vitrinite reflectance and each of total production and D50 production.

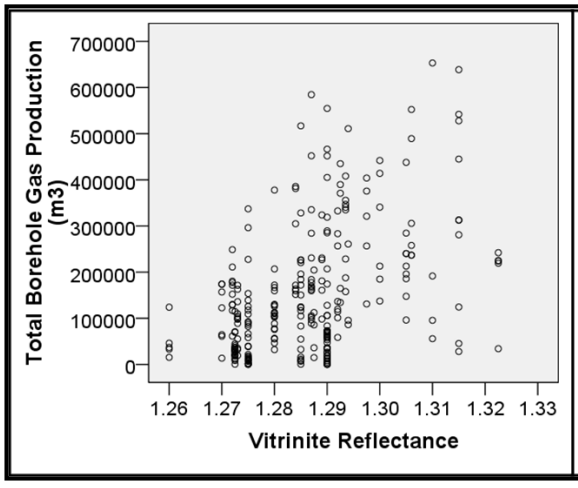

Figure 4.31: Total gas production relative to vitrinite reflectance

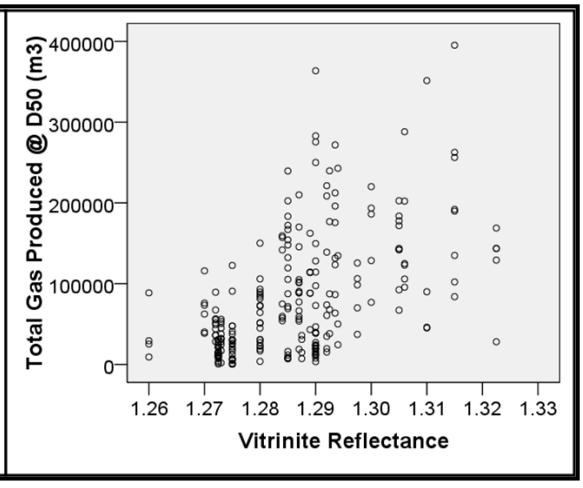

Figure 4.32: D50 gas production relative to vitrinite reflectance

The relationship between vitrinite reflectance and both total and D50 gas production within each cut-through zone was also considered. The gas production data relative to vitrinite reflectance within each cut-through zone is presented in Figure 4.33 and Figure 4.34. The data show highly variable gas production relative to vitrinite reflectance from which it is difficult to identify a relationship, with the exception of the 20-30c/t zone

which suggest increased gas production corresponding to increasing vitrinite reflectance. The range of vitrinite reflectance data within each cut-through zone is quite narrow, with a maximum span of 0.04% in the 10-20c/t zone, which makes it difficult to identify a relationship.

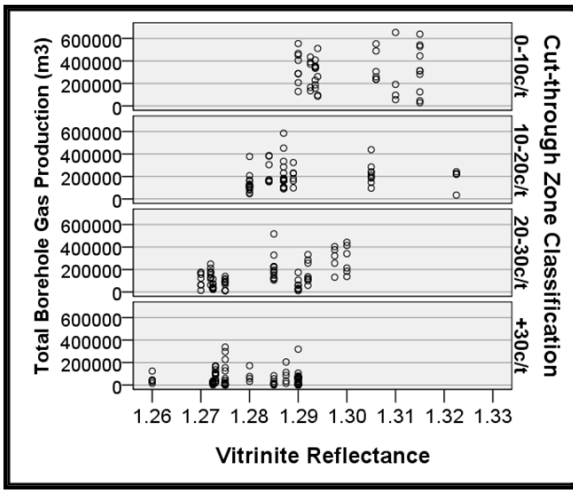

Figure 4.33: Total gas production relative to vitrinite reflectance in each cut-through zone

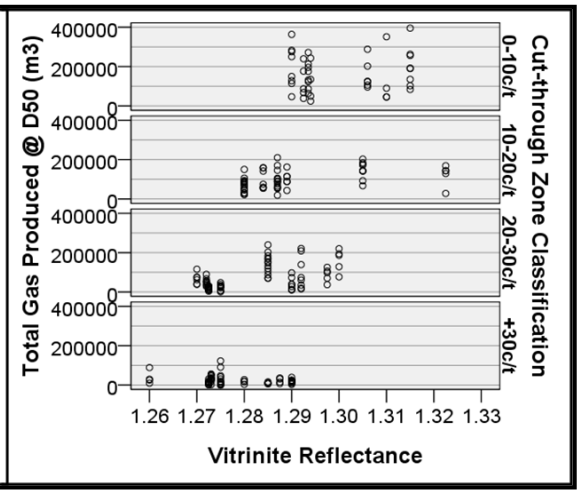

Figure 4.34: D50 gas production relative to vitrinite reflectance in each cut-through zone

This assessment has shown that although increased gas production was achieved from boreholes located in areas which happen to have greater vitrinite reflectance the relationship between the two variables is not particularly strong.

Of the three coal rank components considered, carbon content was found to have the strongest relationship to gas production. While not as strong, there was evidence of a relationship between volatile matter and gas production. Therefore from this analysis it was concluded that a relationship exists between coal rank and gas production with increased gas production from coal of higher rank. This result is contrary to the findings of a study at Metropolitan Colliery, by Battino and Hargraves (1982), which reported decreased gas drainage from areas of higher rank coal.

4.4.2 Coal Type

Testing conducted by Crosdale (1998) indicated maceral composition had little effect on the rate of gas flow from coal. In this section the results of petrographic analysis of coal samples from the mining area, in particular inertinite content, vitrinite content and mineral matter content, has been assessed relative to gas production data to determine whether a relationship exists.

4.4.2.1 Inertinite Maceral Component

Table 4.6 provides a summary of inertinite maceral content from testing conducted on 58 coal samples, reported by Clark (1986-2007). The inertinite content values were used to generate the contour plot, shown relative to current and future mine workings in Figure 4.35.

Table 4.6: Inertinite maceral data source and summary information (after Clark, 1986-2007)

Inertinite maceral content	number of samples	Average (%)	Data range (%)		Sample collection & analysis	
			Minimum	Maximum	From	To
SIS core sample	29	57.5	45.1	67.5	13/08/1986	5/12/2007
UG strip sample	29	56.3	51.0	63.0	8/08/2001	6/08/2007
Combined	58	56.9	45.1	67.5	13/08/1986	5/12/2007

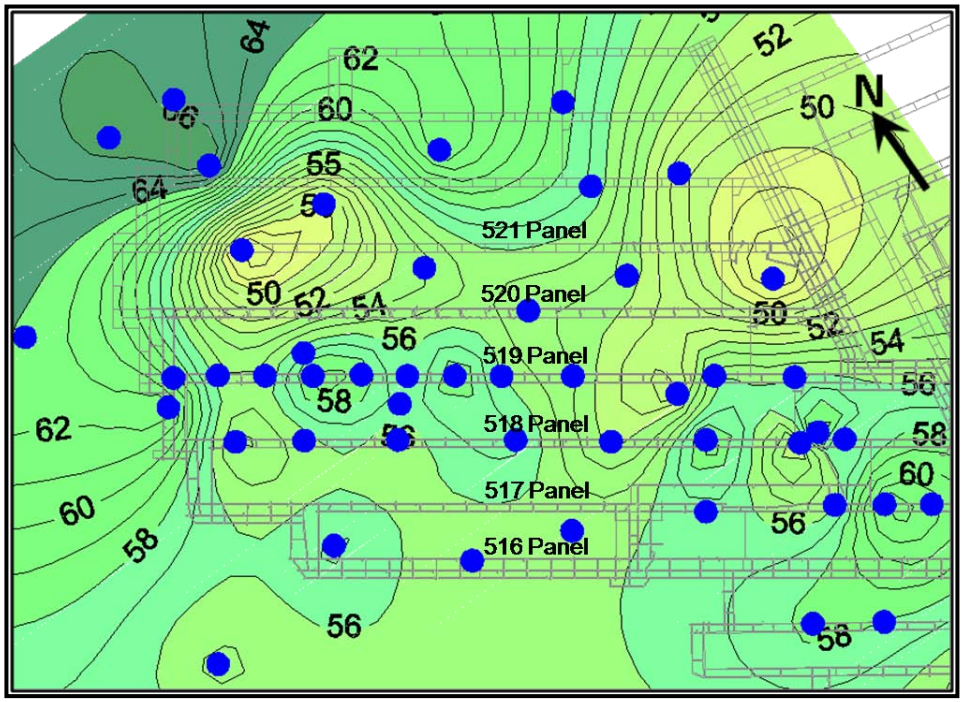

Figure 4.35: Inertinite contours relative to mine workings and coal sample location

Figure 4.36 and Figure 4.37 show the distribution of estimated average inertinite content corresponding to the boreholes in the complete dataset and in each of the four cut-through zones. The average inertinite content of all boreholes in the dataset was 55.4%, with the range extending from a low of 47.0% to a high of 61.5%. The inertinite content was found to increase with distance into the panels, with the average inertinite content in each cut-through zone increasing from a low of 51.7%, in the 0-10c/t zone, to a high of 57.5%, in the +30c/t zone.

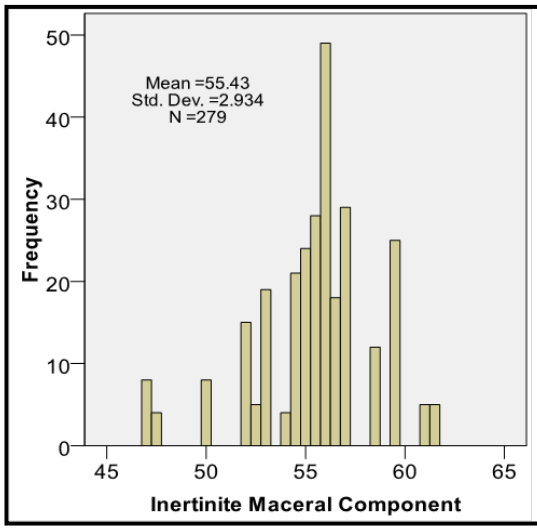

Figure 4.36: Distribution of inertinite content for all boreholes within the complete dataset

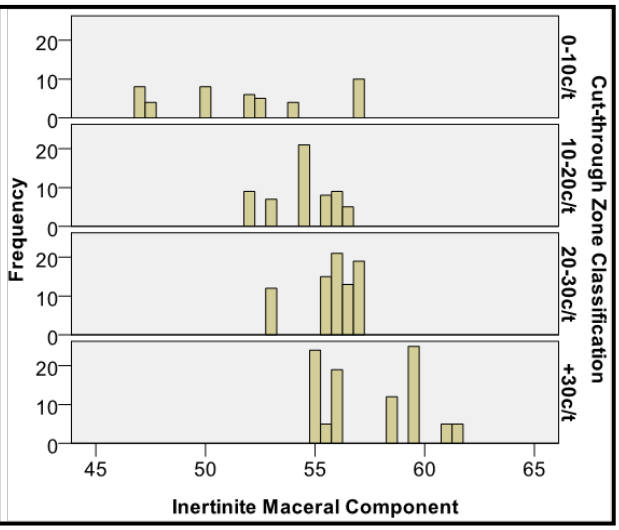

Figure 4.37: Distribution of inertinite content for boreholes in each cut-through zone

Figure 4.38 and Figure 4.39 show the relationship between inertinite content and gas production, which on average indicate increased total and D50 production from boreholes located in areas of reduced inertinite content. Statistical analysis confirmed a negative correlation of –0.440 and –0.410 between inertinite content and both total production and D50 production.

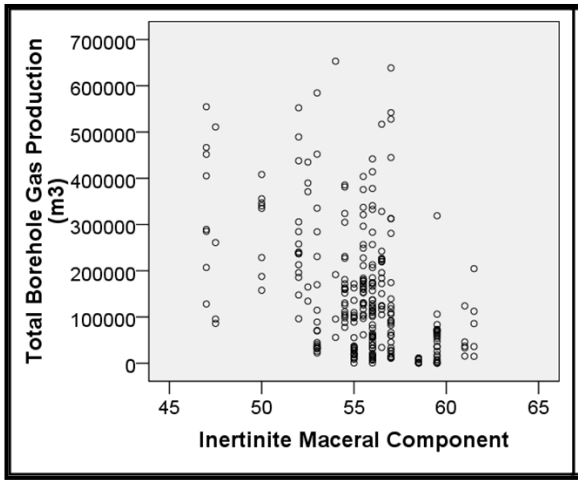

Figure 4.38: Total gas production relative to inertinite content

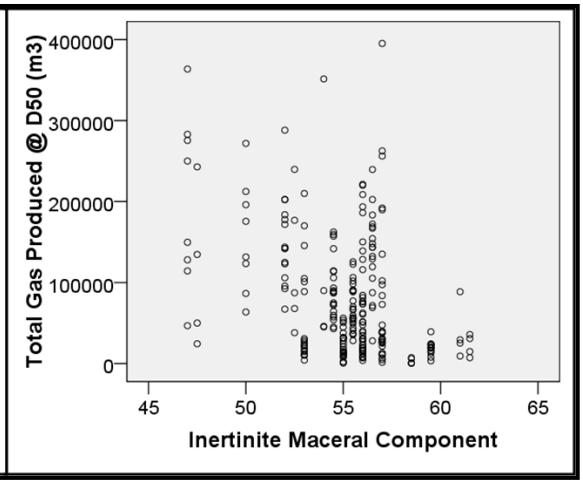

Figure 4.39: D50 gas production relative to inertinite content

The relationship between inertinite content and both total and D50 gas production within each cut-through zone was also considered. As shown in Figure 4.40 and Figure 4.41, within the relatively narrow inertinite content data range considered, there was no discernable relationship between gas production and inertinite content in any of the four cut-through zones. Therefore the relationship observed in the assessment of the total

dataset was considered to be merely a coincidence and the result of the higher producing outbye zone having generally lower inertinite content than the less productive inbye zones.

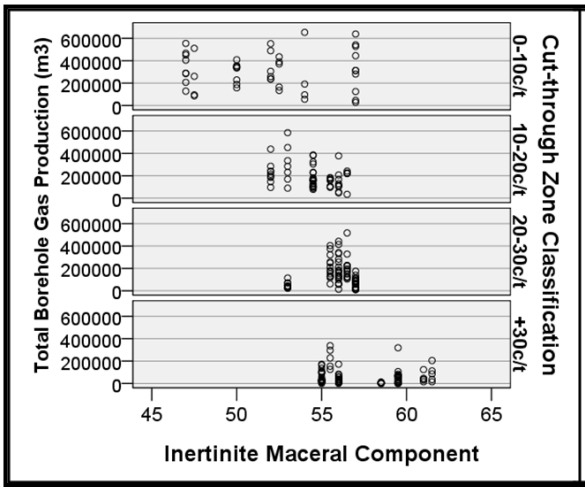

Figure 4.40: Total gas production relative to inertinite content in each cut-through zone

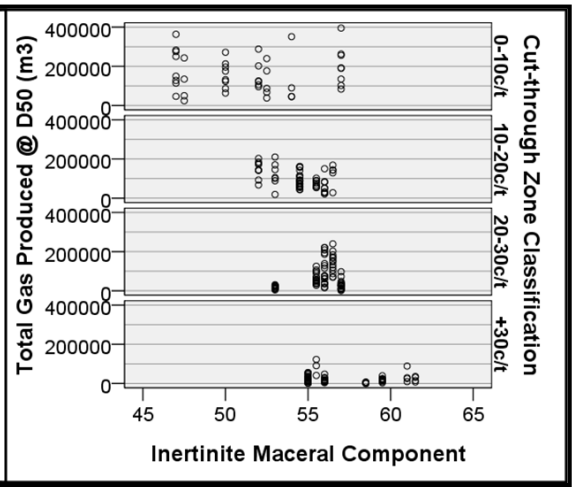

Figure 4.41: D50 gas production relative to inertinite content in each cut-through zone

From this assessment it was concluded that in this case inertinite content has little impact on gas production.

4.4.2.2 Vitrinite Maceral Component

Table 4.7 provides a summary of vitrinite maceral content testing conducted on 58 coal samples, reported by Clark (1986-2007). The vitrinite content values were used to generate the contour plot, shown relative to current and future mine workings in Figure 4.42. The contours show the vitrinite content of the Bulli seam throughout the mining area was variable, however two areas of increased vitrinite content were recorded at opposite ends of the 521 panel.

Table 4.7: Vitrinite maceral data source and summary information (after Clark, 1986-2007)

Vitrinite maceral content	number of samples	Average (%)	Data range (%)		Sample collection & analysis	
			Minimum	Maximum	From	To
SIS core sample	29	42.2	32.5	54.9	13/08/1986	5/12/2007
UG strip sample	29	43.7	36.9	49.0	8/08/2001	6/08/2007
Combined	58	43	32.5	54.9	13/08/1986	5/12/2007

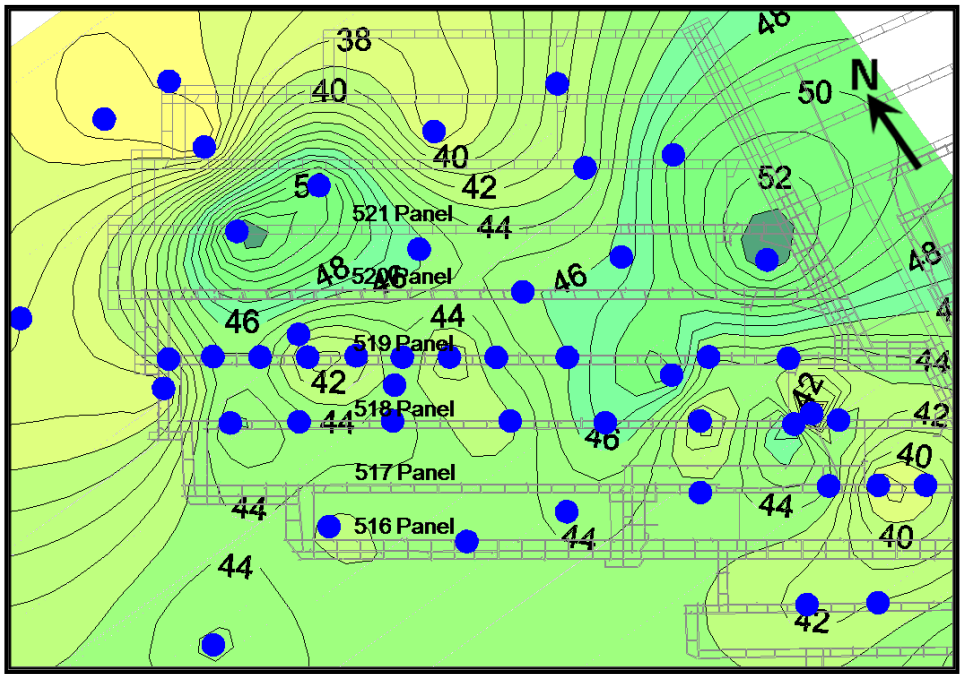

Figure 4.42: Vitrinite contours relative to mine workings and coal sample location

Figure 4.43 and Figure 4.44 show the distribution of estimated average vitrinite content corresponding to the boreholes in the complete dataset and in each of the four cut-through zones. The average vitrinite content of all boreholes in the dataset was 44.6%, with the range extending from a low of 38.5% to a high of 53.0%. Vitrinite content was found to decrease with distance into the panels, with the average vitrinite content in each cut-through zone decreasing from a high of 48.3%, in the 0-10c/t zone, to a low of 42.5%, in the +30c/t zone.

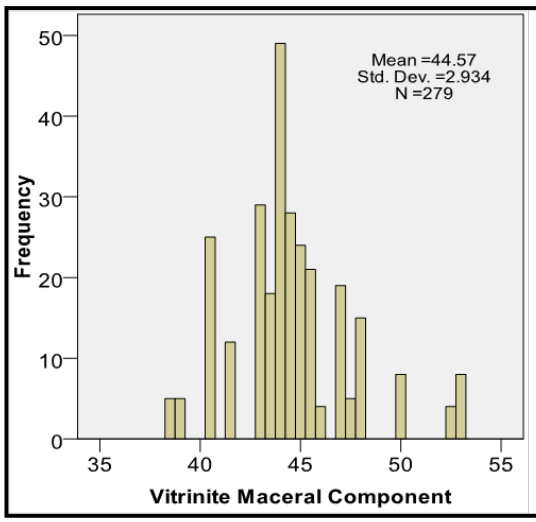

Figure 4.43: Distribution of vitrinite content for all boreholes within the complete dataset

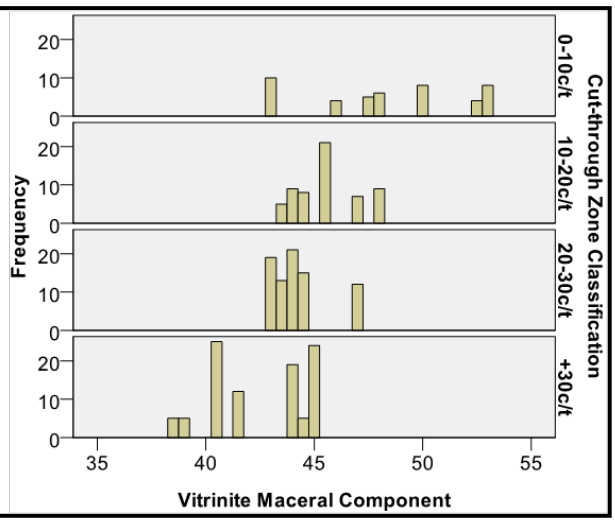

Figure 4.44: Distribution of vitrinite content for boreholes in each cut-through zone

Figure 4.45 and Figure 4.46 show the relationship between vitrinite content and gas production, with greater total and D50 gas production from boreholes located in areas of increased vitrinite content. Statistical analysis confirmed a positive correlation of 0.440 and 0.410 between vitrinite content and each of total production and D50 production.

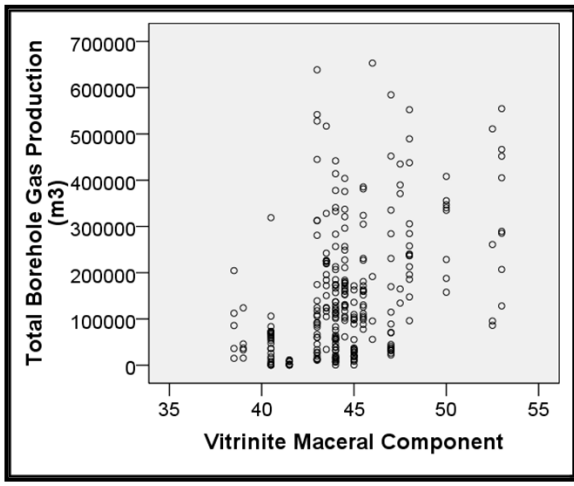

Figure 4.45: Total gas production relative to vitrinite content

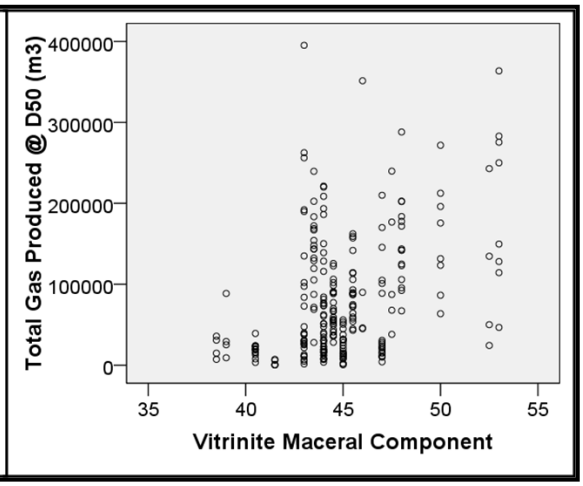

Figure 4.46: D50 gas production relative to vitrinite content

The relationship between vitrinite content and both total and D50 gas production within each cut-through zone was also considered. As shown in Figure 4.47 and Figure 4.48, within the relatively narrow vitrinite content data range considered, there was no discernable relationship between gas production and vitrinite content in any of the four cut-through zones.

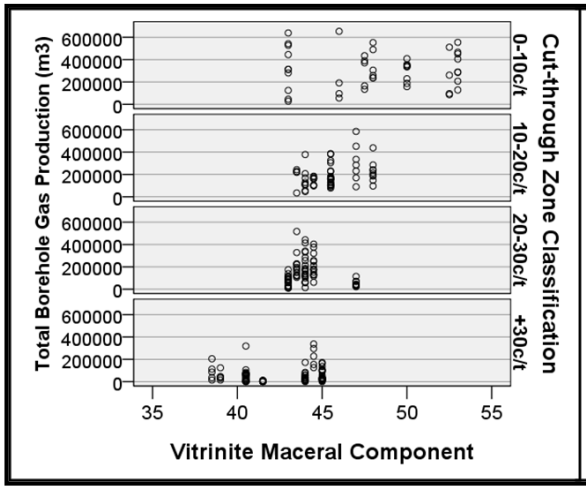

Figure 4.47: Total gas production relative to vitrinite content in each cut-through zone

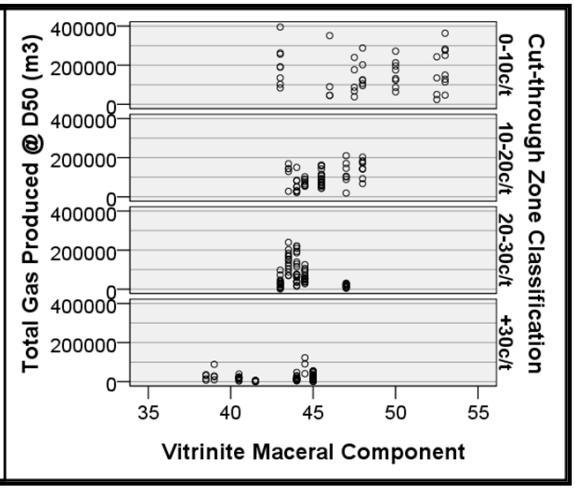

Figure 4.48: D50 gas production relative to vitrinite content in each cut-through zone

From this assessment it was concluded that vitrinite content has little impact on gas production.

4.4.2.3 Mineral Matter Component

Table 4.8 provides a summary of mineral matter content results from petrographic analysis conducted on 58 coal samples, reported by Clark (1986-2007). The results were used to generate the mineral matter contour plot, shown relative to current and future mine workings in Figure 4.49.

Table 4.8: Mineral matter data source and summary information (after Clark, 1986-2007)

Mineral matter content	number of samples	Average (%)	Data range (%)		Sample collection & analysis	
			Minimum	Maximum	From	To
SIS core sample	29	3.7	2.0	8.2	13/08/1986	5/12/2007
UG strip sample	29	3.5	2.0	5.8	8/08/2001	6/08/2007
Combined	58	3.6	2.0	8.2	13/08/1986	5/12/2007

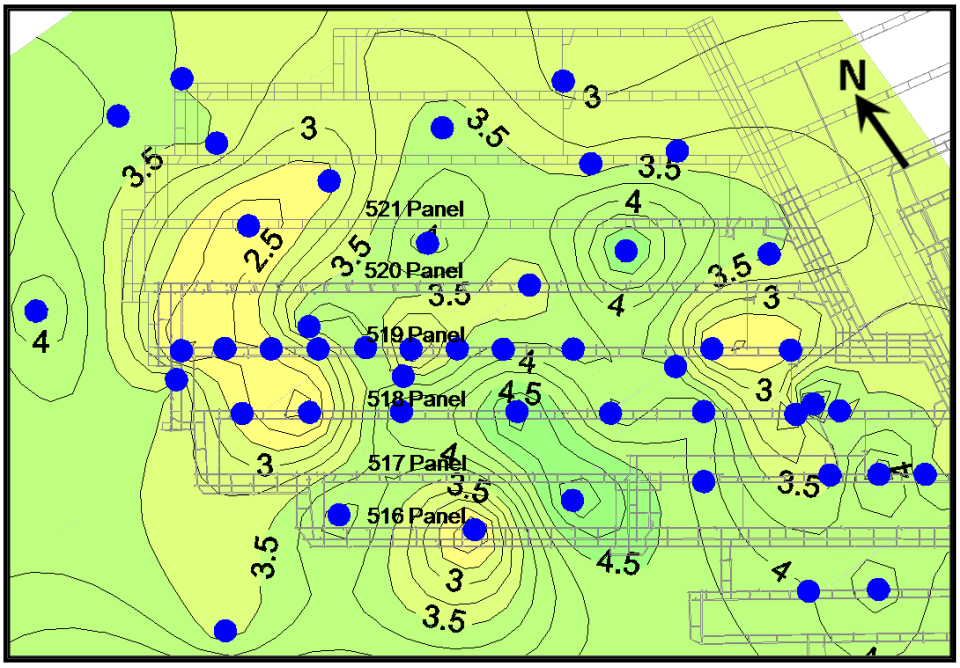

Figure 4.49: Mineral matter contours relative to mine workings and coal sample location

Figure 4.50 and Figure 4.51 show the distribution of estimated average mineral matter content corresponding to the boreholes in the complete dataset and in each of the four cut-through zones. The average mineral matter content of all boreholes in the dataset was 3.3%, with the range extending from a low of 2.4% to a high of 4.6%. Although variable, the average mineral matter in each cut-through zone was found to be reasonably consistent, at approximately 3.6% in the first three cut-through zones, decreasing to 2.8% in the +30c/t zone.

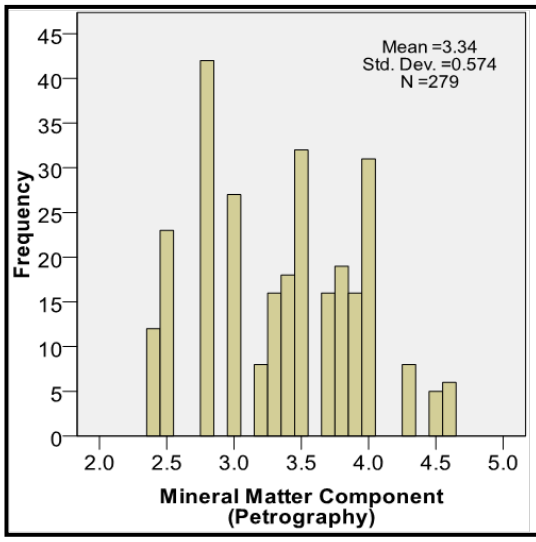

Figure 4.50: Distribution of mineral matter for all boreholes within the complete dataset

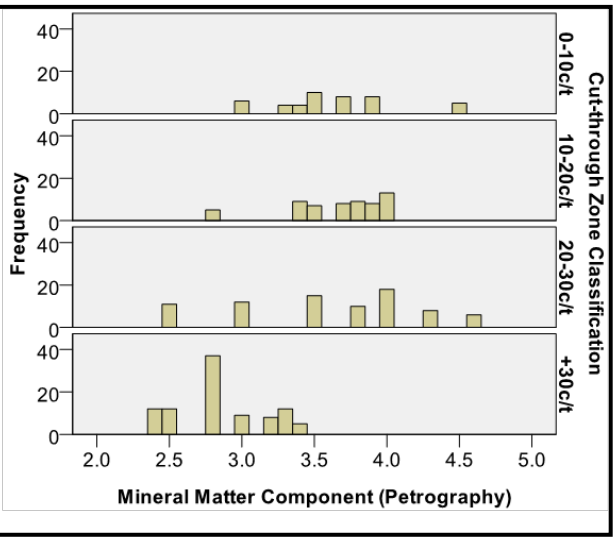

Figure 4.51: Distribution of mineral matter for boreholes in each cut-through zone

Figure 4.52 and Figure 4.53 show the relationship between mineral matter content and gas production, with some indication of increased total and D50 gas production from boreholes located in areas where mineral matter content was between 3.0 and 4.0%.

Statistical analysis confirmed a positive correlation of 0.483 and 0.479 between mineral matter content and each of total production and D50 production.

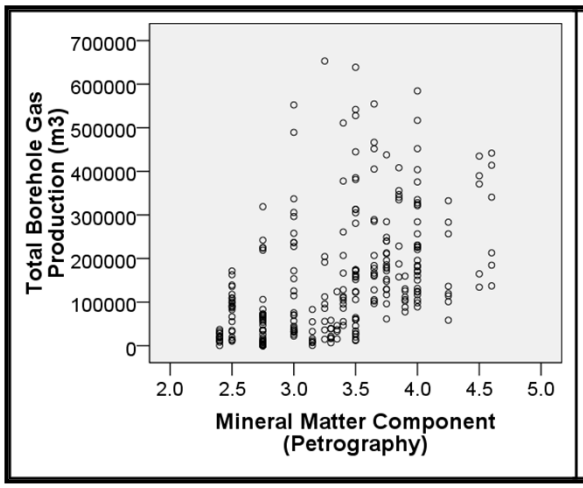

Figure 4.52: Total gas production relative to mineral matter content

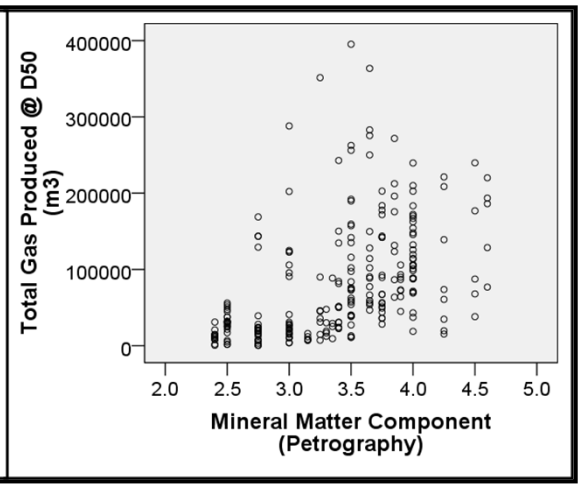

Figure 4.53: D50 gas production relative to mineral matter content

The relationship between mineral matter and both total and D50 gas production within each cut-through zone was also considered. As shown in Figure 4.54 and Figure 4.55, with the exception of the 20-30c/t zone which suggests greater gas production in areas of increased mineral matter content, the data does not support a relationship between mineral matter content and gas production.

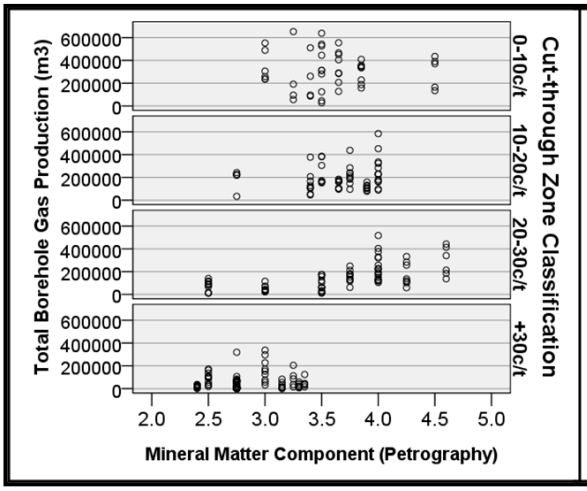

Figure 4.54: Total gas production relative to mineral matter content in each cut-through zone

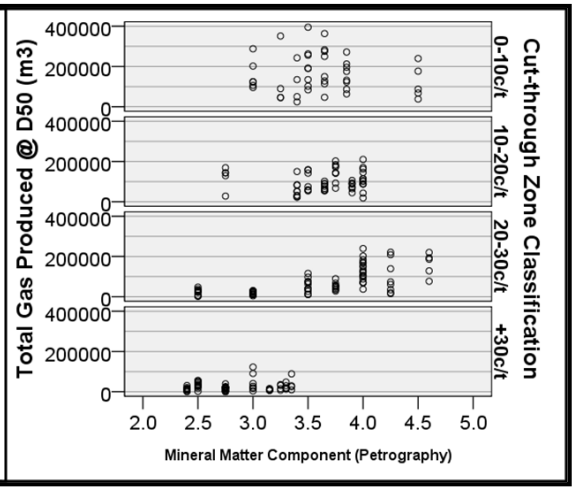

Figure 4.55: D50 gas production relative to mineral matter content in each cut-through zone

This assessment has shown that neither maceral type nor mineral matter content has significant impact on coal seam gas production. This result was consistent with the findings of Crosdale (1998).

4.4.3 Ash Content

The relationship between ash content and coal seam gas production was assessed considering two separate ash measurements. The first, seam ash, also known as raw ash, was determined through density separation whereby the heavier ‘ash’ component was separated from the lighter ‘coal’ component in a density controlled bath. The second, coal ash, was determined through proximate analysis of the ‘coal’ component and constitutes the non-combustible inorganic residue that remains following the burning of the coal (Ward, 1984).

Statistical analysis of the raw seam ash and coal ash values corresponding to each of the 279 boreholes confirmed a weak correlation of 0.291, suggesting the two variables are independent of each other. Considering the distribution of seam ash and coal ash within each of the four cut-through zones, seam ash was found to be relatively consistent along the length of the panels (Figure 4.56), whereas coal ash progressively increased with distance into the panels (Figure 4.57).

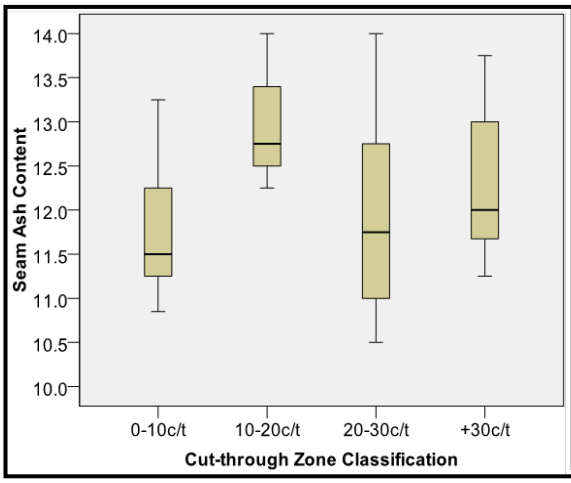

Figure 4.56: Span and average seam ash content in each cut-through zone

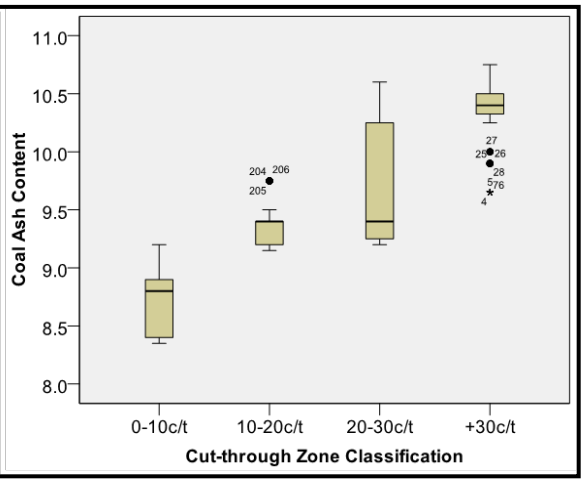

Figure 4.57: Span and average coal ash content in each cut-through zone

Figure 4.58 shows the type and relative percentage of minerals present within the coal ash, determined from proximate analysis testing of 60 coal samples, reported by Clark (1986-2007). The mineral composition of the samples analysed was found to be quite consistent, with the dominant minerals being silicon dioxide (SiO_2) and aluminium oxide (Al_2O_3).

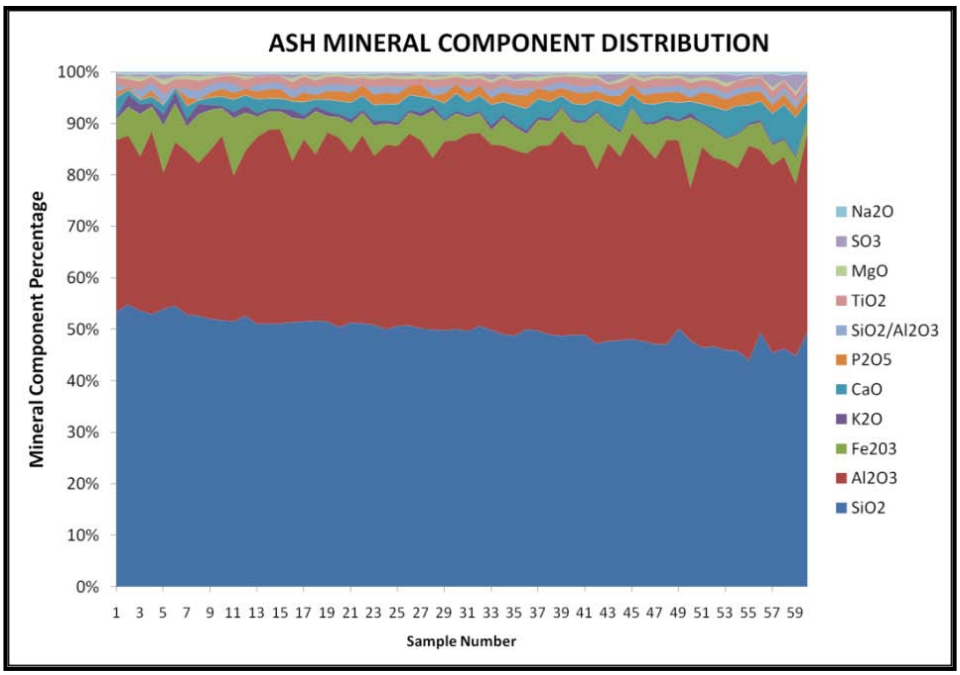

Figure 4.58: Coal ash mineral type and relative percentage

4.4.3.1 Seam Ash

Table 4.9 provides a summary of the results of seam ash content analysis conducted on 62 coal samples, reported by Clark (1986-2007). The seam ash values were used to

generate the contour plot, shown relative to current and future mine workings in Figure 4.59.

Table 4.9: Seam ash data source and summary information (after Clark, 1986-2007)

Seam (raw) ash content	number of samples	Average (%)	Data range (%)		Sample collection & analysis	
			Minimum	Maximum	From	To
SIS core sample	33	11.7	8.8	18.0	13/08/1986	5/12/2007
UG strip sample	29	12.5	8.8	19.6	8/08/2001	6/08/2007
Combined	62	12.0	8.8	19.6	13/08/1986	5/12/2007

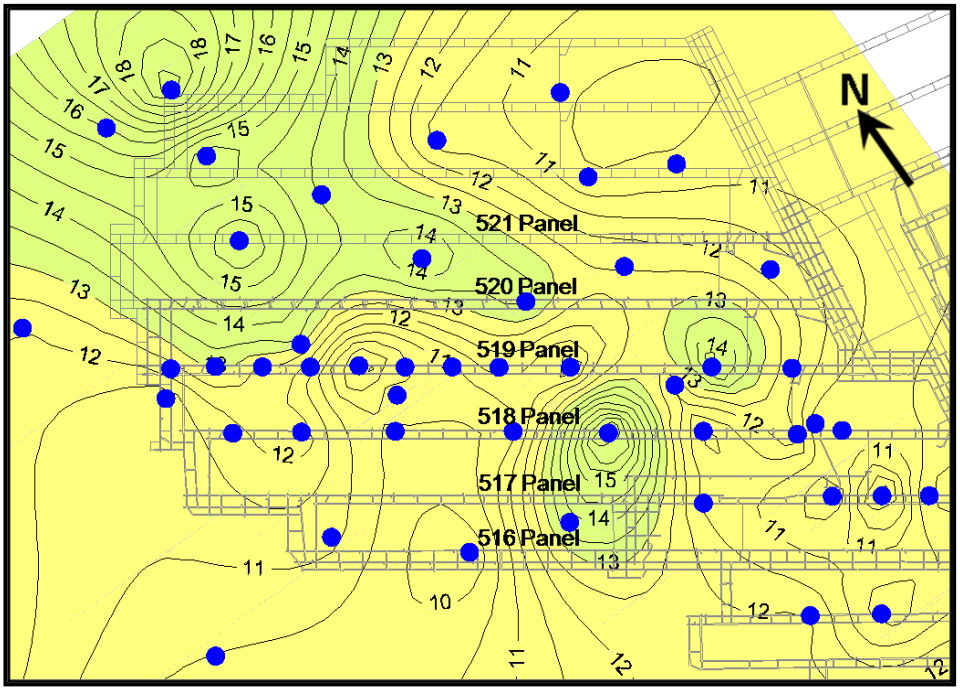

Figure 4.59: Seam ash contours relative to mine workings and coal sample location

Figure 4.60 and Figure 4.61 show the distribution of estimated average seam ash content corresponding to the boreholes in the complete dataset and in each of the four cut-through zones. The average seam ash content of all boreholes in the dataset was 12.2%, with the range extending from a low of 10.5% to a high of 14.0%. With the exception of an area of increased seam ash in the 10-20c/t zone, the seam ash content corresponding to the drill sites assessed was found to be reasonably consistent along the length of the panel. The average seam ash content in cut-through zone 10-20c/t and +30c/t was 12.9% and 12.3% respectively, while the other two zones, 0-10c/t and 20-30c/t, recorded lower average values of 11.8% and 11.9% respectively.

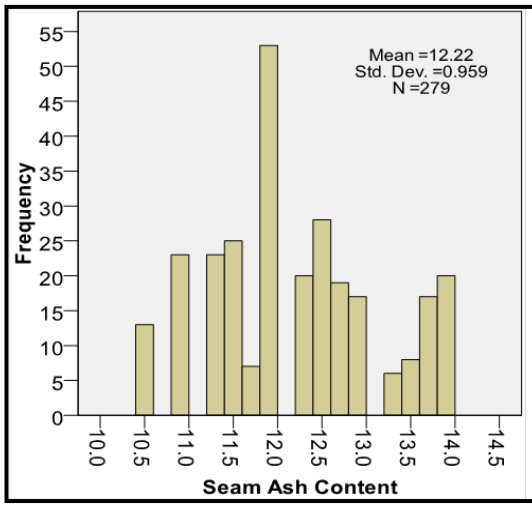

Figure 4.60: Distribution of seam ash content for all boreholes within the complete dataset

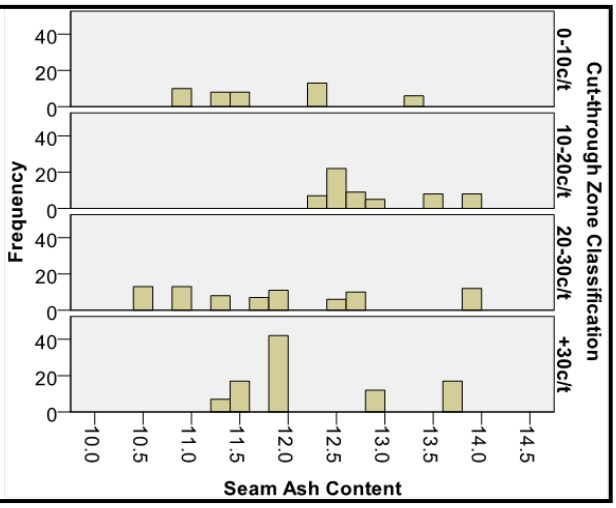

Figure 4.61: Distribution of seam ash content for boreholes in each cut-through zone

Figure 4.62 and Figure 4.63 show the relationship between seam ash and gas production, which indicate increased total and D50 production from boreholes located in areas of lower seam ash content. Statistical analysis determined a low negative correlation of –0.208 and –0.210 between seam ash content and both total and D50 gas production.

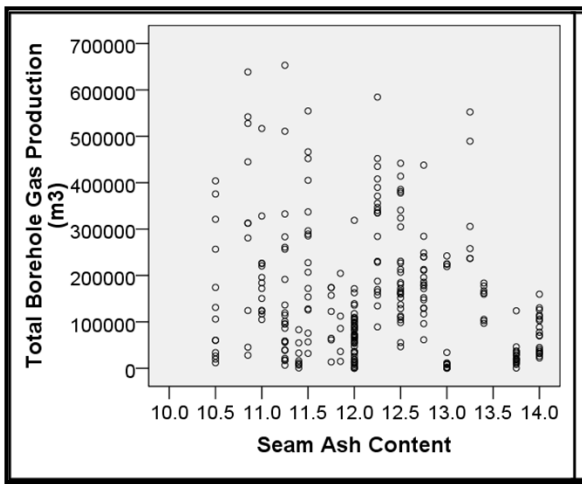

Figure 4.62: Total gas production relative to seam ash content

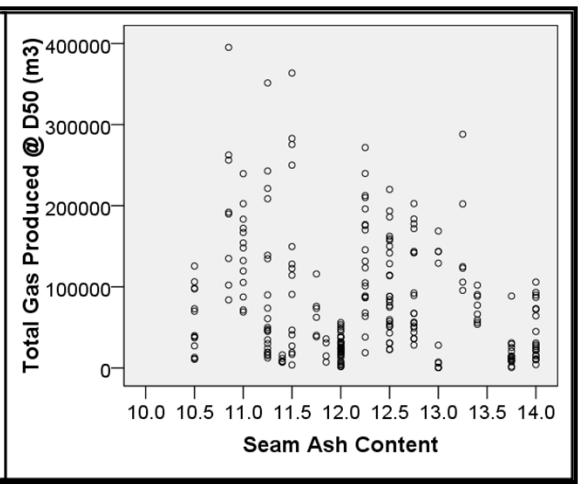

Figure 4.63: D50 gas production relative to seam ash content

The relationship between seam ash and gas production within each cut-through zone was also considered. As shown in Figure 4.64 and Figure 4.65, the maximum total and D50 gas production in each zone tends to be greater in areas of reduced seam ash content. This relationship was particularly evident in the 10-20c/t zone, although the seam ash spans only 2.0%.

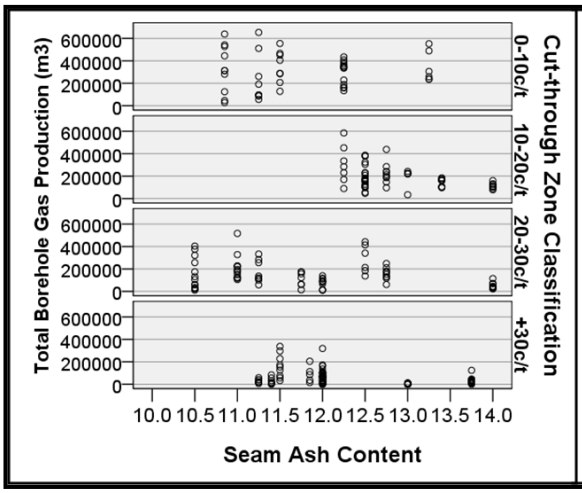

Figure 4.64: Total gas production relative to seam ash content in each cut-through zone

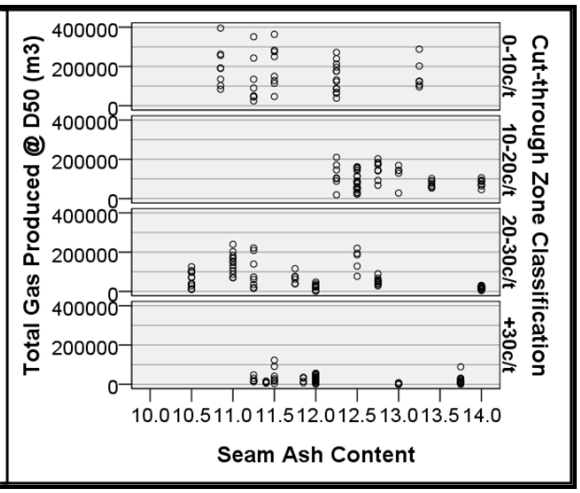

Figure 4.65: D50 gas production relative to seam ash content in each cut-through zone

This assessment has shown increased gas production was achieved from boreholes in areas of reduced seam ash content and this relationship appears to be independent of location along the panels. Therefore the data suggest seam ash content has some impact on gas production.

4.4.3.2 Coal Ash

Table 4.10 provides a summary of the results of coal ash content analysis conducted on 65 coal samples, reported by Clark (1986-2007). The coal ash values were used to generate the contour plot, shown relative to current and future mine workings in Figure 4.66.

Table 4.10: Coal ash data source and summary information (after Clark, 1986-2007)

Coal ash content	number of samples	Average (%)	Data range (%)		Sample collection & analysis	
			Minimum	Maximum	From	To
SIS core sample	34	9.1	8.0	11.5	13/08/1986	5/12/2007
UG strip sample	31	9.1	8.5	10.1	8/08/2001	6/08/2007
Combined	65	9.1	8.0	11.5	13/08/1986	5/12/2007

Figure 4.67 and Figure 4.68 show the distribution of estimated average coal ash content corresponding to the boreholes in the complete dataset and in each of the four cut-through zones. The average coal ash content of all boreholes in the dataset was 9.7%, with the range extending from a low of 8.4% to a high of 10.8%. The coal ash content was found to increase in a north to north-west direction, toward the inbye end of the panels. The average coal ash content of the boreholes located within each of the cut-

through zones increased from a low of 8.8%, in the 0-10c/t zone, to a high of 10.4%, in the +30c/t zone.

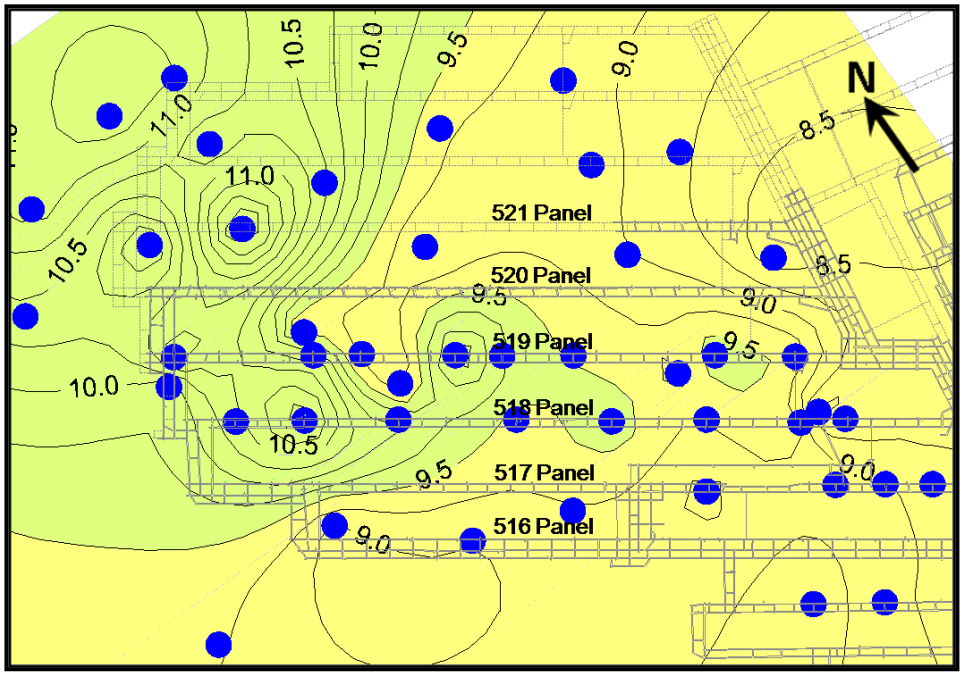

Figure 4.66: Coal ash contours relative to mine workings and coal sample location

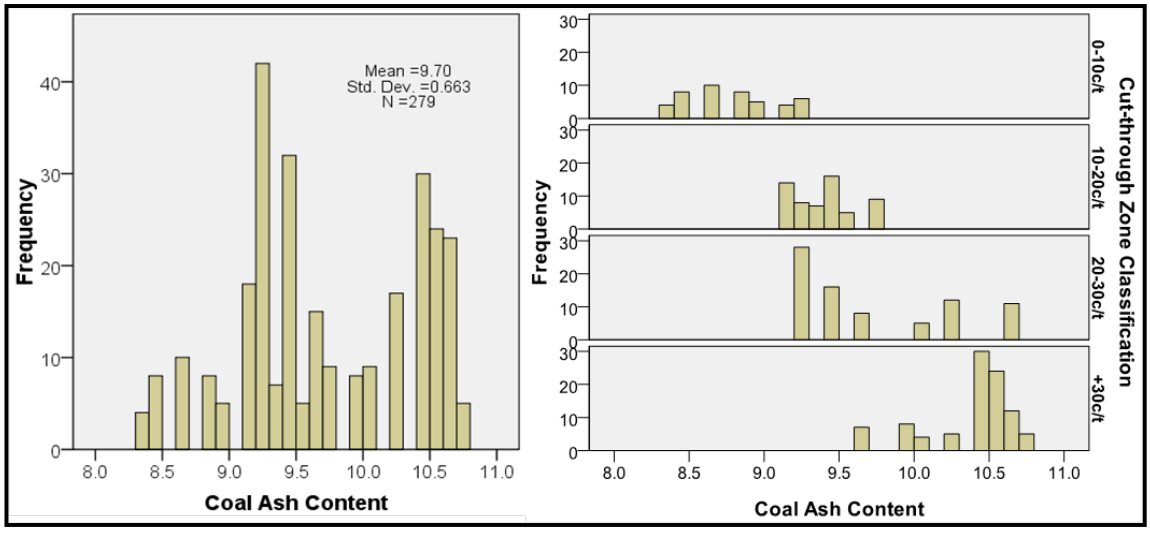

Figure 4.67: Distribution of coal ash content for all boreholes within the complete dataset

Figure 4.68: Distribution of coal ash content for boreholes in each cut-through zone

Figure 4.69 and Figure 4.70 show the relationship between coal ash and gas production, with increased total and D50 production from boreholes located in areas of lower coal ash content. Statistical analysis determined a negative correlation of –0.472 and –0.499 between coal ash content and each of total and D50 production.

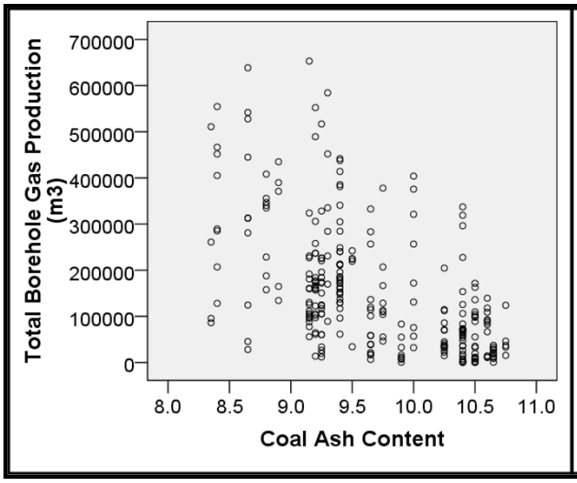

Figure 4.69: Total gas production relative to coal ash content

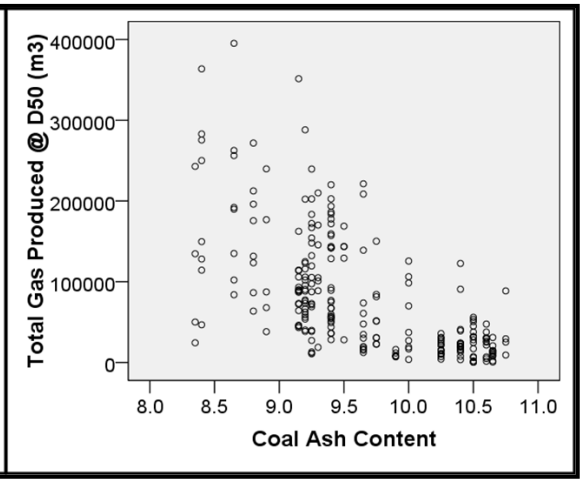

Figure 4.70: D50 gas production relative to coal ash content

The relationship between coal ash and gas production within each cut-through zone was also considered. As shown in Figure 4.71 and Figure 4.72, with the exception of the 0-10c/t zone, the maximum total and D50 gas production in each zone was greater in areas of reduced coal ash content.

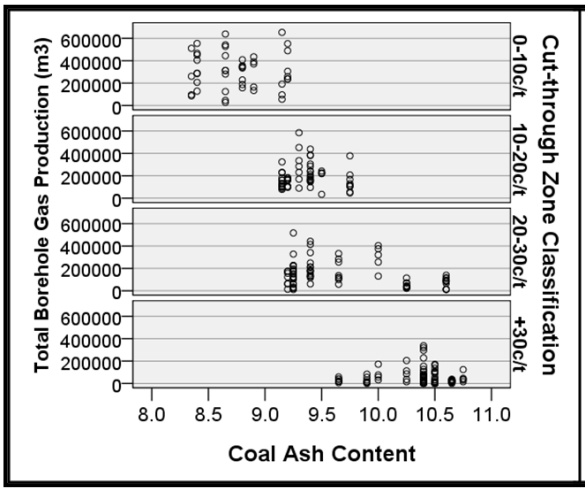

Figure 4.71: Total gas production relative to coal ash content in each cut-through zone

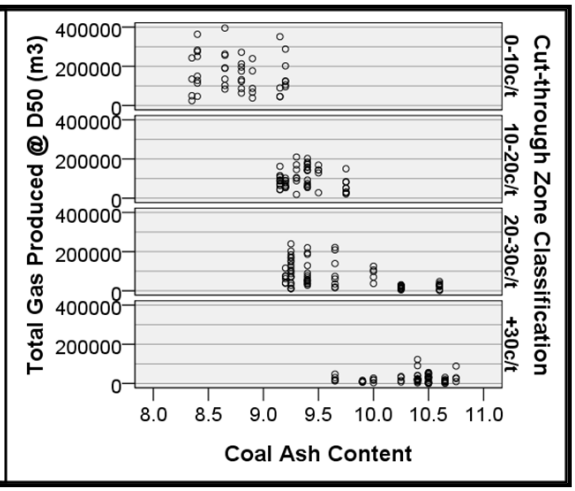

Figure 4.72: D50 gas production relative to coal ash content in each cut-through zone

From this assessment of the relationship between gas production and ash content it was found that gas production was greater in areas where both seam ash and coal ash were lower. The results of the analysis suggest that the relationship between gas production and coal ash content was stronger than the relationship between gas production and seam ash.

4.4.4 Permeability

Permeability is considered by many to have a significant impact on the ability of a coal seam to produce gas (Hayes, 1982; Jones *et al.*, 1982; Clark *et al.*, 1983; Osisanya and Schaffitzel, 1996; Zutshi and Harpalani, 2005; Cui and Bustin, 2006 and Lamarre, 2007). Permeability, which is closely related to the coal fabric (i.e. cleat spacing and aperture width), may vary significantly as fluid pressure changes during coal seam gas production (Cui and Busten, 2006). It has a strong affect on the gas production profile, and gas well performance.

Bulli seam permeability was measured using a combination of injection / falloff and step-rate testing methods (Jackson, 2004) and the results from 31 locations, reported by (Fredericks, 2008), were used to generate the contour plot, shown relative to current and future mine workings in Figure 4.73. The average permeability was 2.2 mD, with the range extending from a low of 0.005 mD to a high of 5.8 mD.

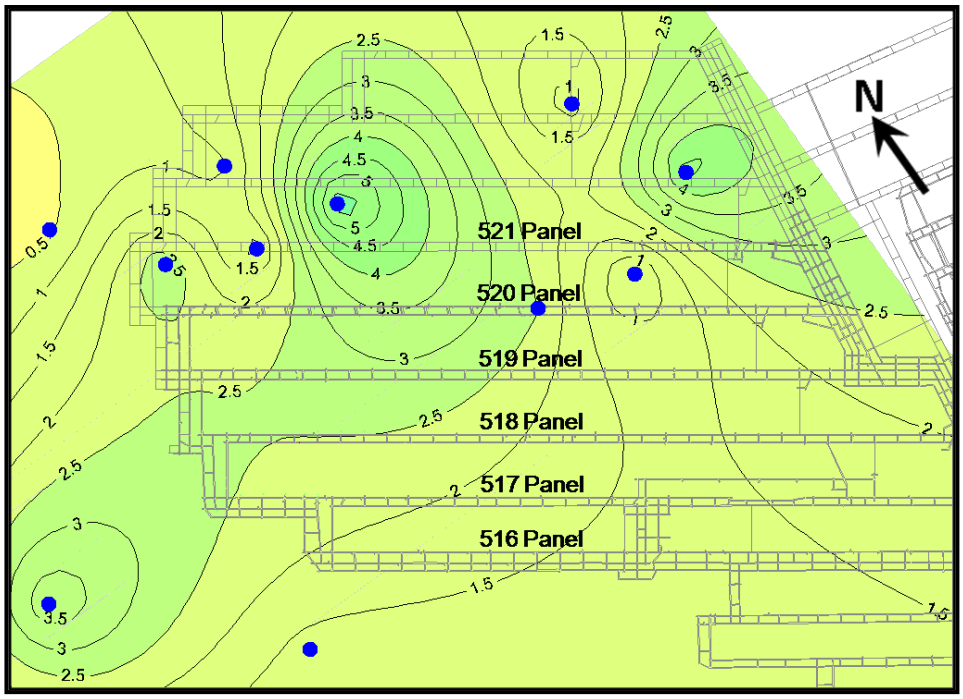

Figure 4.73: Permeability contours (mD) relative to mine workings and measurement locations

As shown, there were few permeability measurement sites within or in close proximity to the mining area. The low number of data points resulted in significant contour smoothing which was considered to reduce the accuracy of the contours within the area of interest to this study. Therefore the permeability contours, although indicative, are not considered to be sufficiently accurate to enable the coal seam permeability to be

reasonably estimated for each UIS borehole. Therefore an analysis of the relationship between permeability and UIS borehole gas production was not undertaken.

4.4.5 Inherent Moisture Content

The presence of water in a coal seam has a significant impact on the ability of that seam to produce gas. Osisanya and Schaffitzel (1996), Cui and Busten (2006), Jahediesfanjani and Civan (2006) and Meszaros *et al.* (2007) explain that water present within the coal cleat system exerts hydrostatic pressure on the adsorbed seam gas, preventing the gas from moving out of the micropores. It is not until the reservoir pressure is reduced that the methane desorbs off the coal surfaces enabling it to diffuse through the matrix to the cleat system where it flows to the borehole for delivery to the surface. At initial reservoir conditions the cleat is typically saturated with water, therefore during the initial production phase a large volume of water may be produced (Jahediesfanjani and Civan, 2006 and Lamarre, 2007). The rate at which water is produced steadily decreases during the initial production phase, whereas the gas production rate steadily increases until it reaches a plateau, or peak gas production rate, following which the gas production rate will decline as per a normal gas well (Lamarre, 2007).

Cui and Busten (2006) state that cleat porosity has an effect on the dewatering rate, and thus the gas production rate, in that the higher the cleat porosity, the greater the volume of water initially stored in the coal seam, and therefore more time is required to reduce the cleat pressure and enhance the gas relative permeability. Jahediesfanjani and Civan (2006) also note that following dewatering some water remains in the coal cleat and matrix system and this residual water may, subject to the nature of the coal seam, have a significant and ongoing impact on the ability to drain gas from the coal seam.

The rate of water production was not recorded as part of the routine UIS gas production borehole data collection protocol, therefore the impact of seam water content and water production rate on gas production was not assessed. There was however data relating to the inherent moisture content of coal samples sourced from within the mining area which was collated for use in this analysis.

Table 4.11 provides a summary of the inherent moisture content, also known as air-dried moisture content, measurement results determined during proximate analysis

testing of 59 samples, reported by Clark (1986-2007). The results were used to generate the contour plot of inherent moisture content, shown relative to current and future mine workings in Figure 4.74.

Table 4.11: Inherent moisture data source and summary information (after Clark, 1986-2007)

Inherent moisture content	number of samples	Average (%)	Data range (%)		Sample collection & analysis	
			Minimum	Maximum	From	To
SIS core sample	31	0.9	0.7	1.2	24/04/1991	5/12/2007
UG strip sample	28	1.0	0.8	1.3	8/08/2001	6/08/2007
Combined	59	1.0	0.7	1.3	24/04/1991	5/12/2007

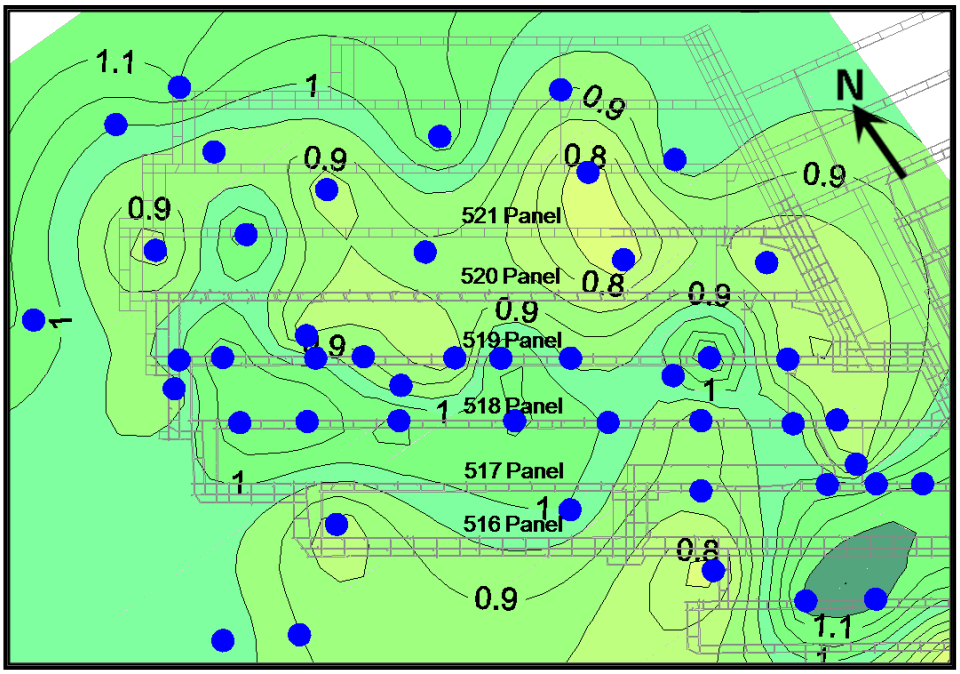

Figure 4.74: Inherent moisture contours relative to mine workings and coal sample location

Figure 4.75 and Figure 4.76 show the distribution of estimated average inherent moisture content corresponding to the boreholes in the complete dataset and in each of the four cut-through zones. The average inherent moisture content of all boreholes in the dataset was 0.94%, with the range extending from a low of 0.78% to a high of 1.05%. The inherent moisture content tended to increase with distance into the panels, with the average in each cut-through zone increasing from a low of 0.85%, in the 0-10c/t zone, to a high of 0.99%, in the +30c/t zone.

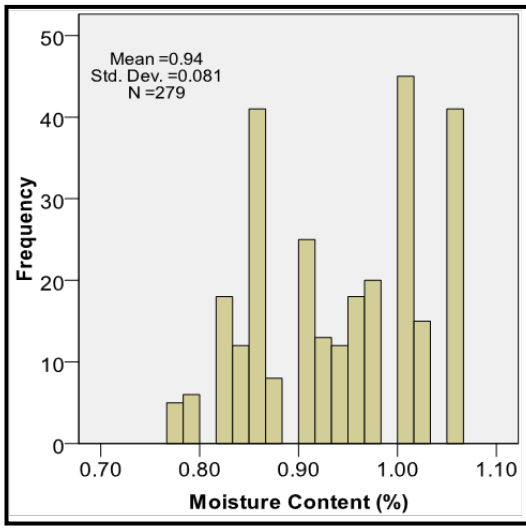

Figure 4.75: Distribution of inherent moisture content for all boreholes within the complete dataset

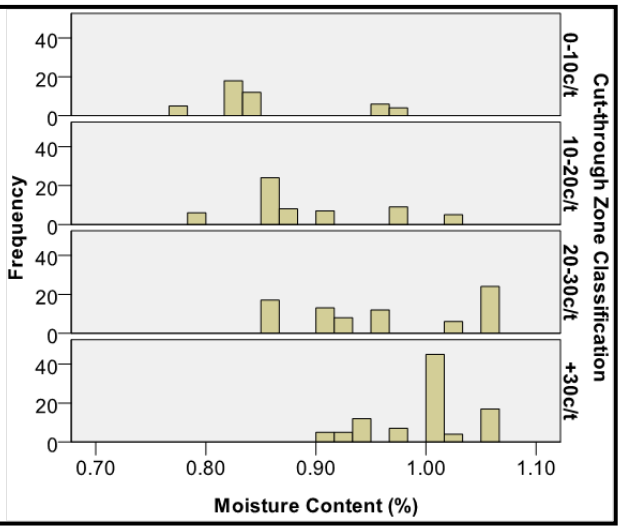

Figure 4.76: Distribution of inherent moisture content for boreholes in each cut-through zone

Figure 4.77 and Figure 4.78 show the relationship between inherent moisture and gas production. There was some evidence of increased gas production from coal with reduced inherent moisture content however there was a high degree of scatter and the relationship was weak. Statistical analysis determined a negative correlation of –0.324 and –0.342 between inherent moisture content and each of the total and D50 gas production figures.

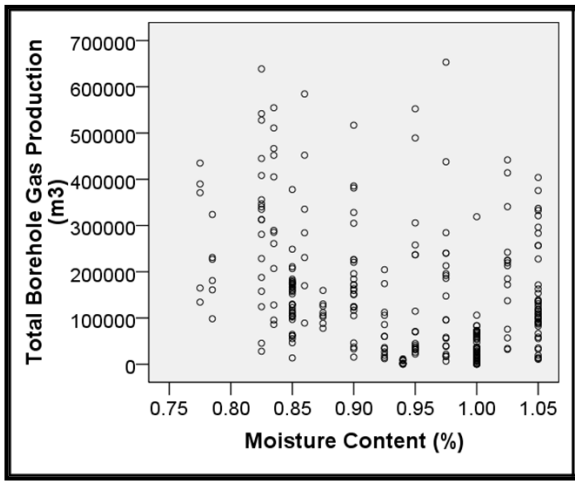

Figure 4.77: Total gas production relative to inherent moisture content

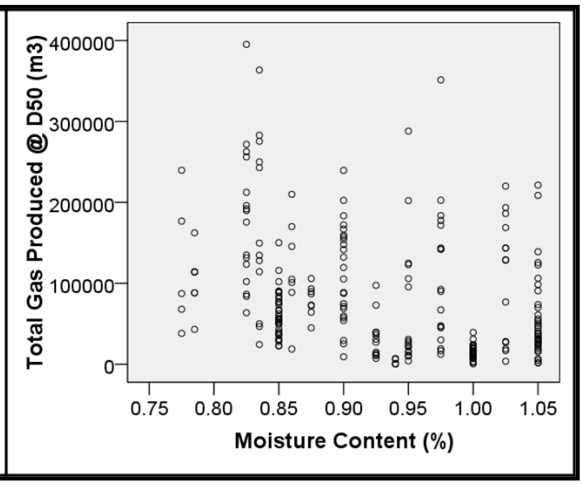

Figure 4.78: D50 gas production relative to inherent moisture content

The relationship between inherent moisture and gas production within each cut-through zone was also considered. As shown in Figure 4.79 and Figure 4.80, there was no evidence to suggest a relationship between inherent moisture and either total or D50 gas production.

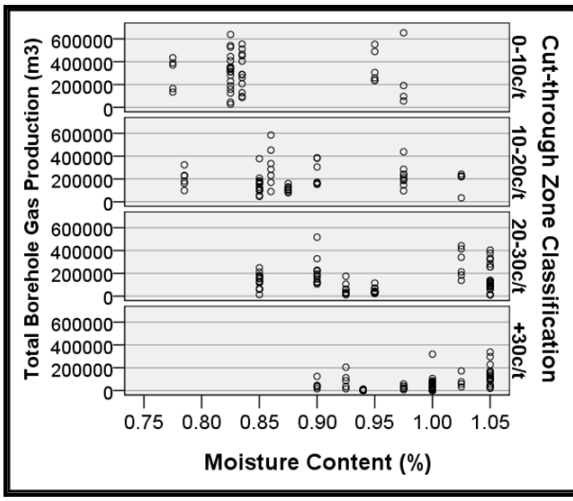

Figure 4.79: Total gas production relative to inherent moisture content in each cut-through zone

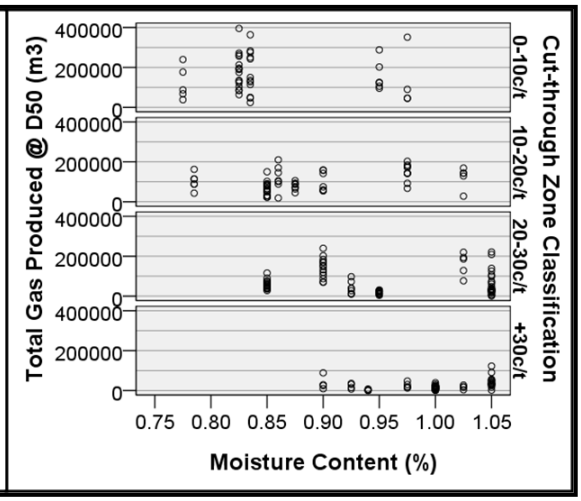

Figure 4.80: D50 gas production relative to inherent moisture content in each cut-through zone

From this assessment it was concluded that within this mining area the inherent moisture content of the coal, which spans a range of 0.78% to 1.05%, does not impact gas production.

4.4.6 Seam Thickness

Table 4.12 provides a summary of seam thickness measurement from 53 sample locations, reported by Clark (1986-2007). The seam thickness values were used to generate the contour plot, shown relative to current and future mine workings in Figure 4.81.

Table 4.12: Seam thickness data source and summary information (after Clark, 1986-2007)

Seam thickness	number of samples	Average (%)	Data range (%)		Sample collection & analysis	
			Minimum	Maximum	From	To
SIS core sample	29	2.6	2.1	3.6	13/08/1986	5/12/2007
UG strip sample	24	2.8	2.2	3.2	8/08/2001	6/08/2007
Combined	53	2.7	2.1	3.6	13/08/1986	5/12/2007

Figure 4.82 and Figure 4.83 show the distribution of estimated average seam thickness corresponding to the boreholes in the complete dataset and in each of the four cut-through zones. The average seam thickness of all boreholes in the dataset was 2.6 m with the range extending from a low of 2.3 m to a high of 2.9 m. Although variable, the average seam thickness in each cut-through zone was found to be reasonably consistent,

at approximately 2.7 m in the first three cut-through zones, reducing to 2.4 m in the +30c/t zone.

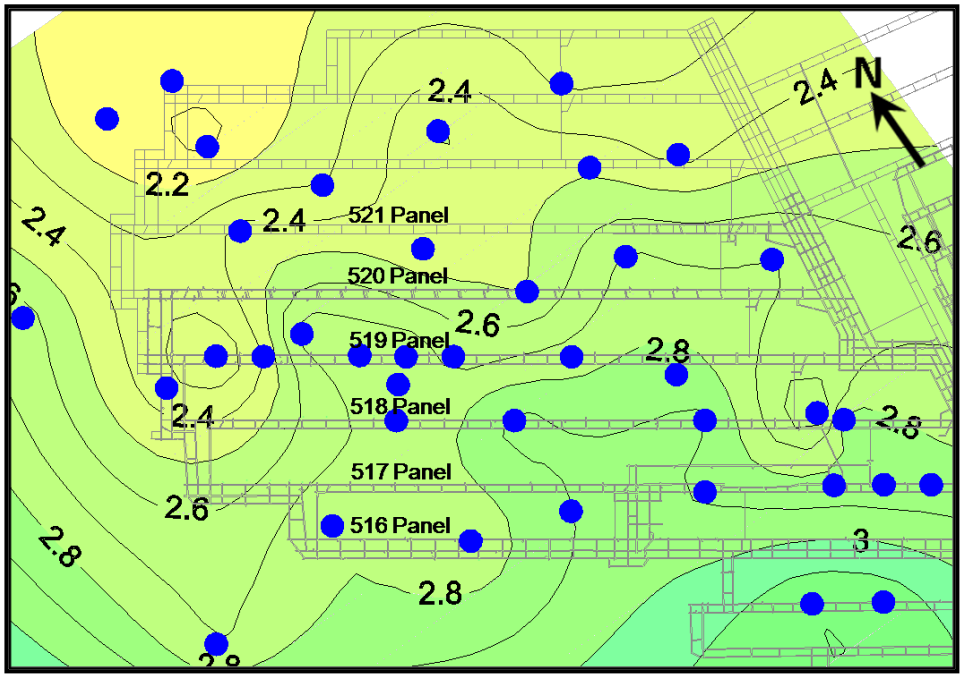

Figure 4.81: Bulli seam thickness contours relative to mine workings and sample location

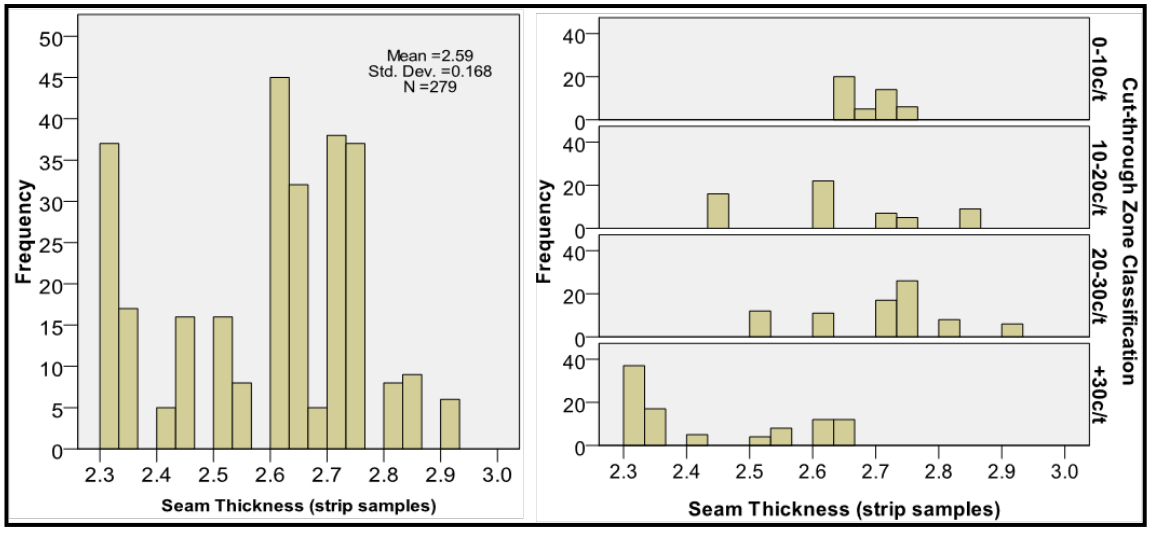

Figure 4.82: Distribution of seam thickness for all boreholes within the complete dataset

Figure 4.83: Distribution of seam thickness for boreholes in each cut-through zone

Figure 4.84 and Figure 4.85 show the relationship between seam thickness and gas production, which indicate increased total and D50 production from boreholes located in areas of increased seam thickness. Statistical analysis determined positive correlation of 0.518 and 0.506 between seam thickness and each of the total production and D50 gas production figures.

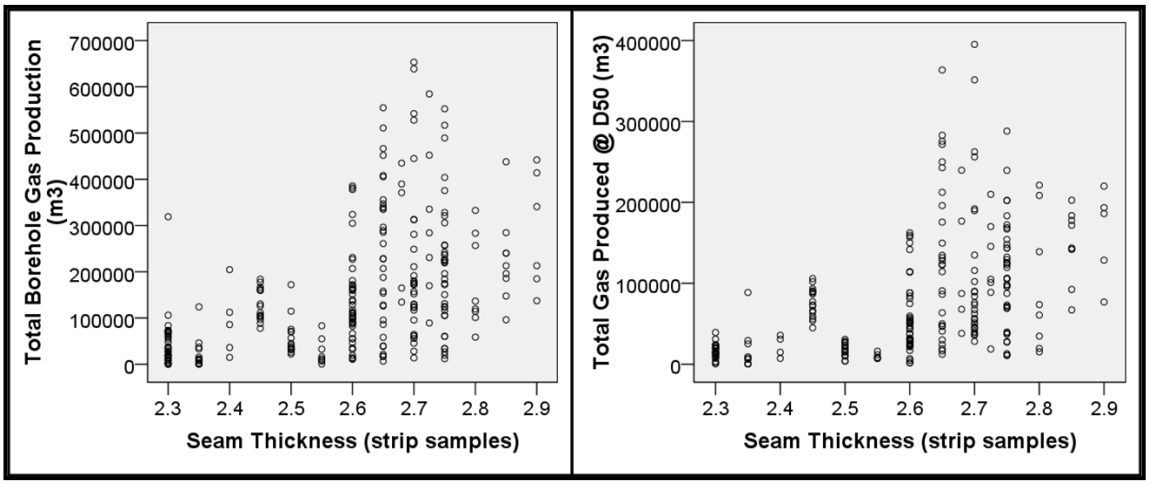

Figure 4.84: Total gas production relative to seam thickness

Figure 4.85: D50 gas production relative to seam thickness

The relationship between seam thickness and each of total and D50 gas production figures within each cut-through zone was also considered. As shown in both Figure 4.86 and Figure 4.87 the maximum gas production in each zone was greater in areas of increased seam thickness.

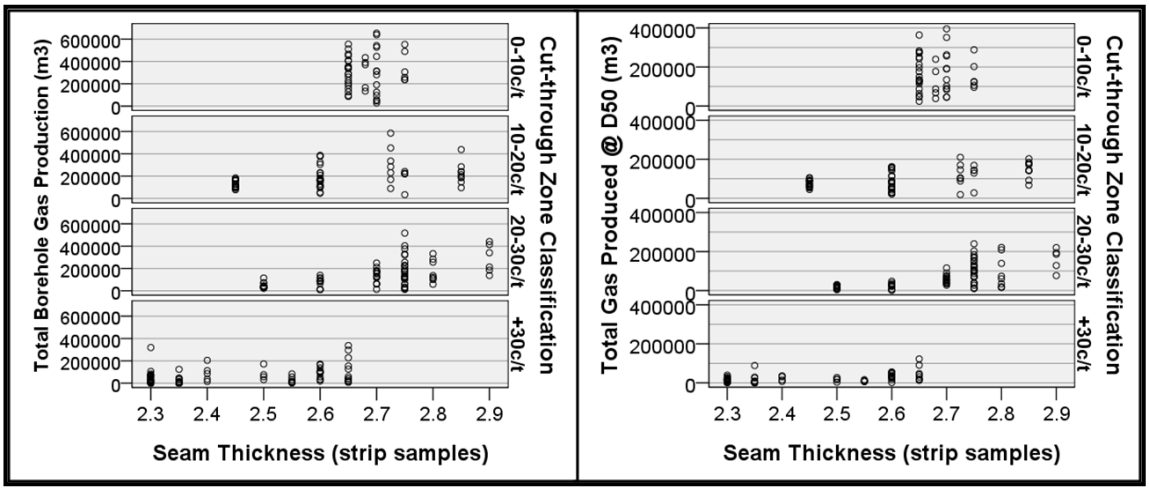

Figure 4.86: Total gas production relative to carbon content in each cut-through zone

Figure 4.87: D50 gas production relative to carbon content in each cut-through zones

This assessment has indicated increased gas production was achieved from boreholes located in areas with greater seam thickness. Therefore in this case the data indicates seam thickness has some impact on gas production.

4.4.7 Coal Seam Gas

Cui and Busten (2006) and Lamarre (2007) suggest that gas production will be greater from coal seams that contain more gas. Factors that impact the total gas present in a coal

seam and impact gas production include seam thickness, gas content, degree of gas saturation and critical desorption pressure (Lamarre, 2007).

Kahil and Masszi (1982) have a somewhat different opinion, suggesting that greater gas content would not necessarily increase the well production but rather extend the life of the well. This statement by Kahil and Masszi was not considered valid given that, in equivalent coal seam conditions, higher gas content equates to a higher total gas volume present in the coal seam and therefore greater total gas volume to be liberated from the coal.

Within the mining area the gas composition ($CH_4/(CH_4+CO_2)$) spans a broad range, from a low of 13% CH_4 to a high of 98% CH_4, whilst the gas content span a much smaller range, from a low of 7.5 m^3/t to a high of 15.5 m^3/t. Figure 4.88 shows the relationship between gas content and gas composition for the boreholes in the complete dataset which highlights the significant difference in gas content between the CH_4 and CO_2 rich areas. Figure 4.89 shows the relationship between gas content and gas composition in each of the four cut-through zones. The coal at the start of the panels was found to have the highest gas content and the seam gas was CH_4 rich. Both gas content and gas composition ($\%CH_4$) decreased with distance into the panels.

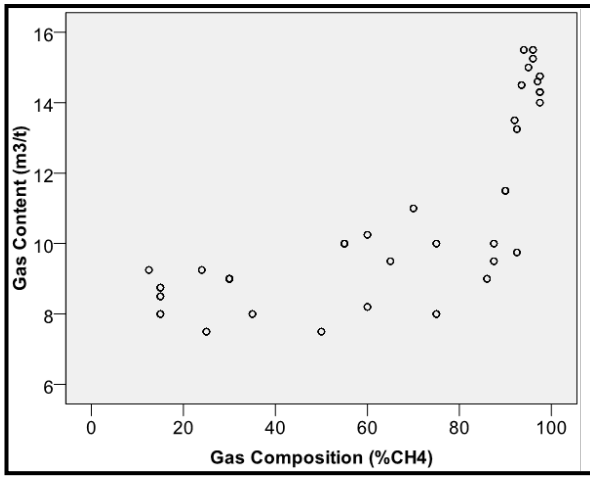

Figure 4.88: Gas content relative to gas composition for all UIS boreholes

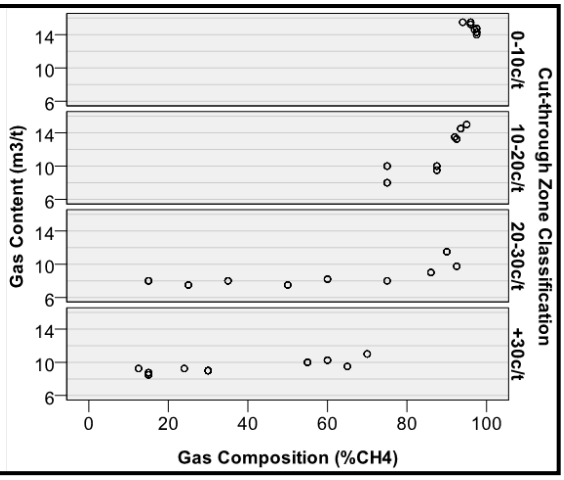

Figure 4.89: Gas content relative to gas composition in each cut-through zone

4.4.7.1 Gas Content

Gas content testing on Bulli seam coal samples was conducted at the BHP Billiton Illawarra Coal Gas Laboratory using the fast desorption gas content testing method, described in AS3980:1999 (SAA, 1999). Gas content data, measured in cubic metres of

gas per tonne of coal (m^3/t), corrected to 10% ash (non-coal matter), representing 82 coal samples collected during surface to seam exploration, was extracted from electronic data files (Armstrong and Kaag, 2008). The data was used to generate the gas content contour plot, shown relative to current and future mine workings in Figure 4.90. Gas content was found to decrease with distance into the panels, reaching a minimum approximately midway along the panels followed by a gradual increase in content toward the inbye end of the panels.

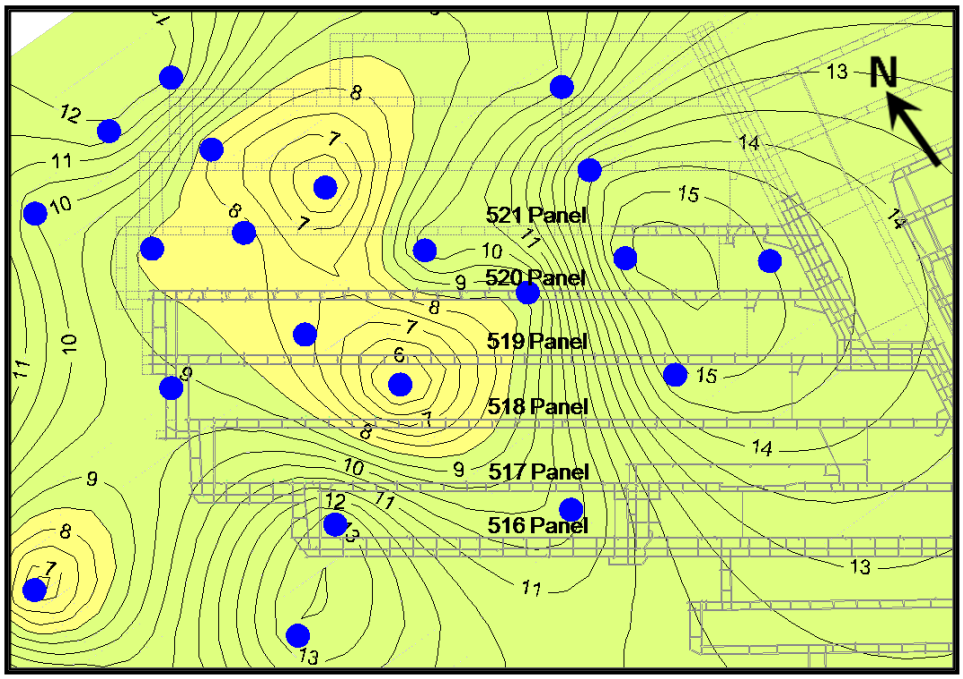

Figure 4.90: Gas content contours relative to mine workings and coal sample location

Figure 4.91 and Figure 4.92 show the distribution of estimated average gas content corresponding to the boreholes in the complete dataset and in each of the four cut-through zones. The average gas content of all boreholes in the dataset was 10.5 m^3/t, with the range extending from a low of 7.5 m^3/t to a high of 15.5 m^3/t. The average gas content in each cut-through zone decreased from a high of 14.9 m^3/t, in the 0-10c/t zone, to a low of 8.7 m^3/t, in the 20-30c/t zone.

Figure 4.93 and Figure 4.94 show the relationship between gas content and gas production, with increased total and D50 production from boreholes located in areas of increased gas content. Statistical analysis determined a positive correlation of 0.548 and 0.608 between gas content and each of the total and D50 production values. This result was consistent with the findings of past studies. According to Hayes (1982) desorption

of gas from coal was proportional to the gas content, providing all other factors remain constant.

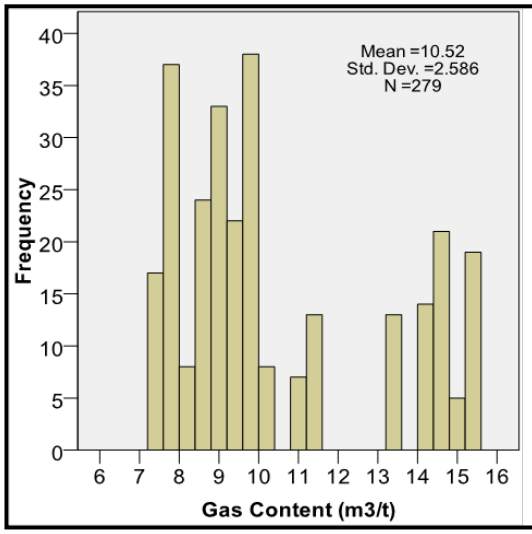

Figure 4.91: Distribution of gas content for all boreholes within the complete dataset

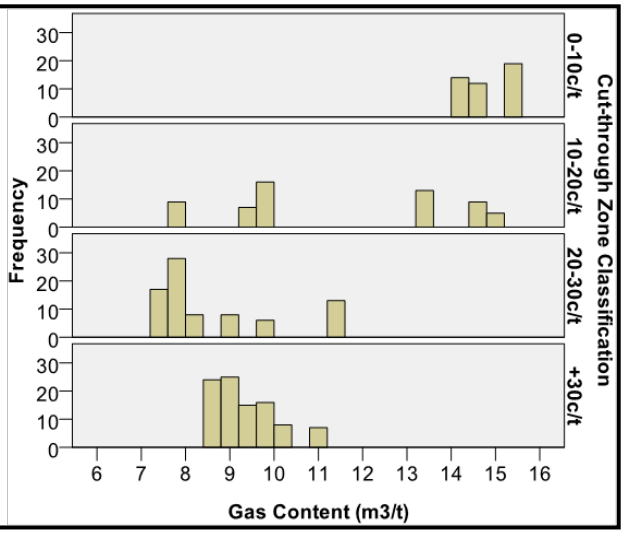

Figure 4.92: Distribution of gas content for boreholes in each cut-through zone

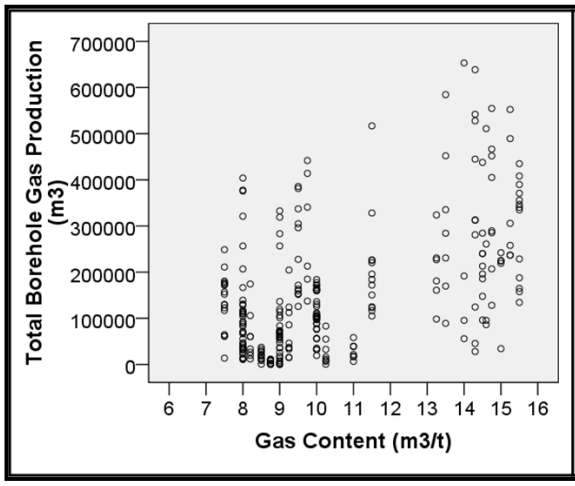

Figure 4.93: Total gas production relative to gas content

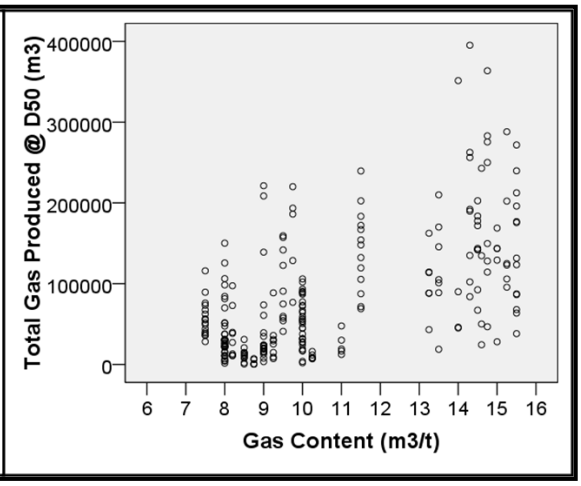

Figure 4.94: D50 gas production relative to gas content

The relationship between gas content and both total and D50 gas production, within each cut-through zone, was also considered. Figure 4.95 and Figure 4.96 provide some indication of a relationship, albeit weak, between gas content and gas production, particularly in the inbye cut-through zones.

The analysis was extended to consider the relationship within three distinct gas content zones, (a) less than 10 m^3/t, (b) between 10 and 14 m^3/t, and (c) greater than 14 m^3/t. As shown in Figure 4.97 there was a reduction in both average and maximum gas

production in response to decreasing gas content. It was also noted that in each gas content zone there were boreholes that achieved very low gas production.

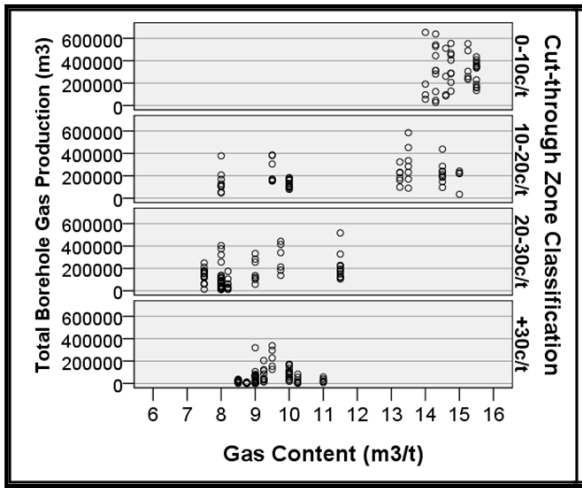

Figure 4.95: Total gas production relative to gas content in each cut-through zone

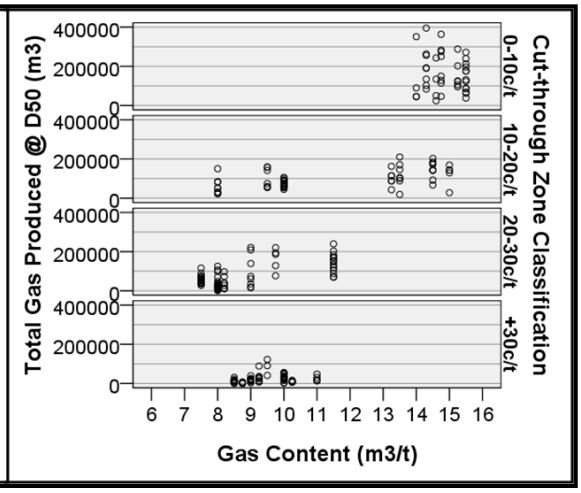

Figure 4.96: D50 gas production relative to gas content in each cut-through zone

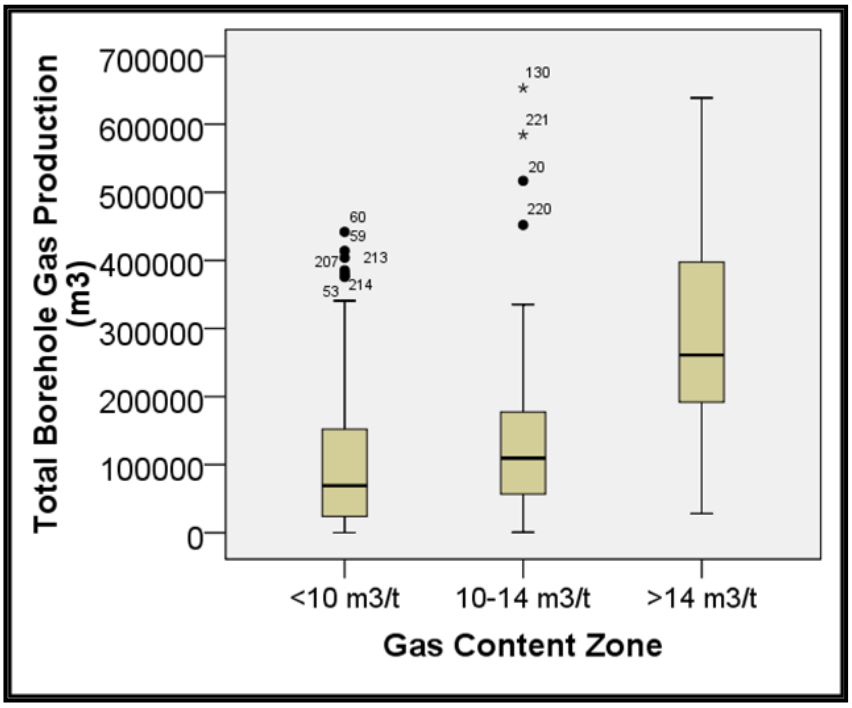

Figure 4.97: Total gas production data range within each gas content zone

Statistical analysis was conducted on the data within each gas content zone to identify significant correlations between gas production and other coal properties. Table 4.13 provides a summary of significant correlations between each of total and D50 gas production and various coal properties. It was noted that the data in the 'Greater than 14 m^3/t' zone spanned a narrow range which adversely impacted the correlation result. In

all three zones gas composition was found to have the greatest and most consistent correlation to gas production. The relationship between gas composition and gas production within each gas content zone was also considered.

Table 4.13: Summary of statistical correlation between gas production and coal properties within each gas content zone

Statistical Correlations	Gas content zone					
	Less than 10 m^3/t		Between 10 and 14 m^3/t		Greater than 14 m^3/t	
Coal Property	Total borehole gas production (m^3)	Total gas production @ D50 (m^3)	Total borehole gas production (m^3)	Total gas production @ D50 (m^3)	Total borehole gas production (m^3)	Total gas production @ D50 (m^3)
Gas composition	0.658	0.666	0.561	0.657	0.237	0.257
Volatile matter	-0.625	-0.629	-0.560	-0.555	0.178	0.092
Fixed carbon	0.616	0.648	0.519	0.576	0.035	0.163
Mineral matter	0.615	0.653	0.420	0.555	0.062	-0.002
Seam thickness	0.593	0.591	0.366	0.432	-0.194	-0.096
Coal ash	-0.468	-0.502	-0.395	-0.538	-0.222	-0.187
Number of samples	147	123	77	73	55	53

Figure 4.98 and Figure 4.99 show increased maximum gas production from areas where the seam gas composition was CH_4 rich, independent of gas content.

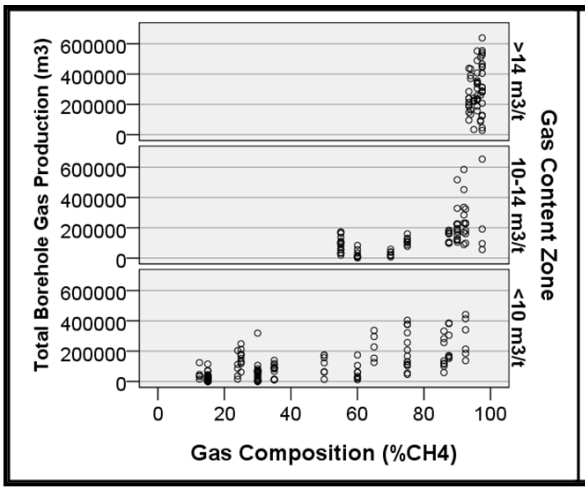

Figure 4.98: Total gas production relative to gas composition in each gas content zone

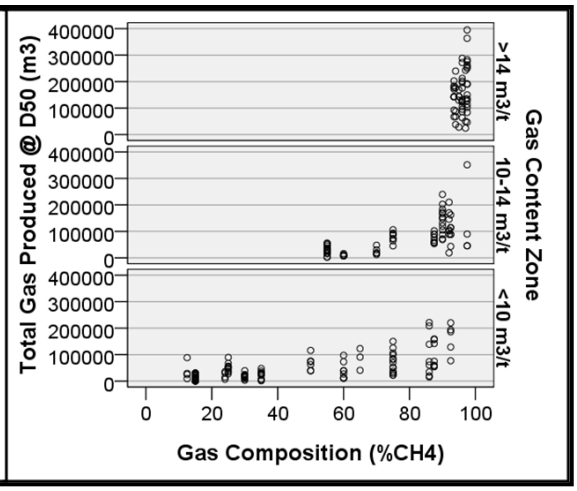

Figure 4.99: D50 gas production relative to gas composition in each gas content zone

This assessment has shown that although increased gas production may be achieved from boreholes located in areas with greater gas content the relationship was not particularly strong. The relationship was considered to be adversely impacted by the large number of boreholes that achieved low total gas production.

4.4.7.2 Gas Composition

The gas composition from the Bulli seam coal samples was determined during gas content testing conducted at the BHP Billiton Illawarra Coal Gas Laboratory. A four channel Varian CP4900 gas chromatograph was used to determine gas composition. Gas composition data was compiled from 67 coal samples collected during surface to seam exploration (Armstrong and Kaag, 2008). The data was used to generate the contour plot of the $CH_4/(CH_4+CO_2)$, shown relative to current and future mine workings in Figure 4.100. As shown, there was a significant change in gas composition along the length of the panels, with the composition shifting from essentially pure CH_4 at the start of the panels to almost pure CO_2 at the inbye-most ends of the panels.

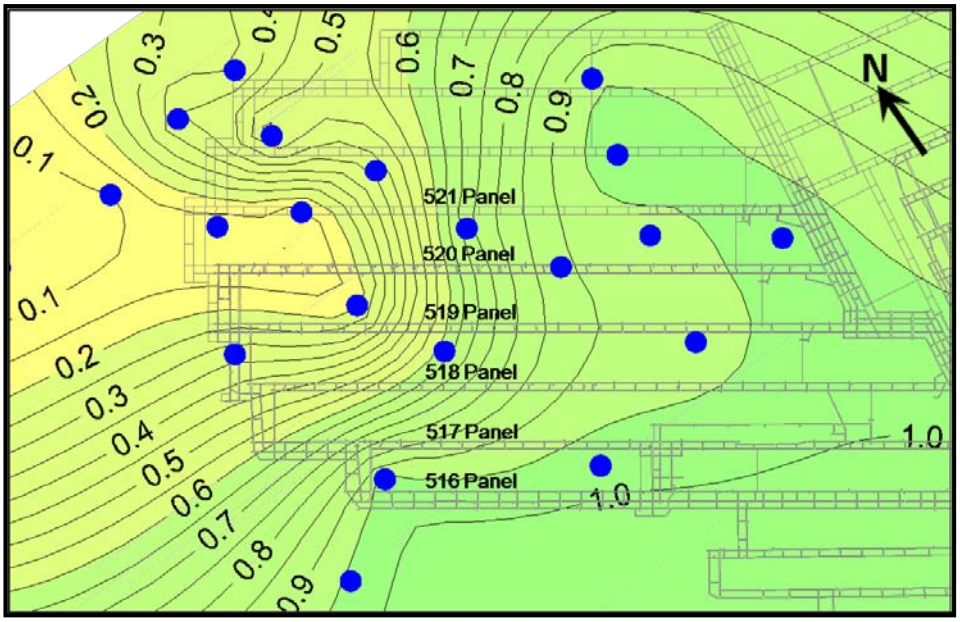

Figure 4.100: Gas composition ($CH_4/(CH_4+CO_2)$) relative to mine workings and sample location

Figure 4.101 and Figure 4.102 show the distribution of estimated average gas composition corresponding to the boreholes in the complete dataset and in each of the four cut-through zones. The average gas composition of all boreholes in the dataset was 62.2% CH_4, with the range extending from a low of 13.0% CH_4 to a high of 98.0% CH_4. The gas composition was found to decrease with distance into the panels, with the average in each cut-through zone decreasing from a high of 96.6% CH_4, in the 0-10c/t zone, to a low of 36.5% CH_4, in the +30c/t zone.

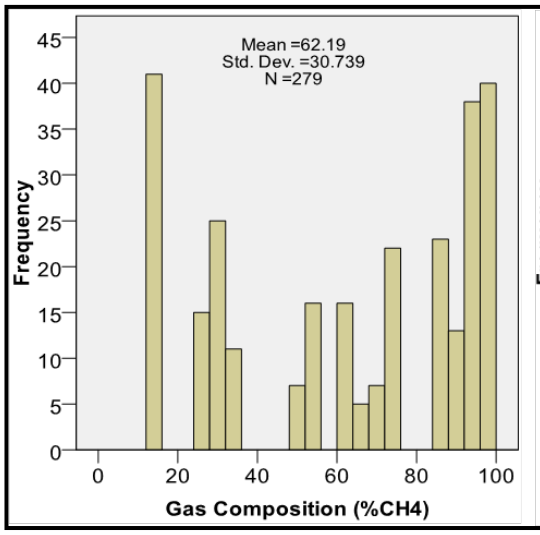

Figure 4.101: Distribution of gas composition for all boreholes within the complete dataset

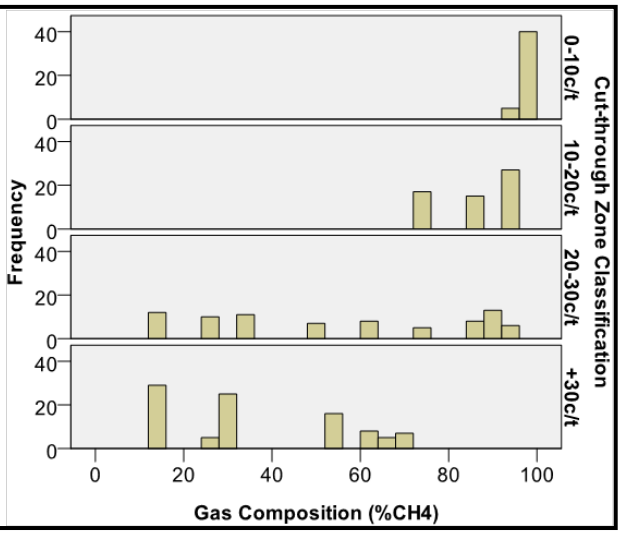

Figure 4.102: Distribution of gas composition for boreholes in each cut-through zone

Figure 4.103 and Figure 4.104 show the relationship between gas composition and each of the total and D50 gas production figures. The data show increasing maximum gas production in response to increasing methane gas composition, particularly where gas composition exceeded 70% CH_4. Statistical analysis determined a positive correlation of 0.626 and 0.657 between gas composition and each of the total and D50 gas production figures.

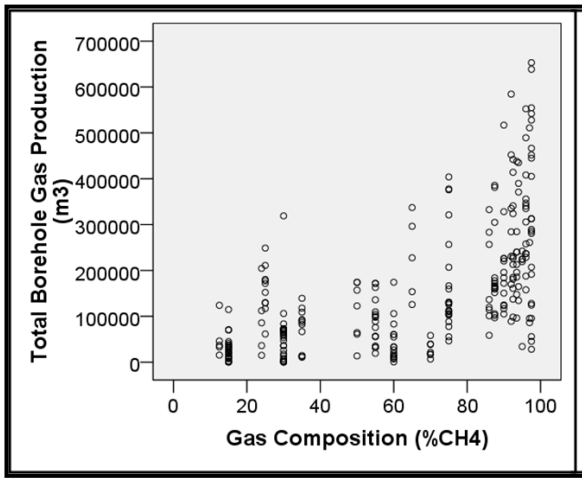

Figure 4.103: Total gas production relative to gas composition

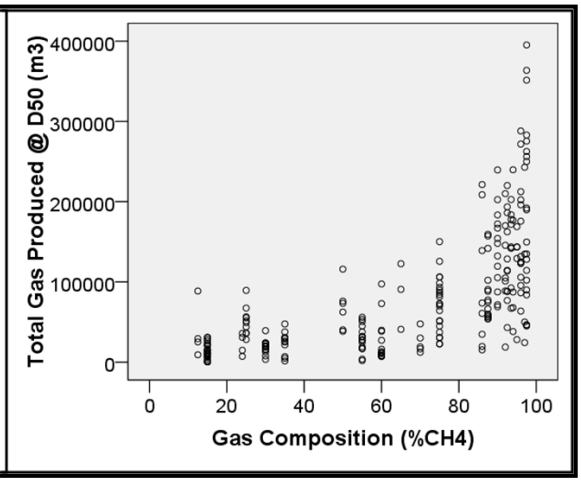

Figure 4.104: D50 gas production relative to gas composition

The relationship between gas composition and both the total and D50 gas production, within each cut-through zone, was also considered. As shown in both Figure 4.105 and Figure 4.106 the maximum gas production in each zone was greater in areas of increased CH_4 gas composition.

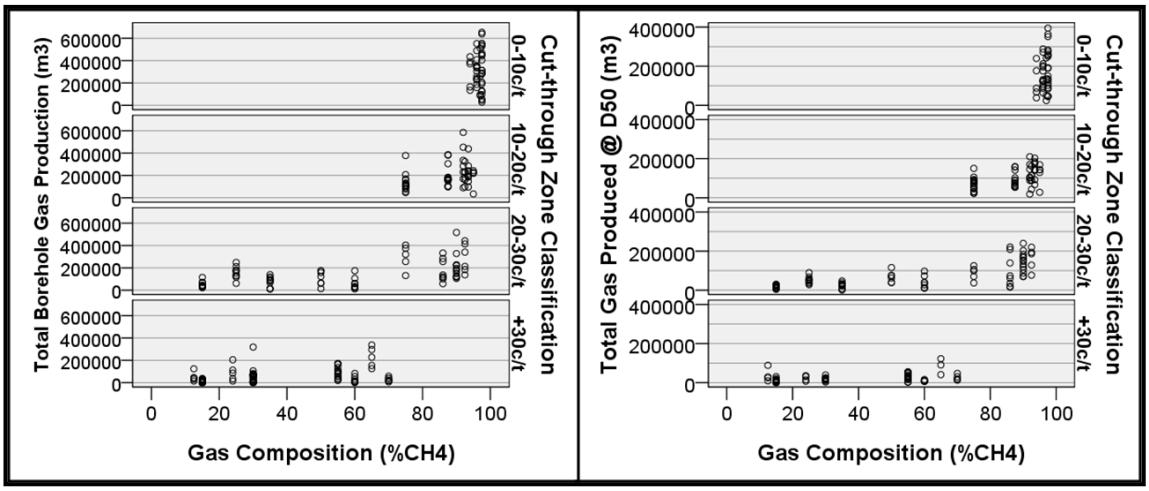

Figure 4.105: Total gas production relative to gas composition in each cut-through zone

Figure 4.106: D50 gas production relative to gas composition in each cut-through zone

The analysis was extended to consider the relationship within three distinct gas composition zones, (a) less than 40% CH_4, (b) between 40 and 80% CH_4, and (c) greater than 80% CH_4. As shown in Figure 4.107 there was a reduction in both average and maximum gas production in response to decreasing CH_4 gas composition. It was also noted that in each gas composition zone there were boreholes that achieved very low gas production.

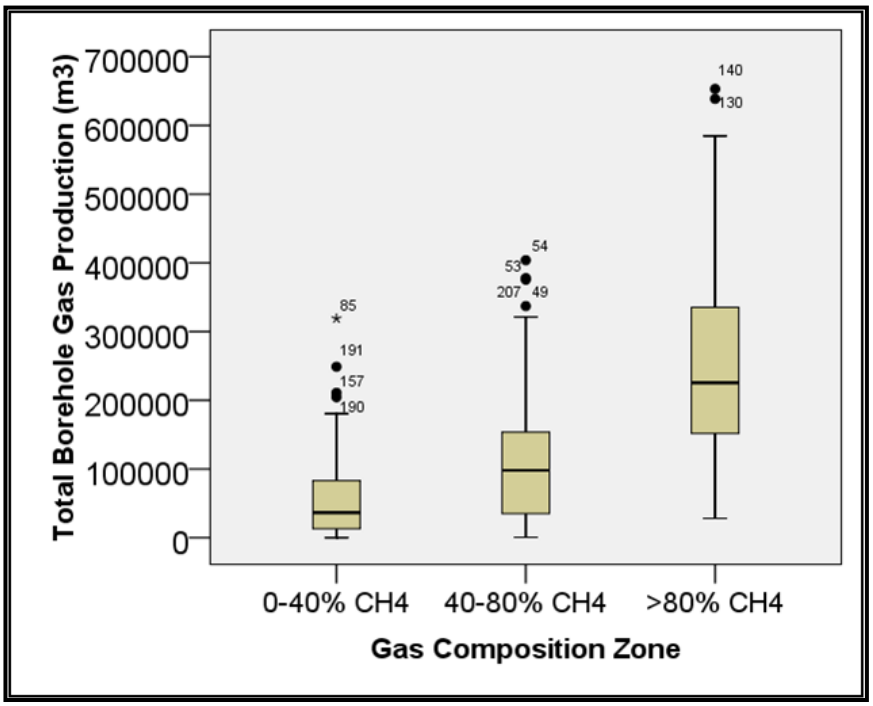

Figure 4.107: Total gas production data range within each gas composition zone

Statistical analysis was conducted on the data within each gas composition zone to identify significant correlations between gas production and other coal properties. Table

4.14 provides a summary of the correlation between total and D50 gas production and the various coal properties considered. Within each gas composition zone no coal property was found to maintain a consistent, strong correlation to gas production,

Table 4.14: Summary of statistical correlation between gas production and coal properties within each gas composition zone

Statistical Correlations	Gas composition zone					
	0-40% CH_4		40-80% CH_4		>80% CH_4	
Coal Property	Total borehole gas production (m^3)	Total gas production @ D50 (m^3)	Total borehole gas production (m^3)	Total gas production @ D50 (m^3)	Total borehole gas production (m^3)	Total gas production @ D50 (m^3)
Gas content	-0.364	-0.357	-0.370	-0.357	0.259	0.257
Volatile matter	-0.058	0.043	-0.526	-0.578	0.056	0.092
Fixed carbon	0.623	0.620	0.214	0.495	0.195	0.176
Mineral matter	0.513	0.596	0.242	0.443	-0.040	-0.056
Seam thickness	0.520	0.515	0.199	0.075	0.078	0.171
Coal ash	-0.570	-0.550	0.178	-0.212	-0.261	-0.273
Number of samples	92	72	73	66	114	111

Further assessment of the relationship between gas content and gas production, within each gas composition zone, was undertaken. Figure 4.108 and Figure 4.109 indicate an apparent negative correlation between gas content and gas production in the zones of low CH_4 composition, where gas content is both low and spans a narrow range. In the >80% CH_4 zone, gas content spans a greater range and the maximum gas production data suggest a positive relationship between gas production and gas content.

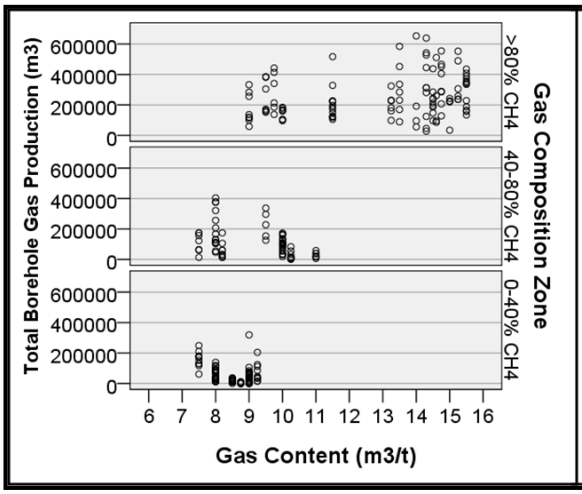

Figure 4.108: Total gas production relative to gas content in each gas composition zone

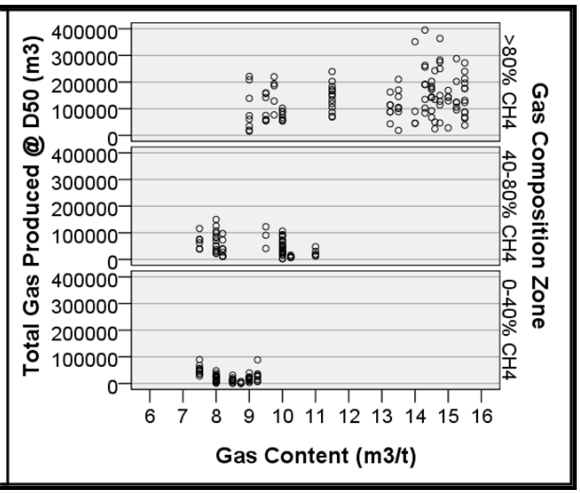

Figure 4.109: D50 gas production relative to gas content in each gas composition zone

This assessment has shown increased gas production was achieved from boreholes located in areas with greater CH_4 seam gas composition and this relationship was

independent of location along the panels. Therefore in this case the data indicates that gas composition does have an impact on gas production. It was also concluded that gas composition had a more significant impact on gas production than gas content.

4.4.7.3 Total Gas in Place

Cui and Busten (2006) and Lamarre (2007) suggest gas production will be greater from coal seams that contain more gas. This view was tested through an assessment of the relationship between total gas in place (GIP) and UIS borehole gas production. The total gas in place (GIP) was determined for each of the 34 drill sites using Equation 4.1.

$$GIP = A \times \rho \times t \times Q_M \quad (m^3) \tag{4.1}$$

where: A = total area drilled from each drill site (m^2);
ρ = average coal density (t/m^3);
t = average coal seam thickness (m); and
Q_M = average measured total gas content (m^3/t)

Statistical analysis was conducted to determine the correlation between GIP and the variables used to calculate GIP. The correlation between GIP and each of the values for area, thickness and gas content was 0.936, 0.257 and 0.310 respectively. The distribution of the values of each of the three variables relative to GIP for each of the 34 drill stubs are shown in Figure 4.110.

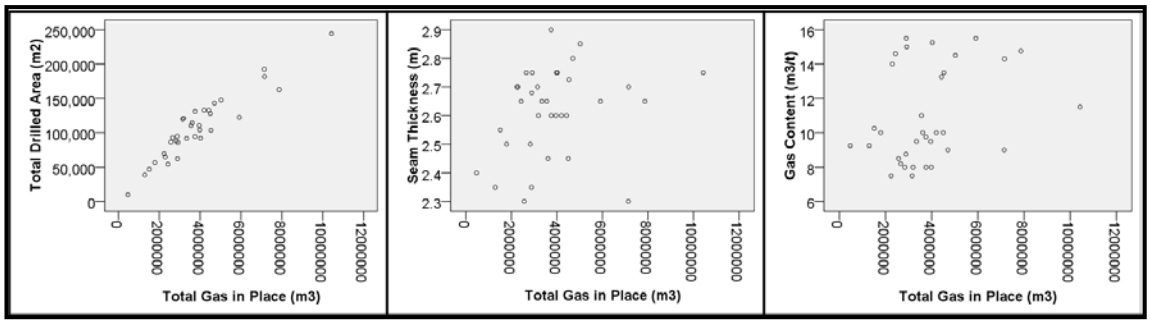

Figure 4.110: GIP relative to each of the values for Area, Thickness and Gas content

Figure 4.111 and Figure 4.112 show the distribution of GIP for all 34 drill sites and the drill sites within each of the four cut-through zones. The average GIP for all drill sites was approximately 3.9 Mm^3, with the range extending from a low of 0.5 Mm^3 to a high of 10.5 Mm^3. The GIP decreased with distance into the panels, with the average in each cut-through zone decreasing from a high of 4.7 Mm^3, in the 0-10c/t zone, to a low of 2.9

Mm^3, in the +30c/t zone. A reduction in the area drilled from each drill site was found to be the dominant factor leading to the lower GIP in the inbye parts of the panels.

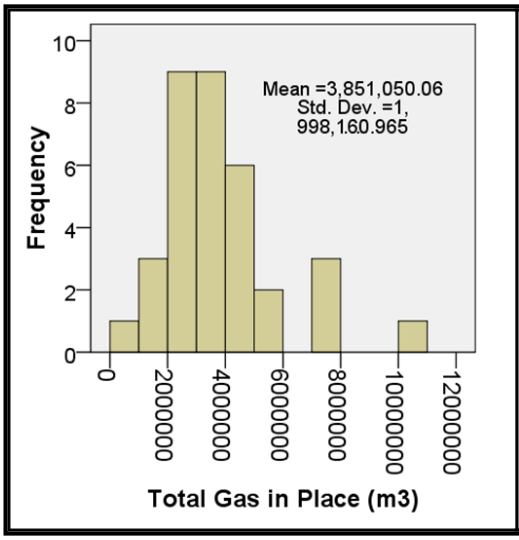

Figure 4.111: Distribution of GIP for drill sites within the complete dataset

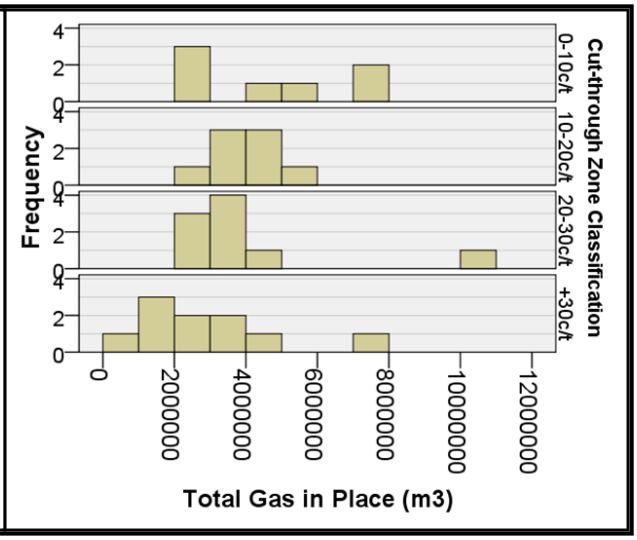

Figure 4.112: Distribution of GIP for drill sites within each cut-through zone

Figure 4.113 shows the relationship between total gas production from the combined boreholes within each drill site relative to the GIP at each site prior to gas production. Statistical analysis determined a positive correlation of 0.773 between gas production and GIP. Further assessment of the relationship between gas production and GIP determined that, within this mining area, 32% of the GIP was removed by UIS gas drainage operations prior to mining. Figure 4.114 shows increased gas production corresponding to increased GIP in each cut-through zone, indicating the relationship between gas production and GIP was independent of location.

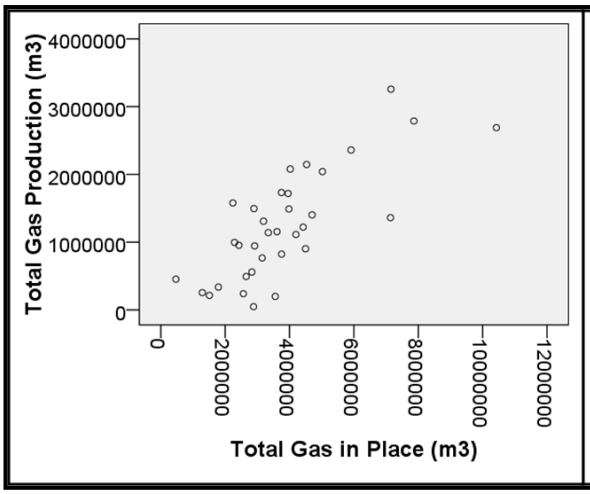

Figure 4.113: Gas production relative to GIP for drill sites within the complete dataset

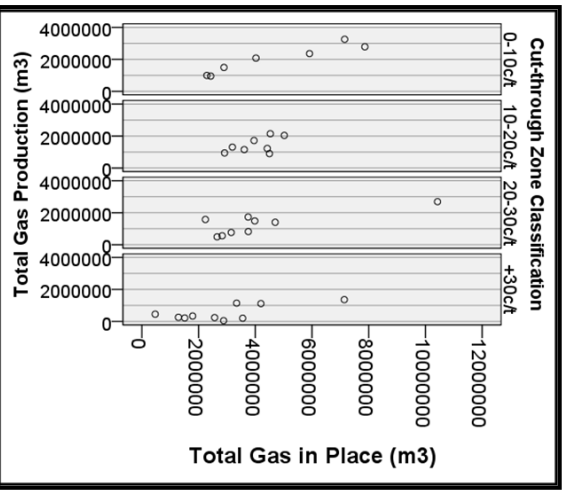

Figure 4.114: Gas production relative to GIP for drill sites within each cut-through zone

The analysis was extended to consider the relationship between gas production and GIP relative to the gas content and gas composition zones previously defined. As shown in Figure 4.115 and Figure 4.116, a consistent relationship was maintained between gas production and GIP. It was also identified that the percentage of GIP removed through gas drainage was lower in the CO_2 rich zones than in CH_4 rich zones.

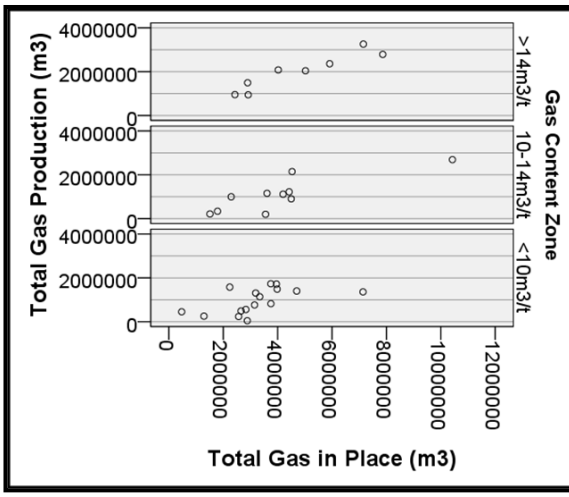

Figure 4.115: Gas production relative to GIP for drill sites within each gas content zone

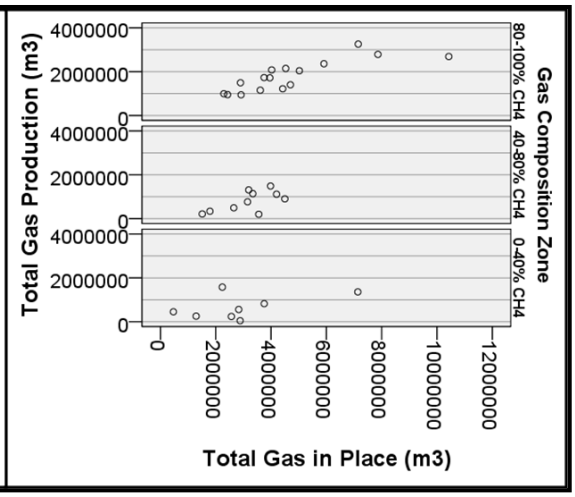

Figure 4.116: Gas production relative to GIP for drill sites within each gas composition zone

This analysis has confirmed a strong relationship exists between gas production and total gas in place, consistent with the views of Cui and Busten (2006) and Lamarre (2007).

It was concluded that seam gas has a significant impact on gas production, with increased gas production expected from areas with greater GIP and, all else being equal, the percentage of GIP drained will be greater in CH_4 rich conditions than in CO_2 rich conditions.

4.4.8 Degree of Saturation

Coal holding the maximum possible amount of gas at reservoir pressure and temperature conditions is said to be ‘saturated’, whereas coal holding less than the theoretical maximum is referred to as ‘undersaturated’. The most successful coalbed methane production occurs in seams that are close to fully saturated (Lamarre, 2007). Slightly undersaturated coals behave similarly to saturated coal with only a short delay prior to first gas production, followed by a steady, strong, rising gas production rate (Lamarre, 2007). In highly undersaturated coal the critical desorption pressure, being

the pressure at which appreciable gas starts to desorb from coal, is significantly less than the initial reservoir pressure and requires extensive dewatering prior to initiation of regular gas production. As indicated in Figure 4.117 (Garbutt, 2004), the duration of Stage 1, where production is dominated by water, is much longer in highly undersaturated coal than in slightly undersaturated coal. The long dewatering (depressurising) period may result in the peak gas production rate being significantly less than that of an equivalent saturated coal (Seidle and O'Connor, 2007).

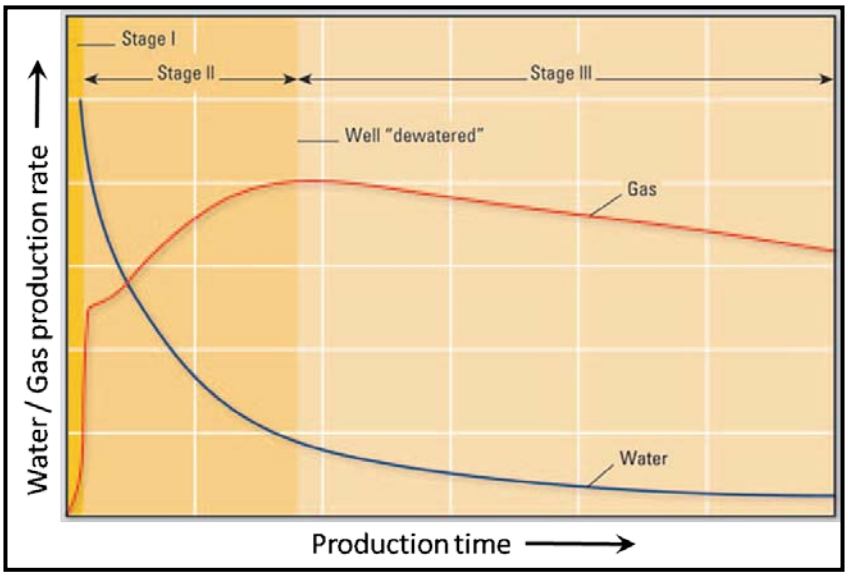

Figure 4.117: Characteristic coalbed water and gas production curves (Garbutt, 2004)

Seidle and O'Connor (2007) suggest many coal deposits throughout the world are undersaturated to some degree. Figure 4.118 illustrates a typical Bulli seam *in situ* gas condition, relative to typical CH_4 and CO_2 isotherms, which represent maximum gas storage capacity of the coal at a given gas pressure. From this figure it can be seen that, when saturated at a given pressure and temperature the volume of CO_2 adsorbed by coal is approximately double the adsorbed volume of CH_4. It can also be seen that the pressure reduction required to reach the critical desorption point in a CO_2 rich environment is much greater than in equivalent CH_4 rich conditions.

In a study of the economic impact of gas saturation on coals in the United States, Seidle and O'Connor (2007) determined that as coal became less saturated, the gas production profile weakened, exhibiting a longer dewatering time and lower peak production rate. Compared to a fully saturated coal, a coal that was 60% undersaturated required five times as long to reach the peak gas production rate and the magnitude was one sixth that

of the saturated coal (Seidle and O'Connor, 2007). Gas saturation is therefore an important coal property and its impact on gas production must be considered.

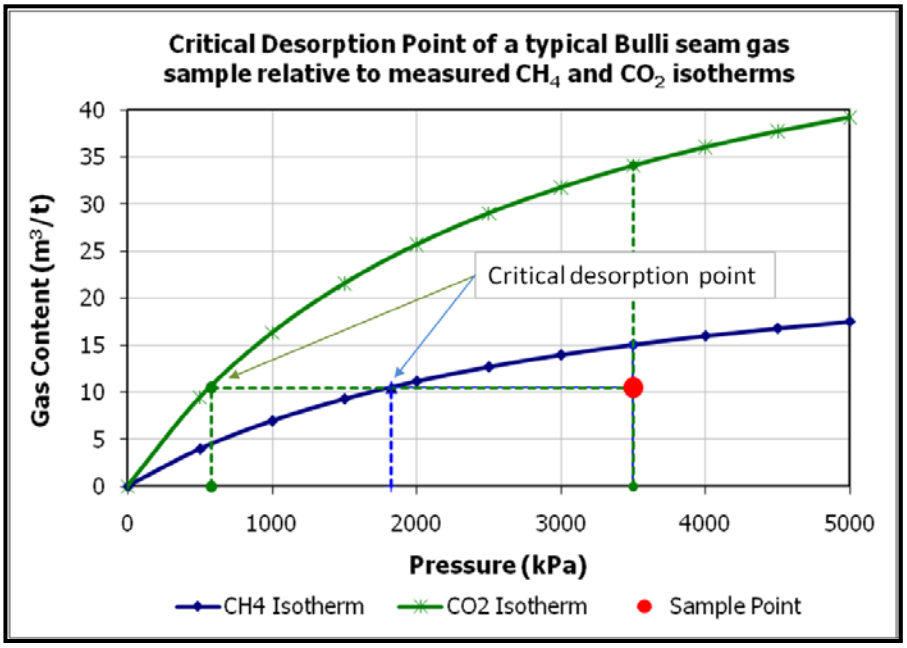

Figure 4.118: Typical Bulli seam *in situ* gas condition relative to CO_2 and CH_4 isotherms

In this analysis, degree of saturation (DoS) represents the ratio of measured to saturated gas content (Equation 4.2). The measured gas content (V_{meas}), also referred to in this document as Q_M, was determined using the method described in Australian Standard AS3980:1999 (SAA, 1999). The saturated gas content (V_{sat}) was calculated using the modified Langmuir equation (Equation 4.3) (Seidle and O'Connor, 2007), which requires prior knowledge of the Langmuir constants of volume (V_L) and pressure (P_L). Both Langmuir constants are determined from gas adsorption testing, and the initial reservoir pressure (P_i) is measured by pressure sensing devices, such as piezometers.

$$DoS = \frac{V_{meas}}{V_{sat}} \cdot 100 \ (\%) \qquad (4.2)$$

where: DoS = degree of saturation (%)
V_{meas} = measured gas content (m^3/t)
V_{sat} = saturated gas content (m^3/t)

$$V_{sat} = V_L \cdot \frac{P_i}{P_i + P_L} \text{ (m}^3\text{/t)} \quad (4.3)$$

where: V_{sat} = saturated gas content (m^3/t)
V_L = Langmuir volume constant (m^3/t)
P_i = initial reservoir pressure (kPa)
P_L = Langmuir pressure constant (kPa)

The Langmuir equation can also be used to determine the critical desorption pressure corresponding to a given measured gas content (Equation 4.4) (Seidle and O'Connor, 2007). The difference between the *in situ* pressure and the critical desorption pressure defines the coal seam pressure reduction required to initiate regular gas production.

$$P_d = P_L \cdot \frac{V_{meas}}{V_L - V_{meas}} \text{ (kPa)} \quad (4.4)$$

where: P_d = critical desorption pressure (kPa)
P_L = Langmuir pressure constant (kPa)
V_L = Langmuir volume constant (m^3/t)
V_{meas} = measured gas content (m^3/t)

Figure 4.119 shows the location of eight coal samples collected for gas sorption testing. The testing determined the maximum CH_4 and CO_2 adsorption capacity of the coal at saturation, through gravimetric testing, along with the Langmuir volume and pressure constants for both gases (Saghafi and Roberts, 2008a and 2008b). Table 4.15 shows the Langmuir volume and pressure constants corresponding to each of the eight coal samples, for CH_4 and CO_2 sorption, at a constant temperature of 27^OC (Saghafi and Roberts, 2008a and 2008b).

Figure 4.120 and Figure 4.121 show the CH_4 and CO_2 isotherm curves for each of the eight coal samples. At 4 000 kPa the saturated gas content of CO_2 was 2.24 to 2.33 times that of CH_4 which was consistent with the results of previous testing of Bulli seam coal by Aziz and Ming Li (1999) who reported a saturated gas content ratio of 2.2, with the coal adsorbing 32 m^3/t of CO_2 and 14.5 m^3/t of CH_4 at 4 000 kPa. Some variability exists among the isotherms shown for each gas type with the difference between the minimum and maximum gas content, measured at 4 000 kPa, being 2.5 m^3/t for CH_4 and 4.8 m^3/t for CO_2.

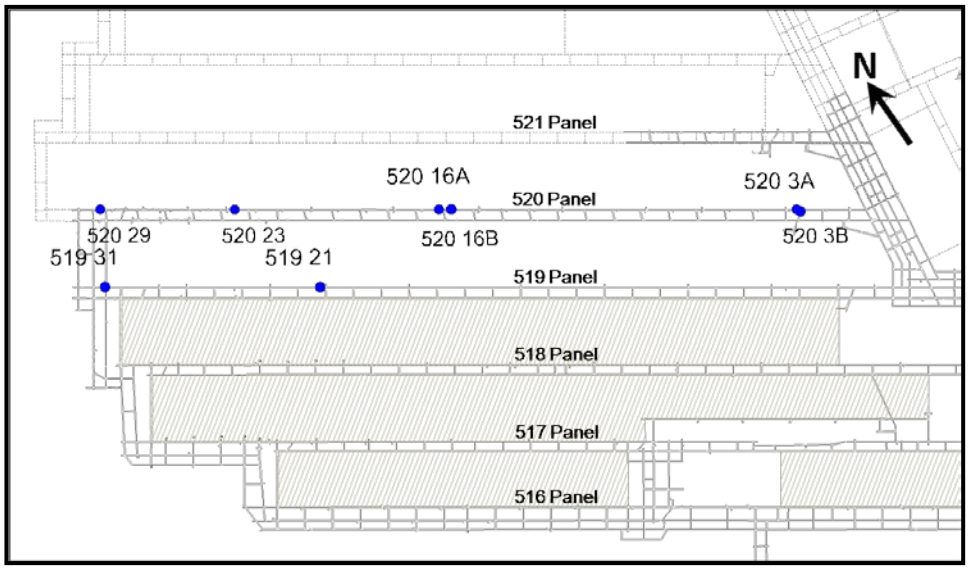

Figure 4.119: Location of coal samples collected for isotherm testing

Table 4.15: Langmuir volume and pressure constants representing CH_4 and CO_2 saturation (after Saghafi and Roberts, 2008a and 2008b)

Sample Reference	CH_4 Gas		CO_2 Gas	
	V_L daf (m^3/t)	P_L (kPa)	V_L daf (m^3/t)	P_L (kPa)
520 3A	27.6	3039	59.5	2708
520 3B	29.4	3045	62.4	2681
520 16A	30.9	3086	65.5	2738
520 16B	29.4	3091	63.0	2715
519 21	26.3	3057	58.4	2694
520 23	39.4	2520	54.2	2303
520 29	28.8	3075	61.3	2691
519 31	26.5	3045	57.3	2722

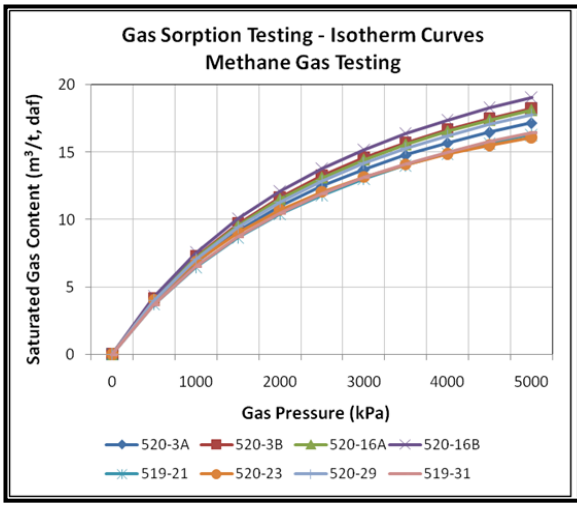

Figure 4.120: CH_4 isotherm curves determined for coal samples within mining area

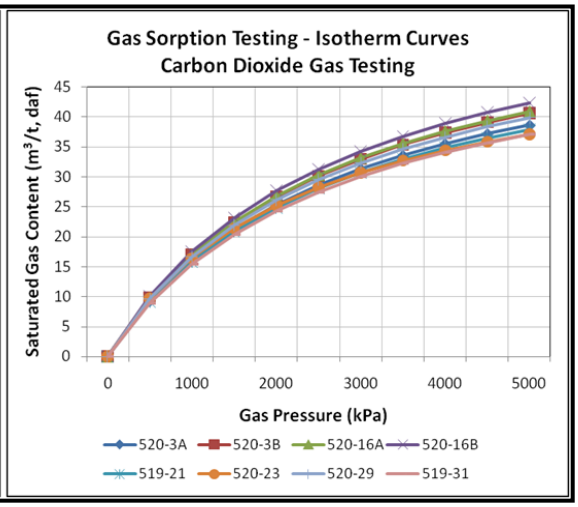

Figure 4.121: CO_2 isotherm curves determined for coal samples within mining area

Piezometers installed into the coal seam as part of the surface-to-seam exploration program provide information relating to the *in situ* pore pressure in the region and subsequent changes in hydrostatic pressure due to the effects of mining and gas drainage.

Data from 18 piezometers installed into the Bulli seam at various locations in and around the mining area was collected (Armstrong and Doyle, 2008). The data, covering an 11 month period from December 2006 to October 2007, was analysed and an average monthly pressure response was calculated for each piezometer location. The piezometer pressure was used to generate a contour plot of pressure distribution for each of the 11 months which, when combined with the monthly progress plans of both mine workings and gas drainage drilling, provided valuable insight into the rate of change and impact on hydrostatic pressure. Figure 4.122 and Figure 4.123 show pore pressure contours (kPa) relative to mine workings and UIS gas drainage boreholes recorded at February 2007 and September 2007, respectively. The complete series of monthly pore pressure contour plots are provided in Appendix 4.2. The results show the naturally occurring hydrostatic pressure within the Bulli seam was in the order of 5 000 kPa, which was expected given the depth of cover to the Bulli seam was approximately 500 m. It was also shown that mining and gas drainage drilling has an effect on reducing the hydrostatic pressure many hundreds of metres beyond the point of activity. Of particular significance was the fact that the hydrostatic pressure within the coal seam immediately prior to roadway development remains quite high at approximately 1 000 kPa. The contour data also indicates a slower rate of pressure reduction from the inbye parts of the mine.

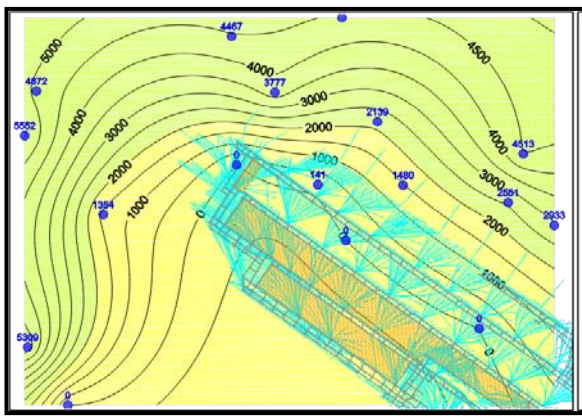

Figure 4.122: Piezometer readings, pressure contours, mine workings and UIS boreholes – February 2007

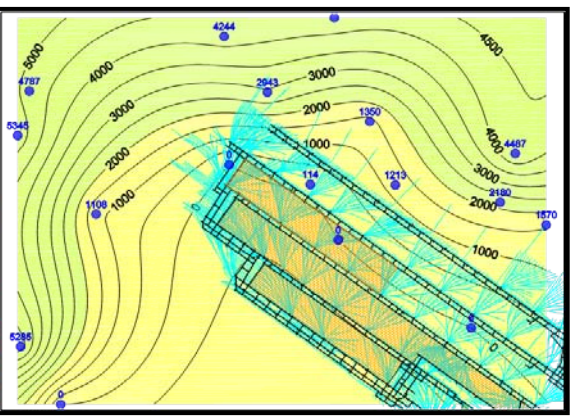

Figure 4.123: Piezometer readings, pressure contours, mine workings and UIS boreholes – September 2007

As discussed previously, the pressure within the coal seam must be reduced to the critical desorption point in order to support efficient gas drainage. Considering the typical Bulli seam example, shown in Figure 4.118, where the average gas content was 10.5 m^3/t and the seam gas is rich in CO_2, the corresponding pressure at the critical desorption point is 570 kPa. In this example, where the hydrostatic pressure within the coal seam remains above 1 000 kPa throughout the life of the gas drainage program, the reservoir pressure remains at least 430 kPa above the critical desorption pressure prior to mining and therefore has an adverse impact on gas desorption. The fact that the reservoir pressure has not been reduced to below the critical desorption pressure was a significant factor in explaining the lower gas production from the inbye, CO_2 rich, areas of the mine. Close and Erwin (1989) present a similar example from the Cameo seam in the Piceance Basin, western Colorado, where appreciable gas production could not be achieved as the reservoir pressure could not be reduced below the critical desorption pressure. Hadden and Sainato (1969) also report measuring high gas pressures in close proximity to freshly exposed, active mine workings during testing at Pocahontas No.3 Colliery, Pittsburgh USA. Pressure testing in the Bulli seam by Lama (1980), using a 40 m UIS borehole drilled at 45^O to the main cleat from 121 Panel at WCC, recorded a maximum gas pressure of 2 670 kPa.

The pressure contours also indicate that within the distance typically drilled for UIS gas drainage the pressure was typically no greater than 2 500 kPa at the time of drilling, which was consistent with measurements reported by Marshall *et al.* (1982). Figure 4.124 show the range of measured gas content values, at an assumed *in situ* gas pressure of 2 500 kPa, relative to the CH_4 and CO_2 isotherms, in each of three zones defined on the basis of seam gas composition. The ‘outbye zone’ comprises all sites where the CH_4 concentration was greater than 70%, the ‘middle zone’ comprises all sites where the CH_4 concentration was between 45 and 70% and the ‘inbye zone’ comprises all sites where the CH_4 concentration was less than 45%. The isotherm curves presented in each zone represent the average isotherm for both CH_4 and CO_2, determined from individual test samples within each zone. In the absence of specific isotherm data for mixed gas combinations linear interpolation was used to determine isotherm values for specific mixed gas combinations. On this basis the saturated gas content was calculated for each drill site location using the applicable $CH_4/(CH_4+CO_2)$ gas composition ratio enabling the DoS to be calculated.

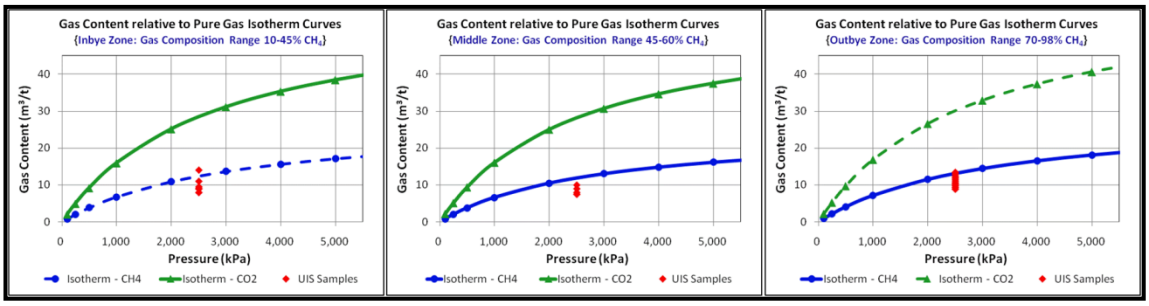

Figure 4.124: Gas content relative to pure gas isotherms within three gas composition zones

Figure 4.125 and Figure 4.126 show gas content and gas composition relative to DoS for each of the 34 drill sites. Where DoS was low, gas content was also low, while gas composition varied significantly. Where DoS was high gas content was also high and the gas composition was methane rich, taking full advantage of the lower methane gas isotherm.

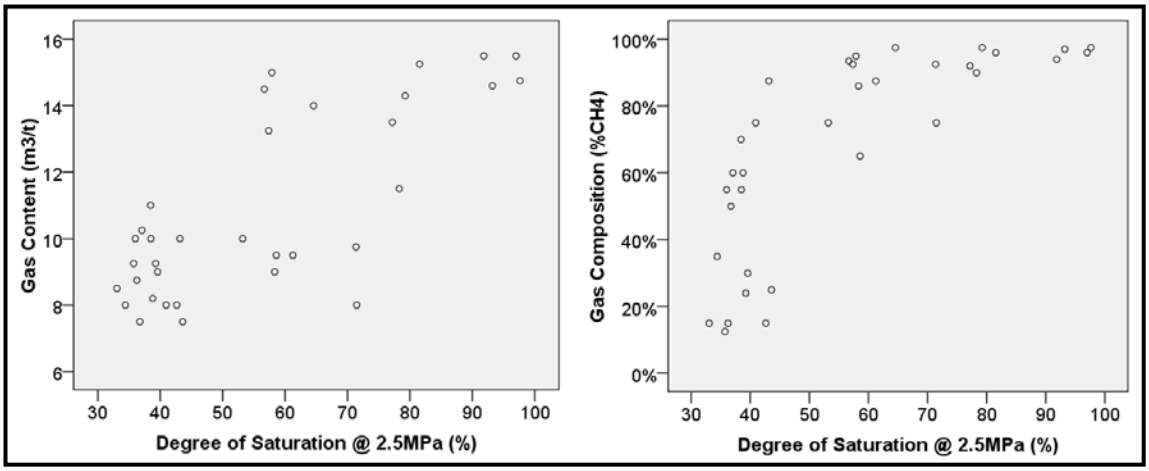

Figure 4.125: Gas content relative to DoS at each drill site

Figure 4.126: Gas composition relative to DoS at each drill site

Figure 4.127 and Figure 4.128 show the relationship between DoS and both total and D50 gas production. A strong relationship was indicated between gas production and DoS, with gas production increasing significantly in response to increasing DoS. Statistical analysis determined the correlation between DoS and each of total and D50 gas production was 0.755 and 0.871 respectively.

The relationship between DoS and both total and D50 gas production, within each cut-through zone, was also considered. As shown in both Figure 4.129 and Figure 4.130 gas production in each zone was consistently greater in areas of increased DoS.

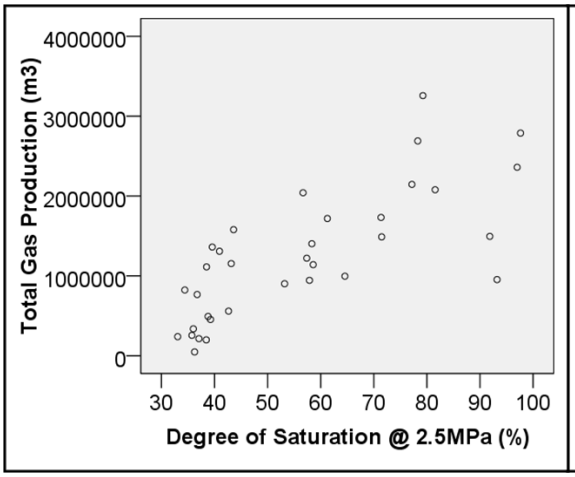

Figure 4.127: Total gas production relative to DoS at each drill site

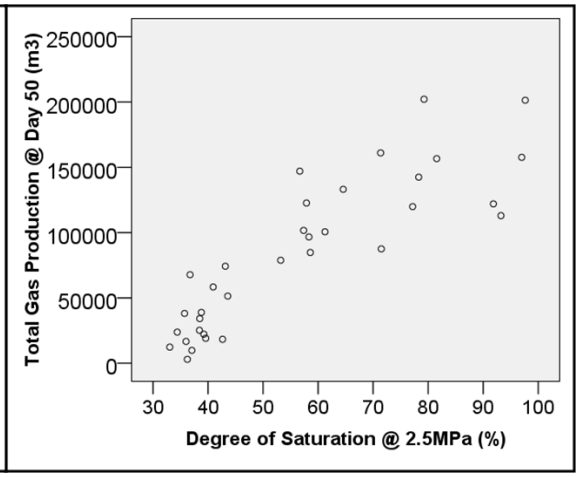

Figure 4.128: D50 gas production relative to DoS at each drill site

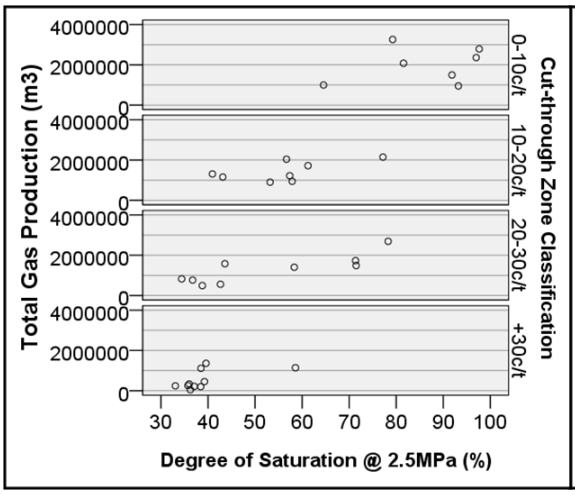

Figure 4.129: Total gas production relative to DoS in each cut-through zone

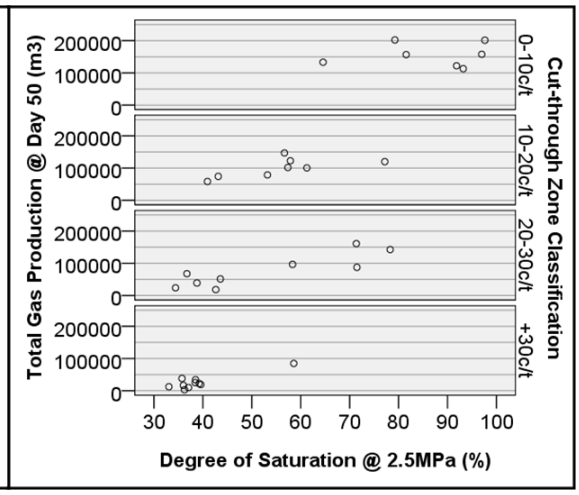

Figure 4.130: D50 gas production relative to DoS in each cut-through zone

Figure 4.131 shows a very strong relationship between DoS and total gas production per borehole within each drill pattern. Gas production per borehole was considered to account for the variable number of gas producing boreholes within each drill site. Statistical analysis determined the correlation between DoS and gas production per borehole was 0.899.

This assessment confirmed a strong relationship between gas production and DoS, consistent with the views of Lamarre (2007) and Seidle and O'Connor (2007). It was also shown that the inbye, CO_2 rich zones are highly undersaturated, requiring substantial pressure reduction prior to achieving appreciable gas production. Given the low saturation in the CO_2 rich inbye area the use of UIS gas drainage generally fails to

reduce reservoir pressure to the critical desorption point prior to mining which is likely to be a major contributing factor in the poor drainage effectiveness from this area.

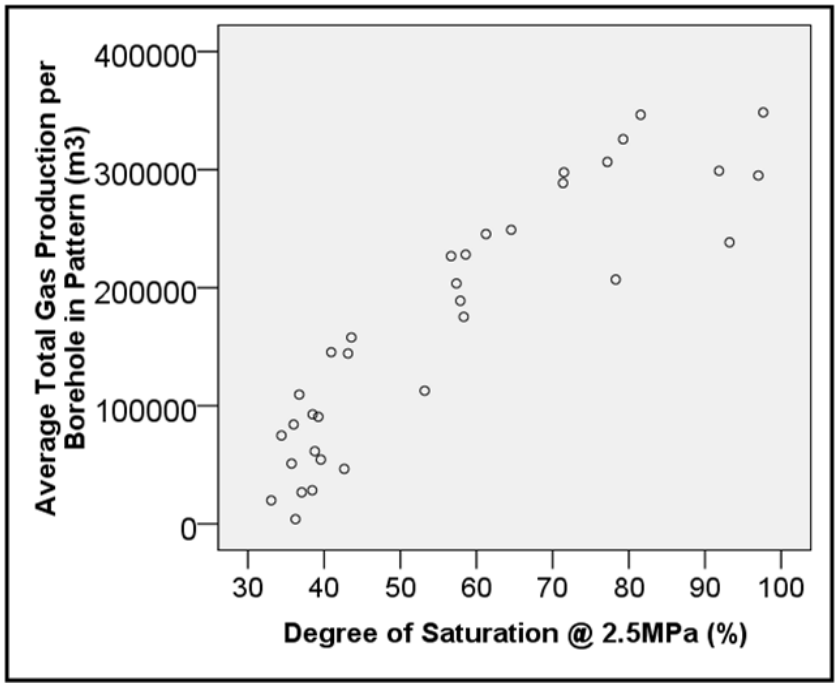

Figure 4.131: Total gas production per borehole in each drill site relative to DoS

4.5 SUMMARY

From this assessment of the impact of coal properties on gas drainage the degree of saturation was found to have the most significant impact on gas production.

Total gas in place, which is the product of seam thickness, drilled area and gas content, was also shown to have a close relationship to gas production.

The impact of gas composition was found to be significant, due to the difference between the CH_4 and CO_2 isotherms and the resulting impact on DoS, with a coal sample in a CO_2 rich area being less saturated than in an equivalent CH_4 rich area.

It was shown that in highly undersaturated CO_2 rich zones the seam gas pressure remains above the critical desorption point throughout the life of the UIS gas drainage boreholes, until immediately prior to mining. Although not analysed in this study, it was likely that the low permeability of the Bulli seam contributes to the slow rate of pressure reduction. The fact that the seam gas pressure was not reduced to below critical

desorption pressure was a significant factor in understanding and explaining the consistently low gas production from the highly undersaturated areas.

Other properties found to have a relationship to gas production include coal rank and ash content, with increased maximum gas production achieved in areas with lower ash content and higher rank. Within this mining area the low ash, high rank coal was located in the more highly saturated, CH_4 rich coal. Given the dominant impact of DoS on gas production the observed relationship between gas production, ash content and coal rank may be coincidental.

No evidence was found to indicate a relationship between gas production and coal type, inherent moisture content or raw ash content.

CHAPTER FIVE – IMPACT OF OPERATIONAL FACTORS ON GAS DRAINAGE

5.1 INTRODUCTION

This chapter examines the impact of a variety of operational factors on gas production from UIS gas drainage boreholes drilled into the Bulli coal seam at WCC, in the mining area, known as Area 5. The operational factors are related to the design and management of the gas drainage system, including the associated gas reticulation network, which is within the control of mine management.

A number of operational factors have been investigated by past researchers to determine their relative impact on the efficiency and overall effectiveness of coal seam gas drainage. These properties include borehole diameter (Battino and Hargraves, 1982 and Clark *et al.*, 1983); borehole length and orientation (Battino and Regan, 1982; Gray, 1982; Kahil and Masszi, 1982 and Clark *et al.*, 1983); borehole spacing (Lama, 1988); drainage time (Clark *et al.*, 1983); and applied suction pressure (Clark *et al.*, 1983 and Lama, 1988a).

When designing a new mine, or new area within an established mine, the impact of mine layout and panel orientation on future gas drainage effectiveness typically does not rank among the major design considerations. Once the orientation of mine workings has been fixed the scope for varying the orientation of UIS gas drainage boreholes becomes constrained, typically limited to drilling across panels, from open roadways, to access the coal ahead of future mine development.

The orientation of the mine workings at WCC was well established; therefore assessment of operational factors relevant to gas production performance was based on data available within the limits of the existing UIS drainage program design.

5.2 DATA ACQUISITION

Figure 5.1 shows the location of the 279 boreholes included in this analysis. In addition to the gas production data, discussed in Chapter 4.2.1, the following data relating to each of the 279 UIS boreholes was measured:

- Total borehole length, including major branches;

- Average orientation of the borehole relative to (a) the primary cleat orientation, (b) principal horizontal stress orientation, and (c) the reference orientation of true north; and
- Average apparent dip of the borehole relative to the strike and dip of the coal seam.

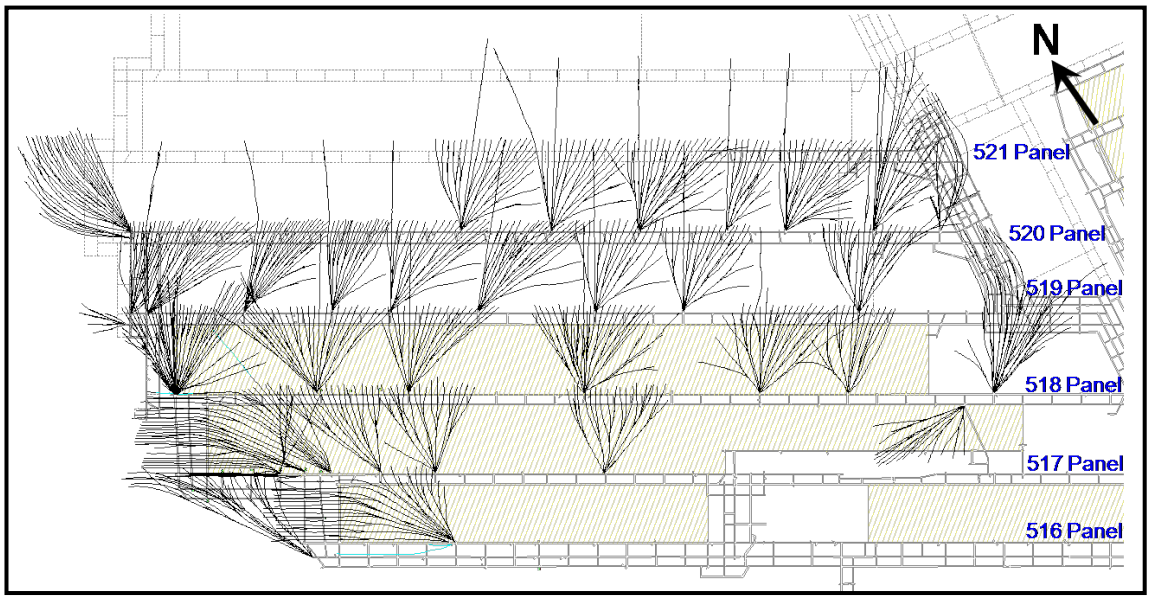

Figure 5.1: Location of UIS boreholes relative to mine workings

Data relating to the assessment of operational factors was gathered from various sources within the operating and technical areas of BHP Billiton Illawarra Coal. Data gathered for analysis includes:

- Cleat orientation and spacing recorded during geological mapping along the length of 519 and 520 panel by an experienced geologist;
- Stress orientation interpreted from borehole logging during surface-to-seam exploration programs;
- Seam dip interpretation from the top of the coal seam measured during surface-to-seam exploration drilling and logging; and
- Drainage time and applied suction pressure data extracted from weekly gas production reports.

5.3 ANALYSIS OF OPERATIONAL FACTORS

The relationship between gas production and each of the operational factors, listed in Table 5.1 is presented. Appendix 5.1 provides a summary of gas production and

operational factor data corresponding to each of the 279 boreholes included in this study.

Table 5.1: Operational factors considered in analysis

Borehole Length	Orientation relative to Cleat	Orientation relative to North
Borehole Diameter	Orientation relative to Stress	Drainage Time
Spacing / Drilling Density	Orientation relative to Seam Dip	Applied Suction Pressure

5.3.1 Borehole Length

The length of the 279 boreholes analysed ranged from 53 to 1 880 m, inclusive of major branches, with the average length measuring 836 m. Figure 5.2 and Figure 5.3 show the distribution of borehole lengths for the boreholes in the complete dataset and in each of the four cut-through zones. More than 50% of the boreholes have a length between 500 and 1 000 m and this trend is reasonably consistent within each cut-through zone. Given the standard fan pattern used in UIS drilling a reasonably consistent borehole length was expected.

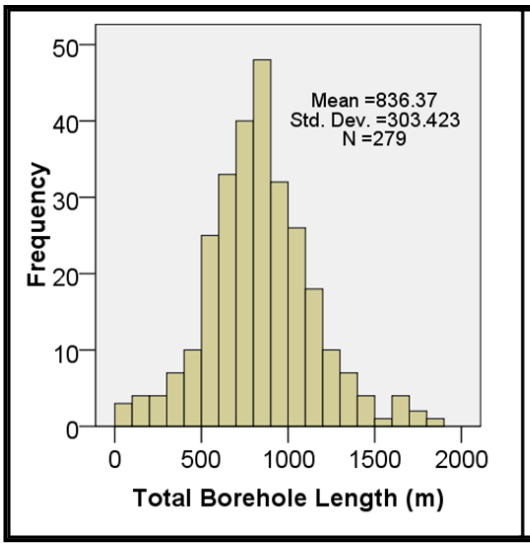

Figure 5.2: Distribution of borehole length for all boreholes within the complete dataset

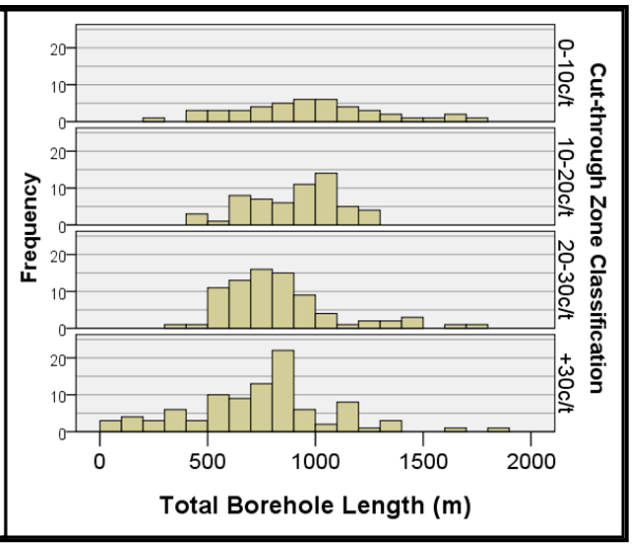

Figure 5.3: Distribution of borehole length for boreholes in each cut-through zone

Figure 5.4 and Figure 5.5 show the relationship between borehole length and gas production, indicates low total and D50 production from shorter boreholes, with

maximum gas production increasing with increasing borehole length. The results also indicate drop in maximum gas production from boreholes whose length exceeded approximately 1 000 m, which may suggest increasing production difficulties from boreholes exceeding the upper limit of an optimum length range.

Statistical analysis determined a positive correlation of 0.306 and 0.368 between borehole length and each of total gas production and D50 gas production.

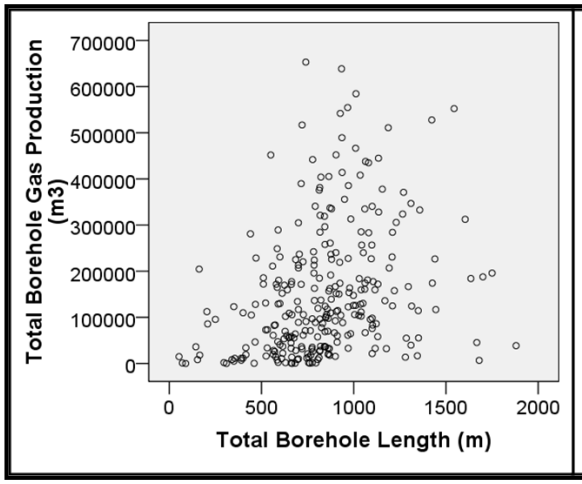

Figure 5.4: Total gas production relative to borehole length

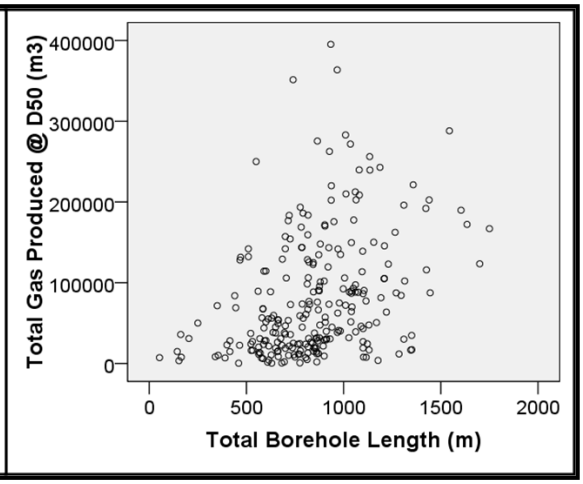

Figure 5.5: D50 gas production relative to borehole length

The relationship between borehole length and both total and D50 gas production, within each cut-through zone, was also considered. The data, presented in Figure 5.6 and Figure 5.7, do not suggest that borehole length has a significant impact on gas production however there was some indication of increased maximum gas production from boreholes ranging in length between approximately 500 and 1 000 m.

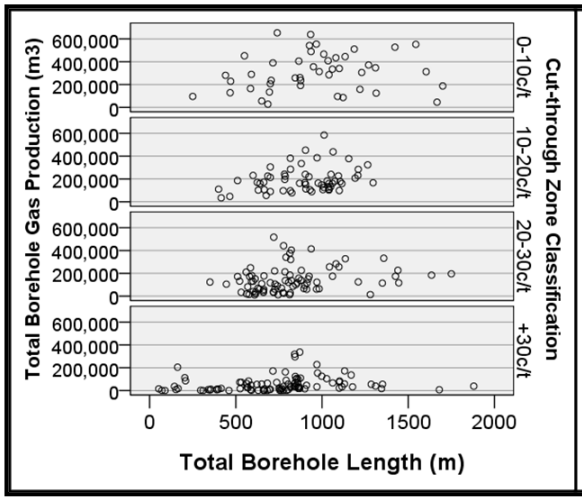

Figure 5.6: Total gas production relative to borehole length in each cut-through zone

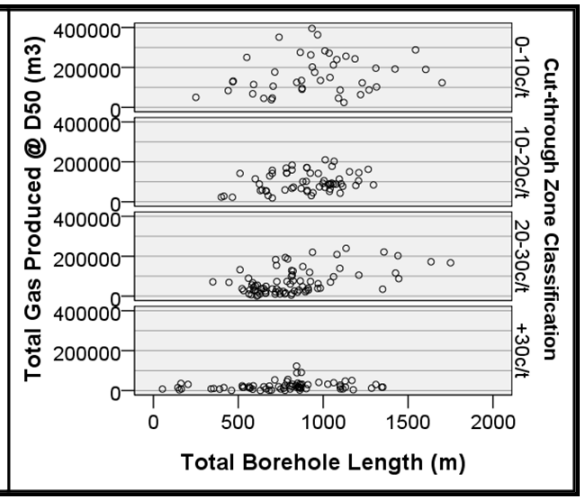

Figure 5.7: D50 gas production relative to borehole length in each cut-through zone

The relationship between borehole length and both total and D50 gas production per unit borehole length was also considered. The data, presented in Figure 5.8 and Figure 5.9, indicate a decrease in gas production per metre from boreholes of increasing length with the maximum gas production rate being achieved from boreholes ranging in length between approximately 500 and 1 000 m.

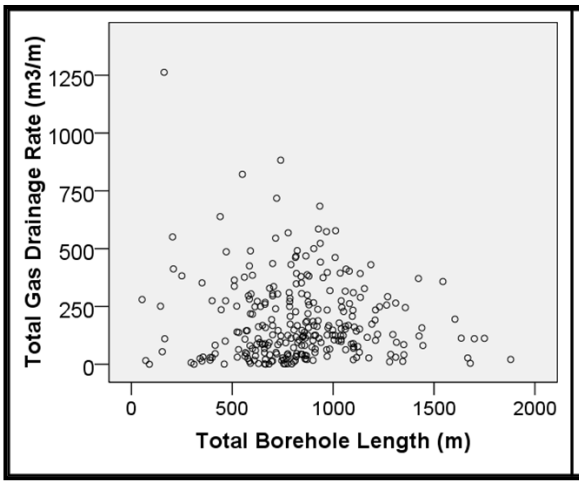

Figure 5.8: Total gas production per unit borehole length relative to borehole length

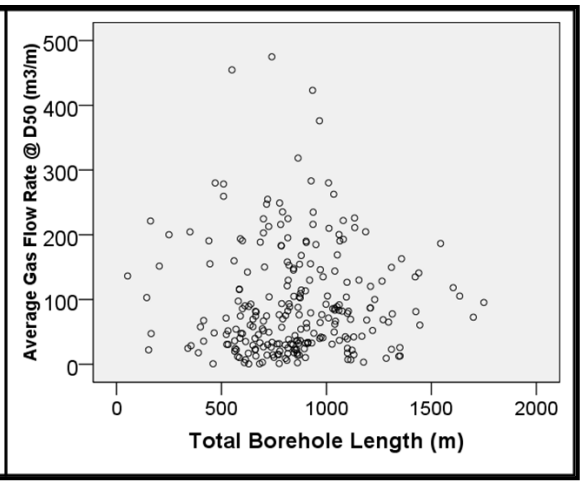

Figure 5.9: D50 gas production per unit length relative to borehole length

Mutmansky (1999) studied the impact of borehole length on gas drainage efficiency and found that in 15 underground mines where boreholes were less than 300 m the drainage efficiency was below 20% whereas in 10 underground mines with boreholes between 300 and 1 300 m the drainage efficiency was up to 40%. Although Mutmansky did not discuss the potential impact of drilling density the results of this study are consistent with Mutmansky's observation in that boreholes less than 500 m in length produce less gas than those of greater length.

This study identified maximum gas production was achieved from boreholes that ranged in length between 500 and 1 000 m. Beyond this range boreholes of increasing length indicated a decrease in both total gas production and gas production per unit length and boreholes less than 500 m long also achieved reduced maximum gas production.

5.3.2 Borehole Diameter

At WCC UIS gas drainage boreholes are drilled using standard 96 mm diameter drill bits. Therefore an analysis of the impact on gas production from changes in drill bit diameter could not be completed. This relationship has been investigated previously by

Battino and Hargraves (1982), who reported a linear increase in gas flow rate from boreholes increasing in diameter from 30 to 130 mm, and Clark *et al*. (1983), who reported a positive correlation between borehole diameter and average gas flow rate per unit borehole length at Metropolitan Colliery. Lama (1988a) suggested that in the very early life of a borehole, a larger diameter will record flow rates proportional to the diameter, but in the later stages, the flow rate will be independent of diameter.

Figure 5.10 shows the gas flow rate recorded from boreholes of various diameters, each being 80 m long, as reported by Battino and Hargraves (1982) and Clark *et al*. (1983). A significant difference exists between the results of the two studies, with Clark *et al*. reporting gas flow rates an order of magnitude greater than those reported by Battino and Hargraves. However both cases reported increased gas production from larger diameter boreholes. The reasons given by Clark *et al*. to support their findings include:

- Holes of larger diameter are less prone to blockages by water and coal fragments;
- The resistance to flow and pressure losses in a borehole decrease with increasing diameter;
- The length of borehole affected by applied suction pressure increases as diameter increases; and
- Larger diameter boreholes achieve greater surface contact with the coal seam and thereby have a greater radius of influence on gas drainage.

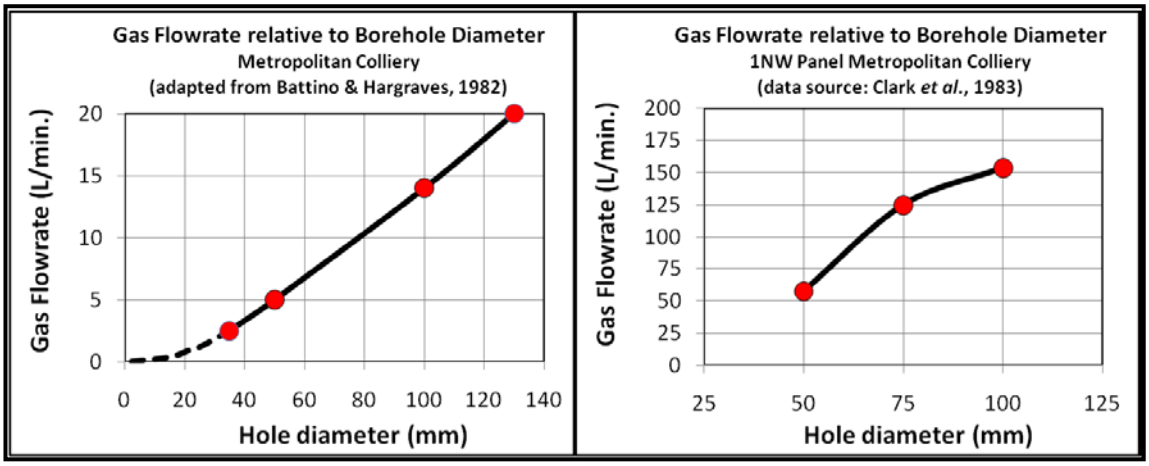

Figure 5.10: Results of gas flow relative to borehole diameter testing by Battino and Hargraves (1982) and Clark *et al.* (1983)

The reported CO_2 gas flow rate from boreholes of 50 and 100 mm diameter, from both studies, was considered in more detail. Battino and Hargraves (1982) reported gas flow rates of 5 and 14 L/min from 50 and 100 mm diameter boreholes, which equate to in-

hole gas flow rate velocities of 0.04 m/s and 0.03 m/s respectively. Clark *et al*. (1983) reported gas flow rates of 57.7 and 150.0 L/min from 50 and 100 mm diameter boreholes, which equate to in-hole gas flow velocities of 0.49 m/s and 0.32 m/s respectively. Using Atkinson's equation (Le Roux, 1990), Equation 5.1, the resulting pressure loss due to frictional resistance along the borehole was calculated. A roughness height of 2 mm was assumed within the borehole.

From the data presented by Battino and Hargraves (1982) the pressure loss along a 100 m borehole, of 50 and 100 mm diameter, was 0.213 Pa and 0.039 Pa respectively for pure CO_2 gas flow, and 0.078 Pa and 0.014 Pa respectively for pure CH_4 gas flow. Both the gas flow velocities and differential pressure loss are extremely low and it is expected that the researchers would have experienced difficulty recording accurate measurements, particularly considering the typically variable nature of gas flow from UIS gas drainage boreholes.

$$P = \frac{k.C.L.}{A^3} . \frac{\rho}{1.2} . Q^2 \qquad (5.1)$$

where: P = pressure loss (Pa)
k = friction factor ($N.s^2/m^4$)
C = borehole perimeter (m)
L = borehole length (m)
A = cross-sectional area (m^2)
ρ = gas density (kg/m^3)
Q = quantity (m^3)

From the data presented by Clark *et al*. (1983) the pressure loss along a 100 m borehole, of 50 and 100 mm diameter, was 28.35 Pa and 4.5 Pa respectively for pure CO_2 gas flow, and 10.38 Pa and 1.65 Pa respectively for pure CH_4 gas flow. These results are considered more reasonable and the levels are such as to support accurate measurement of both gas flow velocity and differential pressure.

The results highlight that resistance, and therefore pressure loss due to friction, along the length of a borehole, carrying pure CO_2 gas, is 2.73 times greater than for the same borehole carrying pure CH_4 gas. This difference is due to the increased gas density of CO_2 (1.83 kg/m^3) which is 2.73 times greater than CH_4 (0.67 kg/m^3).

Further analysis was undertaken, using Atkinson's equation, to evaluate the impact on gas flow velocity and frictional pressure loss through variations in borehole diameter and borehole length. Figure 5.11 and Figure 5.12 show the impact on gas flow velocity and frictional pressure loss along 500 m boreholes having diameters of 50 mm, 100 mm and 150 mm, carrying CH_4 and CO_2 respectively, in response to increasing gas flow rates, from 5 to 700 L/min. The analysis was extended to include the impact of varying borehole length. Table 5.2 and Table 5.3 show gas flow velocity and differential pressure loss for CH_4 and CO_2 gas flow respectively, along boreholes of 250 m, 500 m, 750 m and 1 000 m in length.

The results highlight the significant increase in gas flow velocity and frictional pressure loss in smaller diameter boreholes, with velocity being proportional to the inverse of diameter squared and pressure loss being proportional to length.

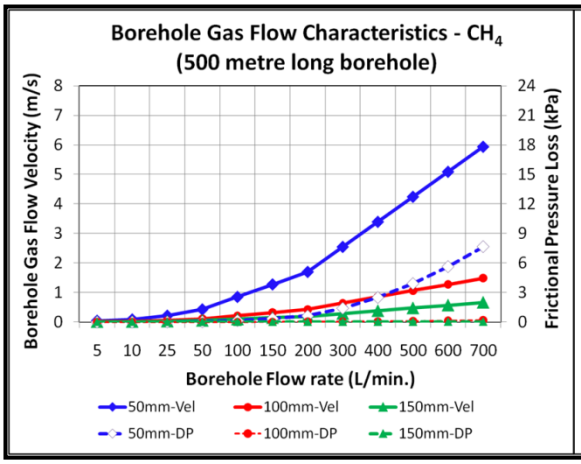

Figure 5.11: Impact of borehole diameter on CH_4 gas flow velocity and pressure loss relative to changes in total gas flow rate

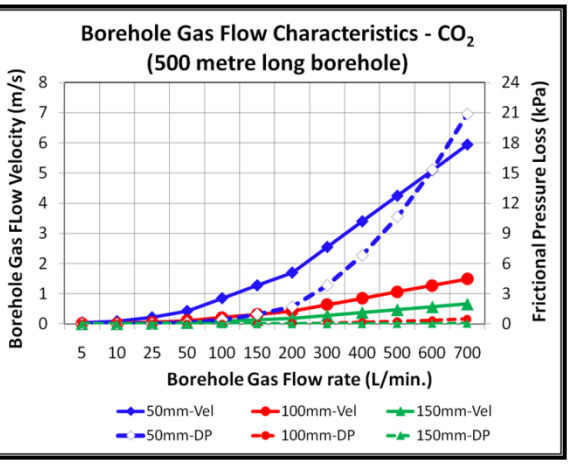

Figure 5.12: Impact of borehole diameter on CO_2 gas flow velocity and pressure loss relative to changes in total gas flow rate

Table 5.2: Impact of diameter, length and flow rate on frictional pressure loss in a borehole carrying CH_4 gas

Flow Rate		CH_4 Gas Flow Velocity (m/s)			Frictional Pressure Loss (kPa) 50mm diameter				Frictional Pressure Loss (kPa) 100mm diameter				Frictional Pressure Loss (kPa) 150mm diameter			
L/min	L/s	50mm Ø	100mm	150mm	250m	500m	750m	1000m	250m	500m	750m	1000m	250m	500m	750m	1000m
5	0.08	0.042	0.011	0.005	0.000	0.000	0.001	0.001	0.000	0.000	0.000	0.000	0.000	0.000	0.000	0.000
10	0.17	0.085	0.021	0.009	0.001	0.002	0.002	0.003	0.000	0.000	0.000	0.000	0.000	0.000	0.000	0.000
25	0.42	0.212	0.053	0.024	0.005	0.010	0.015	0.019	0.000	0.000	0.000	0.000	0.000	0.000	0.000	0.000
50	0.83	0.424	0.106	0.047	0.019	0.039	0.058	0.078	0.000	0.001	0.001	0.002	0.000	0.000	0.000	0.000
100	1.67	0.849	0.212	0.094	0.078	0.156	0.234	0.312	0.002	0.004	0.005	0.007	0.000	0.000	0.001	0.001
150	2.50	1.273	0.318	0.141	0.175	0.351	0.526	0.702	0.004	0.008	0.012	0.016	0.000	0.001	0.001	0.002
200	3.33	1.698	0.424	0.189	0.312	0.624	0.935	1.247	0.007	0.015	0.022	0.029	0.001	0.002	0.002	0.003
300	5.00	2.546	0.637	0.283	0.702	1.403	2.105	2.806	0.016	0.033	0.049	0.066	0.002	0.004	0.006	0.007
400	6.67	3.395	0.849	0.377	1.247	2.494	3.742	4.989	0.029	0.059	0.088	0.117	0.003	0.007	0.010	0.013
500	8.33	4.244	1.061	0.472	1.949	3.897	5.846	7.795	0.046	0.092	0.137	0.183	0.005	0.010	0.016	0.021
600	10.00	5.093	1.273	0.566	2.806	5.612	8.418	11.225	0.066	0.132	0.198	0.264	0.007	0.015	0.022	0.030
700	11.67	5.942	1.485	0.660	3.819	7.639	11.458	15.278	0.090	0.180	0.269	0.359	0.010	0.020	0.031	0.041

Table 5.3: Impact of diameter, length and flow rate on frictional pressure loss in a borehole carrying CO_2 gas

Flow Rate		CO_2 Gas Flow Velocity (m/s)			Frictional Pressure Loss (kPa) 50mm diameter				Frictional Pressure Loss (kPa) 100mm diameter				Frictional Pressure Loss (kPa) 150mm diameter			
L/min	L/s	50mm Ø	100mm	150mm	250m	500m	750m	1000m	250m	500m	750m	1000m	250m	500m	750m	1000m
5	0.08	0.042	0.011	0.005	0.001	0.001	0.002	0.002	0.000	0.000	0.000	0.000	0.000	0.000	0.000	0.000
10	0.17	0.085	0.021	0.009	0.002	0.004	0.006	0.009	0.000	0.000	0.000	0.000	0.000	0.000	0.000	0.000
25	0.42	0.212	0.053	0.024	0.013	0.027	0.040	0.053	0.000	0.001	0.001	0.001	0.000	0.000	0.000	0.000
50	0.83	0.424	0.106	0.047	0.053	0.106	0.160	0.213	0.001	0.003	0.004	0.005	0.000	0.000	0.000	0.001
100	1.67	0.849	0.212	0.094	0.213	0.426	0.639	0.852	0.005	0.010	0.015	0.020	0.001	0.001	0.002	0.002
150	2.50	1.273	0.318	0.141	0.479	0.958	1.437	1.916	0.011	0.023	0.034	0.045	0.001	0.003	0.004	0.005
200	3.33	1.698	0.424	0.189	0.852	1.703	2.555	3.406	0.020	0.040	0.060	0.080	0.002	0.005	0.007	0.009
300	5.00	2.546	0.637	0.283	1.916	3.832	5.748	7.665	0.045	0.090	0.135	0.180	0.005	0.010	0.015	0.020
400	6.67	3.395	0.849	0.377	3.406	6.813	10.219	13.626	0.080	0.160	0.240	0.320	0.009	0.018	0.027	0.036
500	8.33	4.244	1.061	0.472	5.323	10.645	15.968	21.290	0.125	0.250	0.375	0.500	0.014	0.028	0.043	0.057
600	10.00	5.093	1.273	0.566	7.665	15.329	22.994	30.658	0.180	0.360	0.540	0.721	0.020	0.041	0.061	0.082
700	11.67	5.942	1.485	0.660	10.432	20.865	31.297	41.729	0.245	0.490	0.736	0.981	0.028	0.056	0.083	0.111

Another factor that must be considered is the occurrence of borehole breakout in UIS boreholes drilled in the Bulli seam (Mills *et al*., 2006), whereby high vertical stress applied to comparatively weak coal tends to flatten the boreholes leading to failure of the side walls increasing the width of the borehole, as shown in Figure 5.13. An accumulation of coal fines can be seen within the borehole in Figure 5.13 and this may be due to the failure of the coal surrounding the borehole during and subsequent to drilling. The presence of such accumulations may adversely impact gas production and could, in extreme cases, completely block sections of the borehole restricting, or even preventing, gas flow.

Figure 5.13: Borehole breakout in a UIS borehole at WCC

Figure 5.14 shows the results from logging a 50 m section of a UIS borehole within the mining area using the calliper tool developed under ACARP project C12021 (Jeffrey *et al*., 2005). The results confirm the presence of borehole breakout with the measured width increasing in places to double the original diameter.

This analysis has confirmed that the standard drill bit diameter of 96 mm used in UIS gas drainage drilling is effective. Smaller diameter boreholes experience far greater frictional pressure loss and very high gas flow velocity. Larger diameter boreholes require increased diameter drill rods which are more expensive and result in increased weight down-hole which necessitate the use of larger, more expensive, and less flexible drill rigs. Such holes do not achieve appreciable benefits.

In the case of boreholes oriented with the dip of the coal seam there is an increased risk of water and coal fines accumulating within the borehole. Where boreholes are oriented down-dip, high in-hole gas velocity may assist in mobilising the material and blowing it from the borehole to maintain conditions conducive to ongoing degassing. Where the gas velocity is not sufficient to mobilise fines there is a need for an in-hole dewatering and fines removal system.

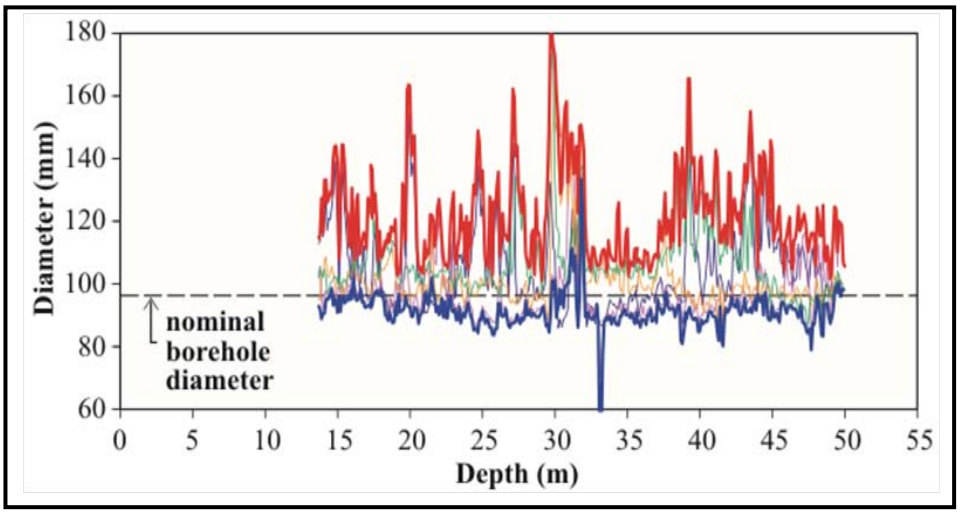

Figure 5.14: Calliper logging of a UIS borehole at WCC (after Mills *et al.*, 2006)

5.3.3 Borehole Density

Lama (1988a) suggests that the spacing between drainage boreholes is an important consideration as the total cost of drilling and equipping holes may make drainage uneconomic when holes are too closely spaced, and if holes are too widely spaced, the

time required to successfully drain may be so long that effective drainage may not be possible.

Borehole spacing is the distance between the end (toe) of each borehole. The spacing between boreholes, or borehole density, is typically a function of the gas content reduction required within the available gas drainage window, with the mine operator increasing the drilling density in areas where gas content is high and the drainage window is short. Figure 5.15 and Figure 5.16 show boreholes drilled from 519 26c/t and 519 11c/t, illustrating the difference in borehole spacing between the inbye and outbye zones of the mining area at WCC. The spacing between boreholes in the inbye zones that drain at a slower rate was less than 12 m whereas, in the outbye, more productive zones, the borehole spacing was typically 20 to 25 m.

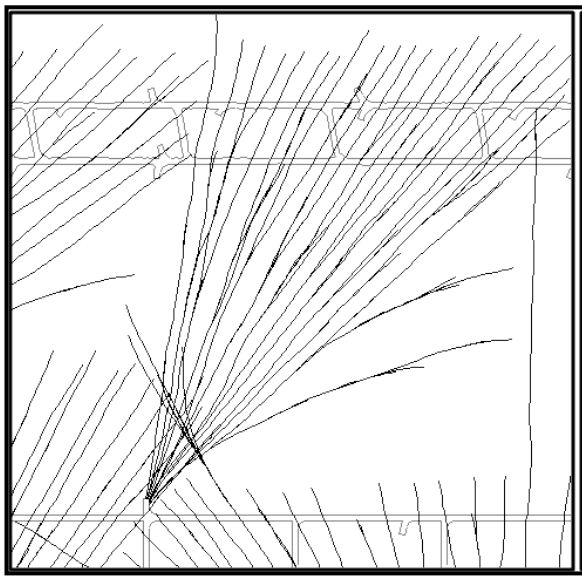

Figure 5.15: 519 26c/t drill pattern showing increased drilling density of the inbye zones

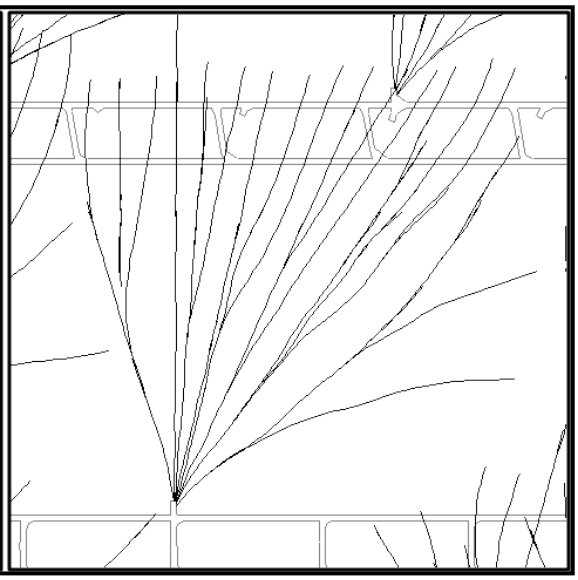

Figure 5.16: 519 11c/t drill pattern showing reduced drilling density of the outbye zones

Figure 5.17 and Figure 5.18 show the distribution of borehole density in metres of boreholes drilled within the total area covered by each drill pattern for all 34 drill sites. The borehole density, which is a measure of total metres drilled (m) within the area drilled (m^2) from each drill site, ranges from a low of 0.04 m/m^2 to a high of 0.13 m/m^2, with an average of 0.07 m/m^2. The borehole density was relatively consistent in the first three cut-through zones, averaging approximately 0.06 m/m^2, however the average increased 50% to approximately 0.09 m/m^2 in the +30c/t zone.

Figure 5.19 and Figure 5.20 show the relationship between borehole density and each of total and D50 gas production. The data suggests a strong relationship between gas production and borehole density, with increased gas production from areas having lower borehole density. This relationship, if taken out of context, appears unreasonable suggesting that increased coal seam gas production may be achieved by increasing the distance between boreholes. However in this case drilling density was increased in an attempt to increase gas production from the highly undersaturated, CO_2 rich coal in the inbye parts of the panels. However the increased drilling density has generally been ineffective in increasing gas production from the inbye drill stubs.

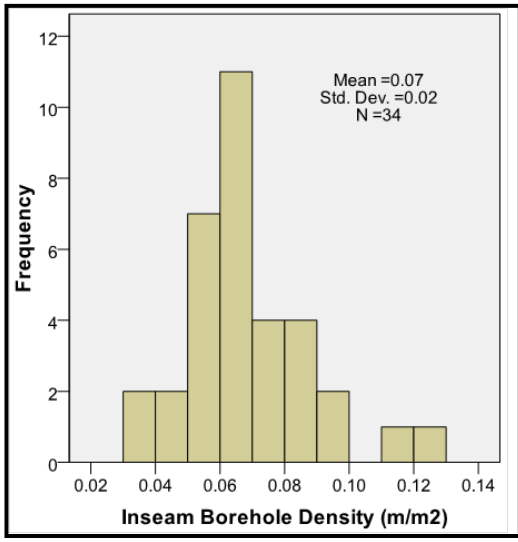

Figure 5.17: Distribution of borehole density for drill sites within the complete dataset

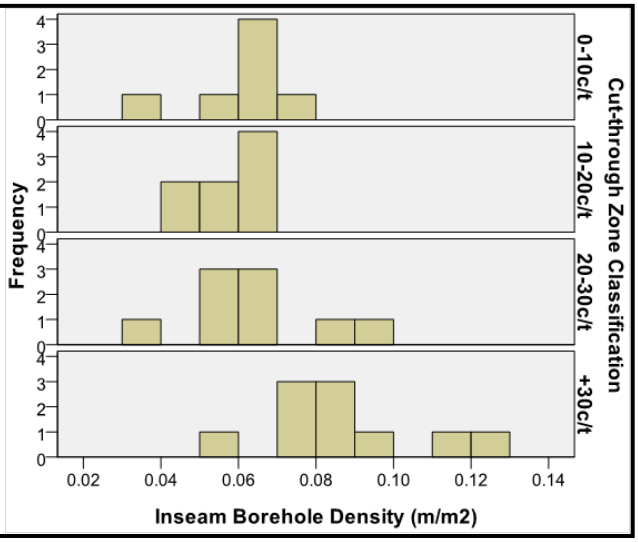

Figure 5.18: Distribution of borehole density for drill sites within each cut-through zone

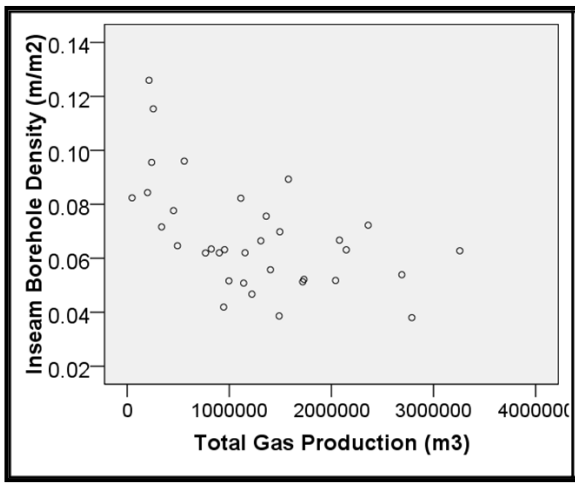

Figure 5.19: Total gas production relative to borehole density

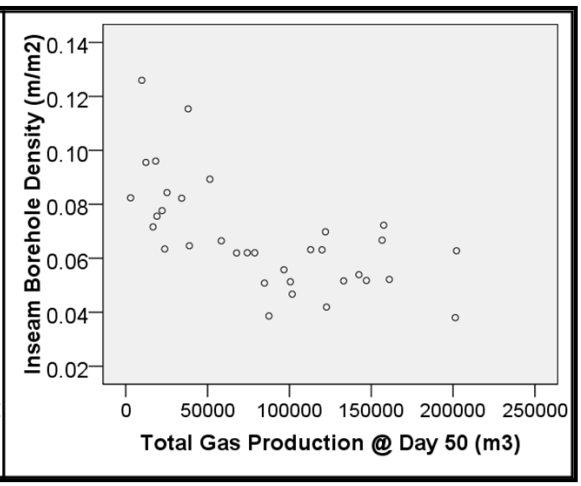

Figure 5.20: D50 gas production relative to borehole density

The relationship between borehole density and both total and D50 gas production, within each cut-through zone, was also considered. As shown in both Figure 5.21 and Figure 5.22 gas production reduces with distance into the panel yet within each cut-through zone there was no evidence to suggest borehole density affects gas production. From this analysis it was concluded that borehole density does not impact gas production and increased drilling in the inbye zones provides no tangible benefit toward increasing gas production.

The cost of drilling UIS boreholes was reported to range between $50 per metre for owner operated and $100 per metre for contracted drilling services (Benson, 2006 and Meyer *et al.*, 2007). Given that the length of a typical UIS borehole is in the order of 400 m the drilling cost ranges between $20 000 and $40 000. The average borehole length, inclusive of major branches, in this mining area, as presented in Section 5.3.1, was 836 m and the cost, given West Cliff runs owner operated drill rigs, is expected to be in the order of $42 000 per borehole. The total cost of a gas drainage program is a function of drilling density; halving the spacing between boreholes effectively doubles the total drilling cost. Therefore the relationship between borehole density and corresponding gas production must be well understood and the design of the gas drainage boreholes should endeavour to avoid over-drilling and to achieve maximum gas production from each drilled metre.

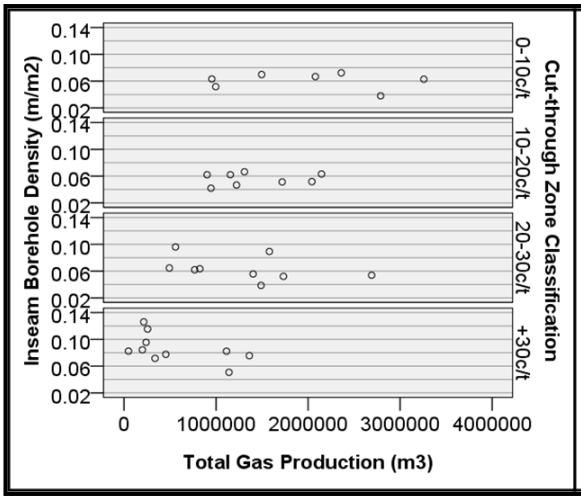

Figure 5.21: Total gas production relative to borehole density in each cut-through zone

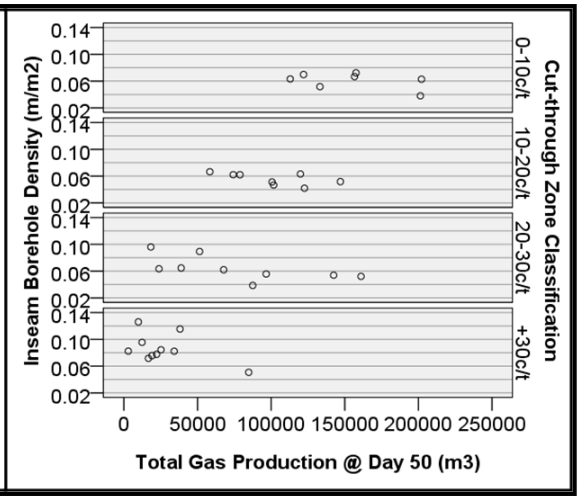

Figure 5.22: D50 gas production relative to borehole density in each cut-through zone

5.3.4 Borehole Orientation

Meszaros *et al*. (2007) suggests gas production is highly dependent upon the properties of the cleat system which include cleat spacing and cleat interconnection. This view was shared by Cui and Busten (2006) who suggested that an increase in cleat spacing increases the length of pathway within the coal matrix through which the gas must diffuse thus reducing the volumetric flux of gas out of the larger coal matrix. Therefore a coal seam with lower cleat spacing and greater cleat aperture can be expected to have better gas production characteristics.

Figure 5.23 illustrates the macroscopic cleat network of a coal seam, consisting of continuous face cleats and discrete butt cleats. Laubach *et al*. (1998) suggest cleat spacing decreases in response to decreasing bed thickness (band thickness), increasing vitrain content, increasing coal rank, and intensity of deformation. Laubach *et al*. also suggest that the most productive coal seams have cleat spacing between 0.001 and 20 mm, and cleat aperture between 0.05 and 20 μm.

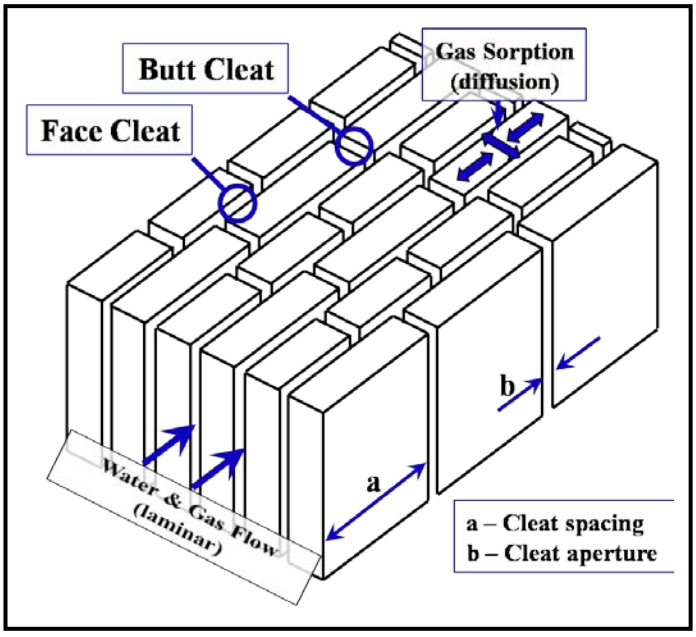

Figure 5.23: Macroscopic cleat network of a coal seam

5.3.4.1 Borehole Orientation Relative to Cleat

Previous studies by Hayes (1982), Hargraves (1983), Hebblewhite *et al*. (1983) and Osisanya and Schaffitzel (1996) suggest gas drainage boreholes drilled perpendicular to the major (face) cleat are more likely to produce a higher volume of gas for a more sustained period than those oriented perpendicular to the minor (butt) cleat. Battino and

Hargraves (1982) reported that testing in the Castor seam at Cook Colliery, using a 21 m long, 43 mm diameter borehole, measured gas flow rates ranging from 85 to 175 L/min from boreholes drilled perpendicular to the major cleat, which was marginally higher than the flow rates from boreholes drilled parallel to the major cleat, which were up to 75 L/min. However, similar testing in the Aries seam at Leichhardt Colliery determined borehole orientation relative to cleat had little influence on gas production.

Geological mapping of 148 locations along the length of the 519 and 520 panels at WCC determined the orientation of the dominant (face) cleat was 100/280^{O} (Newland, 2007). The relationship between gas production and borehole orientation, relative to cleat, has been investigated. As discussed previously, WCC typically utilise standard drilling patterns therefore the distribution of borehole orientation was expected to be reasonably consistent throughout the mine. Figure 5.24 and Figure 5.25 show the distribution of average borehole orientation relative to the face cleat for boreholes in the complete dataset and in each of the four cut-through zones. The average orientation of the boreholes relative to the face cleat for the complete dataset was 49^{O}, with the average in the cut-through zones ranging from a low of 44^{O}, in the 10-20c/t zone, to a high of 52^{O}, in the +30c/t zone.

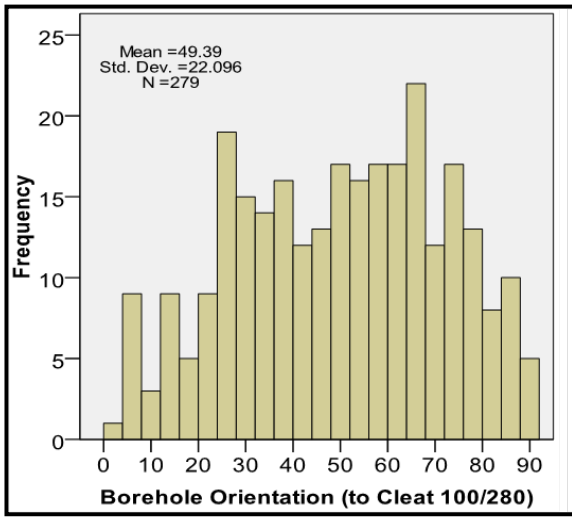

Figure 5.24: Distribution of average orientation relative to cleat (100/280^{O}) for boreholes in the complete dataset

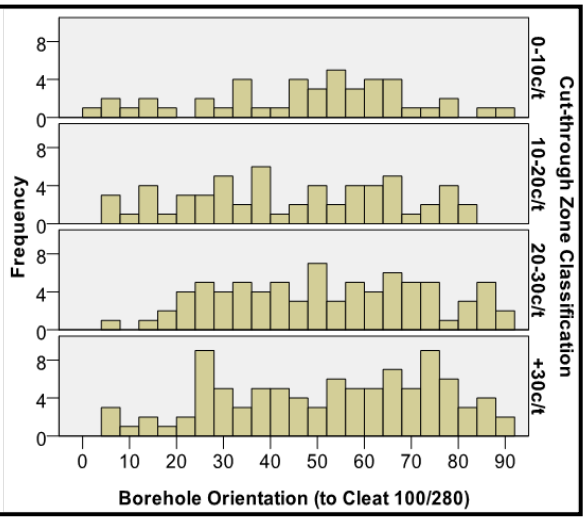

Figure 5.25: Distribution of average orientation relative to cleat (100/280^{O}) for boreholes in each cut-through zone

Figure 5.26 and Figure 5.27 show the relationship between total and D50 gas production relative to the angle between the borehole and the face cleat. Statistical analysis confirmed a weak negative correlation of –0.082 and –0.098 between borehole

orientation relative to face cleat and each of total and D50 gas production. Although there was no apparent relationship between gas production and borehole orientation relative to cleat, the data indicated increased gas production from boreholes oriented between 5 and 60^{O} to the face cleat. The boreholes within this range achieved the highest total gas production, as well as the highest D50 gas production.

Analysis of total gas production data from boreholes oriented between 5 and 60^{O} to the face cleat achieved an average 160 332 m^3 total gas production, 19% greater than the average 135 093 m^3 of the boreholes outside this range. Analysis of D50 gas production from boreholes oriented between 5 and 60^{O} to the face cleat achieved 86 670 m^3, 26% greater than the average 68 838 m^3 of the boreholes outside this range.

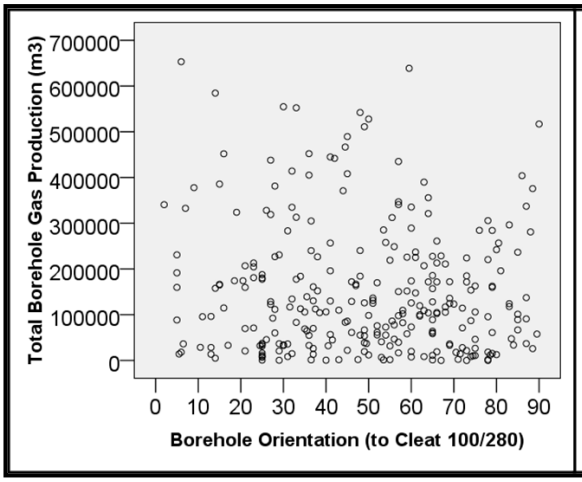

Figure 5.26: Total gas production relative to average borehole orientation to cleat (100/280^{O})

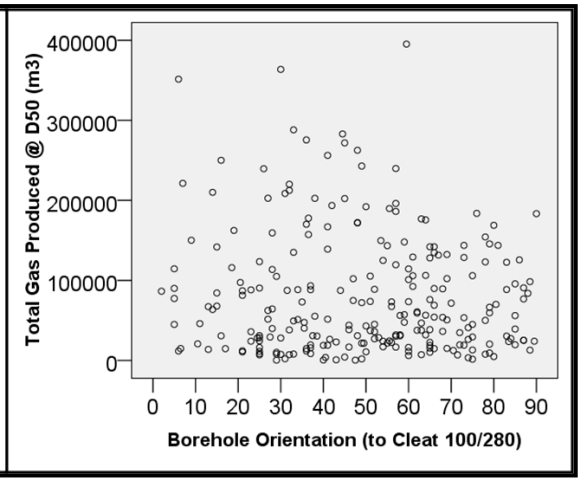

Figure 5.27: D50 gas production relative to average borehole orientation to cleat (100/280^{O})

The relationship between borehole orientation, relative to face cleat and both total and D50 gas production, within each cut-through zone, was also considered. Figure 5.28 and Figure 5.29 indicate increased gas production from boreholes oriented between 5 and 60^{O} to the face cleat, in the 0-10c/t zone and to a lesser extent in the 10-20c/t zone. Borehole orientation relative to cleat had little impact on gas production from boreholes located in the inbye, lower producing, and highly undersaturated cut-through zones.

Contrary to the findings of Hayes (1982), Hargraves (1983), Hebblewhite *et al*. (1983) and Osisanya and Schaffitzel (1996) this analysis indicated maximum gas production was not achieved from boreholes oriented perpendicular to the face cleat. Borehole orientation relative to cleat was shown to have some impact on gas production in the outbye areas with the impact decreasing as the coal became less saturated. In the coal

with greater DoS the data indicate increased gas production from boreholes oriented between 5 and 60^{O} to the face cleat, suggesting neither face or butt cleat was a more dominant path for gas flow. This result was consistent with Lama *et al.* (1980) who suggest that the gas drainage rate from coal at WCC was unlikely to be affected by borehole orientation due to the two cleat systems being more or less equally developed.

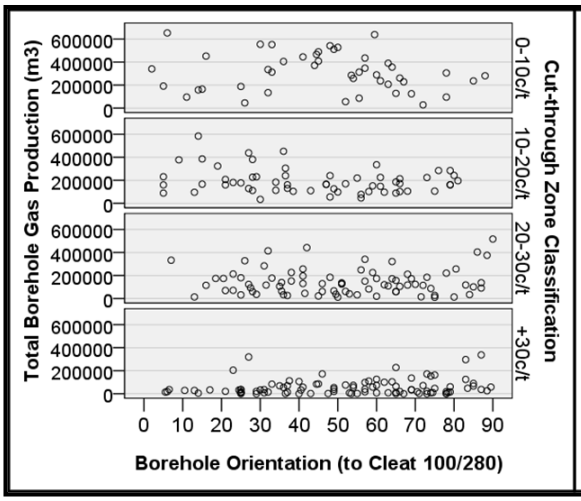

Figure 5.28: Total gas production relative to average borehole orientation to cleat (100/280^{O}) in each cut-through zone

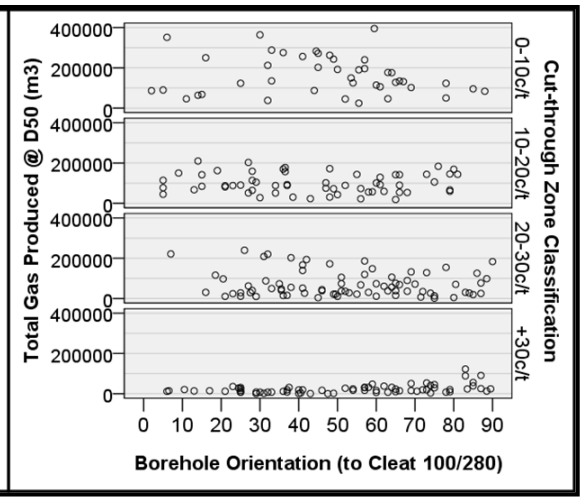

Figure 5.29: D50 gas production relative to average borehole orientation to cleat (100/280^{O}) in each cut-through zone

5.3.4.2 Borehole Orientation Relative to Stress

The orientation of the horizontal stress in the strata above and below the Bulli seam was determined using acoustic scanner logging of surface-based exploration boreholes in advance of mining operations. An acoustic scanner was used to measure and record the orientation of breakout along the wall of the borehole, which typically corresponds to the direction of minimum horizontal stress (Garbutt, 2004), as shown in Figure 5.30. The depth of the breakout cavity provides some indication of the magnitude of the stress, however, this was not considered to be an accurate measurement.

Stress orientation data was available from acoustic logging of ten boreholes located in and around the mining area, shown in Figure 5.31, as reported in BHPBIC (2006). Although there was some difference in stress orientation above and below the seam, the average orientation of the maximum horizontal stress, considered to be representative of the current mining area, was found to be 075/255^{O}. Analysis of the relationship between borehole gas production and borehole orientation, relative to maximum horizontal stress, was conducted. The magnitude of the horizontal stress, based on recorded

breakout and local experience, was expected to be in the range of 15 to 20 MPa at the current mining depth of 450 to 500 m.

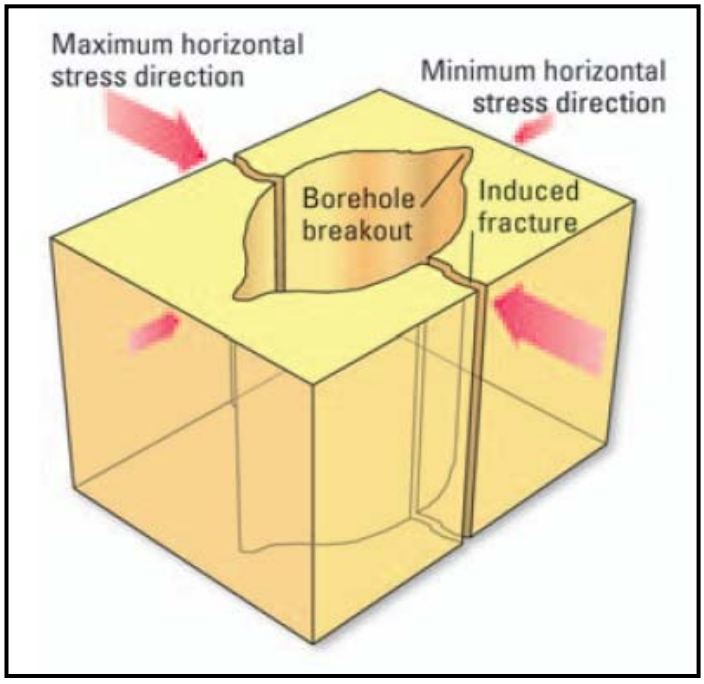

Figure 5.30: Borehole breakout in vertical boreholes aligned with minimum horizontal stress (Garbutt, 2004)

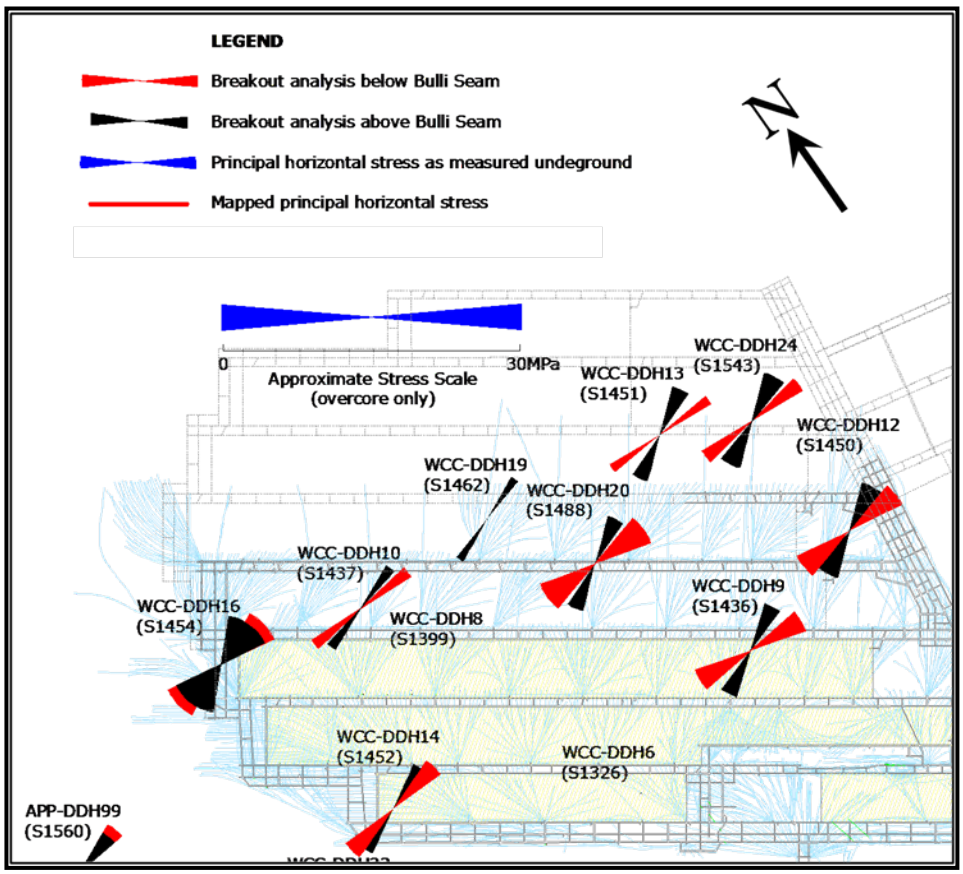

Figure 5.31: Stress measurement locations (after BHPBIC, 2006)

Cui and Busten (2006) suggest boreholes oriented parallel to the maximum horizontal stress are less affected by the impact of stress on cleat permeability and are likely to achieve increased gas production compared to a borehole aligned perpendicular to the principal horizontal stress.

Figure 5.32 and Figure 5.33 show the distribution of average borehole orientation relative to maximum horizontal stress for boreholes in the complete dataset and in each of the four cut-through zones. The average orientation of the boreholes relative to stress for the complete dataset was 38^{O}, with the average in the cut-through zones ranging from a low of 25^{O}, in the 10-20c/t zone, increasing to a high of 52^{O}, in the +30c/t zone.

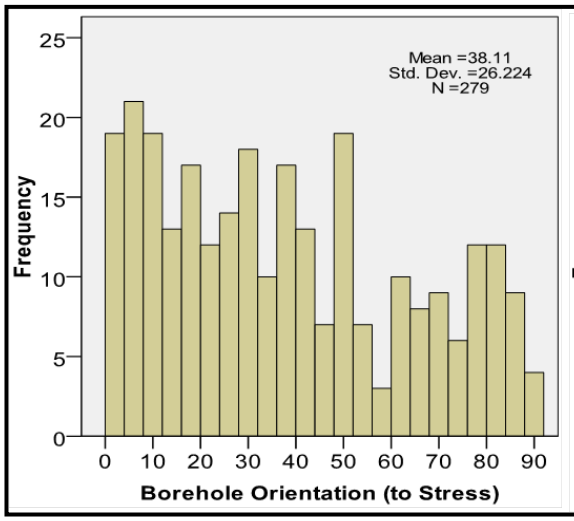

Figure 5.32: Distribution of average orientation relative to stress for boreholes in the complete dataset

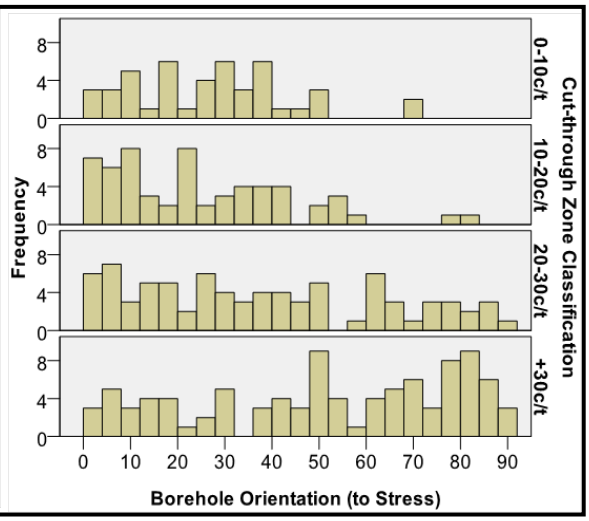

Figure 5.33: Distribution of average orientation relative to stress for boreholes in each cut-through zone

Figure 5.34 and Figure 5.35 show the relationship between total and D50 gas production relative to the angle between the borehole and maximum horizontal stress. Statistical analysis determined a weak negative correlation of –0.205 and –0.184 between borehole orientation relative to stress and each of total and D50 gas production. The data indicate above average gas production from boreholes oriented 0 to 40^{O} relative to the maximum horizontal stress. The boreholes within this range achieved the highest total gas production, as well as the highest D50 gas production.

The average total gas production from boreholes oriented between 0 and 40^{O} to the maximum horizontal stress was 180 141 m^3, 60% greater than the average 112 344 m^3 of the boreholes outside this range. The average D50 gas production of the boreholes

within the range was 93 414 m^3, 52% greater than the average 61 427 m^3 of the boreholes outside this range.

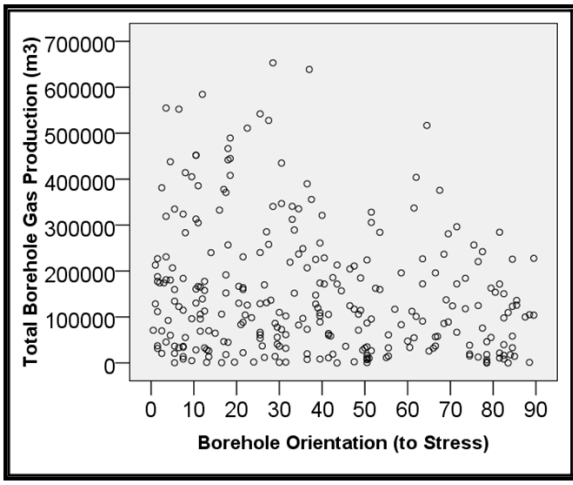

Figure 5.34: Total gas production relative to average borehole orientation to stress (075/255^O)

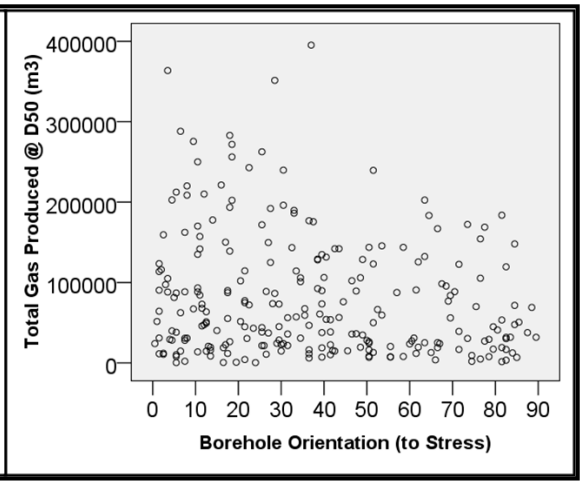

Figure 5.35: D50 gas production relative to average borehole orientation to stress (075/255^O)

The relationship between borehole orientation relative to stress and both total and D50 gas production, within each cut-through zone, was also considered. Figure 5.36 and Figure 5.37 indicate increased gas production from boreholes oriented between 0 and 40^O to stress, in the 0-10c/t zone and to a lesser extent in the 10-20c/t zone. Borehole orientation relative to stress had little impact on gas production from boreholes located in the inbye, lower producing, and highly undersaturated cut-through zones.

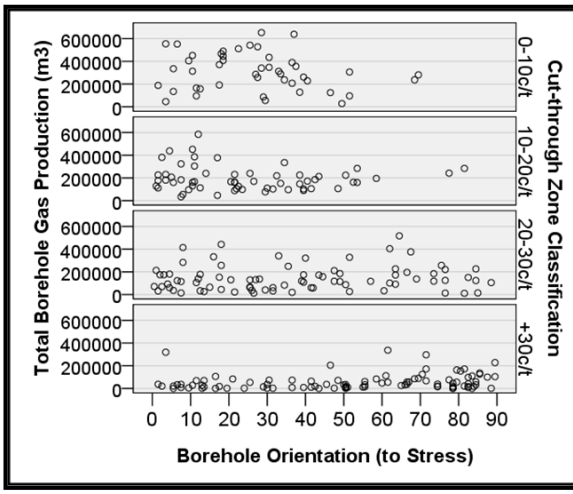

Figure 5.36: Total gas production relative to average borehole orientation to stress (075/255^O) in each cut-through zone

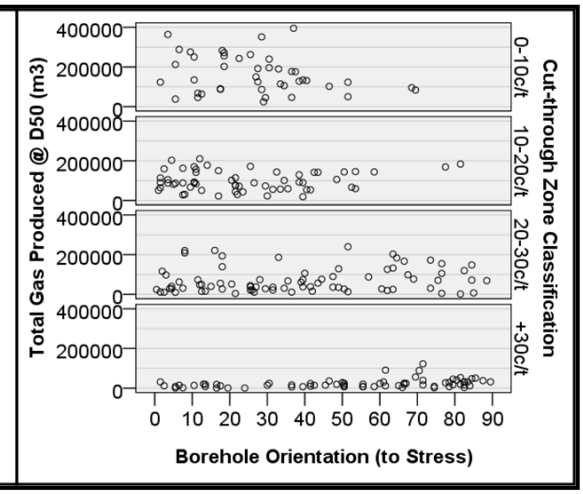

Figure 5.37: D50 gas production relative to average borehole orientation to stress (075/255^O) in each cut-through zone

This analysis has shown increased gas production was achieved from boreholes oriented between 0 and 40^O to the major horizontal stress direction which is consistent with the

work of Cui and Busten, (2006). The impact of borehole orientation on gas production was shown to decrease as the coal became less saturated.

5.3.4.3 Borehole Orientation Relative to Seam Dip

As discussed in Chapter 2 the presence of water within the coal seam has a significant impact on the ability of gas to drain from coal. When boreholes are drilled down-dip or where undulations exist along the length of a borehole, water and fines can accumulate, and there is an increased risk that gas drainage performance will be adversely affected. The impact can be significant, particularly in conditions where the gas pressure and gas production rate are not high enough to displace water and fines from the borehole. Previous studies by Battino and Regan (1982), Hebblewhite *et al.* (1982), Kahil and Masszi (1982) and Clark *et al*. (1983), support the fact that the presence of water in gas drainage boreholes impedes gas production and that suitable dewatering systems must be employed to prevent blockages in order to achieve optimum gas production. Gray (1982) reported on experience in the Gemini seam at Leichardt Colliery where gas drainage boreholes, drilled down-dip, were filled with water. Gas production increased 10 to 15% after the water was purged from these boreholes.

Figure 5.38 shows contours of the base (floor) of the Bulli seam (Armstrong and Kaag, 2008) relative to current and future WCC mine workings which indicate the strike and dip of the coal seam. Within the mining area the Bulli seam generally dips toward the west at a rate of 1 in 39 (1.5^{O}), falling approximately 95m along the 3 700 m length of the gateroad panels.

As discussed in Chapter 3, the process of drilling UIS gas drainage boreholes involves frequent changes in orientation of the down-hole motor assembly and therefore trajectory of the borehole, including frequent roof touches and branching to determine position of the borehole within the seam. This technique results in multiple peaks and troughs along the length of the borehole, as illustrated by the section views of two surveyed inseam boreholes shown in Figure 5.39. Although a borehole may be designed to be drilled up-dip and therefore self-draining of water, the presence of troughs along its length may allow water and/or coal fines to accumulate and restrict or prevent gas flow. No vertical displacement data was available for the UIS boreholes therefore the presence of troughs and the resulting impact on gas production from possible

accumulations of water and fines has not been assessed. In this analysis the apparent dip of each borehole was determined using the average orientation of each borehole, based on its plan view, relative to the average strike and dip of the Bulli seam at each drill site.

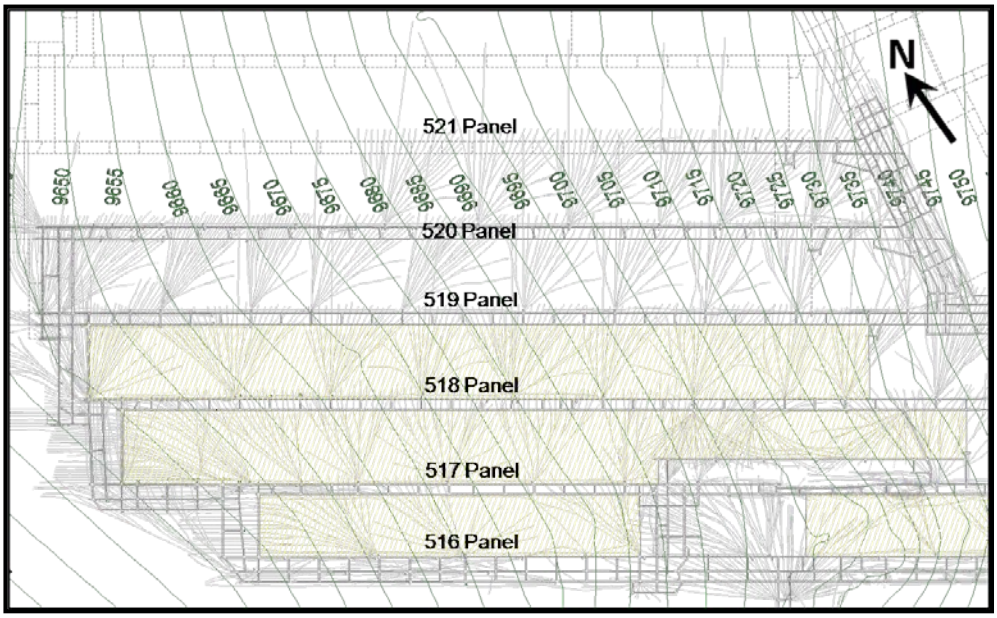

Figure 5.38: Bulli seam floor contours at 5 m interval (after Armstrong and Kaag, 2008)

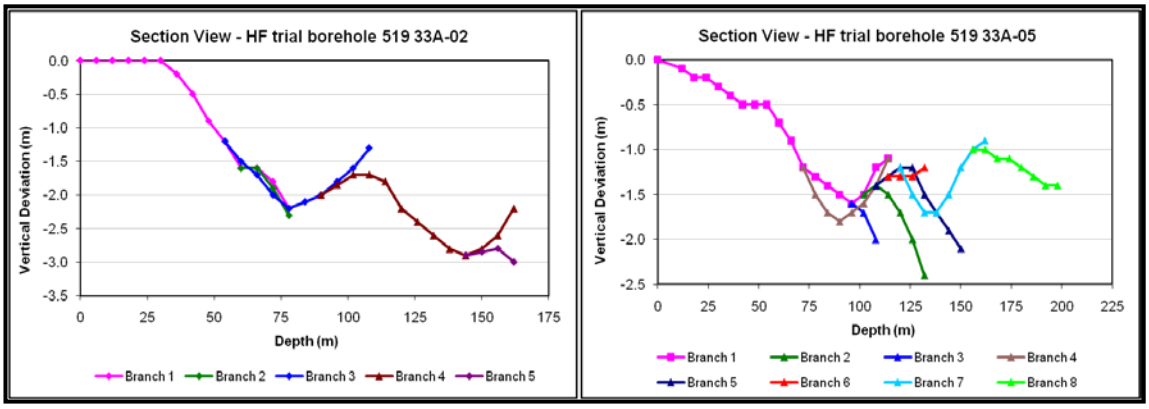

Figure 5.39: Section views of two UIS boreholes (after Black, 2007)

Figure 5.40 and Figure 5.41 show the distribution of average apparent dip of the boreholes in the complete dataset and in each of the four cut-through zones. The average dip for the complete dataset was $+1.3^{O}$, ranging from -2.2^{O} to $+4.0^{O}$. The average dip in the cut-through zones ranged from a high of 1.8^{O}, in the 10-20c/t zone, to a low of 0.8^{O}, in the +30c/t zone.

Figure 5.42 and Figure 5.43 show the relationship between total and D50 gas production relative to the apparent dip of the boreholes. Statistical analysis determined a weak

negative correlation of –0.031 and –0.067 between borehole apparent dip and each of total and D50 gas production. The data indicate above average gas production from boreholes with average apparent dip within the range 0.0 to +3.0 degrees to the horizontal plane. The boreholes within this range achieved the highest total gas production, as well as the highest D50 gas production.

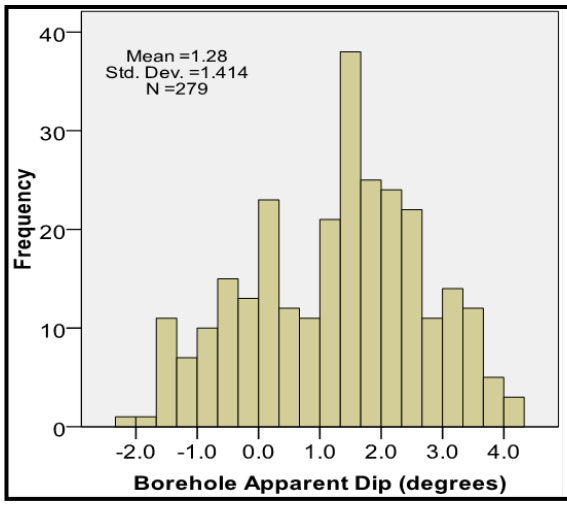

Figure 5.40: Distribution of average apparent dip for boreholes in the complete dataset

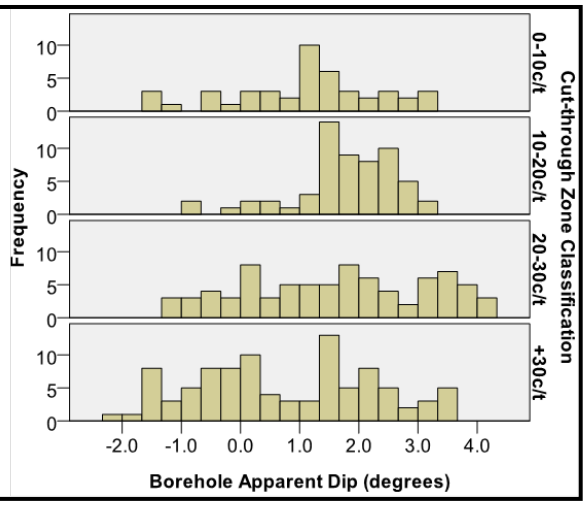

Figure 5.41: Distribution of average apparent dip for boreholes in each cut-through zone

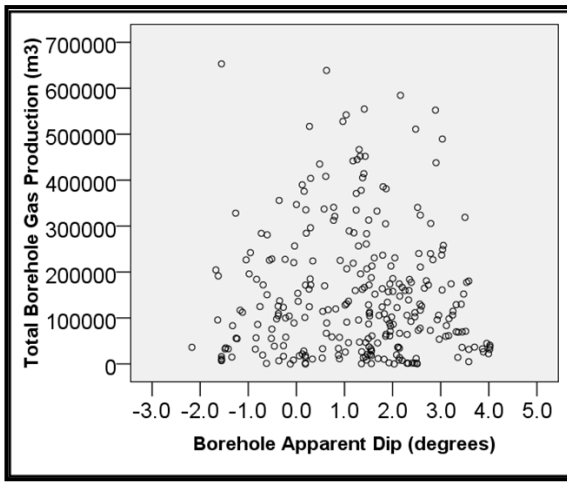

Figure 5.42: Total gas production relative to apparent dip

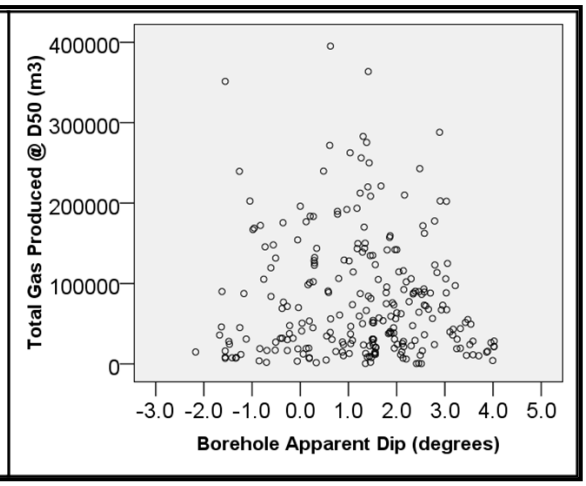

Figure 5.43: D50 gas production relative to apparent dip

The boreholes with apparent dip between 0.0 and $+3.0^{O}$ achieved an average 167 497 m^3 total gas production, 42% greater than the average 118 350 m^3 of the boreholes outside this range. The average D50 gas production of the boreholes within this range was 88 845 m^3, 44% greater than the average 61 664 m^3 of the boreholes outside this range.

The relationship between borehole apparent dip and both total and D50 gas production, within each cut-through zone, was also considered. Figure 5.44 and Figure 5.45 indicate apparent dip had a greater impact on total gas production than on D50 production. The greater effect of apparent dip on total gas production is likely to be due to the reduced production and gas flow velocity from older mature boreholes which decreases the borehole's ability to self-clear accumulations of water and fines. Therefore, following the initial peak production phase, boreholes become more susceptible to the adverse impact, on gas production, from accumulations of water and fines, particularly where drilled down-dip.

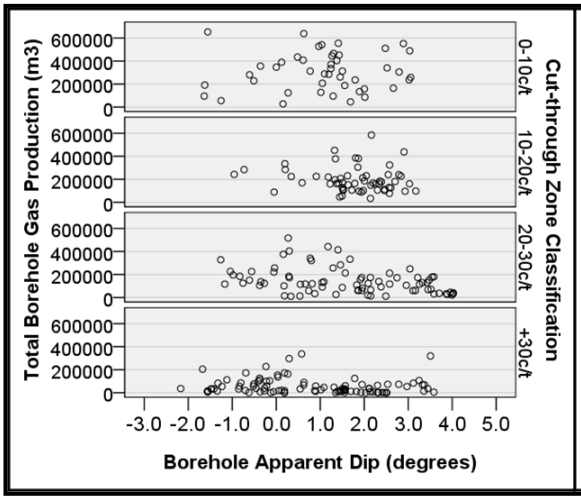

Figure 5.44: Total gas production relative to apparent dip in each cut-through zone

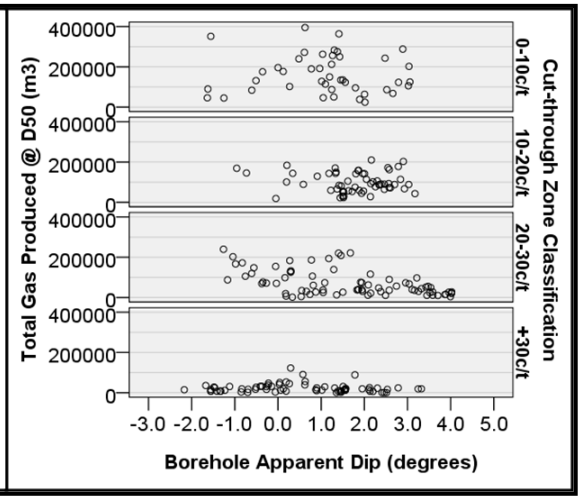

Figure 5.45: D50 gas production relative to apparent dip in each cut-through zone

From this assessment apparent dip was found to impact on total gas production with boreholes drilled up-dip, between 0.0 and $+3.0^{O}$, being less likely to experience restriction or blockage due to water or fines accumulation during the production life of the borehole.

The presence of troughs along the length of the boreholes may allow water and fines to accumulate, potentially restricting or preventing gas flow. Details of the trajectory of the borehole in the vertical plane were not available for analysis; therefore detailed analysis of the nature and position of troughs along the length of the boreholes and their effect on gas production could not be undertaken.

5.3.4.4 Borehole Orientation Relative to North

An assessment of the impact on gas production from boreholes based on their orientation relative to north was considered appropriate as it not only served to consolidate the impact of borehole orientation relative to cleat, stress and apparent dip but also provided specific guidance to the mine operator regarding the most productive drilling orientation to improve the performance of the inseam gas drainage drilling program.

Figure 5.46 and Figure 5.47 show the distribution of borehole orientation relative to north in the complete dataset and in each of the four cut-through zones. The average orientation of the boreholes in the complete dataset was 032^{O}, with the range extending from -132^{O} to $+125^{O}$. The average orientation relative to north in the four cut-through zones varies from a minimum of 012^{O}, in the +30c/t zone, to a maximum 055^{O}, in the 10-20c/t zone.

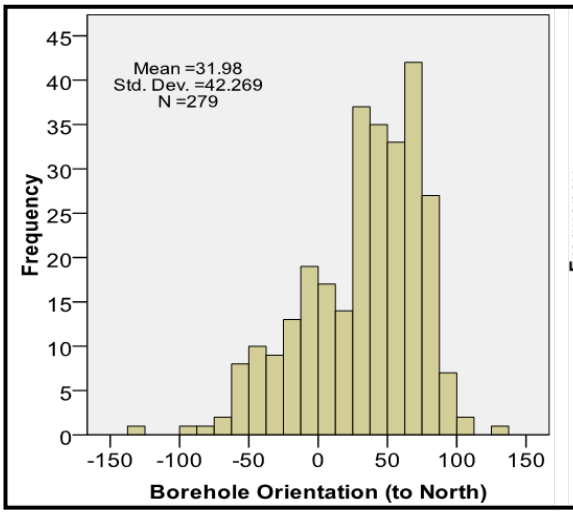

Figure 5.46: Distribution of average orientation relative to north for boreholes in the complete dataset

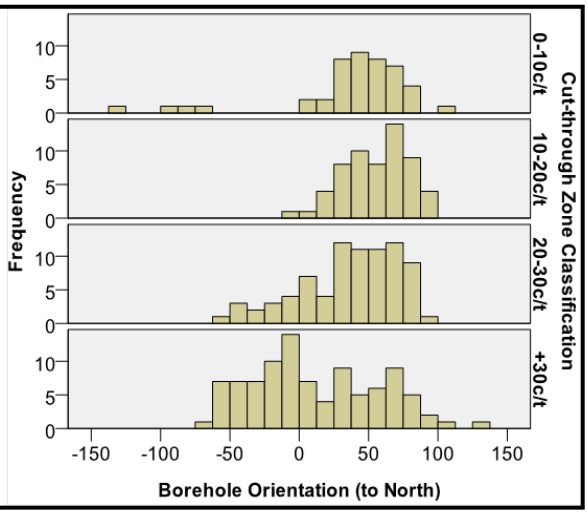

Figure 5.47: Distribution of average orientation relative to north for boreholes in each cut-through zone

Figure 5.48 and Figure 5.49 show the relationship between total and D50 gas production relative to borehole orientation. Statistical analysis determined a weak correlation of 0.173 and 0.149 between borehole orientation and each of total and D50 gas production. With the exception of several boreholes from the 518 A7 drilling pattern, which was a non-standard pattern drilled down-dip, the data indicate above average gas production from boreholes oriented within the range 040^{O} to 090^{O} relative to north.

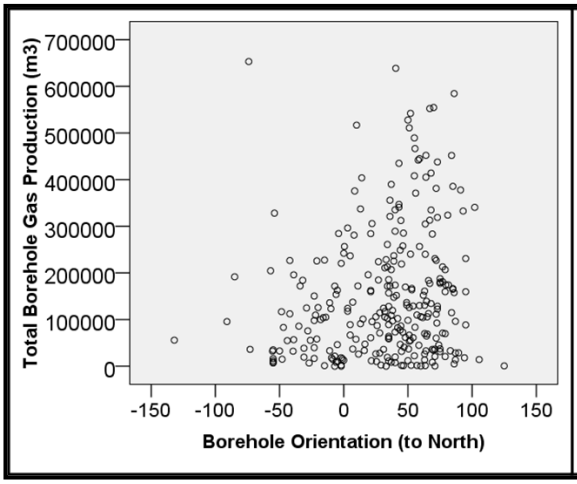

Figure 5.48: Total gas production relative to borehole orientation

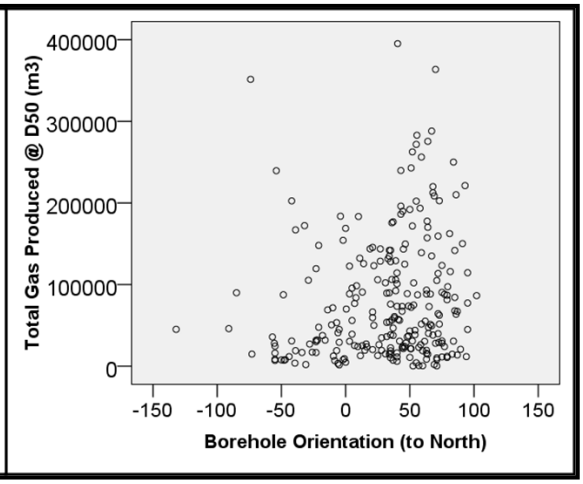

Figure 5.49: D50 gas production relative to borehole orientation

The boreholes oriented between 040^{O} and 090^{O} relative to north achieved an average 188 169 m^3 total gas production, 47% greater than the average 127 731 m^3 of the boreholes outside this range. The average D50 gas production of the boreholes within this range was 92 582 m^3, 34% greater than the average 68 961 m^3 of the boreholes outside this range. Analysis of this subset of borehole data found the distribution of borehole orientation was similar in each cut-through zone however there was a significant decrease in gas production with distance into the panels. The average production in each cut-through zone was 360 000 m^3 in 0-10c/t, 200 000 m^3 in 10-20c/t, 124 000 m^3 in 20-30c/t, and 42 000 m^3 in the +30c/t zone.

The relationship between borehole orientation relative to north and both total and D50 gas production, within each cut-through zone, was also considered. As shown in Figure 5.50 and Figure 5.51, borehole orientation appears to have some impact on gas production from boreholes located in the outbye cut-through zones however, the orientation of the majority of the boreholes drilled in this more productive zone was between 040^{O} and 090^{O}. Therefore it was concluded that borehole orientation had little impact on gas production from UIS boreholes within this mining area, particularly from boreholes located in the inbye, lower producing, and highly undersaturated zones.

Within this mining area, boreholes drilled between 040^{O} and 090^{O} relative to north were aligned approximately parallel to the maximum horizontal stress ($075/255^{O}$), between 10^{O} and 50^{O} to the face cleat ($100/280^{O}$) and were oriented up-dip.

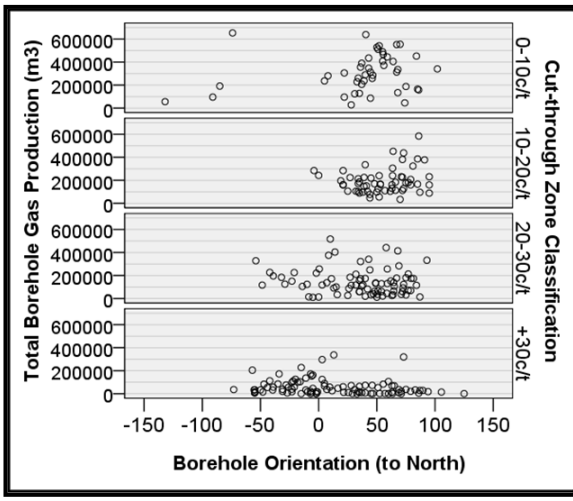

Figure 5.50: Total gas production relative to borehole orientation in each cut-through zone

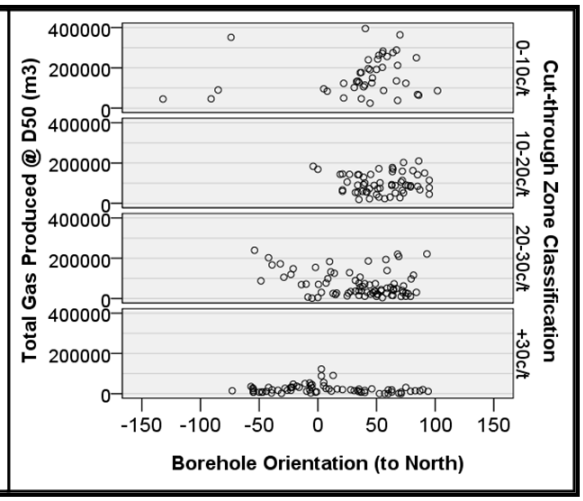

Figure 5.51: D50 gas production relative to borehole orientation in each cut-through zone

Borehole orientation, measured relative to north, was considered a useful reference in this analysis as an identified optimum borehole drilling orientation, such as 040^{O} to 090^{O}, was a common and easily communicated reference able to be incorporated into the mine's UIS gas drainage drilling program by the mine operator.

The analysis has shown borehole orientation, relative to north, cleat and stress, does have some impact on gas production however, the strength of the relationship appears related to degree of saturation (DoS). In the more productive outbye cut-through zones, where the DoS was higher, borehole orientation had a greater impact on gas production than in the less productive inbye zone where DoS was much lower.

Apparent dip was shown to have a greater impact on gas production from boreholes located in highly undersaturated coal and mature boreholes in areas with higher DoS. In such cases, boreholes drilled up-dip, between 0.0^{O} and 3.0^{O}, achieved increased gas production and it was likely that these boreholes had reduced risk of material accumulation and therefore less risk of gas flow restriction or blockage.

It was therefore concluded that, although not a dominant factor governing borehole gas production performance, the orientation of UIS boreholes, relative to the horizontal stress, cleat direction and seam dip, may impact gas production.

5.3.5 Drainage Time

Kahil and Masszi (1982) state that a coal seam is not a conventional reservoir and that regardless of permeability gas production cannot exceed the gas desorption rate.

Therefore, in order to achieve effective gas content reduction ahead of mining the drainage program must be afforded adequate time.

Figure 5.52 and Figure 5.53 show the distribution of drainage time for boreholes in the complete dataset and in each of the four cut-through zones. The average drainage time of all boreholes in the dataset was 157 days, with the range extending from a low of 7 days to a high of 349 days. A number of boreholes drilled from the inbye and outbye ends of the panels, into coal that was not mined, were allowed to produce for extended periods causing the distribution to skew to the right, as seen in the 20-30c/t and +30c/t zones, and the longer drainage times in the 0-10c/t zone. In contrast, approximately 25% of the boreholes in the total dataset achieved an effective drainage time of less than 100 days.

The drainage time in each cut-through zone was reasonably consistent with an average 198 days in the 0-10c/t zone, 140 days in the 10-20c/t zone, 164 days in the 20-30c/t zone, and 142 days in +30c/t zone.

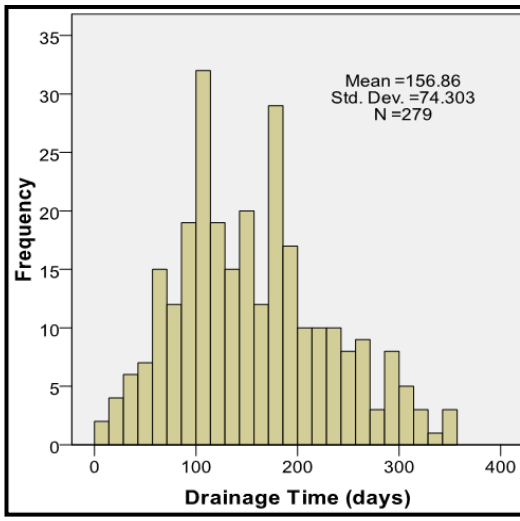

Figure 5.52: Distribution of drainage time for boreholes in the complete dataset

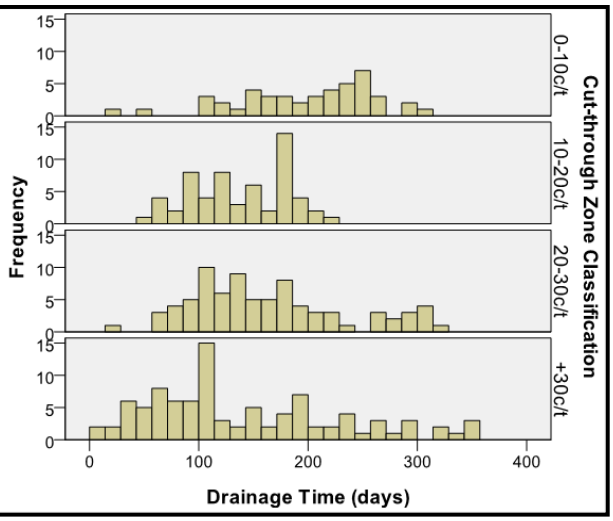

Figure 5.53: Distribution of drainage time for boreholes in each cut-through zone

Figure 5.54 show the relationship between drainage time and total gas production. The data suggest a strong relationship with maximum gas production increasing in response to increasing drainage time. Statistical analysis determined a correlation of 0.441 between drainage time and total gas production.

The relationship between drainage time and total gas production within each cut-through zone was also considered. As shown in Figure 5.55, the maximum gas production in each zone was greater in response to increasing drainage time.

The data indicate that at least 100 days drainage time was required for boreholes to achieve reasonable gas production, and the minimum drainage time required increased with distance into the panels.

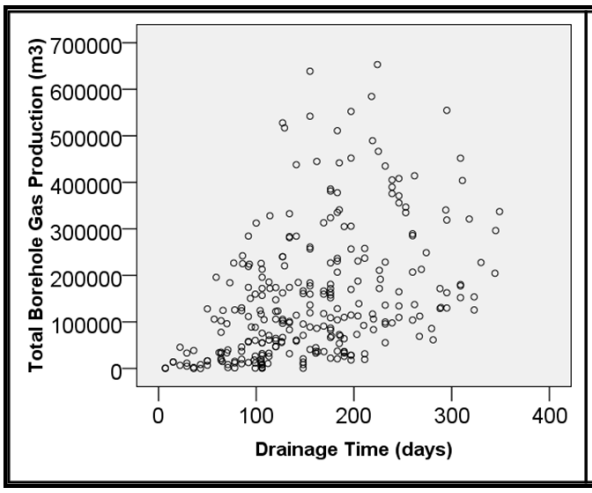

Figure 5.54: Total gas production relative to drainage time

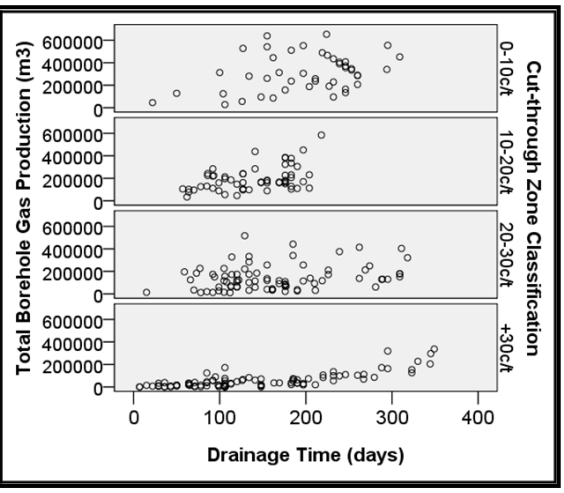

Figure 5.55: Total gas production relative to drainage time for boreholes in each cut-through zone

The analysis was extended to consider the relationship between gas production and drainage time relative to the gas content and gas composition zones previously defined. As shown in Figure 5.56 and Figure 5.57, a consistent relationship was maintained between gas production and drainage time. The data suggest that as methane composition decreased there was an increase in the minimum drainage time required to achieve a notable increase in gas production. It was concluded that for drainage boreholes to exceed a total gas production threshold of 200 000 m^3,the minimum drainage time required is 275 days in the 0-40% CH_4 gas composition zone, 175 days in the 40-80% CH_4 gas composition zone, 75 days in the >80% CH_4 gas composition zone.

This analysis has shown gas production to be strongly impacted by drainage time, with increased drainage time required in areas of reduced CH_4 gas composition. This observation was consistent with findings from the analysis of degree of saturation presented in Chapter 4, Section 4.4.8.

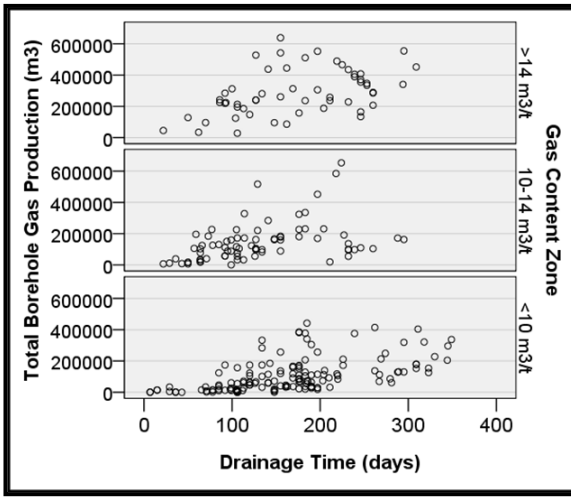

Figure 5.56: Total gas production relative to drainage time in each gas content zone

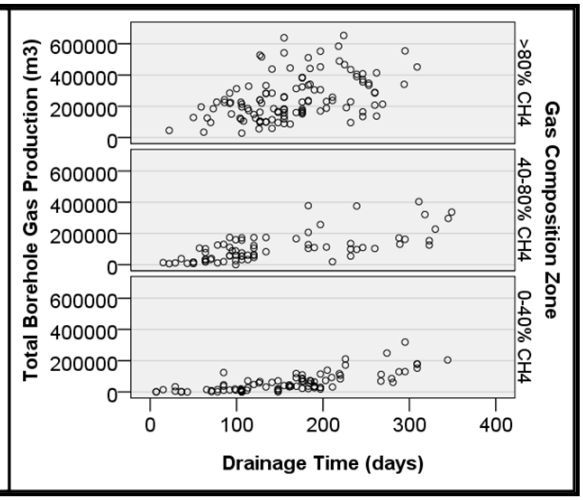

Figure 5.57: Total gas production relative to drainage time for boreholes in each gas composition zone

5.3.6 Applied Suction

At WCC the gas drained from the UIS boreholes was reticulated, initially through flexible hoses, to a network of rigid steel pipes of varying diameter, connected to a surface gas drainage plant. To overcome the internal resistance of the pipes, suction pressure, measured at approximately –50 kPa (gauge), was applied to the surface network connection. A combination of four Nash and one Siemens liquid ring pumps, located in the surface gas drainage plant, generate and maintain the suction pressure to the network (Black and Self, 2008).

Figure 5.58 and Figure 5.59 show the results of testing in a CO_2 rich area at Metropolitan Colliery by Battino and Hargraves (1982) and Clark *et al*. (1983) respectively, that indicate an increase in gas flow rate in response to increased applied suction. It was also shown that leakage, or air dilution into the system, also increased in response to increased applied suction pressure.

Clark *et al*. (1983) concluded that the application of suction benefits coal seam gas drainage and the most productive suction pressure was between 13 and 20 kPa. It was however noted that, at this level of applied suction, air leakage into the system accounted for between 40 to 45% of the total recorded volumetric flow rate.

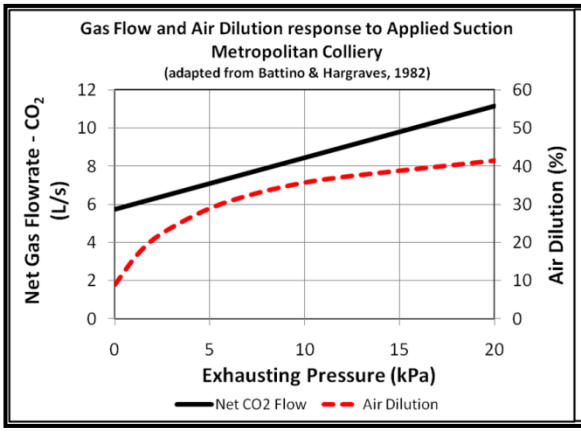

Figure 5.58: UIS borehole gas flow and leakage response to applied suction (after Battino and Hargraves, 1982)

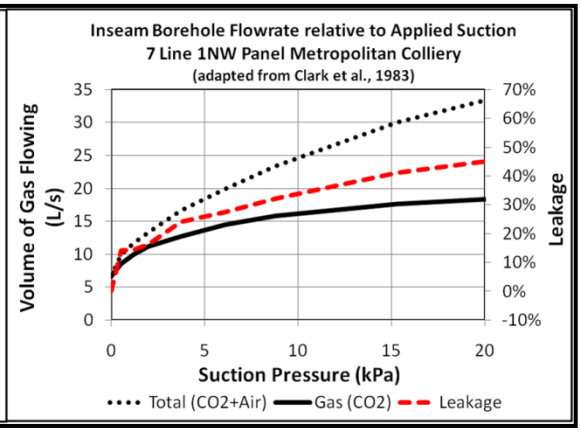

Figure 5.59: UIS borehole gas flow and air dilution response to applied suction (after Clark et al., 1983)

Figure 5.60 present gas flow rate measurements from two UIS boreholes in response to the application of suction pressure during testing conducted in a CH_4 rich area at WCC by Lama (1988a). Although the composition of the seam gas in the area tested by Lama differed from the areas tested by Battino and Hargraves, and Clark *et al.*, the net gas flow rates were of similar magnitude which supports the credibility of the results presented. Lama's results indicate lower air dilution entering the borehole. The reduced dilution was probably the result of improved standpipe design and installation standard which was also a focus of Lama's study (Lama, 1988a).

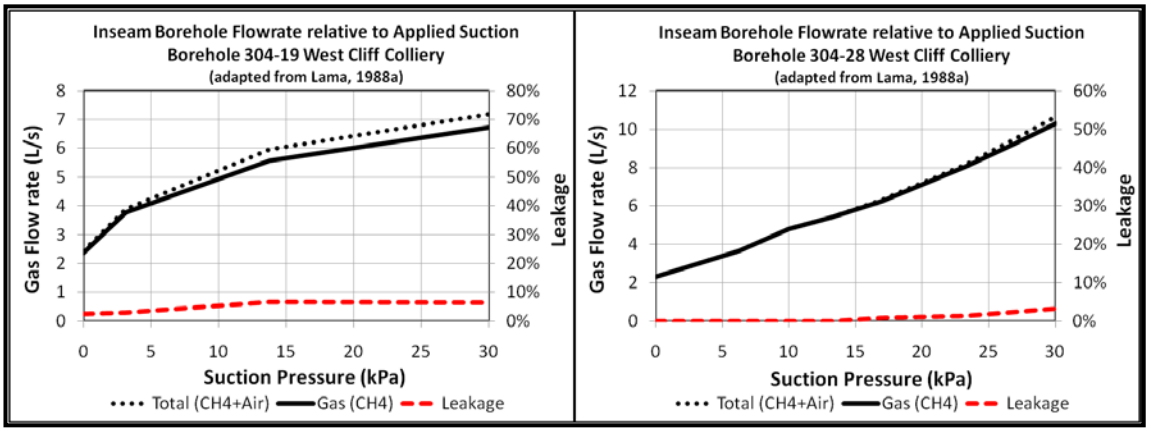

Figure 5.60: UIS borehole gas flow and leakage response to applied suction (after Lama, 1988a)

Figure 5.61 show the results of similar testing conducted by Marshall *et al*. (1982), in a CH_4 rich area at WCC, that recorded increased gas production in response to increasing applied suction pressure, however, the gas flow rates were an order of magnitude lower than those presented by Clark *et al*., Battino and Hargraves, and Lama.

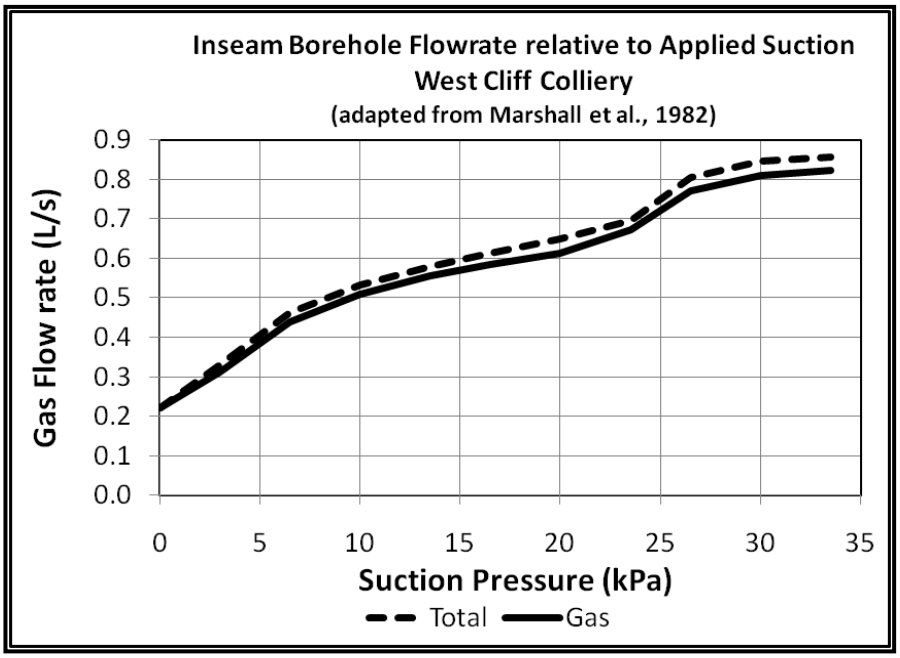

Figure 5.61: UIS borehole gas flow response to applied suction (after Marshall *et al*., 1982)

As part of the gas flow measurement protocol in Area 5 at WCC, the suction pressure applied to each gas drainage borehole was measured at the collar of the borehole. Given the dynamic nature of the gas drainage system the applied suction pressure was found to be highly variable during the operating life of each borehole. The median applied suction pressure was calculated for each of the 279 boreholes and this data was used to assess the relationship between gas production and suction pressure.

Figure 5.62 and Figure 5.63 show the distribution of median suction pressure applied to the boreholes in the complete dataset and in each of the four cut-through zones. The median suction pressure ranged from a low of 1.0 kPa to a high of 31.0 kPa, with an average of 13.6 kPa. The median suction pressure was found to decrease with distance into the panels, with the average in each cut-through zone decreasing from a high of 20.6 kPa, in the 0-10c/t zone, to a low of 9.3 kPa, in the +30c/t zone.

The drop in applied suction pressure along the length of the panels may be the result of increasing internal resistance within the gas reticulation pipe network. Similar investigations into gas drainage system performance at other Bulli seam mines (Black, 2007b) found sections of the gas drainage pipe network that were adversely impacted by accumulations of water and coal fines. These accumulations increased network resistance and reduced both total production capacity and effective suction pressure inbye of the restrictions.

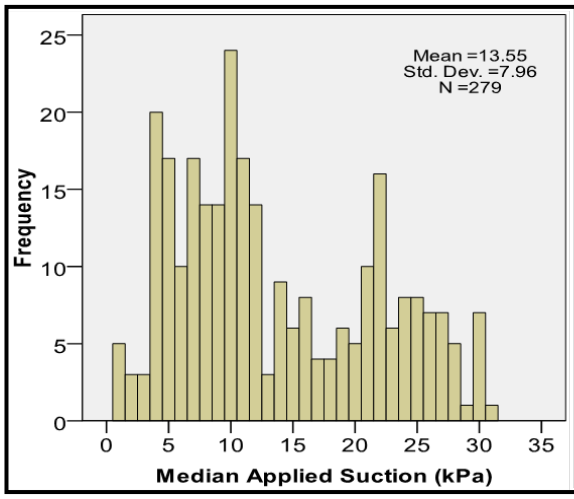

Figure 5.62: Distribution of median suction pressure applied to boreholes in the complete dataset

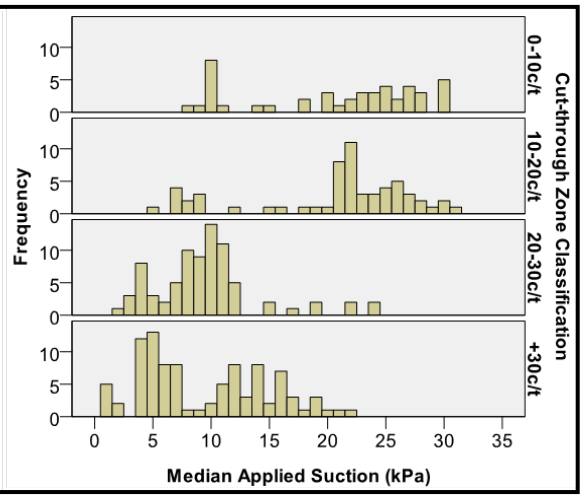

Figure 5.63: Distribution of median suction pressure applied to boreholes in each cut-through zone

Figure 5.64 and Figure 5.65 show the relationship between median applied suction pressure and gas production, which indicate increased total and D50 production from boreholes having greater applied suction pressure. This relationship was consistent with the findings of previous researchers. Statistical analysis determined a positive correlation of 0.412 and 0.322 between median applied suction pressure and each of total production and D50 production.

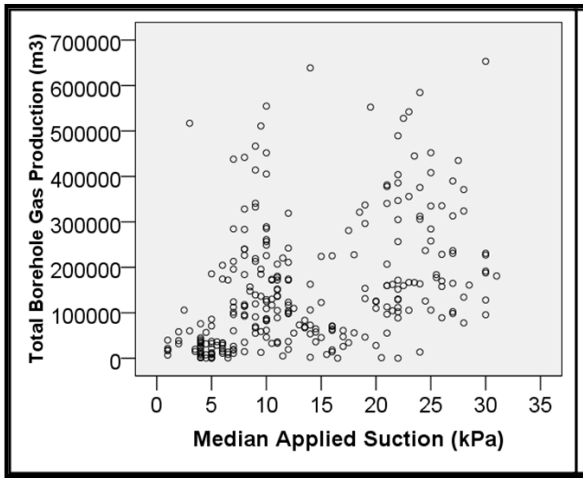

Figure 5.64: Total gas production relative to median applied suction pressure

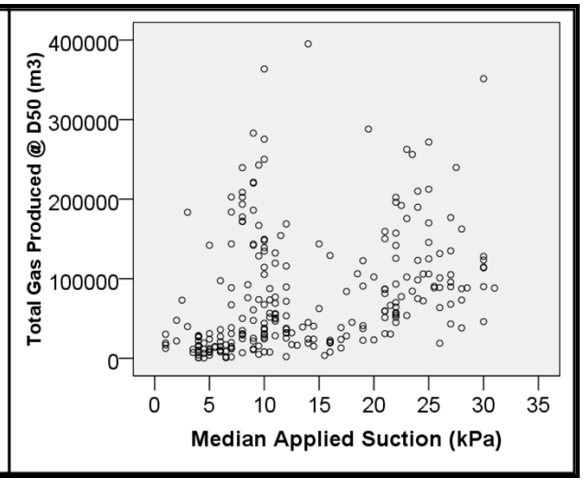

Figure 5.65: D50 gas production relative to median applied suction pressure

The relationship between median applied suction pressure and each of total and D50 gas production within each cut-through zone was also considered. As shown in Figure 5.66 and Figure 5.67 there was no evidence to support a relationship between gas production and applied suction pressure. Therefore the positive relationship between applied suction and gas production appears coincidental, with increased suction pressure applied

to the higher producing outbye area and reduced suction pressure applied to the less productive inbye area. Based on the analysis of data within the four cut-through zones it was concluded that applied suction does not have a significant impact on production from UIS gas drainage boreholes.

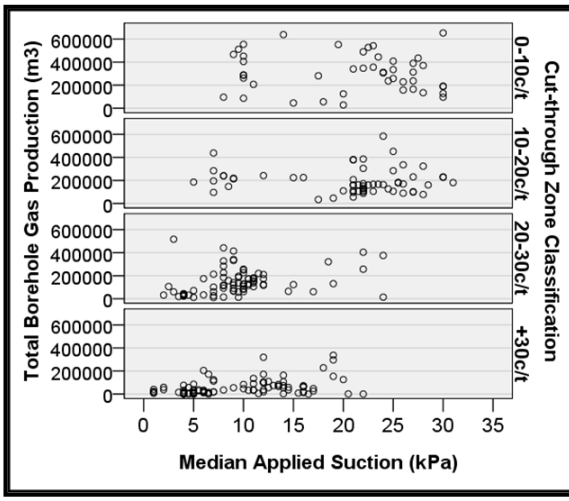

Figure 5.66: Total gas production relative to median applied suction pressure in each cut-through zone

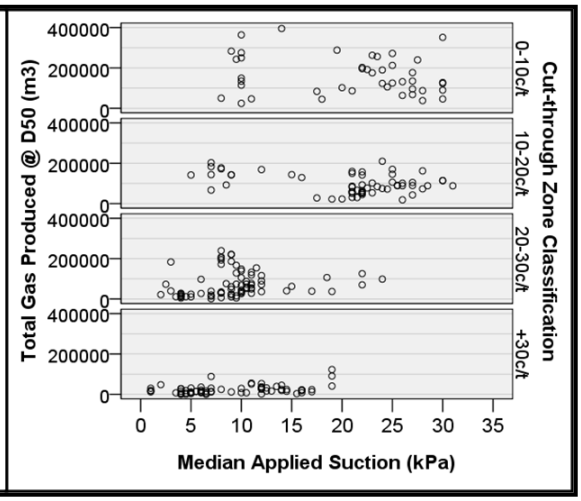

Figure 5.67: D50 gas production relative to median applied suction pressure in each cut-through zone

Previous researchers have identified the risk of potentially significant air leakage into the gas drainage system in response to increased applied suction pressure. Two potential sources of leakage, identified by Black *et al*. (2008), include (a) standpipe leakage, through insufficient length and/or inadequate installation standards, and (b) continued operation of boreholes after having been intersected by advancing mine workings. Where leakage paths exist, increasing the applied suction pressure leads to increased air being drawn into the gas drainage system which reduces the total capacity of the gas drainage system. Therefore the composition of the drainage gas should be monitored to alert the mine operator to the presence of air leakage and the gas drainage system should be operated to minimise leakage.

As part of this research project gas samples were collected periodically from producing inseam gas drainage boreholes for the purpose of analysing changes in gas composition during the operating life of the borehole. The results of analysis from two separate inseam boreholes, shown in Figure 5.68, indicate air leakage accounts for between 10 to 20% of the drainage gas composition. The gas samples in this analysis were collected from boreholes that were liberating gas at atmospheric pressure, with no suction pressure applied at the time of sample collection. It should be noted that where leakage

paths exist the application of suction pressure significantly increases the air leakage into the system.

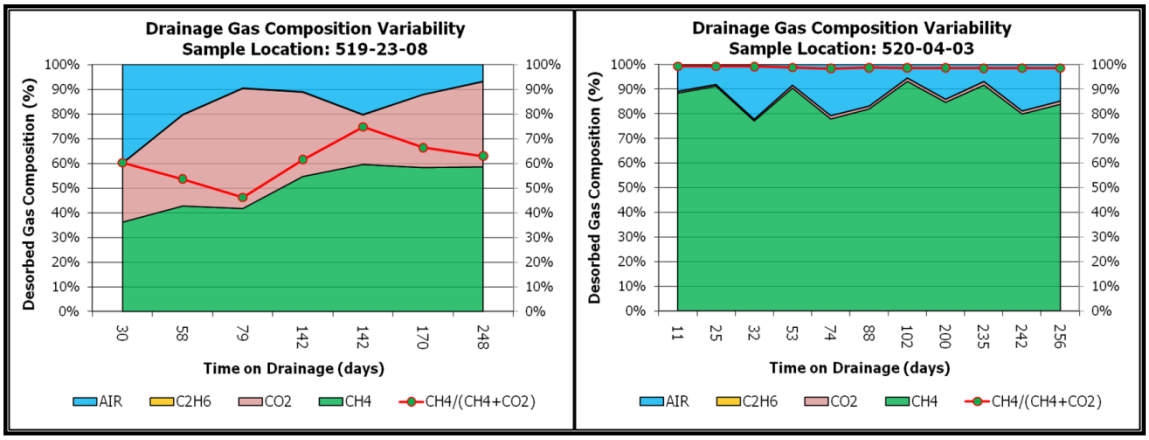

Figure 5.68: Change in drainage gas composition during UIS borehole gas production

Applying suction pressure to the gas drainage system maintains a negative pressure within the pipe network which reduces the risk of gas leaking from the pipes into the underground mine environment. Applying suction to the network compensates for internal pressure losses within the pipe network. However, increasing the suction pressure applied to the collar of a gas drainage borehole may potentially result in a large amount of leakage with minimal improvement in the volume of gas being drained from the coal seam.

From this analysis it was shown that increasing the suction pressure applied to a borehole does not coincide with an increase in gas production.

5.3.7 Gas Drainage System Management

Management of the complete gas drainage system from design, drilling, and production, through to decommissioning, requires dedicated resources to maintain efficiency and gas production capacity.

The most common problems associated with gas drainage system management include (i) accumulation of water and fines within boreholes and throughout the gas reticulation network; and (ii) air leakage into the network.

As discussed in Section 5.3.4.3, accumulations of water and fines impede gas desorption and may result in complete blockage of the borehole. In addition to

groundwater, drilling fluid must also be effectively managed. Separate site investigations confirmed fluid flow between closely spaced boreholes, through the coal seam beyond the end of the standpipe, during UIS drilling. Where the adjacent boreholes had been connected to the gas reticulation network, water and coal fines flowed into the pipe range, accumulating in low sections, increasing system resistance, and reducing total gas production capacity of the drainage system. The impact of material accumulation on reducing the effective area within a 610 mm gas reticulation pipe range at four locations within Appin Colliery, shown in Figure 5.69, was reported by Black and Self (2007).

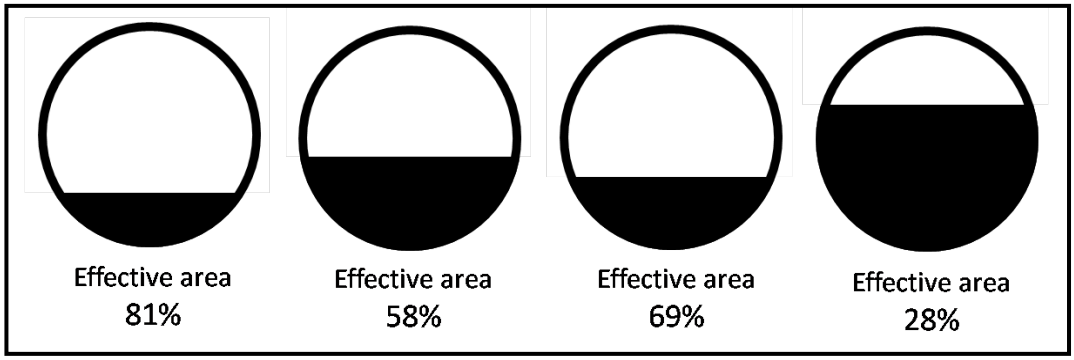

Figure 5.69: Reduction in effective area due to fines accumulation (Black and Self, 2007)

Effective control of water and fines must therefore be an essential consideration in the design and ongoing management of any gas drainage system. Where possible, drill patterns should be designed to maintain separation between boreholes to minimise the risk of gas, water and coal fines passing between boreholes through the coal seam. Fan drilling patterns are preferred by drilling practitioners however control of borehole separation is improved by the use of a parallel drilling pattern which does however require the drill rig to be relocated between each borehole. Where borehole interaction is an issue the standpipe length should be increased and additional drill sites should be considered to reduce the borehole density at each site.

Following completion of drilling water should be removed from the boreholes. Prior to removing the drill rods compressed air may be connected to and blown through the drill rods to clear any accumulated water and coal fines from the borehole. Where boreholes are aligned down-dip, subject to groundwater make, in-hole dewatering systems should be installed and used to maintain conditions conducive to gas drainage.

Lama (1980) suggests providing a water trap, preferably automatic, at each borehole and, if using manual traps, daily emptying may be required in the initial production phase. Water traps should also be installed throughout the gas reticulation pipe network, particularly at the bottom of synclines and other low sections where water is likely to accumulate.

An alternative to maintaining a water trap for each borehole may be the use of a water and fines separator unit to serve each drill site, particularly during the initial production phase of the boreholes. A separator unit, similar to the design shown in Figure 5.70, would be located near to the boreholes and receive all gas, water and coal fines, produced from the boreholes. Once inside the main body of the unit separation occurs with the seam gas exiting the top of the unit to the gas drainage range leaving the water and fines to be pumped and drained from the bottom of unit and removed from the site.

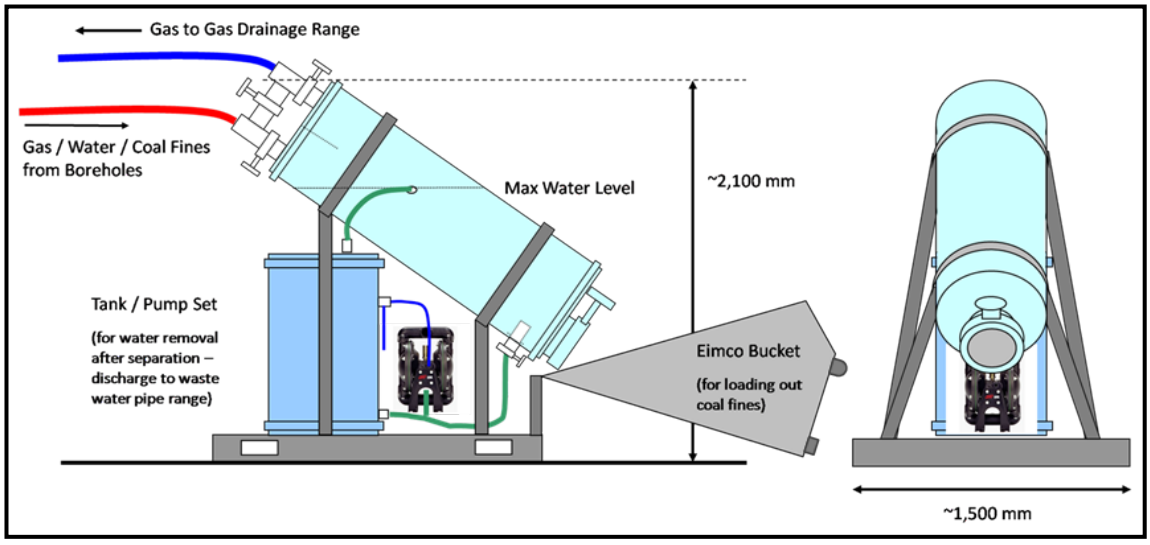

Figure 5.70 – Conceptual gas, water, coal fines separation unit

Air leakage into the gas reticulation network reduces the total capacity of the system to carry seam gas. Gas composition analysis of an underground gas reticulation network, reported by Black and Self (2007), found minimal leakage through victaulic pipe connections, where installed to a high standard, with the most significant leakage occurring close to the working faces where the measured methane purity dropped from 95% to 45% within several hundred metres of the borehole collar. Common sources of leakage included (i) poor hose to pipe connections, (ii) leakage around standpipes due to inadequate standpipe length and inadequate installation standard, and (iii) boreholes,

intersected by mine roadways or compliance boreholes, which had not been effectively sealed and remained open and connected to the network.

Dedicated resources should be assigned to regularly monitor and actively manage the performance of UIS gas drainage boreholes and the complete gas reticulation network. As a minimum, gas flow rate and gas composition should be recorded weekly from all active UIS boreholes. Water production and applied suction pressure should also be recorded to enable more detailed analysis and understanding of site specific gas drainage characteristics. One aspect of the data analysis and reporting must focus on identifying any obvious and unexpected changes in performance, for example a sudden decrease in gas production rate, excessive air dilution, or excessive water production. Regular monitoring enables potential issues to be identified, investigated, and appropriate corrective action to be taken.

If the gas reticulation network is not continuously monitored, measurement of the pressure, flow rate and gas composition within the pipe range should be recorded at least weekly at each drill site, each panel entry, the entry to the surface gas drainage plant and the inbye side of all other significant junctions throughout the network. This information will enable all gas production sources to be quantified as well as identifying sources of leakage and changes in system performance.

5.4 SUMMARY

From the analysis of operational factors, drainage time was found to have the most significant impact on gas production and appeared to be closely related to degree of saturation in that the deeper the undersaturation the greater the drainage time required.

Although not directly assessed, the management of drainage boreholes and the overall gas reticulation system appeared to have a potentially significant impact on gas production and may explain the high number of boreholes, independent of gas composition, degree of saturation and other factors, that achieved low gas production.

Borehole length and orientation were found to have some impact on gas production. Maximum gas production was achieved from boreholes between 500 and 1 000 m long and oriented between 5 and 60^{O} to the face cleat and between 0 and 40^{O} to the maximum horizontal stress. The relationship between orientation and gas production

appeared to be related to degree of saturation with orientation having little impact on highly undersaturated coal. Boreholes drilled up-dip, with an apparent dip between 0.0 and $+3.0^{O}$, also achieved increased gas production, and the relationship was strongest in highly undersaturated coal.

No evidence was found to support a relationship between applied suction pressure and gas production. Although maintaining negative pressure within the gas pipelines reduces the risk of flammable gas being released into the underground environment, increasing suction also increases the risk of air leakage into the pipeline which in turn reduces the gas carrying capacity of the system. Where moderate to high suction pressure is applied to boreholes, standpipes must be installed to a very high standard and supported by regular monitoring to identify and control leakage.

Based on the results of previous studies the standard diameter of 96 mm used in UIS borehole drilling was effective. However borehole breakout was quite common and may lead to material accumulation, or complete blockage, in the boreholes. It was also shown that as the gas production rate reduces so does the gas flow velocity within the borehole which in turn reduces the borehole's ability to self-clear water and fines, particularly in boreholes oriented down-dip.

The gas drainage program should be supported by regular monitoring and active management to identify issues arising within the boreholes and throughout the gas reticulation network. Prompt action should be taken to address issues and restore conditions to support optimum gas production.

CHAPTER SIX – ANALYSIS OF FAST AND SLOW DESORPTION GAS TESTING DATA

6.1 INTRODUCTION

Coal mines operating in seams with moderate to high gas content typically undertake routine gas drainage drilling ahead of mining to reduce gas content for two purposes; compliance with prescribed outburst threshold limits, and compliance with prescribed ventilation air gas concentrations limits. As part of the gas and outburst management process it is typical for drilling and coring to be conducted in three phases. The first phase involves a minimum number of longer boreholes drilled into virgin areas with core samples (virgin core) recovered for testing to provide early insight into the gas content and composition of the future mining areas. This information is used to plan the drainage requirements in these future mining areas. The second phase involves routine drilling of a pattern of gas drainage boreholes for the purpose of reducing gas content ahead of advancing mine development. Typically at least one core sample (standard core) will be recovered for testing from a borehole at each drill site to confirm gas content and gas composition, and the minimum gas content reduction required prior to the area being considered safe to undertake mining activities. The third phase, undertaken immediately prior to mining, involves drilling boreholes ahead of the advancing development roadways to recover core samples (compliance core). The results of compliance core sample testing are used to confirm gas content has been reduced below the prescribed threshold limit and the area is deemed safe and authorised to continue mining. In areas where the content remains above the prescribed limit additional boreholes are drilled in an attempt to rapidly reduce the gas content to avoid mine production delays.

This chapter examines the results from coal core sample gas testing and the nature of coal seam gas emission from both fast and slow desorption testing. The various methods of direct and indirect gas content determination are discussed and the impact of the data analysis on outburst threshold limit determination and gas content estimation are also presented.

6.2 ANALYSIS OF GAS DATA FROM FAST DESORPTION TESTING

Core samples are regularly collected during exploration and gas drainage drilling and tested in accordance with the fast desorption method described in Australian Standard AS3980:1999 (SAA, 1999). The cores are tested to determine the content and composition of seam gas present in the sample. Accurate and timely gas data is required for use in mine planning and decision making to ensure the ventilation, and the gas and outburst risks are effectively managed. The fast desorption method has a short test duration and results are typically provided to the mine within 24 hours.

6.2.1 Data Acquisition – Fast Desorption Gas Testing

The results of fast desorption gas testing conducted at the BHP Billiton Illawarra Coal Gas Laboratories were gathered for 527 core samples collected from UIS drilling within Area 5 at WCC (BHPBIC, 2007). The location of the core samples relative to the mine workings are shown in Figure 4.1. Given the emphasis placed on outburst management and the difficulty experienced at the mine in reducing the gas content from the inbye, CO_2 rich coal, the bulk of the drilling and coring effort was concentrated to the inbye, western side of the mine.

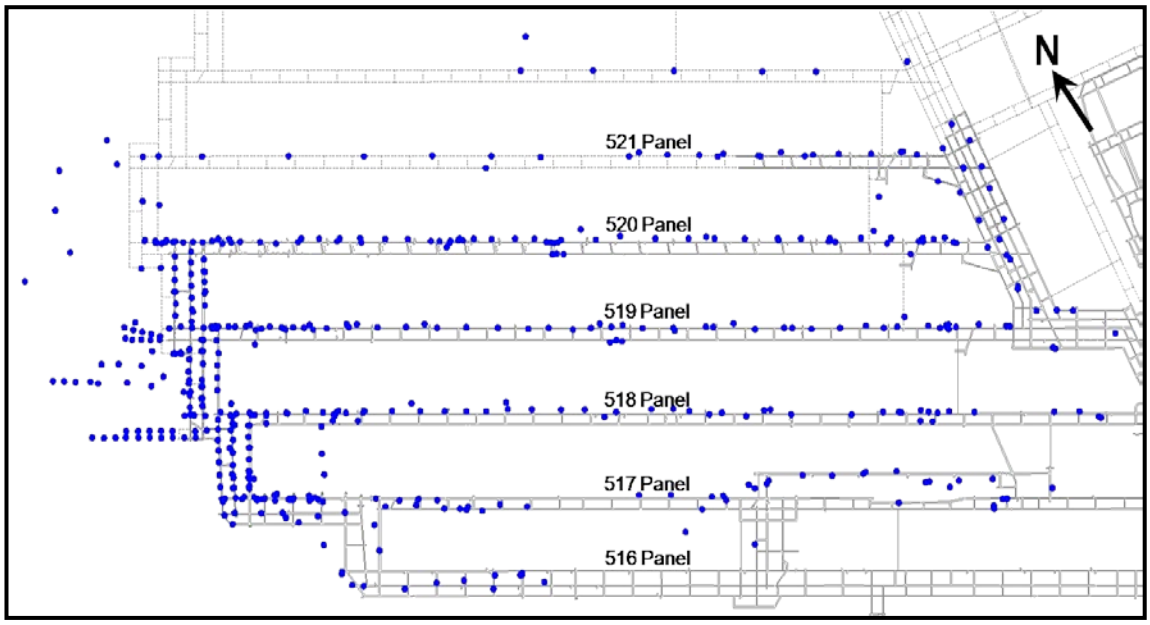

Figure 6.1: Location of core samples tested using the fast desorption method

From each gas test report the following data was extracted and collated for analysis:

- Core sample reference;
- Gas content component volumes – Q_1, Q_2 and Q_3 (m^3/t);
- Gas composition of desorbed gas – CH_4, CO_2 and $CH_4/(CH_4+CO_2)$ (%);
- Initial gas desorption rate – ($mL/min^{0.5}/kg$);
- IDR30 – volume of gas desorbed in the initial 30 minute period (m^3/t); and
- Desorption Rate Index (DRI)

During the course of the analysis a number of potentially significant relationships became evident and additional data was gathered from other Bulli seam mines and mines located in the Bowen Basin and Hunter Valley. As shown in

Table 4.1, 4 785 gas test results were gathered from eight mines, four located in New South Wales and four located in Queensland. In preparing the dataset the results from 600 samples were excluded; 598 due to the combined CH_4 and CO_2 gas concentration being less than 60%, suggesting leakage and possible data error, and two due to the desorption rate index (DRI) value exceeding 3 500. A total of 4 185 gas test results were analysed. A complete list of fast desorption gas test data gathered from each mine is provided in Appendix 6.1.

Table 6.1: Source of UIS gas testing data used in analysis

Mine Reference	State	Seam	Gas Composition	Total Samples	Samples Analysed
Mine A	NSW	Bulli	Mixed CH_4 - CO_2	527	517
Mine B	NSW	Bulli	Mixed CO_2 - CH_4	414	311
Mine C	NSW	Bulli	Mixed CO_2 - CH_4	770	770
Mine D	QLD	Goonyella Middle	CH_4	1 047	1 029
Mine E	NSW	Wynn, Piercefield, Kayuga	CO_2	441	0
Mine F	QLD	Goonyella Middle	CH_4	383	379
Mine G	QLD	German Creek	CH_4	393	376
Mine H	QLD	German Creek	CH_4	810	803
TOTAL SAMPLES				4 785	**4 185**

Table 6.2 presents a summary of the average value of each gas analysis measure, grouped according to gas composition and total gas content. The data highlights the concentration of data in the less than 20% CH_4 and greater than 80% CH_4 categories, with a comparatively low number of data in the mixed gas categories in each gas content group.

Table 6.2: Average gas analysis data grouped according to gas content and gas composition

N = 4185	Subset Samples	Measured Content (m^3/t)	Q_1 (m^3/t)	Q_2 (m^3/t)	Q_3 (m^3/t)	Q_1/Q_M (%)	Q_2/Q_M (%)	Q_3/Q_M (%)	DRI (mL)	IDR 30 (m^3/t)	Initial Desorption Rate (mL/min^0.5/kg)
N = 155		0.0-2.0 m^3/t									
<20% CH_4	13	1.80	0.03	0.16	1.62	1.5%	8.9%	89.6%	254	0.04	5.9
20-40% CH_4	2	1.65	0.10	0.18	1.37	6.6%	11.4%	81.9%	219	0.11	17.2
40-60% CH_4	4	1.45	0.03	0.20	1.22	2.4%	14.9%	82.7%	139	0.08	13.7
60-80% CH_4	3	1.79	0.05	0.10	1.64	2.7%	5.5%	91.9%	200	0.11	18.0
80-100% CH_4	133	1.61	0.03	0.06	1.52	1.9%	3.8%	94.4%	194	0.04	7.2
N = 469		2.0-3.0 m^3/t									
<20% CH_4	86	2.55	0.05	0.20	2.31	1.8%	7.6%	90.5%	341	0.07	12.0
20-40% CH_4	15	2.57	0.27	0.27	2.03	10.1%	10.5%	79.5%	296	0.19	32.0
40-60% CH_4	2	2.81	0.05	0.18	2.58	1.7%	6.5%	91.8%	322	0.07	13.0
60-80% CH_4	3	2.39	0.17	0.28	1.94	7.9%	11.0%	81.2%	206	0.24	42.5
80-100% CH_4	363	2.54	0.06	0.17	2.31	2.2%	6.7%	91.1%	299	0.08	12.9
N = 573		3.0-4.0 m^3/t									
<20% CH_4	96	3.43	0.07	0.27	3.09	1.9%	8.0%	90.1%	444	0.10	16.9
20-40% CH_4	26	3.53	0.11	0.32	3.11	3.0%	8.9%	88.0%	420	0.13	22.1
40-60% CH_4	7	3.50	0.33	0.35	2.82	9.5%	10.3%	80.3%	417	0.22	36.6
60-80% CH_4	10	3.50	0.20	0.38	2.92	5.9%	10.9%	83.3%	423	0.17	29.2
80-100% CH_4	434	3.45	0.09	0.36	3.00	2.6%	10.3%	87.1%	410	0.13	21.9
N = 529		4.0-5.0 m^3/t									
<20% CH_4	84	4.53	0.14	0.45	3.94	3.0%	10.0%	87.0%	573	0.20	33.5
20-40% CH_4	20	4.48	0.32	0.43	3.72	7.2%	9.7%	83.1%	529	0.33	55.5
40-60% CH_4	10	4.40	0.29	0.46	3.65	6.5%	10.6%	83.0%	531	0.24	40.4
60-80% CH_4	8	4.55	0.42	0.66	3.46	9.2%	14.7%	75.9%	460	0.27	45.8
80-100% CH_4	407	4.52	0.15	0.65	3.73	3.2%	14.2%	82.6%	542	0.21	35.6
N = 553		5.0-6.0 m^3/t									
<20% CH_4	92	5.47	0.24	0.66	4.57	4.3%	12.1%	83.5%	700	0.30	49.8
20-40% CH_4	29	5.62	0.24	0.61	4.77	4.2%	10.9%	84.8%	665	0.25	41.1
40-60% CH_4	11	5.42	0.49	0.86	4.08	8.8%	16.0%	75.2%	571	0.33	56.3
60-80% CH_4	7	5.38	0.46	0.82	4.11	8.6%	15.1%	76.4%	658	0.34	57.9
80-100% CH_4	414	5.48	0.24	1.01	4.23	4.4%	18.4%	77.3%	663	0.34	58.1
N = 498		6.0-7.0 m^3/t									
<20% CH_4	107	6.50	0.43	0.86	5.21	6.5%	13.2%	80.3%	817	0.44	74.5
20-40% CH_4	45	6.48	0.43	0.88	5.17	6.7%	13.6%	79.7%	793	0.41	69.8
40-60% CH_4	11	6.27	0.49	0.94	4.84	7.8%	15.1%	77.1%		0.44	75.4
60-80% CH_4	6	6.39	0.55	1.57	4.28	8.5%	24.4%	67.1%	767	0.49	81.9
80-100% CH_4	329	6.48	0.33	1.40	4.74	5.1%	21.6%	73.3%	784	0.47	79.6
N = 418		7.0-8.0 m^3/t									
<20% CH_4	129	7.46	0.40	1.06	6.00	5.4%	14.2%	80.4%	947	0.47	79.9
20-40% CH_4	44	7.42	0.62	1.12	5.69	8.4%	15.0%	76.7%	898	0.51	87.8
40-60% CH_4	9	7.54	0.79	1.27	5.47	10.5%	16.8%	72.7%		0.51	88.9
60-80% CH_4	9	7.49	0.53	1.07	5.89	6.9%	14.5%	78.6%	922	0.46	80.9
80-100% CH_4	227	7.47	0.47	1.81	5.16	6.3%	24.2%	69.2%	911	0.64	108.7
N = 297		8.0-9.0 m^3/t									
<20% CH_4	96	8.45	0.56	1.32	6.58	6.5%	15.6%	77.8%	1054	0.58	97.1
20-40% CH_4	33	8.37	0.70	1.30	6.37	8.3%	15.5%	76.2%	1012	0.60	110.0
40-60% CH_4	16	8.67	0.73	1.50	6.44	8.4%	17.3%	74.3%		0.56	100.3
60-80% CH_4	6	8.64	0.86	1.43	6.35	9.9%	16.7%	73.5%		0.95	172.1
80-100% CH_4	146	8.52	0.68	2.25	5.58	8.0%	26.5%	65.6%	1052	0.86	146.5
N = 206		9.0-10.0 m^3/t									
<20% CH_4	63	9.40	0.52	1.72	7.14	5.5%	18.3%	76.0%	1195	0.71	120.5
20-40% CH_4	15	9.33	1.02	1.88	6.43	11.0%	20.2%	68.7%	1127	0.84	144.2
40-60% CH_4	14	9.35	0.69	1.93	6.74	7.4%	20.6%	72.0%		0.70	125.8
60-80% CH_4	13	9.46	0.90	1.44	7.12	9.5%	15.2%	75.3%		0.82	148.3
80-100% CH_4	101	9.46	0.88	2.53	6.06	9.3%	26.8%	64.0%	1182	1.05	178.5
N = 487		>10.0 m^3/t									
<20% CH_4	110	11.75	1.15	2.86	7.74	9.3%	23.6%	67.1%	1400	1.31	221.5
20-40% CH_4	28	11.82	1.27	2.59	7.95	10.5%	21.9%	67.5%	1391	1.07	177.2
40-60% CH_4	16	11.83	1.23	2.43	8.17	10.0%	20.4%	69.6%		0.96	166.6
60-80% CH_4	15	10.99	0.97	2.49	7.53	8.8%	22.7%	68.6%		0.92	163.4
80-100% CH_4	318	11.97	1.20	4.07	6.70	10.0%	33.5%	56.6%	1520	1.48	250.9

The duration of desorption testing has a significant impact on the relative percentage of Q_M measured during the Q_2 and Q_3 stages of testing. AS3980:1999 states that Q_2 testing

may be deemed complete when the rate of gas evolution approaches an asymptotic value (SAA, 1999). Detailed data relating to the duration and rate of gas emission during Q_2 testing and the transition between the Q_2 and Q_3 measurement was not available for analysis in this study.

At the completion of gas testing coal samples are typically discarded and not tested to determine coal quality and petrography. The absence of coal property data specific to each gas test result prevented the analysis of gas emission from coal samples during fast desorption testing from being extended to consider the impact of coal properties on the results.

6.2.2 Q_1 Gas Content Component

As discussed in Chapter 2, the Q_1 component of measured gas content (Q_M) represents the gas lost from a coal sample, during core recovery, prior to being sealed in a gas desorption canister (SAA, 1999). Figure 6.2 show the distribution of Q_1 gas content data relative to Q_M. The average Q_1 gas content was 0.4 m^3/t, ranging from 0.0 to 4.3 m^3/t. Q_1 increased in response to increasing Q_M. Figure 6.3 shows the distribution of Q_1:Q_M ratio data relative to Q_M. Although a high degree of scatter was evident, statistical analysis confirmed an increase in the Q_1:Q_M ratio corresponding to increased Q_M. The average Q_1:Q_M ratio was 2.7% in the 0-5 m^3/t gas content zone, 6.0% in the 5-10 m^3/t gas content zone and 9.7% in the >10 m^3/t gas content zone.

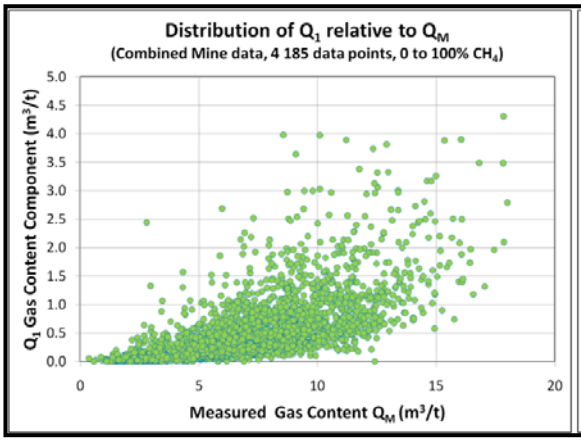

Figure 6.2: Distribution of Q_1 relative to Q_M

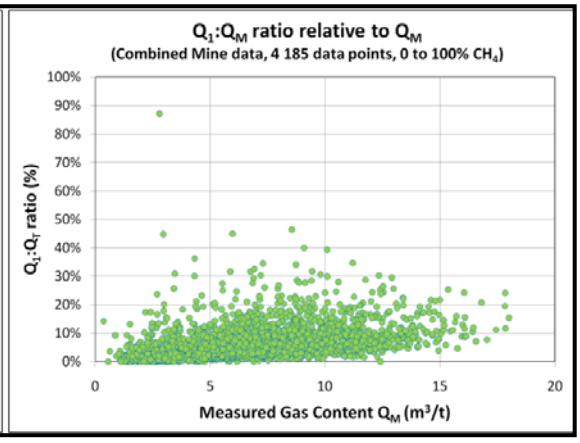

Figure 6.3: Distribution of Q_1:Q_M ratio relative to Q_M

Figure 6.4 show the distribution of Q_1 data relative to the gas composition (CH_4/(CH_4+CO_2)) of each sample. The Q_1 data has a high degree of scatter across the

gas composition range which indicates gas composition had little impact on Q_1 gas emission. Figure 6.5 show the distribution of the Q_1:Q_M ratio data relative to gas composition. The Q_1:Q_M ratio was found to be independent of gas composition with an average Q_1:Q_M ratio of 5.4% in the 0-40% CH_4 gas composition zone, 8.2% in the 40-80% CH_4 gas composition zone and 4.7% in the 80-100% CH_4 gas composition zone.

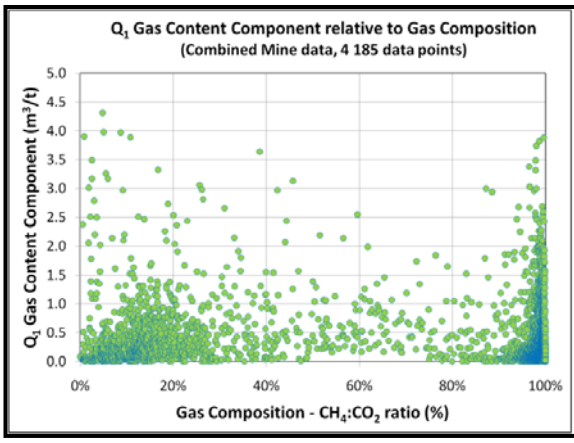

Figure 6.4: Distribution of Q_1 gas content relative to sample gas composition

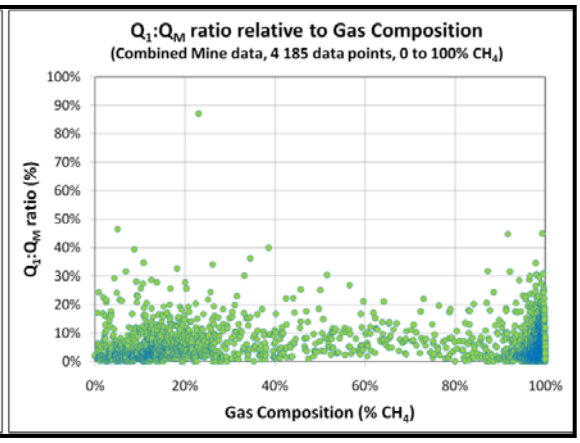

Figure 6.5: Distribution of Q_1:Q_M ratio relative to sample gas composition

Further analysis was undertaken to investigate the relationship between Q_1 and both gas content and gas composition. Figure 6.6 shows a consistent increase in Q_1 in response to increasing Q_M with little change in average Q_1 in each gas composition range.

Figure 6.7 shows the average Q_1:Q_M ratio for data grouped according to total gas content and gas composition. In the gas content range 0.0-2.0 m^3/t, the Q_1:Q_M ratio was approximately 2.0%, increasing in response to increasing Q_M, reaching a maximum of approximately 10% for data in the gas content range >10 m^3/t.

Although there was increased scatter among the mixed gas data, likely due to the low number of data within these categories, the results indicate the Q_1 lost gas content was strongly affected by the total gas content of the sample. Gas composition was shown to have no significant impact on this relationship.

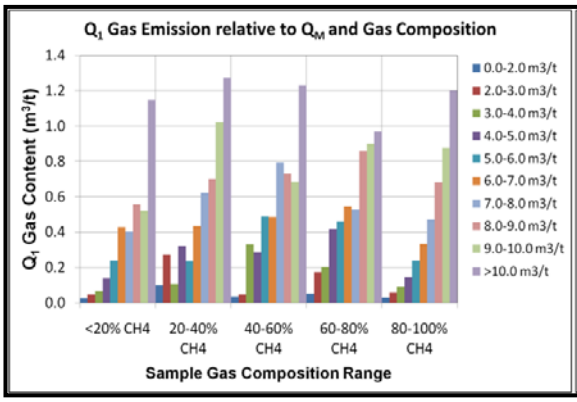

Figure 6.6: Distribution of average Q_1 gas content relative to Q_M and gas composition

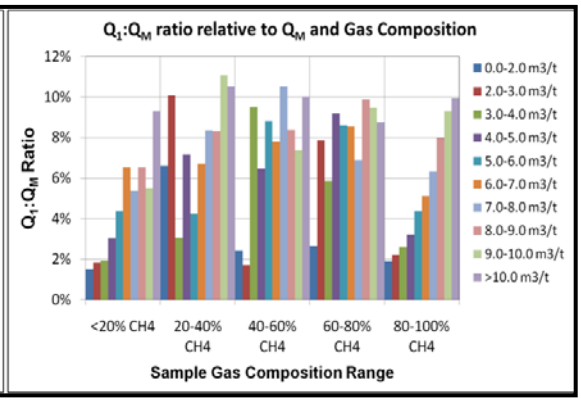

Figure 6.7: Distribution of average Q_1:Q_M ratio relative to Q_M and gas composition

6.2.3 Q_2 Gas Content Component

The Q_2 component of Q_M represents the measurable gas desorbed from a non-pulverised coal sample during laboratory gas emission testing at atmospheric pressure (SAA, 1999). Figure 6.8 shows the distribution of Q_2 gas content data relative to Q_M. The average Q_2 gas content was 1.2 m^3/t, ranging from 0.0 to 11.7 m^3/t. Q_2 increased in response to increasing Q_M. Figure 6.9 shows the distribution of Q_2:Q_M ratio data relative to Q_M. Although a high degree of scatter was evident, statistical analysis confirmed an increase in Q_2:Q_M ratio corresponding to increased Q_M. The average Q_2:Q_M ratio was 9.7% in the 0-5 m^3/t gas content zone, 19.2% in the 5-10 m^3/t gas content zone and 29.9% in the >10 m^3/t gas content zone.

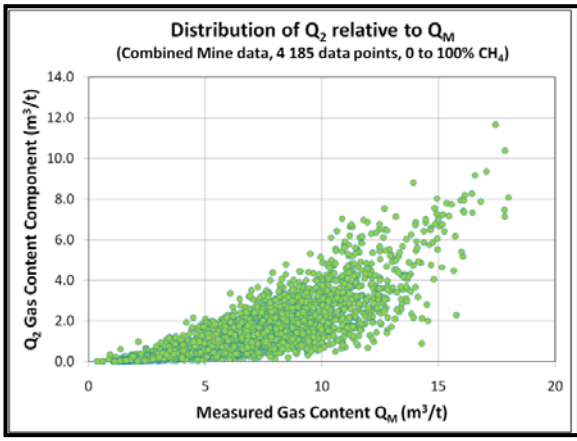

Figure 6.8: Distribution of Q_2 gas content relative to Q_M

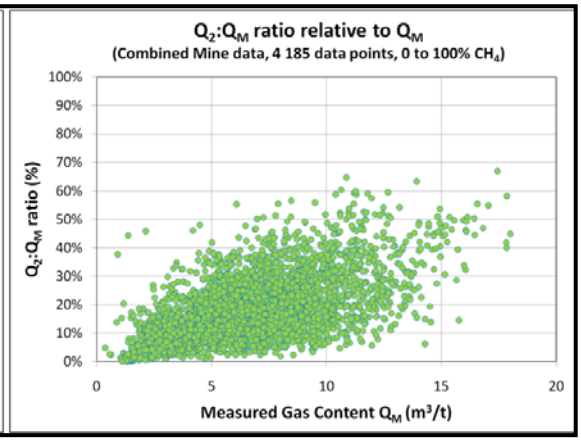

Figure 6.9: Distribution of Q_2:Q_M ratio relative to Q_M

Figure 6.10 shows the distribution of Q_2 data relative to the gas composition of each sample. The Q_2 gas content was generally less than 4.0 m^3/t from the mixed gas samples, increasing to a maximum of 8.0 m^3/t from CO_2 rich samples and a maximum

of 12.0 m^3/t from CH_4 rich samples. Figure 6.11 shows the distribution of Q_2:Q_M ratio data relative to gas composition. The average Q_2:Q_M ratio was slightly greater among CH_4 rich samples with an average Q_2:Q_M ratio of 13.7% in the 0-40% CH_4 gas composition zone, 16.1% in the 40-80% CH_4 gas composition zone, and 17.6% in the 80-100% CH_4 gas composition zone. In many samples, Q_2 accounted for half the Q_M with the Q_2:Q_M ratio reaching a maximum 70% in CH_4 rich samples.

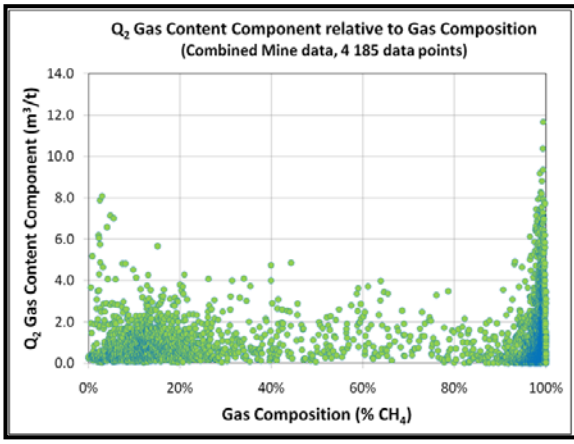

Figure 6.10: Distribution of Q_2 gas content relative to sample gas composition

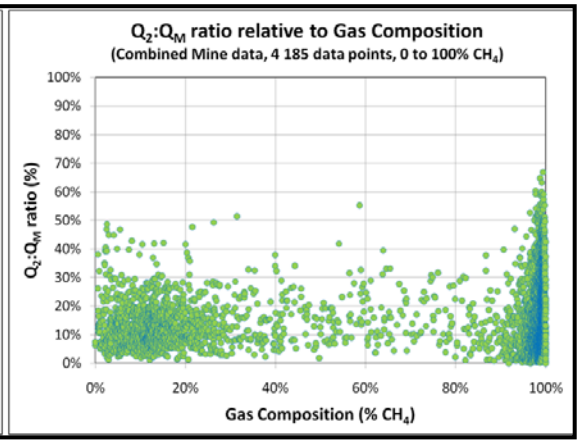

Figure 6.11: Distribution of Q_2:Q_M ratio relative to sample gas composition

Further analysis was undertaken to investigate the relationship between Q_2 and both gas content and gas composition. Figure 6.12 shows a consistent increase in Q_2 in response to increasing Q_M. The average Q_2 value of the samples in each gas content range was similar in the four gas composition ranges between 0 and 80% CH_4, suggesting little impact due to gas composition. However, in the 80-100% CH_4 gas composition range the average Q_2 gas content was approximately 50% greater than in each of the other gas content ranges. Figure 6.13 shows the average Q_2:Q_M ratio for data grouped according to Q_M and gas composition. The data indicate the average Q_2:Q_M ratio increased in response to increasing Q_M. In the 0.0-2.0 m^3/t gas content range the Q_2:Q_M ratio ranged between 4 and 15%, increasing to between 20 and 33% in the >10 m^3/t gas content range.

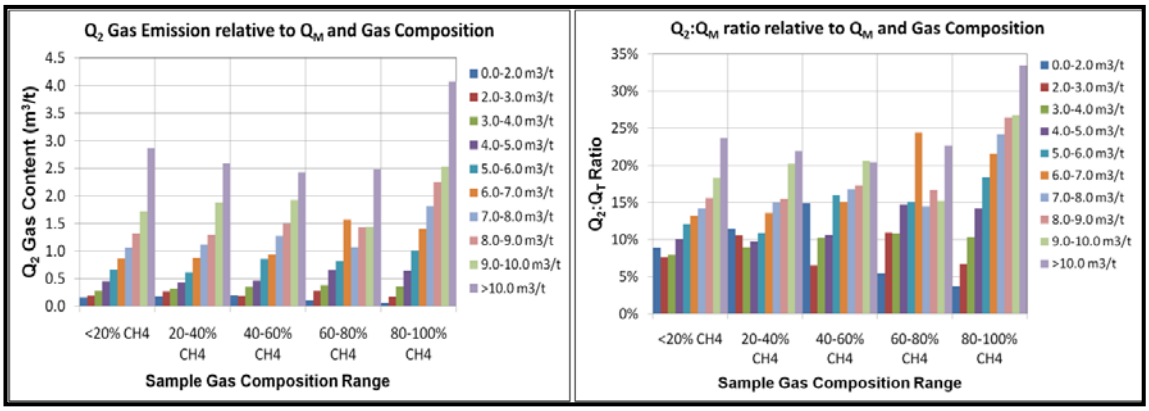

Figure 6.12: Distribution of average Q_2 gas content relative to Q_M and gas composition

Figure 6.13: Distribution of average Q_2:Q_M ratio relative to Q_M and gas composition

6.2.4 Q_3 Gas Content Component

The Q_3 component of Q_M represents the gas released from a coal sample following crushing (SAA, 1999). In fast desorption testing the Q_3 gas content is greater than the residual gas content, which represents the quantity of gas naturally retained within the coal structure at atmospheric pressure.

Figure 6.14 shows the distribution of Q_3 data relative to Q_M. The average Q_3 gas content was 4.5 m^3/t, ranging from 0.3 to 12.7 m^3/t. Q_3 increased in response to increasing Q_M. Figure 6.15 shows the distribution of Q_3:Q_M ratio data relative to Q_M. Although a high degree of scatter was evident, statistical analysis confirmed a decrease in Q_3:Q_M ratio corresponding to increased Q_M. The average Q_3:Q_M ratio was 87.6% in the 0-5 m^3/t gas content zone, 74.8% in the 5-10 m^3/t gas content zone and 60.4% in the >10 m^3/t gas content zone.

Figure 6.16 shows the distribution of Q_3 data relative to the gas composition (CH_4/(CH_4+CO_2)) of each sample. The majority of samples were found to have a Q_3 gas content less than 10.0 m^3/t across the gas composition range 0 to 100% CH_4. Figure 6.17 shows the distribution of Q_3:Q_M ratio data relative to gas composition. The average Q_3:Q_M ratio indicated little impact due to gas composition, with an average Q_3:Q_M ratio of 80.9% in the 0-40% CH_4 gas composition zone, 75.7% in the 40-80% CH_4 gas composition zone and 77.7% in the 80-100% CH_4 gas composition zone.

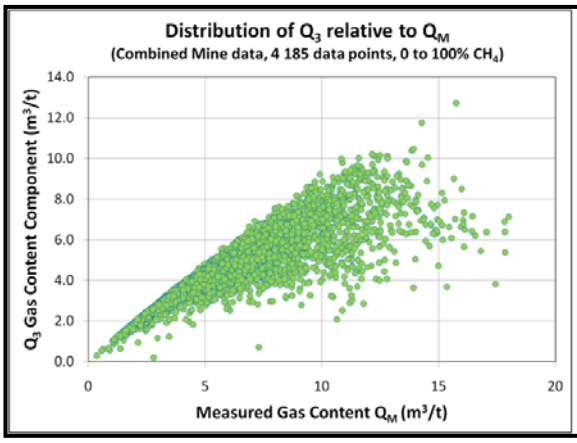

Figure 6.14: Distribution of Q_3 gas content relative to Q_M

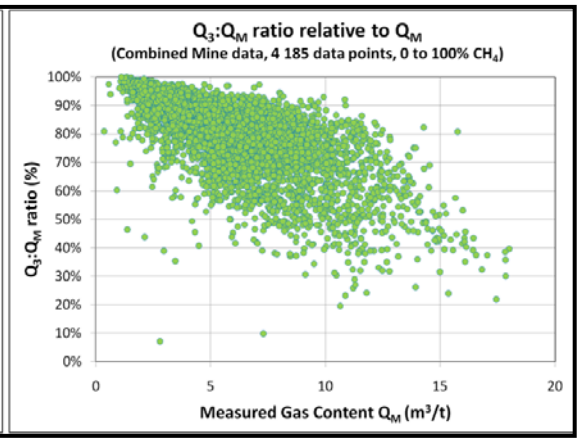

Figure 6.15: Distribution of Q_3:Q_M ratio relative to Q_M

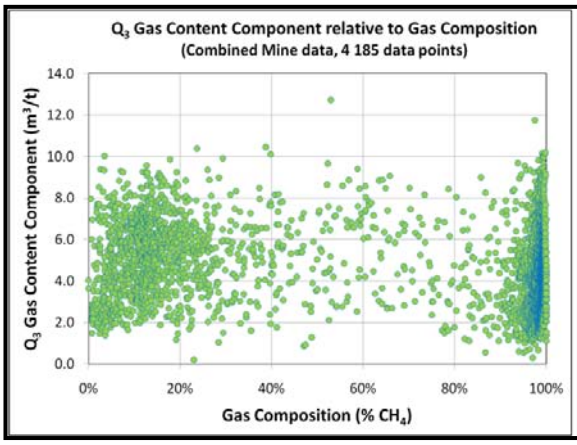

Figure 6.16: Distribution of Q_3 gas content relative to sample gas composition

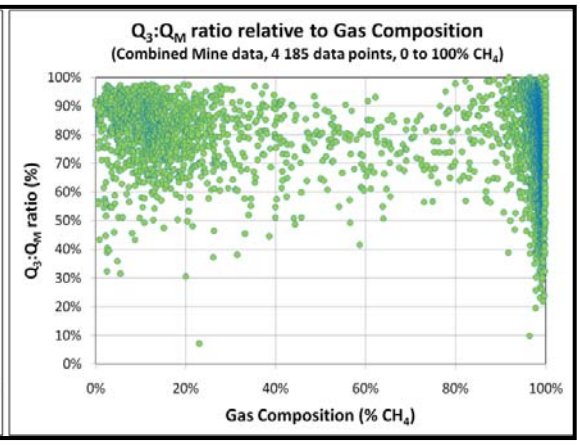

Figure 6.17: Distribution of Q_3:Q_M ratio relative to sample gas composition

The relationship between Q_3 and both gas content and gas composition was also investigated. Figure 6.18 shows a consistent increase in average Q_3 in response to increasing Q_M. This trend appears independent of gas composition for samples having gas composition ranging between 0 and 80% CH_4. The coal samples within the 80-100% CH_4 range indicate a reduction in Q_3 from samples with Q_M greater than 8.0 m^3/t. Figure 6.19 shows a reduction in the Q_3:Q_M ratio in response to increasing Q_M, decreasing from a high of 94% to a low of 57%.

This data indicates that where Q_M was low the bulk of the freely liberated gas has been lost, leaving predominantly the Q_3 component. As Q_M increases so does the volume of gas freely liberated during Q_1 and Q_2 desorption, thereby reducing the Q_3 component percentage.

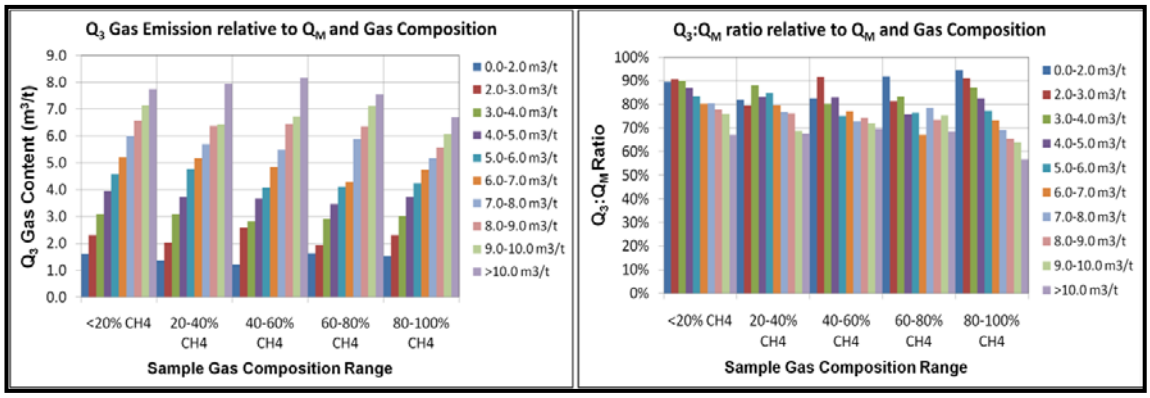

Figure 6.18: Distribution of average Q_3 gas content relative to Q_M and gas composition

Figure 6.19: Distribution of average Q_3:Q_M ratio relative to Q_M and gas composition

6.2.5 Relationship between Gas Content Components

Figure 6.20 shows the results of the gas content component values, Q_1, Q_2 and Q_3, plotted relative to Q_M for each sample. A linear trendline was plotted to represent the average relationship of each gas content component relative to Q_M. In this case $Q_1 = 0.0748.Q_M$, $Q_2 = 0.2306.Q_M$ and $Q_3 = 0.6944.Q_M$.

It can be seen that above $Q_M \approx 7.0$ m^3/t there was an increase in the degree of scatter of each gas content component. Both Q_1 and Q_2 increased and Q_3 reduced, relative to the linear average lines shown, in response to increasing Q_M.

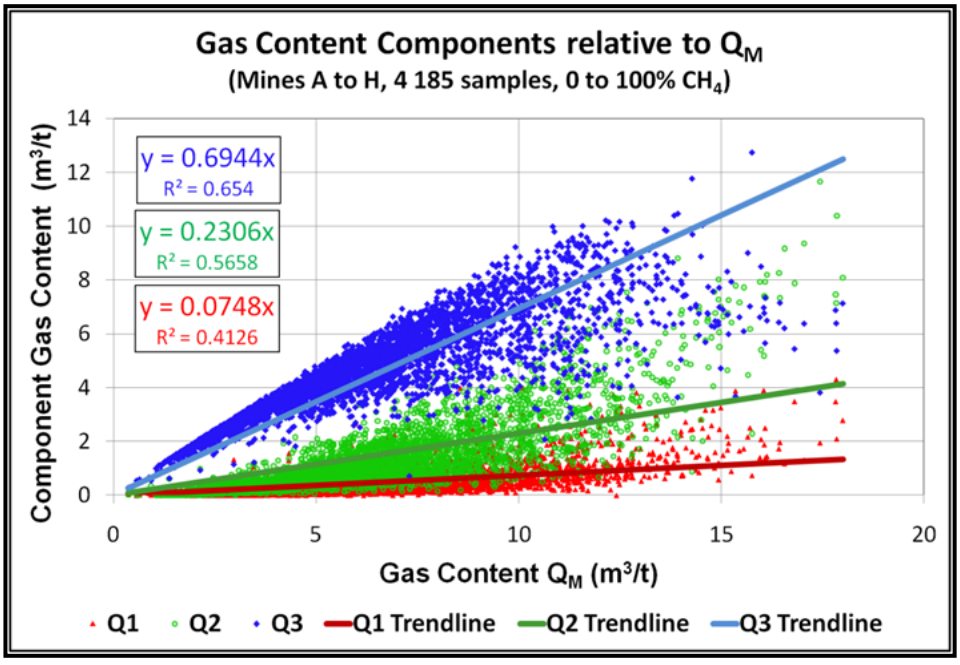

Figure 6.20: Gas content component values plotted relative to Q_M (0-18 m^3/t), including linear trendlines

Figure 6.21 shows the impact of introducing a transition point at Q_M = 7.0 m^3/t in the linear trendline representing each gas content component. For Q_M less than 7.0 m^3/t, the linear average of each gas content component was represented by the following equations $Q_1 = 0.0441.Q_M$, $Q_2 = 0.1561.Q_M$, and $Q_3 = 0.7998.Q_M$. For Q_M greater than 7.0 m^3/t, to the maximum 18.0 m^3/t, the linear average of each gas content component was represented by equations $Q_1 = 0.1723.Q_M - 0.835$, $Q_2 = 0.5345.Q_M - 2.6976$, and $Q_3 = 0.2949.Q_M + 3.5134$. Where total gas content exceeded 14.0 m^3/t, there was less data and increased scatter, therefore these values were excluded to assess the impact on the linear average of each gas content component. Figure 6.22 shows the impact on the linear average trendlines for each gas content component for Q_M between 7 and 14 m^3/t, excluding data having Q_M > 14 m^3/t. For Q_M between 7.0 and 14.0 m^3/t, the linear average of each gas content component was represented by equations $Q_1 = 0.1565.Q_M - 0.6968$, $Q_2 = 0.4531.Q_M - 1.9808$, and $Q_3 = 0.3925.Q_M + 2.654$.

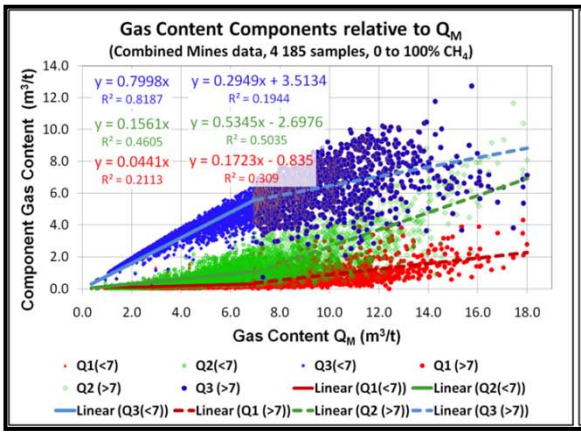

Figure 6.21: Gas content component values plotted relative to Q_M including linear trendlines 0-7 m^3/t and 7-18 m^3/t

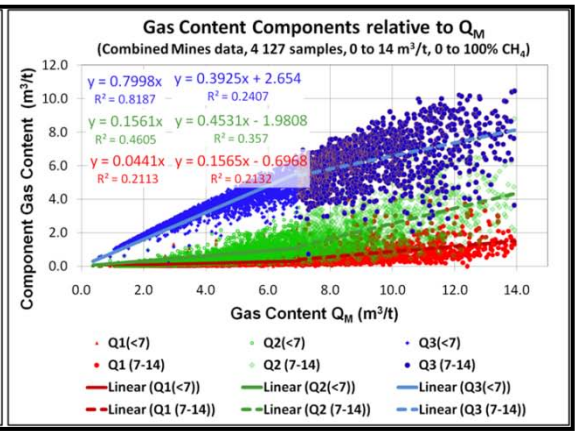

Figure 6.22: Gas content component values plotted relative to Q_M including linear trendlines 0-7 m^3/t and 7-14 m^3/t

Given the trend of increasing Q_1 and Q_2 and decreasing Q_3 corresponding to increasing Q_M, a power relationship was considered to more accurately represent the average of each gas content component relative to Q_M. Figure 6.23, shows each gas content component represented by equations $Q_1 = 0.0064.Q_M^{2.0227}$, $Q_2 = 0.0257.Q_M^{1.9692}$ and $Q_3 = 1.1631.Q_M^{0.7529}$. The statistical correlation achieved using by representing the average relationship of each gas content component was greater compared to using a linear relationship.

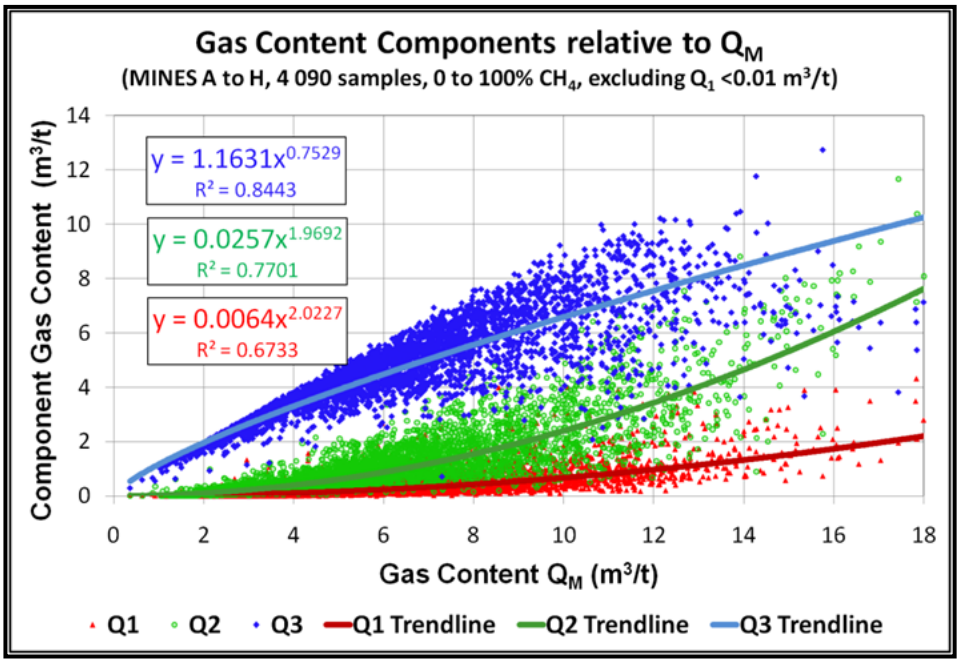

Figure 6.23: Gas content component values plotted relative to Q_M including power formula trendlines representing the average of each component

The comparatively strong correlation indicates that the power formula most accurately represents the relationship between Q_M and each of the three gas content components within this total dataset.

6.2.5.1 Impact of Gas Composition on the Gas Content Component Relationship

The analysis of the relationship between Q_M and each of the three gas content components was extended to consider the impact of gas composition. Gas data from both CO_2 rich (<20% CH_4) and CH_4 rich (>80% CH_4) areas were analysed to determine differences attributable to gas composition.

Figure 6.24 and Figure 6.25 show the distribution of gas content component data relative to Q_M for both CO_2 and CH_4 rich areas respectively. Linear trendlines indicate the average of each component group for Q_M between 0.0 to 7.0 m^3/t and 7.0 to 14.0 m^3/t.

The data show that on average a greater proportion of Q_M was liberated from CH_4 rich coal during Q_2 testing compared to CO_2 rich coal, suggesting that CH_4 was liberated from the core samples at a faster rate than CO_2. The Q_1 gas emission was similar in both cases suggesting the lost gas component was independent of gas composition.

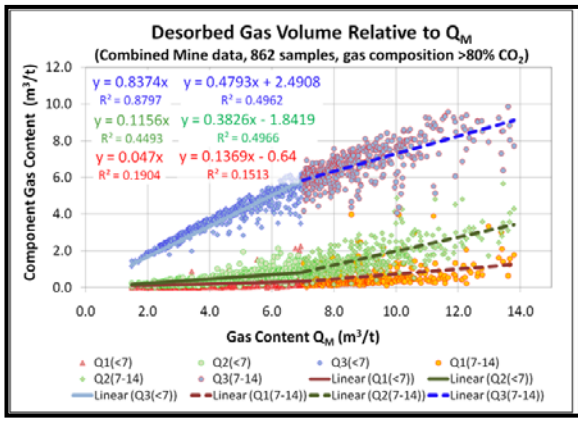

Figure 6.24: CO_2 rich gas content component values plotted relative to Q_M, showing linear trendlines 0-7 m^3/t and 7-14 m^3/t

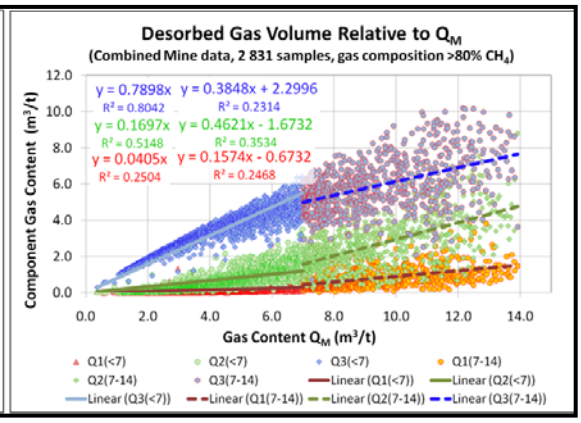

Figure 6.25: CH_4 rich gas content component values plotted relative to Q_M, showing linear trendlines 0-7 m^3/t and 7-14 m^3/t

Figure 6.26 and Figure 6.27 show the use of power formula equations to represent the average relationship between each gas component group and Q_M, for Q_M between 0.0 and 18.0 m^3/t, in CO_2 and CH_4 rich areas respectively.

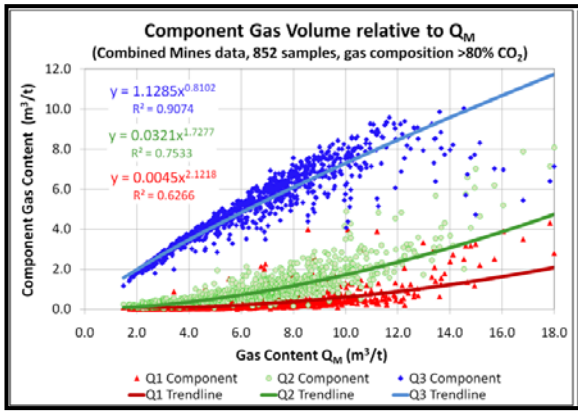

Figure 6.26: CO_2 rich gas content component values plotted relative to Q_M, showing power relationship 0-18 m^3/t

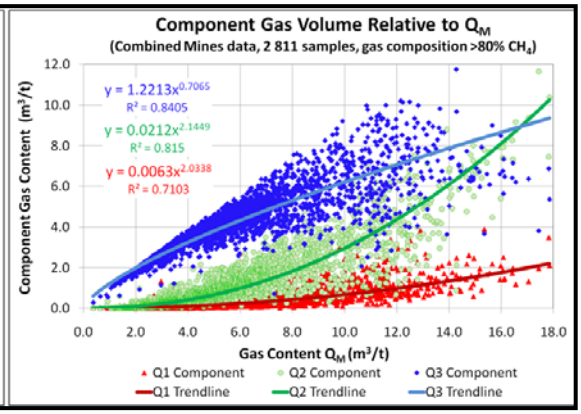

Figure 6.27: CH_4 rich gas content component values plotted relative to Q_M, showing power relationship 0-18 m^3/t

The power relationship achieved comparatively high statistical correlation and was therefore considered to more accurately represent the average relationship between Q_M and each of the three gas content components. The Q_1 gas emission was similar in both cases suggesting the relationship between Q_1 and Q_M was independent of gas composition. A greater proportion of Q_M was liberated during Q_2 testing from CH_4 rich coal compared to CO_2 rich coal suggesting CH_4 desorbs at a faster rate than CO_2.

Figure 6.28 and Figure 6.29 show the difference in average relationship between the three gas content component values relative to Q_M, due to differences in gas composition, represented by linear and power formula respectively.

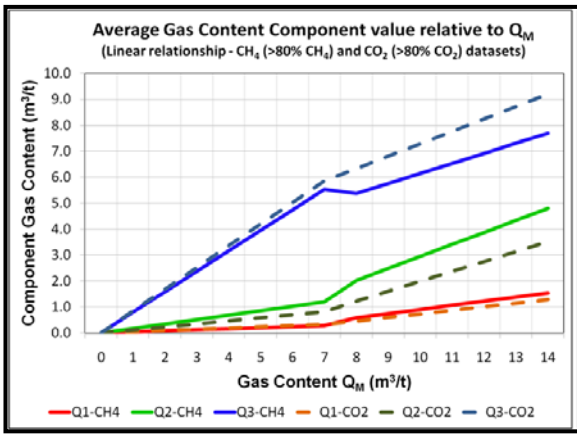

Figure 6.28: Impact of gas composition on average gas content component values relative to Q_M, based on linear average relationship

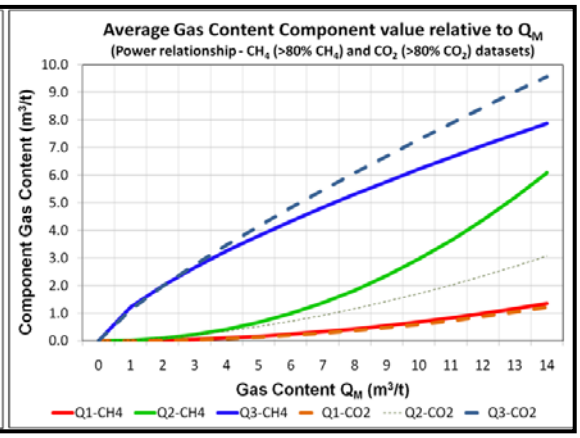

Figure 6.29: Impact of gas composition on average gas content component values relative to Q_M, based on power formula relationship

The Q_1 component was found to be independent of gas composition. Where Q_M was less than 7.0 m^3/t gas composition had little impact on gas emission behaviour. As Q_M increased beyond 7.0 m^3/t it was found that the Q_2:Q_M ratio increased while the Q_3:Q_M ratio decreased. The effect was more significant in CH_4 rich coal samples suggesting, in response to increasing Q_M, CH_4 liberates from coal samples at a faster rate than CO_2.

6.2.5.2 Estimating Average Total Gas Content from Q_1 Lost Gas Content

Given the strong relationship between Q_1 and Q_M, it was proposed that the average Q_M of a coal sample may be estimated using the Q_1 gas content value, once determined in the field. Although only an estimate, an indication of the expected Q_M can be of significant benefit to mine operators, particularly in outburst prone conditions, enabling appropriate response actions to be planned in advance of receiving the gas analysis test result from the laboratory.

The Q_1 gas content was shown to be independent of gas composition and the average Q_M-Q_1 relationship was best represented by a power formula, shown in Equation 6.1, where α and β are variables.

$$Q_{M(ave)} = \alpha \times Q_1^{\beta} \qquad (6.1)$$

Figure 6.30 shows the results of Q_M plotted relative to the Q_1 gas content component for the complete dataset. The value of the two variables, α and β, from Equation 6.1, are 9.3729 and 0.3328 respectively.

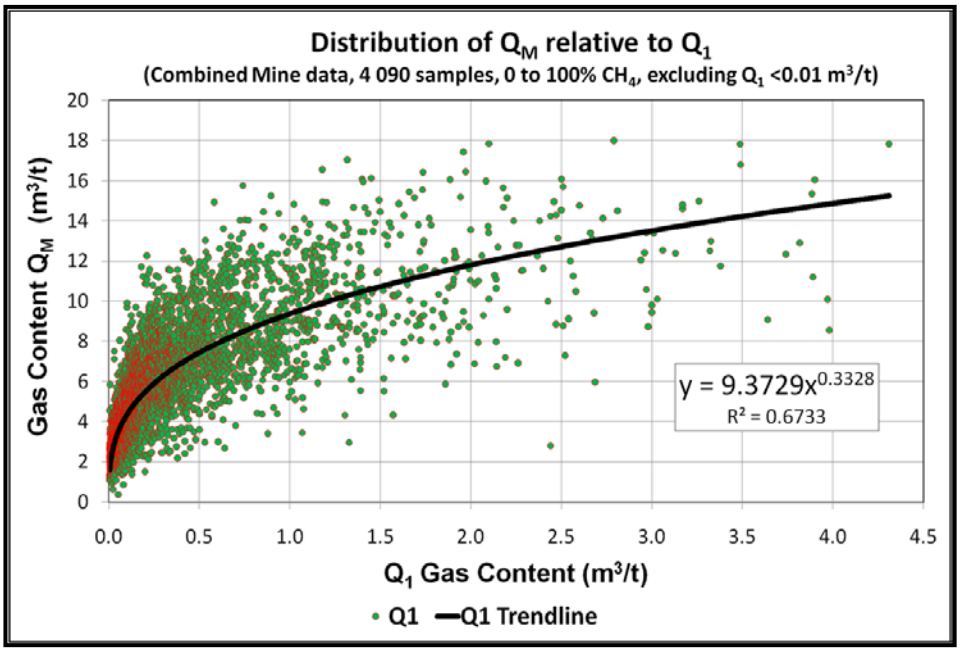

Figure 6.30: Q_M-Q_1 data for the complete dataset, including trendline representing average Q_M relative to Q_1

Figure 6.31 show the average relationship between Q_M and Q_1, represented by the power formula, for the complete dataset and each of five separate gas composition ranges. With the exception of the data within the range 20 to 40% CH_4, the curves representing the average of each gas composition range and the complete dataset are similar. This result suggests, on average, gas composition does not have a significant impact on the relationship between Q_1 and Q_M. Details of the distribution of Q_M and Q_1 for coal samples within each gas composition range are presented in Appendix 6.2.

Figure 6.32 show the average relationship between Q_M and Q_1, represented by the power formula, for the complete dataset and each of the seven mines from which the data was sourced. Analysis of the distribution of Q_M and Q_1 data, presented in Appendix 6.3, suggests that the variation between the average power relationships representing each mine may be partly due to the number and distribution of data. In the case of Mine A and to a lesser extent, Mine D, a greater number of samples of increasing Q_1:Q_M ratio serve to reduce the slope of the curve, whereas in the case of Mine G and to a lesser extent Mine C the increased number of samples with relatively low Q_1:Q_M ratio serve to increase the slope of the curve.

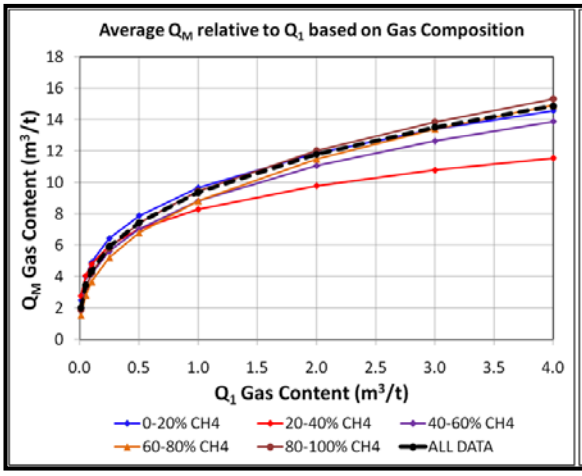

Figure 6.31: Impact of gas composition on the average Q_M to Q_1 gas content relationship

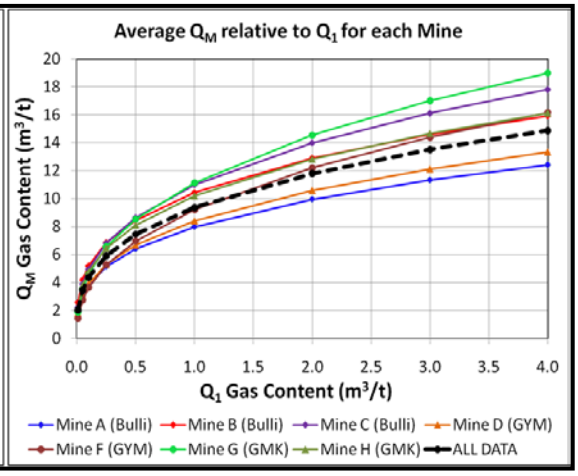

Figure 6.32: Impact of core sample origin on the average Q_M to Q_1 gas content relationship.

6.2.6 Initial Gas Desorption Rate

The initial gas desorption rate (IDR) was investigated to determine if a relationship existed between IDR and each of Q_M and gas composition. A related measure of gas emission rate during early stage gas desorption from coal core samples is known as IDR30. The IDR30 is a measurement of the quantity of gas desorbed from a coal sample per unit mass of the sample in the first 30 minutes of desorption testing (Williams, 2002). Analysis of gas desorption data identified a strong correlation (R^2 = 99%) between IDR and IDR30, with the relationship represented by Equation 6.2.

$$\text{IDR} = 167 \times \text{IDR30} \tag{6.2}$$

The impact of gas content and composition on both IDR and IDR30 was investigated. Figure 6.33 shows a consistent increase in both IDR and IDR30 in response to increasing Q_M. The data suggests that the initial desorption rate was closely related to Q_M and the relationship was independent of gas composition.

Figure 6.34 shows the results of IDR data relative to Q_M for all samples within the dataset. As reported by Williams (2002), samples having an abnormally high IDR and low Q_M may indicate leakage from the desorption canister while in transit between the mine and the gas analysis laboratory. However a highly fractured core can also produce an abnormally high IDR value relative to Q_M. From the mine data presented, a clear upper limit was evident, defining a maximum Q_M envelope relative to IDR.

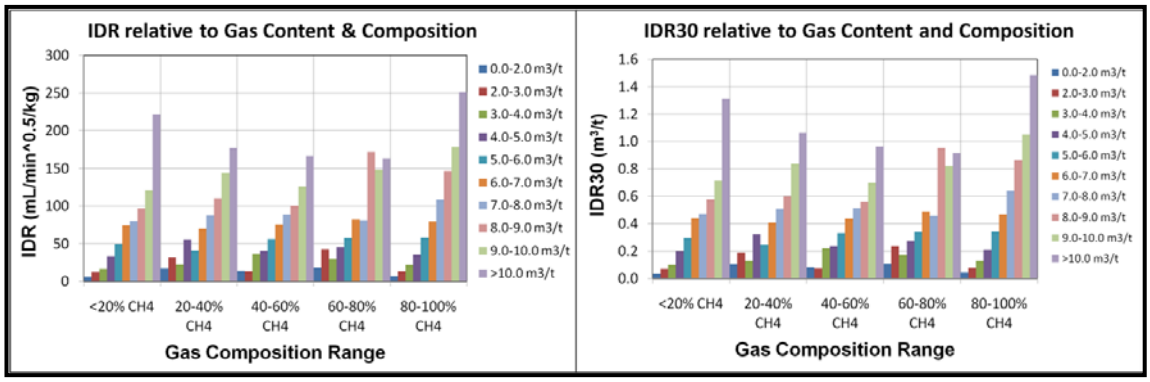

Figure 6.33: Average IDR and IDR30 relative to gas content and gas composition

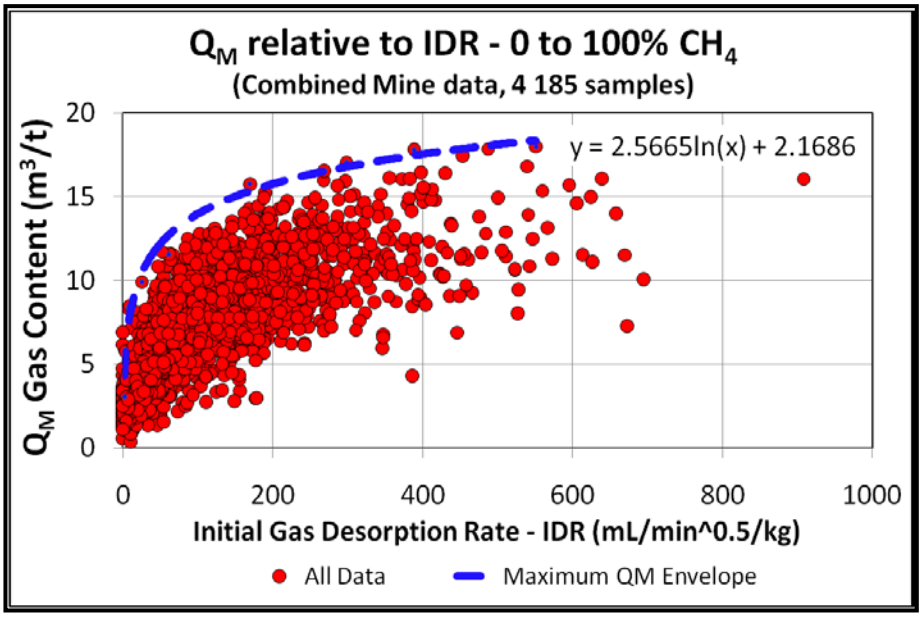

Figure 6.34: Q_M relative to IDR, including maximum Q_M envelope

6.2.6.1 Impact of Gas Composition on Initial Gas Desorption Rate

Analysis of the relationship between Q_M and IDR was extended to consider the impact of gas composition. Mine gas analysis data representing both CO_2 rich (<20% CH_4) and CH_4 rich (>80% CH_4) coal seam gas conditions was analysed to determine differences attributable to gas composition.

Figure 6.35 and Figure 6.36 show the distribution of Q_M relative to IDR from CO_2 and CH_4 rich areas respectively. There was little difference between the maximum Q_M envelopes suggesting the relationship was independent of gas composition.

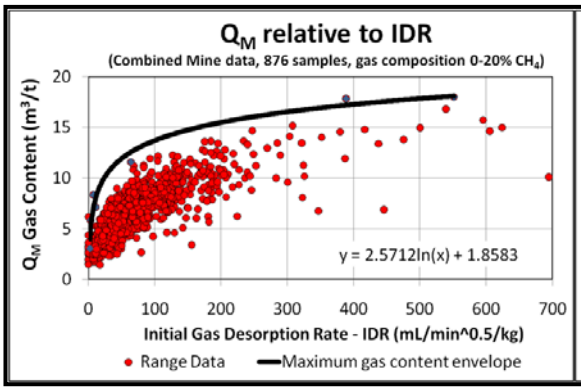

Figure 6.35: Q_M-IDR data from CO_2 rich coal, including $Q_{M(max)}$ envelope

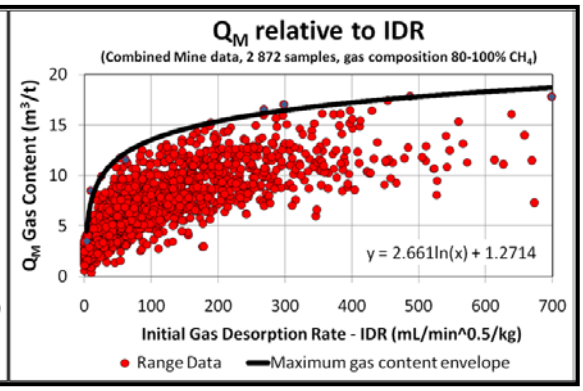

Figure 6.36: Q_M-IDR data from CH_4 rich coal, including $Q_{M(max)}$ envelope

Details of the distribution of Q_M and IDR data within each gas composition range, including the maximum Q_M envelope representing the complete dataset, are presented in Appendix 6.4. The distribution of Q_M and IDR data from each mine, including the maximum Q_M envelope representing the complete dataset, are presented in Appendix 6.5.

6.2.6.2 Estimating Maximum Total Gas Content from the Initial Gas Desorption Rate

From the above assessment of the relationship between Q_M and IDR it was proposed that the maximum Q_M of a coal sample may be estimated using the results of IDR measurements determined in the field. Once the IDR has been determined, this value may be used to estimate the maximum Q_M using Equation 6.3. Although only an estimate, an indication of the maximum expected Q_M can be of significant benefit to mine operators, particularly in outburst prone conditions, enabling appropriate response actions to be planned in advance and prior to receiving the results of gas analysis testing from the laboratory.

$$Q_{M(max)} = 2.5665 \times \ln(IDR) + 2.1686 \quad (6.3)$$

6.2.6.3 Estimating Average Total Gas Content from the Initial Gas Desorption Rate

Figure 6.37 shows the distribution of Q_M relative to the square root of IDR. Presenting the Q_M-IDR data from the combined mine dataset in this manner was found, through statistical analysis, to have a correlation of 0.656.

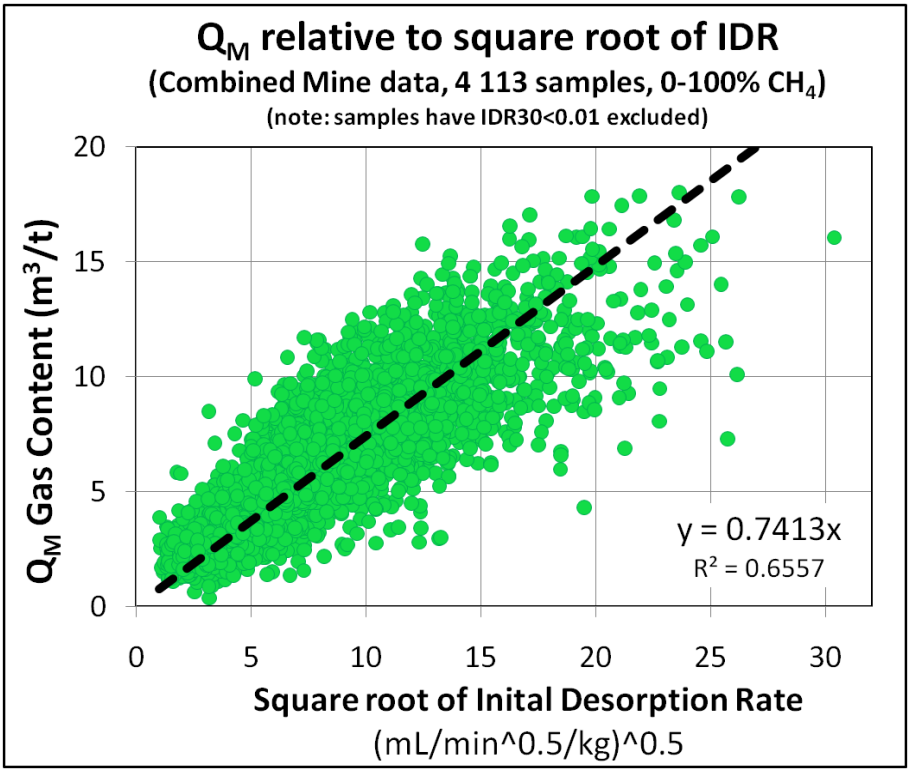

Figure 6.37: Q_M relative to square root of IDR

This analysis was extended to consider the impact of gas composition which confirmed the relationship to be virtually independent of gas composition. Details of the distribution of Q_M relative to the square root of IDR within each gas composition range, including the equation representing the relationship between the two variables, are presented in Appendix 6.6.

From this assessment it was proposed that IDR may be used to estimate average Q_M using the formula shown in Equation 6.4.

$$Q_{M(ave)} = 0.7413 \times \sqrt{IDR} \qquad (6.4)$$

6.2.7 Desorption Rate Index (DRI)

The Desorption Rate Index (DRI) was proposed by Williams and Weissman (1995) as a method of using gas desorption rate to determine outburst threshold limit values (TLV) applicable to coal mines operating in coal seams other than the Bulli seam. As discussed in Chapter 2, DRI is determined by extrapolating the gas volume liberated from crushing a 200 g coal sub-sample for 30 seconds (V_{30}) to calculate the gas volume (DRI)

corresponding to Q_M (Williams, 1996 and Williams, 1997), as represented by Equation 6.5.

$$DRI = Q_M \times \frac{V_{30}}{Q_3} \tag{6.5}$$

DRI data from 3 355 coal samples, collected from five Australian mines, are presented relative to Q_M in Figure 6.38. Statistical analysis confirmed a strong positive correlation of 0.965.

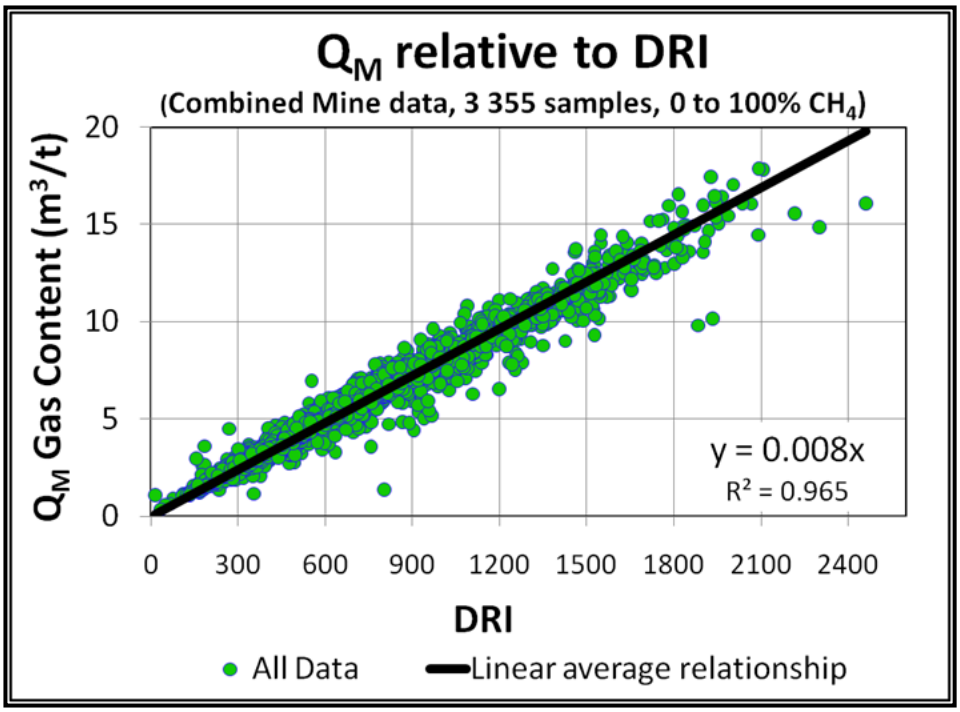

Figure 6.38: Q_M relative to DRI

The relationship between Q_M and DRI was found to be consistent for each of the five mines. The Q_M-DRI data from each mine, including the equation representing the average relationship between the two variables and statistical correlation, are presented in Appendix 6.7. A consistent relationship was identified between Q_M and DRI which appears contrary to the relationship presented by Williams and Weissman (1995), presented in Chapter 2.

Further analysis was undertaken to assess the impact of both gas content and gas composition on DRI. Figure 6.39 shows the average DRI value for samples grouped in accordance with Q_M and gas composition. The results indicate a strong relationship between DRI and Q_M that was independent of gas composition.

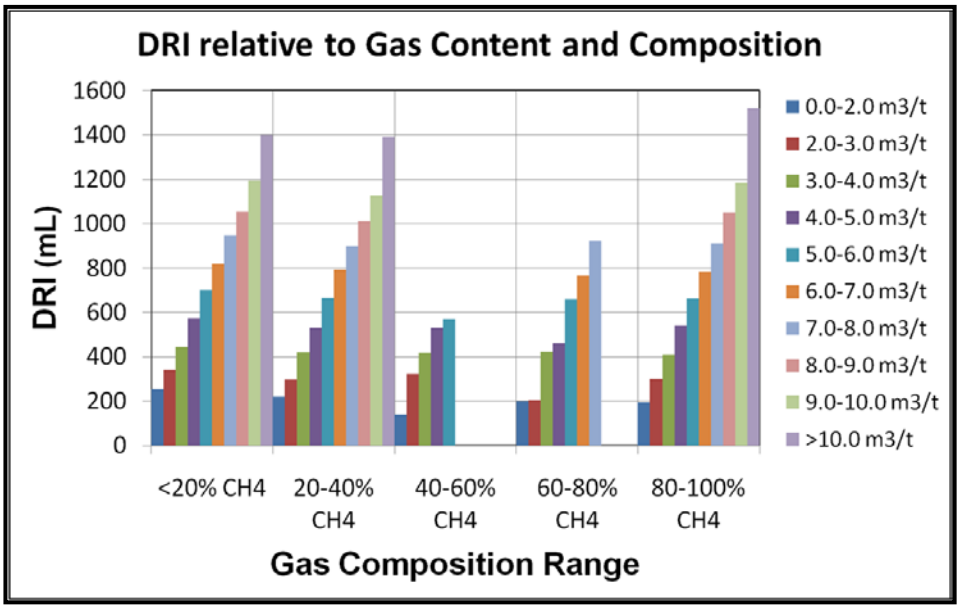

Figure 6.39: Average DRI relative to gas content and gas composition

6.2.7.1 Impact of Gas Composition on Desorption Rate Index

Further analysis was undertaken to confirm the impact of gas composition on the relationship between Q_M and DRI. Figure 6.40 show the relationship between Q_M and DRI for samples in both CO_2 rich (0-20% CH_4) and CH_4 rich (80-100% CH_4) areas of the combined mine dataset. In both cases the data demonstrated a strong correlation and identical linear average relationship between Q_M and DRI, suggesting the relationship was independent of gas composition.

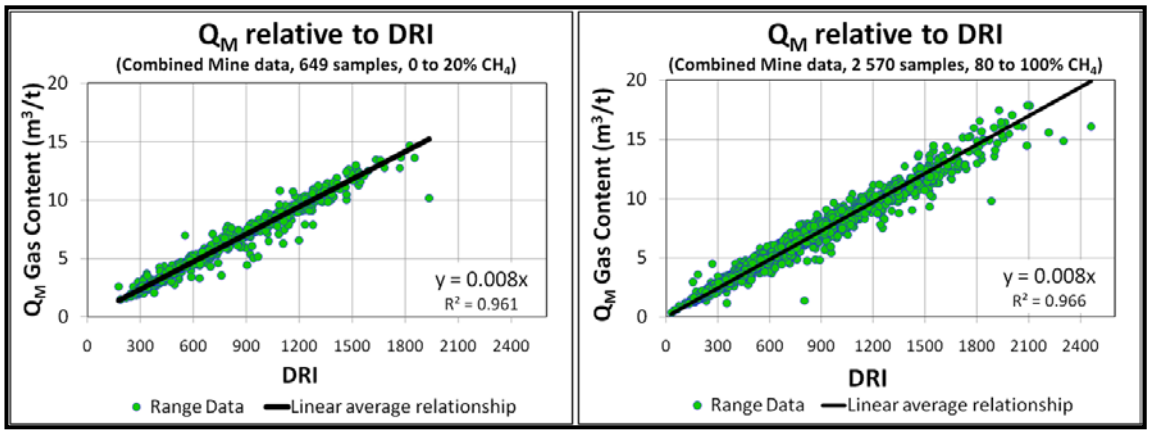

Figure 6.40: Q_M-DRI relationship within CO_2 and CH_4 rich seam gas conditions

Details of the distribution of Q_M and DRI within each gas composition range, including the equation representing the average linear relationship between the two variables, are presented in Appendix 6.8.

This analysis confirmed a strong relationship between Q_M and DRI, independent of both gas composition and mine location, which was represented by Equation 6.5.

$$Q_M = 0.008 \times DRI \quad (6.5)$$

6.2.8 Impact on Outburst Threshold Limits

The strong relationship between Q_M and DRI, represented by Equation 6.5, which appears independent of gas composition and coal seam geological properties, was contrary to the relationship presented by Williams and Weissman (1995), shown in Figure 6.41.

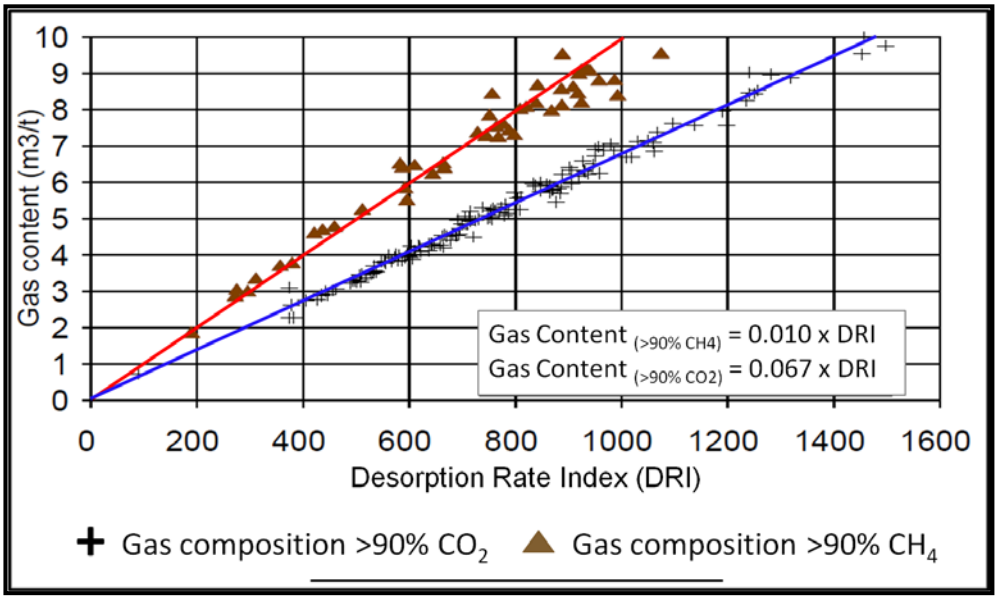

Figure 6.41: Q_M relative to DRI for CH_4 and CO_2 rich Bulli seam coal samples (after Williams and Weissman, 1995)

Figure 6.42 show the relationship between Q_M and DRI of coal samples sourced from five Australian underground coal mines, having gas composition within the range of 90-100% CO_2 and 90-100% CH_4, plotted relative to the Williams and Weissman (1995) data. Although some scatter was evident, statistical analysis confirm a strong correlation (R^2≈97%) among the data from the five mines with little difference between the averages of each gas composition range.

This analysis suggests the relationship between Q_M and DRI, presented by Williams and Weissman (1995), which shows far greater rate of gas emission from CH_4 rich samples, is not representative of current Bulli seam conditions. The similar relationship indicated

between Q_M and DRI, which appears to be independent of gas composition, suggests the DRI900 methodology proposed by Williams and Weissman may no longer be suitable for determining TLV for non-Bulli seam mines.

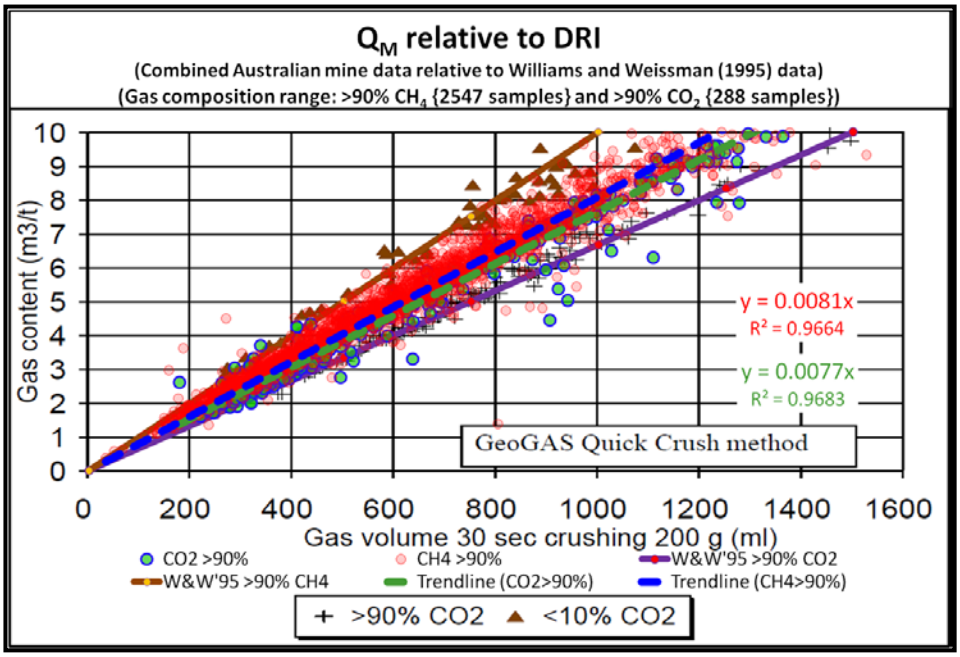

Figure 6.42: Q_M relative to DRI for CH_4 and CO_2 rich Bulli and non-Bulli seam coal samples

Contrary to the methodology proposed by Williams and Weismann (1995), which suggested a single DRI value of 900 as the basis for determining TLV for all non-Bulli seam mines, this study shows a unique DRI value corresponding to each TLV gas content value. In the example presented in Figure 6.43, a TLV of 12 m^3/t corresponds to a DRI of 1 500 and TLV's of 9 m^3/t and 6 m^3/t correspond to DRI values of 1 125 and 750 respectively.

The methodology presented by Williams and Weissman (1995) to determine TLV applicable to non-Bulli seam mines was based upon the relationship between Q_M and DRI being different at each non-Bulli seam mine, and the relationship being impacted by seam gas composition. This analysis identified a common relationship between Q_M and DRI among the mines represented in the dataset that was independent of seam gas composition and variability among other coal properties. The relationship was shown to be consistent not only among Bulli seam mines but also among coal seams located in the Hunter Valley and Central Queensland. The consistency of the relationship between Q_M and DRI among the mines included in this analysis, shown in Equation 6.5, suggests the relationship may also represent many other Australian coal seam conditions. The

potential application of Equation 6.5 to describe the relationship between Q_M and DRI in other coal seams has yet to be investigated and confirmed.

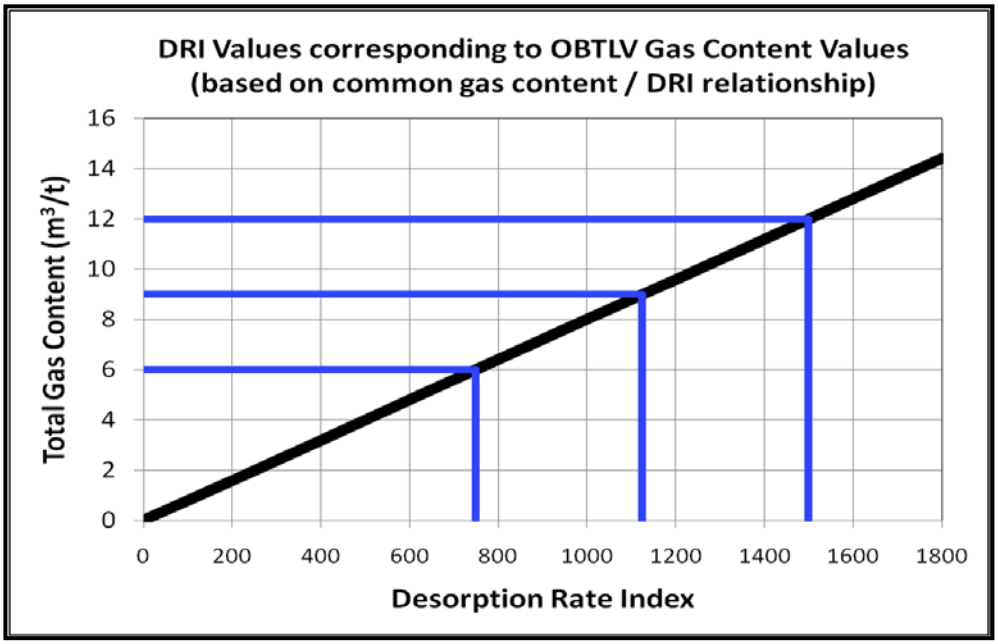

Figure 6.43: Q_M-DRI relationship for determining TLV's applicable to non-Bulli seam mines

This analysis found the relationship between Q_M and DRI, previously proposed by Williams and Weismann (1995), and used as the basis for determining outburst TLV for non-Bulli seam mines, is not representative of current WCC conditions and is not common among all Bulli seam mines. The relationship between Q_M and DRI identified in this study was different to the relationship presented by Williams and Weissman which suggests the use of the DRI900 method for determining TLV applicable to non-Bulli seam mines may no longer be valid and an alternative method must be considered.

Given the apparent common relationship between Q_M and DRI among the Bulli and non-Bulli mines it is suggested that TLV applicable to the Bulli seam may be directly transferrable to non-Bulli seam mines.

6.3 ANALYSIS OF COAL SAMPLE GAS EMISSION – SLOW DESORPTION TESTING

To supplement the data obtained from fast desorption gas testing additional core sample material was gathered and tested using the slow desorption method. The objective of this additional testing was to (a) compare the results of total gas content measurement using separate methods, and (b) analyse the results of slow desorption testing relative to

available coal property data to identify specific relationships that may provide insight into the nature of coal seam gas emission.

6.3.1 Data Acquisition – Slow Desorption Gas Testing

Figure 6.44 shows the location of 35 core samples collected for slow desorption gas content testing from boreholes drilled from the 519 and 520 panels at WCC. Immediately upon recovery from the borehole each coal core sample was removed from the core barrel, separated, inserted into PVC gas desorption canisters and the cap fitted and sealed shut to prevent further loss of gas. The primary core was sent to the BHP Billiton Illawarra Coal Gas Laboratory for fast desorption testing, as per the mine's outburst management procedure. The duplicate core was sent for slow desorption testing at the University of Wollongong Gas Laboratory.

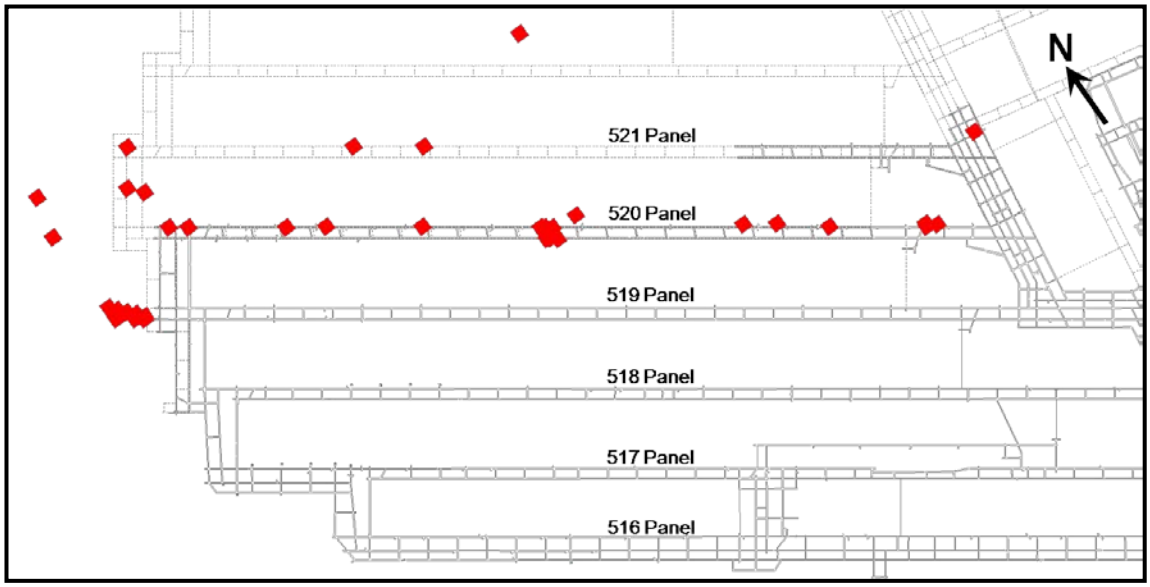

Figure 6.44: Location of core samples tested using slow desorption method

Slow desorption testing was conducted in accordance with the Australian Standard "Guide to the determination of gas content of coal – Direct desorption method" (SAA, 1999).

Figure 6.45 shows both a PVC gas desorption canister, used to store coal core during transport and desorption testing, and the University of Wollongong slow desorption gas testing apparatus, used for measuring the volume of gas liberated from a coal core during slow desorption testing. During slow desorption testing the gas desorption

canisters were connected to the inverted, water filled, graduated cylinders via a nylon tube allowing the volume of gas released from each canister to be accurately measured.

Figure 6.45: PVC core sample gas desorption canister and slow desorption testing apparatus

High concentrations of CO_2 in the gas liberated from the core samples presented a potential risk of gas loss into solution when in contact with water in the measurement cylinders. Therefore contact between the liberated gas and water within the two litre capacity graduated cylinders was kept to a minimum by top-feeding gas into the cylinder and sealing the gas desorption canister between each scheduled gas release.

To account for changes in temperature and barometric pressure at the time of each gas release the desorbed gas volume was corrected to standard conditions, $20^{O}C$ and 101.3 kPa, using Equation 6.7 (SAA, 1999).

$$V_{20^{o}C,101.3\ kPa} = \frac{(V_{bomb} + V_{tube} + V_t) \times P_t \times (T_{20^{o}C} + 273.1)}{(T_t + 273.1) \times P_{101.3}} \qquad (6.7)$$

where: $P_M = P_A - \frac{(V_{CT} - V_t)}{V_{CT}} \times h \times 9.79$ (kPa)

V_t = Volume in cylinder at time of reading t (mL)
V_{CT} = Total volume of cylinder to water level (mL)
h = Height of cylinder zero above water level (m)
T_t = Temperature at time t (^{O}C)
$T_{20^{o}C} = 20^{O}C$
P_t = Corrected barometer at time t (kPa)
$P_{101.3}$ = 101.3 kPa
V_{bomb} = Free volume in bomb (mL)

V_{tube} = Free volume in tube (mL)
P_A = Barometer at time of reading (kPa)
$V_{20^oC,\ 101.3\ kPa}$ = Volume of gas and air in measuring system (mL)

During the course of desorption testing there was a reduction in gas volume liberated at each release. In the latter stages of desorption increased time was allowed between successive gas releases to allow sufficient time for a measurable volume of gas to be liberated from the coal sample. Table 6.3 shows the schedule used to determine the number of days between gas releases during slow desorption testing, based on the volume of gas liberated at each release.

Table 6.3: Slow desorption testing gas release schedule

Measured gas volume liberated	Measurement frequency (days between samples)
Greater than 1 500 mL	1 day
1 000 to 1 500 mL	2 days
500 to 1 000 mL	7 days
150 to 500 mL	14 days
Less than 150 mL	28 days

A glass burette, fitted inline along the nylon tube connecting the desorption canister to the measuring cylinder, was used to collect a sample of the desorbed gas liberated at each release. Subsequent to each gas release the glass burette was sealed, removed from the slow desorption test apparatus, and connected to a four channel Hewlett Packard Quad Micro Gas Chromatograph, shown in Figure 6.46, to measure the composition of the desorbed gas. The relative concentration of the following gases was measured for each sample: helium, hydrogen, oxygen, nitrogen, methane, carbon monoxide, carbon dioxide, ethylene and ethane.

Figure 6.47 shows the cumulative gas emission from two coal samples, WE1203 and WE1185, during slow desorption testing relative to the Q_M value determined by fast desorption testing. The gas content indicated at the commencement of desorption testing (t = 0) represents the Q_1 gas content. At the completion of desorption testing the measured Q_3, residual gas content value, is also shown. A logarithmic trendline was used to represent the nature of gas desorption for each of the 35 samples analysed. Gas emission plots for each sample are presented in Appendix 6.10.

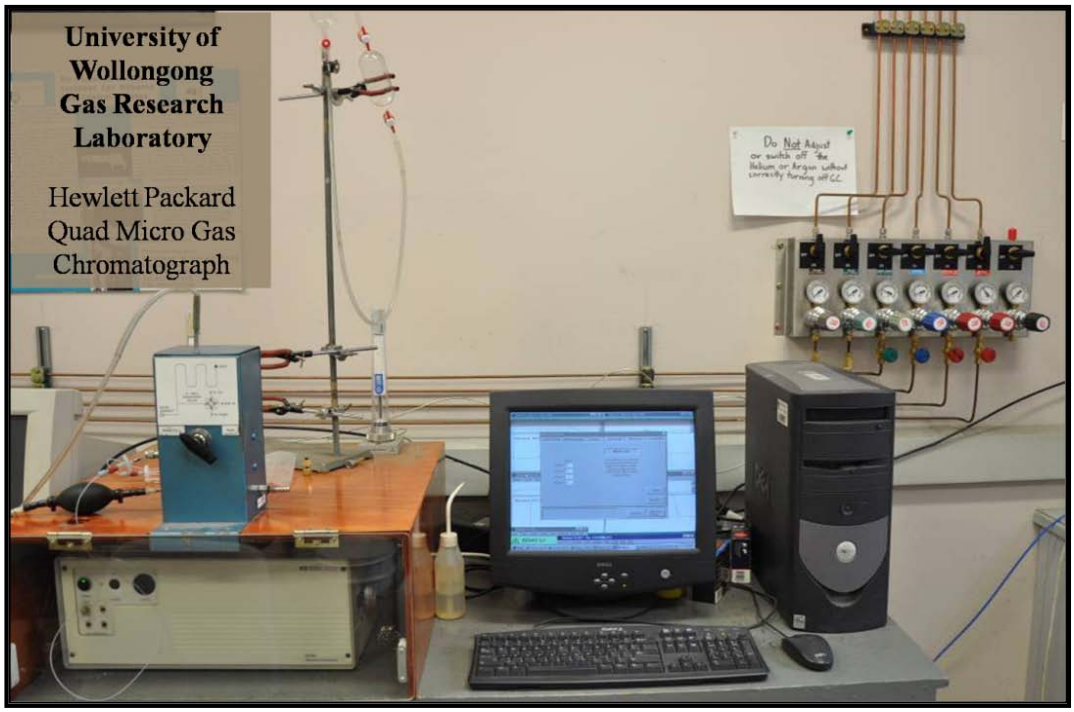

Figure 6.46: Hewlett Packard quad micro gas chromatograph

As shown in Figure 6.47, the Q_M of sample WE1203, determined through slow desorption testing, equals the result obtained from separate fast desorption testing. However, a significant difference exists between the two Q_M values determined for sample WE1185. The much lower Q_M of the WE1185 slow desorption sample was probably the result of gas leakage from the core canister between each gas release, thereby rendering WE1185 an invalid test sample.

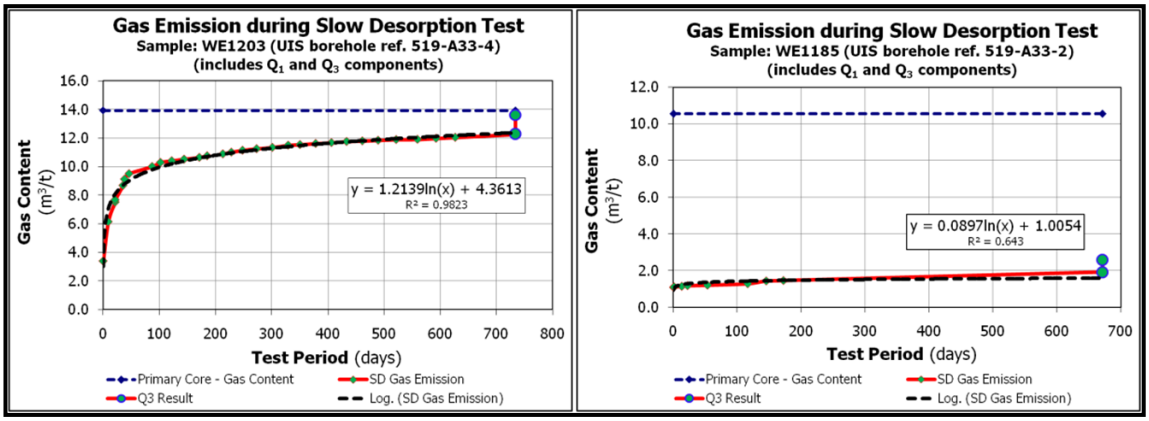

Figure 6.47: Slow desorption gas emission results representing samples WE1203 and WE1185

Analysis of gas emission data from both fast and slow desorption testing was conducted to determine the validity of results from each sample. The analysis considered potential loss of gas through leakage from the gas desorption canister during slow desorption

testing and potential errors in gas content component values from fast desorption testing. In assessing the results from fast desorption testing the value of each gas content component was assessed relative to the average of all mine data with any significant variance indicating possible error. The validity of the fast desorption Q_M values was tested against the average relationship identified between Q_M and each gas content component, represented by the following equations.

$$Q_1 = 0.1196 \times Q_M \tag{6.8}$$

$$Q_2 = 0.1399 \times Q_M \tag{6.9}$$

$$Q_3 = 0.7399 \times Q_M \tag{6.10}$$

Table 6.4 lists samples considered valid, having low risk of data error, including a summary of the validity assessment. Table 6.5 lists samples considered to be invalid. Photographs of each duplicate coal core sample tested using the slow desorption method are shown in Appendix 6.11.

Table 6.4: Assessment of gas emission data listing samples considered to be valid

Sample Reference	Measured Gas Content				Slow Desorption Test		Fast Desorption Test						Comments Observations
					Gas Loss		Possible Errors						
	Fast Desorb.	Slow Desorb.	Diff. (m^3/t)	Diff. (%)	(System Leakage)		Q1 Value		Q2 Value		Q3 Value		
					Yes	No	High	Low	High	Low	High	Low	
WE1188	2.00	2.68	0.68	34%		✓		✓		✓			Low Q1 result - Qt (both FD & SD) may be less than Actual. Low Q2 result - Qt (FD) less than Qt (SD).
WE1180	5.19	4.78	-0.41	-8%		✓		✓					Low Q1 result - Qt (both FD & SD) may be less than Actual.
WE1333	4.33	5.10	0.77	18%		✓		✓		✓			Low Q1 result - Qt (both FD & SD) may be less than Actual. Low Q2 result - Qt (FD) less than Qt (SD).
WE1192	5.35	5.26	-0.09	-2%		✓		✓		✓			Low Q1 result - Qt (both FD & SD) may be less than Actual. Low Q2 result - Qt (FD) less than Qt (SD).
WE1215	6.30	5.32	-0.98	-16%		✓		✓					Low Q1 result - Qt (both FD & SD) may be less than Actual.
WE1183	6.71	5.34	-1.37	-20%	possible								Possibility of some leakage during SD testing resulting in Qt (SD) < Qt (FD).
WE1198	5.38	5.65	0.27	5%		✓		✓		✓			Low Q1 result - Qt (both FD & SD) may be less than Actual. Low Q2 result - Qt (FD) less than Qt (SD).
WE1196	5.99	5.85	-0.14	-2%		✓	✓						High Q1 result - Qt (both FD & SD) may be greater than Actual.
WE1189	6.02	5.92	-0.10	-2%		✓							
WE1246	7.93	6.63	-1.30	-16%		✓			✓				High Q2 result - Qt (FD) greater than Qt (SD).
WE1295	7.08	8.61	1.53	22%		✓		✓					Low Q1 result - Qt (both FD & SD) may be less than Actual.
WE1230	8.15	8.91	0.76	9%		✓		✓					Low Q1 result - Qt (both FD & SD) may be less than Actual.
WE1294	8.99	9.60	0.61	7%		✓							
WE1200	10.78	9.70	-1.08	-10%		✓							
WE1201	10.56	11.02	0.46	4%		✓		✓	✓			✓	Low Q1 result - Qt (both FD & SD) may be less than Actual. High Q2 & Low Q3 result - possibly an extended Q2 (FD) stage.
WE1202	12.19	11.79	-0.40	-3%		✓		✓					Low Q1 result - Qt (both FD & SD) may be less than Actual.
WE1203	13.93	13.61	-0.32	-2%		✓		✓					Low Q1 result - Qt (both FD & SD) may be less than Actual.
WE1199	14.24	15.26	1.02	7%		✓	✓		✓			✓	Low Q1 result - Qt (both FD & SD) may be less than Actual. High Q2 & Low Q3 result - possibly an extended Q2 (FD) stage.

Table 6.5: Assessment of gas emission data listing samples considered to be invalid

Sample Reference	Measured Gas Content				Slow Desorption Test		Fast Desorption Test						Comments Observations
					Gas Loss		Possible Errors						
	Fast Desorb.	Slow Desorb.	Diff. (m^3/t)	Diff. (%)	(System Leakage)		Q1 Value		Q2 Value		Q3 Value		
					Yes	No	High	Low	High	Low	High	Low	
WE1177	5.12	1.76	-3.36	-66%	✓			✓	✓			✓	Significant gas loss during SD testing - Qt (SD) << Qt (FD). Low Q1 result - Qt (both FD & SD) may be less than Actual. High Q2 result is balanced by Low Q3 result.
WE1186	7.97	1.94	-6.03	-76%	✓			✓					Significant gas loss during SD testing - Qt (SD) << Qt (FD). Low Q1 result - Qt (both FD & SD) may be less than Actual.
WE1185	10.55	2.58	-7.97	-76%	✓			✓	✓			✓	Significant gas loss during SD testing - Qt (SD) << Qt (FD). Low Q1 result - Qt (both FD & SD) may be less than Actual. High Q2 result is balanced by Low Q3 result.
WE1193	5.42	3.10	-2.32	-43%	✓								Gas loss during SD testing - Qt (SD) < Qt (FD).
WE1176	10.83	3.61	-7.22	-67%	✓		✓		✓			✓	Significant gas loss during SD testing - Qt (SD) << Qt (FD). High Q1 result - Qt (both FD & SD) may be greater than Actual. High Q2 result is balanced by Low Q3 result.
WE1208	6.19	3.63	-2.56	-41%	✓								Gas loss during SD testing - Qt (SD) < Qt (FD).
WE1205	7.12	4.15	-2.97	-42%	✓			✓					Gas loss during SD testing - Qt (SD) < Qt (FD). Low Q1 result - Qt (both FD & SD) may be less than Actual.
WE1225	8.23	4.21	-4.02	-49%	✓					✓			Significant gas loss during SD testing - Qt (SD) << Qt (FD). Low Q2 result - Qt (FD) understated (Δ masked by SD leakage).
WE1195	9.44	4.57	-4.87	-52%	✓		✓			✓		✓	Significant gas loss during SD testing - Qt (SD) << Qt (FD). High Q1 result - Qt (both FD & SD) may be greater than Actual. Low Q2 & Q3 result - Qt (FD) 'Actual' likely higher than reported.
WE1308	12.54	5.21	-7.33	-58%	✓		✓					✓	Significant gas loss during SD testing - Qt (SD) << Qt (FD). High Q1 result - Qt (both FD & SD) may be greater than Actual. Low Q2 & Q3 result - Qt (FD) 'Actual' likely higher than reported.
WE1209	13.84	5.26	-8.58	-62%	✓			✓					Significant gas loss during SD testing - Qt (SD) << Qt (FD). Low Q1 result - Qt (both FD & SD) may be less than Actual.
WE1206	4.00	6.11	2.11	53%		✓		✓		✓			Low Q1 result - Qt (both FD & SD) may be less than Actual. Low Q2 result - Qt (FD) less than Qt (SD).
WE1173	9.47	7.06	-2.41	-25%		✓			✓			✓	High Q2 result - Qt (FD) greater than Qt (SD).
WE1191	13.91	8.56	-5.35	-38%	possible				✓			✓	Possibility of some leakage during SD testing - Qt (SD) < Qt (FD). High Q2 result - Qt (FD) greater than Qt (SD).
WE1284	6.66	9.61	2.95	44%		✓				✓			Low Q2 result - Qt (FD) less than Qt (SD).
WE1309	8.86	10.55	1.69	19%		✓	✓			✓			High Q1 result - Qt (both FD & SD) may be greater than Actual. Low Q2 result - Qt (FD) less than Qt (SD).
WE1210	14.12	15.84	1.72	12%		✓	✓		✓			✓	Low Q1 result - Qt (both FD & SD) may be less than Actual. Impact of Low Q3 outweighs High Q2 result - Qt (FD) < Qt (SD).

6.3.2 Q_1 Gas Content Component

The volume of gas lost during core recovery, Q_1, was determined from initial desorption measurement of the primary core, as part of the fast desorption testing. In this analysis the Q_1 gas content value, applicable to the slow desorption test samples, was assumed to equal the value determined from fast desorption testing.

Figure 6.48 shows the relationship between Q_1 and Q_M which indicates increasing lost gas volume corresponding to an increase in Q_M. As discussed previously, gas composition was found to have little impact on the volume of gas lost during core sample recovery, also demonstrated in Figure 6.49.

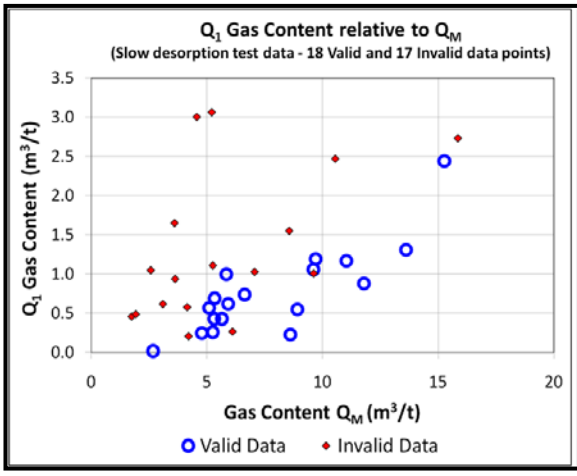

Figure 6.48: Q_1 gas content relative to Q_M

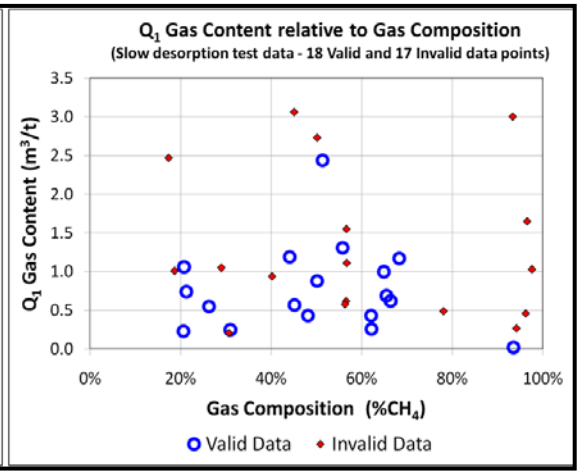

Figure 6.49: Q_1 gas content relative to gas composition

6.3.3 Q_2 Gas Content Component

A strong relationship was identified between Q_2 and Q_M, as shown in Figure 6.50. Figure 6.51 shows gas composition had little impact on the volume of gas liberated during Q_2 desorption testing.

Figure 6.52 indicates an increase in Q_2:Q_M ratio in response to increasing Q_M, whereas no relationship was evident between the Q_2:Q_M ratio and gas composition, as indicated in Figure 6.53.

Further analysis was conducted to assess the impact of gas composition on the rate of gas emission during slow desorption testing. The cumulative desorbed gas volume from each sample during slow desorption testing was plotted for samples having gas composition less than and greater than 50% CH_4, shown in Figure 6.54 and Figure 6.55 respectively. Comparing the emission curves of samples having similar total desorbed gas volumes, the results indicate gas composition had little impact on gas desorption characteristics.

The impact of desorption time was also considered. Figure 6.56 shows Q_2 plotted relative to total desorption time. No relationship was indicated between the two variables which, given the profile of gas emission curves, suggests that little benefit was achieved from continuing desorption for extended periods due to the relatively small volume of additional gas liberated.

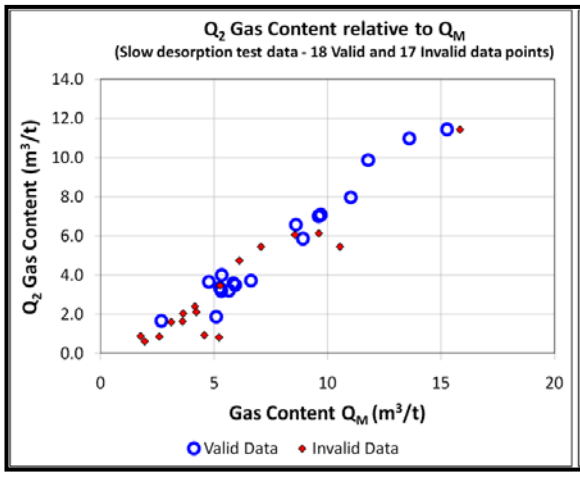

Figure 6.50: Q_2 gas content relative to Q_M

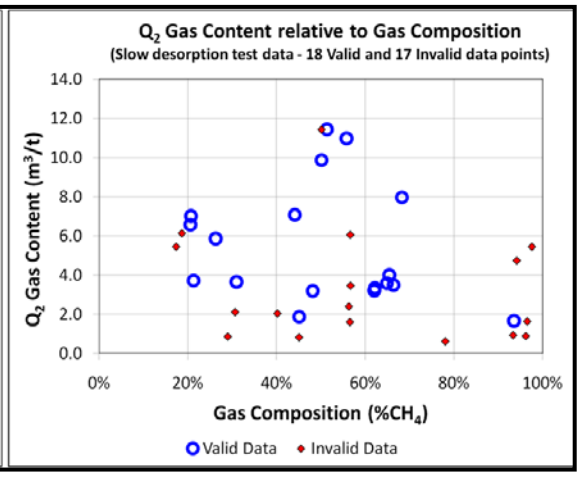

Figure 6.51: Q_2 gas content relative to gas composition

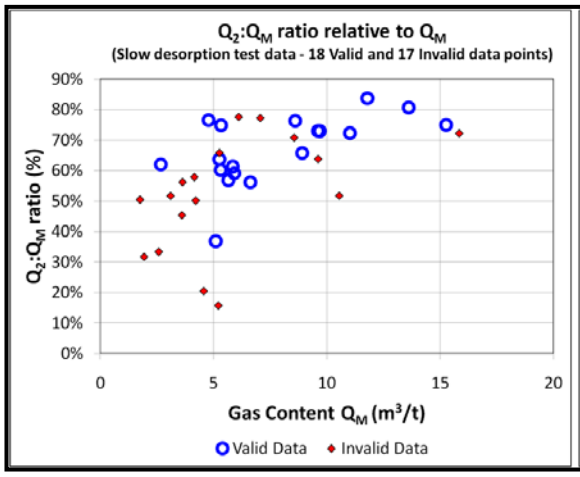

Figure 6.52: Q_2:Q_M ratio relative to Q_M

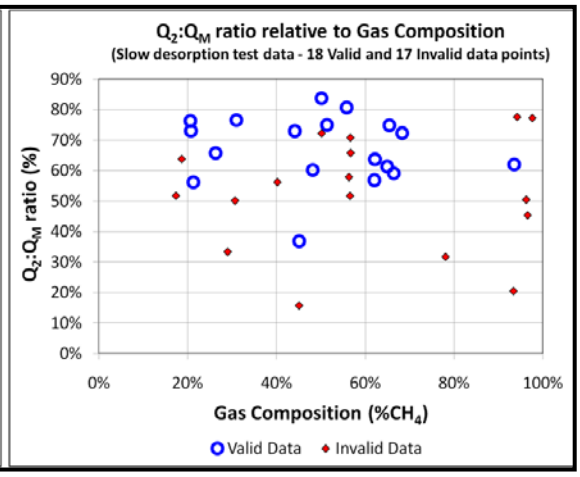

Figure 6.53: Q_2:Q_M ratio relative to gas composition

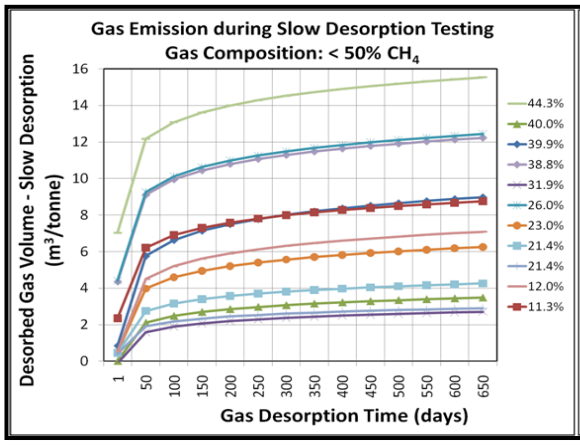

Figure 6.54: Gas emission from valid samples having CH_4 concentration less than 50%

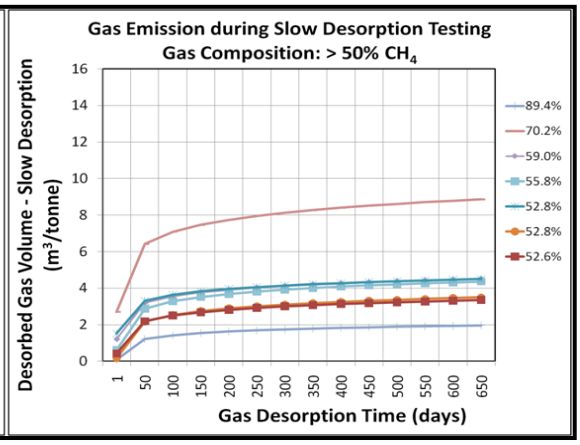

Figure 6.55: Gas emission from valid samples having CH_4 concentration greater than 50%

The number of days taken for coal samples to desorb 65% of Q_M ($65\%Q_{M(d)}$) was also investigated. Time to desorb $65\%Q_{M(d)}$ was considered a more appropriate indicator of the rate of gas emission and therefore provide superior insight into the nature of gas emission from the various coal samples analysed. Figure 6.57 shows the relationship between Q_2 and the number of days to desorb $65\%Q_{M(d)}$. The results indicate samples of increased Q_M desorb gas at a faster rate, with a greater percentage of Q_M liberated during Q_2 testing.

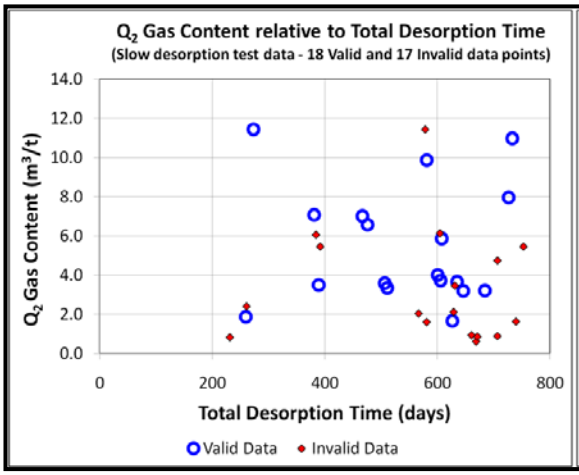

Figure 6.56: Q_2 gas content relative to Q_M

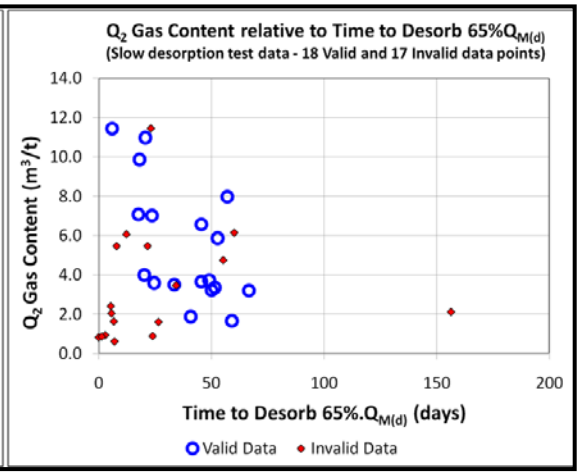

Figure 6.57: Q_2 gas content relative to time to desorb $65\%Q_{M(d)}$

The volume of gas liberated during slow desorption testing was also analysed relative to the results of coal petrographic testing of 34 coal samples which were examined after the slow desorption testing (Hutton, 2008). Figure 6.58 and Figure 6.59 show the value of Q_2 and Q_2:Q_M ratio, determined from slow desorption testing, plotted relative to the vitrinite content, porosity and mineral matter content of each coal sample. The data give some indication of decreasing desorbed gas content from samples of increased vitrinite content however the relationship was not strong. Further investigation suggested the weak relationship between Q_2 and vitrinite content was coincidental and the result of lower Q_M from samples with increased vitrinite content. Porosity and mineral matter content were found to have no apparent impact on desorbed gas content. Therefore it was concluded that coal petrography had little impact on the desorbed gas content, particularly given the broad span of petrographic analysis values for samples having similar desorbed gas content of 4.0 m^3/t.

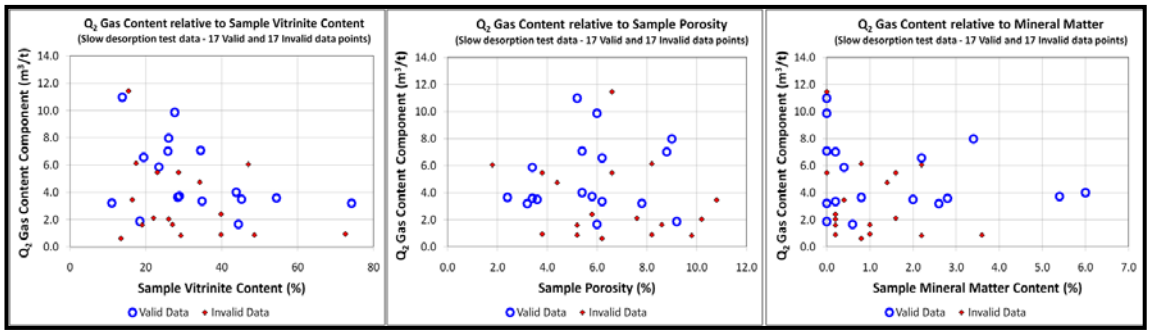

Figure 6.58: Q_2 gas content relative to vitrinite content, porosity and mineral matter content

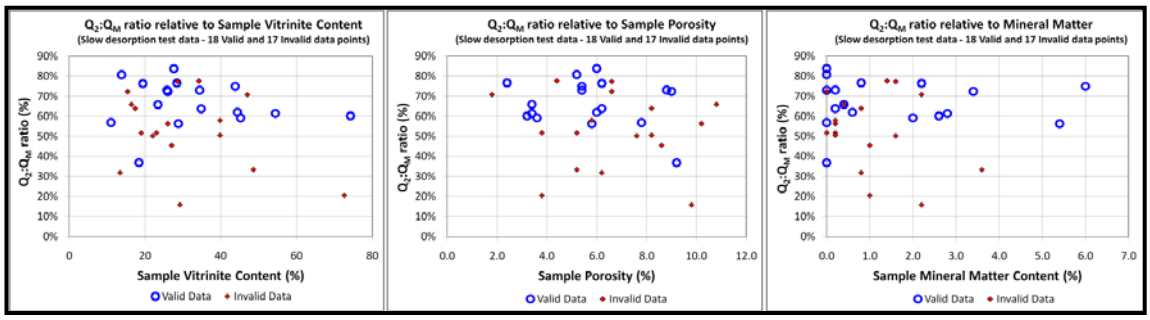

Figure 6.59: Q_2:Q_M ratio relative to vitrinite content, porosity and mineral matter content

Further analysis was conducted to assess the impact of vitrinite maceral composition on the rate of gas emission during slow desorption testing. The logarithmic gas desorption curve representing each sample was plotted for samples having vitrinite content less than and greater than 30%, shown in Figure 6.60 and Figure 6.61 respectively. Comparing the emission curves of samples having similar total desorbed gas volumes it can be seen that vitrinite content has little impact on gas desorption characteristics.

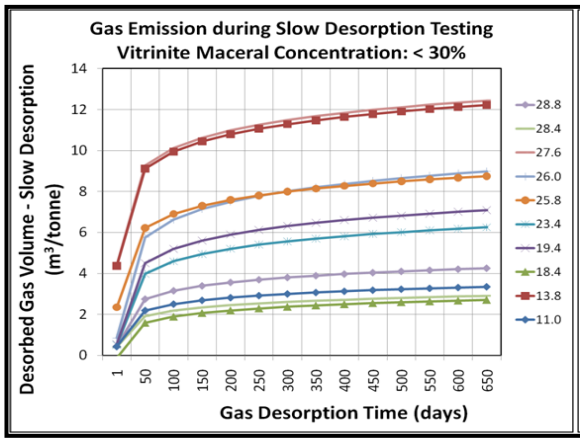

Figure 6.60: Gas emission from valid samples having vitrinite content less than 30%

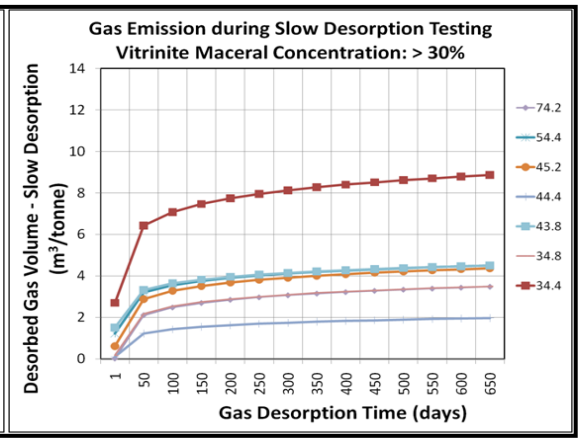

Figure 6.61: Gas emission from valid samples having vitrinite content greater than 30%

6.3.4 Q_3 Gas Content Component

Following completion of slow desorption testing a sub-sample of the coal core from each gas desorption canister was collected and sent to the BHP Billiton Gas Laboratory to determine the residual gas content. Duplicate analysis was conducted for each sample and the average of the two gas content results accepted as the residual gas content of the complete coal sample.

Figure 6.62 shows the relationship between residual gas content (Q_3) and Q_M. The data suggest a possible increase in Q_3 from samples having greater Q_M, although the relationship was not strong. Figure 6.63 shows the relationship between Q_3 and gas composition which indicate increased Q_3 from samples with increased concentration of CO_2.

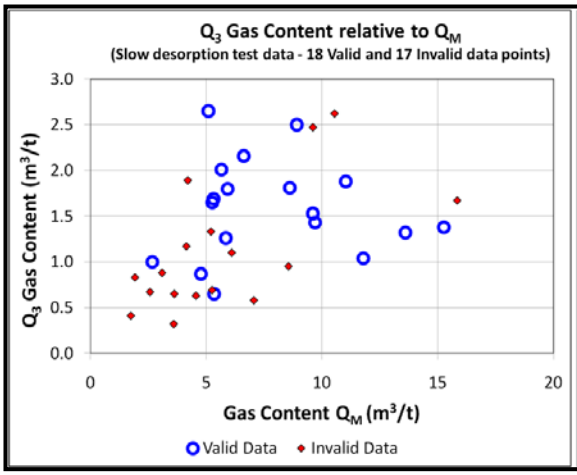

Figure 6.62: Q_3 gas content relative to Q_M

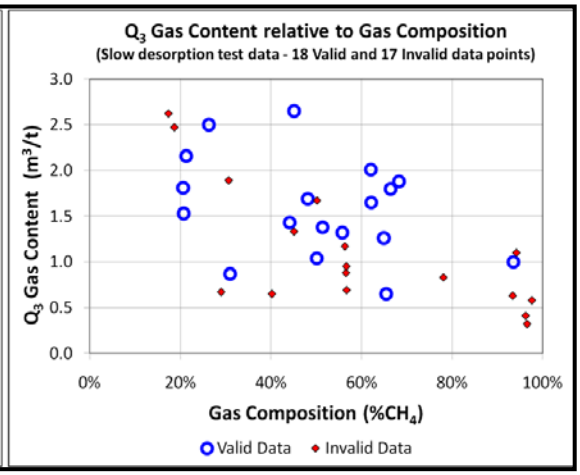

Figure 6.63: Q_3 gas content relative to gas composition

Figure 6.64 indicates a decrease in Q_3:Q_M ratio in response to increasing Q_M, whereas no relationship was evident between the Q_3:Q_M ratio and gas composition, as shown in Figure 6.65.

Figure 6.66 shows Q_3 plotted relative to total desorption time. The data suggest extending the total desorption time beyond 200 days has little impact on Q_3. Figure 6.67 shows the relationship between Q_3 and 65%$Q_{M(d)}$. The data indicate increased residual gas content from samples that desorb gas at a slow rate, i.e. increased time to desorb 65% of Q_M.

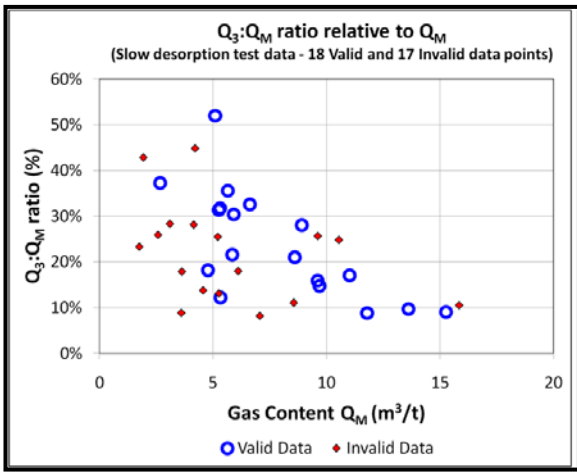

Figure 6.64: Q_3:Q_M ratio relative to Q_M

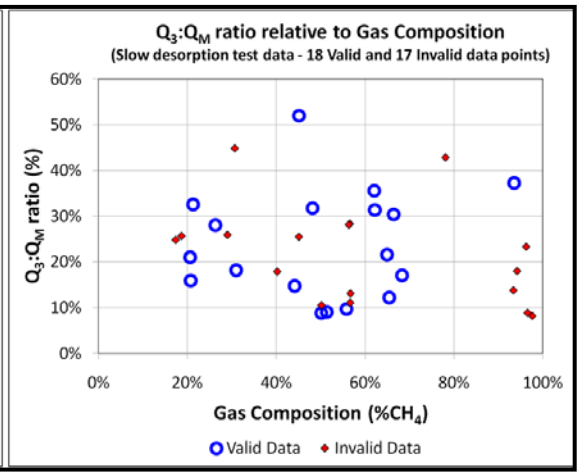

Figure 6.65: Q_3:Q_M ratio relative to gas composition

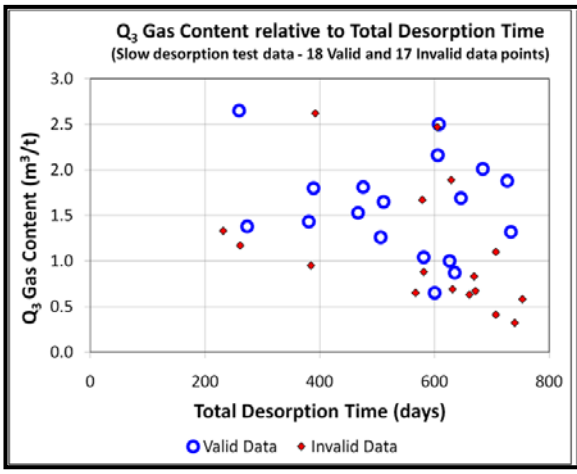

Figure 6.66: Q_3 gas content relative to total desorption time

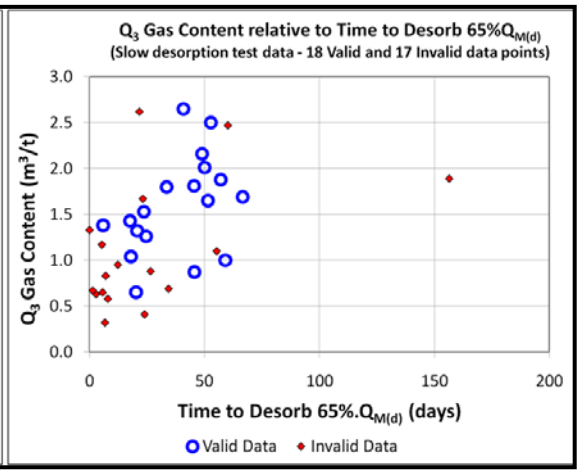

Figure 6.67: Q_3 gas content relative to time to desorb 65%$Q_{M(d)}$

The Q_3 was also analysed relative to the results of coal petrographic testing conducted on 34 coal samples following slow desorption testing (Hutton, 2008). Figure 6.68 and Figure 6.69 show the value of Q_3 and Q_3:Q_M ratio, determined from slow desorption testing, plotted relative to measured vitrinite content, porosity and mineral matter content for each coal sample. A weak relationship may be inferred from the distribution of Q_3 values relative to vitrinite content. The distribution of Q_3 relative to porosity and mineral matter content determined from each sample indicates no apparent impact on residual gas content. Therefore it was concluded that coal petrography has little impact on the Q_3 residual gas content.

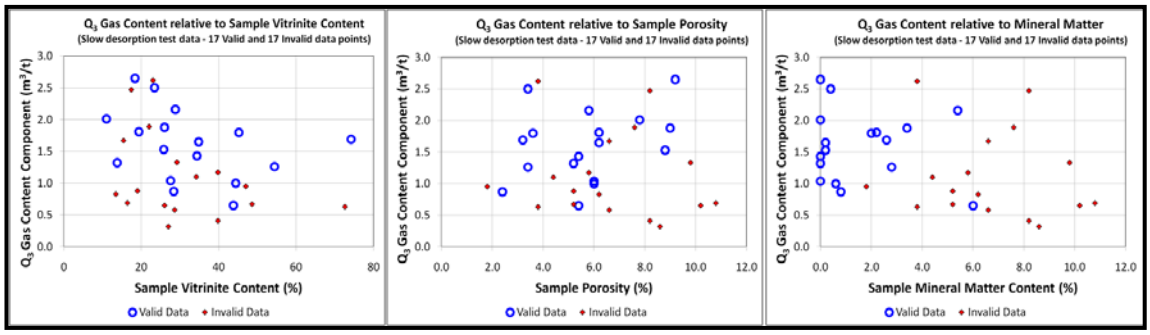

Figure 6.68: Q_3 gas content relative to vitrinite content, porosity and mineral matter content

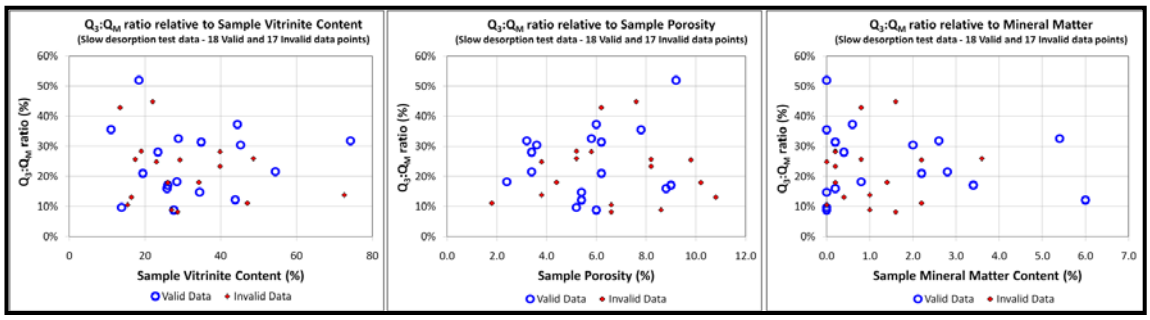

Figure 6.69: Q_3:Q_M ratio relative to vitrinite content, porosity and mineral matter content

From this analysis it was found that coal samples with low Q_M required increased desorption time and therefore had a slower desorption rate. The Q_3 component percentage of Q_M (Q_3:Q_M ratio) was shown to be greater from samples with low Q_M compared to samples with higher Q_M. There was some indication of reduced Q_3 from coal samples having increased CH_4 concentration and increased vitrinite content, however the correlation was low and the relationship considered weak.

6.3.5 Relationship between Gas Content Components

The relationship between each of the three gas content components determined from slow desorption testing was analysed relative to Q_M and gas composition (CH_4/(CH_4+CO_2)). The results from slow desorption testing on the 18 valid coal samples were analysed and compared to the results from fast desorption testing on the primary core sample.

6.3.5.1 Gas Content

Figure 6.70 shows the values of each gas content component, Q_1, Q_2 and Q_3, determined from slow desorption testing, plotted relative to Q_M for each of the 18 valid slow desorption test samples. Figure 6.71 shows the gas content component values, plotted

relative to Q_M, determined from fast desorption testing for the same 18 samples. It can be seen that Q_2 represents the majority of gas liberated during slow desorption testing whereas in fast desorption testing the majority of gas is liberated during Q_3 testing.

The results of slow desorption testing indicate that in response to increasing Q_M there was an increase in both the volume and component percentage of gas lost during core recovery and desorbed during Q_2 testing. The residual gas content varied between 0.5 and 2.5 m^3/t. The Q_3 component percentage of Q_M (Q_3:Q_M ratio) decreased in response to increasing Q_M and was greatest from samples with Q_M less than 4.0 m^3/t, with little gas lost during core recovery.

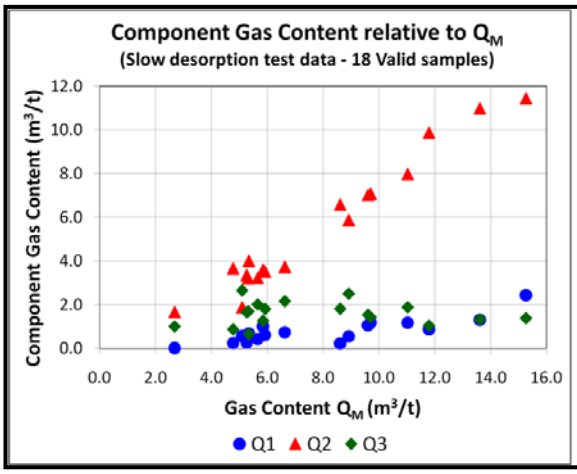

Figure 6.70: Slow desorption gas content component values relative to Q_M

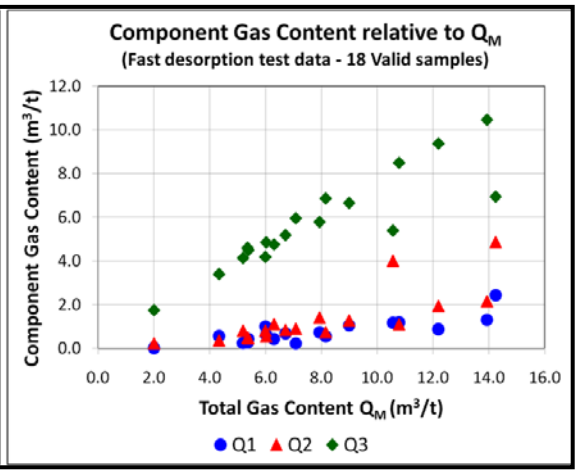

Figure 6.71: Fast desorption gas content component values relative to Q_M

A similar trend was identified from fast desorption testing however there was a distinct difference in the component percentage of both Q_2 and Q_3 relative to Q_M, with the Q_3 component representing a much greater portion of Q_M due to the significantly shorter period afforded for Q_2 desorption. Figure 6.72 and Figure 6.73 show the average gas content component percentage of Q_M within four Q_M groups, 0-4 m^3/t, 4-8 m^3/t, 8-12 m^3/t and 12-16 m^3/t, determined from slow and fast desorption testing respectively.

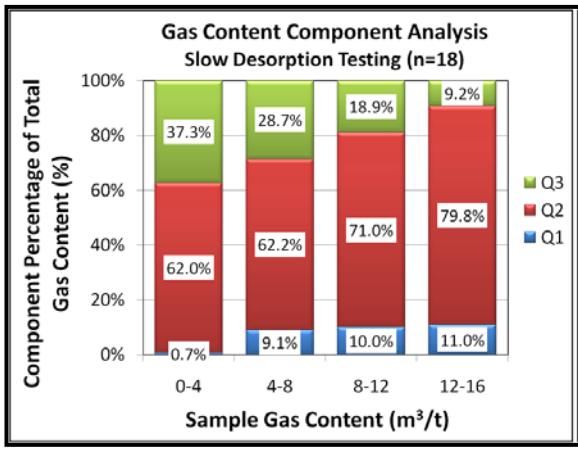

Figure 6.72: Average slow desorption Q_M component percentage assessed relative to Q_M

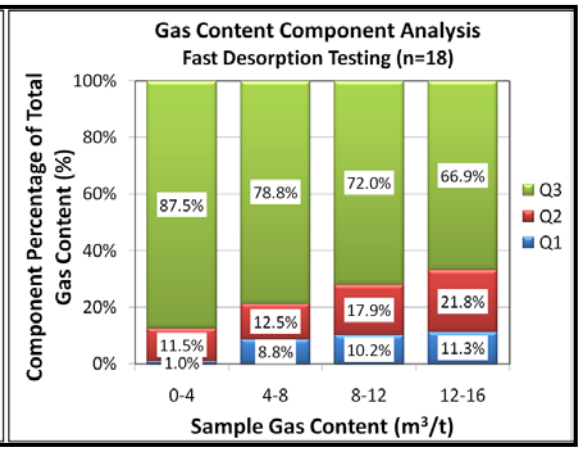

Figure 6.73: Average fast desorption Q_M component percentage assessed relative to Q_M

6.3.5.2 Gas Composition

The impact of gas composition on the percentage of Q_M within the three gas content components was also assessed. The results of the 18 valid samples were divided into five gas composition groups based on CH_4 concentration ($CH_4/(CH_4+CO_2)$), 0-20%, 20-40%, 40-60%, 60-80% and 80-100%. Figure 6.74 shows average Q_M and component percentage of Q_M determined from slow desorption testing for the samples within each gas composition group. Although average Q_M varies between each gas composition group, gas composition does not appear to have a significant impact on the relative percentage of Q_M within each gas content component.

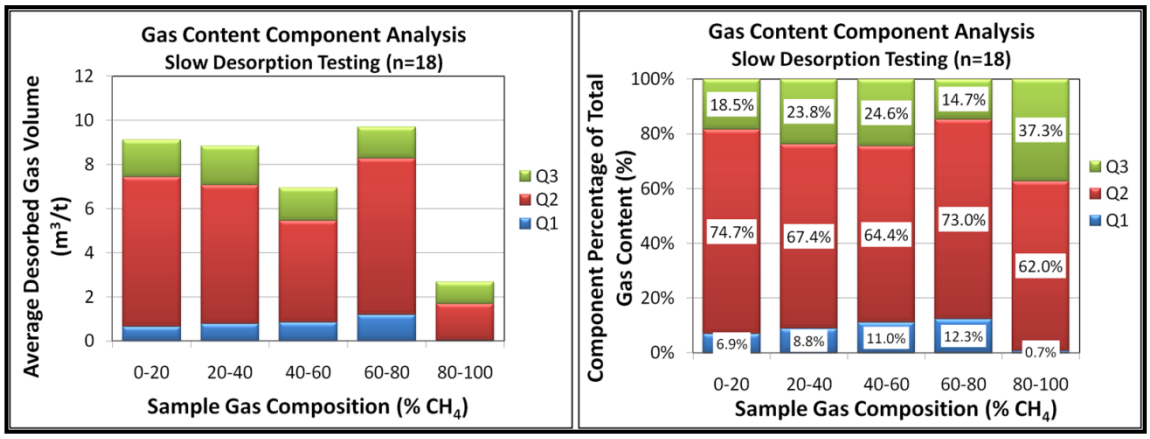

Figure 6.74: Average slow desorption Q_M and gas content component percentage assessed relative to gas composition

The assessment of the impact of gas composition on gas content component emission also compared results obtained from fast desorption testing on the same 18 coal samples, shown in Figure 6.75. Similar to the results from slow desorption testing, the

data indicate gas composition had little impact on the relative percentage of Q_M within each gas content component.

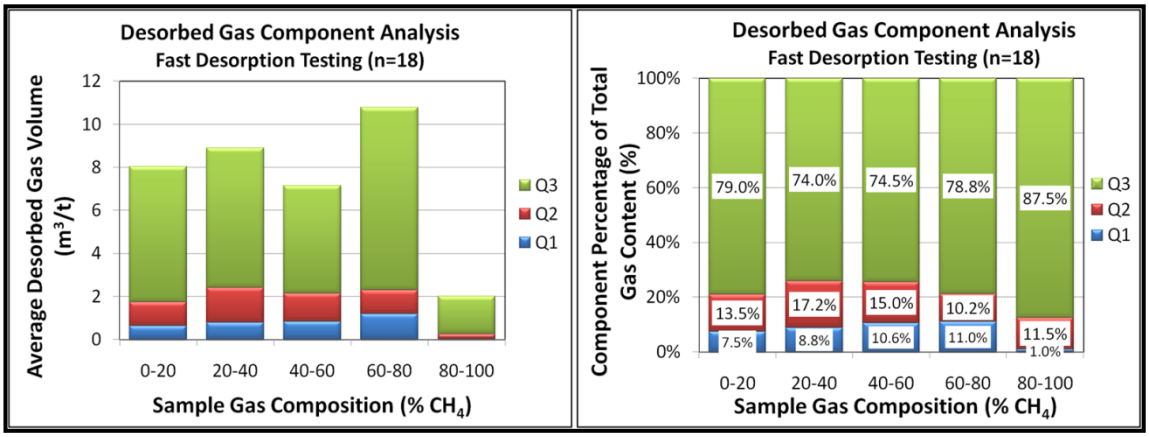

Figure 6.75: Average fast desorption Q_M and gas content component percentage assessed relative to gas composition

6.3.6 Analysis of Gas Composition during Desorption

Representative samples of desorbed gas collected from each coal sample during slow desorption were tested and the results of gas composition analysis compiled and analysed to identify changes in composition. Changes in gas composition during desorption may provide an insight into the rate of emission of various seam gases.

Gas samples were also collected from producing inseam gas drainage boreholes and analysed using a gas chromatograph to determine composition. The gas composition data from the inseam boreholes was also compiled and analysed to identify changes in composition.

6.3.6.1 Gas Composition during Slow Desorption Testing

From mixed gas isotherm studies by Lama *et al.* (1984), Williams (1991), Mavor *et al.* (1992) and Crosdale (1998), CH_4 was reported to be preferentially liberated from *in situ* coal in response to pressure reduction due to coal's affinity for CO_2, with CO_2 being retained until later in the desorption test period.

In contrast, Williams (1991), Lama (1995a) and Cui and Busten (2006) suggest gas emission from coal core samples is governed more by diffusion than by sorption affinity, therefore in mixed gas conditions CO_2 is liberated more rapidly than CH_4.

Gas composition was monitored during the course of slow desorption testing of 35 coal samples collected from WCC. In addition to recording changes in concentration of CH_4, CO_2, N_2, C_2H_6 and air, the $CH_4/(CH_4+CO_2)$ ratio was also determined. Figure 6.76 shows the result from two samples, WE1206 and WE1246. Details of the change in gas composition and the emission rate of each gas during slow desorption testing from all 35 coal samples are presented in Appendix 6.12. In the majority of cases excess N_2 was detected during early stage desorption. The presence of the excess N_2 may be an indication of oxidation of the coal sample within the canister however specific investigation of the source of the N_2 was not undertaken.

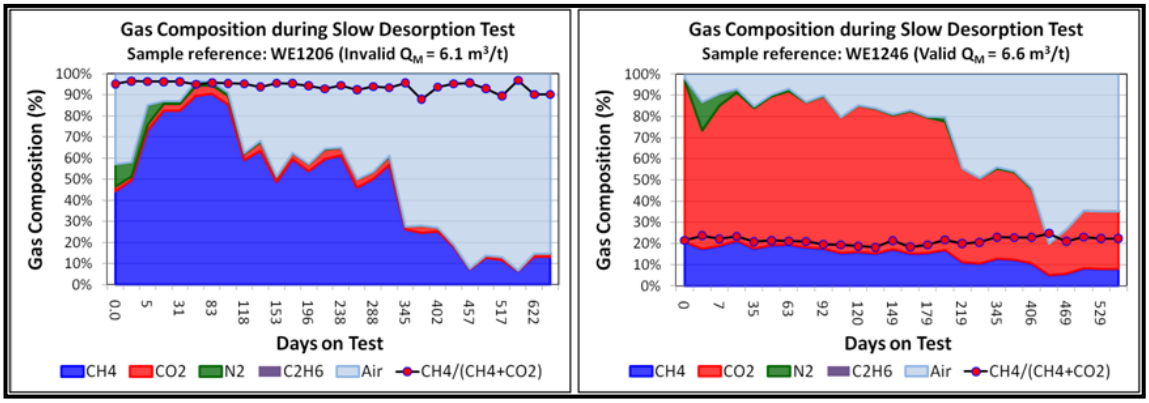

Figure 6.76: Gas composition during slow desorption testing – results of samples WE1206 and WE1246

Analysis of gas emission from coal core samples during slow desorption testing indicate inconsistent gas emission characteristics, particularly the $CH_4/(CH_4+CO_2)$ ratio which in many cases varied significantly during desorption. Of the 35 samples analysed, 26 demonstrated progressive CH_4 enrichment to varying degrees, while the $CH_4/(CH_4+CO_2)$ ratio remained relatively stable in 3 cases and decreased in 6 cases. Further analysis of the data related to each coal sample was unable to explain the variability in gas composition during desorption.

Figure 6.77 shows the variability in desorbed gas composition during slow desorption testing, indicating average, maximum, minimum and median $CH_4/(CH_4+CO_2)$ ratio for each of the 35 coal samples tested. The results highlight increased variability in gas composition from samples with mixed seam gas composition, located in the mid-panel region, compared to the samples in the CH_4 rich outbye zone and the CO_2 rich inbye zone.

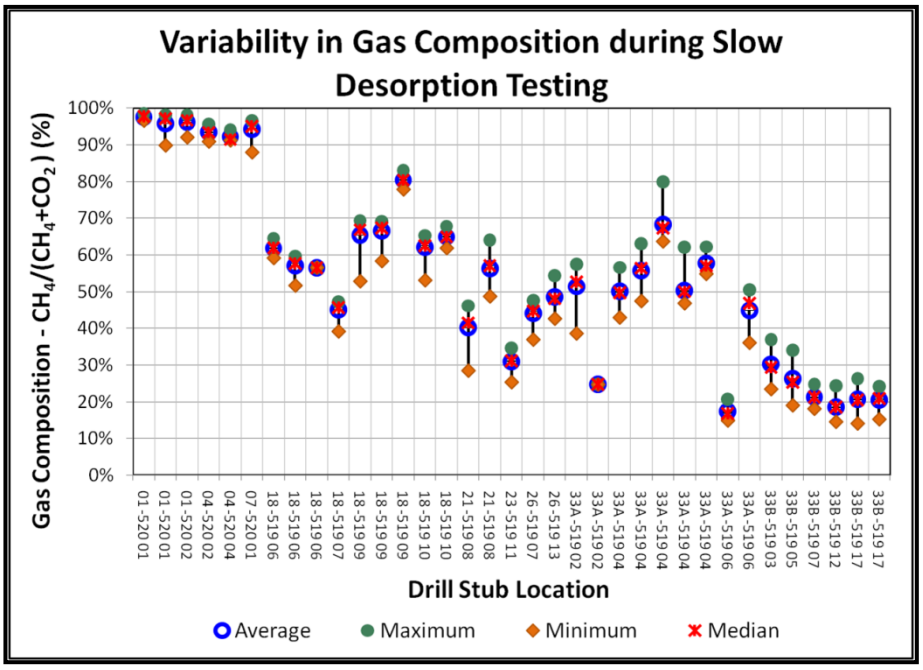

Figure 6.77: Variability in gas composition during slow desorption testing

Significant changes in gas composition were evident in the results from seven samples during late stage desorption, within several readings prior to completing desorption testing. In six cases a large drop in CH_4 concentration occurred and in one case the CH_4 concentration increased. Figure 6.78 shows two examples of rapid change in $CH_4/(CH_4+CO_2)$ ratio during late stage desorption. The rapid change in composition was considered to be an error due to the adverse impact of high air content measurement accuracy and introduced error into the air-free and normalisation calculations.

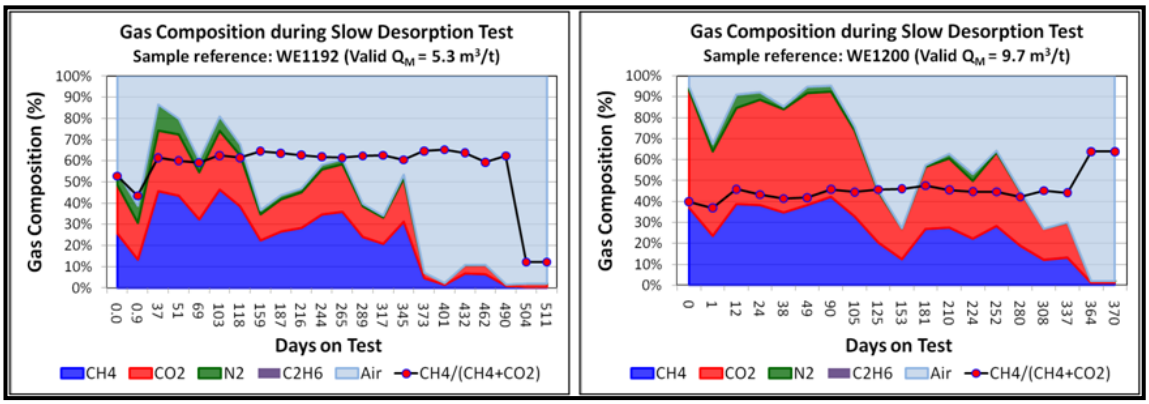

Figure 6.78: Changes in gas composition during late stage desorption

Due to the expectation of low gas content and the potentially adverse impact on measurement accuracy, the composition of the gas liberated from the West Cliff coal samples during Q_3 residual gas content testing was not determined. Crosdale (1998)

reported reduced CH_4 concentration of gas liberated from coal during residual gas content testing following the completion of slow desorption testing.

Crosdale (1998) conducted slow desorption testing on 10 coal samples collected from Dartbrook and South Bulli Collieries. The gas composition during desorption from the 10 samples, presented in Appendix 6.13, was inconsistent as the CH_4 concentration increased in some cases and decreased in others. Crosdale (1998) indicated the decrease in CH_4 concentration was expected based on the results of isotherm studies and the preferential release of CH_4 from coal at high pressure whereas the cause of the increase in CH_4 concentration could not be adequately explained.

Analysis of gas composition during slow desorption has shown a steady increase in CH_4 concentration in 26 of the 35 samples tested. This behaviour was consistent with the results of Lama (1988b), Lama (1995a) and Cui and Busten (2006) who suggest gas emission from these samples was governed primarily by diffusion rather than sorption affinity. In contrast, the CH_4 concentration was found to decrease in six samples, consistent with the view of Mavor *et al.*, (1992) and Crosdale (1998), who suggest CH_4 will be preferentially liberated from coal in response to reducing pressure, with CO_2 being retained until the pressure has been reduced to below 0.7 MPa.

The composition of gas liberated from core samples during the fast desorption test was compared to the results collected during slow desorption testing. The results from each of the 18 valid and 17 invalid samples, presented in Figure 6.79, show the CH_4 concentration from fast desorption testing was, in the majority of cases, less than the values determined from slow desorption testing. The results are consistent with the findings of Lama (1995a) and Cui and Busten (2006), suggesting the early liberation of CO_2 is followed by progressive CH_4 enrichment during desorption. In the majority of the 35 cases the average and median CH_4 concentration, determined during slow desorption, was greater than the fast desorption result.

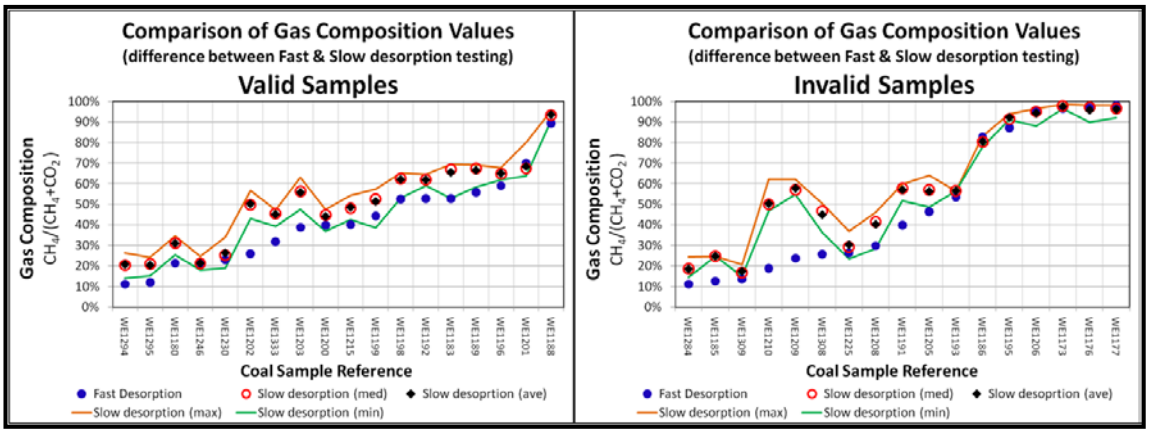

Figure 6.79: Comparison of gas composition values from fast and slow desorption testing

The Q_M values, from fast and slow desorption testing, were considered to determine whether the differences in Q_M correlated with differences in gas composition. Figure 6.80 shows Q_M results from fast and slow desorption testing. The results from the valid samples are similar whereas large differences exist between the results of the invalid samples. Given the similar Q_M of the valid samples it was concluded that the difference in gas composition was not due to loss of gas during testing.

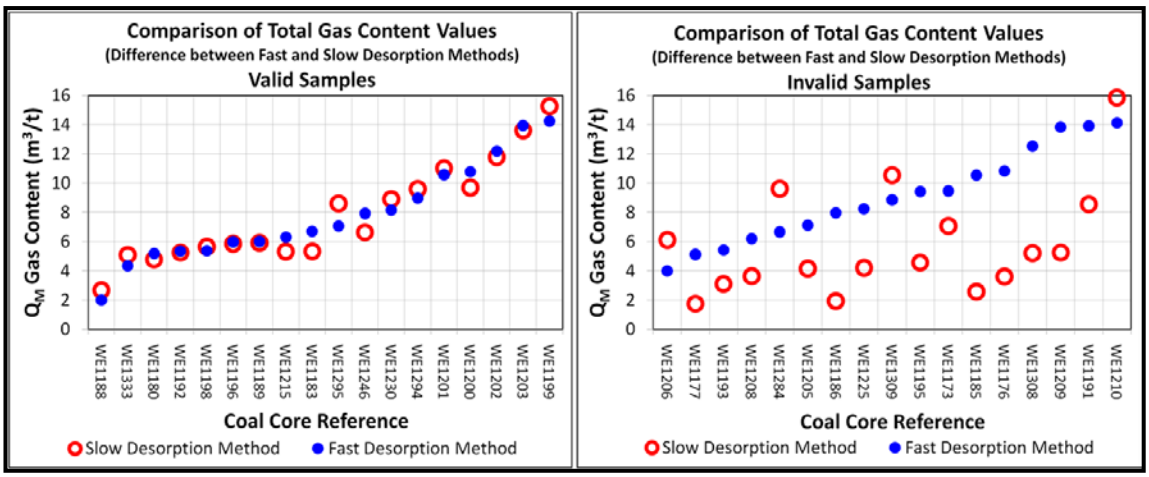

Figure 6.80: Comparison of Q_M values from fast and slow desorption testing

6.3.6.2 Analysis of Gas Composition during Inseam Borehole Gas Production

Cui and Busten (2006) suggest coal seam gas production involves two stages controlled by different mechanisms, diffusion and desorption. During initial gas production, diffusion is the dominant mechanism whereby gas diffuses from the coal matrix to the borehole. Following the initial production phase, for the balance of the borehole's production life, gas production is primarily controlled by equilibrium desorption from the coal. In a coal seam with mixed CH_4 and CO_2 seam gas, the increased diffusivity of

CO_2 will result in the produced seam gas being relatively CO_2 rich during initial production, with progressive CH_4 enrichment toward the transition zone where the dominant gas production mechanism changes from diffusion to desorption. Subsequent to the transition from diffusion to desorption the produced gas will be relatively CH_4 rich, followed by progressive CO_2 enrichment (Cui and Busten, 2006). Figure 6.81 illustrates the mechanisms that control coal seam gas production and the change in composition of gas produced from a mixed seam gas environment during inseam borehole gas production. Cui and Busten (2006) also suggest the dominance of either mechanism in coal seam gas production is controlled by the coal fabric which determines permeability to gas and water flow as well as the path length for gas diffusion through the coal matrix.

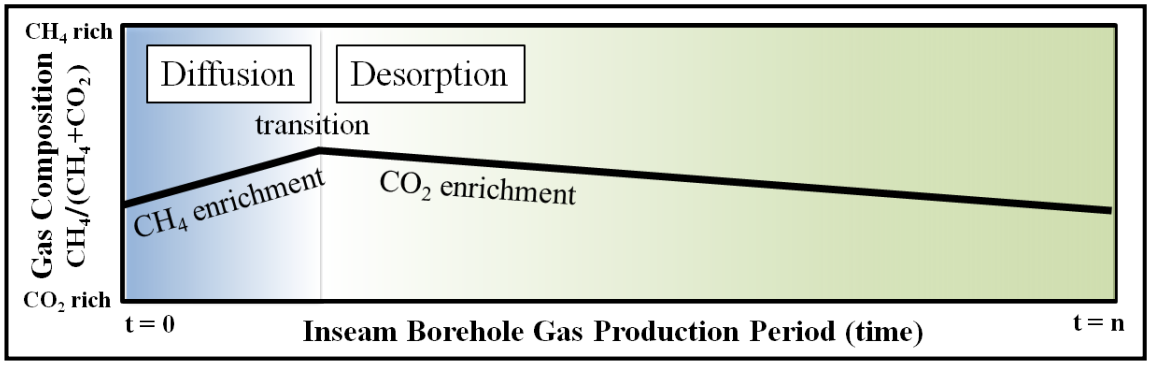

Figure 6.81: Gas production mechanisms and change in produced gas composition during inseam borehole gas production (after Cui and Busten, 2006)

Gas desorption measurements during mixed gas isotherm studies conducted by Mavor *et al.* (1992) and Harpalani and Pariti in 1993 and Greaves *et al.* in 1993, cited in Crosdale (1998), suggest coal's affinity for CO_2 results in preferential liberation of CH_4 in response to reducing pressure, with coal retaining CO_2 until the pressure was less than 0.7 MPa. Mavor *et al.* (1992) suggest the significance of this behaviour is that boreholes producing predominantly CH_4 during the early periods of operation may produce an increased concentration of CO_2 as the reservoir becomes depleted.

Samples of produced gas were periodically collected from UIS boreholes drilled from 17 separate drill stubs located along 519 and 520 panel at WCC. The gas samples were analysed using a gas chromatograph to determine the relative concentrations of the gases, CH_4, CO_2, N_2, O_2, C_2H_6, CO and C_2H_4. In addition to the individual component gases, air dilution and the $CH_4/(CH_4+CO_2)$ ratio was calculated.

Figure 6.82 show the change in composition of the gas produced from the boreholes drilled from each of the 17 drill stubs. The results highlight the variable composition of gas produced from the mid panel zone, between 18 and 26c/t, where the seam gas composition transitions from CH_4 rich at the start of the panel to CO_2 rich in the inbye areas. Details of the change in gas composition during production from individual boreholes drilled from 16 separate drill stubs, excluding 18c/t 520 panel due to limited data, are presented in Appendix 6.14. The results show little change in composition from the samples in CH_4 rich conditions, whereas the composition of produced gas from mixed gas areas did change during the life of the borehole, however the nature of the change was inconsistent. Many of the boreholes recorded a reduction in the CH_4 concentration with increasing time on drainage, which was consistent with the findings of Mavor *et al.* (1992) and Crosdale (1998), while the remaining boreholes demonstrated progressive CH_4 enrichment.

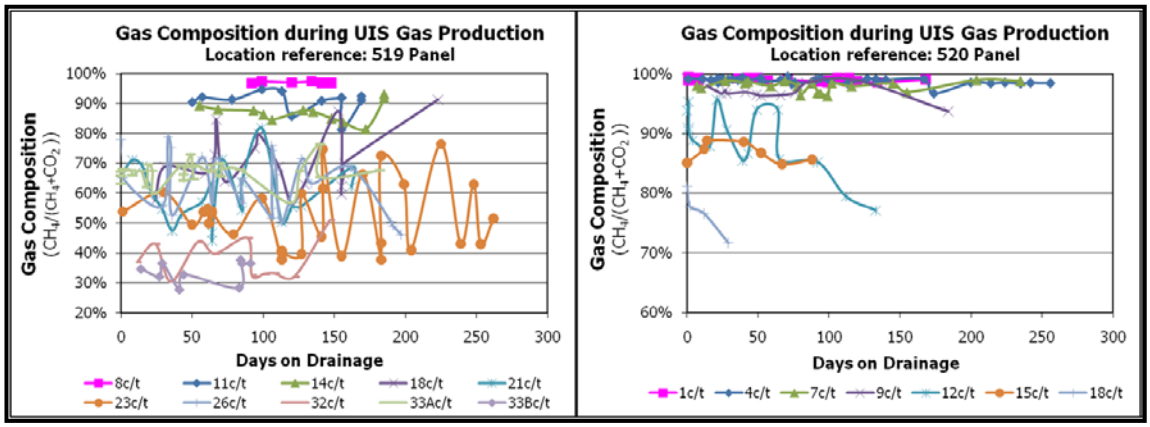

Figure 6.82: Composition of gas produced from UIS boreholes drilled along 519 and 520 panel

Where a minimum of five separate gas composition measurements were recorded from individual boreholes the results were consolidated and presented graphically to show the change in composition during gas production. Graphs were prepared for 12 separate boreholes, presented in Appendix 6.15. Minimal change in gas composition was recorded in gas produced from boreholes drilled into CH_4 rich coal. The composition of gas produced from inseam boreholes drilled into coal with seam gas comprised of a mixture of CH_4 and CO_2 exhibited increased variability with the measured $CH_4/(CH_4+CO_2)$ ratio increasing and decreasing during the life of the borehole. Figure 6.83 shows the gas composition during desorption from two boreholes, one (519-26-02)

shows reducing CH_4 while the other (519-33A-04) shows increasing CH_4 during production.

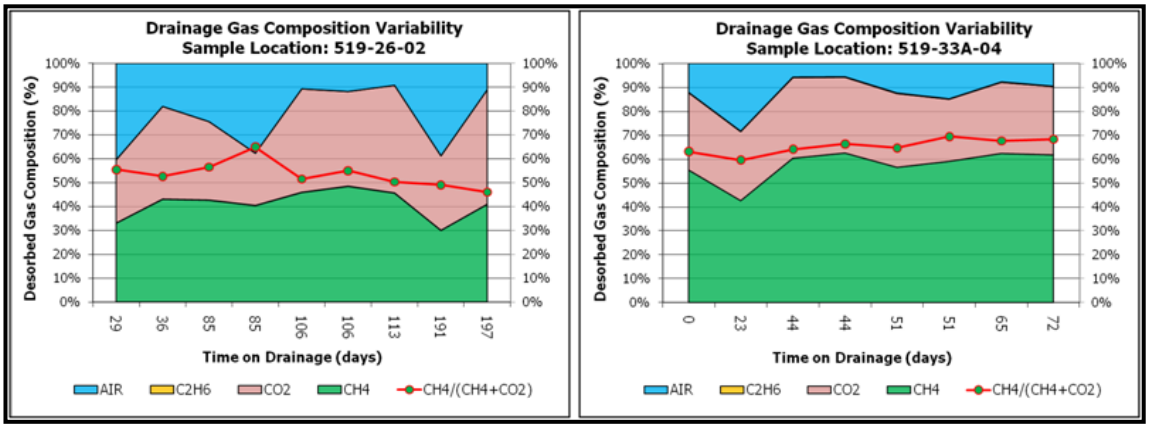

Figure 6.83: Composition of gas produced from individual UIS drainage boreholes

The composition of gas from inseam drainage boreholes was analysed relative to the gas composition measurements from core samples collected during UIS drilling and analysed using both the fast and slow desorption methods. The location of the UIS boreholes and various core samples used in the assessment of gas composition are shown in Figure 6.84.

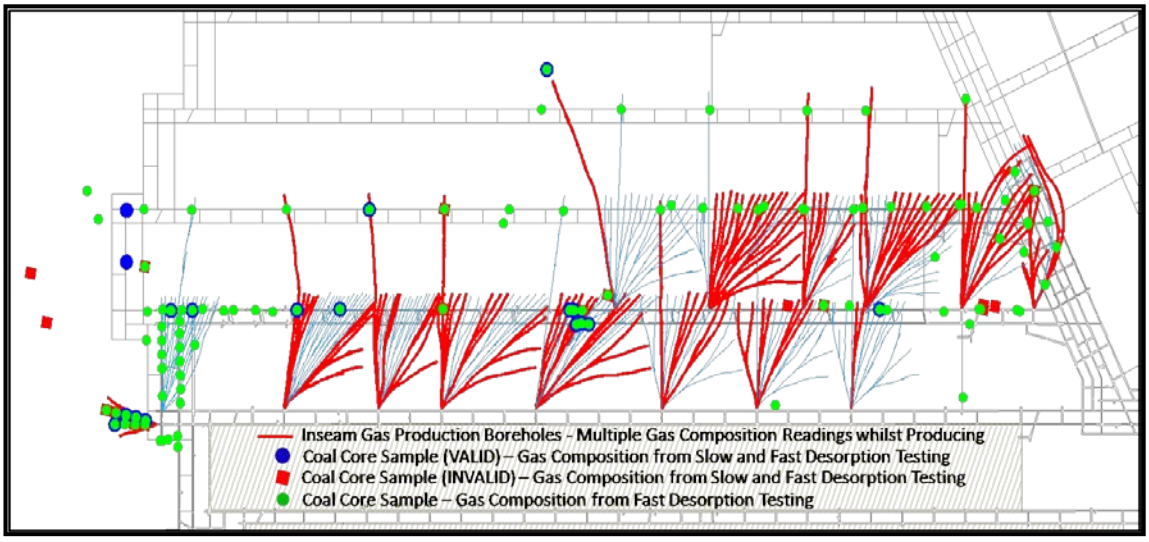

Figure 6.84: Location of UIS boreholes and core samples used to determine gas composition

The inseam borehole, 519-33A-04, was the only borehole from which multiple core samples were collected for slow desorption gas analysis. The five core samples, three valid (WE1201, WE1202, WE1203) and two invalid (WE1209 and WE1210), demonstrated CH_4 enrichment during desorption, consistent with the CH_4 enrichment

measured from borehole 519-33A-04. Each of the five core samples recorded a different gas composition. The $CH_4/(CH_4+CO_2)$ ratio measured from core WE1201 was marginally greater than the value recorded from the UIS borehole, while the $CH_4/(CH_4+CO_2)$ ratio recorded from the other four core samples was less than that of the borehole. This result suggests a large portion of the total gas produced from borehole 519-33A-04 may have originated from the coal seam adjacent to the location of core sample WE1201 and/or from zones along the length of the UIS borehole which intersect a particular coal ply from which the core sample was extracted.

Table 6.6 provides a summary of gas composition measurements from UIS boreholes and core samples collected from drill stubs along 519 and 520 panel. The results highlight changes in gas composition from core samples collected along the length of the boreholes. In all cases the average $CH_4/(CH_4+CO_2)$ ratio of gas produced from UIS boreholes was greater than from core samples recovered along, or adjacent to, the boreholes. This result suggests increased gas production from zones of increased $CH_4/(CH_4+CO_2)$ ratio along the length of the borehole, with comparatively higher degree of saturation. Increased gas production from discrete zones along the length of inseam drainage boreholes was previously recorded during in-hole incremental flow measurement by Gray (1982).

Table 6.6: Summary of gas composition (%CH_4) results recorded from different sample sources

Location	INSEAM BOREHOLE DESORBED GAS COMPOSITION				SLOW DESORPTION GAS COMPOSITION				FAST DESORPTION GAS COMPOSITION		INSEAM CORE SAMPLE GAS COMPOSITION			
	Average	Maximum	Minimum	Median	Average	Maximum	Minimum	Median	Average	Median	Average	Maximum	Minimum	Median
01-520	99%	99%	99%	99%	97%	98%	93%	97%	97%	97%	97%	98%	96%	97%
04-520	99%	100%	97%	99%	93%	95%	91%	92%	88%	88%	95%	99%	84%	98%
05-519	98%	98%	98%	98%							95%	98%	86%	96%
07-520	98%	99%	96%	98%	94%	97%	88%	95%	95%	95%	95%	98%	83%	98%
08-519	97%	97%	97%	97%							84%	98%	71%	84%
09-520	97%	99%	94%	97%							88%	93%	83%	88%
11-519	91%	95%	81%	92%							57%	57%	57%	57%
12-520	89%	96%	77%	90%							74%	93%	63%	71%
14-519	87%	93%	81%	87%							80%	80%	80%	80%
15-520	87%	89%	85%	87%							53%	53%	53%	53%
18-519	70%	91%	57%	69%	62%	65%	57%	63%	53%	53%	60%	83%	53%	55%
18-520	77%	81%	72%	77%							66%	85%	32%	72%
21-519	60%	82%	44%	58%	48%	55%	39%	49%	38%	38%	38%	46%	30%	38%
21-520	79%	79%	79%	79%										
23-519	52%	76%	38%	52%	31%	35%	25%	31%	21%	21%	21%	21%	21%	21%
26-519	63%	79%	46%	65%	46%	51%	40%	46%	40%	40%	41%	70%	14%	40%
31-520	23%	25%	21%	23%							12%	16%	9%	12%
32-519	38%	51%	30%	37%							18%	36%	4%	18%
33A-519	67%	76%	57%	67%	47%	53%	41%	47%	30%	26%	28%	44%	8%	26%
33B-519	34%	38%	28%	35%	23%	28%	17%	23%	18%	17%	19%	49%	11%	16%

Figure 6.85 shows the median gas composition values from each data source relative to the drill stub from which the data was collected. In addition to the increased CH_4 concentration of produced gas from inseam boreholes, the results indicate increased

CH_4 concentration of gas liberated during slow desorption relative to the results obtained from fast desorption analysis.

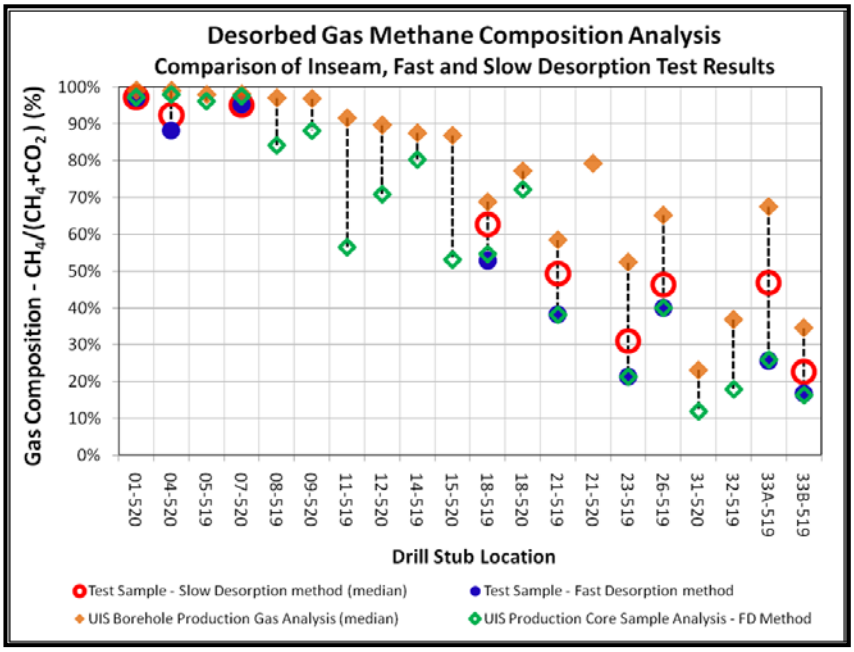

Figure 6.85: Comparison of median gas composition of samples from UIS boreholes and coal core samples

Two possible reasons for the $CH_4/(CH_4+CO_2)$ ratio of the samples tested using the slow desorption method being greater than the fast desorption result include:

1. Preferential desorption of CO_2 early in the slow desorption test followed by progressive CH_4 enrichment results in fewer gas composition measurements early in the test, while CO_2 was preferentially liberated, relative to a high number of gas composition measurements being taken during progressive CH_4 enrichment. The shift in composition of the liberated gas during slow desorption testing tends to skew the median and average gas composition to reflect an increased $CH_4/(CH_4+CO_2)$ ratio compared to the measurement recorded during fast desorption testing; and
2. The composition of the gas released during residual gas content testing of the slow desorption samples was not measured which, based on the work of Crosdale (1998), may have reduced the apparent CH_4 concentration. If this were the case the CO_2 retained in the Q_3 sample would have biased the measured slow desorption gas composition toward an increased $CH_4/(CH_4+CO_2)$ ratio, greater than the composition measured during fast desorption testing, which included the gas from the crushed coal component.

6.4 ELECTRONIC GAS TESTING APPARATUS

Gas emission rate and changes in composition during coal seam gas production are considered important factors in the economic assessment of CBM reservoirs and coal mine outburst risk. The fast desorption method for gas content testing, although important for outburst risk management, is incapable of providing data relating to desorption rate or changes in gas composition during gas production. The slow desorption method has the potential to provide valuable information relating to gas emission rate, changes in gas composition during desorption and residual gas content. However, the quality of information and accuracy of results from slow desorption testing is considered to be adversely impacted by current equipment design that utilises a water column to measure desorbed gas volume. In addition to system leakage, the loss of soluble gases, such as CO_2 and N_2, through contact with the water column is a known source of measurement error (Saghafi *et al.*, 1998; Schatzel and Garcia, 1999 and Danell *et al.*, 2003). Replacement of water with an acid brine solution and use of linseed oil to create a barrier between the gas mixture and the water column was trialled to reduce the risk of gas loss into solution however, gas desorption canisters typically remain sealed between each gas release to reduce contact exposure (Saghafi *et al.*, 1998). Danell *et al.* (2003) report the results of testing on acid brine solutions and linseed oil barriers to assess the impact on the rate of CO_2 loss into solution (Figure 6.86), which indicate potentially significant gas loss through contact with water.

Through periodic gas release the true nature of gas emission is not accurately recorded as the emission rate is governed by the time between each gas release. Also, between each gas release, particularly during early stage desorption, the pressure within the gas desorption canister increases, applying pressure to the coal sample, which has the potential to slow the gas emission rate (Lama and Bartosiewicz, 1982 and Close and Erwin, 1989).

The large free volume within the measuring cylinder and tubing, used to connect the measuring cylinder to the desorption canister, has been shown to impact the accuracy of gas composition measurement, particularly during late stage desorption when the gas volume liberated represents a small percentage of the total free volume.

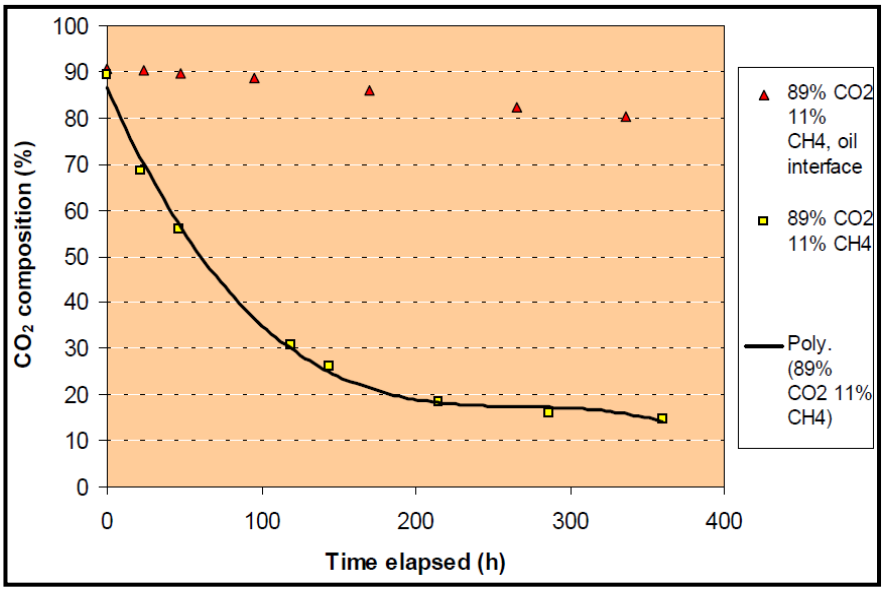

Figure 6.86: Time-dependent composition change of a CO_2 rich gas in contact with a water column of (a) acidified water column, and (b) a linseed oil barrier (Danell *et al.*, 2003)

To account for changes in environmental conditions at the time of each gas release it is recommended that gas volume be corrected to normal conditions of $20^{O}C$ and 101.3 kPa using Equation 6.7 (SAA, 1999). Inaccurate recording of temperature and barometric pressure at the time of each reading may adversely impact the accuracy of the liberated gas volume measurement.

The Portable Modified Direct Method Testing Apparatus was proposed as an alternative to water column systems for conducting slow desorption testing (Schatzel and Garcia, 1998 and Diamond *et al.*, 2002). Through the use of modern electronics and sensors the unit is reported to achieve increased sensitivity and accuracy in the measurement of gas emissions from coal and rock samples, particularly from samples with low gas content.

Figure 6.87 shows a simplified schematic of an alternative to current systems available for core sample gas testing. The electronic gas testing apparatus incorporates electronic sensors to monitor and record critical data such as pressure, temperature and flow rate from each gas desorption canister connected to the system. All sensors are connected to a data logger that records data from each sensor.

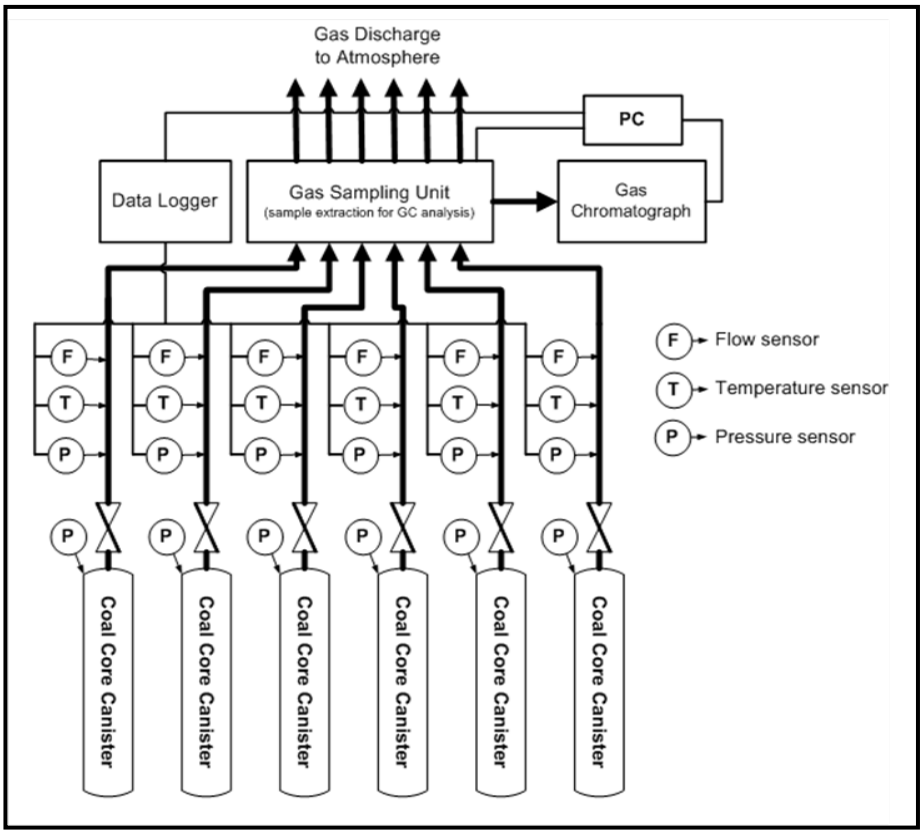

Figure 6.87: Simplified schematic of electronic gas testing apparatus

Gas flow from the desorption canister is continuous, passing through a gas sampling unit prior to being discharged to atmosphere. Within the sampling unit, gas from each discharge line is analysed in sequence using an integrated gas chromatograph to measure changes in gas composition during desorption. The data logger, gas sampling unit and gas chromatograph are each connected to a personal computer which consolidates data from each sample enabling the accurate and near continuous recording of gas emission rate and gas composition throughout the test.

The development of the electronic gas testing apparatus is the subject of ongoing research and development at the University of Wollongong.

6.5 SUMMARY

The results of fast desorption gas testing from 4 185 coal core samples, collected from eight separate Australian underground coal mines have been investigated. The following notable relationships were identified.

- Q_1 and the Q_1:Q_M ratio increased in response to increasing Q_M and the relationship was independent of gas composition;

- Q_2 and the Q_2:Q_M ratio increased in response to increasing Q_M. Where Q_M was less than 7.0 m^3/t, average Q_2 emission appeared not to be impacted by gas composition. As Q_M increased above 7.0 m^3/t the Q_2:Q_M ratio was greater from CH_4 rich samples indicating CH_4 desorbs from coal core samples at a faster rate than CO_2;
- Q_3 increased, while the Q_3:Q_M ratio decreased, in response to increasing Q_M. Where Q_M was less than 7.0 m^3/t, average Q_3 emission appeared not to be impacted by gas composition. As Q_M increased above 7.0 m^3/t, the Q_3:Q_M ratio of the CH_4 rich samples was lower indicating a greater portion of seam gas had been desorbed from the CH_4 rich coal core samples during Q_2 testing than from the CO_2 rich samples;
- In coal samples with low Q_M much of the free and desorbed gas components had been previously released from the coal leaving predominantly Q_3 as the major gas content component, hence the comparatively high Q_3:Q_M ratio of samples with low Q_M;
- Both linear and power formulae were used to represent the average of each gas content component relative to Q_M. The power formula was shown to have the highest correlation. Equations found to represent the average of each gas content component relative to Q_M are:
  - $Q_1 = 0.0064 \times Q_M^{2.0227}$
  - $Q_2 = 0.0257 \times Q_M^{1.9692}$
  - $Q_3 = 1.1631 \times Q_M^{0.7529}$
- Given the strong relationship between Q_1 and Q_M, which appeared independent of gas composition, it was proposed that an average Q_M value may be estimated for a particular coal sample using the Q_1 gas content value, once determined in the field. The power formula relationship, based on the results of 4 090 samples, with Q_1 >0.01 m^3/t, is represented by the equation:
  - $Q_{M(ave)} = 9.3729 \times Q_1^{0.3328}$
- Initial gas desorption rate (IDR) was shown to increase in response to increasing Q_M, with the IDR:Q_M ratio also increasing in response to increasing Q_M. Analysis of changes in seam gas composition indicated the relationship was independent of gas composition. From the distribution of the Q_M and IDR data a clear maximum Q_M envelope was evident. The following equation was found to represent the

maximum Q_M envelope, from which the maximum likely Q_M may be estimated for a given coal sample using the IDR value, once determined in the field.

- $Q_{M(max)} = 2.5665 \times \ln(IDR) + 2.1686$

- Plotting Q_M relative to the square root of IDR indicated a linear relationship between the two variables from which the following equation was proposed to enable an estimate of average Q_M to be calculated for a given coal samples using an IDR value, once determined in the field.
  - $Q_{M(ave)} = 0.7413 \times \sqrt{IDR}$
- Analysis of the desorption rate index (DRI) values, determined from crushed coal testing, plotted relative to Q_M demonstrated a strong relationship, that appeared to be independent of both seam gas composition and site specific coal property variations. The relationship between Q_M and DRI was found to be represented by the equation:
  - $Q_M = 0.008 \times DRI$
- The strong relationship between Q_M and DRI, based on the results of 3 355 samples collected from five separate mines, was found to be different to the relationship presented by Williams and Weissman (1995) which was used as the basis for the DRI900 methodology to determine outburst TLV applicable to non-Bulli seam mines. The fact that the relationship between Q_M and DRI found to be common among the five mines considered in this analysis is different to the relationship reported by Williams and Weissman the validity of the DRI900 methodology for determining outburst TLV applicable to non-Bulli seam mines is questioned and an alternative method for TLV determination must be established. Given the strong and seemingly generic nature of the relationship between Q_M and DRI among the Australian coal seams considered in this analysis it was suggested that a TLV applicable to the Bulli seam may be directly transferrable to non-Bulli seam mines.

During the course of core sample collection for fast desorption testing duplicate coal core samples were collected from 35 locations and tested using the slow desorption method. The characteristics of gas emission from coal core samples tested using the slow desorption method were investigated and the availability of results from fast desorption testing enabled direct comparison of the two methods. Comparison of Q_M results from both methods highlighted significant differences which were investigated.

Gas loss due to leakage was considered to be the dominant contributing factor along with several questionable gas content component values reported from fast desorption testing. Of the 35 samples analysed the results of 18 were considered credible while 17 samples were deemed invalid.

- Q_1 was not measured for the slow desorption samples with values determined from the fast desorption test assumed to be directly transferrable between methods.
- Q_2 indicated a strong near linear relationship to Q_M. The relationship appeared independent of changes in seam gas composition. The rate of gas desorption was shown to be faster from samples with increased Q_M whilst extended desorption time (>200 days) had no discernable effect on Q_2 or the Q_2:Q_M ratio.
- Analysis of Q_2 and the Q_2:Q_M ratio relative to the measured vitrinite content, porosity and mineral matter content of each sample found no relationship suggesting the nature of desorbed gas emission was independent of coal petrography.
- Q_3 did not vary significantly in response to increasing Q_M whereas the Q_3:Q_M ratio reduced. The results indicate coal samples with high Q_M, having increased DoS, desorb gas at a faster rate and the Q_3:Q_M ratio was less than from samples with reduced Q_M. Extended desorption time (>200 days) had little effect on the Q_3 residual gas content.
- Analysis of Q_3 and the Q_3:Q_M ratio relative to the measured vitrinite content, porosity and mineral matter content of the coal samples indicated residual gas content was independent of coal petrography.
- Although gas emission from coal samples tested by fast and slow desorption methods exhibited similar characteristics, the most significant difference between the two methods was the percentage of Q_M liberated during Q_2 and Q_3 testing. In fast desorption testing the greatest volume of gas was liberated during Q_3 testing whereas in slow desorption testing the greatest volume of gas was liberated during Q_2 testing. Comparing the Q_2:Q_M and Q_3:Q_M ratio determined from fast and slow desorption testing, for samples with low gas content (Q_M between 0 and 4 m^3/t), the average Q_2:Q_M and Q_3:Q_M ratio was 62.0% and 37.3% respectively from slow desorption testing, and 11.5% and 87.5% from fast desorption testing. In response to increasing Q_M, the volume of gas liberated during Q_2 was found to increase relative to Q_3. For samples with high gas content (Q_M between 12 and 16 m^3/t), the

average Q_2:Q_M and Q_3:Q_M was 79.8% and 9.2% respectively from slow desorption testing and 21.8% and 66.9% respectively from fast desorption testing.

Changes in gas composition during slow desorption testing and during inseam gas production from the Bulli seam were also considered. The results of the two studies were compared and assessed relative to gas composition results obtained from fast desorption testing.

- Previous studies report conflicting changes in the composition of gas liberated from coal, some workers propose CH_4 was preferentially liberated from coal due to equilibrium desorption while others propose CO_2 desorbed at a faster rate than CH_4 from coal core due to the increased diffusivity of CO_2.
- Analysis of gas emission from 35 coal core samples during slow desorption testing identified 26 cases of progressive CH_4 enrichment, while the $CH_4/(CH_4+CO_2)$ ratio remained relatively stable in 3 cases and decreased in 6 cases.
- Lama (1988b), Lama (1995a) and Cui and Busten (2006) suggest diffusivity is the primary mechanism governing gas emission resulting in the preferential liberation of CO_2 from the coal core due to its increased diffusivity relative to CH_4. While Cui and Busten (2006) suggest changes in composition of gas liberated from coal are due to the coal fabric which controls the dominance of either gas emission mechanism, diffusion or desorption.
- The $CH_4/(CH_4+CO_2)$ ratio of gas liberated from inseam drainage boreholes was greater than from core samples collected within and adjacent to the same borehole. This observation suggests preferential gas emission from zones of increased CH_4 concentration intersected by the borehole. The increased CH_4 concentration from inseam boreholes may also be from more highly saturated coal plies with increased CH_4 concentration that liberate gas at a faster rate than the highly undersaturated CO_2 coal plies intersected along the length of the borehole.

During slow desorption testing several issues and opportunities were recognised with respect to the design of the testing equipment. Current slow desorption testing equipment necessitates the periodic release of gas to minimise contact with the water column to reduce the risk of gas loss into solution. Between each gas release the coal core remains sealed in the desorption canister which has the potential to impede gas emission thereby slowing the process and not accurately representing the true nature of coal seam gas emission. An electronic gas testing apparatus, which builds upon the

portable modified direct method testing apparatus proposed by Schatzel and Garcia (1998), offers continuous monitoring and analysis of gas emission during slow desorption testing, without the risk of gas loss through contact with water, enabling the rate of gas emission and changes in gas composition to be accurately and continuously monitored throughout the complete desorption test period.

CHAPTER SEVEN – CONCLUSIONS AND RECOMMENDATIONS

7.1 CONCLUSIONS

From an analysis of operational factors and geological properties that impact gas production and assessment of methods to improve drainage effectiveness, the following conclusions have been made:

- Degree of saturation (DoS) had the greatest impact on coal seam gas production and appeared to have a dominant influence over the relationship between gas production and other factors. The rate of gas production and total gas produced from highly undersaturated coal is less than from an equivalent saturated coal. Based on piezometer data analysis, the use of the underground-to-inseam (UIS) gas drainage method in highly undersaturated, CO_2 rich and low permeability areas of the Bulli seam at West Cliff Colliery was found to be ineffective in reducing reservoir pressure to the critical desorption point within the available drainage time.
- Drainage time had a significant impact on gas production. A minimum of 275 days drainage was shown to be required in the highly undersaturated coal, CO_2 rich coal (0-40% CH_4), with reduced drainage time required in coal with increased DoS.
- Accumulation of water and fines within gas drainage boreholes impedes gas desorption. The design, installation and ongoing management of drainage boreholes must aim to maintain all boreholes free of material and fluid accumulations. Boreholes should ideally be drilled up-dip to encourage self-drainage. Where seam conditions and mine layout necessitate drilling boreholes down-dip, in-hole dewatering systems should be provided, particularly in highly undersaturated areas where low gas production rate is incapable of flushing material from the borehole.
- The tortuosity of UIS boreholes presents a risk to borehole stability and creates multiple troughs along each borehole where water and fines may accumulate. The use of drilling guidance systems in UIS drilling has the potential to improve drilling performance, increase borehole length and improve the quality of gas drainage borehole installations; thereby increasing the total quantity of gas drained.

- Lack of pressure control within the borehole during UIS drilling was shown to have a significant impact on downhole conditions with the potential to create borehole instability and reduce the permeability of the coal seam surrounding the borehole.
- The gas reticulation system should be designed to remain free of water and accumulation of fines. Material accumulation within the pipe range reduces the capacity of the system to reticulate gas from the mine. In addition to providing dewatering points, strategically located in low areas throughout the pipe network, gas/water separators should be maintained at each of the active drill stubs to prevent water and fines from the boreholes flowing directly into the gas reticulation pipe range.
- Although not directly assessed, the management of drainage boreholes and the total gas reticulation system has a potentially significant impact on gas production. Approximately half of all UIS gas drainage boreholes drilled in Area 5 at West Cliff Colliery produced less than 100 000 m^3, independent of location, gas composition, degree of saturation and other factors. It is suggested that frequent monitoring and proactive management of the gas drainage system will identify poor producing boreholes permitting actions to be taken to optimise system performance and increase total gas production.
- A weak relationship was indicated between gas production and the length and orientation of gas drainage boreholes. Maximum gas production was achieved from boreholes ranging in length between 600 and 1 100 m. Boreholes oriented between 0 and 40^O to the principal horizontal stress produced more gas than boreholes oriented perpendicular to the principal horizontal stress. The orientation of boreholes relative to cleat was shown to have a comparatively weak impact on total gas production which was consistent with previous studies in the Bulli seam at West Cliff Colliery.
- Increased gas production was indicated in areas with reduced coal ash content and increased rank. However the low ash, high rank coal was located in the area of increased DoS. Given the dominant impact of DoS on gas production, the observed relationship between gas production, coal ash content and coal rank was considered to be coincidental.

- No evidence was found to indicate a relationship between gas production and coal type, inherent moisture content or raw ash content.
- No evidence was found to support a relationship between applied suction pressure and gas production. Maintaining negative pressure within the gas reticulation pipe network reduces the risk of positive pressure within the range causing seam gas to leak into the underground environment. However, high suction pressure increases the risk of air leakage into the pipeline which effectively reduces the gas carrying capacity of the system. Where moderate to high suction pressure is applied to the boreholes, gas reticulation pipes and the standpipe at each borehole must be installed to a very high standard to minimise the risk of leakage.
- In highly undersaturated coal, where the minimum drainage time exceeds the relatively short drainage window associated with the UIS drainage method, alternative surface-based drilling and drainage enhancement methods must be utilised. Drilling methods such as radius drilling and stimulation methods such as hydraulic fracturing have been considered however both methods rely on pressure decline and should be installed at least five years ahead of mining activity.
- A new method involving cyclic inert gas injection into the coal seam has been proposed as an alternative to existing gas drainage and stimulation methods that rely on decreasing reservoir pressure to the critical desorption point. The proposed method, which involves repeated cycles of gas injection, hold and release, has the potential to significantly enhance gas desorption, particularly from highly undersaturated, low permeability coal seams.
- The volume of gas liberated from a coal sample during each stage of fast desorption gas content testing, Q_1, Q_2 and Q_3, increased in response to increasing Q_M. The relative percentage of Q_M liberated during each stage of the test differed in response to increasing Q_M; Q_1:Q_M and Q_2:Q_M both increasing, the latter at a greater rate, whereas Q_3:Q_M decreased.
- In coal samples with low Q_M the majority of gas was released during Q_3 testing, with a greater Q_3:Q_M ratio than samples with high Q_M. This relationship suggests much of the free and readily desorbed gas had been liberated from the coal prior to collection and testing, leaving predominantly the Q_3 residual gas content component.

- The relationship between each gas content component and Q_M, recorded during fast desorption testing, was shown to be most accurately represented by power equations, achieving greater statistical correlation than linear equations. The average relationship between each gas content component and Q_M was found to be represented by the following equations:
  - $Q_1 = 0.0064 \times Q_M{}^{2.0227}$
  - $Q_2 = 0.0257 \times Q_M{}^{1.9692}$
  - $Q_3 = 1.1631 \times Q_M{}^{0.7529}$
- The composition of the seam gas present in the coal sample was found to have little impact on the relationship between Q_1 and Q_M, for all samples tested using the fast desorption method. Gas composition was also found to have minimal impact on the relationship between Q_2 and Q_3 relative to Q_M for all samples where Q_M was less than 7.0 m^3/t, as determined using the fast desorption method. As Q_M increased above 7.0 m^3/t, the Q_2:Q_M ratio increased at a greater rate and the rate of increase of Q_3:Q_M reduced from CH_4 rich samples. The results indicate that as Q_M increased and the DoS increased, CH_4 desorbed from coal core samples at a faster rate than CO_2.
- Based on the strong relationship between Q_1 and Q_M, which is suggested to be independent of gas composition, several methods are proposed to estimate likely average and total Q_M of a coal sample, and therefore the coal seam from which the sample was recovered, using results from initial gas desorption measurement. From the results of fast desorption testing the following equations are proposed as semi-direct methods for estimating average and maximum coal seam gas content:
  - $Q_{M(ave)} = 9.3729 \times Q_1{}^{0.3328}$
  - $Q_{M(ave)} = 0.7413 \times \sqrt{IDR}$
  - $Q_{M(max)} = 2.5665 \times \ln(IDR) + 2.1686$
- The relationship between Q_M and DRI was shown to be very strong and consistent among the five mines, located throughout QLD and NSW, included in the analysis. The relationship was shown to be independent of changes in seam gas composition. The following equation represents the common relationship between Q_M and DRI.

- $Q_M = 0.008 \times DRI$

- Outburst threshold limit values (TLV) prescribed for use in Bulli seam mines are considered conservative when used in conjunction with intensive inseam gas drainage drilling and core sampling programs which are integral elements of modern outburst risk management. Two Bulli seam mines have demonstrated an ability to continue to operate without outburst after having raised outburst TLV.
- The DRI900 methodology used to determine outburst TLV applicable to non-Bulli seam mines is no longer considered valid. Given the recent success of Bulli seam mines in raising TLV the DRI900, originally based on TLV prescribed to Bulli seam mines in 1994, is considered conservative in cases where mines utilise intensive gas drainage drilling and outburst risk management. Based on the relationship between Q_M and DRI presented in 1994 by Williams and Weissman a DRI of 1200 is considered to be a more appropriate Level 2 TLV.
- Analysis of gas data from five mines identified a common relationship between Q_M and DRI, which is contrary to the relationship presented by Williams and Weissman and used as the basis for the DRI900 methodology for determining TLV applicable to non-Bulli seam mines. From the relationship identified it is suggested that a separate DRI value corresponds to each TLV gas content value.
- Given the strong and seemingly generic nature of the relationship between Q_M and DRI among the Australian coal seams considered in this analysis it is proposed that an outburst TLV applicable to Bulli seam mines is directly transferrable to non-Bulli seam mines. Therefore a TLV of 9 m^3/t, which corresponds to a DRI value of 1 125, is considered to be equally applicable for use in other non-Bulli coal seams.
- Significant differences were found between Q_M determined using the fast and slow desorption methods in 17 of the 35 samples. Gas loss due to leakage was considered to be the most probable reason for the difference between Q_M determined using the two testing methods. This finding was based on comparison of duplicate coal core samples were collected from 35 locations and tested using the fast and slow desorption methods.
- From slow desorption testing, a strong linear relationship was indicated between Q_2 and Q_M, with increased Q_2 and Q_2:Q_M ratio from samples with increased Q_M. Gas

desorbed at a faster rate from samples with increased Q_M. The relationship between Q_2 and Q_M and the gas emission rate appeared to be independent of changes in seam gas composition and independent of changes in coal petrography.

- The residual gas content (Q_3), measured at the completion of slow desorption testing, did not vary significantly in response to increasing Q_M whereas a reduction in the Q_3:Q_M ratio was evident. The residual gas content of coal samples that desorbed at a faster rate was found to be less than the residual gas content of slower desorbing samples. The relationship between Q_3 and Q_M appeared to be independent of changes in seam gas composition and coal petrography.
- Samples with increased Q_M were found to desorb gas at a faster rate than samples of lower Q_M.
- Extending the slow desorption test period beyond 200 days was found to have little impact on the volume of gas desorbed from, or the residual gas content of, the coal samples with virtually no change in the Q_2:Q_M ratio or the Q_3:Q_M ratio.
- Comparing the results obtained from fast and slow desorption testing the major difference identified was the relative percentage of Q_M liberated during Q_2 and Q_3 testing. In slow desorption testing the greatest volume of gas was liberated during Q_2 testing whereas in fast desorption testing the greatest volume of gas was liberated during Q_3 testing. In both tests the Q_2:Q_M ratio increased and the Q_3:Q_M ratio decreased in response to increasing Q_M.
- Analysis of the composition of seam gas liberated from 35 coal core samples during slow desorption testing identified 26 cases of progressive CH_4 enrichment, while the CH_4:CO_2 ratio remained relatively stable in 3 cases and decreased in 6 cases. Consistent with the work of Lama (1988b), Lama (1995a) and Cui and Busten (2006), the results indicate early liberation of CO_2 from coal core samples, due to the increased diffusivity of CO_2 relative to CH_4, followed by progressive CH_4 enrichment during desorption. Cui and Busten (2006) also suggest changes in composition of gas liberated from coal are due to the coal fabric which controls the dominance of either gas emission mechanism, diffusion or desorption.
- Gas sampled during production from inseam boreholes was found on analysis to have a higher CH_4:CO_2 ratio than coal samples collected from within the same borehole during drilling and tested using the slow and fast desorption method. This

observation suggests preferential gas emission from zones of increased CH_4 concentration along the length of the borehole that liberate gas at a faster rate than highly undersaturated zones or plies with comparatively higher CO_2 concentration.

- Several issues and opportunities were identified with respect to the design of the equipment used for slow desorption testing. Current slow desorption testing equipment necessitates the periodic release of gas to minimise contact with the water column to reduce the risk of gas loss into solution. Between each gas release the coal core remains sealed in the desorption canister which has the potential to impede gas emission thereby slowing the process and not accurately representing the true nature of coal seam gas emission. An electronic gas testing apparatus has been proposed which offers continuous monitoring and analysis of gas emission during slow desorption testing, without the risk of gas loss through contact with water, enabling the rate of gas emission and changes in gas composition to be accurately and continuously monitored throughout the complete desorption test period.

7.2 RECOMMENDATIONS

The following matters were identified and are recommended as topics for further research:

- Conduct laboratory study to investigate the characteristics of gas emission from undersaturated coal. Many coal seams are undersaturated in gas however laboratory sorption testing is presently limited to testing on saturated coal samples.
- Expand the analysis of the relationship between Q_M and DRI to include additional Australian coal mines. A common relationship was identified among the five mines included in this analysis and it is recommended that further research be undertaken to expand the dataset and investigate the relationship between Q_M and DRI from other coal seams.
- Alternative methods for determining outburst TLV applicable to non-Bulli seam mines should be investigated. It is proposed that TLV applicable to Bulli seam mines may be directly transferred to non-Bulli seam mines. This proposal should be investigated, considering coal seam gas conditions present at the location of outburst incidents in non-Bulli seam mines.

- A number of inherent limitations were identified with equipment presently used to conduct gas content testing. An electronic gas content testing apparatus is proposed as an alternative to the current apparatus that relies on the use of a water column to measure the gas volume liberated from a coal sample. It is recommended that a prototype electronic gas testing apparatus be developed for use in comparative analysis alongside existing equipment to confirm the proposed benefits.
- Cyclic inert gas injection requires further research and development to demonstrate the ability of this method to increase gas production from highly undersaturated and low permeability coal. This should include both laboratory studies to evaluate the impact of varying pressure, temperature and inert gas type in enhancing coal seam gas production and field studies to define and optimise the injection and treatment process.

REFERENCES

Advanced Mining Technologies (AMT), 2008. DGS and DDM-MECCA Product Brochures [online]. Available from: http://www.advminingtech.com.au/Default.aspx?tabid=108 [Accessed: September 2010].

Allen, B, 2002. Industry impacts – outburst and gas management, in *Proceedings of the 3rd Australian Coal Operators' Conference COAL2002*, Australasian Institute of Mining and Metallurgy, Wollongong, 6-8 February, pp.30-33.

Apex Energy NL, 2008. Stratigraphic section of the Sydney basin from Bulli to Burragorang [online]. Available from: http://www.apexenergy.com.au/general-information/ [Accessed: May 2010].

Armstrong, M and Doyle, J, 2008. Bulli seam piezometer data files, Internal Report (unpublished).

Armstrong, M and Kaag, H, 2006. Review of Bulli seam gas drainage limits and the impact on future mining in Douglas and West Cliff, Internal Report (unpublished).

Armstrong, M and Kaag, H, 2008. Bulli seam exploration data files, Internal Report (unpublished).

Arrow Energy, 2008. Capitalising on Asia's CBM resources, Coalbed Methane Conference, Singapore, 29 July [online]. Available from: http://www.arrowenergy.com.au/icms_docs/30978_CBM_Conference.pdf [Accessed: November 2010].

Australian Bureau of Agriculture and Resource Economics (ABARE), 2009a. Energy in Australia, Chapter 5 – Coal production and trade [online]. Available from: http://www.abare.gov.au/interactive/09_auEnergy/htm/chapter_5.htm [Accessed: May 2010].

Australian Bureau of Agriculture and Resource Economics (ABARE), 2009b. Energy in Australia, Chapter 6 – Gas production and trade [online]. Available from: http://www.abare.gov.au/interactive/09_auEnergy/htm/chapter_6.htm [Accessed: May 2010].

Australian Bureau of Agriculture and Resource Economics (ABARE), 2010. Australian Energy Resource Assessment [online]. Available from: http://www.abare.gov.au/publications_html/energy/energy_10/ga_aera.html [Accessed: May 2010].

Australian Government Department of Climate Change (AGDCC), 2009. National greenhouse gas inventory accounting for the Kyoto target May 2009, Australia's National Greenhouse Accounts [online]. Available from: http://www.climatechange.gov.au/climate-change/~/media/publications/greenhouse-report/national-greenhouse-gas-inventory-pdf.ashx [Accessed: May 2010].

Aziz, N I, 2006. Rank of coal seam, *Coal Mining Science and Technology Website*, University of Wollongong [online]. Available from: http://www.uow.edu.au/eng/outburst/html/rank.html [Accessed: May 2010].

Aziz, N I and Ming-Li, W, 1999. The effect of sorbed gas on the strength of coal – an experimental study, *Geotechnical and Geological Engineering*, Volume 17, Numbers 3-4, pp 387-402.

Badri, M, Dare, D, Rodda, J, Thiesfield, G and Blauch, M, 2000. Keys to successful application of hydraulic fracturing in an emerging coalbed methane prospect – an example from the peat coals of Australia, *SPE Asia Pacific Oil and Gas Conference*, Society of Petroleum Engineers, Brisbane, Australia, 16-18 October, 15p. (SPE-64493).

Battino, S and Hargraves, A J, 1982. Seam gas drainage experiments in some collieries of B.H.P., *Seam gas drainage with particular reference to the working seam*, (ed: A J Hargraves), University of Wollongong, Wollongong, Australia, pp 157-171.

Battino, S and Regan, R, 1982. Methane drainage under the No.7 longwall block Appin Colliery, *Seam gas drainage with particular reference to the working seam*, (ed: A J Hargraves), University of Wollongong, Wollongong, Australia, pp 254-267.

Beamish, B B and Crosdale, P J, 1995. The influence of maceral content on the sorption of gases by coal and the association with outbursting, *International Symposium on Management & Control of High Gas Emissions & Outburst in Underground Coal Mines*, (ed: R D Lama), Wollongong, 20-24 March, pp 353-361.

Beamish, B B, Crosdale, P J and Gamson, P D, 1993. Characterising the methane sorption behaviour of banded coals in the Bowen Basin, in *Proceedings of the 1993 International Coalbed Methane Symposium*, University of Alabama, Tuscaloosa, pp 145-148.

Beamish, B B and O'Donnell, G, 1992. Microbalance applications to sorption testing of coal, *Symposium on Coalbed Methane Research and Development in Australia*, Coalseam Gas Research Institute – James Cook University, Townsville, 19-21 November, Volume 4, pp 31-41.

Beamish, B B, Williams, R J, Hungerford, F and McKavanagh, B M, 1985. Outburst research, End of Grant Report No. 495, National Energy Research, Development and Demonstration Program.

Bell, G J and Jones, A H, 1989. Variation of mechanical strength with rank of gassy coals, in *Proceedings of the 1989 International Coalbed Methane Symposium*, The University of Alabama, Tuscaloosa, 17-20 April, pp 65-74.

Benson, D J, 2006. West Cliff Colliery, BHP Billiton Illawarra Coal, Personal Communication.

Bertard, C, Bruyet, B and Gunther, J, 1970. Determination of desorbable gas concentration of coal (direct method), International Journal of Rock Mechanical and Mining Sciences and Geomechanics, Volume 7, Issue 1, pp 43-65.

BHP, 1995. Outburst awareness, Tower Colliery Training Manual, BHP Collieries Division, pp 1-48.

BHP Billiton, 2001. BHP Chronology [online]. Available from: http://www.bhpbilliton.com/bbContentRepository/docs/AboutUs/history/BHPChronology.pdf [Accessed: September 2010].

BHP Billiton Illawarra Coal (BHPBIC), 2006. Westcliff 5 geotechnical report – preliminary February 2006, Internal Report (unpublished).

BHP Billiton Illawarra Coal (BHPBIC), 2007. Total gas content report, Standard Form QS-SGM-SF010, Electronic Gas Analysis Data Files.

Bishop, R and Battino, S, 1989. Extraction and utilisation of coalseam methane – the Australian experience, *Proceedings of the 1989 International Coalbed Methane Symposium*, University of Alabama, Tuscaloosa, 17-20 April, pp 107-115.

Black, D J, 2007. Hydraulic fracturing development and demonstration project – West Cliff Colliery trial 519-33A, BHP Billiton Illawarra Coal Gas & Ventilation, Confidential Report.

Black, D J and Aziz, N I, 2009. Reducing coal mine GHG emissions through effective gas drainage and utilisation, in *Proceedings of the 2009 International Coalbed and Shale Gas Symposium*, University of Alabama, Tuscaloosa, 18-22 May, Paper No.0912.

Black, D J, Aziz, N I, Jurak, M J and Florentin, R M M, 2009. Outburst threshold limits – are they appropriate?, in *Proceedings of the 9th Underground Coal Operator's Conference COAL2009*, University of Wollongong and Australasian Institute of Mining and Metallurgy, (eds: N I Aziz and J Nemcik), Wollongong, 12-13 February, pp 185-192 [online]. Available from: http://ro.uow.edu.au/coal/99/ [Accessed: November 2010].

Black, D J, Ren, T X and Aziz, N I, 2010. Development of a cyclic inert gas injection method to enhance methane gas capture and reduce coal mine fugitive emissions, University of Wollongong, Project Funding Application, EPA-OAR-CCD-10-02.

Black, D and Self, A, 2007. Appin gas drainage system improvement project, BHP Billiton Illawarra Coal Gas & Ventilation, Confidential Technical Report.

Black, D and Self, A, 2008. West Cliff Colliery gas and ventilation strategy, BHP Billiton Illawarra Coal Gas & Ventilation, Confidential Report.

Black, D, Self, A and Hockey, M, 2008. Appin Colliery ventilation & gas drainage strategy, BHP Billiton Illawarra Coal Gas & Ventilation, Confidential Report.

British Broadcasting Corporation (BBC), 2010. Deadly explosion in Slovakia mine [online]. Available from: http://news.bbc.co.uk/2/hi/europe/8194505.stm [Accessed: December, 2010].

Britt, L K, Smith, M B, Haddad, Z, Lawrence, P, Chipperfield, S and Hellman, T, 2006. Water-fracs: we do need proppant after all, *SPE Annual Technical Conference and Exhibition*, Society of Petroleum Engineers, San Antonio, Texas, 24-27 September, 15p. (SPE-102227).

Brown, K, Casey, D A, Enever, J R, Facer, R A and Wright, K, 1996. New South Wales coal seam methane potential, *Geological Survey of NSW Coal and Petroleum Geology*, Department of Mineral Resources, Petroleum Bulletin 2.

Brown, M, 2007. West Cliff Colliery, BHP Billiton Illawarra Coal, Personal Communication.

Brunner, D J, 2005. Modern methane drainage strategies [online], 29p. Available from: http://www.epa.gov/cmop/docs/cmm_conference_apr05/dan_brunner.pdf [Accessed: September 2010].

Brunner D J and Schwoebel, J J, 2010. Directional drilling for methane drainage and exploration in advance of mining and recent advances and applications [online]. Available from: http://www.reidrilling.com/pdf/REI%20Drilling%20Technical%20Paper.pdf [Accessed: September 2010].

Brunner, D J, Schwoebel, J J and Thomson, S, 2008. Directional drilling for methane drainage and exploration in advance of mining [online], 10p. Available from: http://www.advminingtech.com.au/Default.aspx?tabid=108 [Accessed: September, 2010].

Busch, A, Gensterblum, Y, Kroos, B and Littke, R, 2004. Methane and carbon dioxide adsorption-diffusion experiments on coal: upscaling and modelling, *International Journal of Coal Geology*, Volume 60, pp 151-168.

Cameron, J R, Palmer, I D, Lukas, A and Moschovidis, Z A, 2007. Effectiveness of horizontal wells in CBM, in *Proceedings of the 2007 International Coalbed Methane Symposium*, University of Alabama, Tuscaloosa, 23-24 May, paper no. 0716, 18p.

Carlson, F M, 2006. Technical and economic evaluation of undersaturated coalbed methane reservoirs, *SPE Europec/EAGE Annual Conference and Exhibition*, Vienna, Austria, 12-15 June, 13p. (SPE-100224).

Carter, R A, 1990. Underground developments in methane recovery, *COAL*, vol. 95, No. 12, December, pp 55-59.

Caudill, D, 2008. Target drilling hits mark with borehole record [online]. Available from: http://www.longwalls.com/StoryView.asp?StoryID=171458 [Accessed: April 2008].

Clark, B, 1986-2007. Coal analysis reports – various, *BHP Billiton Illawarra Coal*, Internal Reports.

Clark, D A, 1983. Prevention of instantaneous outbursts of coal and gas by pre-drainage, *Alleviation of Coal and Gas Outbursts in Coal Mines – Seminar 3*, Coordinating Committee on Outburst Research, September.

Clark, D A, Battino, S and Lunarzewski, L, 1983. Prevention and control of outbursts by pre-drainage of seam gas at Metropolitan colliery – a review, *Alleviation of Coal and Gas Outbursts in Coal Mines – Seminar 3*, Coordinating Committee on Outburst Research, September.

Clarke, M, 1994. Notice pursuant to Section 63 Coal Mines Regulation Act 1982, New South Wales Department of Mineral Resources – Coal Mining Inspectorate and Engineering Branch, 11 May.

Clarkson C R and Bustin R M, 1999. The effect of pore structure and gas pressure upon the transport properties of coal: a laboratory and modelling study, *Fuel*, Volume 78, pp 1345-1362.

Close, J C and Erwin, T M, 1989. Significance and determination of gas content data as related to coalbed methane reservoir evaluation and production implications, in *Proceedings of the 1989 International Coalbed Methane Symposium*, University of Alabama, Tuscaloosa, 17-20 April, pp 37-55.

Cram, K, 1995-2010. Australian longwall mine production statistics, *Australian Longwall Magazine and International Longwall News* [online]. Available from: http://www.longwalls.com [Accessed: March 2010].

Cram, K, 2009. Overview of Australian black coal mining operations, Coal Services Pty Ltd, Personal Communication (May 2010).

Cramer, D D, 2008. Stimulating unconventional reservoirs: lessons learned, successful practices, areas for improvement, *SPE Unconventional Reservoirs Conference*,

Society of Petroleum Engineers, Keystone, Colorado, 10-12 February, 19p. (SPE-114172).

Creedy, D P, Saghafi, A and Lama R, 1997. Gas control in underground coal mining, *IEA Coal Research*, Organisation for Economic Co-operation and Development, London.

Crosdale, P J, 1998. Degassing of methane and carbon dioxide: prediction of gas composition, Australian Coal Association Research Program, Project Report C5037.

Crosdale, P J, Beamish, B B and Valix, M, 1998. Coalbed methane sorption related to coal composition, *International Journal of Coal Geology*, Volume 35, pp 147-158.

Crosdale, P J, Moore, T A and Mares, T E, 2008. Influence of moisture content and temperature on methane adsorption isotherm analysis for coals from a low-rank, biogenically-sourced gas reservoir, *International Journal of Coal Geology*, Volume 76, pp 166-174.

CSIRO, 2007. Petrology and gas composition of Bulli coal samples from boreholes West Cliff 58 and 61, *CSIRO Petroleum*, Confidential Report, Number 07-096.

Cui, X and Busten, R, 2006. Controls of coal fabric on coalbed gas production and compositional shift in both field production and canister desorption tests, *SPE Journal* March, pp 111-119. (SPE-89035).

Curl, S J, 1978. Methane prediction in coal mines, *IEA Coal Research*, London, Report Number ICTIS/TR04.

Danell, R E, Saghafi, A, Williams, R J and Wood, J, 2003. Reproducibility of gas content measurements using the fast desorption technique, *Australian Coal Association Research Program*, Project Report C8024.

Diamond, W P and Levine, J R, 1981. Direct method determination of the gas content of coal: procedures and results, *United States Department of the Interior*, Bureau of Mines Report of Investigations RI8515, 40p. [online]. Available from: http://www.cdc.gov/NIOSH/Mining/pubs/pdfs/ri8515.pdf [Accessed: November 2010].

Diamond, W P, Murrie, G W and McCulloch, C M, 1976. Methane gas content of the Mary Lee group of coalbeds, Jefferson, Tuscaloosa, and Walker Counties, Ala., *United States Department of the Interior*, Bureau of Mines Report of Investigations RI8117, 13p. [online]. Available from: http://www.cdc.gov/niosh/mining/pubs/pdfs/ri8117.pdf [Accessed: November 2010].

Diamond, W P and Oyler, D C, 1987. Effects of stimulation treatments on coalbeds and surrounding strata, *United States Department of the Interior*, Bureau of Mines Report of Investigations RI9083, 53p. [online]. Available from: http://www.cdc.gov/niosh/mining/pubs/pdfs/ri9083.pdf [Accessed: November 2010].

Diamond, W P and Schatzel, S J, 1998. Measuring the gas content of coal: a review, *International Journal of Coal Geology*, Volume 35, pp 311-331.

Diamond, W P, Schatzel, S J, Garcia, F and Ulery, J P, 2002. The modified direct method: a solution for obtaining accurate coal desorption measurements, in *Proceedings of the 2001 International Coalbed Methane Symposium*, University of Alabama, Tuscaloosa, 14-18 May, pp 331-342 [online]. Available from: http://www.cdc.gov/niosh/mining/pubs/pdfs/mdmsoa.pdf [Accessed: May 2010].

Dougherty, H N and Karacan, C Ö, 2010. Methane drainage and degasification – general concepts, *NIOSH Short Course – Control of Methane Gas in Underground Mining Operations*, 12 June, Sudbury, Ontario.

Durucan, S and Shi, J, 2009. Improving the CO_2 well injectivity and enhanced coalbed methane production performance in coal seams, *International Journal of Coal Geology*, Volume 77, pp 214-221.

Dutta, P, Harpalani, S and Prusty, B, 2008. Modelling of CO_2 sorption on coal, *Fuel*, Volume 87, pp 2023-2036.

Eddy, G E, Rightmire, C T and Byrer, C W, 1982. Relationship of methane content of coal rank and depth theoretical vs. observed, *SPE/DOE Symposium on unconventional gas recovery*, Pittsburgh, Pennsylvania, pp 117-122.

Elder, C H, 1977. Effects of hydraulic stimulation on coalbeds and associated strata, *United States Department of the Interior*, Bureau of Mines Report of Investigations RI8260, 25p. [online]. Available from: http://www.cdc.gov/niosh/mining/pubs/pdfs/ri8260.pdf [Accessed: November 2010].

Enever, J R, Jeffrey, R G and Vlahovic, W, 1995. Hydraulic fracture development in Australian coal seams, *International Symposium on Management & Control of High Gas Emissions & Outburst in Underground Coal Mines*, (ed: R D Lama), Wollongong, 20-24 March, pp 257-265.

Esterle, J S, 2007. Coalification processes and coal rank, grade and type, Department of Earth Sciences, University of Queensland [online], Available from: http://www.earthsciences.uq.edu.au/Course_Information/2007/MINE2106/2106_JE_CoalificationRankGradeType.pdf [Accessed: March 2008].

Every, R L and Dell'Osso, J, 1977. Method for removing methane from coal, *US Patent* 4043395 [online]. Available from: http://www.freepatentsonline.com/4043395.html [Accessed: November 2010].

Faiz, M M, 1993. Thermal history and geological controls on the distribution of coal seam gases in the southern Sydney basin, Australia, *PhD Thesis*, Department of Geology, University of Wollongong.

Faiz, M M, Aziz, N I, Hutton, A C and Jones, B G, 1992. Porosity and gas sorption capacity of some eastern Australian coals in relation to coal rank and composition, *Symposium on Coalbed Methane Research and Development in Australia*, Coalseam Gas Research Institute – James Cook University, Townsville, 19-21 November, Volume 4, pp 9-20.

Faiz, M M and Cook, A C, 1991. Influence of coal type, rank and depth on the gas retention capacity of coal in the southern coalfield, NSW, *Symposium on Gas in Australian Coals*, (eds: W J Bamberry and A M Depers), Geological Society of Australia, Sydney, Volume 2, pp 19-29.

Faiz, M M and Hutton, A C, 1995. Geological controls on the distribution of CH_4 and CO_2 in coal seams in the Southern Coalfield, NSW, Australia, *International Symposium on Management & Control of High Gas Emissions & Outburst in Underground Coal Mines*, (ed: R D Lama), Wollongong, 20-24 March, pp 375-383.

Faiz, M M, Saghafi, A, Barclay, S A, Stalker, L, Sherwood, N R and Whitford, D J, 2007a. Evaluating geological sequestration of CO_2 in bituminous coals: The southern

Sydney basin, Australia as a natural analogue, *International Journal of Greenhouse Gas Control*, Volume 1, No.2, April, pp 223-235.

Faiz, M M, Saghafi, A, Sherwood, N and Wang, I, 2007b. The influence of petrological properties and burial history on coal seam methane reservoir characterisation, Sydney Basin, Australia, *International Journal of Coal Geology*, Volume 70, pp 193-208.

Fredericks, L, 2008. Bulli seam permeability data files – 2003 to 2006, *BHP Billiton Illawarra Coal Exploration – Confidential Test Reports.*

Gamson, P D and Beamish, B B, 1992. Coal type, microstructure and gas flow behaviour of Bowen Basin coals, *Symposium on Coalbed Methane Research and Development in Australia*, Coalseam Gas Research Institute – James Cook University, Townsville, 19-21 November, Volume 4, pp 43-64.

Garbutt, D, 2004. Schlumberger unconventional gas – white paper [online]. 12p. Available from: http://www.slb.com/~/media/Files/industry_challenges/unconventional_gas/white_papers/uncongas_whitepaper_of03056.ashx [Accessed: July 2010]

GeoGAS Systems Pty Ltd, 2004. Analysis of selected areas input data for modelling, West Cliff Colliery. Confidential Report.

Gleeson, D, 2010. Methane drilling / detection, *International Mining*, June, pp 53-54. [online]. Available from: http://www.infomine.com/publications/docs/InternationalMining/Gleeson2010c.pdf [Accessed: September 2010].

Gray, I, 1982. A study of seam gas drainage in Queensland, in *Proceedings of the Symposium on Seam Gas Drainage with Particular Reference to the Working Seam*, (ed: A J Hargraves), Australasian Institute of Mining and Metallurgy – Illawarra Branch, University of Wollongong, Wollongong, Australia, 11-14 May, pp 218-231.

Gray, I, 1987. Reservoir engineering in coal seams: part 1 – the physical process of gas storage and movement in coal seams, *SPE Reservoir Engineering*, Volume 2, Number 1, pp 28-34. (SPE-12514).

Gray, I, 1994. Optimisation of longhole drilling equipment, *Australian Coal Association Research Program*, Project Report C3023.

Gray, I, 1997. Development of torque, thrust and rpm sensors, *Australian Coal Association Research Program*, Project Report C3073.

Gray, I, 1998. Borehole pressurisation system, *Australian Coal Association Research Program*, Project Report C3072.

Gray, I, 2000. Surface to in-seam drilling for methane drainage and exploration [online]. Available from: http://www.sigra.com.au/ppr_sinblurb.html [Accessed: February 2008].

Gray, I, Clemence, P, Paradise, G, Charlton, S, Dixon, R and Hatherly, P, 2002. The development of geosteering sensors for in-seam drilling, *Australian Coal Association Research Program*, Project Report C5029. Demonstration of bit torque, load, rpm and survey tool, *Australian Coal Association Research Program*, Project Report C7023. Proving field trials for the Sigra geosteering tool, *Australian Coal Association Research Program*, Project Report C10007.

Gurba, A, Gurba, L, Ward, C and Wood, J, 2003. Gas drainability and outburst risk assessment based on the distribution of micro-markers in coal seams, *Australian Coal Association Research Program*, Project Report C11057.

Hadden, J D and Sainato, A, 1969. Gas migration characteristics of coalbeds, *United States Bureau of Mines Methane Control Program, Technical Progress Report – 12*, 13p. [online]. Available from: http://www.cdc.gov/niosh/mining/pubs/pubreference/outputid1906.htm [Accessed: November, 2009].

Ham, Y and Kantzas, A, 2008. Development of coalbed methane in Australia: unique approaches and tools, *CIPC/SPE Gas Technology Symposium*, Society of Petroleum Engineers, Calgary, Alberta, 16-19 June, 8p. (SPE-114992).

Hanes, J, 2004. Outburst Scoping Study, ACARP Project 10012, Australian Coal Association Research Program [online]. Available from: http://www.uow.edu.au/eng/outburst/Outburst_Scoping_Study_BWR_304.doc [Accessed: December 2006].

Hargraves, A J, 1983. Prevention of instantaneous outbursts of coal and gas, *Alleviation of Coal and Gas Outbursts in Coal Mines – Seminar 3*, (ed: R D Lama), Co-ordinating Committee on Outburst Research.

Harpalani, S, 1989. Permeability changes resulting from desorption, *Quarterly Review of Methane from Coal Seams Technology*, Gas Research Institute, Volume 6, Numbers 3 and 4, pp 58-61.

Harpalani, S and Chen, G, 1992. Effect of gas production on porosity and permeability of coal, *Symposium on Coalbed Methane Research and Development in Australia*, Coalseam Gas Research Institute – James Cook University, Townsville, 19-21 November, Volume 4, pp 67-78.

Harpalani, S and Schraufnagel, R A, 1990. Influence of matrix shrinkage and compressibility on gas production from coalbed methane reservoirs, *Proceedings of the 65th Annual Technical Conference and Exhibition of the Society of Petroleum Engineers*, Los Angeles, pp 171-179. (SPE-20729).

Harpalani, S and Zhao, X, 1989. An investigation of the effect of gas desorption on coal permeability, in *Proceedings of the 1989 International Coalbed Methane Symposium*, University of Alabama, Tuscaloosa, 17-20 April, pp 57-64.

Hartman, C and Pratt, T J, 2005. A preliminary study of the effect of moisture on the carbon dioxide storage capacity in coal, in *Proceedings of the 2005 International Coalbed Methane Symposium*, University of Alabama, Tuscaloosa. 18-19 May. Paper No.0533.

Harvest Tool Company, 2010. Cavity underreamer [online]. Available from: http://www.harvesttool.com/cavityunderreamer.html [Accessed: November 2010].

Harvey, C R and Singh, R N, 1998. A review of fatal outburst incidents in the Bulli seam, in *Proceedings of the 1st Australasian Coal Operators' Conference COAL98*, University of Wollongong, 18-20 February, pp 649-658.

Hatherly, P, Dixon, R, Murray, W, Tchen, T, Pollock, J T A, Jecny, Z, Williams, C J and Cervolo, C, 1996. Sensing and logging for in-seam boreholes, *Australian Coal Association Research Program*, Project Report C4037.

Hays, J, 2010. Coal mine deaths in China [online]. Available from: http://factsanddetails.com/china.php?itemid=321&catid=13&subcatid=85 [Accessed: December 2010].

Hayes, P J, 1982. Factors affecting gas release from the working seam, in *Proceedings of the Symposium on Seam Gas Drainage with Particular Reference to the Working Seam*, (ed: A J Hargraves), Australasian Institute of Mining and Metallurgy – Illawarra Branch, University of Wollongong, Wollongong, Australia, 11-14 May, pp 62-69.

Hebblewhite, B, Richmond, A and Allan, J, 1982. Factors affecting gas release from the working seam, in *Proceedings of the Symposium on Seam Gas Drainage with Particular Reference to the Working Seam*, (ed: A J Hargraves), Australasian Institute of Mining and Metallurgy – Illawarra Branch, University of Wollongong, Wollongong, Australia, 11-14 May, pp 202-217.

Hebblewhite, B K, Sheppard, J and Nixon, L K, 1983. The use of gas drainage and role of structural geology in outburst prevention, *Alleviation of Coal and Gas Outbursts in Coal Mines*, Coordinating Committee on Outburst Research.

Hildenbrand, A, Kroos, B M, Busch, A and Gaschnitz, R, 2006. Evolution of methane sorption capacity of coal seams as a function of burial history – a case study from the Campine Basin, NE Belgium, *International Journal of Coal Geology*, Volume 66, pp 179-203.

Holditch, S A, Ely, J W and Carter, R H, 1989. Development of a coal seam fracture design manual, in *Proceedings of the 1989 International Coalbed Methane Symposium*, University of Alabama, Tuscaloosa, 17-20 April, pp 299-320.

Holditch, S A, Ely, J W, Carter, R H, Hinkel, J and Jeffrey, R G, 1988. Enhanced recovery of coalbed methane through hydraulic fracturing, in *Proceedings of the 63rd Annual Technical Conference and Exhibition of the Society of Petroleum Engineers*, Society of Petroleum Engineers, Houston, Texas, 2-5 October, 9p. (SPE-18250).

Humphries, P, Ogden, A and Li, F, 2006. Pre-mining gas drainage technologies optimisation, *Australian Coal Association Research Program*, Project Report C13020.

Hungerford, F, 2008. In-seam directional drilling [online], ACARP Gas and Outburst Seminar, Wollongong, 26 November. Available from: http://www.uow.edu.au/eng/outburst/html/outburst_pres.html [Accessed: September 2010].

Hutton, A, 2008. Results of petrographic analysis of coal samples following slow desorption testing, Unpublished report.

International Longwall News (ILN), 2000. Valley develops innovative surface to in-seam drilling method [online]. Available from: http://www.longwalls.com/storyview.asp?storyid=2094&sectionsource=s89&highlight=survey [Accessed: September 2010].

International Longwall News (ILN), 2009a. Xinxing death toll hits 108 [online]. Available from: http://www.longwalls.com/storyview.asp?storyid=1039279&sectionsource=s89&highlight=gas [Accessed: June 2010].

International Longwall News (ILN), 2009b. Exporters to gain from Chinese safety shutdowns [online]. Available from: http://www.longwalls.com/storyview.asp?storyid=1036674&sectionsource=s89&highlight=gas [Accessed: June 2010].

International Longwall News (ILN), 2009c. Another 21 deaths in Chinese coal industry [online]. Available from: http://www.longwalls.com/storyview.asp?storyid=1027228&sectionsource=s89&highlight=gas [Accessed: June 2010].

International Longwall News (ILN), 2009d. Explosion devastates Indo coal mine [online]. Available from: http://www.longwalls.com/storyview.asp?storyid=1003332&sectionsource=s89&highlight=gas [Accessed: June 2010].

International Longwall News (ILN), 2010a. Explosion claims 10 lives at Chinese coal mine [online]. Available from: http://www.longwalls.com/storyview.asp?storyid=1135482&sectionsource=s89&highlight=gas [Accessed: June 2010].

International Longwall News (ILN), 2010b. Gas explosion kills 2 at Chinese colliery [online]. Available from: http://www.longwalls.com/storyview.asp?storyid=1134142&sectionsource=s89&highlight=gas [Accessed June 2010].

International Longwall News (ILN), 2010c. More bodies retrieved from Colombian mine disaster [online]. Available from: http://www.longwalls.com/storyview.asp?storyid=1137033&sectionsource=s89&highlight=gas [Accessed: June 2010].

International Longwall News (ILN), 2010d. Russian safety blitz [online]. Available from: http://www.longwalls.com/storyview.asp?storyid=1135689&sectionsource=s89&highlight=coal [Accessed June 2010].

International Longwall News (ILN), 2010e. Subsidence hampers Turkish mine rescue [online]. Available from: http://www.longwalls.com/storyview.asp?storyid=1135905&sectionsource=s89&highlight=zonguldak, [Accessed June 2010].

International Longwall News (ILN), 2010f. MSHA releases preliminary UBB report [online]. Available from: http://www.longwalls.com/storyview.asp?storyid=1134635&sectionsource=s89&highlight=coal [Accessed: June 2010].

International Longwall News (ILN), 2010g. Mourning for lost Pike miners [online]. Available from: http://www.longwalls.com/storyview.asp?storyid=1587349&sectionsource=s89&highlight=pike [Accessed: December 2010].

International Longwall News (ILN), 2010h. Death toll at gassy mine accident could be 37 [online]. Available from: http://www.longwalls.com/storyview.asp?storyid=1541456&sectionsource=s89&highlight=gas [Accessed: December 2010].

International Longwall News (ILN), 2010i. Gas kills 21 at Chinese colliery [online]. Available from: http://www.longwalls.com/storyview.asp?storyid=1135690&sectionsource=s89&highlight=gas [Accessed: December 2010].

Jackson, M, 2004. Permeability testing procedure, *BHP Billiton Illawarra Coal Exploration / Coal Bed Methane*, Internal Operating Procedure, document reference - CBM-12-010.

Jahediesfanjani, H and Civan, F, 2006. Effect of resident water on enhanced coal gas recovery by simultaneous CO2/N2 injection, *SPE Annual Technical Conference and Exhibition*. Society of Petroleum Engineers, San Antonio, Texas, 24-27 September, 18p. (SPE-102634).

Jeffrey, R G, Connell, L and Mills, K, 2005. Optimising sand-propped hydraulic fracture stimulation of in-seam gas drainage holes, *Australian Coal Association Research Program*, ACARP Report C12021.

Jeffrey, R G, Enever, J R, Ferguson, T, Bride, J, Phillips, R and Davidson, S, 1993. Small-scale hydraulic fracturing and mineback experiments in coal seams. in *Proceedings of the 1993 International Coalbed Methane Symposium*, Birmingham, Alabama, 17-21 May.

Jeffrey, R G, Hinkel, J J, Nimerick, K H and McLennan, J, 1989. Hydraulic fracturing to enhance production of methane from coal seams, in *Proceedings of the 1989 International Coalbed Methane Symposium*, University of Alabama, Tuscaloosa, 17-20 April, pp 385-394.

Jeffrey, R G, Settari, A and Smith, N P, 1995. A comparison of hydraulic fracture field experiments, including mineback geometry data, with numerical fracture model simulations, *SPE Annual Technical Conference & Exhibition*, Dallas, 22-25 October, pp 591-606. (SPE-30508).

Jeffrey, R G, Vlahovic, W, Doyle, R P and Wood, J H, 1998. Propped fracture geometry of three hydraulic fractures in the Sydney basin coal seams, *SPE Asia Pacific Oil & Gas Conference*, Perth, Australia, 12-14 October, pp 191-201. (SPE-50061).

Jeffrey, R G, Weber, C R, Vlahovic, W and Enever, J R, 1994. Hydraulic fracturing experiments in the Great Northern coal seam, *Asia Pacific Oil and Gas Conference*, Melbourne, 7-10 November, pp 361-371. (SPE-28779).

Jenkins, C and Boyer, C M, 2008. Coalbed- and shale-gas reservoirs, *Journal of Petroleum Technology*, Society of Petroleum Engineers, February, Distinguished Author Series, pp 92-99. (SPE-103514).

Johnson, D, 2010. Perspectives on new CBM production, gas markets and carbon trading in Australia [online], *Metgasco Limited*, 15p. Available from: http://www.metgasco.com.au/files/623758.pdf [Accessed: November 2010].

Johnson, R L, Scott, S and Herrington, M, 2006. Changes in completion strategy unlocks massive Jurassic coalbed methane resource base in the Surat Basin, Australia, *SPE Asia Pacific Oil & Gas Conference*, Adelaide, Australia, 11-13 September, pp 191-201, 16p. (SPE-101109).

Jones, A H, Ahmed, U, Abou-Sayed, A S, Mahyera, A and Sakashita, B, 1982. Fractured vertical wells versus horizontal boreholes for methane drainage in advance of mining U.S. coals, in *Proceedings of the Symposium on Seam Gas Drainage with*

Particular Reference to the Working Seam, (ed: A J Hargraves), Australasian Institute of Mining and Metallurgy – Illawarra Branch, University of Wollongong, Wollongong, Australia, 11-14 May, pp 172-201.

Kahil, A A and Masszi, D, 1982. Technical considerations for the design of a demethanation program, in *Proceedings of the Symposium on Seam Gas Drainage with Particular Reference to the Working Seam*, (ed; A J Hargraves), Australasian Institute of Mining and Metallurgy – Illawarra Branch, University of Wollongong, Wollongong, Australia, 11-14 May, pp 99-104.

Kelly, M, 1983. Practical in-seam drainage at Appin Colliery, *Alleviation of Coal and Gas Outbursts in Coal Mines – Seminar 3*, (ed: R D Lama), Co-ordinating Committee on Outburst Research.

Kim, A G, 1977. Estimating methane content of bituminous coalbeds from adsorption data, *United States Department of the Interior*, Bureau of Mines Report of Investigations RI8245.

Kissell, F N, 2006. Handbook for methane control in mining, *National Institute for Occupational Safety and Health*, NIOSH Information Circular No.9486, 191p. [online]. Available from: http://www.cdc.gov/niosh/mining/pubs/pdfs/2006-127.pdf [Accessed: November 2010].

Kissell, F N and Edwards, J C, 1975. Two-phase flow in coalbeds, *United States Department of the Interior*, Bureau of Mines Report of Investigations RI8066, 20p. [online]. Available from: http://www.cdc.gov/niosh/mining/pubs/pdfs/ri8066.pdf [Accessed: November 2010].

Kravits, S, Rusby, B, Reilly J and DuBois, G, 1999. Reaching greater depths, [online]. 7p. Available from: http://www.targetdrilling.com/pdf/pubs/REACHING-GREATER-DEPTHS.pdf [Accessed: September 2010].

Kravits, S J and Schwoebel, J J, 1994. Directional drilling techniques for exploration in-advance of mining [online], 8p. Available from: http://www.targetdrilling.com/pdf/pubs/Directional-Drilling-Techniques-explor.pdf [Accessed: September 2010].

Lama, R D, 1980. Drainage of methane from the solid at West Cliff Colliery – Optimisation of drainage hole design parameters, *Commonwealth Scientific and Industrial Research Organisation, Division of Applied Geomechanics*, Geomechanics of coal mining report No.18.

Lama, R D, 1981. The use of adsorption/desorption isotherms in predicting outburst conditions, *Commonwealth Scientific and Industrial Research Organisation*, Report No. 21.

Lama, R D, 1983. Alleviation of methane controlled outbursts by advance drainage, *Alleviation of Coal and Gas Outbursts in Coal Mines – Seminar 3*, (ed: R D Lama), Co-ordinating Committee on Outburst Research.

Lama, R D, 1988a. Improving the efficiency of gas drainage systems, *Australian Coal Association Research Program*, ACARP Project Report C0574. Also published as *National Energy Research, Development and Demonstration Program*, End of Grant Report number 7.01, October 1986.

Lama, R D, 1988b. Adsorption and desorption of mixed gases on coal and their implications in mine ventilation, in *Proceedings of the Fourth International Mine Ventilation Congress*, (ed: A D S Gillies), Brisbane, 3-6 July, pp 161-174.

Lama, R D, 1991. Methane emissions from coal mining in Australia: estimates and control strategies, in *Proceedings of the IEA/OECD conference on coal, the environment and development: technologies to reduce greenhouse gas emissions*, Sydney, 18-22 November, pp 255-266.

Lama, R D, 1995a. Errors in gas content measurements in underground sampling of coal using cores, *International Symposium on Management and Control of High Gas Emissions and Outbursts in Underground Coal Mines*, (ed: R D Lama), Wollongong, 20-24 March, pp 557-567.

Lama, R D, 1995b. Evaluation of in-seam borehole stability in coal mines, *Australian Coal Association Research Program*, ACARP Project Report C3029.

Lama, R D, 1995c. Safe gas content threshold value for safety against outbursts in the mining of the Bulli seam, *International Symposium on Management and Control of High Gas Emissions and Outbursts in Underground Coal Mines*, (ed: R D Lama), Wollongong, 20-24 March, pp 175-189.

Lama, R D and Bartosiewicz, H, 1982. Determination of gas content of coal seams, in *Proceedings of the Symposium on Seam Gas Drainage with Particular Reference to the Working Seam*, (ed: A J Hargraves), Australasian Institute of Mining and Metallurgy – Illawarra Branch, University of Wollongong, Wollongong, Australia, 11-14 May, pp 36-52.

Lama, R D and Bodziony, J, 1996. Outbursts of gas, coal and rock in underground coal mines, *R. D. Lama and Associates*, Wollongong.

Lama, R D, Chan, L and Tomczyk, W, 1984. Improving the efficiency of underground gas drainage systems, *National Energy Research, Development and Demonstration Program*, NERDDC Project Number 574, Progress Report March 1984.

Lama, R D, Marshall, P and Griffiths, L, 1980. Methane drainage investigations as a method of control of outbursts at West Cliff Colliery, in *Proceedings of the Symposium on The Occurrence, Prediction and Control of Outbursts in Coal Mines*, Australasian Institute of Mining and Metallurgy – Southern Queensland Branch, pp 223-239.

Lama, R D and Saghafi, A, 2002. Overview of gas outbursts and unusual emissions, in *Proceedings of the 3rd Australasian Coal Operators' Conference COAL2002*, Australasian Institute of Mining and Metallurgy, Wollongong, 6-8 February, pp 74-88.

Lamarre, R A, 2007. Downhole geomechanical analysis of critical desorption pressure and gas content for carbonaceous reservoirs, *SPE Annual Technical Workshop on Coalbed Methane*, Society of Petroleum Engineers, Durango, Colorado, 27-29 March, 31p. (SPE-111091).

Larsen, J W, 2004. The effects of dissolved CO_2 on coal structure and properties. *International Journal of Coal Geology*, Volume 57, pp.63-70.

Laubach, S E, Marrett, R A, Olsen, J E and Scott, A R, 1998. Characteristics and origins of coal cleat: a review, *International Journal of Coal Geology*, Vol.35, pp 175-207.

Laxminarayana, C and Crosdale, P J, 1999. Role of coal type and rank on methane sorption characteristics of Bowen Basin, Australia coals, *International Journal of Coal Geology*, Volume 40, pp 309-325.

Le Roux, W L, 1990. Le Roux's notes on mine environmental control, *The Mine Ventilation Society of South Africa*, Fourth Edition, p.50.

Levine, J R, 1992. Influences of coal composition on coal seam reservoir quality: a review, *Symposium on Coalbed Methane Research and Development in Austral*ia, Coalseam Gas Research Institute – James Cook University, Townsville, 19-21 November. Volume 1, pp i-xxviii.

Levine, J R, 1996. Model study of the influence of matrix shrinkage on absolute permeability of coal bed reservoirs, *Coalbed Methane and Coal Geology*, (eds: R Gayer and I Harris), Geologic Society Special Publication, No.109, pp 197-212.

Levy, J H, Day, S J and Killingley, J S, 1997. Methane capacities of Bowen Basin coals related to coal properties, *Fuel*, Volume 76, Number 9, pp 813-819.

Levy, J H, Killingley, J S, Day, S J and Liepa, I, 1992. Measurement of coalbed methane isotherms for Australian coals, *Symposium on Coalbed Methane Research and Development in Australi*a, Coalseam Gas Research Institute – James Cook University, Townsville, November 19-21. Volume 3, pp 1-7.

Loftin, P, 2009. Tips and tricks for finding, developing and operating a coalbed methane field [online], *24th World Gas Conference*, Argentina, 5-9 October, 17p. Available from: http://www.igu.org/html/wgc2009web/admin/archivosCom/Loftin-Philip%20%5BCompatibility%20Mode%5D.pdf [Accessed: November 2010].

Logan, T L, Clark, W F and McBane, R A, 1989. Comparing different coalbed methane completion techniques, hydraulic fracture and openhole cavity, at the Northeast Blanco unit, San Juan Basin, in *Proceedings of the 1989 International Coalbed Methane Symposium*, University of Alabama, Tuscaloosa, 17-20 April, pp 265-272.

Logan, T L, Schwoebel, J J and Horner, D M, 1987. Application of horizontal drainhole drilling technology for coalbed methane recovery, in *Proceedings of the SPE/DOE Low Permeability Reservoirs Symposium*, Society of Petroleum Engineers, Denver, Colorado, 18-19 May, pp 195-206. (SPE-16409).

Lunarzewski, L W, 2001. Gas drainage practices [online], in *Proceedings of Coal 2001: Coal Operators' Geotechnical Colloquium*, (ed: N I Aziz), University of Wollongong and Australasian Institute of Mining and Metallurgy, 15 February, pp 34-44. Available from: http://www.uow.edu.au/eng/outburst/presentations_publications/coal_2001/Lunarzewski%202001.pdf [Accessed: November 2010].

Marshall, P, Lama, R D and Tomlinson, E, 1982. Experiences on pre-drainage of gas at West Cliff colliery, in *Proceedings of the Symposium on Seam Gas Drainage with Particular Reference to the Working Seam*, (ed: A J Hargraves), Australasian Institute of Mining and Metallurgy – Illawarra Branch, University of Wollongong, Wollongong, Australia, 11-14 May, pp 141-156.

Mastalerz, M, Gluskoter, H and Rupp, J, 2004. Carbon dioxide and methane sorption in high volatile bituminous coals from Indiana, USA, *International Journal of Coal Geology*, Volume 60, Issue 1, 22 October, pp 43-55.

Mavor, M J, 1994. Coal gas openhole well performance, in *Proceedings of University of Tulsa Centennial Petroleum Engineering Symposium*, Society of Petroleum Engineers, Tulsa, Oklahoma, 29-31 August, pp 369-382. (SPE-27993).

Mavor, M J, Close, J C and Pratt, T J, 1992. Review of recent US coalbed natural gas reservoir research, in *Proceedings of the Symposium on Coalbed Methane Research and Development in Australia*, Coalseam Gas Research Institute – James Cook University, Townsville, November 19-21, Volume 2, pp 109-152.

Mavor, M J and Logan, T L, 1994. Recent advances in coal gas-well openhole well completion technology, *Journal of Petroleum Technology*, Society of Petroleum Engineers, July, pp 587-593. (SPE-26211).

Mazumder, S, van Hemert, P, Busch, A, Wolf, K-H A A and Tejera-Cuesta, P, 2006. Flue gas and pure CO_2 sorption properties of coal: a comparative study, *International Journal of Coal Geology*, Volume 67, pp 267-279.

Mazumder, S and Wolf, K H, 2008. Differential swelling and permeability change of coal in response to CO_2 injection for ECBM, *International Journal of Coal Geology*, Volume 74, pp 123-138.

McCulloch, C M, Levine, J R, Kissell, F N and Deul, M, 1975. Measuring the methane content of bituminous coalbeds, *United States Department of the Interior*, Bureau of Mines Report of Investigations RI8043, 25p.

Meszaros, G, Boonen, P and Hale, M, 2007. New tools enable CBM horizontal drilling [online], *E&P Journal*, pp 50-53. Available from: http://www.epmag.com/archives/features/536.htm [Accessed: August 2009].

Meyer, T, Lugg, P and Black, D J, 2007. Coiled tubing drilling system development – risk mitigation, *Australian Coal Association Research Program*, 2007 Project Proposal, Reference number C27132.

Mills, K, Jeffrey, R G, Black, D J, Meyer, T, Carey, K, Goddard, S, 2006. Developing methods for placing sand-propped hydraulic fractures for gas drainage in the Bulli seam, in *Proceedings of the 7th Underground Coal Operators' Conference COAL2006*, University of Wollongong and The Australasian Institute of Mining and Metallurgy, (eds: N I Aziz and W Keilich), Wollongong, 5-7 July, pp 190-199.

Monaghan, W D, Trevits, M A, Mucho, T P and Wood, J, 2003. Recent national institute for occupational safety and health research using ground penetrating radar for detection of mine voids [online], in *Proceedings of the Geophysical Techniques for Detecting Underground Coal Mine Voids – An Interactive Forum*, Lexington, Kentucky, 29-30 July, 29p. Available from: http://www.cdc.gov/niosh/mining/pubs/pdfs/rnifos.pdf [Accessed: September 2010].

Mones, C G, 2001. System for improving coalbed gas production, *US Patent* 6244338 B1 [online]. Available from: http://www.freepatentsonline.com/6244338.html [Accessed: November 2010].

Mones, C G, 2002. Enhanced coalbed gas production system, *US Patent* 6450256 B2 [online]. Available from: http://www.freepatentsonline.com/6450256.html [Accessed: November 2010].

Moore, R D and Hanes, J, 1980. Bursts in coal at Leichardt Colliery, Central Queensland and the apparent benefits of mining by shotfiring, in *Proceedings of the Symposium on the Occurrence, Prediction and Control of Outbursts in Coal Mines*,

Australasian Institute of Mining and Metallurgy – Southern Queensland Branch, pp 71-83.

Murray, W, Williams, C, Lewis, C and Hatherly, P, 1999. Borehole dielectric probe for the detection of mylonite zones and other structures, *Australian Coal Association Research Program*, Project Report C6026.

Mutmansky, J M, 1999. White Paper: Guidebook on coalbed methane drainage for underground coal mines [online]. Available from: http://www.epa.gov/cmop/docs/red001.pdf [Accessed: January 2007].

New South Wales Department of Mineral Resources (NSWDMR), 1995. Outburst Mining Guideline MDG No.1004, Coal Mining Inspectorate and Engineering Branch, Department of Mineral Resources New South Wales.

Newland, A, 2007. West Cliff 519 and 520 panel cleat mapping data, Unpublished data.

Olsen, T N, Brenize, G and Frenzel, T, 2003. Improvement processes for coalbed natural gas completion and stimulation, *SPE Annual Technical Conference and Exhibition*, Denver, Colorado, 5-8 October, 16p. (SPE-84122).

Osisanya, S A and Schaffitzel, R F, 1996. A review of horizontal drilling and completion techniques for recovery of coalbed methane. *SPE International Conference on Horizontal Well Technology*, Society of Petroleum Engineers, Calgary, Canada, 18-20 November, 13p. (SPE-37131).

Oudinot, A Y, Schepers, K C and Reeves, S R, 2007. Gas injection and breakthrough trends as observed in ECBM sequestration pilot projects and field demonstrations, in *Proceedings of the 2007 International Coalbed Methane Symposium*, University of Alabama, Tuscaloosa, 24-25 May, 13p. Paper No.0714.

Palmer, I D, 1992. Review of coalbed methane well stimulation, *SPE International Meeting on Petroleum Engineering*, Society of Petroleum Engineers, Beijing, China, 24-27 March, pp 679-703. (SPE-22395).

Palmer, I D, 1993. Induced stresses due to propped hydraulic fracture in coalbed methane wells, *SPE Rocky Mountain Regional Meeting and Low Permeability Reservoirs Symposium*, Society of Petroleum Engineers, Denver, Colorado, 12-14 April, pp 221-232. (SPE-25861).

Palmer, I D, 2008. CBM well completions: principles and best practices, *ASIA Pacific Coalbed Methane Symposium*, University of Queensland, Brisbane, 21 September.

Palmer, I D, Fryar, R T, Tumino, K A and Puri, R, 1991. Comparison between gel-fracture and water-fracture stimulations in Black Warrior Basin, in *Proceedings of the 2001 International Coalbed Methane Symposium*, University of Alabama, Tuscaloosa, 13-16 May, 10p. (SPE-23415).

Pan, Z, Connell, L D, Camilleri, M and Connelly, L, 2010. Effects of matrix moisture on gas diffusion and flow in coal, *Fuel*, Volume 89, pp 3207-3217.

Patching, T H, 1970. The retention and release of gas in coal – a review, *Canadian Mining and Metallurgical Bulletin*, Vol.63, pp 1302-1308.

Perkins, J H and Cervik, J, 1969. Sorption investigation of methane on coal, *United States Department of the Interior*, Bureau of Mines Methane Control Program, Technical Progress Report – 14 [online], 9p. Available from:

http://www.cdc.gov/niosh/mining/pubs/pubreference/outputid1908.htm [Accessed: November 2009].

Puri, R, King, G E and Palmer, I D, 1991. Damage to coal permeability during hydraulic fracturing, *SPE Rocky Mountain Regional Meeting and Low Permeability Reservoirs Symposium*, Society of Petroleum Engineers, Denver, Colorado, 15-17 April, pp 109-115. (SPE-21813).

Puri, R and Stein, M H, 1989. Method of coalbed methane production, *US Patent* 4883122.

Reward, H, 2006. Volumetric changes in coal due to changes to gas sorption, *Undergraduate Thesis*, School of Civil, Mining and Environmental Engineering, University of Wollongong.

REI Drilling, 2004. Horizontal heading [online], *American Longwall Magazine*, pp 20-21. Available from: http://www.reidrilling.com/pdf/Horizontal%20headings.pdf [Accessed: September 2010].

Richards, D J, 1980. Seam gas drainage as a means of outburst control, in *Proceedings of the Symposium on the Occurrence, Prediction and Control of Outbursts in Coal Mines*, Australasian Institute of Mining and Metallurgy – Southern Queensland Branch, pp 217-221.

Roy, M, 2008. Personal communication, AGL Gas Developments, 09 January.

Saghafi, A, (2009). Enhanced coal bed methane (ECBM) and CO_2 storage in Australian coals [online], The Australian Institute of Energy, 43p. Available from: http://aie.org.au/Content/NavigationMenu/SydneyBranch/PastTechnicalMeetings/saghaficsm.pdf [Accessed November 2010].

Saghafi, A, Faiz, M and Roberts, D, 2007. CO_2 storage and gas diffusivity properties of coals from Sydney basin, Australia, *International Journal of Coal Geology*, Volume 70, Issues 1-3, 2 April, pp 240-254.

Saghafi, A and Roberts, D, 2008a. Measurement of CO_2 and CH_4 reservoir properties of coal from West Cliff mine, CSIRO Investigation Report ET/IR 1033R.

Saghafi, A and Roberts, D, 2008b. Results of coal gas reservoir property testing, Raw Data – Unpublished.

Saghafi, A, Roberts, D, Fry, R, Quintanar, A, Day, S, Lange, T, Hoarau, P, Dokumcu, C and Carras, J, 2008. Evaluating a tier 3 method for estimating fugitive emissions from open cut coal mining, *Australian Coal Association Research Program*, Project Report C15076.

Saghafi, A and Williams, D J, 1998. Factors influencing the accuracy of measurement of gas content of coal: Inter-comparison of the quick crush technique, *Australian Coal Association Research Program*, Project Report C6023.

Saghafi, A, Williams, D J and Battino, S, 1998. Accuracy of measurement of gas content of coal using rapid crushing techniques [online], in *Proceedings of the 1st Australasian Coal Operators' Conference COAL98*, University of Wollongong, 18-20 February, pp 551-559. Available from: http://www.uow.edu.au/eng/outburst/presentations_publications/coal_1998/Saghafi-1998.pdf [Accessed: November 2010].

Schatzel, J and Garcia, F, 1999. Apparatus for measuring the gas content of coal or rock core samples [online], *National Institute for Occupational Safety and Health*, NIOSH Technology News No.478. Available from: http://www.cdc.gov/niosh/mining//pubs/pdfs/tn478.pdf [Accessed: November 2008].

Schatzel, S J, Karacan, C Ö, Krog, R B, Esterhuizen, G S and Goodman, G V R, 2008. Guidelines for the prediction and control of methane emissions on longwalls [online], *National Institute for Occupational Safety and Health*, NIOSH Information Circular No.9502. Available from: http://www.cdc.gov/niosh/mining/pubs/pdfs/2008-114.pdf [Accessed: April 2009].

Scott, A R, 2002. Hydrogeologic factors affecting gas content distribution in coal beds, *International Journal of Coal Geology*, Volume 50, Issues 1-4, May, pp 363-387.

Seidle, J P and O'Connor, L S, 2007. The impact of undersaturation on coal gas economics, *SPE Rocky Mountain Oil & Gas Technology Symposium*, Society of Petroleum Engineers, Denver, Colorado 16-18 April, 12p. (SPE-107731).

Sereshki, F, 2005. Improving coal mine safety by identifying factors that influence the sudden release of gases in outburst prone zones, *PhD Thesis*, University of Wollongong.

Shi, J and Durucan, S, 2003. Gas storage and flow in coalbed reservoirs: implementation of a bidisperse pore model for gas diffusion in coal matrix, *SPE Annual Technical Conference and Exhibition*, Denver, Colorado, 5-8 October, 9p. (SPE-84342).

Singh, A and Singh, B D, 1999. Methane gas: an unconventional energy resource. *Indian Academy of Science – Current Science Online* [online] Available from: http://www.ias.ac.in/currsci/jun25/articles15.htm [Accessed: January 2008]

Siriwardane, H J, Gondle, R K and Smith, D H, 2009. Shrinkage and swelling of coal induced by desorption and sorption of fluids: theoretical model and interpretation of a field project, *International Journal of Coal Geology*, Volume 77, pp 188-202.

Snyder, S G, Jockel, D W and Lopez, A W, 2007. Improved fracturing technology for coalbed methane gas wells in Western Pennsylvania increases gas production over offset and historic wells in Mount Pleasant CBM field, *SPE Eastern Regional Meeting*, Society of Petroleum Engineers, Lexington, Kentucky, 17-19 October, 6p. (SPE-111206).

Solano-Acosta, W, Mastalerz, M and Schimmelmann, A, 2007. Cleats and their relation to geologic lineaments and coalbed methane potential in Pennsylvanian coals in Indiana, *International Journal of Coal Geology*, Volume 72, Issues 3-4, 22 November, pp 187-208.

Standards Association of Australia (SAA), 1998. Coal petrography part 2: maceral analysis, *Australian Standard*, AS2856.2:1998.

Standards Association of Australia (SAA), 1999. Guide to the determination of gas content of coal – direct desorption method, *Australian Standard*, AS3980:1999.

Steffen, R M, 1948. Apparatus for oil sand heating, *US Patent* 2444755.

Stevenson, M D, Pinczewski, W V and Downey, R A, 1993. Economic evaluation of nitrogen injection for coalseam gas recovery, *SPE Gas Technology Symposium*, Society of Petroleum Engineers, Calgary, Canada, 28-30 June, 14p. (SPE-26199).

Stewart, W J and Barro, L, 1982. Coal seam degasification by use of hydraulic fracturing in vertical wells case histories, in *Proceedings of the Symposium on Seam Gas Drainage with Particular Reference to the Working Seam* (ed: A J Hargraves), Australasian Institute of Mining and Metallurgy – Illawarra Branch, University of Wollongong, Wollongong, Australia, 11-14 May, pp 89-98.

Tahmoor Colliery, 2003. Outburst management plan: monitoring progress under "limited advance rate" thresholds, *Tahmoor Colliery Work Instruction*, Document No.:W1111, Rev.0.

Thakur, P C and Dahl, H D, 1982. Methane drainage, *Mine Ventilation and Air Conditioning* (eds: H Hartman, J M Mutmansky and Y J Wang), John Wiley & Sons, New York, pp 69-83.

Thomson, S, 1998. The role of directional drilling for safety in coal mining [online], in *Proceedings of the 11th Turkish Coal Congress*, Bartin-Amasra, Turkey, 10-12 June, 10p. Available from: http://www.advminingtech.com.au/Default.aspx?tabid=108 [Accessed: September, 2010].

Thomson, S, 2007. Developments in inseam drilling technology [online], *ACARP Coal and Gas Outburst Seminar*, Wollongong, November. Available from: http://www.uow.edu.au/eng/outburst/html/outburst_pres.html [Accessed: May 2010].

Thompson, S, 2009. Review of inseam drilling practice [online], *ACARP Gas and Outburst Seminar*, Wollongong, 11 November. Available from: http://www.uow.edu.au/eng/outburst/html/outburst_pres.html [Accessed: September 2010].

Thomson S and Adam, S, 2007. Intelligent drilling systems, *Australian Coal Association Research Program*, Project Report C14034.

Thomson, S, Adam, S and Hatherly, P, 2005. Comparative study of in-seam surveying technology (coal interface detection project), *Australian Coal Association Research Program*, Project Report C12024.

Thomson, S, Adam, S and Hatherly, P, 2007. Enhanced geological modelling through advances in logging and interpretation of inseam boreholes, in *Proceedings of the 2007 International Coalbed Methane Symposium*, University of Alabama, Tuscaloosa, 24-25 May, 13p.

Thomson, S, Lukas, A and MacDonald, D, 2003. Maximising coal seam methane extraction through advanced drilling technologies, in *Proceedings of the 2nd Australian Coal Seam and Mine Methane Conference*, 19-20 February, 13p.

Thomson, S and MacDonald, D, 2003. The application of medium radius directional drilling for coal bed methane extraction [online], 11p. Available from: http://www.lucas.com.au/eWebUploadedFiles/MRD%20for%20coal%20seam%20gas.pdf [Accessed: January 2007].

Thomson, S and Qzn, Z, 2009. Review of inseam drilling practice, *Australian Coal Association Research Program*, Project Report C15075.

Thungsuntonkhun, W and Engler, T W, 2001. Well deliverability of undersaturated coalbed reservoir, *SPE Rocky Mountain Petroleum Technology Conference*, Society of Petroleum Engineers, Keystone, Colorado, 21-23 May, 11p. (SPE-71068).

Trevits, M A, Hanson, M E and Ward, V L, 1982. Methane drainage: identification and evaluation of the parameters controlling induced fracture geometry, *Unconventional*

Gas Recovery Symposium, Society of Petroleum Engineers, Pittsburgh, 16-18 May, pp 253-260. (SPE-10820).

United States Environmental Protection Agency (USEPA), 2009. Coal mine methane recovery: a primer, *Coalbed Methane Outreach Program*, Report No. EPA-430-R-09-013 [online]. Available from: http://www.epa.gov/cmop/docs/cmm_primer.pdf [Accessed: November 2010].

University of Wyoming (UWYO), 2002a. The anatomy of a coal forming swamp [online], *The Science and Mathematics Teaching Centre*, University of Wyoming Available from: http://www.wsgs.uwyo.edu/coalweb/swamp/anatomy.aspx [Accessed: March 2008].

University of Wyoming (UWYO), 2002b. Coalification [online], *The Science and Mathematics Teaching Centre*, University of Wyoming. Available from: http://www.wsgs.uwyo.edu/coalweb/swamp/coalification.aspx [Accessed: March 2008].

Ward, C R, 1984. Coal geology and coal technology, Blackwell Scientific Publications, Carlton, Victoria, Australia.

Ward, H, 1980. Outburst occurrences at Metropolitan Colliery, in *Proceedings of the Symposium on the Occurrence, Prediction and Control of Outbursts in Coal Mines*, Australasian Institute of Mining and Metallurgy – Southern Queensland Branch, pp 63-68.

West Cliff Colliery, 2007. West Cliff Colliery Major Hazard Management Plan – Outburst Management Plan, Document No: WCMP0010, Revision 11, 05 June.

Williams, R J, 1991. Carbon dioxide and methane emission at Tahmoor Colliery, *Gas in Australian coals, a symposium on seam gas* (eds: W J Bamberry and A M Depers), University of New South Wales, pp 141-155.

Williams, R J, 1996. Application of gas content test data to the evaluation of gas emission and hazards during longwall development and extraction, *Symposium on Geology in Longwall Mining*, Coalfield Geology Council of New South Wales, pp 35-40.

Williams, R J, 1997. Definition of outburst threshold limits from core testing [online]. Available from: http://www.geogas.com.au/files/u2/OutburstThresholdOct1997.pdf [Accessed: March 2008].

Williams, R J, 2002. Gas content testing for outburst management compliance, in *Proceedings of the 3rd Australasian Coal Operators' Conference COAL2002*, Australasian Institute of Mining and Metallurgy, Wollongong, 6-8 February, pp 47-52 [online]. Available from: http://www.uow.edu.au/eng/outburst/presentations_publications/coal_2002-3/Williams%202002.pdf [Accessed: November 2010].

Williams R J, 2010. Personal Communication, 30 August.

Williams, R J, Hungerford, F, Beamish, B B and Gray, I, 1983. Gas drainage as a means of outburst alleviation at No.2 mine, Collinsville – A summary of investigations from 1977, *Alleviation of Coal and Gas Outbursts in Coal Mines – Seminar 3* (ed: R D Lama), Co-ordinating Committee on Outburst Research.

Williams, R J and Weissman, J, 1995. Gas Emission and Outburst Assessment in Mixed CO_2 and CH_4 Environments, *ACIRL Seminar – Prosperity with Safety in a Hostile Environment*, University of New South Wales, pp 1-13.

Wight, D, 2005. Unconventional plays: enhancing performance with new technologies [online]. Available from: http://energy.ihs.com/NR/rdonlyres/4EA9831E-99AA-4F1D-A09B-EEDF75212610/0/wight.pdf [Accessed: November 2010].

Wood, J H and Hanes, J, 1983. Development of techniques for prevention of outbursts, *Alleviation of Coal and Gas Outbursts in Coal Mines – Seminar 3* (ed: R D Lama), Co-ordinating Committee on Outburst Research.

Yi, J, Akkutlu, I Y, Karacan, C Ö and Clarkson, C R, 2009. Gas sorption and transport in coals: A poroelastic medium approach [online], *International Journal of Coal Geology*, Volume 77(1-2), pp 137-144. Available from: http://www.cdc.gov/niosh/mining/pubs/pubreference/outputid3065.htm [Accessed: November 2009].

Zahid, S, Bhatti, A A, Khan, H A, Ahmad, T, 2007. Development of unconventional gas resources: stimulation perspective, *SPE Production and Operations Symposium*, Society of Petroleum Engineers, Oklahoma City, Oklahoma, 31 March – 3 April, 11p. (SPE-107053).

Zutshi, Z and Harpalani, S, 2005. Gas flow characterization of Illinois coal: assessment for recovery of coalbed methane and carbon sequestration potential, in *Proceedings of the 2005 International Coalbed Methane Symposium*, University of Alabama, Tuscaloosa, 18-19 May, paper no.0514, 10p.